

Hydrogeology of the Main Karoo Basin: Current Knowledge and Future Research Needs

AC Woodford and L Chevallier (Editors)



TT 179/02



Water Research
Commission

Hydrogeology of the Main Karoo Basin: Current Knowledge and Future Research Needs

**Prepared for the
Water Research Commission**

by

AC Woodford and L Chevallier (editors)

Contributors:

**JF Botha
D Cole
MR Johnson
R Meyer
M Simonic
GJ Van Tonder
B Th Verhagen**

Obtainable from:

**Water Research Commission
Private Bag X03
GEZINA
0031**

The publication of this report emanates from a project entitled: *The Preparation of a Handbook on the Hydrogeology of the Karoo Supergroup* (WRC Project No. 860)

DISCLAIMER

This report has been reviewed by the Water Research Commission (WRC) and approved for publication. Approval does not signify that the contents necessarily reflect the views and policies of the WRC, nor does mention of trade names or commercial products constitute endorsement or recommendation for use.

**ISBN No 1 86845 851 2
Printed in the Republic of South Africa**

ACKNOWLEDGEMENTS

The Project Team would like to express their gratification to the following instances:

- The Water Research Commission for its funding and assistance of the research project,
- Members of the Working Group for their time and invaluable input into ensuring the success of the project. The inaugural August 1997 Steering Committee consisted of the following persons:
 - Mr. A.G. Reynders (Water Research Commission) - Chairman
 - Mr. K. Pietersen (Water Research Commission) - Chairman
 - Mr. A. Woodford (Department Water Affairs & Forestry)
 - Dr. L. Chevallier (Council for Geoscience)
 - Prof. J.F. Botha (University of the Free State)
 - Prof. G.J. van Tonder (University of the Free State)
 - Prof. B. Th. Verhagen (Witwatersrand University)
 - Mr. M. Simonic (Hydromedia Solutions)
 - Mr. R. Meyer (CSIR)
 - Prof. C. Hartnady (Univeristy of Cape Town)
 - Dr. M.R. Johnson (Council for Geoscience)
 - Dr. W. Colliston (University of the Free State)
 - Mr. J. Looock (University of the Free State)
 - Mr. J.R. Vegter (Consultant)
 - Mr. N. Andersen (NJB Andersen Consulting)

Dedication

This manuscript is dedicated to the memory of Tony Reynders, who initiated and enthusiastically guided this project, but was not able to see its fruition.



The editors at an exploration site on a dolerite sill in the Victoria West District, during the drilling of an artesian borehole with a drillstem yield of 80 ℓ/s

TABLE OF CONTENTS

	Page No.
1. INTRODUCTION	1
1.1 BACKGROUND TO THE PROJECT	3
1.2 SCOPE	3
1.3 TARGET AUDIENCE	3
1.4 PHYSIOGRAPHY, CLIMATE AND SURFACE HYDROLOGY	4
1.5 GEOLOGICAL OVERVIEW	8
1.5.1 Sediments of the Karoo Supergroup	8
1.5.2 Karoo Basalt and Dolerite Magmatism	12
1.5.3 Kimberlite Intrusives	14
1.6 MODERN GEOMORPHOLOGY	14
2. GEOLOGY AND HYDROLOGICAL PROPERTIES	15
2.1 LITHOSTRATIGRAPHY AND DEPOSITIONAL HISTORY	15
2.1.1 Dwyka Group	15
2.1.1.1 Lithofacies	15
2.1.1.2 Depositional Environment and Sediment Source	17
2.1.2 Eccca Group	18
2.1.2.1 Prince Albert Formation (Lower Eccca)	20
2.1.2.2 Whitehill Formation (Lower Eccca)	20
2.1.2.3 Collingham Formation (Upper Eccca)	22
2.1.2.4 Vischkuil Formation (Upper Eccca)	23
2.1.2.5 Laingsburg Formation (Upper Eccca)	23
2.1.2.6 Ripon Formation (Upper Eccca)	24
2.1.2.7 Fort Brown Formation (Upper Eccca)	24
2.1.2.8 Waterford Formation of the Southern Zone (Upper Eccca)	25
2.1.2.9 Tierberg Formation (Upper Eccca)	25
2.1.2.10 Skoorsteenbergr Formation (Upper Eccca)	26
2.1.2.11 Kookfontein Formation (Upper Eccca)	26
2.1.2.12 Waterford Formation of Western Zone (Upper Eccca)	27
2.1.2.13 Waterford Formation of the North-Western Zone (Upper Eccca)	27
2.1.2.14 Pietermaritzburg Formation	28
2.1.2.15 Vryheid Formation	28
2.1.2.16 Volksrust Formation	29
2.1.2.17 Depositional Environment and Source of Sedimentation	29
2.1.3 Beaufort Group	30
2.1.3.1 Adelaide Subgroup	30
2.1.3.2 Tarkastad Subgroup	31
2.1.4 Molteno, Elliot and Clarens Formations	33
2.1.4.1 Molteno Formation	33
2.1.4.2 Elliot Formation	34
2.1.4.3 Clarens Formation	36

2.2	HYDROSTRATIGRAPHY	37
2.2.1	Dwyka Group	37
2.2.2	Ecca Group	38
2.2.3	Beaufort Group	38
2.2.4	Molteno, Elliot and Clarens Formations	39
2.2.5	Primary Hydraulic Properties of Karoo Rocks	40
2.3	KAROO MAGMATISM	46
2.3.1	Extrusives	46
2.3.1.1	Drakensberg Lavas	46
2.3.2	Intrusives	48
2.3.2.1	Karoo Dolerites	48
2.3.2.2	Breccia Plugs and Volcanic Vents	113
2.3.2.3	Kimberlite and Associated Alkaline Intrusive Complexes	122
2.4	NON-INTRUSIVE TECTONIC FEATURES	133
2.4.1	Regional Lineaments	133
2.4.1.1	Description	133
2.4.1.2	Hydrological Properties	135
2.4.2	Folding	135
2.4.2.1	Description	135
2.4.2.2	Hydrological Properties	136
2.4.3	Vertical Faulting and Master-Jointing	143
2.4.3.1	Description	144
2.4.3.2	Distribution	144
2.4.3.3	Jointing Mechanisms	145
2.4.3.4	Hydrological Properties	146
	<i>Case Study: Flooding of the Orange-Fish River Tunnel</i>	149
2.4.4	Bedding-Plane Fracturing	153
2.4.4.1	Description	153
2.4.4.2	Hydrological Properties	154
2.5	SEISMICITY, NEOTECTONICS AND UNLOADING	155
2.5.1	Seismo-neotectonic Provinces	155
2.5.2	Uplifting and Erosional Unloading	157
2.5.3	Hydrological Implications	157
2.6	GEOMORPHOLOGY, FLUVIAL TERRACES AND PEDOCRETES	158
2.6.1	Geomorphology	158
2.6.1.1	First Order Features	158
2.6.1.2	Second Order Features	158
2.6.1.3	Hydrological Significance	162
2.6.2	Fluvial Terraces and Floodplains	162
2.6.2.1	Description	162
2.6.2.2	Hydrological Properties	164
2.6.3	Pedocretes	167
2.6.3.1	Description	167
2.6.3.2	Hydrological Significance	169

2.7	DIAGENESIS, PALEO-FLUID MOVEMENTS AND THERMO-METAMORPHISM	170
2.7.1	Description	170
2.7.2	Hydrological Implications	170
2.8	WEATHERING	171
2.8.1	Sediment Weathering	172
2.8.1.1	Dwyka Diamictite	172
2.8.1.2	Mudrock	173
2.8.1.3	Sandstone	173
2.8.2	Dolerite Weathering	173
2.8.3	Hydrological Implications	176
3.	PHYSICAL AND CHEMICAL DESCRIPTION OF KAROO AQUIFERS	178
3.1	GROUNDWATER FLOW AND BEHAVIOUR OF KAROO FRACTURED AQUIFERS	178
3.1.1	Introduction	178
3.1.2	Nature of Groundwater Flow in Fractured Aquifers	179
3.1.2.1	General	179
3.1.2.2	Fracture Hydraulics	182
3.1.2.3	Fracture Mechanics	186
3.1.2.4	Summary	188
3.1.3	Theoretical Models of Fractured-Aquifers	189
3.1.4	Flow Regime Characteristics	193
3.1.4.1	Inner Boundary Conditions	194
3.1.4.2	Outer Boundary Conditions	196
3.1.4.3	Typical Water-level Drawdown Plots	197
3.1.4.4	Derivative Plots of Water-level Drawdown	198
3.1.4.5	Summary of Drawdown Graph Characteristics	198
3.1.4.6	Characteristics of Derivative Drawdown Graphs	200
3.1.4.7	Examples of Drawdown and Derivative Graphs	204
	<i>Case Study: Borehole GR3 at Graaff-Reinet</i>	207
3.2	MACRO-CHEMICAL CONSTITUENTS AND WATER QUALITY	212
3.2.1	Introduction	212
3.2.2	Solute-forming Processes	212
3.2.2.1	Physical Weathering	212
3.2.2.2	Weathering of Dolerite	213
3.2.2.3	Weathering of Sedimentary Rocks	213
3.2.2.4	Role of Carbon Dioxide	214
3.2.2.5	Ion Exchange and Sorption	214
3.2.2.6	Evapotranspiration	215
3.2.2.7	Redox Controlled Reactions	216
3.2.3	Spatial Distribution of Major Constituents	217
3.2.3.1	Approach	217
3.2.3.2	Summary of Chemical Parameters	219
3.2.3.3	Major Cations	223
3.2.3.4	Major Anions	229
3.2.4	Variability of the Major Constituents	236

3.2.5	Groundwater Quality with Respect to Drinking Water Guidelines	237
3.2.6	Fluoride and Possibilities for Deep-seated Groundwater in the Karoo Basin	238
3.3	ENVIRONMENTAL ISOTOPE HYDROLOGY	243
3.3.1	Principles and Applications to the Geohydrology of the Karoo Basin	243
3.3.2	Environmental Isotopes Used in Hydrology	243
3.3.2.1	Definitions	244
3.3.2.2	Radioactive Isotopes	246
3.3.2.3	Non-Radioactive or Stable Isotopes	256
3.3.2.4	Dissolved Gases	261
3.3.2.5	Unsaturated or Vadose Zone	262
3.3.3	Isotope Studies of Groundwater in the Main Karoo Basin	263
3.3.3.1	Irrigation Return Flow in the Fish River Valley, Eastern Cape Province	263
3.3.3.2	Philipolis Study, Southern Free State	264
3.3.3.3	De Aar - Dewetsdorp Study	265
3.3.3.4	Beaufort West Study	267
3.3.3.5	Doornberg Fault Zone Study	270
3.3.3.6	Waste Disposal Impact on Groundwater, Bloemfontein	271
3.3.3.7	Study of Groundwater at Dewetsdorp Using Environmental CFCs	271
3.3.4	Isotope Studies of Karoo Aquifers in the Kalahari Basin	272
3.3.4.1	Surface Water and Groundwater Interaction in Gordonia	272
3.3.4.2	Jwaneng Mine, Botswana	274
3.3.4.3	Karoo Aquifers at Orapa, Botswana	275
3.3.5	Concluding Remarks	276
4.	RESOURCE DEVELOPMENT AND EVALUATION	277
4.1	GROUNDWATER EXPLORATION AND DEVELOPMENT	277
4.1.1	Remote-Sensing	277
4.1.1.1	Introduction	277
4.1.1.2	Commonly Used Satellite Imagery	278
4.1.1.3	Geological Lineament Mapping and Structural Analysis in Groundwater Exploration	284
4.1.1.4	Exploration of Karoo Aquifers	289
4.1.2	Structural, Stress and Spatial Analysis	289
4.1.2.1	Lineament Mapping	290
4.1.2.2	Structural and Stress Analysis	294
4.1.2.3	Spatial Analysis of Lineaments and Borehole Productivity Borehole Database	295
	Spatial Analysis	296
	Development of a Hydro-tectonic Groundwater Map	299

4.1.2.4	Loxton Case Study - Exploration Drilling of Lineaments	
	Site 1: Loxton Allotment	301
	Site 2 : De Wilg	302
	Site 3 : Midlands	302
	Site 4 : Nuweland	304
	Site 5 : Taaiboschfontein	305
	Site 6 : Moreson	305
	Discussion	305
4.1.3	Geophysics	307
4.1.3.1	Introduction	307
4.1.3.2	Description of Techniques Already Applied in the Karoo Basin	
	Ground Magnetic Surveys	308
	Aeromagnetic Imagery	308
	Radiometrics	309
	Electrical and Electromagnetic Techniques	309
	Gravity Techniques	310
	Seismic Techniques	311
	Radar Techniques	311
	<i>Ground Penetrating Radar (GPR)</i>	311
	<i>Borehole Radar</i>	311
	Geophysical Borehole Logging	311
	Tomography Techniques	312
	<i>Radiowave Tomography</i>	312
	<i>Seismic Tomography</i>	313
	<i>Resistivity Tomography</i>	314
4.1.3.3	Examples of Groundwater Exploration Techniques Routinely Applied to Groundwater	314
	Target Features	314
	Magnetic Techniques	314
	Electrical and Electromagnetic Techniques	324
	Geophysical Borehole Logging	333
4.1.3.4	Examples of Techniques Primarily Applied in Research Environments	
	Deep Resistivity-Soundings And -Profiling	333
	Tomographic Techniques	334
	Soekor Deep Seismic Reflection	340
	Radiometric Surveys	340
	Geophysical Borehole Logging	341
	Radar Techniques	341
4.1.3.5	Concluding Remarks	341
4.1.4	Drilling Techniques and Borehole Construction	342
4.1.4.1.	Historical Perspective of the Influence of Drilling Technology on the Utilisation of Karoo Aquifers	342
4.1.4.2	Drilling Methods	
	Cable-Tool or Percussion Drilling (Rigs)	343
	Rotary-Percussion Air Drilling	344
	Mud-Rotary Drilling	345

4.1.4.3	Borehole Construction	
	Production Boreholes	345
	<i>Fractured Hardrock Aquifers</i>	346
	<i>Intergranular Semi- to Unconsolidated Aquifers</i>	347
	Monitoring Boreholes	353
	Artesian Boreholes	354
4.2	GROUNDWATER RESOURCE EVALUATION AND MANAGEMENT	355
4.2.1	Aquifer Pump-Testing	355
	<i>Case Study: Putdam Pumping Test</i>	359
4.2.1.1	Test Pumping Procedures	361
	Slug Tests	361
	Multiple-Rate Discharge Test	362
	Constant Rate Discharge Test	363
	Recovery Test	363
4.2.2	Simplified Methods Currently Used in Karoo Rocks for Sustainable Borehole Yield Estimation	364
4.2.2.1	Justification for the Use of the Cooper-Jacob Approximation of the Theis Equation for Interpreting Test Pump Data	365
4.2.2.2	Estimating Sustainable Borehole Yields	366
	Maximum Drawdown Method	367
	<i>Case Study: Borehole T26325A</i>	368
	<i>Case Study: Borehole CHB754B</i>	369
	Recovery Test Method	371
	Transmissivity Method	373
	Methods Based on the Theis Equation	374
	<i>Late-T Method</i>	375
	<i>Case Study: Example 1</i>	376
	<i>Case Study: Example 2</i>	376
	<i>Drawdown-to-Boundary Method</i>	377
	<i>Distance-to-Boundary Method</i>	378
	RPTSOLV (Radial Two-Dimensional Numerical Model)	380
	<i>Case Study: Production Borehole GR2 at the Mimosadale Wellfield, Graaff-Reinet</i>	381
	<i>Discussion</i>	383
	Square-Root of Time Method	385
	Flow Characteristic (FC) Method	386
	<i>Theoretical Formulation of the FC-Method</i>	387
	Estimation of Factor F1	388
	Estimation of Factor F2 from the Drawdown Derivative Graph	389
	The Effect of Boundaries on the Derivative Graph	390
	Calculation of Transmissivity from the Drawdown Derivative Graph	392
	<i>Case Study: Campus Borehole UP15</i>	393
	<i>Case Study: GR2 at Mimosadale Wellfield, Graaff-Reinet</i>	396
	<i>Case Study: Borehole Bacl-01 at Ramatshowe, Northern Province</i>	398
	Pseudo-Steady-State Management Method	402

4.2.2.3	General Discussion of Methods	404
	Late-T Method	404
	Drawdown-to-Boundary Method	405
	Distance-to-Boundary Method	405
	Recovery Method	405
	RPTSOLV Program	405
4.2.3	Estimation of Recharge	406
4.2.3.1	Introduction	406
4.2.3.2	Mechanisms of Recharge	406
4.2.3.3	Water Quality Mass Balance	
	Chloride Method	408
4.2.3.4	Saturated Water Balance Method	410
4.2.3.5	Modified Hill Method	412
4.2.3.6	Cumulative Rainfall Departure (CRD) Method	
	Classical CRD method	412
	Long- and Short-Term Memory of an Aquifer System	413
	<i>Case study: De Aar – Dewetsdorp</i>	414
4.2.3.7	Concluding Remark	415
4.2.4	Groundwater Flow Modelling	416
4.2.5	Groundwater Management Principles	419
	<i>Case Study: Meadhurst Site</i>	420
	Concluding Remarks	421
4.3	POLLUTION POTENTIAL AND AQUIFER VULNERABILITY	422
4.3.1	Aquifer Vulnerability and Risk Management	422
4.3.2	Pollution Hazard	423
4.3.2.1	Vulnerability	423
4.3.2.2	Exposure Consequences	424
4.3.3	Contamination Susceptibility of Karoo Aquifers	425
4.3.3.1	Main Factors Determining Vulnerability	425
4.3.3.2	Assessment Guidelines	426
4.3.3.3	Uncertainty and Limitations	427
4.3.4	Case Studies	427
4.3.4.1	Impact of Gold Mining in Free State	427
4.3.4.2	Municipal Waste Disposal	428
4.3.4.3	Fuel Leaks from Service Stations and Storage Facilities	429
4.3.5	Experimental Work at Institute for Groundwater Studies	430
4.3.5.1	Borehole Dilution Test	431
4.3.5.2	Radial Convergence Test	431
4.3.6	Capture Zones in Karoo Auifers	433
4.3.6.1	Purposes	433
4.3.6.2	Conceptual Models	433
	Circular Zone	434
	<i>Vertical Fracture</i>	435
	<i>Horizontal Fracture</i>	436
4.3.6.3	Discussion	
	Establishing Regional Water-Level Gradient	438
	Dealing with Parameter Uncertainty	438

4.4	NATIONAL GROUNDWATER QUALITY MONITORING IN KAROO AQUIFERS – PRELIMINARY RESULTS AND TRENDS	441
4.4.1	National Groundwater Quality Monitoring Network	441
4.4.2	Karoo Groundwater Quality	442
4.4.2.1	Determination of Regional Trends between 1994 and 1999	442
4.4.2.2	Identification of Hydrochemical Classes	444
4.4.3	Time Trend Detection	454
4.4.3.1	Statistical Method	454
	Computed Temporal Trends	455
	Detected Trends for Scenario 1	455
	Detected Trends for Scenario 2	456
4.4.4	Conclusions	458
5.	RECCOMENDATION FOR FUTURE RESEARCH	460
5.1	WATER RESOURCE MANAGEMENT	461
5.1.1	Groundwater Quantification	461
5.1.1.1	Hydrostratigraphy	462
5.1.1.2	Reserves	462
5.1.1.3	Flow Dynamics	463
5.1.2	Groundwater Development and Environment	463
5.1.2.1	Availability and Needs	463
5.1.2.2	Environmental Issues	
	Groundwater and Ecosystems	463
	Water Quality	464
	Isotopes	464
5.2	TECHNOLOGY TRANSFER	464
5.2.1	Information Technology	464
5.2.1.1	Data Archiving and Accessibility	464
5.2.1.2	Access to Technology	465
5.2.1.3	Layman Book	465
5.2.1.4	Website	465
5.2.2	Education	465
5.2.2.1	Training Courses	465
5.2.2.2	Internet ‘Online’ Training	466
5.3	CONCLUSION	466

LIST OF FIGURES

	Page No.
1.1 Topography and drainage of the Main Karoo Basin	5
1.2 Distribution of Median Annual Runoff in the Main Karoo Basin	6
1.3 Distribution of (a) Mean Annual Precipitation, (b) Evaporation and (c) Rainfall Deficit/Surplus	7
1.4 The Main Karoo Basin in its restored position within Gondwanaland	9
1.5 Extent of the Southern African Karoo Basin	10
1.6 Cross-section of the Main Karoo Basin	10
1.7 Simplified geology of the Karoo Supergroup in South Africa	10
1.8 The extent of the Karoo basaltic lavas and their associated dolerite intrusion in the context of the early stage of the Gondwana break-up.....	12
1.9 Satellite image showing the influence of dolerite ring-complexes on the geomorphology and drainage system of the Queenswood area, Eastern Cape	13
2.1 Schematic areal distribution of lithostratigraphic units in the Main Karoo Basin	16
2.2 Generalised stratigraphy and lithology of the Karoo Supergroup of the Main Karoo Basin	17
2.3 (a) Source areas of the Dwyka glacial sediment (b) Depositional environment of the Dwyka glacial sediments with glacially-excavated paleo-valley facies inland and Diamictite-dominated platform facies offshore	19
2.4 (a) Source areas for the Southern and Western Ecca Formations (b) and the northern Pietersburg, Vryheid and Volksrust Formations	21
2.5 (a) Sediment source areas for the Beaufort Group (b) Depositional environment of the Beaufort Group in the Southern Karoo Basin	32
2.6 (a) Sediment sources of the Molteno and Elliot Formations (b) Depositional environment and lateral facies relationships of the Molteno and Elliot Formations in the Main Karoo Basin	35
2.7 Depositional environment of the Clarens Formation in the Main Karoo Basin	37
2.8 Location of SOEKOR and other relevant deep core-boreholes in the Main Karoo Basin ...	41
2.9 Porosity and permeability variations in the Sandstone/Siltstones of the Karoo Basin	42
2.10 Porosity and bulk density variations in shales of the Karoo Basin	42
2.11 Beaufort Sandstone – primary porosity variation with depth	44
2.12 Ecca Sandstone – primary porosity variation with depth	44
2.13 Stratigraphy of the Barklay East Formation and its relation with the Clarens Sandstone at Tafelkop	47
2.14 Dolerite dykes of the Karoo Basin	49
2.15 Structural domains and mechanism of emplacement of dolerite dykes	51
2.16 (a) En-echelon dolerite dyke (b) Dyke showing vertical tectonic and horizontal thermal jointing and (c) Fissures related to tectonic reactivation and jointing related to weathering/erosional unloading	53
2.17 Borehole yield versus distance from dyke contact	61
2.18 Borehole yield versus distance from dolerite dyke contact in the Loxton – Victoria West area	63
2.19 Borehole yield versus distance from the Tweeling-Brandwag Dyke, Beaufort West	63
2.20 Dyke width versus yield of boreholes drilled into dykes in the North-East Free State	65
2.21 Borehole yield versus dyke width in the Loxton-Victoria West area, Western Karoo	66
2.22 Borehole site selection on dolerite dykes	67
2.23 Geohydrology of the Sandwerf Dolerite Dyke and Sill, east of Calvinia	68

2.24	Geohydrology of the (a) Waterloo inclined sheet and (b) Perries/Welgevonden dykes, north of Graaff-Reinet	69
2.25	Vertical dislocation of the De Wilg Shear Dyke, southwest of Loxton	70
2.26	Geohydrology of the Lehman's Drift (a) Inclined sheet and (b) Dyke, Queenstown	72
2.27	Geohydrology of the MX4 Dyke / Sill Intersection Zone, Queenstown	73
2.28	Geohydrology of the Dunblane Dyke, Middelburg	75
2.29	Correct siting of exploration boreholes alongside dykes cutting drainage features	76
2.30	Morphology of the Tweeling-Brandwag Shear Dyke, Beaufort West	78
2.31	Distribution of borehole yields along the northern contact of the Tweeling-Brandwag dyke	79
2.32	Dolerite sill/sediment ratios of the Karoo Basin	82
2.33	Dolerite sill distribution in the Karoo Basin, extracted from the 1/1 000 000 geological map	83
2.34	Major dolerite sill and ring complex systems in the Eastern and Western Karoo	83
2.35	Geological map and cross-section of the Queenstown dolerite sill and ring-complexes	85
2.36	Geological section showing the stratigraphy and attitude of dolerite sills and ring-complexes between Nieuwoudtville and Williston	87
2.37	Different types of fractures associated with sill and ring-complexes	89
2.38	Two mechanisms of emplacement of the dolerite sill/ring systems (a) the ring dyke model of Chevallier and Woodford (1999), and (b) the laccolith model of Burger et.al	90
2.39	Location of exploration drilling sites targeting the Victoria West dolerite sill- and ring-complex	92
2.40	Exploration drilling sites indicated on 3D enhanced satellite image of the Victoria West dolerite sill- and ring-complex	93
2.41	Geological cross-sections across the Victoria West dolerite sill and ring-complex showing the position of drilling sites	94
2.42	Victoria West sill- and ring-complex – Exploration Drill Site 2	96
2.43	Victoria West sill- and ring-complex – Exploration Drill Site 3	97
2.44	Victoria West sill- and ring-complex – Exploration Drill Site 4	98
2.45	Victoria West sill- and ring-complex – Exploration Drill Site 5	99
2.46	Victoria West sill- and ring-complex – Exploration Drill Site 6	100
2.47	Victoria West sill- and ring-complex – Exploration Drill site 7	101
2.48	Histogram showing percentages of water-interceptions and relative percentages of drillstem yields per 10 m drilling depth intervals below ground surface	102
2.49	Geological map and cross-section of the Philippolis area, Free State	104
2.50	Detailed locality map of exploration drilling site A, Philippolis	105
2.51	Geohydrological cross-section through the Philippolis inclined-sheet	105
2.52	Hydrogeology of the Williston dolerite ring-complex	107
2.53	Geohydrology of the inclined sheet of the Vanwyksvlei Dolerite Ring-Complex	108
2.54	Geohydrology of an extensive, undulating sill, not related to a dolerite sill- and ring-complex	109
2.55	The occurrence of groundwater on the weathered lower contact of an inclined-sheet, Middelburg	110
2.56	Geohydrology of the Roodekraal inclined-sheet, De Aar	111
2.57	Hydro-morphotectonic model of a dolerite sill- and ring-complex, detailed fracture pattern for inclined sheet indicated in Figure 2.37	112
2.58	Distribution of mapped Breccia Plugs and Volcanic Vents in the Karoo Basin	114
2.59	Geological logs of core-boreholes drilled into breccia plugs and a stratigraphic borehole ...	117
2.60	Geological log of stratigraphic borehole LA1/68, near Ladybrand	119

2.61	Distribution of Cretaceous Kimberlites and Carbonatites in the Karoo Basin (after Chevallier, 1997, modified)	123
2.62	Kimberlite Swarms and Sub-Swarms of (a) the Victoria West – Beaufort West area (b) Proposed Vertical Geometry of a swarm (Woodford and Chevallier, 2001)	125
2.63	Geohydrology of the Jagersfontein kimberlite diatreme (after Kok, 1982)	131
2.64	Deep-seated Pre-Karoo structures (geophysical anomalies), major faults (Thomas et al., 1992) and morphological lineaments (this study)	134
2.65	Fold axes and master joints of the southwestern Karoo (after Woodford and Chevallier, 2001 and Chevallier, unpublished data). Fold axes are only shown for Quadrant	137
2.66	Schematic structural profile along the Rhemhoogte road across units of the Ecca Group (taken from Coetzee, 1983)	137
2.67	Geological cross-section of the Vorster Syncline, Graaff-Reinet	138
2.68	Leeu-Gamka – Borehole productivity and associated structural features	140
2.69	Leeu-Gamka – Groundwater level fluctuations during 1985-86	141
2.70	De Aar – Groundwater quality variations in an alluvial/bedrock aquifer following abnormally high rainfall in 1988 (Woodford, unpublished data)	143
2.71	Rose diagram of joint orientations at Graaff-Reinet and Beaufort West	145
2.72	Development of systematic and non-systematic joints of the Western Karoo (after Woodford and Chevallier, 2001)	146
2.73	Borehole yield distribution with distance from fracture zone	148
2.74	The Orange-Fish River Tunnel Scheme showing the flooding zone near Shaft 2 (after Olivier, 1972)	150
2.75	Plan showing boreholes and fractures at the point of flooding (after Olivier, 1972)	150
2.76	Relationship between total dissolved solids and source depth of the groundwater	152
2.77	Map of seismic epicentres (Fernandez & Du Plessis, 1992) and seismotectonic provinces (Hartnady, 1998; Du Plessis et al., 1997) of South Africa	156
2.78	The African and Post-African land surfaces in South Africa (after Partridge and Maud, 1987)	159
2.79	Digital elevation model indicating the regional topographic anomaly associated with the Middelburg Dolerite ring-complex	160
2.80	The influence of dolerite sill-ring complexes on the drainage system near Victoria West ...	161
2.81	Schematic distribution of major Late Tertiary - Early Quaternary fluvial terrace and pedocrete (excluding gypcrete) deposits of the Main Karoo Basin	163
2.82	Geohydrological section across the Caroluspoort alluvial-bedrock aquifer, De Aar (Woodford, unpublished data)	167
2.83	Distribution of gypcrete in Southern Africa (after Visser et al., 1963)	169
2.84	Climatic N-values of 2, 5 and 10 in Southern Africa (Weinert, 1974)	172
3.1	Schematic illustration of groundwater flow, towards a borehole in a Karoo Aquifer	180
3.2	Appropriate areal extent of the horizontal water-bearing fracture in the campus test site aquifer	181
3.3	Schematic illustration of the parallel plate model for a fracture	183
3.4	Response of the piezometric heads in the three-layered aquifer system on the Campus Test Site, as measured in Piezometer UO18 during the constant-rate on the Borheole UP16.	184
3.5	Drawdowns observed during a constant-rate test on a high-yielding borehole at Kokstad ..	184
3.6	Water-level response in boreholes UOF, U011, UP15 and U020 during a constant-discharge test on pumped borehole UP15	185

3.7	Acoustic scanner image Borehole UO5 on the campus test site. The orientation of the oblique fracture above 23 m in UO5 is 085 65.....	187
3.8	Pump test results at the Meadhurst site	192
3.9	Pump test results at the Meadhurst site	192
3.10	Hantush pseudo T-value estimation for production borehole at Meadhurst site	193
3.11	Early time-drawdown curve of borehole UP16 at the campus site showing inner-boundary conditions	195
3.12	Typical derivative graph for various boundary conditions	204
3.13	Water-level drawdown and derivative graph indicating borehole storage, radial flow and boundary effects	204
3.14	Water-level drawdown and derivative plot showing flow to an infinite conductive fracture	205
3.15	Water-level drawdown and derivative plot showing a constant head – type boundary	205
3.16	Water-level and derivative plot showing dual-porous flow	206
3.17	Water-level drawdown, and the different derivative plots for borehole	207
3.18	Flow characteristic analysis of drawdown derivative plot for borehole GR2	207
3.19	Cooper-Jacob plot of borehole GR2 showing position of fractures and boundary	208
3.20	Log-log Theis plot of borehole GR2	208
3.21	Difference between drawdown and derivative is equal to 4 until 140 min, indicating a good fracture network	209
3.22	Square root of time plot. After the linear flow period, a flow period is evident where water is derived from the matrix	209
3.23	After well bore storage a period of bilinear flow is occurs, where water is derived from both the fracture and the matrix	210
3.24	Inverse square root time graph showing ‘sharp bend’ indicating that the fracture is finite ..	210
3.25	Graph of residual recovery indicating that recovery was incomplete	211
3.26	Samples collected since 1990 as per cent of total sample count	218
3.27	Ranges of total dissolved solids (TDS) expressed as geometric means over representative lithological units	221
3.28	Mean pH for representative lithological units	222
3.29	Calcium concentrations expressed as a geometric mean within each lithological unit	224
3.30	Magnesium concentrations expressed as geometric mean over elementary lithological units	225
3.31	Total harness of groundwater in the Karoo Basin	226
3.32	Sodium concentrations expressed as geometric mean over elementary lithological units ...	227
3.33	Spatial distribution of the Na/Cl ratio in the Karoo Basin	228
3.34	Total alkalinity expressed as geometric mean over elementary lithological units	229
3.35	Carbon dioxide activity expressed as mean log pCO ₂ over representative lithological units .	231
3.36	Chloride concentrations expressed as geometric means over representative lithological units	233
3.37	Sulphate concentrations expressed as geometric means over representative lithological units	234
3.38	Nitrate concentrations expressed as geometric means over representative lithological units	235
3.39	Fluoride concentrations expressed as geometric means over representative lithological units	236
3.40	Variability of major ions	237
3.41	Fluoride distribution in the Southern Karoo Basin	241
3.42	Tritium in Southern African rainfall showing the thermonuclear “peak”	247

3.43	Radiocarbon in southern hemisphere atmospheric CO ₂	248
3.44	Idealised flow-lines for a confined aquifer receiving recharge only in the outcrop area	251
3.45	Idealised flow-lines for an isotropic, unconfined, phreatic aquifer receiving uniform diffuse recharge	252
3.46	Expected tritium values calculated with the exponential model for an idealized Southern African phreatic aquifer as a function of a mean residence time (MRT) for 1998	253
3.47	Radiocarbon values expected at present calculated with the exponential model for an idealized Southern African phreatic aquifer as a function of the mean residence time (MRT) for 1998 and 100% atmospheric	254
3.48	Radiocarbon values plotted against tritium values calculated with the exponential model for different MRTs	255
3.49	$\delta^2\text{H}$ vs. $\delta^{18}\text{O}$ plot, showing the world meteoric water line (WMWL) and a typical evaporation line	258
3.50	Values of $\delta^{15}\text{N}$ for different dissolved nitrogenous species derived from different Sources	260
3.51	Atmospheric concentrations of a number of different chlorofluorocarbons (CFCs) as a function of time	262
3.52	Plot of radiocarbon vs. tritium for ground water in the Phillipolis area showing a near-linear relationship	265
3.53	$\delta^2\text{H}$ and $\delta^{18}\text{O}$ values as a function of time for a number of rainfall events at Dewetsdorp ...	266
3.54	$\delta^2\text{H}$ vs $\delta^{18}\text{O}$ plot for rain water and ground water at De Aar and Dewetskorp	267
3.55	Plot of tritium vs. radiocarbon for ground water at Beaufort West	269
3.56	$\delta^2\text{H}$ vs $\delta^{18}\text{O}$ plot for Gordonia groundwater, showing the WMWL and the two groups of values for groundwater near to, and further away from, the Kuruman River bed, respectively	273
3.57	Schematic section of the alluvial-fan aquifer at Jwaneng, showing radiocarbon values at different wells and inferred groundwater flow paths from recharge at the aquifer sub-outcrop to leakage into the aquitard	275
4.1	Comparison of the spectral resolution of commonly used satellite imagery	280
4.2	LANDSAT TM and ERS satellite imagery of the Loxton area in the Western Karoo Basin	283
4.3	Fracture patterns caused by a major compressive horizontal force	285
4.4	LINAIR – Lineaments captured from aerial-photographs, existing geological maps and field mapping	291
4.5	LINCOMP – Integrated map containing lineaments from LINAIR, LANDSAT TM and aeromagnetic imagery	292
4.6	A comparison of lineament datasets from the Loxton area (a) LINAIR, (b) LINCOMP, (c) SPOT-1 and (d) SPOT-2	293
4.7	Borehole GIS indicating positional accuracy of data	296
4.8	Lineaments with orientations ranging between N70 ⁰ and N130 ⁰ , correlated with higher than average yielding boreholes	297
4.9	‘Wet’ borehole yield variations associated with 2 km wide corridors of major lineaments in the Loxton-Victoria West area	298
4.10	Fracture spatial density map showing positions of accuracy classes I and II boreholes	298
4.11	Dolerite sill and ring-complexes of the study area showing the position of ON-and OFF-Sill ‘wet’ boreholes in Positional Accuracy Class I, as well as ‘wet’ Boreholes in Accuracy Class II	299

4.12	Hydro-tectonic map showing mean groundwater yield showing exploration boreholes used in the case study	300
4.13	Hydro-tectonic map showing Median Groundwater Yield, showing exploration boreholes used in the case study	301
4.14	Lineament map indicating exploration drill-sites in the Loxton Area. Inset map indicates various structural types of dolerite dykes that developed along the Jurassic E-W dextral shear zone	302
4.15	Detail plans of exploration drilling sites at Loxton	303
4.16	Magnetic fabric map of the Queenstown-East London area, clearly showing the dolerite ring-complexes and mega-dykes	316
4.17	High-resolution [A] and [B] aeromagnetic surveys of the Victoria West area showing prominent dolerite dykes and sills	317
4.18	The effect of the depth of burial on a dyke anomaly	319
4.19	Interpretation of contacts of a dolerite dyke from the vertical intensity magnetic anomaly, Loch Lamind No. 157, Bethlehem	320
4.20	Geological sections and geophysical anomalies across dolerite dykes in the Odendaalsrus area	321
4.21	Type curves for magnetic anomalies over dipping dolerite dykes in South Africa	323
4.22	Variation in magnetic anomalies along strike of a dolerite dyke at Odendaalsrus	325
4.23	Magnetic anomaly across an inclined-sheet, showing exploration drilling results, Steynsrus area (Lindley District)	326
4.24	Magnetic anomaly across the intersection of an inclined-sheet and an inner-sill, showing exploration drilling results, Steynsrus area (Lindley District)	327
4.25	Relationship between electrical resistivity and borehole yield	329
4.26	Resistivity method used to site boreholes on dolerite ring-structures, Petrus Steyn	331
4.27	Schlumberger depth-sounding curves used to delineate an alluvial aquifer overlying the Prince Albert Formation shale, Strydensburg	332
4.28	Schlumberger deep resistivity sounding at the Shaft No2 inflow point, showing depth to dolerite sill	335
4.29	Plan showing borehole positions on the Institute for Groundwater Studies campus test site.....	336
4.30	Radio-tomograph between boreholes on the campus test site, showing position of main fractures	337
4.31	Campus test site – 30 MHz background difference images between boreholes UO3 and UO5, showing zone of horizontal jointing	338
4.32	Campus test site – 12MHz background difference images between boreholes UO3 and UO5, showing zone of horizontal jointing	339
4.33	Typical production borehole design for a fractured hardrock aquifer	347
4.34	Typical production borehole design for an intergranular aquifer	349
4.35	Schematic plan of well-point system	350
4.36	Schematic plan of a collector well system	351
4.37	Typical low-yield production borehole design for an alluvial-bedrock aquifer	352
4.38	Multi-piezometer monitoring borehole	353
4.39	Constant discharge test at Rhodenbeck, Bloemfontein	357
4.40	Constant discharge test at Kokstad	357
4.41	Constant discharge test at Grootegeluk, Ellisras	358
4.42	Constant discharge test on borehole G39973, Clavinia	358
4.43	Putsdam constant rate test at 2.6 l/s	360
4.44	Slug test: Recovery time versus yield of borehole	362

4.45	A comparison between transmissivity values obtained using the Coope-Jacob and the Boulton-Streltsova methods in different hydro-lithologies	366
4.46	Drawdown in borehole T26325A at current production rates	368
4.47	Drawdown in borehole CHB754B at a production rate of 4.2 l/s	369
4.48	Recovery curve showing t/t' intercept	373
4.49	Modelled drawdown curve based on the drawdown-to-boundary method	378
4.50	Distance to boundary values	380
4.51	Borehole GR2 - Constant discharge test at 28.6 l/s	382
4.52	Borehole GR2 - Recovery test	382
4.53	Borehole GR2 – Water-level and rainfall data	384
4.54	RPTSOLV's fit of borehole GR2	386
4.55	Drawdown parameters used to calculate factor F1	389
4.56	Derivative plot of drawdown showing various boundary conditions	391
4.57	Constant discharge test on Borehole UP15 – drawdown versus time	394
4.58	Constant discharge test on Borehole Up 15 – derivative versus time	395
4.59	Constant discharge test of Borehole GR2 – derivative versus time	397
4.60	Step-down test on borehole Bacl-01 – drawdown versus time	398
4.61	Constant discharge test on borehole Bacl-01 – drawdown versus time	399
4.62	Constant rate discharge test of Back-01 – derivative versus time	399
4.63	Back-01 step-drawdown test – specific drawdown curve	400
4.64	Constant rate discharge on Borehole Back-01 – recovery	402
4.65	Pseudo steady-state method applied to borehole F4 at Meadhurst	403
4.66	Relationship between mean annual rainfall and chloride content	409
4.67	Lobatse – Relationship between average chloride content of rainwater and mean annual precipitation	409
4.68	Relationship between recharge and annual rainfall for Dewetsdorp	411
4.69	Relationship between the cumulative rainfall departure curve and water-level for borehole D6N519, at De Aar	414
4.70	CFC groundwater age determinations in the Dewetsdorp aquifer	416
4.71	Mean annual groundwater recharge from precipitation	418
4.72	Reaction of water-level in a production borehole at pump rates in excess of the yield of the fractures	420
4.73	Water-level decline in a production borehole that is being over-exploited	421
4.74	Scale dependency of Hydraulic Conductivity (K)	432
4.75	Approximation of the travel time ellipse and ZOC Boundary	433
4.76	Effect of recharge on radius of influence	434
4.77	Ellipsoidal protection zone along a vertical fracture or dyke	435
4.78	Borehole protection area for an interbedded aquifer with a horizontal fracture zone	437
4.79	Comparison of analytical BPA with approximate BPA taken as a conservative approach ..	438
4.80	Effect of random K values on simulated BPA ellipses	440
4.81	Geographic distribution of sampled stations (1999) and their cluster membership for a 3-cluster model	445
4.82	Geographic distribution of sampled stations (1999) and their cluster membership for a 5-cluster model	447
4.83	Geographic distribution of sampled stations (1999) and their cluster membership for a 7-cluster model	448
4.84	Schoeller diagram of cluster centers for the 7-cluster model	449
4.85	Piper diagram representation of cluster centers (7-cluster model)	449

4.86	Relation between calcium and sodium, showing a trend-line with a 2:1 slope indicating ion-exchange processes	450
4.87	Relation between magnesium and sodium, with a trend line (2:1 slope) indicating ion-exchange processes	452
4.88	Relation between magnesium and silica indicating the precipitation of kaolinite (all Karoo monitoring points used up to the 1999 sampling run)	453
4.89	Saturation levels in groundwater with respect to calcite	453

LIST OF PLATES

1.1	View of concrete structure erected by the Municipality of Bloemfontein over the spring, after which the city is supposedly named	2
1.2	Typical landscape of the Western Karoo Basin showing the classical ‘koppie’ or butte capped by a dolerite sill rising above the featureless and flat-lying plains	6
2.1	N-S Rooiaar dolerite dyke, near Loxton (a) reactivated contact between dyke (left) and host-rock (right). (b) Cretaceous aged calcite filled vertical shear and tension gashes related to Kimberlite activity (after Woodford and Chevallier, 2001)	55
2.2	Tectonic Reactivation of a NNW dyke in the De Jagers Pass, Beaufort West	56
2.3	N-S dolerite dyke (red - foreground) delineated in the distance by a dense line of taller bushes (Farm: Meltonwold, Sheet 3122 DA)	58
2.4	The Kwecka Sill-Ring Complex, near Victoria West	81
2.5	Breccia Plugs (a) the positive-relief Jagkop plug on the Farm Lower Zwartrand in the Carnarvon district (3022CD), (b) tourmaline-rich breccia, showing flow alignment of sediment blocks, on the Farm Bo-Downes in the Calvinia area	116
2.6	(a) Kimberlite fissure and pipe on the farm Nuweland (Loxton) and (b) Cross-section of kimberlite body on the farm Meltonwold (Victoria West) – note thin kimberlite, calcite and calcrete stringers parallel to the main body	124
2.7	(a) Prominent systematic NNW master joints with orthogonal a non-systematic set responsible for the ‘ladder’ effect, Hillcrest, Sheet 3122DC (b) Superimposition of two orientations of master jointing, namely NNW and NNE at Loxton, Sheet 3122CB	147
2.8	Calcretized river-terrace overlying mudstone of the Middleton Formation, Graaff-Reinet	163
2.9	Fractured and weathered dolerite dyke, north of Victoria West	174
2.10	Fractured and decomposed dolerite sheet, Victoria West	176

Chapter 1

INTRODUCTION

Water, particularly fresh or potable water, is indispensable for all man's activities on earth. Approximately 75% of the total volume of freshwater on earth is frozen in glaciers, whilst rivers and lakes hold approximately 0.33%. The remaining 24.67% occurs as groundwater (Chorley, 1969; Zumberge and Nelson, 1984). Since the water in glaciers is not available for general consumption, groundwater forms the largest source of freshwater available to man.

The situation in South Africa, however, is complicated because of the nature of the aquifer systems. Here groundwater is usually regarded as an unreliable source of water. The result is that groundwater contributes only 10% to the national water budget (Department of Water Affairs, 1986). The surface water resources, however, have now almost been exploited to their limits. South Africa, therefore, will have to make greater and more efficient use of its groundwater resources in the future, to meet the demand of the growing population. This is especially true in the semi-arid and arid central and western regions of South Africa, which cover approximately 66% of the country (Department of Water Affairs, 1986), where there are no major rivers, or other surface water sources. The majority of the inhabitants in these areas therefore depend upon groundwater for their water supply. A large part of these regions, and approximately 50% of the country as a whole, is underlain by the so-called Karoo Supergroup of geological formations. The potential thus exists that aquifers in the Karoo Supergroup can make a significant contribution to the water budget of the country.

A major characteristic of the Karoo Supergroup, which consists mainly of sandstone, mudstone, shale and siltstone, is their low permeability. The majority of boreholes drilled in Karoo formations therefore have very low immediate yields (<1 ℓ/s). Indeed, the common view is that Karoo aquifers do not contain large quantities of groundwater, hence the name Karoo, which is the Hottentot word for dry. However, large volumes of groundwater are pumped from wellfields supplying towns, mines and the basements of buildings on a daily basis in areas underlain by the Karoo formations, which is not what one would expect from aquifers with a limited yield.

Karoo aquifers have a very complex and unpredictable behaviour, as outlined above. The oogeneral view is thus that Karoo aquifers are not reliable sources of water. However, there is no doubt that these aquifers played a significant part in the development of the Republic of South Africa. This is evident in numerous place and area names, such as De Aar, Bitterfontein, Koffiefontein, Springfontein, Lelieput, Syfergat, and Putsonderwater. It is also known that the Voortrekkers often used natural springs, wells dug by the Khoi, or dug new wells during the Great Trek. The City of Bloemfontein was founded by Major Henry Warden in 1848 at its present site, not only for strategic reasons, but also because the perennial Bloemenfontein spring (**Plate 1.1**).



Plate 1.1: *View of concrete structure erected by the Municipality of Bloemfontein over the spring, after which the city is supposedly named*

The Khoi probably dug the first water-wells in the South Africa, judging from their proximity to the cave paintings, some of which are thousands of years old. It is unclear when or where the first borehole in South Africa was drilled. The earliest South African windpump to be described or illustrated appears in the foreground of a watercolour by Johannes Cornelius Poorteremans of Brink's farm Saldanha Bay in 1848. The first record of an imported windpump is that of a Halladay Standard imported in 1874 by the farmer P.J. du Toit and installed on his farm Kaffersdam in the district of Hopetown (Walton, 1998).

1.1 **BACKGROUND TO THE PROJECT**

The Water Research Commission (WRC) has co-ordinated and funded numerous research projects aimed at understanding the hydrogeology, flow characteristics and exploitability of Karoo fractured-aquifers over the past 20 years. The research was conducted by various research institutions, governmental organisations and private consultants, involving both intensive localised and more extensive regional studies.

During its 1996 annual review of research proposals the Water Research Commission (WRC) management decided that instead of funding new and possibly overlapping projects, it was time to review and collate the vast amount of existing knowledge on Karoo fractured-aquifers and thereby identify future research priorities.

1.2 **SCOPE**

This document aims to:

- collate and summarise all known information on the hydrogeology of the *Main Karoo Basin*,
- provide an inventory of all relevant published material on Karoo fractured-aquifers,
- convey this information to practitioners in a systematic and understandable way, and
- to identify future research priorities in Karoo aquifer systems.

The report deals specifically with the hydrogeology of the Main Karoo Basin, but in certain instances more general physical or chemical information relating to Karoo rocks outside of the Main Basin have been included.

1.3 **TARGET AUDIENCE**

This document is aimed primarily at the *groundwater practitioners* working in Karoo fractured-rock aquifers, especially those involved in rural water supply projects and WRC-funded research projects. The level of information presented is also useful to other professionals with only limited groundwater knowledge.

1.4 PHYSIOGRAPHY, CLIMATE AND SURFACE HYDROLOGY

The Main Karoo Basin encompasses an area of approximately 630 000 km², including the greater part of the central plateau region of South Africa (**Figure 1.1**). The surface altitude ranges between 800 and 3 650 m above mean sea level, with the exception of a narrow belt along the south and the south-eastern coastal zone, and the Tankwa Basin in the west. Altitudes are highest in the east, decreasing gradually as the surface slopes down to the west. The generally flat-relief is broken by the upwarped plateau edges and the escarpment, which are most prominent in the Drakensberg region around the Kwa-Zulu Natal-Lesotho border.

A prominent feature of the Karoo landscape are flat-topped hills or ‘butte’, which are often capped by the more resistant dolerite sills or sandstone beds, separated by wide plains with pediments and bahadas, as shown in **Plate 1.2**. Outcrops are rare between the hills, because of the surficial cover of calcrete, windblown sand, alluvium, colluvium and soil.

The river-flow is highest in the east due to increased rainfall in these areas. The major drainage features are the Orange River and its perennial tributaries, the Vaal and Caledon Rivers. Other drainage is mostly peripheral, with the high-gradient rivers flowing from the escarpment to the coast. In the central and western Karoo Basin the river are mainly ephemeral, flowing only for short periods of time following heavy rainfalls. A number of perennial easterly draining rivers occur along the eastern edge of the Basin (i.e. east of 28° longitude) – **Figure 1.2**.

The greater part of the Karoo Basin is classified as a summer rainfall region, with the exception of the south-eastern coastal zone that receives both summer and winter rains. During the summer months warm, moisture-laden air flows in from the Indian Ocean, penetrating the interior and giving rise to thunderstorm activity and rain. Intensified high-pressure systems during the winter months causes an inversion layer that prevents maritime air from reaching the interior, thereby minimising winter rainfall. From **Figure 1.3(a)** it is apparent that mean annual precipitation decreases from east to west, with the central regions receiving less than 200 mm per annum. The highest values (up to 2 000 mm per annum) are noted in the eastern escarpment area, corresponding well with altitude. Evaporation is greatest during the hot summer months, further depleting the available moisture in the arid areas (**Figure 1.3(b)**), this deficit is clearly illustrated in **Figure 1.3(c)**.

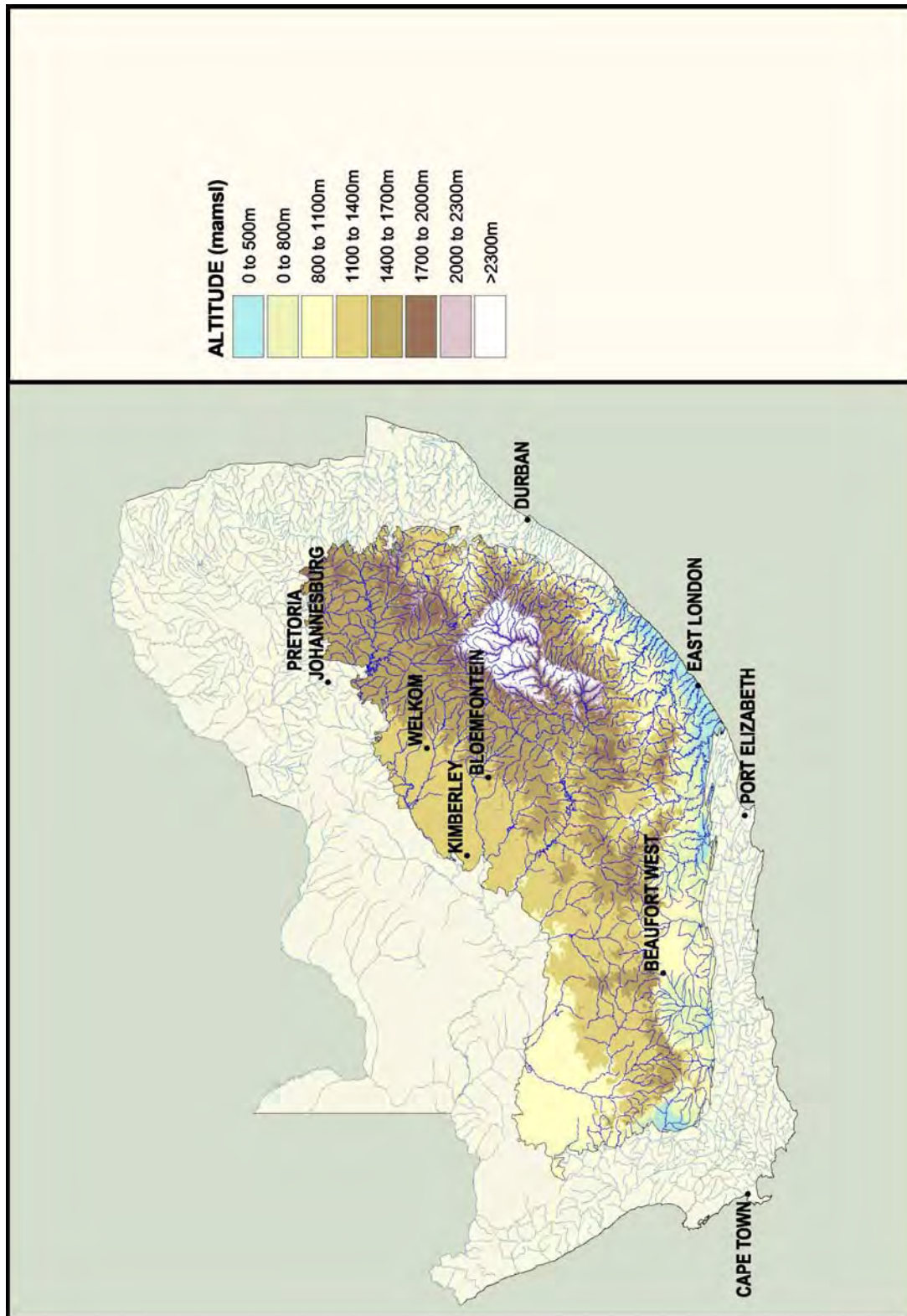


Figure 1.1: Topography and drainage of the Main Karoo Basin



Plate 1.2: Typical landscape of the Western Karoo Basin showing the classical ‘koppie’ or butte capped by a dolerite sill rising above the featureless and flat-lying plains

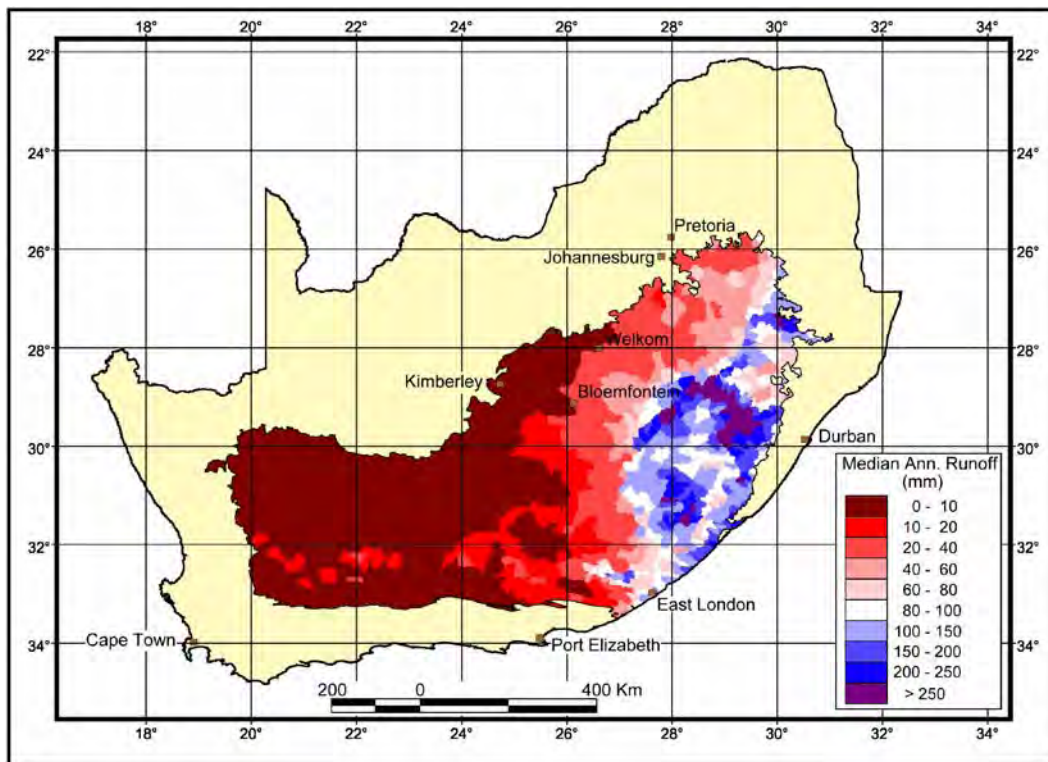


Figure 1.2: Distribution of Median Annual Runoff in the Main Karoo Basin

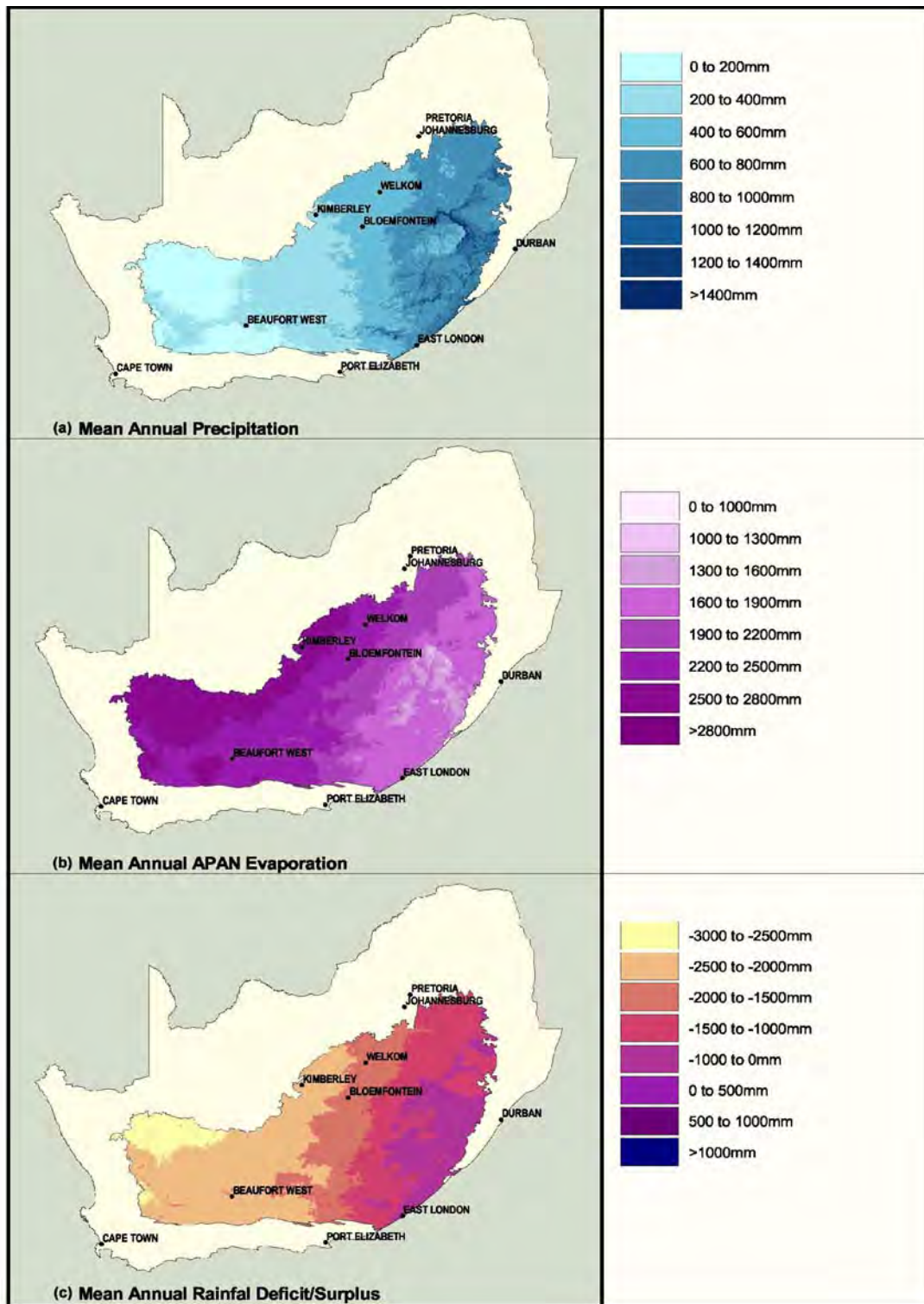


Figure 1.3: Distribution of (a) Mean Annual Precipitation
(b) Evaporation and
(c) Rainfall Deficit / Surplus

1.5 GEOLOGICAL OVERVIEW

The Main Karoo Basin was controlled by four major geodynamic events:

1. Deposition of the Karoo sediments and the uplift of the Cape Fold Belt,
2. intrusion of Karoo basalt and dolerite, and the break-up of Gondwanaland,
3. intrusion of kimberlite and localised mantle up-welling,
4. modern geomorphology, deposition of recent sediments, uplift, and cessation of regional tectonism.

1.5.1 SEDIMENTS OF THE KAROO SUPERGROUP

The Karoo Basin is a retro-arc foreland basin bounded by (1) a fold-thrust belt (Cape Fold Belt) lying along the southern margin of the basin, (2) the cratonic basement to the west, north and northeast, and (3) the Indian Ocean to the southeast. In its restored position within Gondwana (**Figure 1.4**), the Karoo Basin included the Falkland Islands, inverted by 180° to a position southeast of South Africa (Veevers et al., 1994). A magmatic arc developed to the south of the fold-thrust belt (**Figure 1.4**) and was associated with subduction of the Palaeo-Pacific (Panthalassan) plate beneath the Gondwana plate. Other fold-thrust belts and retro-arc foreland basins also formed in Patagonia, the Ellsworth Mountains and Transantarctica. Visser (1997) suggested that the 'foredeep' of the Karoo Basin was initiated due to crustal sagging, possibly associated with sinking of denser material at the site of the Southern Cape Conductive Belt, which presently lies north of the Cape Fold Belt (Veevers et al., 1994). Alternatively, the loss of Gondwana heat leading to thermal subsidence could also have initiated basin development (Visser and Praekelt, 1996). These latter authors proposed that the east-west elongation of the basins in southwestern Gondwanaland (**Figure 1.4**) was due to an early phase of transpressive strike-slip caused by oblique subduction along the Palaeo-Pacific plate, which preceded development of the fold-thrust belt and retro-arc basins.

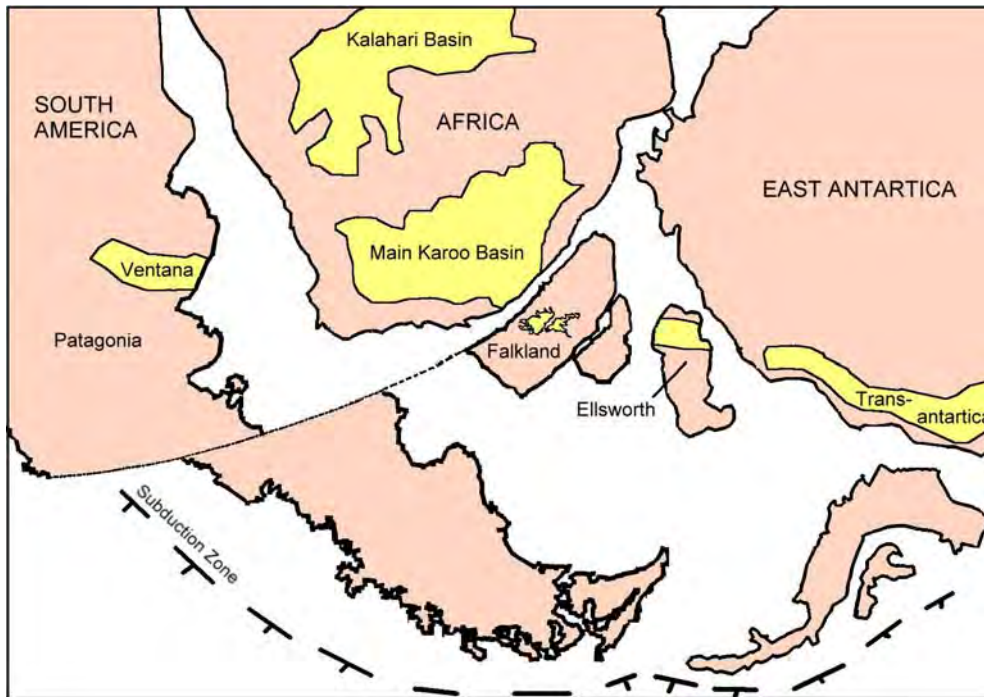


Figure 1.4: *The Main Karoo Basin in its restored position within Gondwanaland*

Today, the Main Karoo Basin outcrops over more than half of South Africa (**Figure 1.5**), and is infilled with up to 12 km of sedimentary strata which are capped by a 1.4 km thick unit of basaltic lava (**Figure 1.6**; Cole, 1992). The sediments were deposited during the Late Carboniferous (310 Ma; Visser, 1997) through to the Mid Jurassic (185 Ma; Catuneanu et al., 1998) times, with the thickest pile developed in the foredeep on the landward side of a rising Cape Fold Belt.

The major lithostratigraphic units of the Karoo Supergroup are shown in **Figure 1.7**. Each Group corresponds to progressively changing depositional environments. The sediments (glacial ice-shelf deposits of Dwyka Group and the marine shales of Ecca Group) were initially deposited in an extensive basin, covering much of south-western Gondwanaland, located in the polar latitudes (Visser, 1987). The Basin became progressively smaller as a result of a rising and northward-migrating Cape Fold Belt, and it had shrunk to its present size by the Middle Jurassic (Veevers et al., 1994).

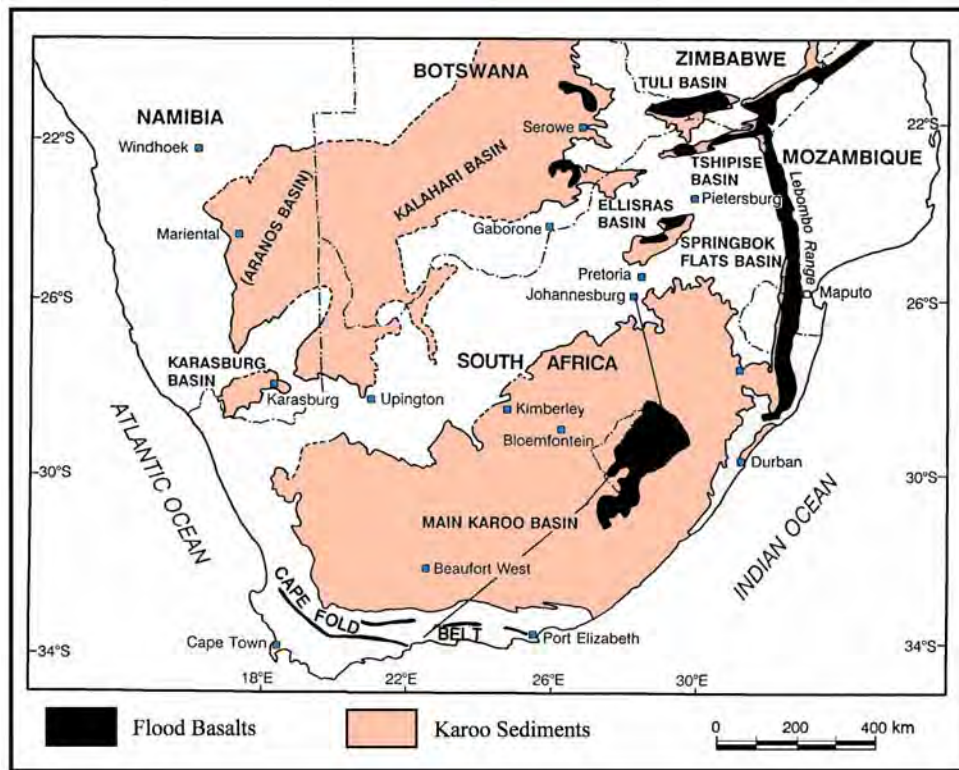


Figure 1.5: Extent of the Southern African Karoo Basins

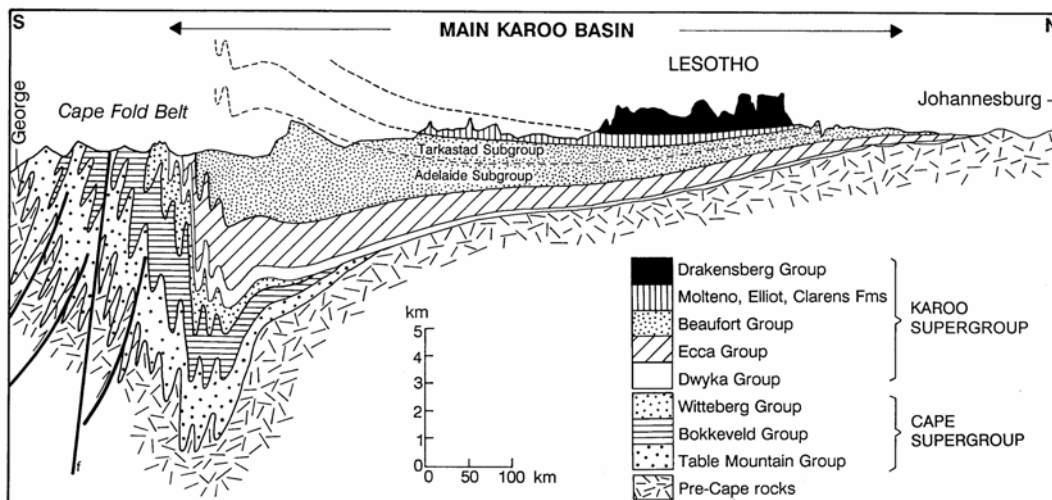


Figure 1.6: Cross-section of the Main Karoo Basin (see section-line, Figure 1.5)

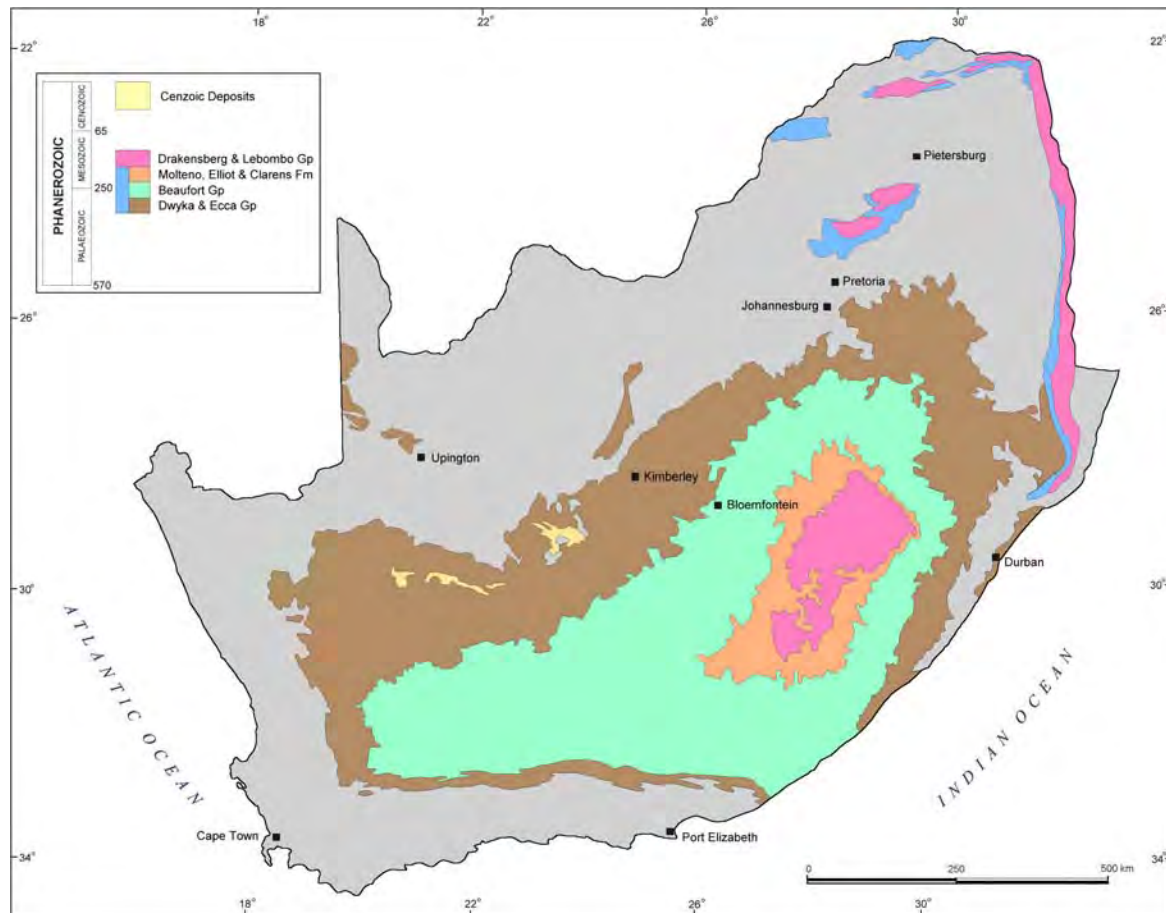


Figure 1.7: Simplified geology of the Karoo Supergroup in South Africa

This was accompanied by progressive infilling and concomitant shallowing of the Basin, with only subaerial depositional environments being present by Permo-Triassic times (mudstone, siltstone and sandstone of the Beaufort Group). Progressive aridification also occurred as south-western Gondwanaland migrated from the polar latitudes to sub-tropical latitudes (sandstone of the Stormberg Group) (Smith, 1990). A detailed description of the lithostratigraphy and depositional environment of the Karoo Supergroup is presented in **Chapter 2**. During the period 278 to 215 Ma, the Cape Orogeny severely deformed the southern margin of the Karoo Basin by episodic tectonism (Hälbich et al., 1983; Cole, 1992; Catuneanu et al., 1998), while the remaining interior portion of the basin was gently folded with a centripetal dip ($< 5^\circ$) towards Lesotho. Fluid migration and progressive diagenesis accompanied the development of the Main Karoo Basin and the Cape Fold Belt (Duane and Brown, 1992).

1.5.2 KAROO BASALT AND DOLERITE MAGMATISM

The Mid-Jurassic aged Karoo basalt (180 Ma: Duncan et al., 1997; 190-160 Ma: Fitch and Miller, 1984; Richardson, 1984) extruded onto the surface of the Karoo sediments during a period of extensive magmatic activity that took place over the entire Southern African subcontinent and which was accompanied by one of the early stages of the break-up of Gondwanaland (Eales et al., 1984; Bristow and Saggerson, 1983; Hunter and Reid, 1987, White, 1997; Marshall, 1994). The total volume of magma is estimated at 10 million km³ (White, 1997), making this event one of the largest flood-basalt outpourings in the World. It is widely accepted that the flood basalts originated from large mantle plumes or ‘convection-cells’, which caused the upwelling of abnormally hot material from the base of the lithosphere. A mantle plume situated off the eastern coast of Southern Africa is proposed by Storey and Kyle (1997) (**Figure 1.8**).

This magmatic activity also generated extremely large volumes of hypabyssal dolerite dykes and sills, now outcropping over an area covering almost two-thirds of South Africa. On a regional scale, these sills and dykes often exhibit circular patterns that control the geomorphology and drainage system of the Karoo Basin, clearly visible on satellite imagery (**Figure 1.9**). It is unlikely that all the dolerite intrusions within the Main Karoo Basin led to volcanic eruptions at the surface.

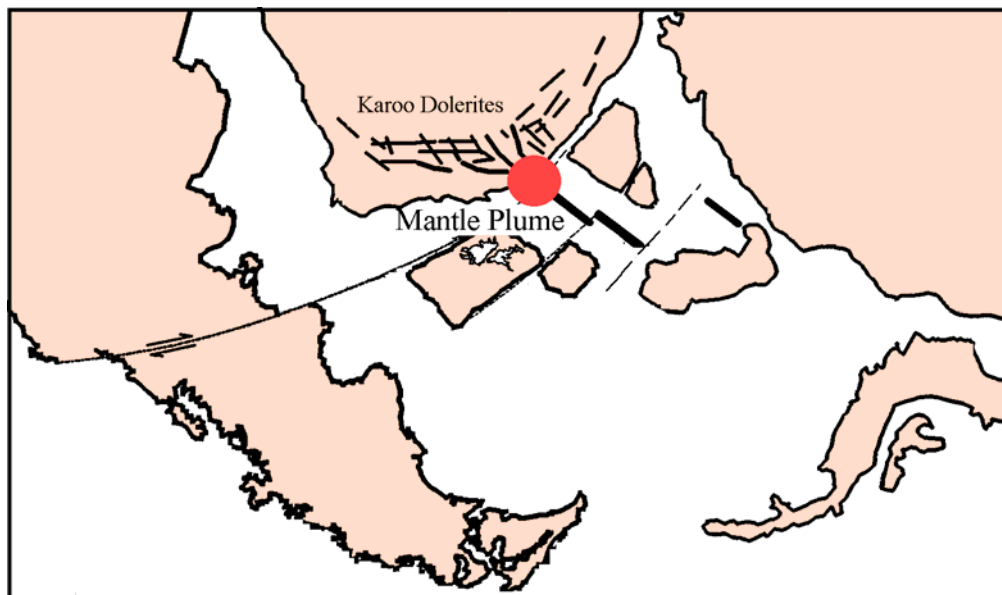


Figure 1.8: *The extent of the Karoo basaltic lavas and their associated dolerite intrusion in the context of the early stage of the Gondwana break-up (adapted from Marshall, 1994; Storey and Kyle, 1997)*

The tremendous heat flow generated by the intrusives was responsible for the general hydrothermal metamorphism of the sediments (White, 1992; Rowsell and De Swart, 1976).

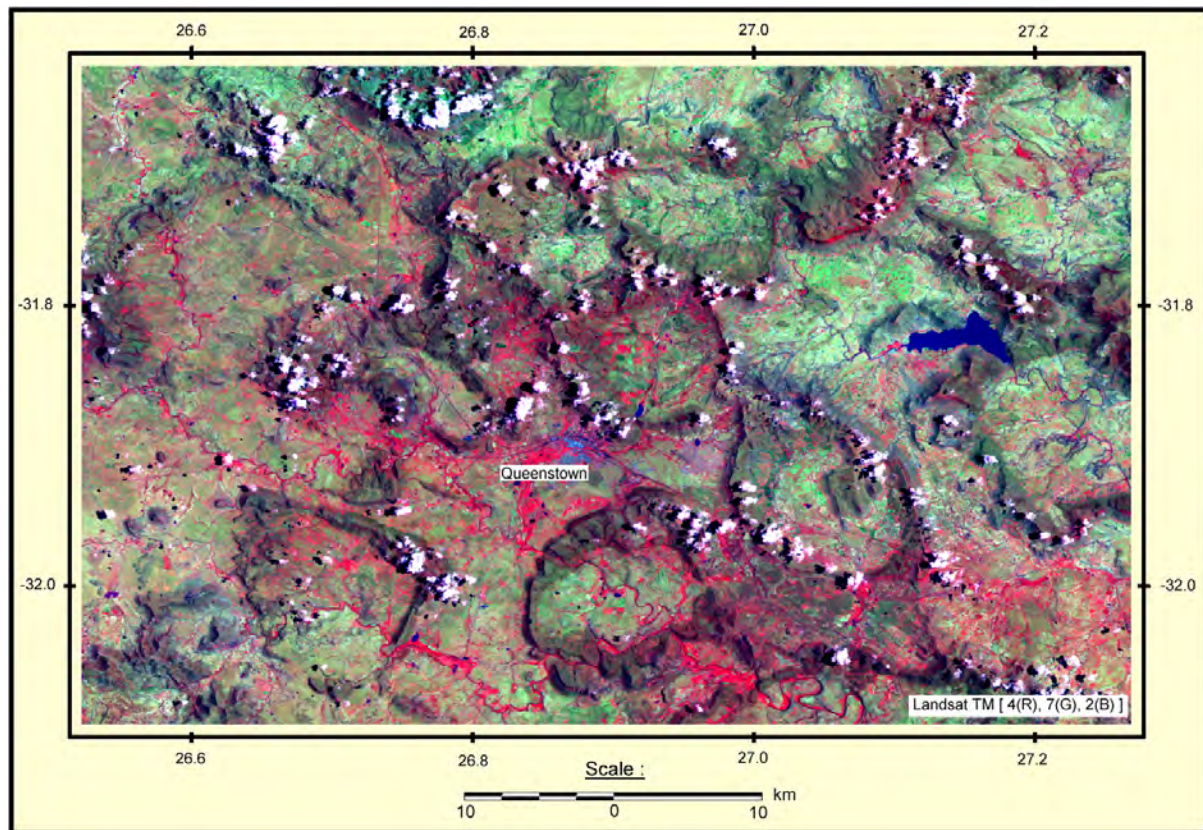


Figure 1.9: *Satellite image showing the influence of dolerite ring-complexes on the geomorphology and drainage system of the Queenstown area, Eastern Cape*

1.5.3 KIMBERLITE INTRUSIVES

Relatively small volumes of kimberlite and associated alkaline-rich igneous rocks (i.e. carbonatite, olivine melilitite), and basaltic lavas were intruded into the Main Karoo Basin during the Cretaceous period between 130 Ma to 70 Ma (Allsop et al., 1986; Duncan et al., 1978; Smith et al., 1985; Smith et al., 1994). Some radiometric dating also indicate ages between 140 and 190 Ma (Davis, 1977; Nixon et al., 1983; Smith et al., 1994), indicating that some of the kimberlite may have been intruded directly after the Karoo dolerite. Kimberlite, however, originates in the mantle (>200 km) and therefore has a totally different origin and composition to that of dolerite or basalt.

Kimberlite fissures or dykes and diatremes ('pipes') occur in clusters and their activity did not produce any noticeable regional geomorphological features. Furthermore, they did not result in any significant regional or even local contact metamorphism due to a lack of high and sustained heat flow during intrusion.

1.6 MODERN GEOMORPHOLOGY

Major uplift during the Miocene and Plio-Pliostocene resulted in the development of the Great Escarpment, the present course of the Orange River and the African Cycle of erosion and weathering (Du Toit, 1933; Partridge and Maud, 1987). Recent sediments include terrace gravel, soil development, modern alluvium and calcrete deposits.

Whether or not the South African continent is presently undergoing a renewal of tectonic activity is still a matter of much controversy. For some authors neotectonics and seismicity in South Africa are indicative of a renewed era of tectonic activity (Partridge, in press; Hartnady, 1990, 1998). For others the African Plate has been at rest with respect to the mantle for the past 40-30 My (Burke, 1996). The fact, however, remains that there has been no volcanism, plate movement or major geological compressive event recorded on the Southern African subcontinent during the recent geological times. The distribution of present day seismic activity over Southern Africa, however, indicates a number of distinctive seismo-tectonic provinces that could be linked to the development of a new structural and plate tectonic framework.

Chapter 2

GEOLOGY AND HYDROLOGICAL PROPERTIES

The sedimentary strata of the Main Karoo Basin range in age from Late Carboniferous to Early Jurassic and attain a maximum cumulative thickness of approximately 12 km in the southern portion of the basin. Today the Karoo strata outcrop over an area of approximately 700 000 km² or more than half of South Africa.

2.1 LITHOSTRATIGRAPHY AND DEPOSITIONAL HISTORY

The lithostratigraphic units of the Karoo Supergroup outcrop concentrically around the Main Karoo Basin (**Figure 2.1**). More detailed sections portraying the entire stratigraphic succession in different parts of the basin are contained in Figure 2.2. Lateral facies changes, particularly in the lower half of the succession, have given rise to intertonguing of formations in various parts of the basin. No major regional unconformities are known to exist within the basin, with the possible exception of one at the base of the Molteno Formation (Veevers et al., 1994; Catuneanu et al., 1998). The description which follows is a summary from Veevers et al., (1994) and Johnson et al., (1997), to which readers are referred for more detail, including additional literature references. Other recent reviews of the Main Karoo Basin are those by Cole (1992), Tankard et al. (1982), Smith (1990), Smith et al. (1993) and Visser (1991).

2.1.1 DWYKA GROUP

2.1.1.1 Lithofacies

The dwyka sediments were deposited during late Carboniferous to early Permian times by glacial processes and the underlying rocks, particularly in the north, display well-developed striated glacial pavements in places. The group consists mainly of diamictite (tillite) which is generally massive with little jointing, but it may be stratified in places. Subordinate rock types are conglomerate, sandstone, rhythmite and mudrock (both with and without dropstones). In the southern part of the basin, under the influence of the Cape Fold Belt, the diamictite display a distinctive ‘tombstone’ morphology as a result of selective weathering along axial-plane cleavage.

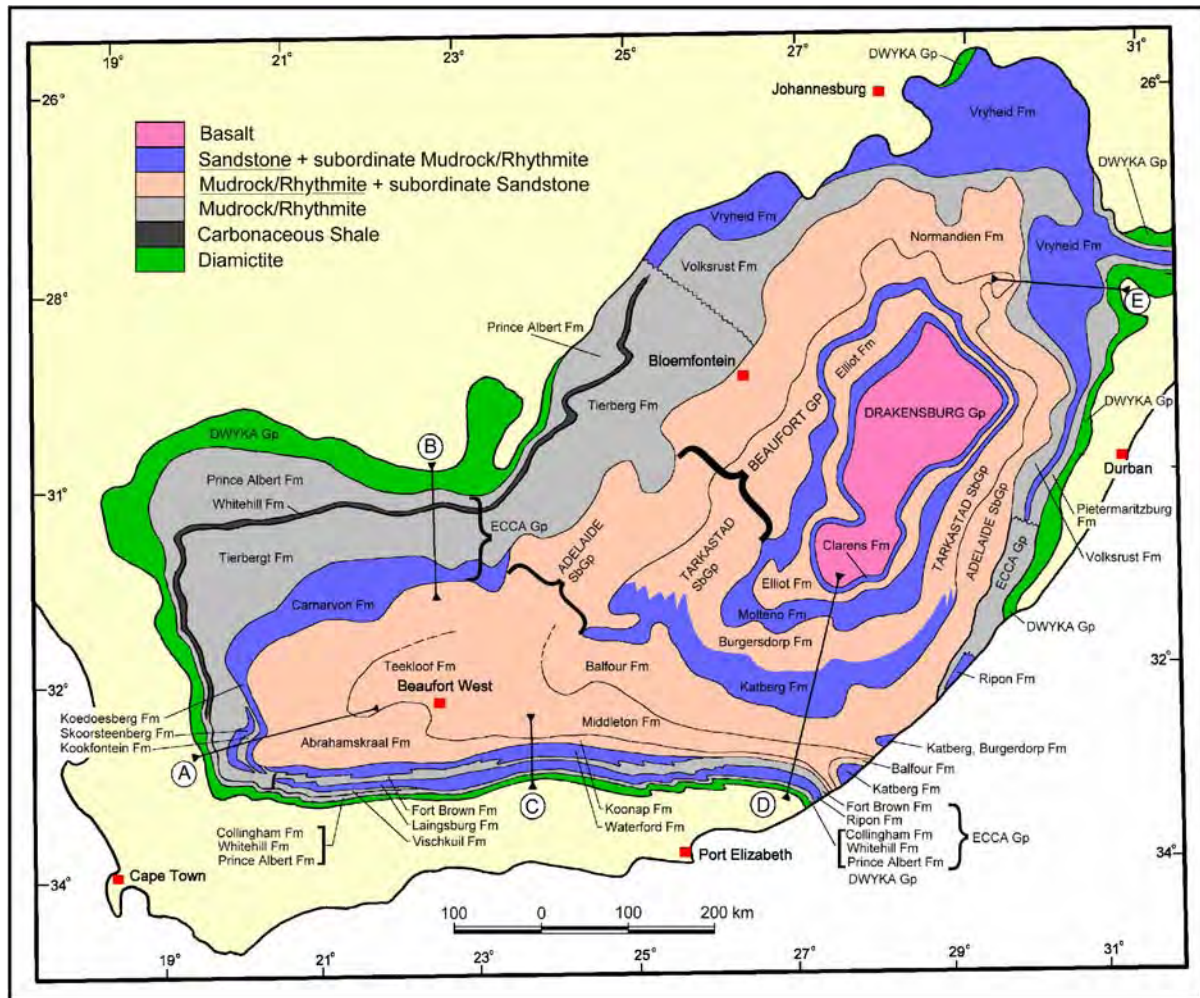


Figure 2.1: Schematic areal distribution of lithostratigraphic units in the Main Karoo Basin (after Johnson et al., 1997)

The Dwyka Group shows distinct lithological differences over the Basin, which led to the recognition of a *northern valley inlet* and *southern platform facies* (Visser, 1986). The northern facies mainly belongs to the Mbizane Formation and is characterised by rapid thickness changes (up to 200 m variations within short distances), a highly variable lithology, and a low, massive diamictite (~20%) and high mudrock (~40%) content. The southern facies constitutes the Elandsvlei Formation and is characterised by a regular increase in thickness towards the south (from about 100 m to 800 m), a fairly uniform lithology, and a high, massive diamictite (~70%) and low mudrock (~8%) content. The Dwyka diamictite consists of angular to rounded clasts of basement rock embedded in a clay and silt matrix. Individual clasts measure up to 3 m in diameter.

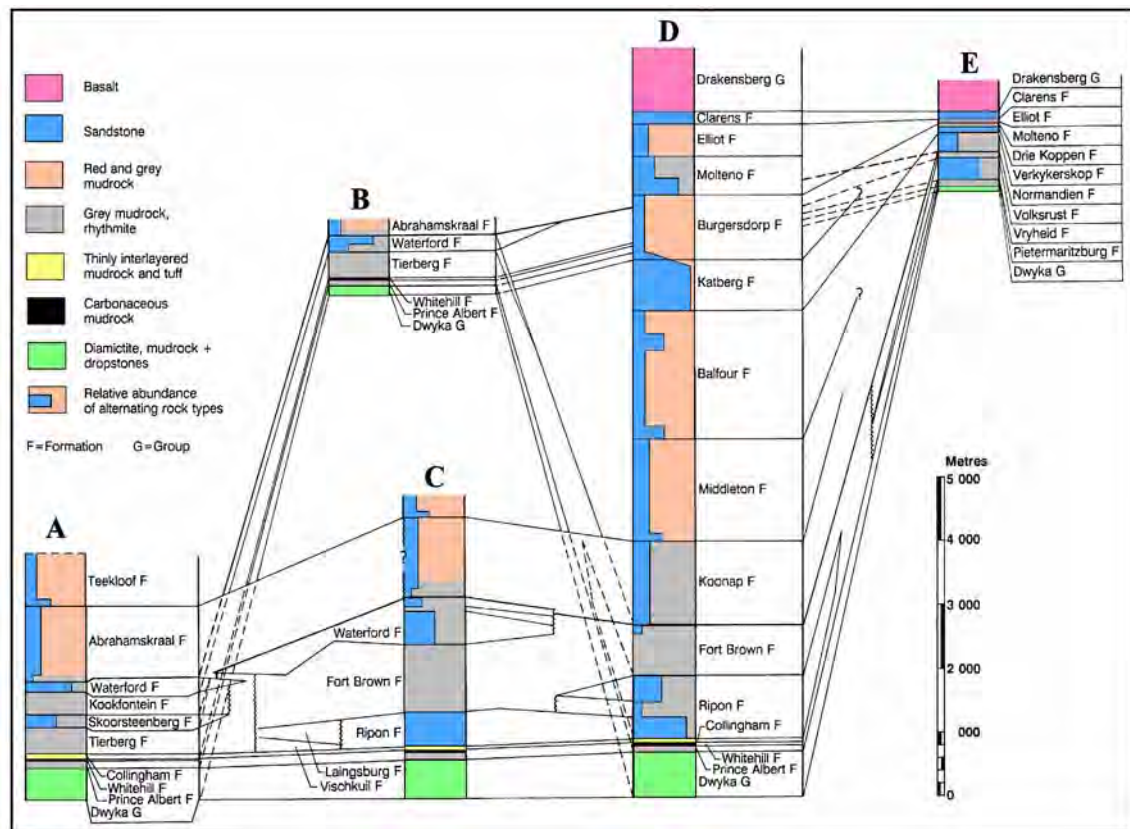


Figure 2.2: Generalised stratigraphy and lithology of the Karoo Supergroup of the Main Karoo Basin (Johnson et al., 1997)

2.1.1.2 Depositional Environment and Sediment Source

The depositional environment and source of the Dwyka Group are summarised in **Figure 2.3**. The *northern valley/inlet facies* were deposited within several southward-trending, glacially-excavated paleo-valleys, where sub-glacial lodgement, supra-glacial ablation tills, marginal moraines, debris-rain sediments and outwash sands and gravels have been recognised (Visser, 1986). The *southern platform facies* extends southwards from the foot of a prominent east-west trending palaeo-escarpment with the diamictite-dominated assemblage, which was deposited as sub-glacial tills of grounded ice, sub-aqueous rain-out from floating ice-sheets and re-worked deposits in the form of debris flows (Visser, 1986; 1997). The water body was marine as shown by the presence of marine fossils - palaeoniscid fish, gastropods, the bivalve *Eurydesma*, cephalopods, brachiopods, echinoids, crinoids, asteroids, radiolaria and foraminifera - in mudstone units of the Dwyka Group and lowermost part of the overlying Ecca Group (Smith, 1990; Veevers et al., 1994; Visser, 1997).

Four deglaciation sequences have been recognised in the Main Karoo Basin (Theron and Blignault, 1975; Visser et al., 1997), with each sequence emanating from an ice-

spreading centre that progressively shifted from an initial location to the north of the Basin to a location south-east of the Basin (Visser et al., 1997).

A complete deglaciation sequence consists of a massive basal diamictite, up to 250 m thick, overlain by a combination of, up to 200 m thick, stratified diamictite, diamictite containing sandstone bodies, rhythmite and mudrock, with or without ice-rafted material. Visser et al., (1997) suggested that the duration of the deglaciation sequences, which are related to major sea-level changes, varied between 9 and 11 million years. Deposition of the first sequence began at about 310 Ma, while the final sediments of the fourth sequence were deposited at about 275 Ma and already belong to the Prince Albert Formation of the Eccca Group. Such dates are supported by U-Pb ages of 302 Ma and 288 Ma for juvenile zircons derived from bentonitic tuffs within the Dwyka Group (Bangert et al., 1998) and unpublished ages of 270 Ma for zircons from tuffs in the Collingham Formation of the Eccca Group (Bangert, 1998, pers. comm.).

Since this ice movement from the south and southeast coincides with the early phase of the Cape Orogeny (278 Ma, Hälbig et al., 1983), it is possible that the compressional paroxysm was associated with uplift of the magmatic arc, which became an ice-spreading centre near the southern margin of Gondwanaland (**Figure 2.3.(b)**).

2.1.2 ECCA GROUP

The Permian-aged Eccca Group comprises a total of 16 formations, reflecting the lateral facies changes that characterise this succession. Except for the fairly extensive Prince Albert and Whitehill Formations, the individual formations can be grouped into three geographical zones, the *southern*, *western - northwestern* and *northeastern*.

The basal sediments in the southern, western and northwestern zones (Prince Albert and Whitehill Formations) of the basin will first be described, followed by the southern Collingham, Vischkuil, Laingsburg, Ripon, Fort Brown and Waterford Formations. The remaining western and northwestern sediments of the Tierberg, Skoorsteenberg, Kookfontein and Waterford Formations and the northeastern Pietermaritzburg, Vryheid and Volksrust Formations will then be considered. In addition, a relatively small area along the eastern flank of the Basin, between the southern and north-eastern outcrop areas, contains 600 – 1 000 m of undifferentiated Eccca mudrock, which has not yet been studied in detail (**Figure 2.1**).

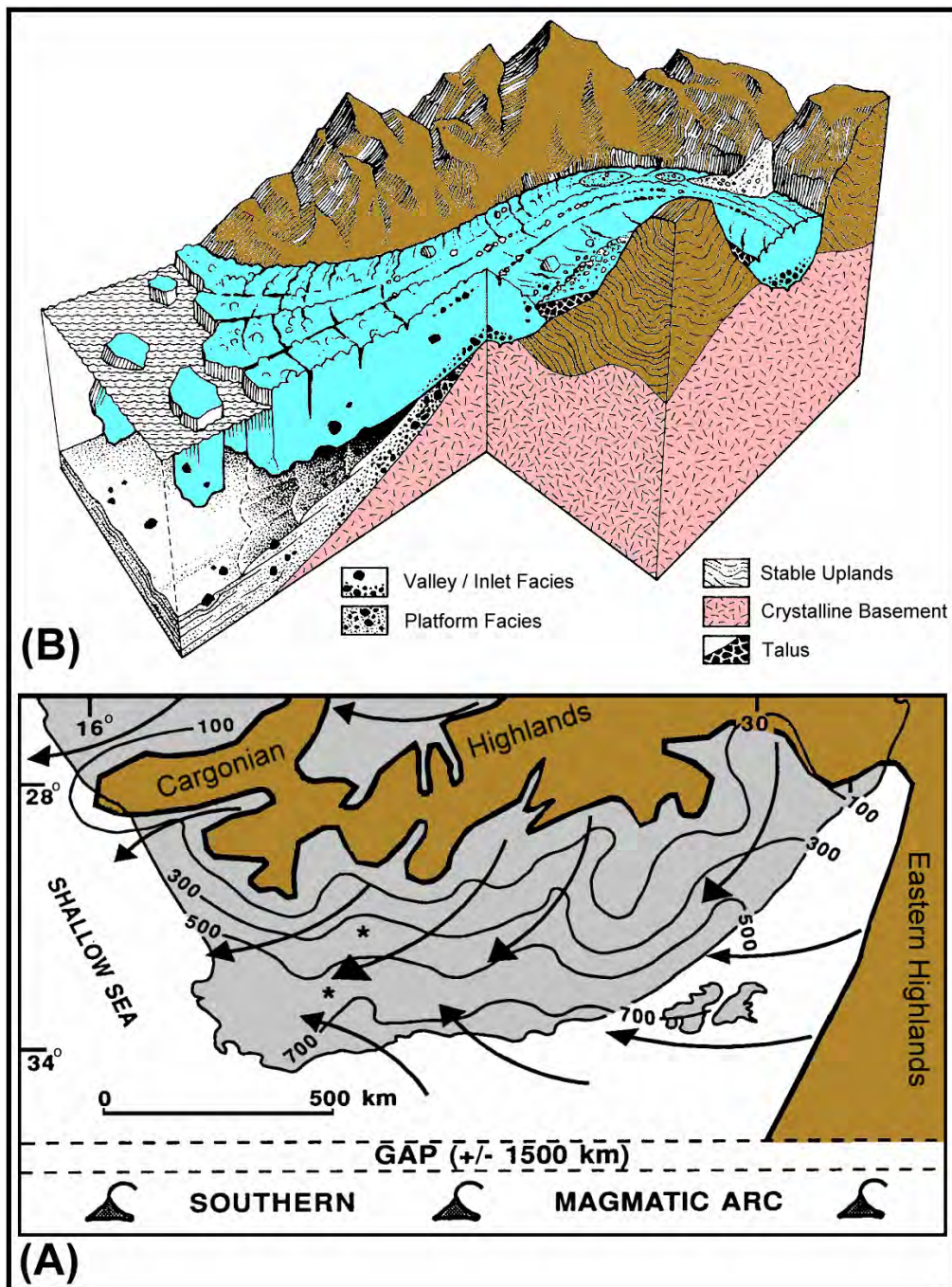


Figure 2 3: (A) Source areas of the Dwyka glacial sediment (after Cole, 1992). (B) Depositional environment of the Dwyka glacial sediments with glacially-excavated paleo-valley facies inland and diamictite-dominated platform facies offshore (after Smith et al., 1993)

2.1.2.1 Prince Albert Formation (Lower Ecca)

The Prince Albert Formation is confined to the south-western half of the Karoo Basin (**Figure 2.1**). Towards the northeast it thins and locally pinches out against the basement or merges with the Vryheid and/or Pietermaritzburg Formations. Along the western and southern outcrop belt its thickness is highly variable (40 – 150 m), while borehole data indicate a maximum thickness of up to 300 m (Veevers et al., 1994).

It is possible to recognise a northern and a southern facies in the Formation. The northern facies is characterised by the predominance of greyish to olive-green, micaceous shale and grey, silty shale, as well as a pronounced transition from the underlying glacial deposits. Dark-grey to black carbonaceous shale and fine- to medium-grained feldspathic arenite and wacke are also present. The southern facies is characterised by the predominance of dark-grey, pyrite-bearing, splintery shale, siltstone and the presence of dark-coloured chert and phosphatic nodules and lenses.

The shale represents suspension settling of mud and the siltstone represents turbidites (Visser, 1991), whereas the arenite and wacke in the northern part of the basin are probably the result of deltaic sedimentation (**Figure 2.4**) (Cole and McLachlan, 1991). The lower part of the formation was deposited following final melting of the Dwyka ice-sheets (Visser, 1997) and the presence of marine invertebrate fossils and phosphorite are indicative of marine conditions (Visser, 1992) at least in the lower part (Veevers et al., 1994).

2.1.2.2 Whitehill Formation (Lower Ecca)

The mudrocks of this formation weather white on surface, making it a very useful marker unit (**Figure 2.1**). In fresh outcrop and in the subsurface the predominant facies is black, carbonaceous, pyrite-bearing shale. The shale is very thinly laminated and contains up to 14 per cent carbonaceous material (Du Toit, 1954). The thickness varies from 10 to 80 m and it contains the fossilized reptile *Mesosaurus*.

The Whitehill Formation loses its distinctive lithological character towards the northeast with its lower part containing siltstone and very fine-grained sandstone. It can be regarded as a distal equivalent of part or all of the Vryheid Formation (Cole and McLachlan, 1991; Visser, 1992).

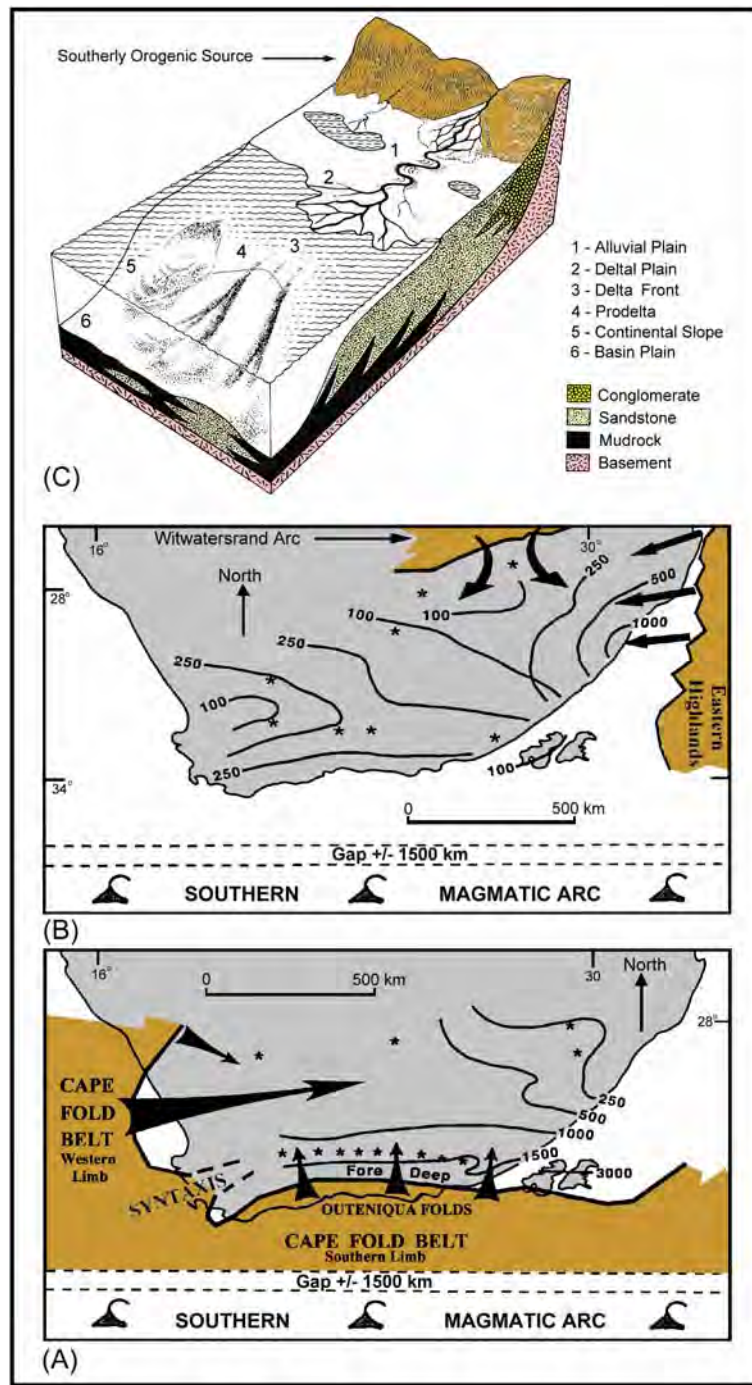


Figure 2 4: (A) Source areas for the Southern and Western Ecca Formations (B) and the northern Pietermaritzburg, Vryheid and Volksrust Formations (after Cole, 1992). (C) Depositional environment of the Ecca Group in the southern Karoo trough (after Smith et al., 1993 and Wickens, 1994).

The black, organic-rich shales are thought to represent suspension-settling of mud under reducing conditions, but the salinity remains unresolved with some researchers proposing:

- a marine water body (Oelofsen and Araujo, 1987; Visser, 1992),
- a non-marine brackish water body with no connection to the world oceans (Veevers et al., 1994), with a maximum water-depth of 80 m (i.e. within the photic zone), under anoxic conditions being restricted to the basin floor by benthic microbial mats (Cole and McLachlan, 1991),
- a huge freshwater lake that spanned much of south-western Gondwana and was characterised by algal blooms (Faure and Cole, 1999), and / or
- a sea-level highstand under restricted oceanic circulation (Visser, 1992, 1993).

The depositional environment cannot therefore be depicted in **Figure 2.4**.

2.1.2.3 Collingham Formation (Upper Ecca)

Outcrops of the Collingham Formation are confined to the southern and western margins of the Main Karoo Basin (**Figure 2.1**). The formation is generally between 30 and 70 m thick and comprises a rhythmic alternation of thin, continuous beds (average 5 cm) of hard, dark grey, siliceous mudrock and very thin beds (average 2 cm) of softer yellowish tuff (K-bentonite). In the western part of the area minor sandstone and siltstone units occur in the upper half of the formation, while the distinctive Matjiesfontein Chert Bed (0.2 - 0.6 m thick) is present in the lower half (Viljoen, 1994). Unpublished U-Pb ages of 270 Ma for juvenile zircons derived from the tuffs (Bangert, 1998, pers. comm.) indicate deposition during early-late Permian times.

The sediments were deposited by suspension settling of hemi-pelagic and pelagic detritus of aeolian origin, by underflow and overflow suspensions and from distal, low density, mud-rich turbidity currents (Viljoen, 1994). These deposits were periodically interrupted by the deposition of fall-out tephra (K-bentonites). The sandstone and siltstone in the upper half of the formation represent fine-grained turbidites and are interpreted as basin plain and outer fan deposits (Viljoen, 1994) (**Figure 2.4**).

2.1.2.4 Vischkuil Formation (Upper Ecca)

The predominantly argillaceous Vischkuil Formation overlies the Collingham Formation in the southwestern part of the basin (**Figure 2.1**). The Vischkuil Formation becomes more arenaceous towards the east and grades into the Ripon Formation. A western cut-off is located where the overlying Laingsburg Formation pinches out. The formation varies in thickness between 200 and 400 m.

The Vischkuil Formation consists essentially of dark shale, alternating with subordinate fine-grained sandstone, siltstone and minor yellowish tuff layers. The shale units are thinly laminated or structureless, and contain phosphatic and calcareous lenses, and ferruginous layers with liesegang structures. Sandstone (greywacke) beds vary from 0.3 to 1.5 m in thickness and increase in abundance upwards.

The shale represents basin-plain suspension settling of clays, interrupted by sporadic influxes of muddy turbidite flows, whereas the sandstone represents more proximal turbidites (Wickens, 1994). The presence of minor tuff beds in the shale, indicates continued volcanic activity in the southern magmatic arc region. The upward increase in the thickness and abundance of sandstone has been interpreted as active progradation (Theron, 1967) from a southerly and southwesterly source area that was probably situated to the south of the present coastline (**Figure 2.4**).

2.1.2.5 Laingsburg Formation

This formation usually comprises four sandstone-rich units separated by shale units and is approximately 400 m thick in its type area. It wedges out towards the west and north. A vertical cut-off is located in the east where the underlying Vischkuil Formation merges with the Ripon Formation (**Figures 2.1** and **2.2**).

The thick massive sandstone units (up to 30 m thick, with individual beds up to 4m thick) are fine- to medium-grained with sharp upper and lower contacts. They grade upward into planar-laminated siltstone and shale, which commonly contain coalified plant fragments and lenticular calcareous concretions.

The four sandstone-rich units represent arenaceous submarine fan systems, which are separated by basin-plain shale units (Wickens, 1994) (**Figure 2.4(C)**).

2.1.2.6 Ripon Formation

The Ripon Formation is generally 600 – 700 m thick, but is over 1 000 m in the eastern part of its outcrop area. It consists of poorly sorted, fine- to very fine-grained lithofeldspathic sandstone alternating with dark grey clastic rhythmite and mudrock. In the eastern area the formation has been subdivided into a lower Pluto's Vale Member (mainly sandstone), a middle Wonderfontein Member (mudrock/ rhythmite) and an upper Trumpeters Member (alternating sandstone and mudrock) by Kingsley (1981). Sandstones of the upper member pinch out towards the west, where the Ripon is correspondingly thinner (**Figure 2.1**). Drilling has shown that the sandstones wedge out rapidly northwards.

The sandstone units of the lower 50 m of the succession are on average about 0.3 m thick. The average sandstone thickness increases to 12 m for the overlying rocks, where a maximum thickness of 44 m has been recorded. Most of the sandstone layers are tabular and consist of a number of individual sedimentation units. The lower boundaries are sharp, while the upper boundaries are gradational into mudrock or rhythmite over an interval ranging from a few millimetres to a few metres. Roughly spherical calcareous concretions of 10–15 cm in diameter are fairly common in these sandstones, while larger brown-weathering calcareous bodies of 30–150 cm in diameter are also present in places.

The sandstones have been interpreted as turbidites deposited within submarine fan environment, while the mudrocks are thought to represent basin-plain suspension and distal turbidites (Kingsley, 1981). A source area to the south of the present coastline is postulated (**Figure 2.4**).

2.1.2.7 Fort Brown Formation

The Fort Brown Formation consists of rhythmite and mudrock with minor sandstone intercalations and displays an overall coarsening-upward tendency. At certain localities, one or more fairly prominent sandstone units occur some distance below the upper contact. The average thickness is about 1 000 m, with values ranging from about 500 m to 1 500 m. Outcrops are confined to the southern margin of the basin.

Individual sand/silt and silt/clay layers comprising rhythmite units of similar thickness, ranging from a few millimetres to a few centimetres, are laterally persistent. The sand/silt layers display a general upward increase in thickness within the Formation. Calcareous concretions 30–100 cm in diameter and 10–30 cm thick occur sporadically.

The rhythmite and mudrock were deposited in a prodelta environment ahead of a prograding delta front. The deltas also supplied sand to the submarine fan sediments of the Collingham, Vischkuil, Laingsburg and Ripon Formations, as a result of slumping, which generated turbidity currents (Kingsley, 1981; Wickens, 1994) (Figure 2.4).

2.1.2.8 Waterford Formation of the Southern Zone (Upper Ecca)

The arenaceous Waterford Formation overlies the Fort Brown Formation to the west of longitude 26°E, where its thickness generally varies between 200 and 800 m. The formation comprises alternating very fine-grained, lithofeldspathic sandstone and mudrock or clastic rhythmite units. The Britskraal Shale Member in the upper part of the Waterford Formation in the eastern outcrop area averages 100 m in thickness and consists essentially of dark grey mudrock and rhythmite.

The average and maximum thickness of individual sandstone units is 6 m and 18 m, respectively. Well-developed oscillation ripples and ball-and-pillow, and related deformation structures are characteristic features of the Waterford Formation. Thin mud-flake conglomerate layers are occasionally present. Brown-weathering calcareous concretionary bodies occur in both the sandstones and the argillaceous rocks.

The arenaceous Waterford Formation was probably deposited in delta front and distributary-mouth bar environments within a highly constructive delta system, that prograded from the south (Smith, 1990; Veevers et al., 1994; Wickens, 1994) (Figure 2.4).

2.1.2.9 Tierberg Formation (Upper Ecca)

The Tierberg Formation is a predominantly an argillaceous succession which reaches a maximum thickness of approximately 700 m along the western margin of the basin, thinning to about 350 m towards the northeast. It rests with a sharp contact on the Collingham or Whitehill Formations and grades upward into the arenaceous Waterford Formation or, where the latter is absent, into the Adelaide Subgroup (Beaufort Group). Where it is overlain by sandstone of the Skoorsteenberg Formation the contact is fairly sharp and the formation is about 460 m thick.

The bulk of the Tierberg Formation comprises well-laminated, dark grey to black shale. Some yellowish tuffaceous beds up to 10 cm thick occur in the lower part of the succession along the western and northern margins of the Basin. Calcareous concretions are common towards the top of the formation. Clastic rhythmites occur at various levels in the sequence.

The transition zone at the top of the formation consists of a number of upward-coarsening sequences of 2–10 m thick mudstone, siltstone and very fine-grained sandstone layers. Thin clay-pellet conglomerates are present while calcareous concretions occur relatively frequently.

The bulk of the Formation represents a basin-plain and prodelta environment, while the upward-coarsening transition sequences at the top of the formation correspond to a distal delta-front depositional environment (Veevers et al., 1994) (**Figure 2.4**).

2.1.2.10 Skoorsteenberg Formation (Upper Ecca)

The Skoorsteenberg Formation is a lenticular, arenaceous unit located between the Tierberg and Kookfontein Formations in the southwestern part of the basin. It attains a maximum thickness of approximately 200 m at its type locality, where it comprises five sandstone-rich units up to 65 m thick with shale units separating them. Individual sandstone layers attain a maximum thickness of 6m and are parallel-sided with sharp upper and lower boundaries and are fairly persistent along strike.

The six sandstone-rich units represent arenaceous submarine fan deposits, which are separated by equally thick basin-plain shale units (Wickens, 1994). The provenance was located towards the west and southwest of the Basin (**Figure 2.4**).

2.1.2.11 Kookfontein Formation (Upper Ecca)

The Kookfontein Formation overlies the Skoorsteenberg Formation with a sharp contact and grades upwards into the Waterford Formation. It is a lateral equivalent of the upper part of the Tierberg Formation and is approximately 300 m thick at its type locality.

The lower part of the formation comprises horizontally laminated dark-grey shales alternating with clastic rhythmities, which form minor upward-thickening cycles. The cycles become more prominent towards the top of the Formation where they are up to 15m thick and consist of alternating siltstone and thin sandstone beds, capped in places by a thick sandstone bed. The lithologies represent prodelta sedimentation in a gradually shallowing water body (Visser, 1993) (**Figure 2.4**).

2.1.2.12 Waterford Formation of the Western Zone (Upper Ecca)

The Waterford Formation, formerly the known as the Koedoesberg Formation, outcrops along the western flank of the Basin (**Figure 2.1**) and overlies the Kookfontein and Tierberg Formations with a gradational contact. The contact with the overlying Abrahamskraal Formation is relatively sharp. The Formation has a mean thickness of 130 m.

The major rock types are fine- to medium-grained sandstone, siltstone, shale and rhythmite. The lower part of the Formation is characterized by upward-coarsening cycles of sediments, which are capped by extensive sheet-like sandstones and alternating chaotic, slump and slide deposits. The upper portion of the Formation consists of sandstone (± 8 m thick), siltstone, ball-and-pillow layers and channel-fill deposits.

The Formation displays an overall coarsening upward pattern, grading from the argillaceous Tierberg Formation through alternating sandstone, siltstone and mudstone into a sandstone-dominated interval at the top.

The Waterford Formation has a similar origin to that in the Southern Zone, i.e. delta front and distributary-mouth bar deposits within a highly constructive delta system that prograded from the west (**Figure 2.4**).

2.1.2.13 Waterford Formation of the North-Western Zone (Upper Ecca)

The Waterford Formation, formerly named the Carnarvon Formation, outcrops along the north-western margin of the Basin (**Figure 2.1**) and is up to 250 m thick in the vicinity of Carnarvon. The sediments consist of fine- to very fine-grained tabular sandstones that are up to 8m thick, siltstone, shale and rhythmite (Siebrits, 1987). Brown-weathering, calcareous concretions with a maximum diameter of 2 m are present in all the rock types. Wavy bedding, including hummocky cross-bedding and symmetrical ripples are predominant, as well as slump structures, ball-and-pillow structures and load-casts. The different facies commonly form upward-coarsening sequences ranging in thickness from 4 to 38 m.

Deposition probably took place in a shallow sea, where wave action was the controlling process (Rust et al., 1991). The nearest shoreline was more than 200 km towards the west in the vicinity of Calvinia (Rust et al., 1991) (**Figure 2.4**).

2.1.2.14 Pietermaritzburg Formation

The Pietermaritzburg Formation comprises dark, upward coarsening, silty mudrock, which is heavily bioturbated. Pene-contemporaneously deformed sandy and silty beds appear near the top of the formation. Outcrops of the Pietermaritzburg Formation are confined to the eastern margin of the basin, but extensive drilling has shown that it underlies the Vryheid Formation over much of the northeastern part of the basin. It attains a maximum thickness of over 400 m in the southeast (Du Toit, 1954), thinning towards the north and pinching out against the Dwyka Group or against a palaeo-scarp near the northern margin of the Basin. Towards the south, where the Vryheid Formation pinches out, it merges with the Volksrust Formation. The contact between the Pietermaritzburg and Vryheid Formations is strongly diachronous, with sandstones successively higher up in the succession shelving out towards the south.

The mudrock-dominated formation has been interpreted as a prodelta deposit, which fronted upon a succession of north and northeasterly prograding delta fronts (Hobday, 1973; Van Vuuren and Cole, 1979) (**Figure 2.4**).

2.1.2.15 Vryheid Formation

The Vryheid Formation thins towards the north, west and south from a maximum of approximately 500 m in the Vryheid-Nongoma area. The uneven pre-Karoo topography in the vicinity of the northern and northwestern margins of the basin where the Vryheid rests directly on pre-Karoo rocks or the Dwyka Group gives rise to marked variations in thickness. In these areas, the Vryheid pinches out against numerous local basement highs. Thinning and pinch-out towards the southwest and south is due to a facies gradation of its lower and upper parts into shales of the Pietermaritzburg and Volksrust Formations respectively (**Figure 2.1**).

The Vryheid Formation comprises mudrock, rhythmite, siltstone and fine- to coarse-grained sandstone (pebbly in places). The Formation contains up to five (mineable) coal seams. The different lithofacies are mainly arranged in upward-coarsening deltaic cycles (up to 80m thick in the southeast). Linear coastline cycles are, however, fairly common particularly in the thin northwestern part where they constitute the entire Vryheid in places (**Figure 2.4**).

A relatively thin fluvial interval (60 m thick) which grades distally into deltaic deposits towards the southwest and south occurs approximately in the middle of the formation in the east and northeast. Fining-upward fluvial cycles, of which up to six are present in the east, are typically sheet-like in geometry, although some form valley-fill deposits. They comprise coarse-grained to pebbly, immature sandstones - with an abrupt upward transition into fine-grained sediments and coal seams.

2.1.2.16 Volksrust Formation

The Volksrust Formation is a predominantly argillaceous unit, which interfingers with the overlying Beaufort Group and underlying Vryheid Formation. Where the latter pinches out towards the southwest the Volksrust merges with the Tierberg Formation in the northern outcrop area or with the Pietermaritzburg Formation in the undifferentiated Ecca Group in the southeast (**Figure 2.1**). Drilling has shown that it reaches a thickness of 380m about 120km northeast of Bloemfontein, thinning to 250 m in the east (Taverner-Smith et al., 1988) and to 100 m towards the northern margin of the basin.

The Formation consists of grey to black, silty shale with thin, usually bioturbated, siltstone or sandstone lenses and beds, particularly towards its upper and lower boundaries. Thin phosphate and carbonate beds and concretions are relatively common.

A shallow water shelf environment has been proposed (Smith et al., 1993), with the upward-coarsening transition into the Beaufort Group representing a prodelta and distal delta front environment (Cadle and Hobday, 1977; Visser and Looek, 1978) (**Figure 2.4**).

2.1.2.17 Depositional Environment and Source of Sedimentation

Ecca Group sediments were predominantly derived from a provenance located to the south and west of the Basin, which included:

detrital material from the Cape Fold Belt,
volcanic ash exhaled from the magmatic arc situated along the Gondwana Plate subduction zone, and
sediments reworked in the Basin (Cole and Wipplinger, in press) (**Figure 2.4(A)**).

The Ecca sediments were deposited within a rapidly downwarping foredeep trough by prograding submarine fans and turbidites (Prince Albert, Collingham, Vischkuil, Laingsburg, Ripon, Skoorsteenberg Formations), as well as prodeltas and deltas (Fort Brown, Waterford, Tierberg, Kookfontein Formations) (**Figure 2.4(C)**). A continental provenance located north and northeast of the Basin supplied fluvial to deltaic sediments to the Prince Albert, Pietermaritzburg, Vryheid and Volksrust formations (Veevers et al., 1994) (**Figure 2.4(B)**), as well as extensive shallow lake deposits (Whitehill Formation).

2.1.3 BEAUFORT GROUP

2.1.3.1 Adelaide Subgroup

In the southeastern part of the basin, the late Permian Adelaide Subgroup comprises the Koonap, Middleton and Balfour Formations. In the west, the Abrahamskraal and Teekloof Formations are the approximate equivalents of the Koonap and Middleton Formations, respectively (**Figures 2.1 and 2.2**). While the Middleton and Teekloof Formations are characterised by a greater relative abundance of red mudstone compared to the underlying and (in the case of the former) overlying units, in practice the boundaries are linked to specific sandstone-rich marker units (members). Thus the arenaceous Poortjie and Oudeberg Members constitute the base of the Teekloof and Balfour Formations, respectively. In the northeastern region, only a single formation, the Normandien Formation, is present.

The Adelaide Subgroup attains a maximum thickness of about 5000m in the southeast, which decreases rapidly to about 800 m in the centre of the Basin and thereafter more gradually to around 100–200 m in the extreme north. The Koonap Formation attains a maximum thickness of about 1 300 m, the Middleton 1 600 m (although it may be as much as 2 500 m to the north of Port Elizabeth) and the Balfour 2 000 m. In the west, the Abrahamskraal and Teekloof Formations are up to 2500 m and 1400 m thick, respectively. The Normandien Formation is approximately 320 m thick in its type area (Groenewald, 1989).

In the southern and central parts of the Basin the Adelaide Subgroup consists of alternating bluish-grey, greenish-grey or greyish-red mudrock and grey, very fine to medium-grained, lithofeldspathic sandstone. In the northern part of the Basin, coarse to very coarse sandstone, or even granulestone, are also common in the Normandien Formation. Sandstone generally constitutes 20–30% of the total thickness, but in certain areas may be as little as 10%, while some sandstone-rich intervals may in places contain up to 60 % sandstone.

Individual sandstone units are thickest in the south (averaging 6 m; maximum 60 m) and become thinner northwards, except for the extreme northeast where thick, laterally extensive units are also present in the Normandien Formation. They generally extend laterally for a few hundreds metres to a few kilometres, but many are markedly lenticular. Calcareous concretions 20-100 cm in diameter are present in some sandstone layers.

In the Daggaboersnek Member, which occurs towards the middle of the Balfour Formation in the southeastern part of the basin, the sandstones tend to be thin and tabular, possibly reflecting a lacustrine depositional environment.

Palaeocurrent data indicate that the bulk of the sediment was derived from a source area situated to the south and southeast of the Basin, with subordinate influxes from

the southwest, west-northwest and northeast (**Figure 2.5(a)**). The source area situated to the south, southeast and southwest of the Basin coincides with the second major tectonic paroxysm of the Cape Fold Belt, dated at ± 258 Ma (Hälbich et al., 1983). The margin of the Basin was probably close to the present South African coastline (Cole, 1998). Source areas to the west-northwest and northeast were sited on the continental regions of western Namaqualand / north-eastern Patagonia and the Mozambique Ridge / East Antarctica respectively (Cole, 1998).

Except in the lower part of the Normandien Formation, where coarsening-upward cycles of sedimentation are present, the sandstone units normally form fining-upward cycles. The cycles vary from a few metres to a few tens of metres in thickness and were probably formed by the lateral migration of meandering rivers (**Figure 2.5(B)**). The subordinate, horizontally bedded sandstone units that show no upward change in grain-size were deposited by ephemeral sheet-floods. The mudstone represents deposition in a flood plain and lacustrine environment.

2.1.3.2 Tarkastad Subgroup

The early Triassic Tarkastad Subgroup is characterized by a greater abundance of both sandstone and red mudstone when compared with the Adelaide Subgroup. The boundary between these two subgroups is the only one in the Beaufort Group that can be traced with certainty throughout the Main Karoo Basin. The subgroup has a maximum thickness of nearly 2 000 m in the south, decreasing to approximately 800 m in the mid-Basin and 50 m or less in the far northern extremity of the Basin (Groenewald, 1989).

In the south, the Tarkastad Subgroup comprises a lower, sandstone-rich Katberg Formation and an upper, mudstone-rich Burgersdorp Formation. Sandstone constitutes over 90% of the Katberg Formation in the small coastal exposures in the vicinity of East London, where the unit is over 900 m thick, and in the southernmost part of the main outcrop area. However, the sandstone : mudstone ratio decreases steadily northwards until the Formation becomes indistinguishable from the Burgersdorp Formation. The latter is around 1 000 m thick in the southern outcrop area, with the overall sandstone content diminishing from approximately 50% in the coastal exposures to around 20–30 per cent or less further north within the main outcrop area. In the extreme northeast Groenewald (1989) recognized a lower Verkykerskop Formation comprising up to 80 m of fine- to very coarse-grained sandstone and an upper Driekoppen Formation, which is up to 70 m thick and consists almost entirely of mudstone.

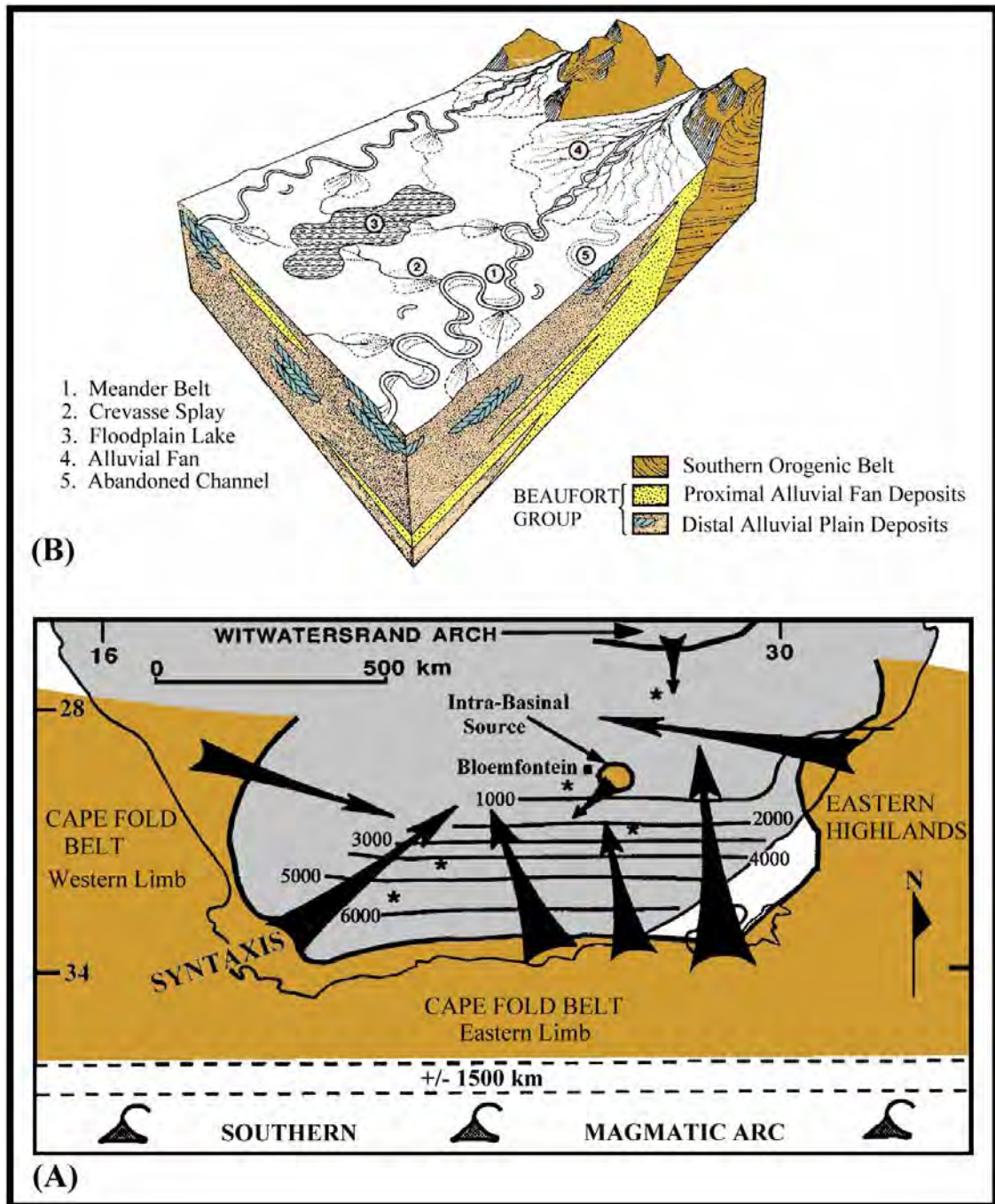


Figure 2.5: (A) Sediment source areas for the Beaufort Group (after Cole, 1992).
 (B) Depositional environment of the Beaufort Group in the Southern Karoo Basin (after Smith et al., 1993).

The Katberg Formation sandstones are light brownish grey to greenish grey, fine- to medium-grained and contain scattered pebbles up to 15 cm in diameter within the coastal outcrops. Oval to spherical calcareous concretions, 3–10 cm in diameter, are also common. The Burgersdorp Formation sandstones are greenish grey to light brownish grey and are fine-grained. The average thickness of sandstone units in the central portion of the Formation in the main outcrop area is 2 m.

Intraformational mud-pellet conglomerates are common in both the Burgersdorp and Katberg Formations. The mudstone units in both Formations are predominately red coloured. Reptile, amphibian and to a much lesser extent fish remains are relatively common in the Tarkastad Subgroup.

Except for the Katberg Formation in the south, which was probably deposited in a braided stream environment, the sandstone and mudstone units of the Tarkastad Subgroup tend to form fining-upward cycles comparable to those of the Adelaide Subgroup. Meandering streams or, in the case of the Burgersdorp Formation, flood basin and lacustrine palaeo-environments may therefore have predominated (**Figure 2.5(b)**).

Palaeo-current data for the Tarkastad Subgroup suggest a northerly to northwesterly regional palaeo-slope, similar to that prevailing during deposition of the underlying Adelaide Subgroup. Once again, the major source area must have been located to the southeast of the basin (**Figure 2.5(a)**). The rapid increase in the quartz content at the expense of feldspar in the Katberg Formation would appear to reflect strong uplift and denudation of the Cape Fold Belt, located between the magmatic arc and the Basin. Catuneanu et al., (1998) postulated that the Tarkastad Subgroup was deposited during a period of orogenic loading and foredeep subsidence that terminated with a tectonic paroxysm dated at ± 239 Ma (Hälbich, 1983).

For his Verkykerskop Formation in the northeastern part of the basin, Groenewald (1989) postulated the continued existence of a granitic source lying to the east of the Basin.

2.1.4 MOLTENO, ELLIOT AND CLARENS FORMATIONS

2.1.4.1 Molteno Formation

The late Triassic Molteno Formation attains a maximum thickness of close to 600 m in its southern outcrop area. It is less than 10 m thick in the extreme north. The Formation comprises alternating medium- to coarse-grained, ‘glittering’ sandstones and grey mudrocks, with well-preserved plant fossils and sporadic coal seams. In the south, the arenaceous Bamboesberg Member forms the base of the Molteno Formation. Elsewhere, the Indwe Sandstone Member, which is the only

representative of the Molteno Formation in the north, constitutes the base and may rest unconformably on the Beaufort Group in places.

Deposition was predominantly by braided rivers flowing from a tectonically active source area, probably the Cape Fold Belt, situated to the south and southeast (**Figure 2.6(a)**). An additional source area in the form of a fault-controlled, uplifted, cratonic basement east-southeast of the Basin has recently been advocated (Turner and Thompson, 1998).

If the age estimates in the literature are correct, a Middle Triassic lacuna lasting about 10 million years must have separated the Middle Triassic Burgersdorp Formation from the Late Triassic Molteno Formation (Catuneanu et al., 1998; Hancox, 1998). At the end of the Middle Triassic, the Cape Fold Belt was reactivated by four major paroxysms dated at 230 Ma (Hälbich et al., 1983). These events resulted in the downwarping of the Main Karoo Basin below its base-level and a renewed cycle of sedimentation was initiated to form the Molteno Formation (Veevers et al., 1994). Catuneanu et al., (1998), however, suggest that the lacuna coincided with a change from orogenic compression to extension in the Cape Fold Belt, with the depocentre shifting towards the craton from the foredeep to the fore-sag zone.

2.1.4.2 Elliot Formation

The late Triassic to early Jurassic Elliot Formation comprises an alternating sequence of mudrock and subordinate fine- to medium-grained sandstone. It attains a maximum thickness of about 500 m in the south (Visser and Botha, 1980), thinning to ~100 m in the north. Contacts with the underlying Molteno and the overlying Clarens Formations are gradational.

The maroon and green-grey mudrock units typically range in thickness between 25 and 100 m in the type area and contain vertebrate (mainly dinosaur) fossils. The sandstone layers are yellowish grey to pale red and are up to 22 m thick (generally 6–15 m). Their bases are characteristically erosive and contain numerous mudrock intraclasts.

The Elliot Formation comprises a lower arenaceous unit with fining-upward cycles, reflecting meandering river sedimentation and an upper mudrock-dominated unit interpreted as a playa deposit (**Figure 2.6(b)**). Palaeocurrent patterns suggest northerly to north-westerly transport from a source area coinciding with the Cape Fold Belt (**Figure 2.6(a)**).

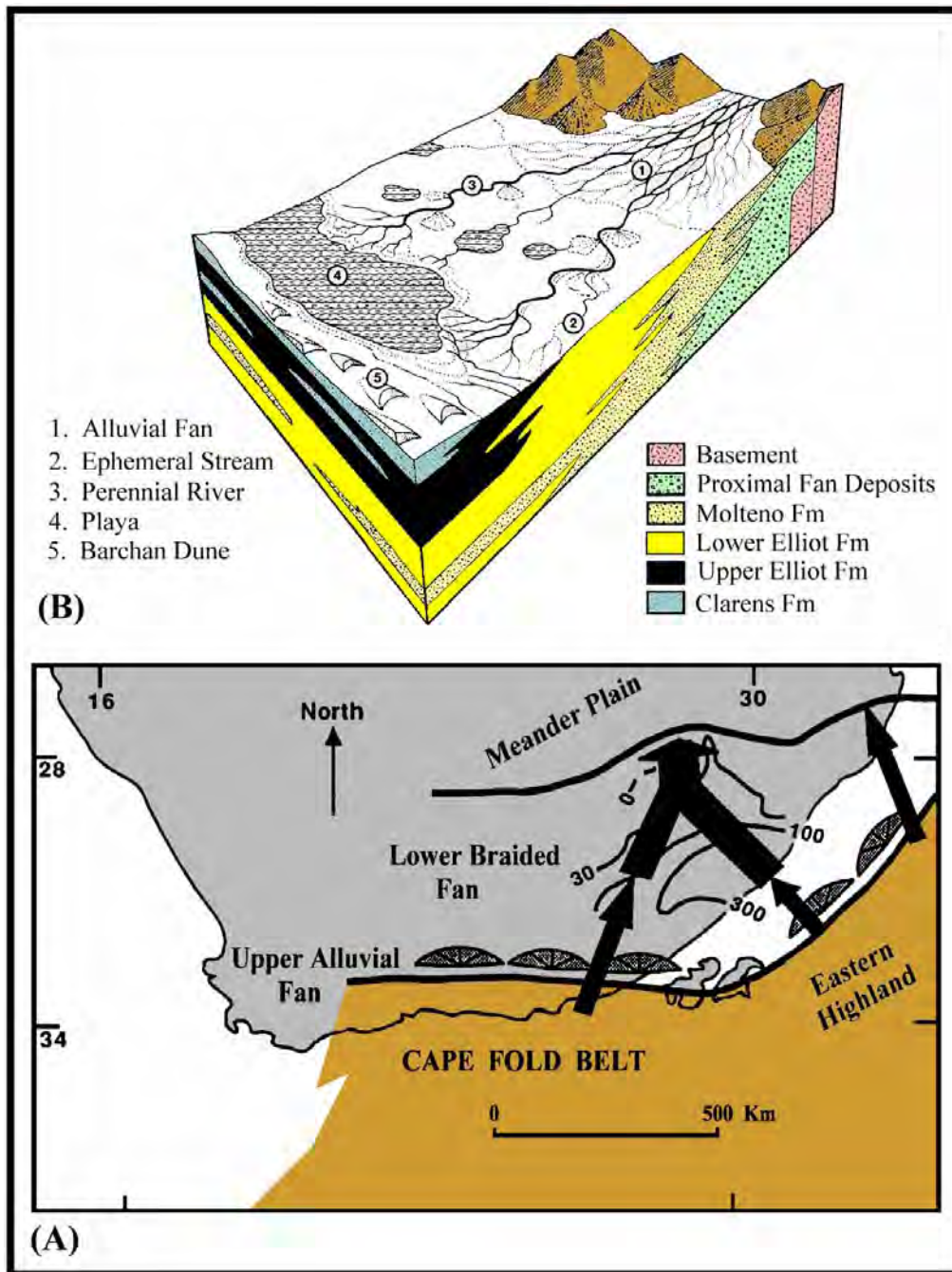


Figure 2.6: (A) Sediment source areas of the Molteno and Elliot Formations (after Cole, 1992).
 (B) Depositional environment and lateral facies relationships of the Molteno and Elliot Formations in the Main Karoo Basin (after Smith et al., 1993).

2.1.4.3 Clarens Formation

The early to middle Jurassic Clarens Formation (Catuneanu et al., 1998) represents the final phase of the Karoo sedimentation and consists mainly of wind-blown, fine-grained sandstone and siltstone (**Figure 2.7**). Channel-filled wadi sandstones and horizontally-laminated sheet-flood sandstone are also present. Minor interbedded sandstone, siltstone and mudstone represent localised playa lake deposits. The northern Clarens Formation is usually in the order of 100m thick, but it is up to 300m thick in the south.

Palaeo-winds were from the west (Beukes, 1970), which are thought to have transported silty and fine-grained sandy material from exposed Carboniferous glacial deposits in Brazil (Eriksson, 1981). Material was also reworked from the wadi, sheet-flood and playa lake deposits (Smith et al., 1993). The former two deposits were derived from the same south-eastern source area as that which supplied the Molteno and Elliot Formations, indicating that the Cape Fold Belt was still an important provenance.

Minor basaltic lava flows interlayered with sandstone occur in the uppermost part of the Clarens, which signals the commencement of magmatic activity that led to the termination of sedimentation in the Main Karoo Basin.

2.2 HYDROSTRATIGRAPHY

This section outlines the general hydrological characteristics of the various litho-stratigraphic units, related more to the processes of sedimentation and diagenesis (i.e. the *primary hydraulic properties*). These properties are more important when considering the longer-term sustainable utilisation of the Karoo aquifers (storativity), rather than individual borehole yields.

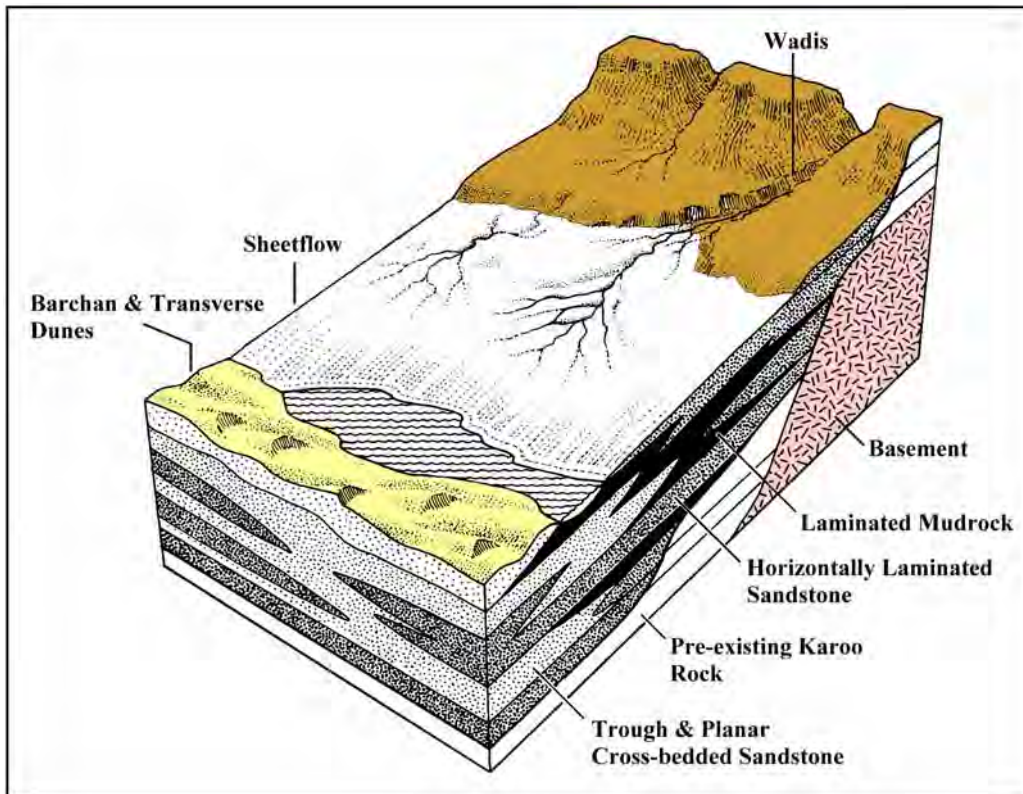


Figure 2.7: *Depositional environment of the Clarens Formation in the Main Karoo Basin (after Smith et al., 1993)*

2.2.1 DWYKA GROUP

The Dwyka diamictite and shale have very low hydraulic conductivities [$\sim 10^{-11}$ to 10^{-12} m.s⁻¹ (Driscoll, 1986)], and virtually no primary voids. The Dwyka Group constitutes a very low-yielding fractured aquifer and water is confined within narrow discontinuities like jointing and fracturing. They therefore tend to form aquitards rather than aquifers. The few sandstone bodies deposited in the glacial valleys of the northern facies are very limited in extent, and sealed off by the diamictite or mudrock. Since the Dwyka sediments were deposited mainly under marine conditions, the water in these aquifers tends to be saline. Exploitable aquifers

thus only exist at few localities in the Basin, where sand and gravel were deposited on beaches or where the Dwyka Group was fractured significantly. In general, the Dwyka Group is thus not an ideal unit for the large-scale development of groundwater.

The folded Dwyka rocks in the southern Karoo Basin are well fractured to great depths, as evidenced by the SOEKOR deep core-boreholes (**Chapter 2.4.5**). Deep core-drilling by DWAF in the Calvinia district of the Western Karoo indicated that the Dwyka diamictite is massive at depth, i.e. below 150 m.bgl.

2.2.2 ECCA GROUP

The Eccla Group consists mainly of shales, with thicknesses varying from 1 500 m in the south, to 600 m in the north. Since the shales are very dense, they are often overlooked as significant sources of groundwater. However, as illustrated in **Figure 2.10**, their porosities tend to decrease from ~0.10% north of latitude 28°S, to < 0.02% in the southern and southeastern parts of the Basin, while their bulk densities increase from ~2 000 to > 2 650 kg.m⁻³. The possibility thus exists that economically viable aquifers may exist in the northern parts of the Basin underlain by the Eccla shale. It is therefore rather surprising to find that there are areas, even in the central parts, where large quantities of water are pumped daily from the Eccla formations. For example, some 4 500 ha are irrigated from boreholes drilled into the Eccla shales in the Petrusburg district (central Free State), compared to the 2 000 ha from the Modder River. One should thus not neglect the Eccla rocks as possible sources for groundwater, especially the deltaic sandstone facies. Rowsell and De Swardt (1976) report that the permeabilities of these sandstones are usually very low. The main reason for this is that the sandstones are usually poorly sorted, and that their primary porosities have been lowered considerably by diagenesis.

The deltaic sandstones represent a facies of the Eccla sediments in which one would expect to find high-yielding boreholes. Unfortunately, Rowsell and De Swardt (1976) have found that the permeabilities of these sandstones are also usually very low. The main reason for this is that the sandstones are usually poorly sorted, and that their primary porosities have been lowered considerably by diagenesis. However, the Vryheid Formation sandstones in KwaZulu-Natal (west of Pietermaritzburg) appear to be more permeable, with a median borehole yield of 0.33 ℓ/s and 62% yielding greater than 1 ℓ/s (KwaZulu-Natal project, 1995, unit 8).

2.2.3 BEAUFORT GROUP

The main sediment source area for the Beaufort rocks lay along the high-lying, southern margin of the Basin. The coarser grained rocks are, therefore, found near the Cape Fold Belt (alluvial fan and braided stream environments), while mudstone, shale

and fine-grained sandstones dominate the more distal central and northern portion (meandering river and floodplain environment) of the Basin. The sedimentary units in the Group therefore usually have very low primary permeabilities. The geometry of these aquifers is complicated by the lateral migration of meandering streams over a floodplain. Aquifers in the Beaufort Group will thus not only be multi-layered, but also multi-porous with variable thicknesses.

The contact plane between two different sedimentary layers will cause a discontinuity in the hydraulic properties of the composite aquifer. The pumping of a multi-layered aquifer will thus cause the piezometric pressure in the more permeable layers to drop faster than in the less permeable layers. It is therefore possible to completely extract the more permeable layers of the multi-layered Beaufort aquifers, without materially affecting the piezometric pressure in the less permeable layers. This complex behaviour of aquifers in the Beaufort Group is further complicated by the fact that many of the coarser, and thus more permeable, sedimentary bodies are lens-shaped. The life-span of a high-yielding borehole in the Beaufort Group may therefore be limited, if the aquifer is not recharged frequently.

2.2.4 MOLTENO, ELLIOT AND CLARENS FORMATIONS

The characteristics and depositional history of the *Molteno Formation* indicate that the Formation should form an “ideal” aquifer. This applies not only to the pebble conglomerates and coarse-grained sandstones at the base of the Formation, but also to the other sedimentary bodies. These sedimentary bodies are more persistent than those of the Beaufort Group and are sheet-like (Theron, 1970), which represents a more favourable aquifer geometry in terms of groundwater storativity. It may therefore be worthwhile to study the groundwater potential of this Formation in more detail.

The largest part of the *Elliot Formation* consists of red mudstone. The Formation thus represents more of an aquitard than an aquifer. One approach to exploiting the groundwater potential of these relatively impermeable but highly porous rocks is to drill boreholes through the Elliot Formation into the Molteno Formation and restrict the pumping of water to the latter, more permeable Formation. This will allow water from the Elliot Formation to ‘leak’ downwards into the Molteno Formation.

The *Clarens Formation* consists almost entirely of well-sorted, medium- to fine-grained sandstones, deposited as thick consistent layers (Visser, 1984). It is thus the most homogeneous Formation in the Karoo Supergroup. With this type of geometry, the Formation should be an ideal aquifer. Although the Formation has a relatively high and uniform porosity (average 8.5%), as shown in **Table 2.3**, it is poorly fractured and has a very low permeability. The Formation may therefore be able to store large volumes of water, but is unable to release it quickly.

The previous conjecture is supported by the large number of springs that constantly flow from the base of Clarens Formation. The optimal method for utilising such low-permeability aquifers is to abstract smaller volumes over larger areas, which would not be economically feasible using standard borehole techniques. The use of ancient Persian qanats (Issar, 1985) is one approach that would satisfy small-scale water supply schemes.

2.2.5 PRIMARY HYDRAULIC PROPERTIES OF KAROO ROCKS

The Southern Oil Exploration Corporation (SOEKOR) was established in 1965 to investigate whether or not any economic accumulations of oil or gas existed in South Africa. This program involved the drilling of a number of deep core-borehole into the Karoo Basin by SOEKOR, the Geological Survey and a number of Mining Houses. The borehole locations are indicated in **Figure 2.8**, while **Table 2.1** summarizes the relevant borehole and geological information. The drill-core was subjected to a number of tests in order to assess the host-rocks potential as an oil reservoir, some of which are of importance to the geohydrologist – permeability and porosity.

The sandstones in the southern Karoo Basin, south of latitude 29°S, have extremely low *primary* porosity and permeability (**Figure 2.8**). The porosity and permeability of middle Ecca sandstones to the north of latitude 29°S tend to improve from south to north. This trend is in agreement with a general decrease in diagenesis from south to north over the Main Karoo Basin.

Van Wyk (1963) and Vegter (1992) state that the porosity of Karoo sediments appears to be higher nearer the earth's surface (**Table 2.5**), probably due to weathering and leaching of the rocks within the upper 30 m. Similarly, the primary porosity of the sediments is expected to decrease with depth due to increasing lithostatic pressures and temperatures.

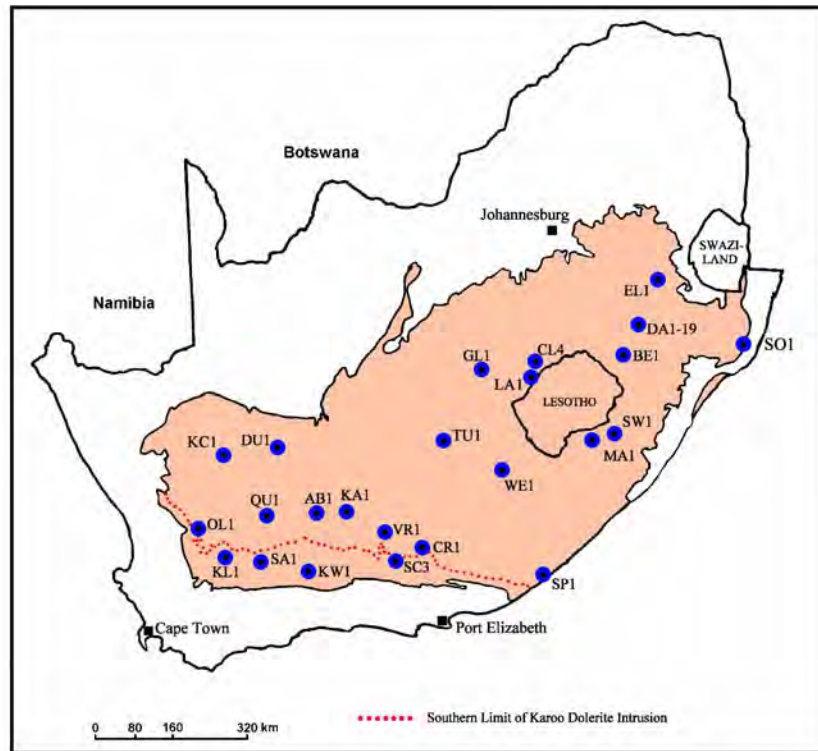


Figure 2.8: Location of SOEKOR and other relevant deep core-boreholes in the Main Karoo Basin (after Roswell and De Swardt, 1976)

Table 2.1: Borehole and geological information from deep core-boreholes located in the Main Karoo Basin (after Roswell and De Swardt, 1976)

Bore No.	Total depth (m)	Total thickness of dolerite (m)	Depth to base of Karoo (m)	Rock type at total depth	Borehole number in Figure 2.8
KL 1/65	3 460	170	2 035	TMS	KL1
QU 1/65	2 531	434	2 411	Granite	QU1
AB 1/65	-	622	-	-	AB1
KA 1/66	2 600	121	2 531	Gneiss, Granulite	KA1
SA 1/66	4 169	15	3 572	TMS	SA1
WE 1/66	3 746	956	3 732	Gneiss	WE1
SC 3/67	5 560	0	5 288	Bokkeveld	SC3
KW 1/67	5 555	0	-	Dwyka	KW1
VR 1/66	3 948	55	3 307	Gneiss, Granite	VR1
CR 1/68	4 658	27	4 290	TMS	CR1
SW 1/67	1 420	172	-	Ecca	SW1
GN 1/67	2 947	278	773	Granite	GL1
SP 1/69	4 557	198	4 282	TMS	SP1
MA 1/69	1 892	385	-	Ecca	MA1
TU 1/50	1 344	586	1 344	Ventersdorp Lava	TU1

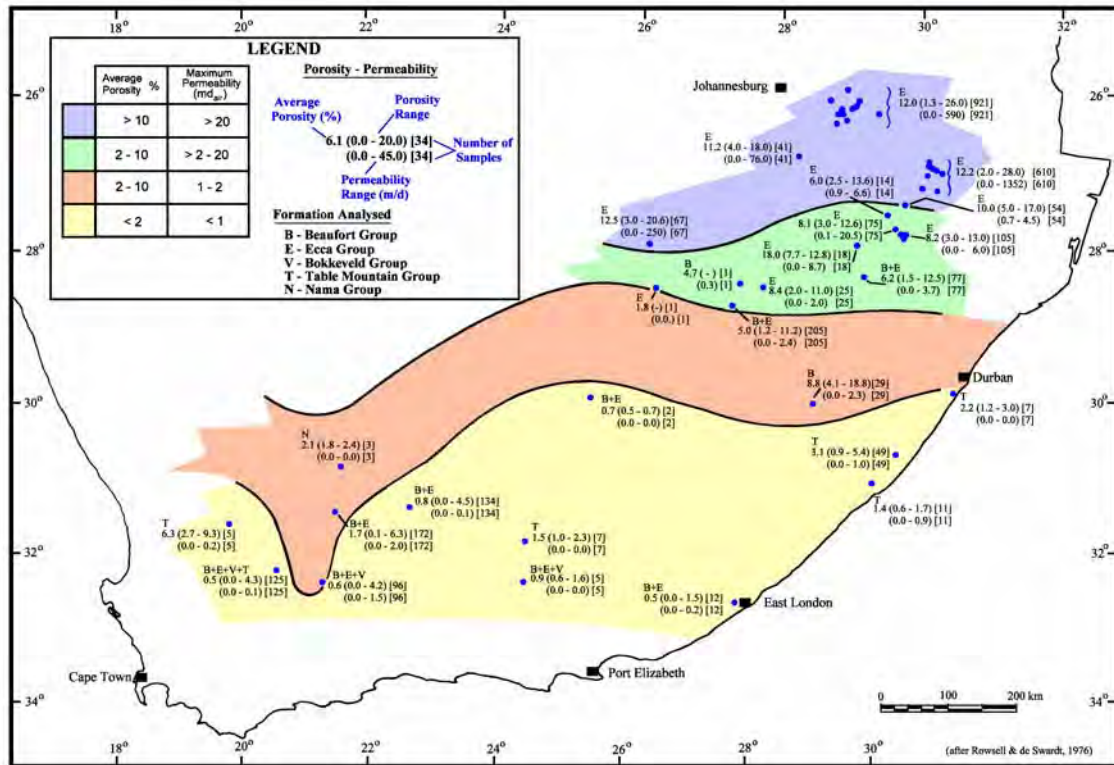


Figure 2.9: Porosity and permeability variations in the Sandstone/Siltstones of the Karoo Basin (after Roswell and De Swardt, 1976)

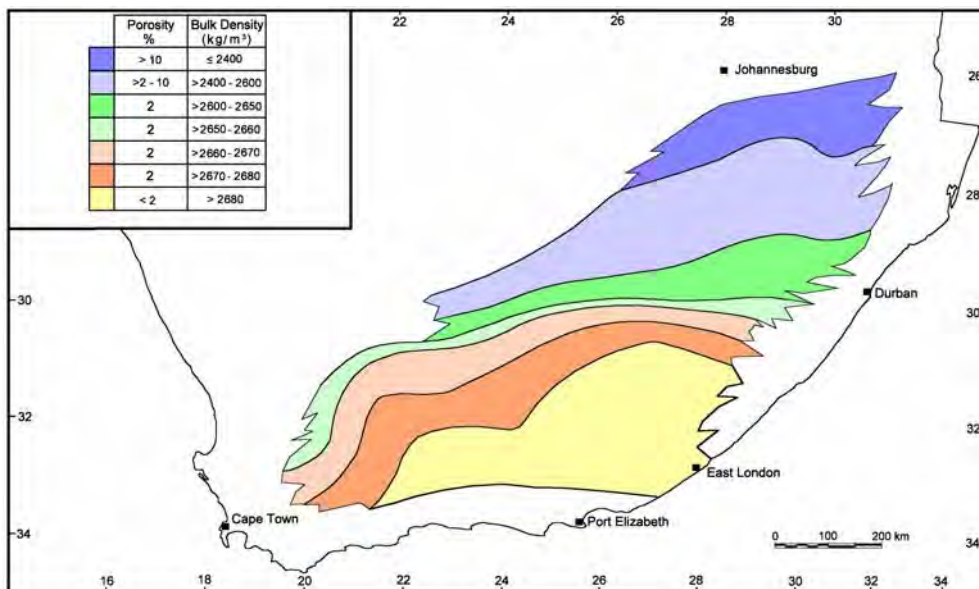


Figure 2.10: Porosity and bulk density variations in shales of the Karoo Basin (after Roswell and De Swardt, 1976)

Table 2.2: Porosity and permeability values of sandstone/siltstone obtained from deep core-boreholes located in the Main Karoo Basin (after Roswell and De Swardt, 1976)

Bore No.	Formation analyzed	Depth interval (m)	No. of samples	Percentage porosity		Permeability range (md)
				Average	Range	
KL1	Beaufort	7	1	1.9	1.9	-
	Ecca	14 - 1341	41	0.6	0.1 - 1.9	0.0 - 0.1
SA1	Beaufort	34 - 1215	84	0.5	0.2 - 2.9	0.0 - 1.5
	Ecca	520	1	13.6	13.6	-
		1296 - 1429	3	0.5	0.4 - 0.5	0.0
QU1	Beaufort	7 - 778	132	1.8	0.1 - 6.3	0.0 - 0.9
AB1	Beaufort	283 - 746	134	1.3	0.3 - 3.7	0.0 - 2.0
	Ecca	761 - 1563	?	0.8	0.0 - 4.5	0.0 - 0.1
SC3	Ecca	?	4	0.9	0.4 - 1.3	0.0
SP1	Beaufort	601 - 1938	12	0.5	0.0 - 1.5	0.0 - 0.2
TU1	Beaufort + Ecca	78 - 1311	2	0.7	0.5 - 0.9	0.0
MA1	Beaufort	427 - 1390	29	8.8	3.1 - 18.1	0.0 - 2.3
LA1	Beaufort	210 - 1240	138	4.7	1.2 - 10.7	0.0 - 2.4
	Ecca	1540 - 1600	67	5.6	1.2 - 11.2	0.0 - 1.5
F1 + W1	Ecca	450 - 1500	25	8.4	2.0 - 11.0	0.0 - 2.0
GL1	Ecca	635	1	1.8	1.8	0.0
CL4	Beaufort	700	1	4.7	4.7	0.3
BE1	Beaufort + Ecca	80 - 850	77	6.2	1.5 - 12.5	0.0 - 3.7
ME1	Middle Ecca	780 - 900	18	11.0	7.7 - 12.8	0.0 - 8.7
OM1	Middle Ecca	640 - 670	14	6.0	2.5 - 13.6	0.9 - 6.6

Note: Permeability (milli-darcy to air)

Table 2.3: Drill information from shallow core-boreholes located in the Main Karoo Basin

Rock type	Geological formation / group	Number of samples	Depth interval (m) [Bore No.]	Permeability range (md _{air})	Porosity (%)	
					Average	Range
Very fine Sandstone ¹	Clarens	-	-	-	-	6.2 - 9.8
Cross-bedded Sandstone ¹	Clarens	-	-	-	-	8.9 - 10.8
Sandstone ^{3**}	Clarens	43	26 - 130	1.0 - 73.0 (27 samples >1)	15.1	4.7 - 21.0
Sandstone ⁴	Clarens	-	-	-	8.46	6.19 - 10.75
Mudstone ²	Beaufort	33	-	-	-	25.4 - 26.9
Sandstone ²	Beaufort	23	-	-	-	5.4 - 6.8
Sandstone ³	Beaufort	1	7 [KL1]	0.0 - 0.1	1.9	1.9
Shale ²	Upper Ecca	5	-	-	-	2.5 - 2.7
Shale ²	Middle Ecca	17	-	-	-	1.8 - 2.5
Sandstone ²	Middle Ecca	11	-	-	-	4.0 - 12.9
Shale ²	Lower Ecca	19	-	-	-	1.5 - 3.1
Shale ^{3*}	Ecca	67	10 - 40	0.0 - 250	12.5	1.5 - 12.5
Diamictite ²	Dwyka	7	-	-	-	0.5 - 1.3

Notes: 1 - after Beukes (1969). 2 - samples from Natal, after Van Wyk (1963).
 3 - after Rowsell & De Swardt (1976). 4 - after Beukes (1969)
 * - boreholes in the Welkom-Virginia area
 ** - SOEKOR borehole at Barkly East.

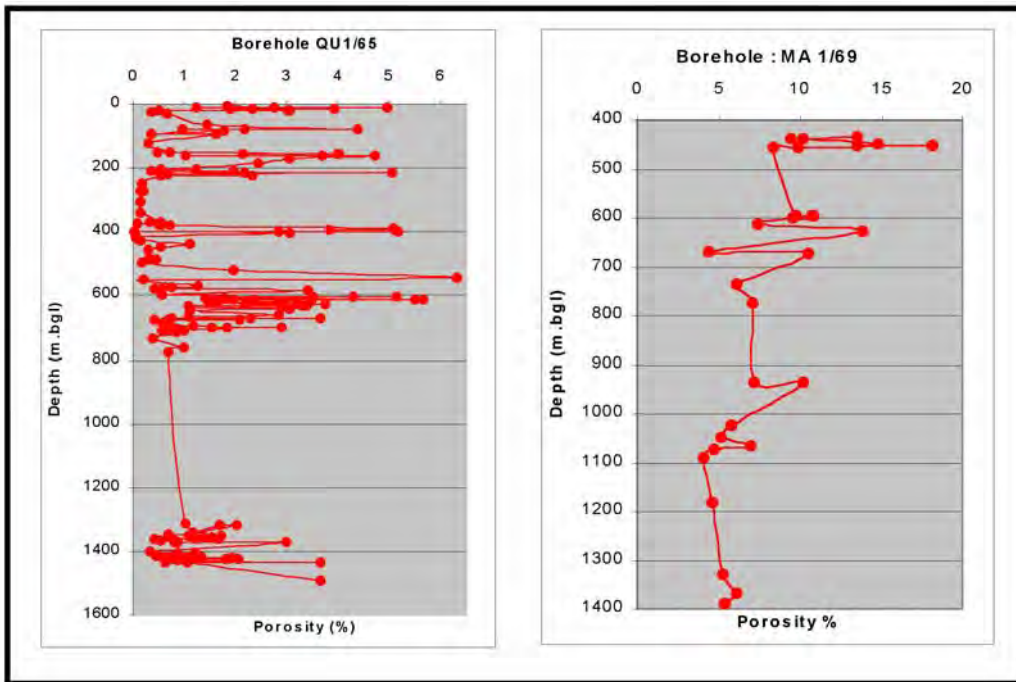


Figure 2.11: *Beaufort Sandstone - primary porosity variation with depth*

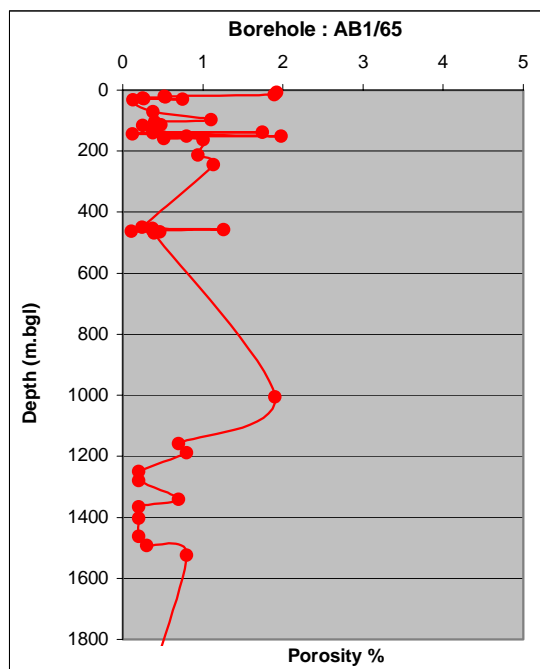


Figure 2.12: *Eccca Sandstone - primary porosity variation with depth*

The SOEKOR field porosity determinations on sandstones of the Beaufort and Ecca Groups do in general corroborate this point of view (**Figures 2.11** and **2.12**; **Tables 2.2** and **2.3**), although highly variable with depth. This trend is clearly not evident in the Beaufort sandstone in borehole QU1/65 (**Figure 2.11**). Note that the porosity of Beaufort sandstones in borehole MA 1/69 (**Figure 2.11**), are anomalously high (**Table 2.2**).

The broad geographical variations in *shale porosity* and *bulk density* in the Karoo Basin are indicated in **Figure 2.10**, based upon the analysis of SOEKOR drill-cores. In the northern Karoo, the porosity and density of shales varies between 2-10% and 2 400-2 600 kg/m³, respectively. The shale porosity is generally less than 2% to the south of latitude 31°S. There is very little, if any, increase in shale porosity or density with depth in most of the boreholes. In the deeper northern Karoo boreholes there is a more definite tendency for the density to increase with depth (Rowsell and De Swardt, 1976).

Significant secondary fracture porosity is known to be present at depth. Rowsell and de Swardt (1976) reported that water was struck at 3 700 m in the Dwyka diamictite in borehole SP1/69, near East London.

2.3 KAROO MAGMATISM

2.3.1 EXTRUSIVES

2.3.1.1 Drakensberg Lavas

Lithostratigraphy

The tholeiitic basalts cover 80 % of Lesotho and represent the remnants of a larger lava flood, the palaeo-extent of which is unknown (**Figure 2.1**). The idea that the basalts covered an area similar to the one occupied by the outcropping dolerite dykes and sills of the Main Karoo Basin (compare **Figures 2.1** and **2.14**) remains speculative. In fact, geochemical (mantle plume), structural (the proximity of an inferred triple-junction), stratigraphic (thicker sills beneath Lesotho) and eruptive dynamic factors (the presence of many vents around Lesotho) would argue towards a restricted extension of the basalt surface and eruptive activity. However, the presence of basalt blocks within the kimberlite breccias pipe at Finch (Northern Cape) would indicate that lava was extruded some distance away from the main Drakensberg flood (Field, pers. comm.)

The lava pile in Lesotho has an average thickness of 1000 m and attains a maximum thickness of 1400 m in the northwest. It consists mainly of a monotonous succession of individual lava flows varying from 1 to 50 m in thickness, accompanied by local pyroclastites at the base of the series and volcanic vents. Despite the presence of palaeo-valleys filled with lava material, no significant palaeosol or sedimentary deposits are found within the sequence. Recent dating shows that the Drakensberg lavas were extruded in a very short period of time around 180 Ma (Duncan, 1997). Recent work on lava floods in other part of the world suggest that only eruptions exceeding 10 years along fissures several kilometres long and producing lava fountains up to 1500 m high, would be able to generate these amounts of basalt in such a short time (Self and Thordarson, 1998). The basalt pile has been subdivided into two Formations and 11 stratigraphic units, based upon geochemical criteria (Marsh et al., 1997). The lower Barkley East Formation is 200 m thick and consists of thin flows, is of restricted geographical distribution and diverse geochemical character. The upper Lesotho Formation represents the bulk of the sequence with thick flows of more uniform composition.

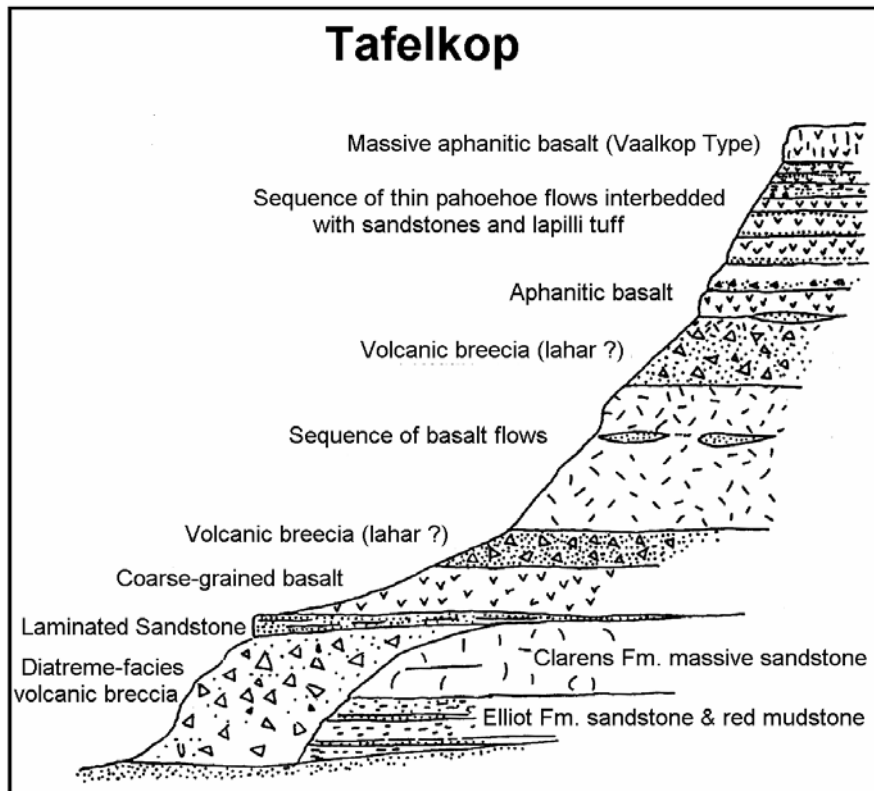


Figure 2.13: *Stratigraphy of the Barkley East Formation and its relation with the Clarens Sandstone at Tafelkop (Marsh, 1991)*

The relationship between the lower Barkley East Formation and the underlying Karoo sediments is complex and interesting from a geohydrological point of view. The early phases of the volcanic activity occurred intermittently during the deposition of the upper Clarens sandstone units and intercalation of basalt and sandstone beds (Figure 2.13 - see Figure 2.57 for location) can be seen at many localities (i.e. Barkley East, Maclear, Tafelkop). Explosive activity seems to have occurred during the early stages of the development of many of the volcanic vents (pyroclastites maar, hydrothermal breccia pipes). Prior to the deposition of the main lava sequence the volcano- sedimentary pile was eroded leaving topographic relief of up to 100m in height and many basaltic units can be seen locally wedging against the Clarens Formation sandstone. (Lock et al., 1974).

Hydrological Properties

Lava flows, especially basalts are heterogeneous rocks showing a wide range of facies: massive flows, scoria, lava tubes etc. Massive lava flows always exhibit open thermal joints with good interconnectivity and thus basaltic sequences often are highly permeable. Groundwater commonly percolates downwards within the lava succession, until an impermeable horizon/contact is reached (i.e. palaeosols or palaeo-valleys), where after it flows laterally along this discontinuity. This often results in an alignment of springs along a major stratigraphic contact within the volcanic pile.

Aquifers are expected to be poorly developed in the massive, 1200 m thick, upper Lesotho lava sequences, although the rocks are characterised by a high permeability. The contact between the lower Barkley East and upper Lesotho sequences could represent a suitable discontinuity along which groundwater could circulate. This contact has thus far not been mapped. The base of the Drakensberg lavas, with interbedded sediment and paleo-reliefs, constitutes favourable zones for groundwater movement and storage. Numerous springs located along the Drakensberg / Clarens Formations contact point to the geohydrological significance of this discontinuity. Boreholes drilled within the Drakensberg basalt in KwaZulu-Natal often intersect water at the fractured and weathered zone contact with the sediment (KwaZulu-Natal Project, 1995).

2.3.2 INTRUSIVES

2.3.2.1 Karoo Dolerite

Dolerite intrusions represent the roots of the volcanic system and are presumed to be of the same age as the extrusive lavas (Fitch and Miller, 1984). The level of erosion that affected the Main Karoo basin has revealed the deep portions of the intrusive system, which displays a high degree of tectonic complexity.

Early mapping of the dolerite intrusives was carried out by Rogers and Du Toit (1903) in the Western Cape and Du Toit (1905) in the Eastern Cape. Further contributions on their tectonic and structural aspects include Du Toit (1920), Mask (1966) and Walker and Poldervaart (1949). More recently the Geological Survey have published most of the 1/ 250 000 maps of the entire Karoo Basin. Detailed mapping of dolerite occurrences at specific localities in the southern Orange Free State were conducted by Burger et al. (1981) and in the Western Karoo by Chevallier and Woodford (1999).

The Karoo dolerite, which includes a wide range of petrological facies, consists of an interconnected network of dykes and sills and it is nearly impossible to single out any particular intrusive or tectonic event. It would, however, appear that a very large number of fractures were intruded simultaneously by magma and that the dolerite intrusive network acted as a shallow stockwork-like reservoir.

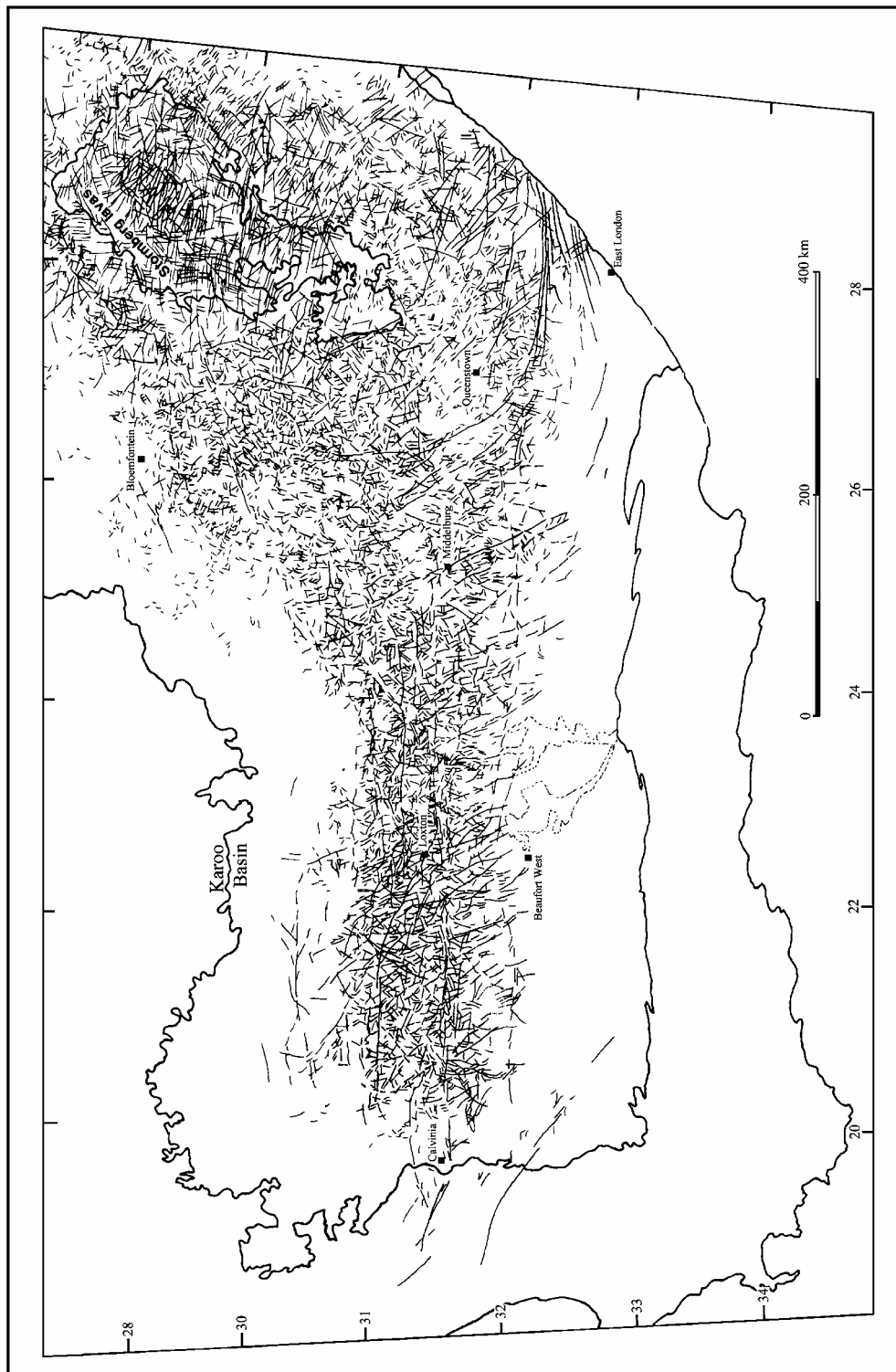


Figure 2.14: Dolerite Dykes of the Karoo Basin (from Woodford and Chevallier, 2001)

Dykes

Distribution

A map of the Karoo dolerite dykes has been compiled from existing 1/250 000 scale geological maps (Chevallier and Woodford, 1999) and completed by aerial photograph and satellite lineament interpretation over Lesotho (Chevallier, 1998, Norman et al., 1977, Binnie and Partners, 1971) (**Figure 2.14**). It would appear that there is a lithological control on the emplacement of dykes within the Western Karoo Basin: a sharp decrease in intrusion density is noted at the boundary between the lower Ecca and the upper Ecca. This boundary corresponds to the appearance of the first sandstone units in the Karoo Basin. Even if many dykes can still be seen within the lower Ecca and Dwyka Formations, as well as the Nama basement, the bulk of the dykes are strata bound and concentrated in the Upper Ecca and Beaufort Group. This means that they propagate laterally along strike and not vertically and that their magmatic source was not everywhere under the Karoo Basin but concentrated at one spot (the East London triple junction).

The different dyke swarms form three major structural domains (**Figures 2.14 and 2.15**):

- (1) **Western Karoo Domain:** extending from Calvinia to Middelburg and is characterised by two distinctive structural features (Woodford and Chevallier, 2001):

- (i) *E-W Dyke Intrusion*

Some of these dykes are extensive and continuous and can be followed over 500 km. They were intruded along a major right lateral E-W dislocation/shear zone and are accompanied by NW Riedel shears and NE P-type fractures.

- (ii) *NNW Dyke Intrusion*

They are also extensive structures and are regularly spaced from east to west across the domain. The trend of these dykes varies along their trajectory, curving from WNW in the south to NS in the north. Two dyke systems are specifically well developed: the Middelburg Dyke delimiting the Western Karoo domain in the east and the Loxton Fracture Zone in the centre of the domain. A further major feature, the Hantam Escarpment near Calvinia, delimits the domain boundary to the west. It corresponds to a decrease in the density of dykes and the abrupt cessation of E-W magnetic anomalies (Thomas et al., 1992).

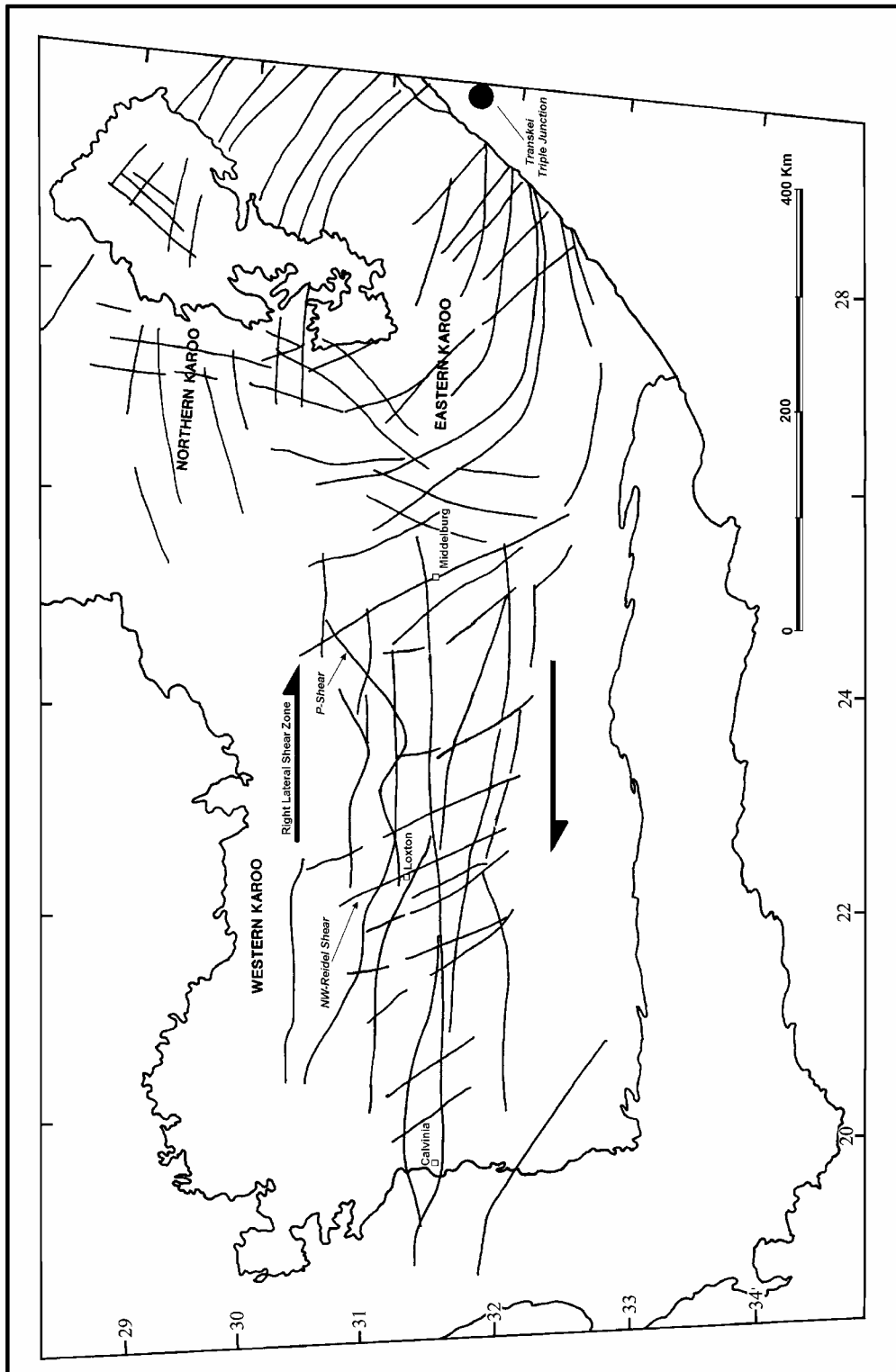


Figure 2.15: Structural Domains and mechanism of emplacement of Dolerite Dykes (Woodford and Chevallier, 2001).

- (2) **Eastern Karoo Domain** extending from East London to Middelburg and comprises two major dyke swarms, namely:
- (i) An arcuate swarm of extensive dykes diverging from a point offshore of East London. They display a strong curvi-linear pattern, trending approximately E-W along the coast and curving NNW to NS inland. It seems likely that the Middelburg dyke was fed from one of these diverging intrusive systems. The dykes are characteristically very thick - widths of up to 300 m are reported.
 - (ii) Minor NNE trending dykes represent the extension and probably the termination of the Lesotho NE trend described below.
- (3) **Transkei-Lesotho-Northern Karoo Domain** consists of major two swarms:
- (i) NW trending dykes in the Transkei region, curving to EW in the Free State. However, some of these NW intrusives do not curve and may form part of an extensive swarm (1 000 km long) called the *Transkei-Southern Namibian Dyke Swarm* by Hunter and Reid (1987).
 - (ii) NE trending dykes mainly occurring within and alongside the Lesotho basalts and that seem to converge towards the *the Limpopo - Lebombo Triple Junction* (Hunter and Reid, 1987).

Geometry, Structure and Mechanism of Emplacement

Emplacement Mode

Dolerite dykes, like many other magmatic intrusions, develop by rapid hydraulic fracturing via the propagation of a fluid-filled open fissure, resulting in a massive magmatic intrusion with a neat and transgressive contact with the country rock. This fracturing mechanism is in contrast to the slow mode of hydraulic fracturing responsible for breccia-intrusions (i.e. kimberlite). For the intrusion to develop the magma pressure at the tip of the fissure must overcome the tensile strength of the surrounding rock. Dykes can develop vertically upwards or laterally along-strike over very long distances, as long as the magma pressure at the tip of the fissure is maintained. The intrusion of dolerite and basaltic dykes are therefore never accompanied by brecciation, deformation or shearing of the host-rock, at least during their propagation.

Dyke Attitude

All the dykes are sub-vertical with a dip rarely below 70°. Kruger and Kok (1976) report dips of dykes in the northeastern Free State varying between 65° to 90°. The attitude of dykes often change with depth (i.e. are curved or dislocated), as observed from many detailed borehole logs (**Figure 2.16(a)**). This phenomenon can be attributed to vertical offsetting as a result of vertical *en-échélon* segmentation or due to interconnecting of dykes between sediment layers.

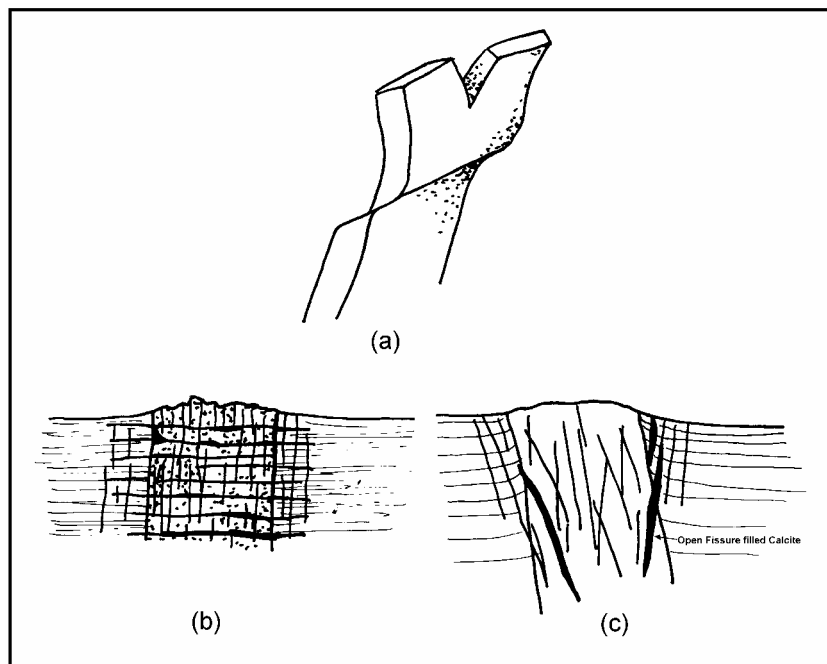


Figure 2.16: (a) *En-échélon Dolerite Dyke*
 (b) *Dyke showing Vertical Tectonic and Horizontal Thermal Jointing and*
 (c) *Fissures related to Tectonic Reactivation and Jointing related to weathering / erosional unloading.*

Dyke Width

The average thickness of Karoo dolerite dykes ranges between 2 and 10 m (Woodford and Chevallier, 2001). In general, the width of a dyke is a function of its length. In other words, the wider a dyke is, the longer it will be (this probably also applies to the vertical extension of the feature). For example, the major E-W dykes of Western Karoo Domain can attain widths of up to 70 m, while the Middelburg dyke is 80 m wide. The radiating E-W dykes of Eastern Karoo have widths of up to 300 m in places. No relationship has been found between trend and thickness (Woodford and Chevallier, 2001).

En-échelon Pattern

Dolerite dykes often exhibit an *en-échelon* pattern along strike, which are clearly detected by mapping. This is especially the case with the E-W shear dykes and their associated riedel-shears (**Figure 2.16(a)** and **2.30**). Displacements in the vertical section also occur, often associated with horizontal, transgressive fracturing (**Figure 2.25**). These offsets are not often observed, except through drilling.

Dyke Related Fracturing

The country rock is often fractured during and after dyke emplacement. These fractures form a set of master joints parallel to its strike over a distance that does not vary greatly with the thickness of the dyke (between 5 and 15 m). The dolerite dykes are also affected by thermal- or columnar- jointing perpendicular to their margins (**Figure 2.16(b)**). These thermal joints also extend into the host rock over a distance not exceeding 0.3 – 0.5 m from the contact. Van Wyk (1963) observed two types of jointing associated with dyke intrusions in a number of coalmines in the Vryheid-Dundee area, namely:

- (1) three sets of pervasive-thermal, columnar joints that are approximately 120° apart, and
- (2) joints parallel to the contact, confined mainly to the host rock alongside the dyke.

Many cases of tectonic reactivation of the dolerite dykes have been observed in the Loxton-Victoria West area (Woodford and Chevallier, 2001), especially on the N-S dykes that have been reactivated by Cretaceous kimberlite activity or by more recent master jointing (**Figure 2.16(c)**). Reactivation often results in sub-vertical fissures within the country rock and/or dyke itself, which are commonly highly weathered and filled with secondary calcite/calcrete (width of up to 150 mm – **Plate 2.1**), uplifting or brecciation of the sediment along the dyke contact (**Plate 2.2**).

Deformation and Contact Metamorphism of Host Rock

Localized upwarping of the country rock is often observed adjacent to dipping dykes (**Figure 2.16(c)**). Hydraulic fissure propagation, as mentioned above, cannot be responsible for this phenomena, as the magma would have to be cool and become viscous in order cause such deformation. This upwarping of the country rock is commonly a near-surface phenomenon related to supergene formation of clays with a high expansion coefficient resulting in the ‘swelling’ of the rockmass.

In nearly every case, the dolerite magma shows marked chilling against the sediments into which it has been injected. The chill zone generally exhibits the effects of contact metamorphism, where argillites are altered to hornfels or lydianite and arenaceous units are recrystallized to quartzite. Enslin (1951) and Van Wyk

(1963) state that the jointed contact zone is less than 30 cm wide, irrespective of dyke thickness.

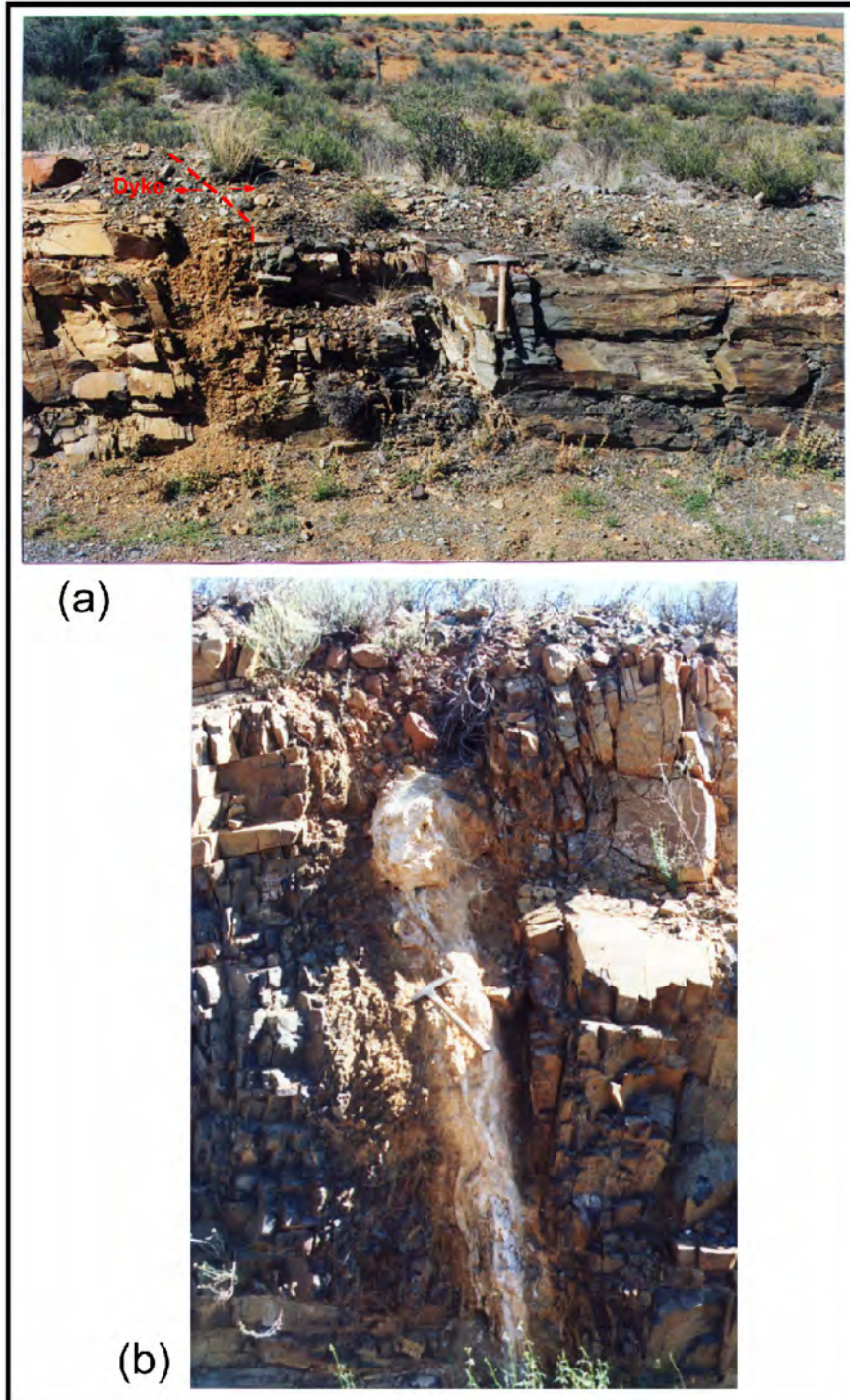


PLATE 2.1 *N-S Rooiaar dolerite dyke, near Loxton (a) reactivated contact between dyke (left) and host-rock (right). (b) Cretaceous aged calcite filled vertical shear and tension gashes related to Kimberlite activity (after Woodford and Chevallier, 2001)*

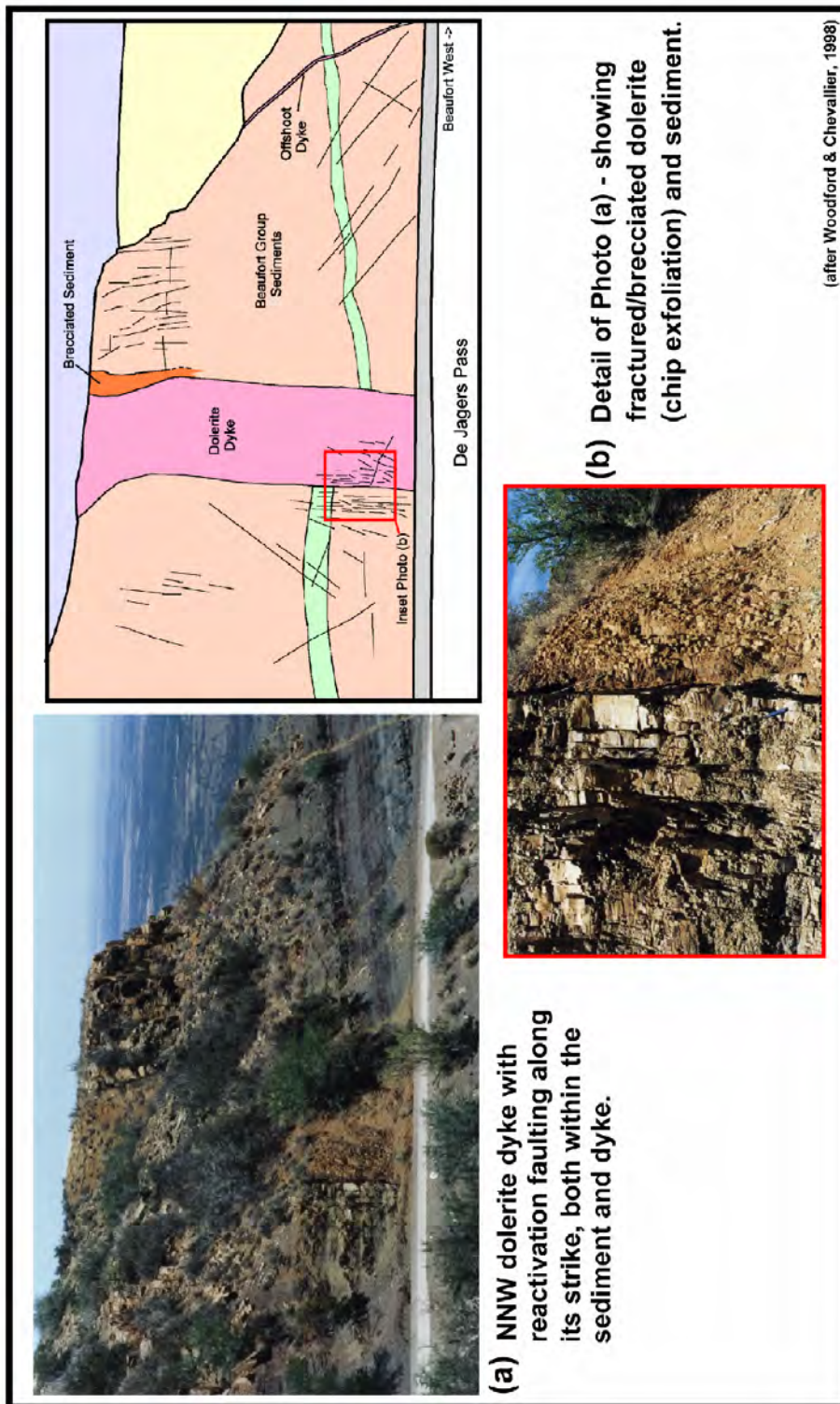


Plate 2.2 – *Tectonic Reactivation of a NNW dyke in the De Jagers Pass, Beaufort West*

Petrography and Dyke Weathering

The effect of variable cooling of dykes following intrusion is also apparent in the way in which dykes weather in the Western Karoo, namely:

1. Thick dykes (>8 m) generally exhibit a prominent chill-margin containing a fine grained, porphyritic, melanocratic dolerite that weathers to produced well-rounded, small, white-speckled boulders (i.e. spheriodal weathering). This zone is normally only 0.5 to 1.5 m wide and exhibits well-developed thermal-shrinkage joints. The central portion of such dykes consist of medium- to coarse-grained, mesocratic and occasionally leucocratic dolerite that decomposes to a uniform 'gravelly' material, which exhibits an exfoliation type of pattern. Sporadic fractures or meta-sedimentary veins are encountered in this zone and they often do not extend into the country rock. Magnetic traverses across these features normally produce two distinctive peaks.
2. Thin dykes (<3 m) commonly consist of fine-grained, porphyritic, melanocratic dolerite (Vandoolaeghe, 1979). These tend to be more resistant to weathering than the thicker dykes and in outcrop exhibit a uniform pattern of shrinkage-joints. The dyke weathers to produce small rounded, white-speckled boulders set in a finer angular groundmass.

Continental-scale Geodynamics of Dyke Emplacement

A debate is still ongoing among geologists as whether or not an extensive subcrustal magma chamber underlay the entire dolerite outcrop area or whether such a chamber was restricted in dimension to the Lesotho area.

A sub-crustal magma chamber the size of a diapir-shaped, mantle convective cell (or mantle plume) that generated the flood basalts is probable beneath the Main Karoo Basin. In contrast, however, the general distribution of dykes along the eastern coast would be in agreement with an extensive continental rifting event and a more localized magmatic source. Two curved dyke swarms diverge from a point off the East Coast (**Figure 2.15**). Their distribution and geometry is very typical of fan-shaped mega-swarms linked to crustal extension (Fahrig, 1987, Greenough and Hodych, 1990). These dykes probably represent the products of a failed triple-junction system located east of East London that may have been the magma source for most of the Karoo dolerite intrusions. This suggests that the dykes propagated laterally along strike from the triple junction and may explain why many of the dykes are confined to the same stratigraphic level (Chevallier et al., 2001).

The NE-trending swarm of dykes that extend across Lesotho may represent the southern extension of one of the arms of the Limpopo - Lebombo triple junction, situated further north.

The E-W dextral shear zone and NNW dominated pattern of dyke intrusion are typical features found in transform fault systems that developed between two rifts (Courtilot et al., 1974; Fox and Gallo, 1983). The Western Karoo dolerite shear zone might therefore represent a major offset (or step) between one of the arms of the Eastern Karoo triple-junction and another failed rift zone along the South African / Namibian West Coast (Chevallier et al., 2001) (**Figure 2.15**).

Groundwater Occurrence and Hydrological Properties

Dolerite dykes are vertical to sub-vertical discontinuities that, in general, represent thin, linear zones of relatively higher permeability which act as conduits for groundwater flow within the aquifer. They may also act as semi- to impermeable barriers to the movement of groundwater. The dykes are commonly expressed on the surface as a line of green bushes, which can be readily observed during the dry season (**Plate 2.3**).



Plate 2.3: *N-S dolerite dyke (red - foreground) delineated in the distance by a dense line of taller bushes (Farm: Meltonwold, Sheet 3122 DA)*

Dolerite dykes have always been and still are the preferred drilling target for groundwater in the Karoo. Both geohydrologists and groundwater-dowsers have sited many successful boreholes on these structures. There are a number of reasons why these features are preferred for groundwater exploration, namely:

- there exists an apparent higher probability of drilling a wet borehole in or next to a dyke than in the host rock away from the dyke,
- they are easily detected on remotely-sensed imagery, by relatively simple geophysical techniques (the magnetometer) and are clearly visible to both the skilled and unskilled eye in the field (i.e. if not outcropping, they are often conspicuous as lines of vegetation or animal-burrows).
- their relatively simple and regular 3D geometry makes it easy to conceptualize and site an exploration borehole in the field, and
- they are thus a very cost effective groundwater target.

Van Wyk (1963) states that more than 80% of the successful boreholes ($> 0.13 \ell/s$) drilled into Karoo sediments in Northern Kwazulu Natal are directly or indirectly related to dolerite intrusions.

A hydrocensus covering 11 600 km² of the Victoria West 1/250 000 mapsheet showed that more than 25% of the 3 194 boreholes surveyed were drilled into or alongside dolerite dykes (Woodford and Chevallier, 2001).

The Department of Water Affairs & Forestry, research institutions, groundwater consultants and private landowners have drilled many dolerite dykes throughout the Karoo Basin. There are a large number of reports documenting these results (Campbell, 1975; Vandoolaege, 1978, Vegter 1990), whilst others also provide guidelines to siting successful boreholes on dykes (Paver et al., 1943; Enslin, 1951; Kruger and Kok, 1976).

Enslin (1951, p195) expresses the classical hydrological conceptualization of Karoo dykes - *“the effect of induration and crushing of the sedimentary rock is that the permeability has been increased and the contact zone has been changed into an aquifer lying between the solid dyke and the saturated, low permeability country rock”*.

Van Wyk (1963) states that the high permeability of the dyke contact zones is a result of shrinkage joints developed during cooling of the intrusion. He based this finding on observations in 5 coalmines in the Vryheid and Dundee area, where groundwater issues from isolated joints in the dyke contact zone only. Van Wyk found that two types of jointing typically developed, namely:

- (1) three sets of columnar joints that are approximately 120° apart, and
- (2) joints parallel to the contact.

In the Vryburg – Dundee area the columnar joints are most prominently developed within the dolerite and parallel joint mainly confined to the sediments alongside the dyke.

Several aspects appear to affect occurrence of groundwater and the productivity of boreholes located in or near dolerite dykes:

- *Contact Metamorphism and Distance from Dyke Contact:*

There is considerable debate concerning to what distance away from a dyke the host rock is metamorphosed and jointed – thereby effecting the yield of a borehole drilled into this zone. Campbell (1975) refers to a “rule-of-thumb” width of <3 m, but states that the Tweeling-Brandwag dyke did not conform to the this rule. Enslin (1951) illustrates this relationship in **Figure 2.17**, where the highest borehole yields are obtained within 1m of the dyke contact. Note that because distances from the dyke edge are measured at the surface, the dip of the dyke must also be considered. Also of importance is whether the dyke itself is water-bearing or not. Many researchers have found that drilling into the middle of solid dolerite dykes is often unsuccessful (Enslin, 1951, Van Wyk, 1963), while others have found that the dykes themselves are fractured (Vegter, 1968; Woodford and Chevallier, 2001).

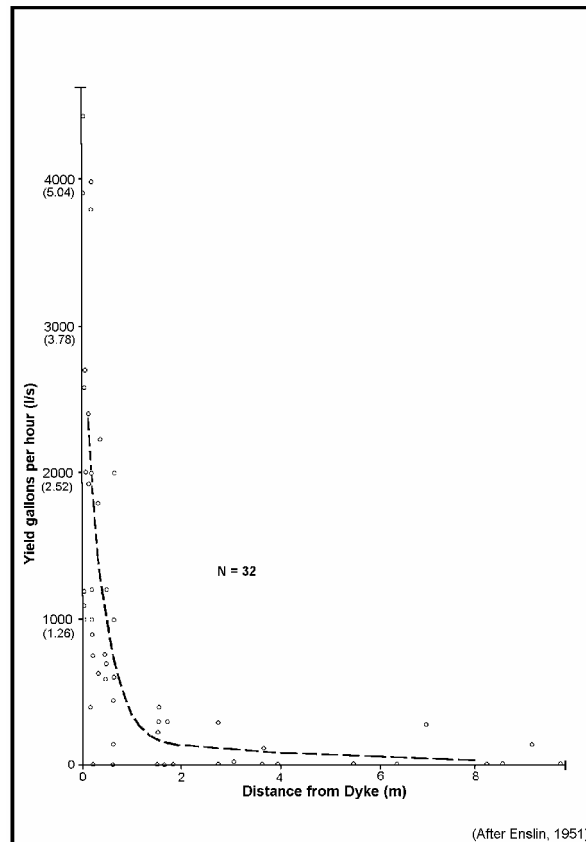


Figure 2.17: *Borehole yield versus distance from dyke contact*

Kruger and Kok (1976) analyzed hydrocensus information and drilling logs from 3 637 and 219 borehole, respectively, in the Bethlehem, Ficksburg, Fouriesburg and Senekal districts. The pertinent results of their work are presented in **Table 2.4**.

Their work illustrates a number of important points, namely:

1. that the probability of a borehole striking $> 0.14 \text{ l/s}$ in the Stormberg Group sediments is extremely low,
2. boreholes drilled alongside dykes, i.e. into the upper and lower contacts, are more likely to be successful than those sited away from the structure in the country rock.
3. the dykes themselves are almost always fractured and significantly higher yields can be obtained in these structures.

Table 2.4: Borehole Yield Data for the North-Eastern Free State

Borehole Position	Number of Boreholes	% Successful Boreholes (> 0.5 m ³ /hr)	Ave. Depth (m) of Successful Boreholes	Ave. Borehole Yield (m ³ /hr) [ℓ/s]
Dyke Contact (Upper)	417	19	28	1.80 [0.50]
Dyke Contact (Lower).	75	76	46	5.80 [1.61]
Dyke Only	144	99	54	15.00 [4.17]
Stormberg Sediments, away from dolerite.	3220	1	25	0.95 [0.26]
TOTAL	3856			

Woodford and Chevallier (2001) studied the relationship between yield data gathered from 594 privately drilled boreholes and their distance from a dyke contact, measured in the field (**Figure 2.18**).

Only a weak statistical correlation was found between borehole yield and distance drilled from the dyke contact. Line A (blue) represents the upper-boundary of a zone into which the bulk of the data plot – indicating that yields of up to 5-7 ℓ/s can occur within 20 m of a dyke, where after less than 5 ℓ/s is more common. A similar result was obtained for 169 boreholes drilled into and alongside the Tweeling-Brandwag (**Figure 2.19**) – which indicates that borehole yields of 6 – 18 ℓ/s occur within 5 m of the dyke, where after borehole yields of less than 6 ℓ/s are typically encountered.

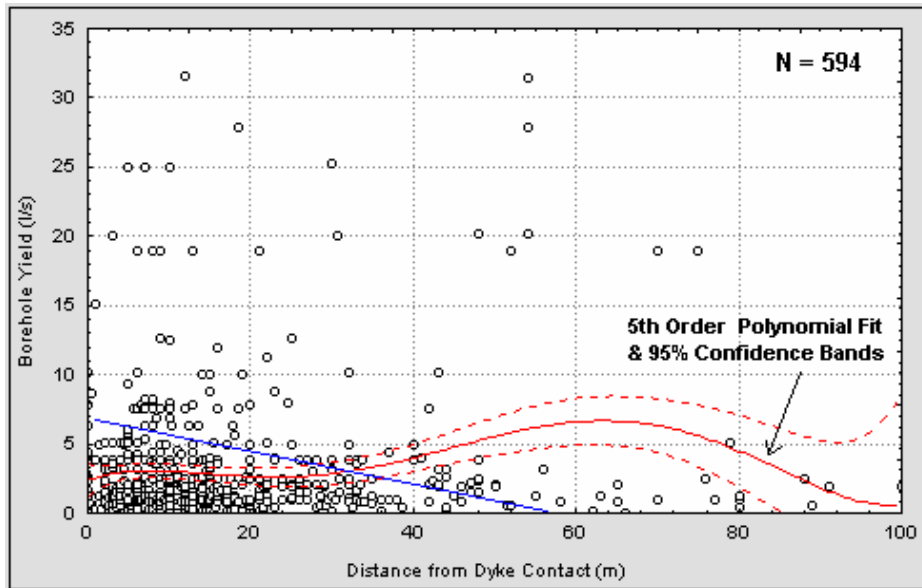


Figure 2.18: *Borehole yield versus distance from dolerite dyke contact in the Loxton – Victoria West area*

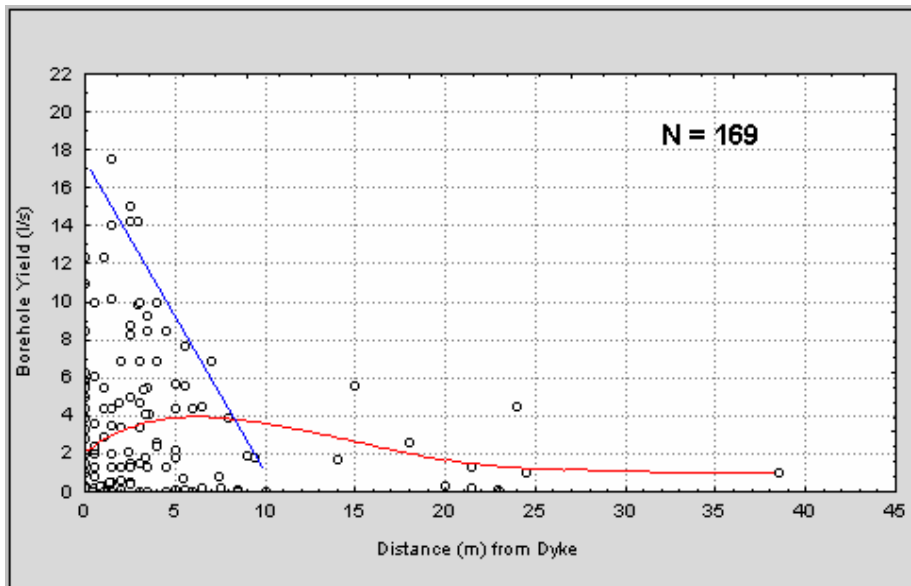


Figure 2.19: *Borehole Yield versus Distance from the Tweeling-Brandwag Dyke, Beaufort West*

Intrusion of dolerite results in localised metamorphism of the country rock. This zone of metamorphism is commonly less than or equal to the width/thickness of the intrusive body. Van Wyk (1963) conducted a number of porosity determinations on specimens of the same rock-type obtained at different distances from dolerite

intrusions (**Tables 2.5** and **2.6**). The results clearly indicate a marked decline in the porosity of the host-rock within the contact metamorphic aureole of the intrusive, mainly as a result of re-crystallisation of the host-rock silicates and infiltration/cementation by magmatic silica.

Table 2.5: *Host-rock porosity variations with distance from the contact of dolerite intrusions (after Van Wyk, 1963)*

Rock Type	Intrusion	Distance from Intrusion (m)	Porosity (%)
Middle Ecça Sandstone	Dyke (7.6m wide)	7.6*	8.65
		3.0	7.37
		0.9	1.16
		0.0	0.36
Lower Ecça Shale	Dyke (3.7m wide)	4.6*	2.51
		1.5	1.12
		0.3	0.47
Middle Ecça Sandstone	Sill (24-30m thick)	7.6	0.95
		1.8	0.39
		0.6	0.06

Note: * - unaffected host-rock.

Table 2.6: *Host-rock porosity variations with depth and distance from a dolerite dyke at Ntabamhlope in the Escourt District (after Van Wyk, 1963)*

Rock Type	Depth Sampled (m)	Distance from Dyke (m)		Porosity (%)	
		Bore N	Bore L	Bore N	Bore L
Mudstone	9.1	2.6	9.5	9.7	20.3
Sandstone	16.8	1.7	8.5	6.5	7.8
Sandstone	21.3	1.1	7.9	4.9	7.2
Sandstone	24.4	0.8	7.6	3.6	7.1
Sandstone	26.2	0.5	7.2	5.4	-
Sandstone	27.4	0.3	7.0	2.7	7.2
Sandstone	30.2	0.2	6.9	1.8	5.9

- *Width of Dyke*

Enslin (1951) states that Karoo dolerite dykes are seldom wider than 18.5 m and generally between 2 to 8 m in width. Many researchers have tried to relate the width of a dolerite dyke in the Karoo to the expected yield of a borehole sited on it. During 1964 to 1967, Kruger and Kok (1976) evaluated drilling results along dykes in the vicinity of Bethlehem, Ficksburg, Fouriesburg and Senekal, in the northeastern Free State. They found a relationship between the width of a dyke and borehole yield (**Figure 2.20**), after analysing the results 177 boreholes on drilled on dykes - where dykes of between 4.5 and 14 m produced yields of 2 to 5 ℓ/s. They concluded that the highest borehole yields could be obtained on dykes of 7 to 11 m wide. Vandoolaeghe (1980, p 39) found that higher borehole yields are obtained alongside dykes that are wider than 5 m in the Queenstown area.

Woodford and Chevallier (2001), however, could not find a significant correlation between dyke width and yield of 539 privately-drilled boreholes in the Western Karoo (**Figure 2.21**). It is, however, apparent that thin dykes (≤ 2 m) do not deliver more than 4 ℓ/s.

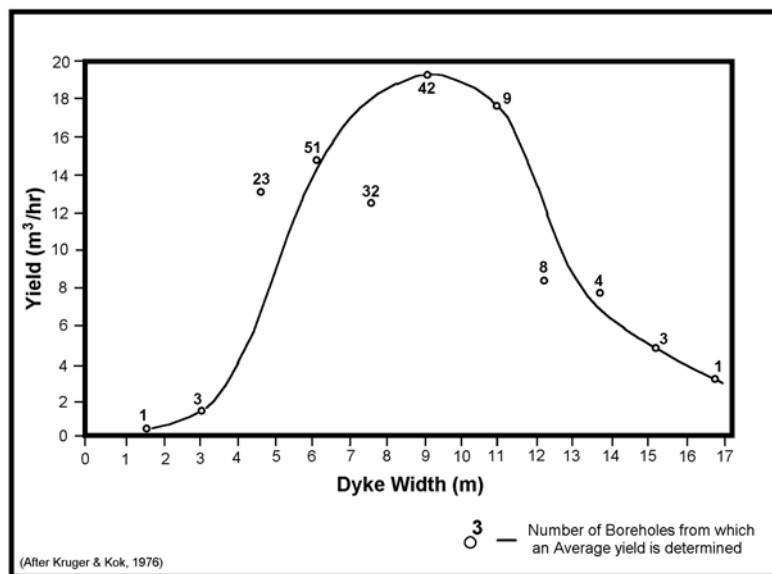


Figure 2.20: *Dyke width versus yield of boreholes drilled into Dykes in the North-East Free State (after Kruger & Kok, 1976)*

- *Dip of Dyke*

The dip of a dolerite dyke per se does not appear to have a major influence on the yield of boreholes drilled on it (Enslin, 1951; Vandoolaeghe, 1980), but it is important for siting of a successful borehole. Boreholes can be sited to intersect the “upper” or “lower” dyke contact depending on its attitude. Kruger and Kok (1976) produced a schematic diagram showing where boreholes should be sited in order to maximize groundwater yield (**Figure 2.22**), based on a detailed analysis of dyke drilling results in the northeastern Free State (**Table 2.6**). Various authors have also expressed the need to take into account the dyke attitude in relation to the direction of the local drainage (Paver et al., 1943).

Landowners have reported many successful boreholes drilled into the upper-contact of dipping dykes. The Zandwerf dyke east of Calvinia produced high yields in this contact zone (**Figure 2.23**). Note that the water-bearing fractures do not follow the contact of either the dyke or the sill and that they transgress both intrusions. Other examples are the Welgevonden and the Perries dyke north of Graaff-Reinet (**Figure 2.24(b)**).

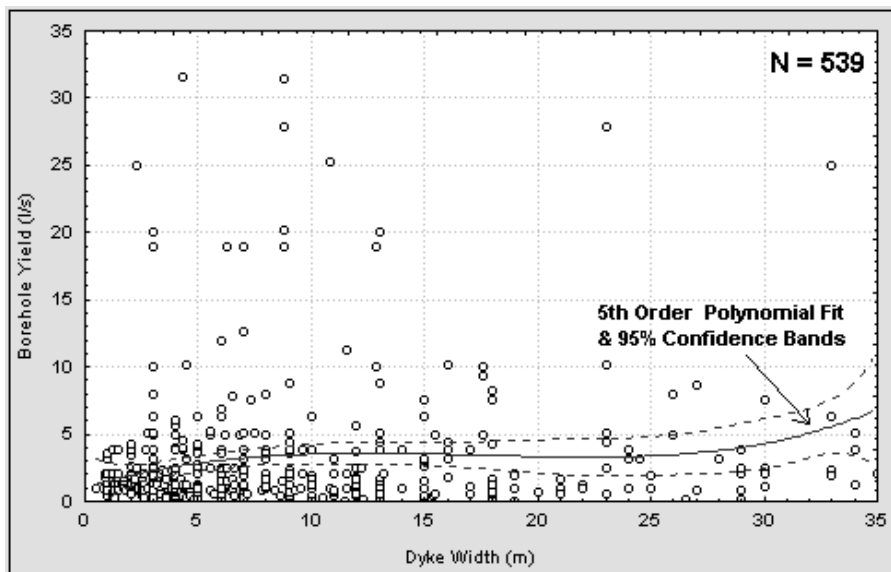


Figure 2.21: *Borehole yield versus dyke width in the Loxton-Victoria West Area, Western Karoo (after Woodford and Chevallier, 2001)*

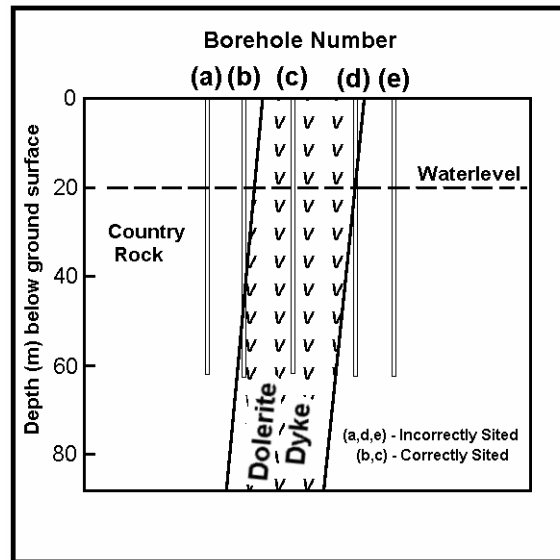


Figure 2.22: *Borehole Site Selection on Dolerite Dykes*

- *En-échelon Dyke Segmentation*

Lateral displacement or en-échelon segmentation often occurs along the major E-W dykes, such as the Tweeling-Brandwag dyke at Beaufort West. This dyke represents the southernmost extensive a major E-W dyke system within the Western Karoo and is approximately 11 m wide (**Figure 2.29**). Note that the point of dislocation marks a change in the attitude of the dyke.

Vertical offsets of the parent dyke are also observed in these structures, where intense fracturing and high groundwater yields are common. **Figure 2.25** is a typical example of a 20 m wide, E-W shear dyke on the farm De Wilg to the southwest of Loxton (Woodford and Chevallier, 2001).

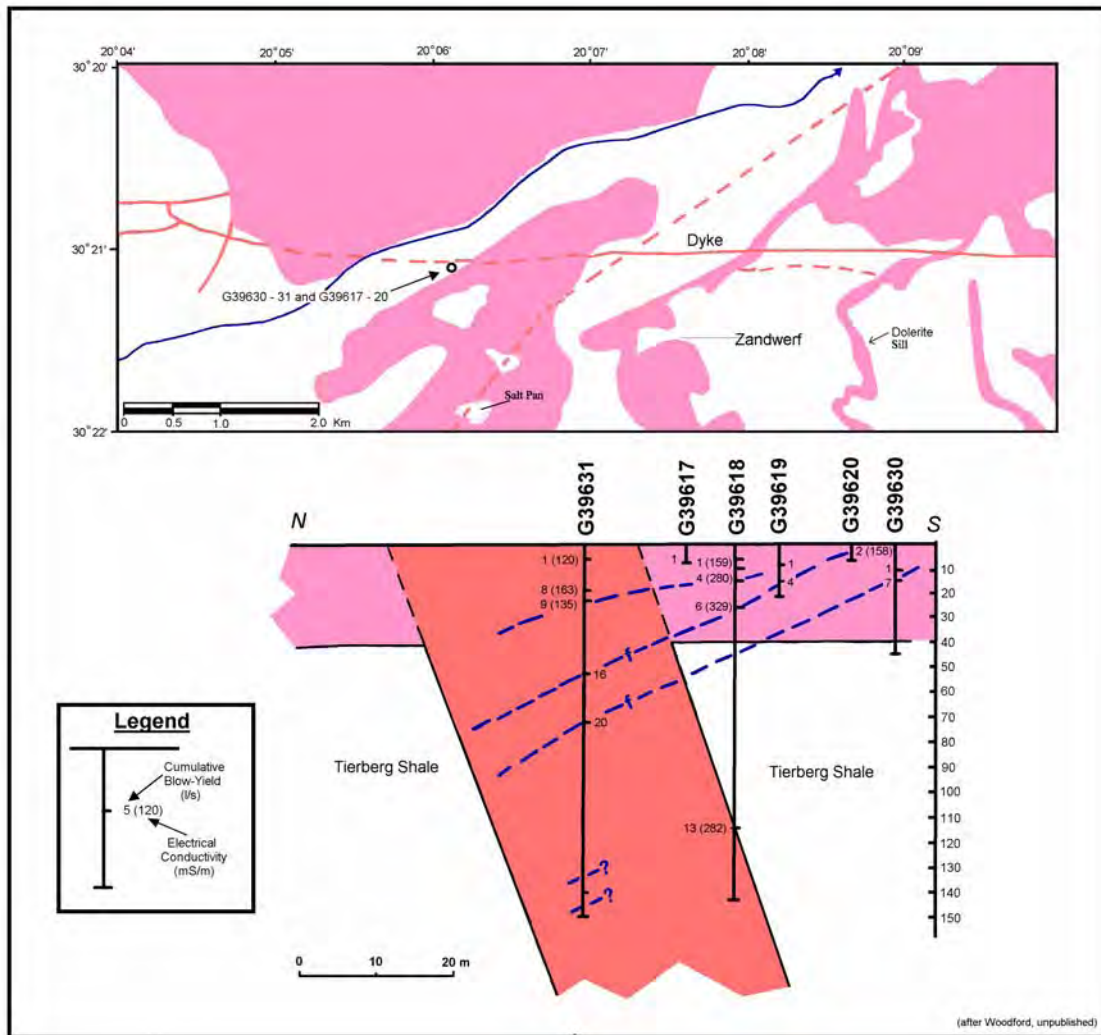


Figure 2.23: Geohydrology of the Zandwerf Dolerite Dyke and Sill, east of Calvinia

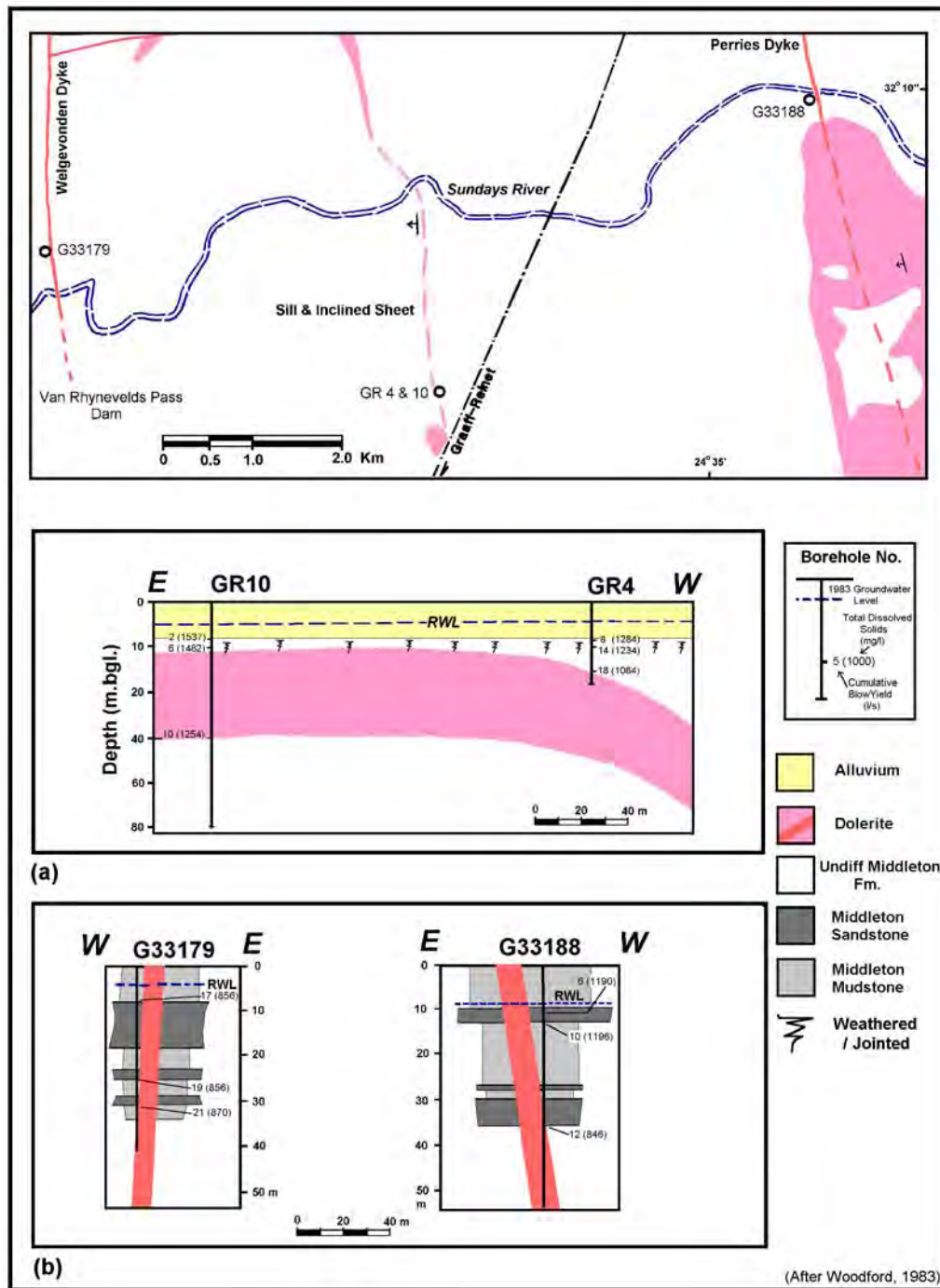


Figure 2.24: Geohydrology of the (a) Waterloo Inclined Sheet and (b) Perries / Welgevonden Dykes, north of Graaff-Reinet

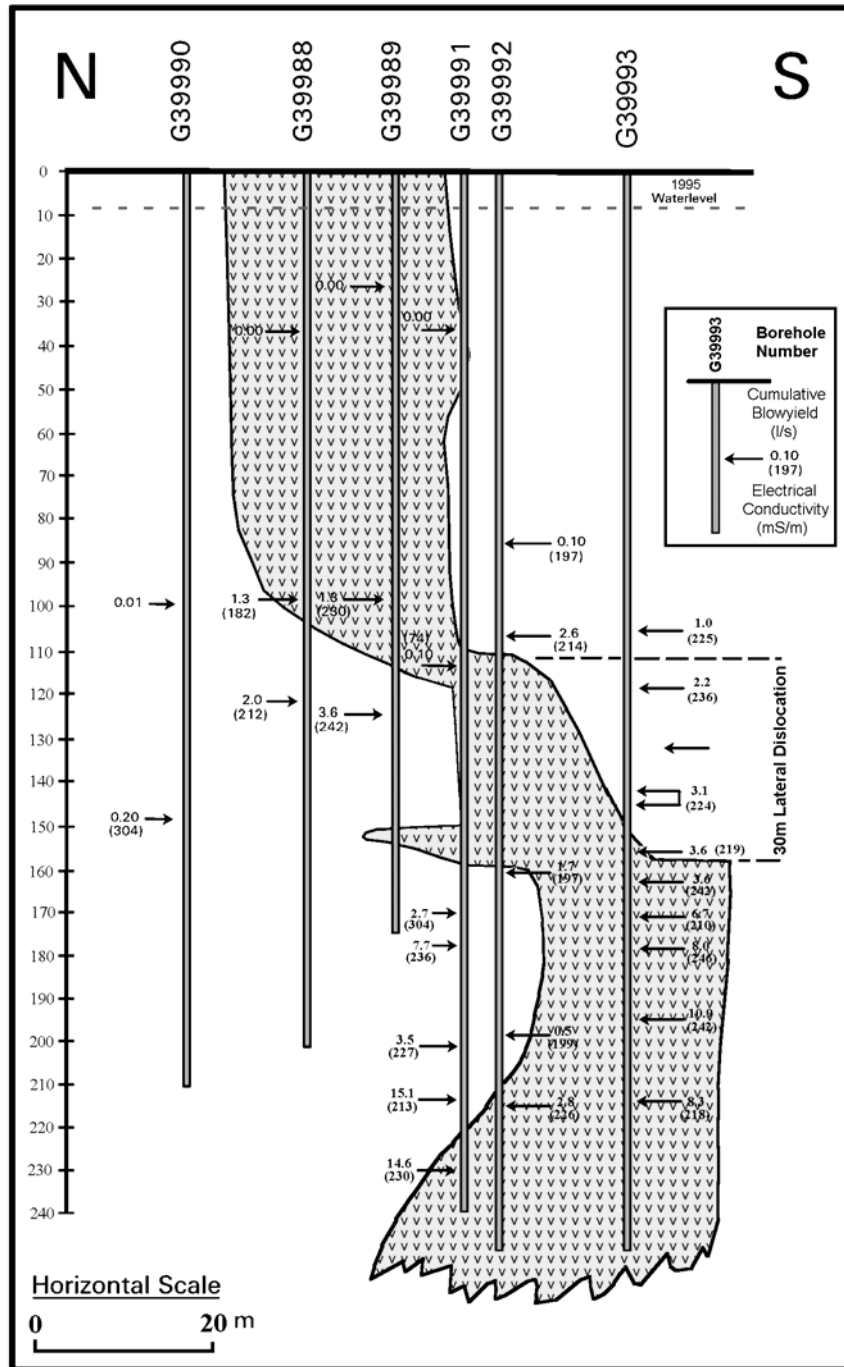


Figure 2.25: Vertical Dislocation of the De Wilg Shear Dyke, southwest of Loxton (Woodford and Chevallier, 2001)

- *Transgressive Fracturing*

Large volumes of groundwater are often intercepted in discrete, open-fractures or fissures that transgress the dyke, and extend some distance into the country rock (typically up to 15 m away from the contact). Examples included here are the Zandwerf dyke (**Figure 2.23**) near Calvinia, and the MX4 dyke (**Figure 2.27**) and Lehman's Drift dyke (**Figure 2.26(b)**) near Queenstown. The fractures are commonly sub-horizontal in attitude ($< 50^\circ$).

Vandoolaeghe (1980) concluded that horizontal- and oblique-fractures within the dolerite and adjacent sediments are the dominant water-bearing features in the Queenstown area.

These fractures occasionally extend several tens of metres away from the dyke into the country rock, i.e. a sub-horizontal, transgressive fracture in the vicinity of the 20 m wide Dunblane Dyke near Middelburg, is reported to extend some 90 m away from the dyke contact (**Figure 2.28**). The dyke forms part of an extensive NNW dyke system and can be traced from some 80 km south in the Cradock district. The Dunblane dyke transgresses some of the dolerite ring-complex systems in the Middelburg area. This phenomenon was reported by Campbell (1975) at a few localities along the Tweeling-Brandwag dyke. These extensive sub-horizontal fractures are only observed in the near-surface where an advanced stage of weathering has taken place. Note that the deeper-seated transgressive, sub-horizontal open-fractures at 100-150 m below surface (**Figure 2.25**) in the De Wilg dyke do not extend more than 5 m into the host rock.

- *Jointing Parallel to the Dyke Contact*

Enslin (1951) and Boehmer (1986) proposed that Karoo dolerite dykes are jointed along a narrow zone that parallels the two contacts.

Enslin (1951) states that "*some dolerite dykes (themselves) have vertical joints and fractures near their contacts at depth and that these zones in the dyke will then yield very large supplies of water. Owing to uncertainties of the existence of such joints at depth and technical difficulties that may be encountered if a borehole is drilled into this zone, boreholes are preferably sited to strike water in the indurated sediments alongside the dyke*".

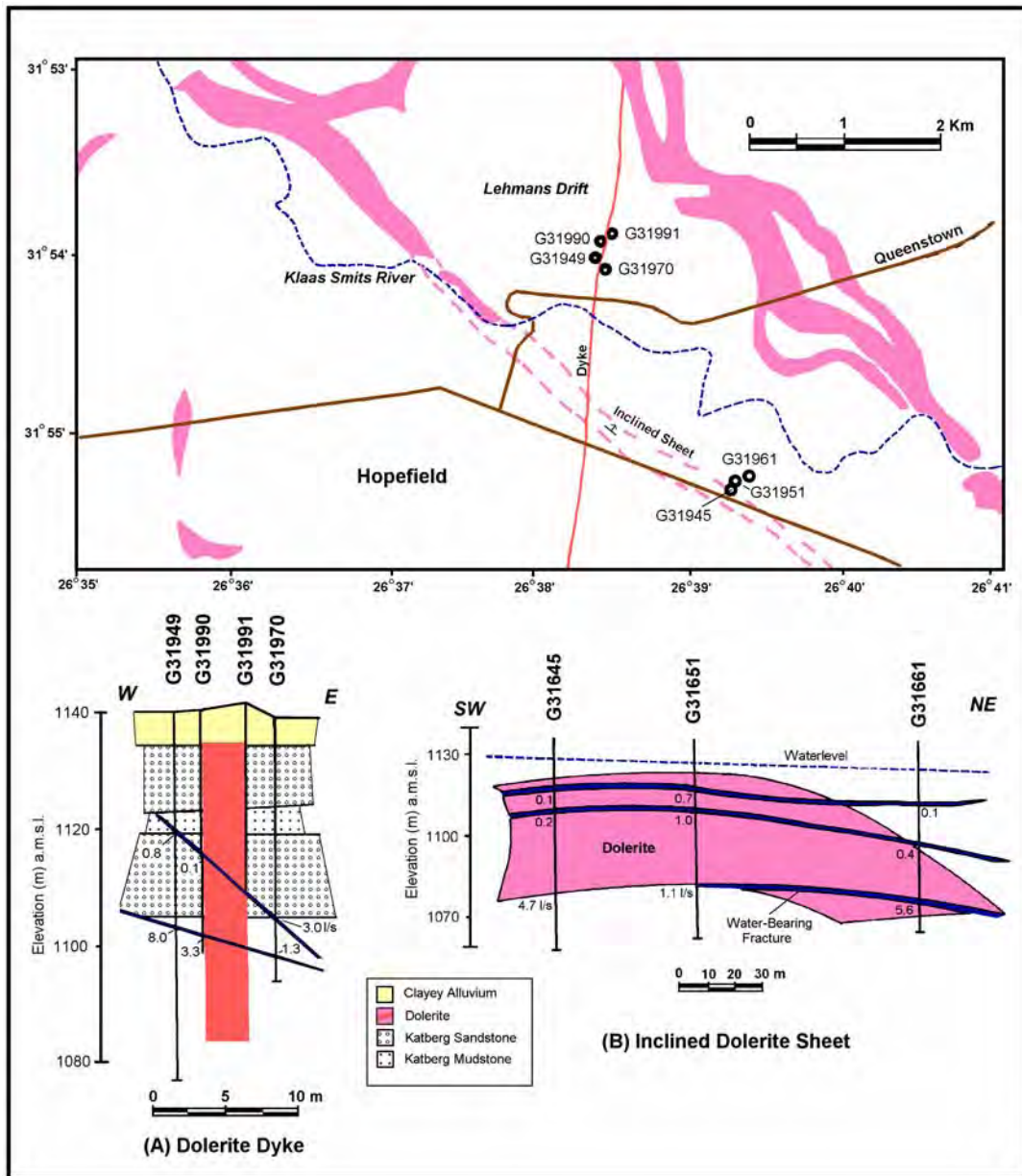


Figure 2.26: Geohydrology of the Lehman's Drift (a) Inclined Sheet and (b) Dyke, Queenstown (after Vandoolaeghe, 1980)

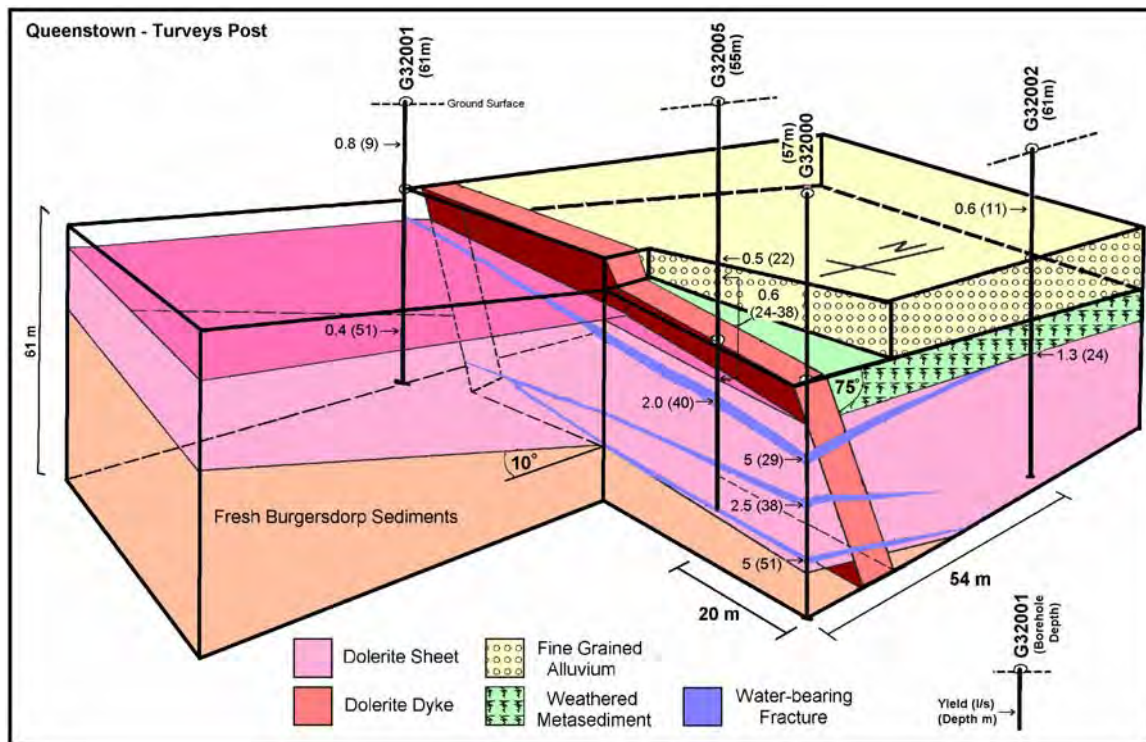


Figure 2.27: *Geohydrology of the MX4 Dyke / Sill Intersection Zone, Queenstown (after Vandoolaeghe, 1980)*

- *Effect of Dyke Attitude and Drainage*

In the past, a number of authors have proposed that higher yields are obtained in boreholes sited on the upstream contact of dykes cutting drainage systems, where dykes are assumed to act as an impermeable barrier to groundwater flow. Paver et al., (1943) states that boreholes should, in such cases, be sited as follows:

- if the dyke is vertical or near vertical then a site should be chosen on the drainage side of its outcrop and close to the contact (**Figure 2.29(a)-(c)**).
- if the dyke dips steeply downstream a site should be chosen downstream from its outcrop, and at such a distance from it that the borehole will penetrate the dyke, and tap water trapped on the upstream side (**Figure 2.29(d)**).

- if a dyke dips steeply upstream a site should be chosen upstream from its outcrop and such a distance from it that the borehole will reach the waterlevel before penetrating the dyke (**Figure 2.29(e)**).
- if the dyke cuts the drainage obliquely a site should be chosen in accordance with the above and towards the side of the valley where the dyke is furthest downstream (**Figure 2.29 (f)**).

It is the experience of the authors that there are no valid grounds for such thinking, as it is the mechanisms and degree of dyke fracturing that determines the yield of the borehole. Impermeable dykes cutting across the groundwater flow path may result in elevated waterlevels on the upstream side of the dyke and the development of springs.

- *Dyke / Sill Intersections*

Dolerite dykes (younger) that cut sills are often good targets for groundwater, especially in a valley-bottom situation where the sill material is highly weathered. The dyke-sill contact zone is generally not as wide or permeable as that of the dyke-sediment contact (Paver et al., 1943, Van Wyk, 1963). This may be due to the more intense development of thermal-joints along dolerite-sediment contacts as a result of differential cooling caused by the greater contrast in thermal conductance between the two rock types. Transgressive fractures are often well developed in the vicinity of the dyke/sill contacts and are similar to those illustrated in (**Figure 2.16(b)**). For example, the Zandwerf dyke-sill intersection (**Figure 2.23**), where several high yielding transgressive fractures were intercepted within the weathered sill material and fresh dolerite dyke. This fracturing probably resulted during the simultaneous cooling of the dyke and the sill. A similar fracture pattern is developed at the MX4 dyke-sill contact (**Figure 2.27**). Note the upper contact of the sill is weathered and decomposed, while the intruding finer grained dyke is not.

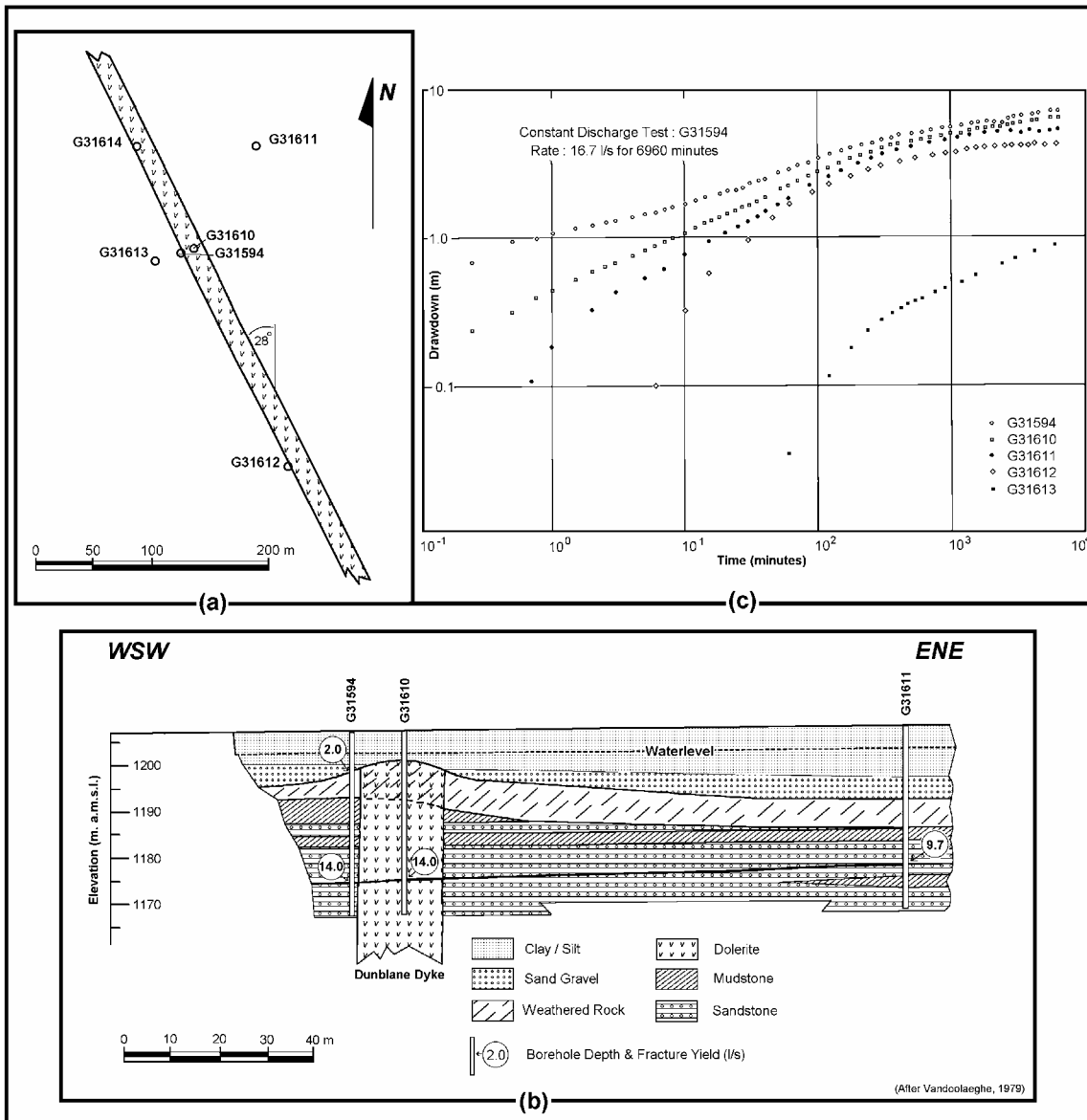


Figure 2.28: Geohydrology of the Dunblane Dyke, Middelburg (after Vandoolaeghe, 1979)

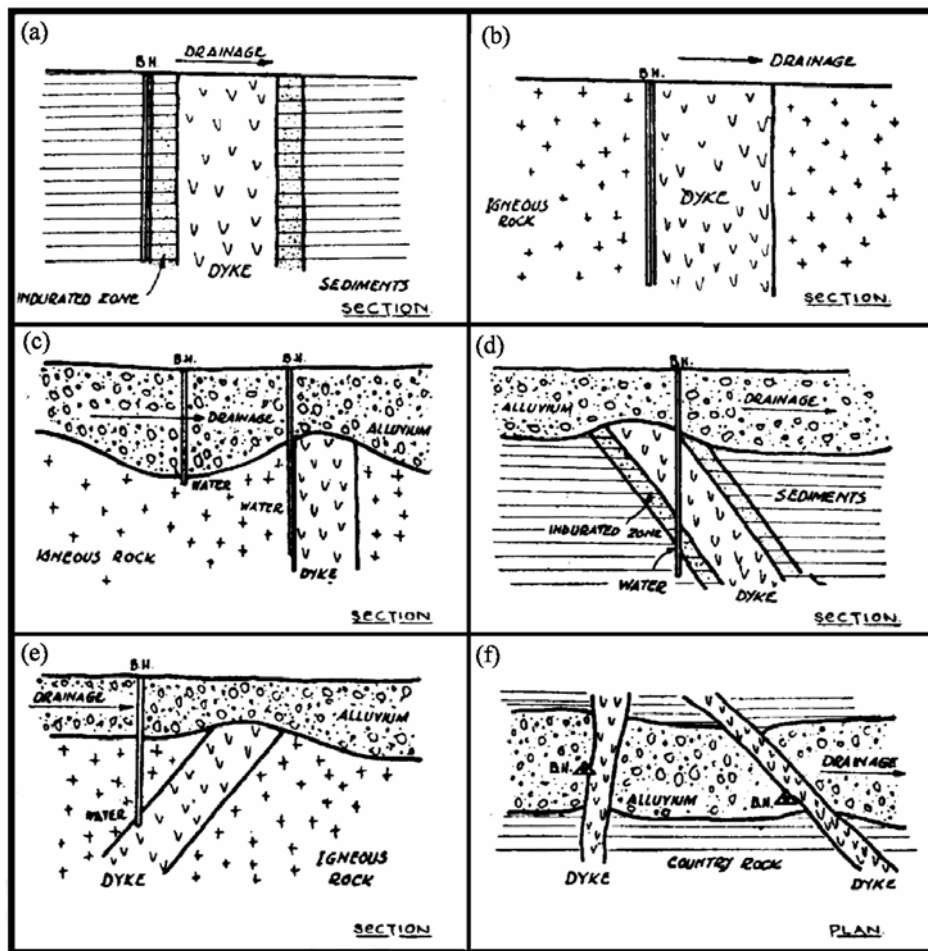


Figure 2.29: *Correct Siting of Exploration Boreholes alongside Dykes cutting Drainage Features (after Paver et al., 1943)*

Jointing is commonly developed along the contact of the dyke (thermal) and within the adjacent baked, disturbed sediment. Boreholes drilled into this zone are generally higher yielding than those drilled away from the dyke in the undisturbed host rock. Syn- or post- intrusion tectonic and/or hydrothermal reactivation of the structure often results in the development of more discrete fractures or fissures that transgress the dyke and extend into the country rock. Boreholes intercepting such fractures often produce exceptionally high-yields.

Summary

On a regional scale, the structural domains indicated in **Figure 2.15** have not as yet been shown to influence the regional hydrogeology. However, the wide and extensive dykes such as the E-W Victoria West dyke, the NNW Middelburg dyke and the curved “gap” dykes near East London, were major magma feeders which were accompanied by extensive fracturing (shearing and jointing). They form regional discontinuities that, although likely to have propagated laterally, extend to great depths within the earth’s crust. In theory these structures could form part of a fracture network wherein deeper-seated groundwater flows on a more regional scale. Boreholes correctly drilled into these features are anticipated to deliver high-yields, as is the case of the E-W Victoria West dyke.

On the local scale, the geometry, attitude, grain size, degree of weathering and fracturing of dykes influence the hydrological properties of individual structures. For example, thick dykes do not necessarily deform the country rocks more than do thin dykes, but the former may be more porous because of their granularity upon weathering. Emplacement of an *en-échelon* dyke is associated with complex stress fields and strong deformation of the host-rock, which make it a good drilling target for high-yielding boreholes. The hydrology of a particular dyke is related to a complex interplay of these parameters and can thus vary dramatically along the strike of the structure.

Case Study: Tweeling-Brandwag Dyke

The Tweeling-Brandwag dyke near Beaufort West represents the most southerly extension of a major E-W dyke shear system in the Western Karoo (**Figure 2.15**). It exhibits typical *en-échelon* segmentation and the dyke is believed to have intruded into the fold-axis of a low amplitude syncline, with inferred dips of 1° to 2° (Campbell, 1975).

The Department of Water Affairs (Campbell, 1975) drilled 208 boreholes along an 11 km portion of the Tweeling-Brandwag dyke, (**Figure 2.30**). The dyke varies in thickness between 5 and 11 m and dips between 82° to 90° either to the north or south. The attitude of the dyke changes abruptly along strike at offset points. The dyke is offset by ±250 m on the Tweeling Farm.

Analysis of groundwater-levels fluctuations in the vicinity of the dyke indicated that it impeded rather than impounded the southward movement of groundwater (Campbell, 1975).

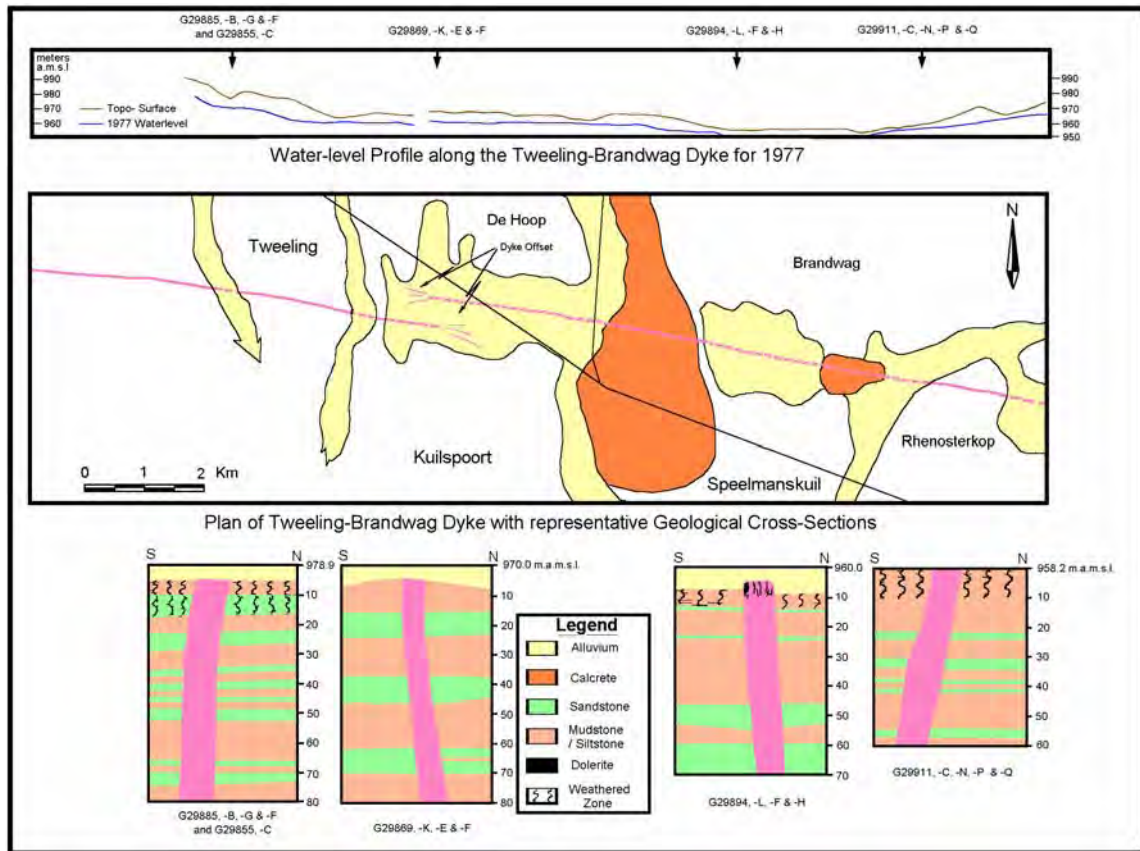


Figure 2.30: Morphology of the Tweeling-Brandwag Shear Dyke, Beaufort West (after Campbell, 1975)

Variations in the median blow-tests yields of boreholes situated along the northern contact (upstream) of the dyke are presented in **Figure 2.31**. The relationship between the median borehole yield and thickness of the saturated alluvium / weathered bedrock is clearly displayed, where the high water strikes are associated with the weathered and jointed bedrock. The highest borehole yields occurring in the floodplain of the Platdorings River. The central portion of the dyke is deeply weathered, down to 25 m on the Brandwag Farm, where it is obscured by silty alluvium and well-developed calcrete.

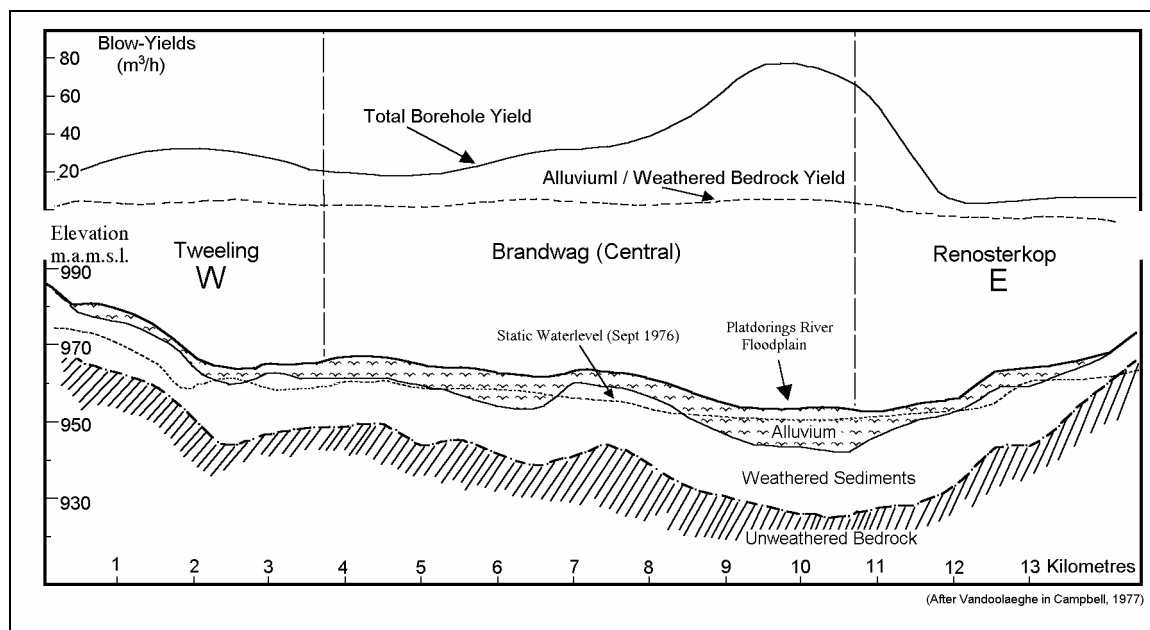


Figure 2.31: Distribution of Borehole Yields along the Northern Contact of the Tweeling-Brandwag Dyke (after Campbell, 1975)

Sill and Ring-Complexes

One of the most prominent features of the present Karoo landscape is the large number of dolerite sills and ring-complexes. These structures are easily recognized on satellite images (**Figure 1.9**), where they often display a sub-circular saucer-like shape, the rims of which are commonly exposed as topographic highs and form ring-like outcrops. Du Toit (1905, 1920) first described these structures in the vicinity of Queenstown.

Stratigraphic and Regional Distribution.

The Karoo dolerite sills and ring-complexes have the same geographical distribution as the dolerite dykes and they are by far the most common type of intrusion in the Karoo basin, to a large extent controlling the geomorphology of the landscape (**Plate 2.4**). The dolerite sills and dykes form a complex intrusive network that probably acted as a shallow magma storage system. The lithology of the country-rock strongly controlled the emplacement of the sills. Du Toit (1920) pointed out the existence of preferential horizons of emplacement of dolerite sills, i.e. the Dwyka-Ecca Group contact, the Prince Albert-White Hill Formation contact, the Upper Ecca-Lower Beaufort Group contact and other lithological boundaries within the Beaufort Group. Drilling in the Karoo has confirmed the presence of these preferential

stratigraphic levels of intrusion (De la Rey Winter and Venter, 1970). The dolerite / sediment ratio decreases from west to east, reflecting the increase of sill intrusion toward the top of the Karoo sedimentary pile in the more elevated portions the Eastern Karoo (**Figure 2.32**).

On a regional scale, Karoo dolerite sills form large coalescing circular, oval or kidney-shaped structural units. Each unit is in itself composed of several sub-units of smaller size which in turn are made of even smaller units and so on, resulting in the so called ‘*ring-within-ring*’ patterns (**Figure 2.33**).

Five major regional ring-complex units can be recognized extending from the Western to the Eastern Karoo (**Figure 2.34**). These are clearly defined on the topographic map of the Karoo Basin - the Sutherland, Victoria West, Middelburg, Queenstown and the Umtata mega-basins. No major basins have been mapped in the Northern Karoo. One of the more obvious reasons for this is that a greater degree of weathering and denudation has taken place in the Basin to the north of Bloemfontein and Umtata.

The dolerite ring-structures of the Queenstown area in the Eastern Cape (Queenstown mega-basin), were initially described by Du Toit (1905) and later by Meyboom and Wallace (1978) and may be regarded as a ‘type-area’ for these structures. Chevallier and Woodford (2000) compiled detailed geological cross-sections of the area, which illustrate the structural complexity of these features and their intricate interconnectivity (**Figure 2.35**). The typical “*ring-within-a-ring*” pattern is also clearly indicated. The outline of the dolerite sill and ring-complexes, although “circular” in broad terms, are in reality often irregular and may intersect one another. In fact, many dolerite ring systems are composed of many linear to curvi-linear segments that tend to follow the regional trend of dykes and fractures. The sills and rings display important vertical stacking. An inclined sheet can feed two superimposed sills of the same size, resulting in the characteristic ‘box-like’ pattern (**Figure 2.35**).

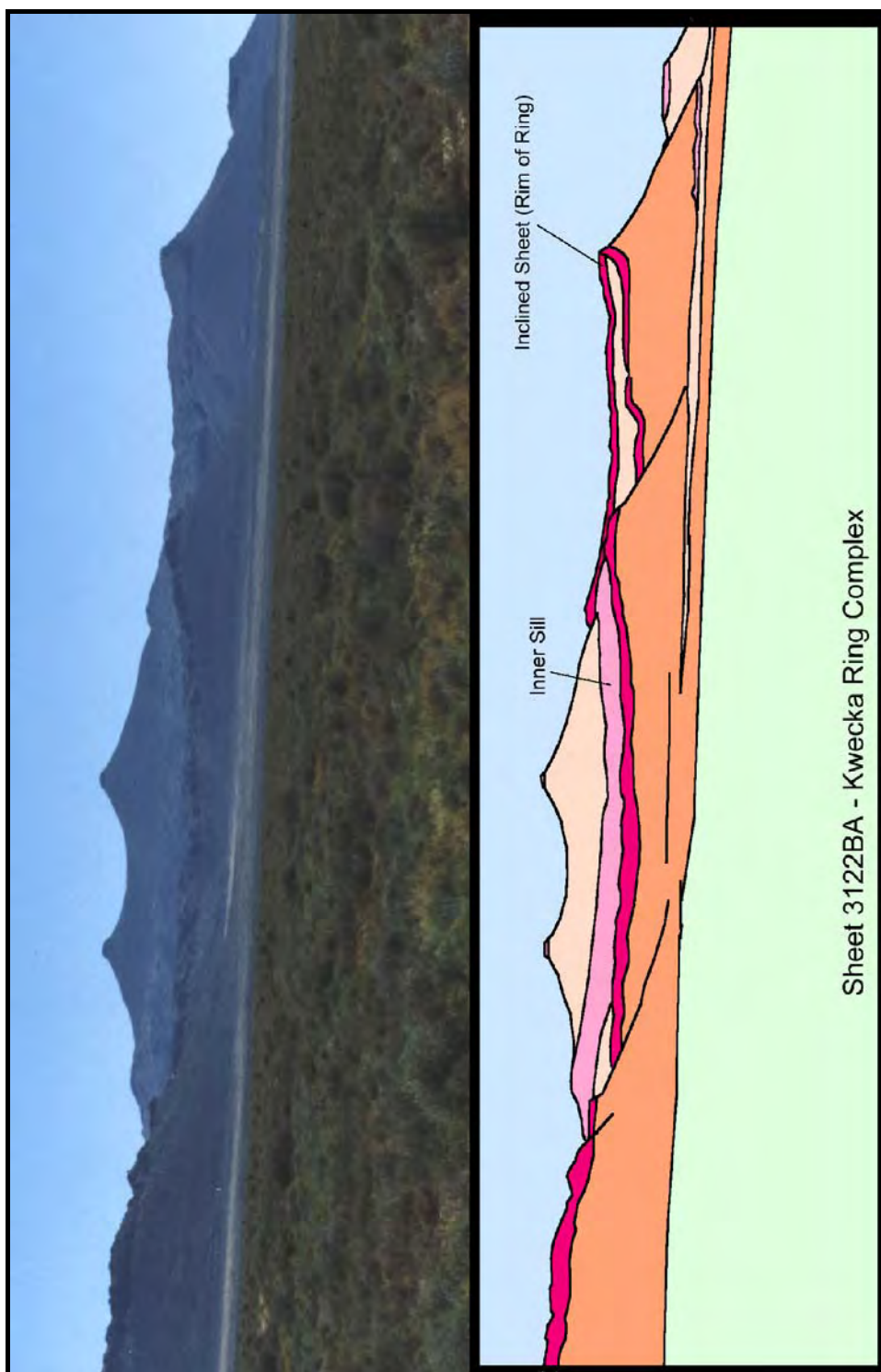


Plate 2.4 : The Kweeka Sill-Ring Complex, near Victoria West

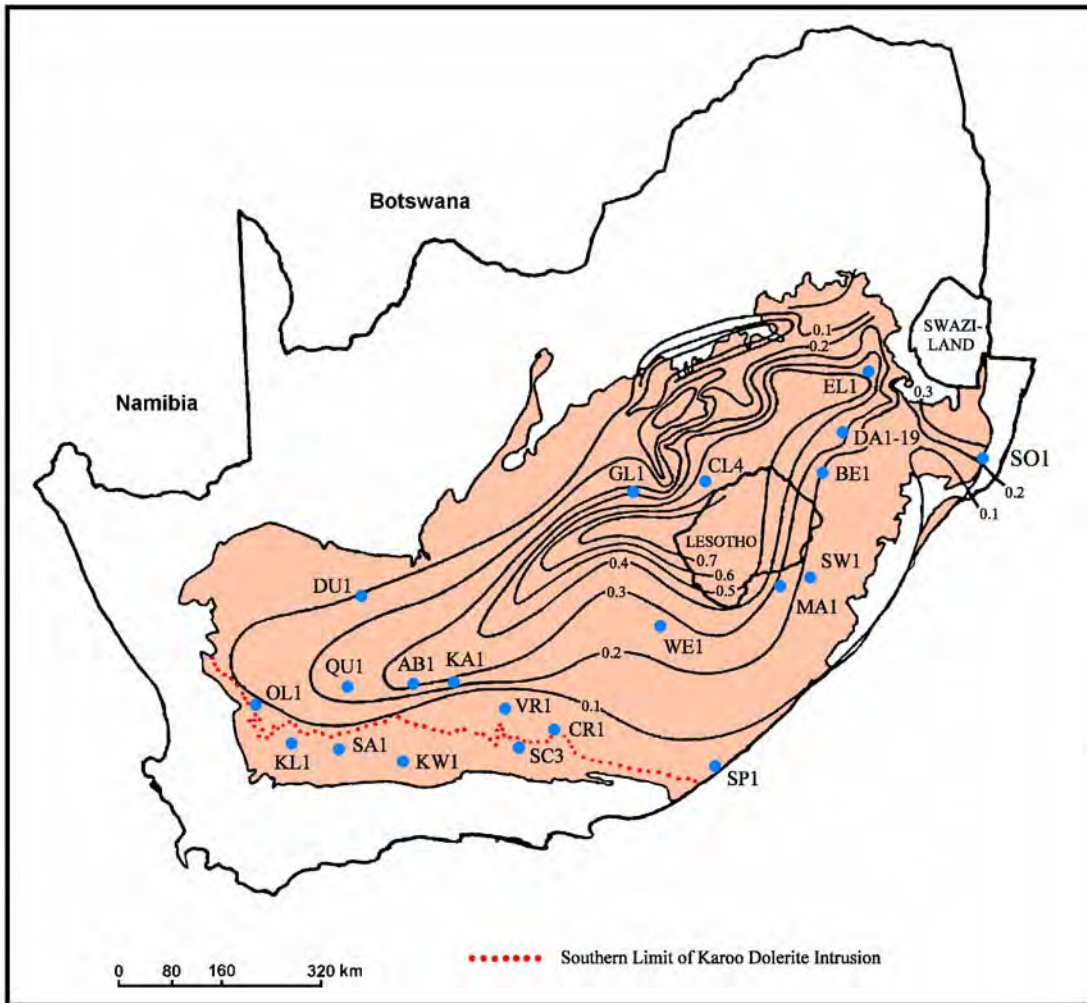


Figure 2.32: Dolerite Sill / Sediment Ratios of the Karoo Basin (after De la Rue and Winter, 1970)

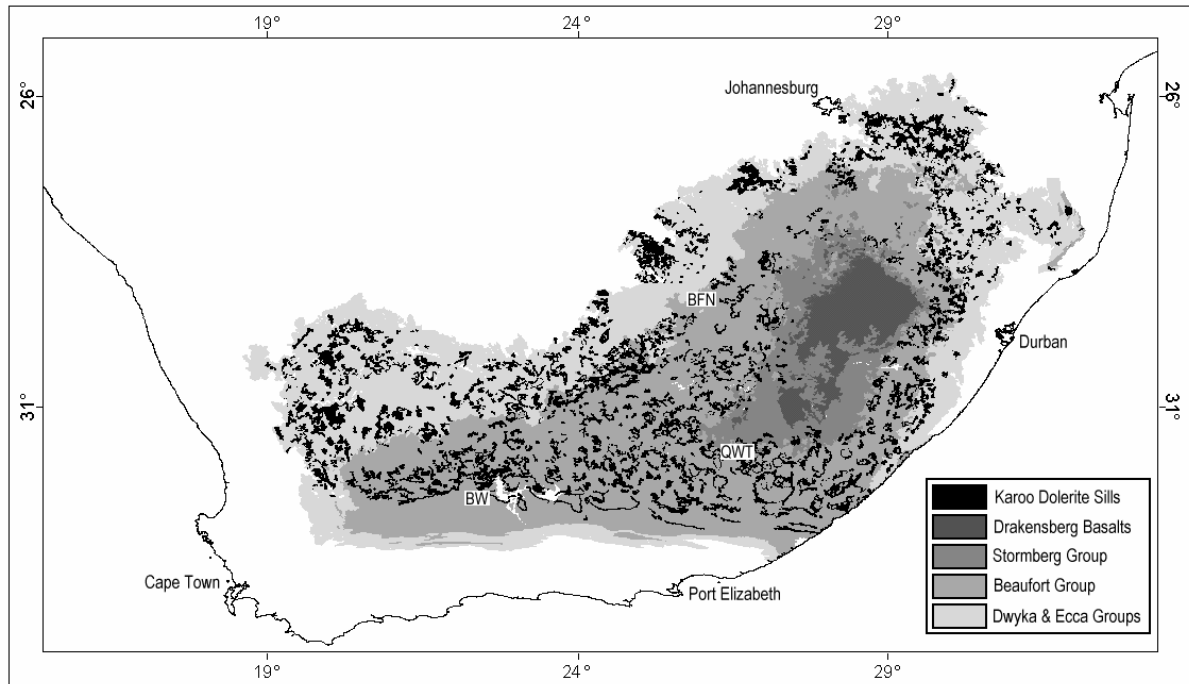


Figure 2.33: Dolerite sill distribution in the Karoo Basin, extracted from the 1/1 000 000 Geological Map

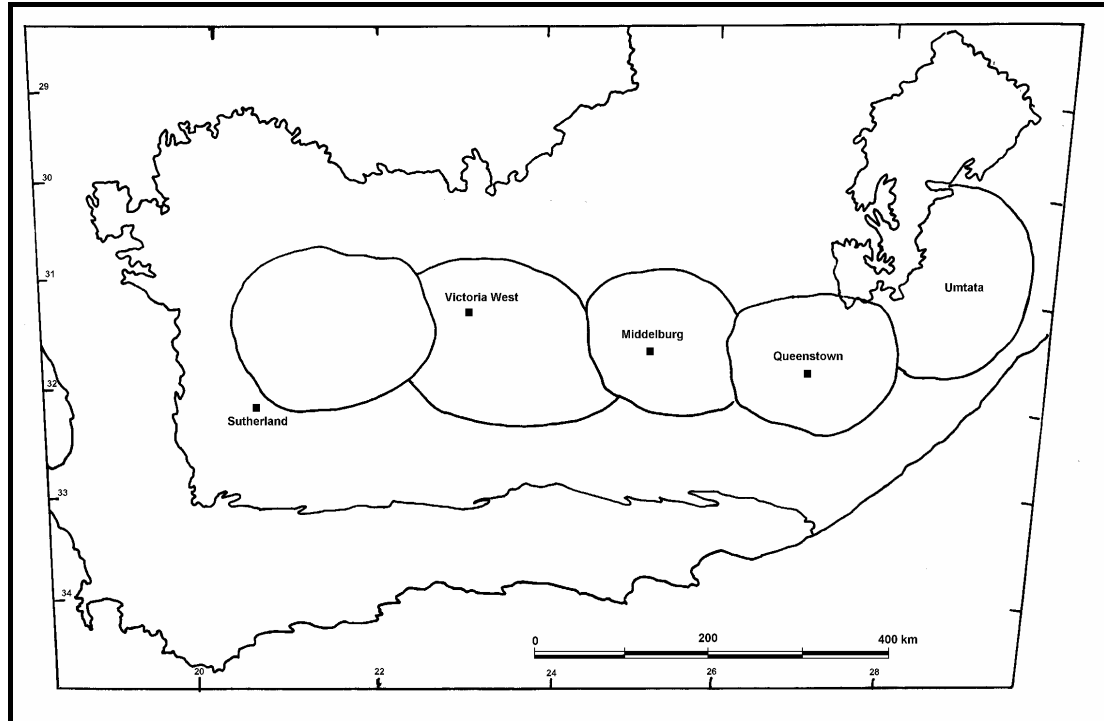


Figure 2.34: Major Dolerite Sill and Ring Complex Systems in the Eastern and Western Karoo (after Chevallier and Woodford, 2000)

On a regional scale, the attitude and stratigraphic level of intrusion of these sills are highly variable. A relationship exists between the size of the dolerite basins and Karoo Supergroup stratigraphy. The more extensive sills forming these mega-structures have been intruded near the base of the Karoo sediments, while the smaller structures (diameter of 10 km and less) have been intruded into the upper parts of the Karoo Supergroup (**Figure 2.35**). The shape and attitude of sills also changes from the bottom to the top of the stratigraphic sequence:

- Laterally extensive and long wave-length, undulating sills occur at the base of the Karoo sequence, i.e. along the contact of the Dwyka Group in the Prince Albert Formation and Prince Albert-Whitehill Formations,
- well developed saucer-like structures dominate the middle portions, i.e. within the upper Ecca and Beaufort Groups, and
- flat-lying sills reappear towards the top of the Karoo succession, i.e. directly below the Lesotho basaltic pile.

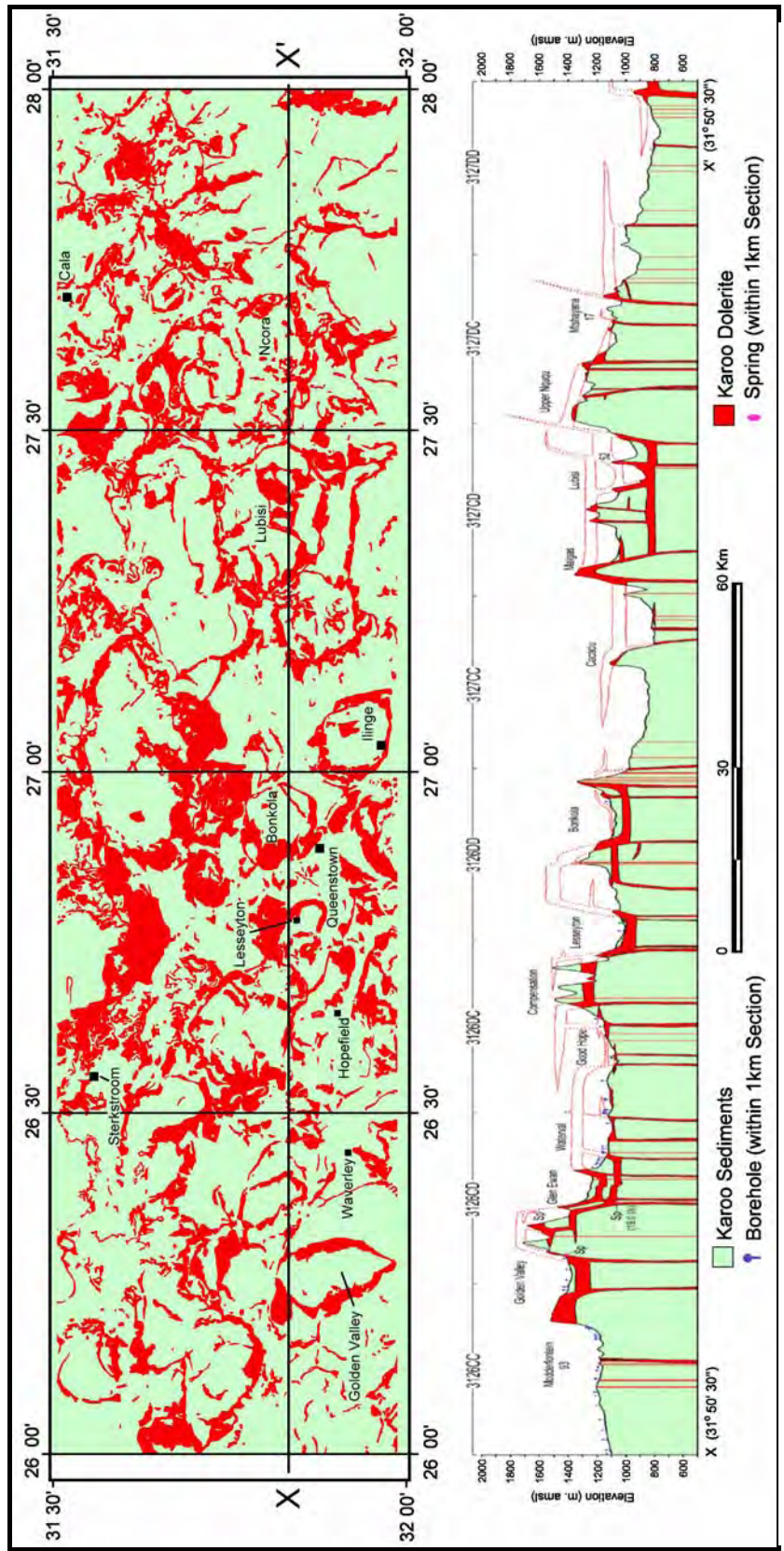


Figure 2.35: Geological map and cross-section of the Queenstown dolerite sill and ring-complexes

Geometry and Structure

The larger Karoo dolerite sill and ring-complexes, within the 10 to 50 km diameter range, exhibit a “saucer-shape”- (Chevallier and Woodford, 1999), or “disc-laccolithic shape” (Burger et al., 1981) morphology and not the “basin & dome” structure as originally proposed by Du Toit (1905) or subsequently by Meyboom and Wallace (1978). **Figure 2.40** indicates the typical surface morphological expression of these structures. Each intrusion consists of four distinctive morpho-tectonic units (**Figures 2.37, 2.35, 2.36 and Plate 2.4**), (Chevallier and Woodford, 1999), namely:

- (a) A flat-lying *inner sill* forming the bottom of the saucer, (also referred as a laccolith by Burger et al., 1981). The thickness of the sill commonly varies between 30 and 60 m. Vegter (1992) reports an average sill thickness of 30 m in the De Aar area. However, very thick sills are also encountered near Lesotho (up to 1 000 m for Insizwa; Mask, 1966) and in Natal.
- (b) A flat-lying *outer sill* showing extensive fracturing and jointing. The thick sills which intruded into the base of the Karoo basin are outer sills and can extend for hundred of kilometres. Undulation is very shallow (less than 2°), which can only be detected on large-scale maps. The thickness of these sills, usually between 50 and 100 m, do not appear to be any different from that of the inner sills. The ring-structures of the northeastern Karoo Basin commonly do not show a prominent outer sill on outcrop.
- (c) A peripheral, *inclined sheet* with dips of up to 60° towards the centre of the basin, leaving a topographic ring after erosion (also referred as the “horn” by Burger et al., 1981). Vandoolaeghe (1979, 1980) reports that inclined sheets exhibit inward dips ranging from 3-70° and 10-35° in the Middelburg and Queenstown areas, respectively. The “inclined sheet” is commonly 20 to 40 m in thickness, but may actually exceed that of the sills (Chevallier and Woodford, 2000).

Inclined sheets in the Southern Free State dip at angles of 30° to 80°, whilst their thicknesses varies from 36 m to 150 m, as measured in road-cuttings (Burger et al., 1981). In the coal-mines of the northern Karoo Basin, a similar situation is evident, where sills often extend over large areas along the Dwyka-Ecca contact and abruptly curve-upward into the overlying rocks at angles in excess of 80° to form a ring-structure on the surface (Burger et al., 1981).

- (d) Abundant *feeder dykes* which branch into or out of the sill and ring complexes, or cut through them.

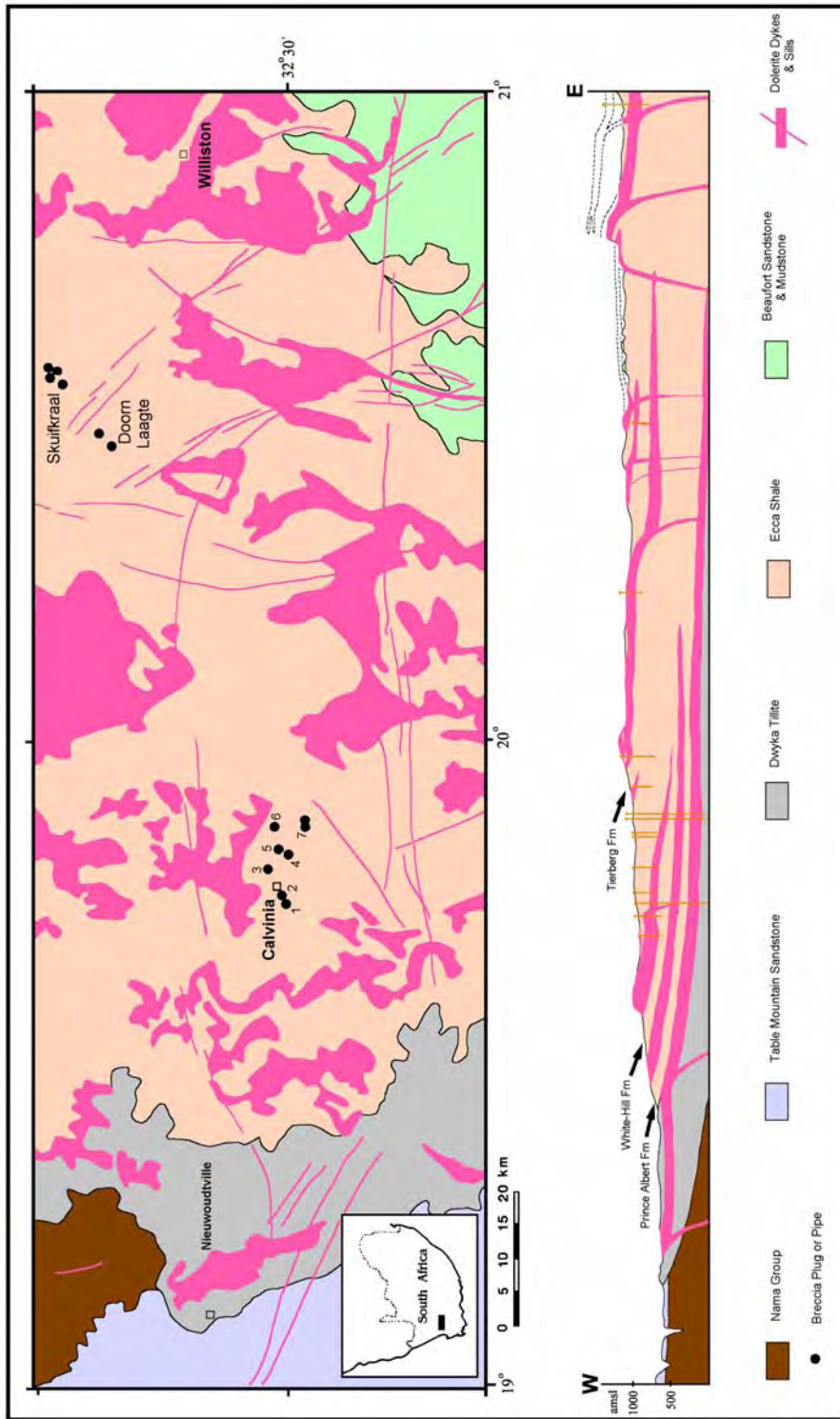


Figure 2.36: Geological Section showing the stratigraphy and attitude of dolerite sills and ring-complexes between Nieuwoudtville and Williston

Relationship between Sills and Dykes

The relationship between the dykes and sill-ring complexes are extremely intricate. In the Western Karoo, many dolerite dykes can be observed to feed inclined sheets and thus control the shape of the ring-complexes, which sometimes results in a jagged rim (Vandoolaeghe, 1979; Chevallier and Woodford, 1999). Some dykes also branch out of one ring and coalesce with an adjacent ring. In the Eastern Cape, dolerite dykes often transgress sills or rings and are clearly younger (Vandoolaeghe, 1979, 1980). In the Queenstown-Tarkastad and Middelburg areas, the rings are typically oval in shape, with the long-axis trending NNW (Vandoolaeghe, 1979, 1980). This coincides with the dominant dyke/joint direction in the area (**Figure 2.15**). In the Tarkastad area a transgressive NNW dyke is intruded along the axis of basin elongation.

Fracturing associated with Sills and Ring-Complexes

Chevallier et al., (2001) identify three major types of fracturing within a dolerite sill and ring complex (**Figure 2.37**), namely:

- (a) Vertical thermal columnar jointing. This is well developed within the flat-lying sill (*f1*). From air photo examination and satellite imagery it appears that the outer sill often displays a very dense system of columnar jointing.
- (b) Fractures parallel to the strike of the intrusion are dominant within the inclined sheet. Air photo and satellite imagery show that the actual circular inclined-sheet is the most fractured part of the complex (*f2*).
- (c) Well-developed, oblique or sub-horizontal open fractures develop within curved portions of the sill. In the Western Karoo, these fractures are often infilled with secondary calcite (*f3*). Vandoolaeghe (1980) made similar observations in the Eastern Karoo.

In the country-rocks, conjugated vertical jointing is often observed in the sediments above the sill or inclined sheet. Burger et al., (1981) suggest that, based upon their laccolith model of intrusion, these fractures are open. Botha et al., (1998) also mentioned that sills with laccolith shapes could have contributed to the existence of bedding-parallel fractures in the host rock.

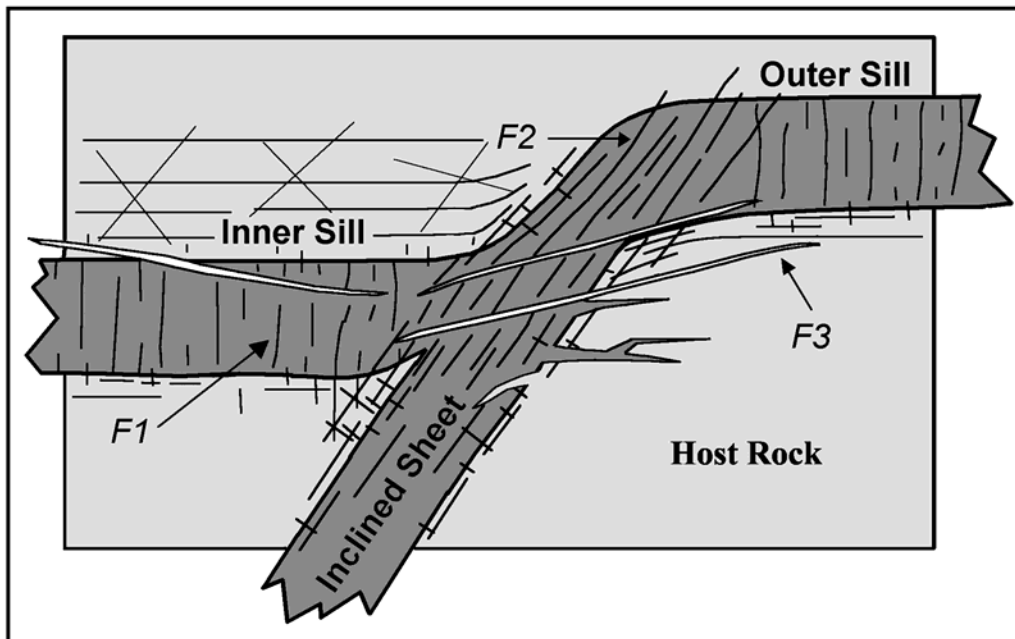


Figure 2.37: *Different Types of fractures associated with sill and ring-complexes (after Chevallier et al., 2001)*

Mechanism of emplacement of Karoo dolerite sills

Various attempts have been made in the past to develop a mechanism of emplacement for the sill and ring-structures. The following more recent tectonic interpretations are based on extensive geomorphological and geological observations and have been partly confirmed by drilling:

1. Burger et al., (1981), from observations made in the Northern Karoo (Free State), proposed that the sills have the form of a laccolith which thickens from the outer rim towards the centre of the structure. In this model the feeder to the laccolith is a central forming plug or dyke. The rings were envisaged as peripheral offshoots formed as a result of warping of the overlying sedimentary country-rock. Bending of the roof of the laccolith would also create open-vertical fractures that are devoid of magma (**Figure 2.38(b)**).
2. Chevallier and Woodford (1999) from observations made in the Western Karoo, proposed a different model and invoked a feeding system of magma along the inclined sheet or along the ring itself using a coalescing ring-dyke network. In this model, the 60° inward-dipping inclined-sheet thus changes into an upper outer sill, feeding a lower inner sill at the same time (**Figure 2.38(a)**).

From a geohydrological perspective, the two tectonic models propose that the rim of the ring-structure is the most tectonised unit within the sill/ring complex. However

the two models can vary considerably especially concerning the development of fracturing below the ring and above the centre of the inner sill.

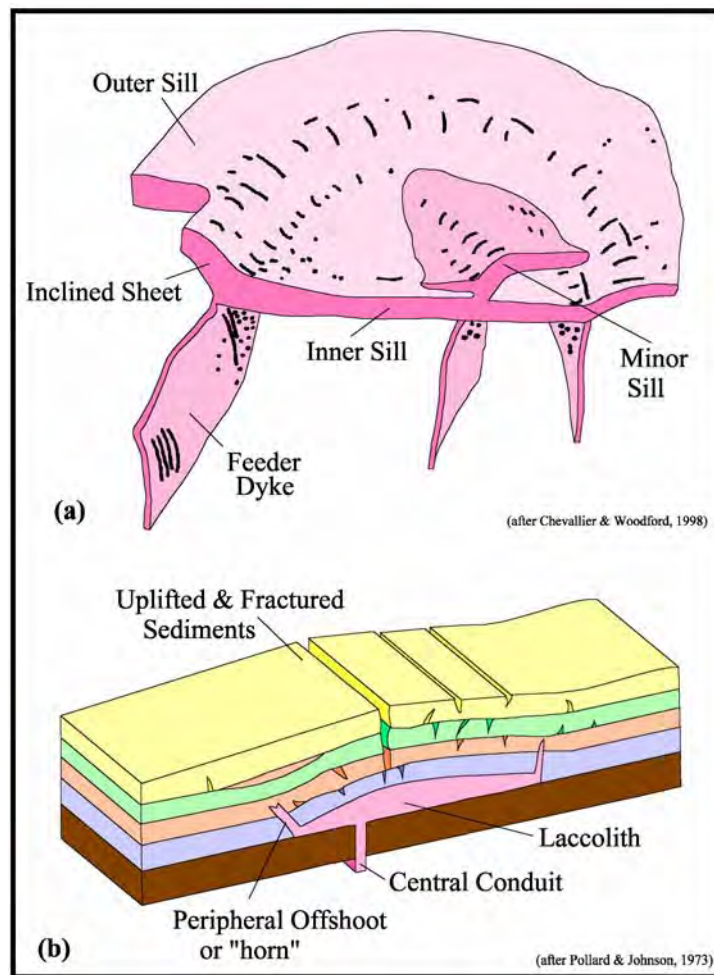


Figure 2.38: *Two mechanisms of emplacement of the dolerite sill/ring systems (a) the ring dyke model of Chevallier and Woodford (1999), (b) the laccolith model of Burger et al., (1981)*

Groundwater Occurrence and Hydrological Properties

The dolerite ring-complexes and associated sills have largely been over-looked by most geohydrologists and drillers, because of their size, thickness, rock hardness and structural complexity. Relatively few boreholes have been drilled by landowners on these structures, mainly because they commonly use water-dowsers to site their boreholes and they tend to site on the multitude of easier linear targets (dykes, fissures etc.). The Department Water Affairs (Vandoolaeghe, 1979, 1980; Burger, 1981;

Chevallier et al., 2001) investigated different portions of the dolerite ring-complexes. Vandoolaeghe (1979, 1980) apparently did not fully understand the morphology of these structures – when he was puzzled by boreholes sited on steeply-inclined sheets in the Queenstown and Middelburg areas that unexpectedly struck dolerite at shallow depths.

In the following sections a number of groundwater investigations of dolerite ring-structures are presented:

Victoria West Complex

The Water Research Commission and Department of Water Affairs and Forestry (DWAF) funded a hydrogeological investigation of the prominent ring-structure at Victoria West. This study represents the most recent and detailed assessment of the occurrence of groundwater associated with these features (Chevallier et al., 2001). The study area covers six 1:50 000 scale mapsheets (**Figure 2.39**). This structure exhibits the typical ‘ring-within-a-ring’ intrusion of dolerite that consists of many coalescing circular or arcuate structures of different sizes, attitudes and stratigraphic level of emplacement. All of these units are interconnected and belong to the same intrusive phase.

During 1999 to 2000, the Directorate: Geohydrology (DWAF) drilled 67 exploration boreholes on the northern part of the complex, where, at least, three systems of sills and rings are intruded at different stratigraphic levels (**Figures 2.39** and **2.40**). Seven drilling sites were chosen to explore the various morpho-tectonic intrusive units and structural complexities associated with these features (**Figure 2.37** and **2.41**). A profile of exploration boreholes, extending down to a maximum depth of 300m below surface, was drilled at each site. The objectives of the drilling programme was twofold, namely:

1. to assess the geometry of these intrusive units at depth, and more specifically to determine the location and vertical extent of the ring-feeder dykes – which are not always visible at the surface; and
2. to assess the occurrence of groundwater in terms of strike depth, frequency and yield, as well as to rank the water-bearing potential of the various intrusive units. The geometry and stacking of the various intrusive units are indicated in the geological cross-sections at the seven exploration drilling sites (**Figure 2.41**), whilst detailed cross-sections and water interceptions at drill sites 2 to 7 are indicated in **Figures 2.42** to **2.47**. The pertinent geohydrological results of the exploration-drilling programme are summarised in **Table 2.7**.

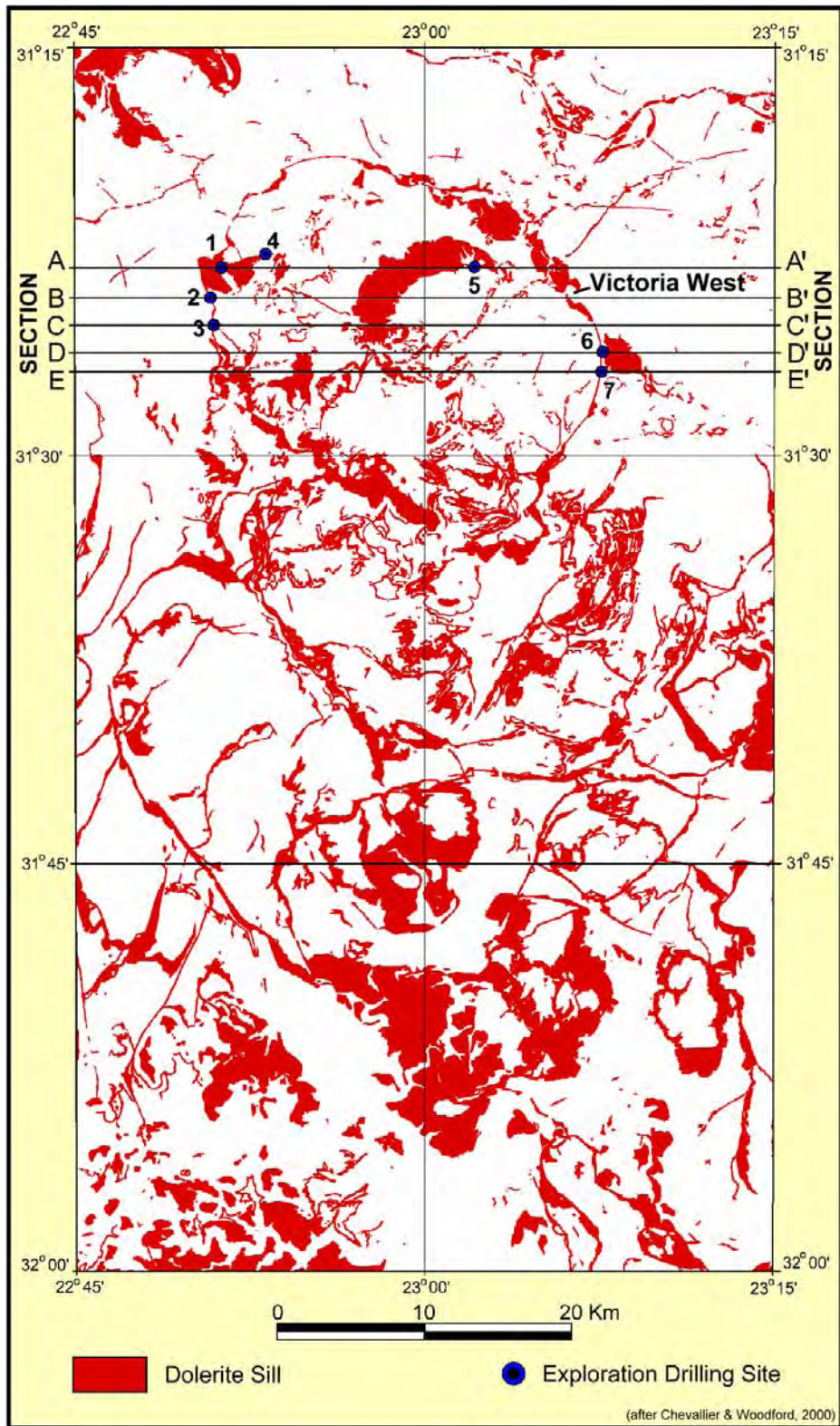


Figure 2.39: Location of exploration drilling sites targeting the Victoria West dolerite sill- and ring-complex

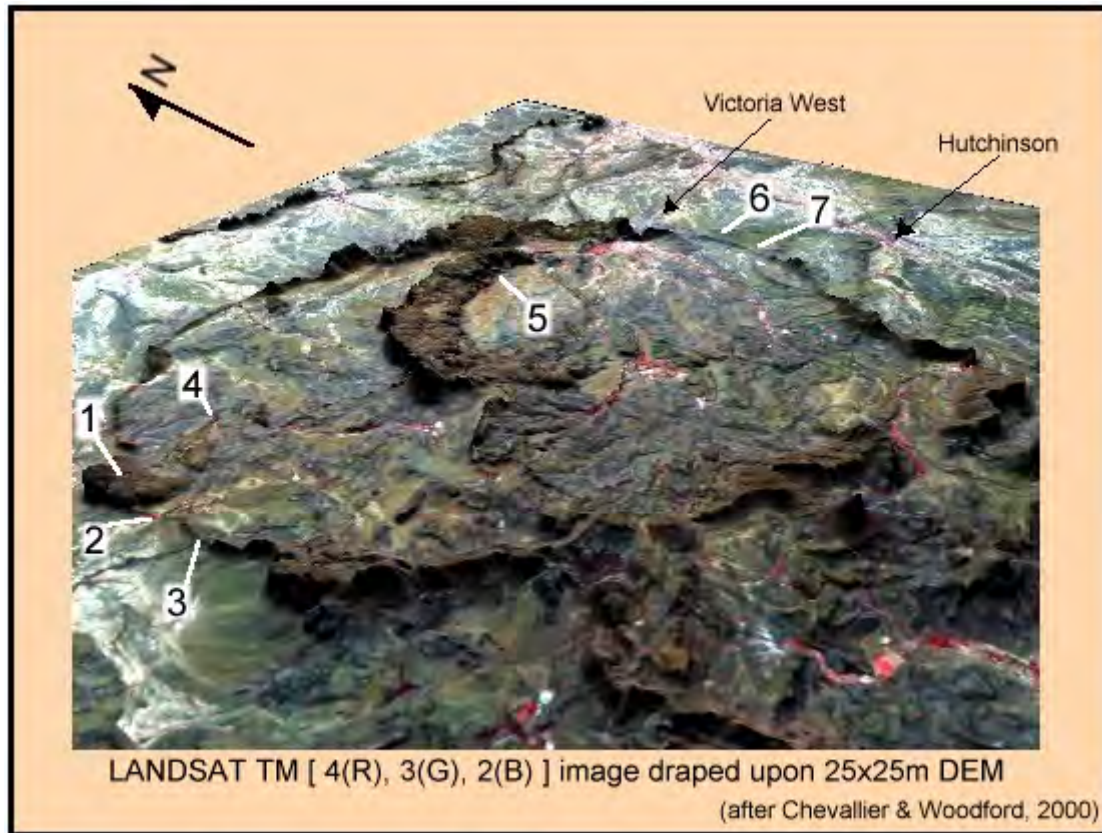


Figure 2.40: *Exploration drilling sites indicated on 3D enhanced satellite image of the Victoria West dolerite sill- and ring-complex*

The footwall of the steeply inclined sheet often exhibits an irregular contact with the sediment host rock and offshoots of thin dolerite or ‘open’ fractures (Sites 2, 3 and 7, **Figures 2.42, 2.43 and 2.47**, respectively), but only low to moderate yields were intercepted along these footwalls. The hanging-wall of the inclined sheet does not show any irregular contact with the sediment.

The flat inner-sill was explored at most of the sites. Very few water-bearing fractures were intercepted at the contact between the top of the inner-sill and the host-rock (Site 2, **Figure 2.42**). Horizontal water-bearing dolerite offshoots or fractures are found in the host-rock on the footwall contact of the inclined sheet at the same elevation as the top and the bottom of the inner-sill (Sites 2 and 7). High-yields were intercepted at these locations, as well as at the base of the sill, (drillstem blowyields of up to 24 ℓ/s) (Site 2). Moderate to high yields were also intercepted in the sediments above the inner sill, about 20 m below ground surface and some distance away from the hanging wall (Sites 2 and 7). This is probably the result of weathering combined

with the near surface release of residual compressive stress developed inside the saucer during intrusion.

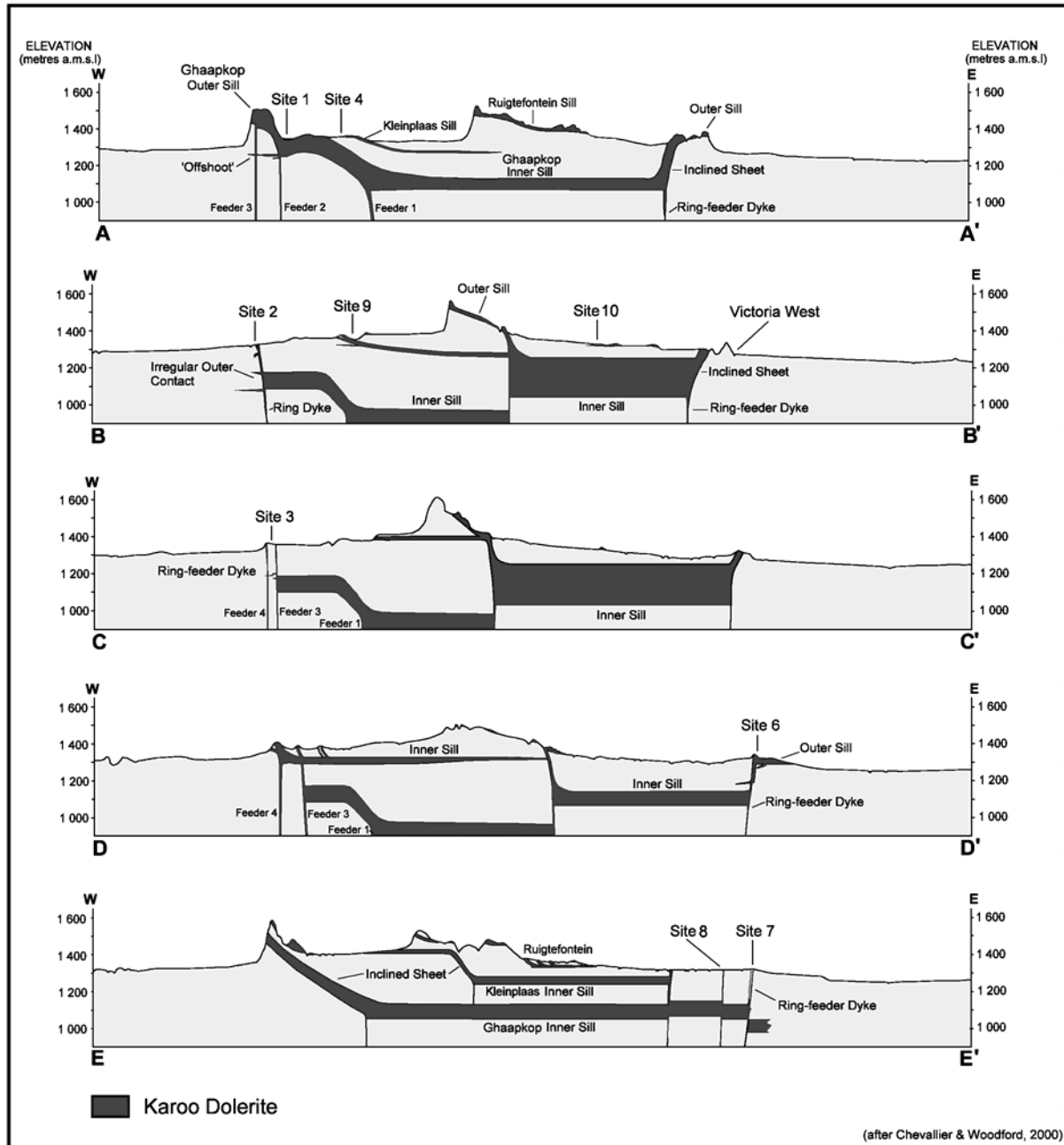


Figure 2.41: Geological cross-sections across the Victoria West dolerite sill and ring-complex showing the position of drilling sites

Up-stepping sills forming shallow inclined sheets were drilled at Sites 4 and 5 (**Figures 2.44** and **2.45**, respectively). Many water strikes were intercepted below the sill and along sub-horizontal, transgressive fractures in the sill. Site 4 produced the highest yielding boreholes (blow-yields of up to 80 ℓ/s).

The groundwater bearing potential of the outer-sill was only tested at Site 6, due to inaccessibility of these features (**Figure 2.46**). Blow-yields of 5 ℓ/s were intercepted at the intersection between the outer-sill and the inclined feeder dyke.

The drilling results are in line with what one has come to expect from groundwater exploration in Karoo fractured-rock aquifers, where dry boreholes and high-yielding borehole are drilled within relatively short distances of one another. The statistical analysis of the groundwater interceptions in the 67 exploration boreholes (total drilling depth of 13 799 m) indicates that (**Figure 2.48**):

- A high frequency of water-strikes extending from the regional waterlevel to some 60 m below ground surface. Thereafter, the frequency of water-bearing fractures decreases markedly. Approximately 73% of all water interceptions occur within 80 m of the surface.
- The first water strike commonly occurred at 40 m.bgl (median 34 m.bgl), which is below the mean drilling depth (28 m, number records 837) of private boreholes in the area. The mean depth to the waterlevel is 16.2 m.bgl (median 13.9 m.bgl).
- The proportion of high-yielding fractures tends to increase with increasing drill depths and individual water strikes in excess of 12 ℓ/s only occur below 40 m.bgl.
- Approximately 62% of the individual water-strikes yielded less 3 ℓ/s , 10% yielded between 3 and 5 ℓ/s , 9% yielded between 5 and 8 ℓ/s , 5% yielded between 8 and 12 ℓ/s and 14 % yielded in excess of 12 ℓ/s .
- The groundwater quality in these fractured-rock aquifers is good, with a total salt content of generally less than 600 mg/ ℓ (total dissolved solids).

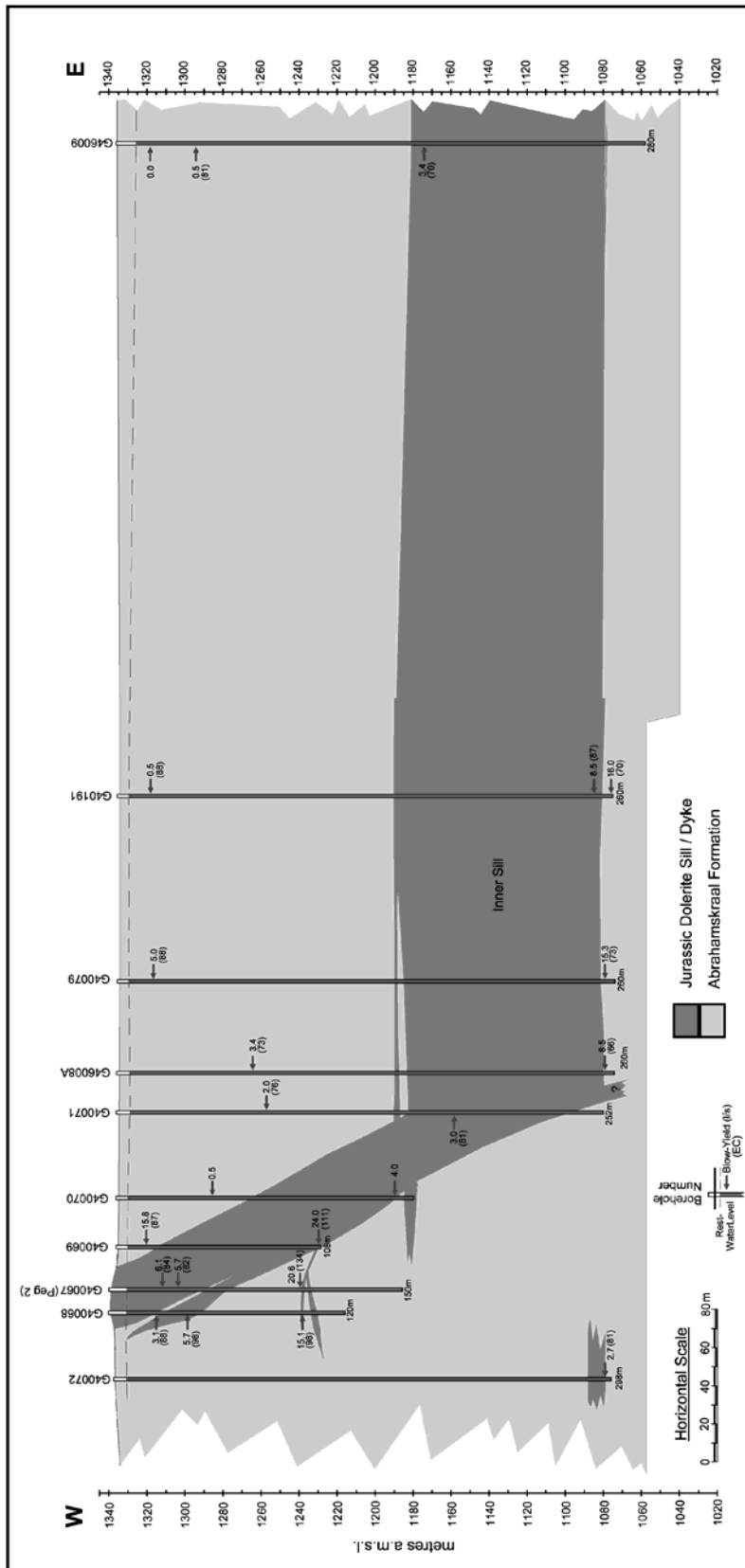


Figure 2.42: Victoria West sill and ring complex - Exploration Drill Site 2

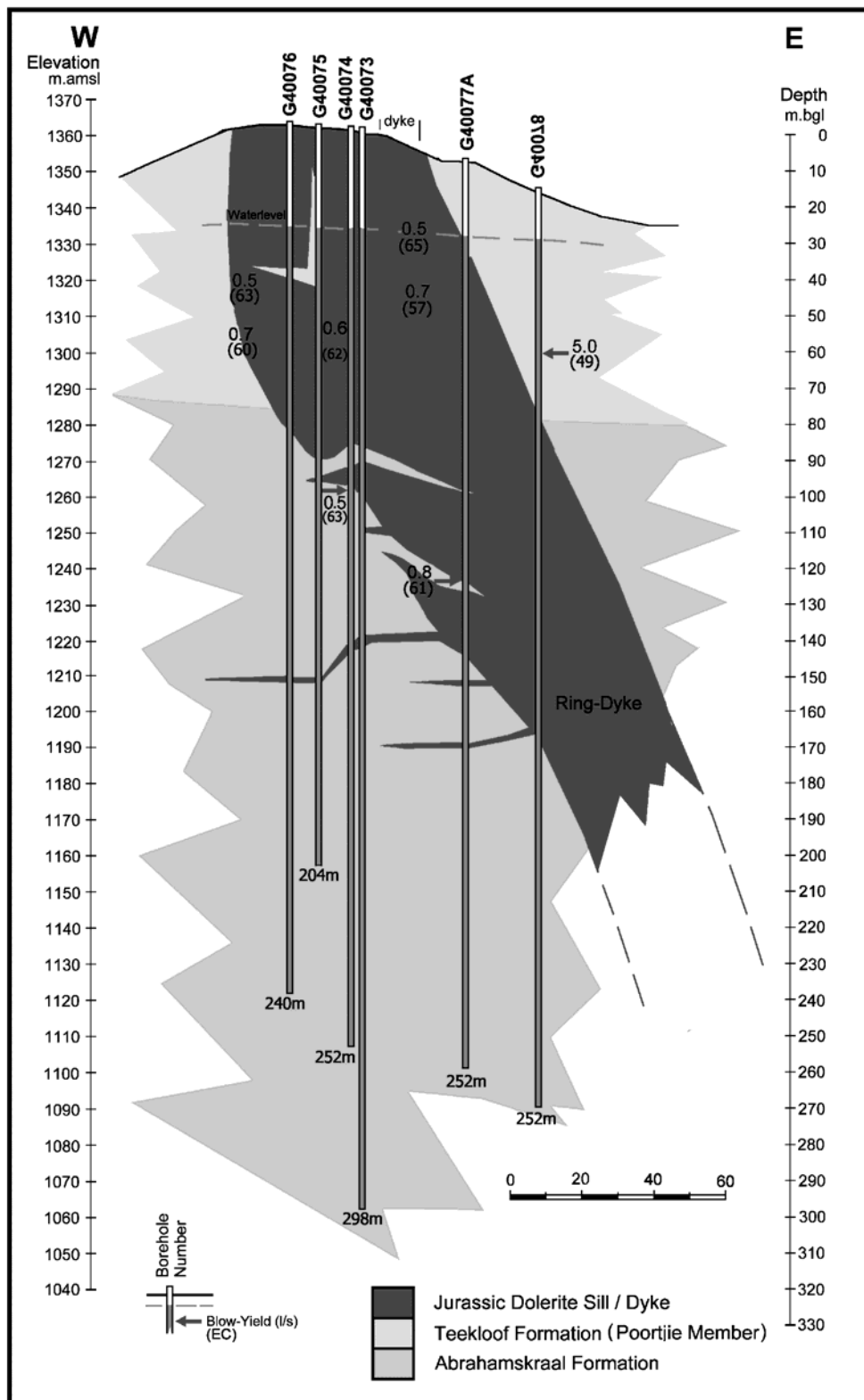


Figure 2.43: Victoria West sill- and ring-complex - Exploration Drill Site 3

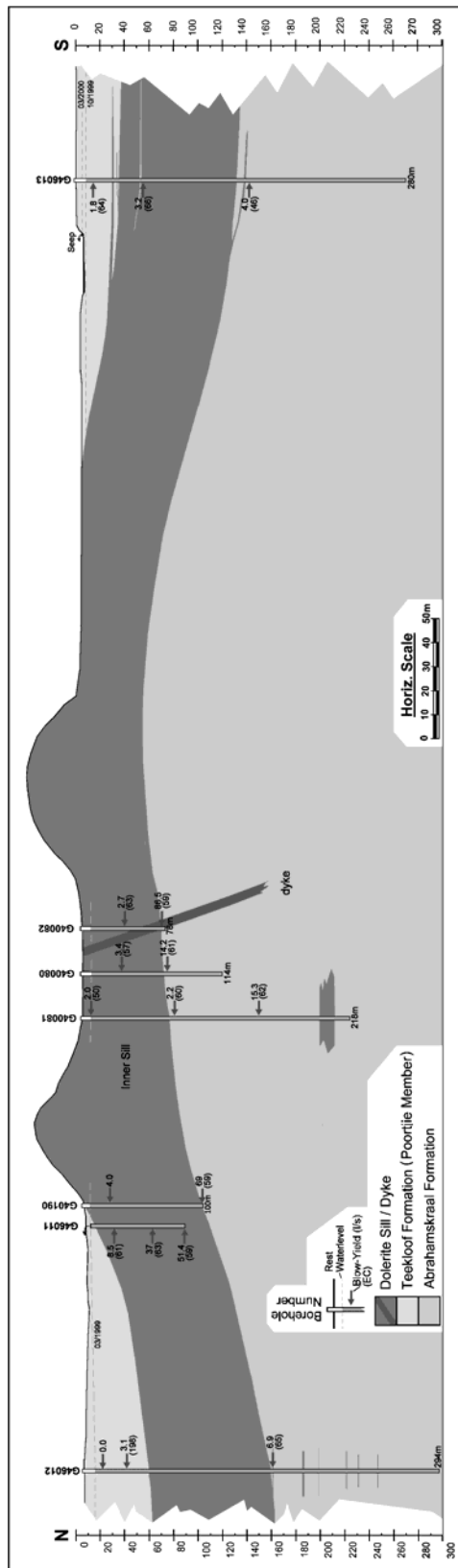


Figure 2.44: Victoria West sill- and ring-complex - Exploration Drill Site 4

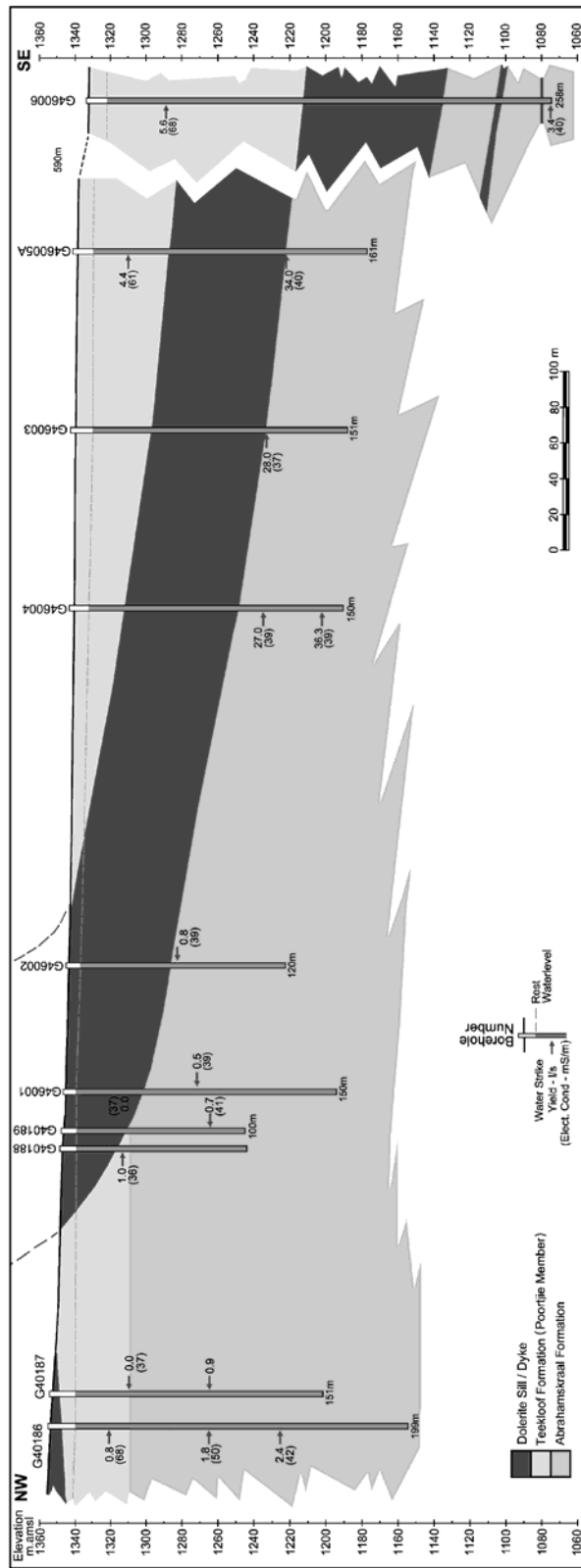


Figure 2.45: Victoria West sill and ring complex - Exploration Drill Site 5

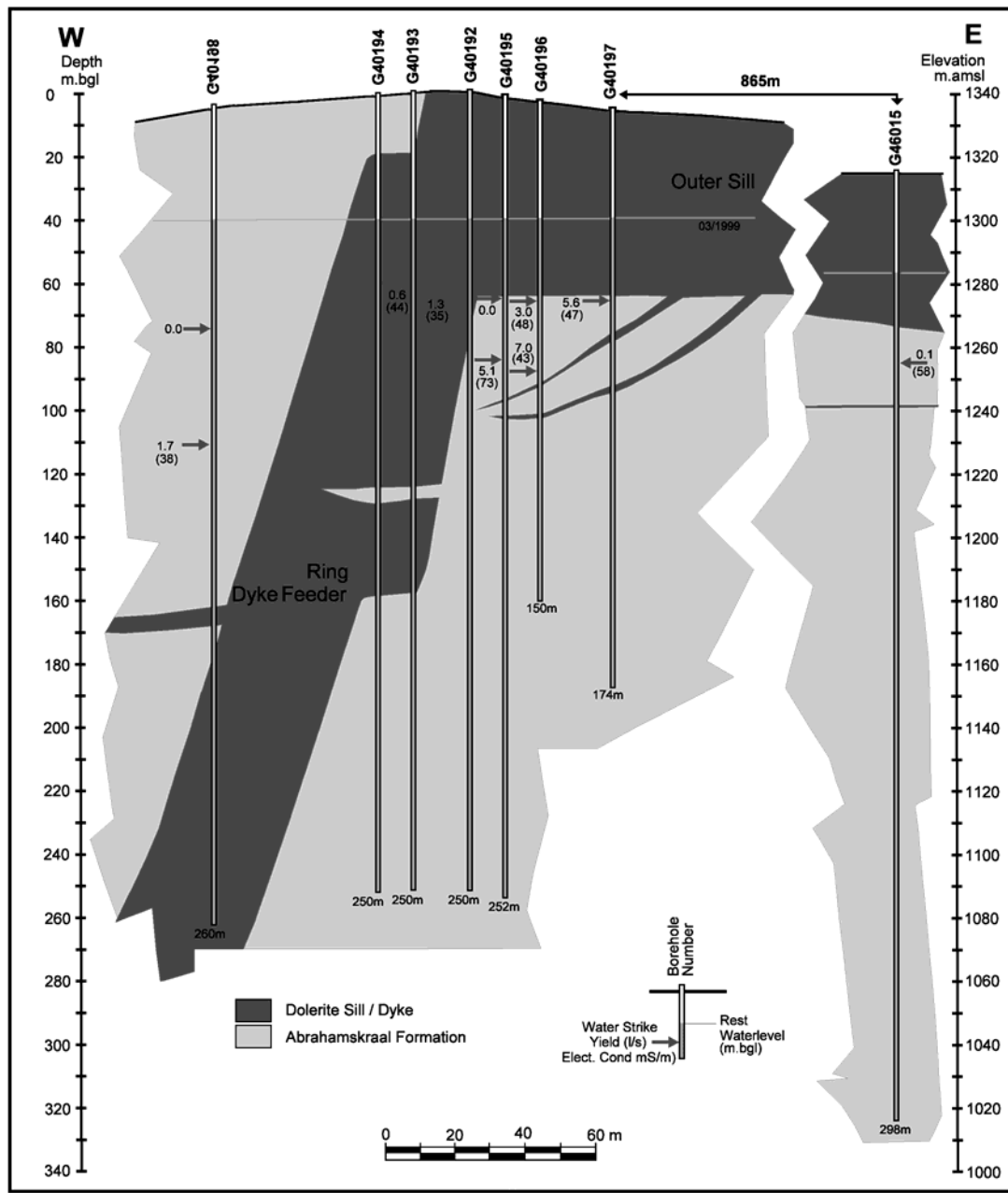


Figure 2.46: Victoria West sill- and ring-complex - Exploration Drill Site 6

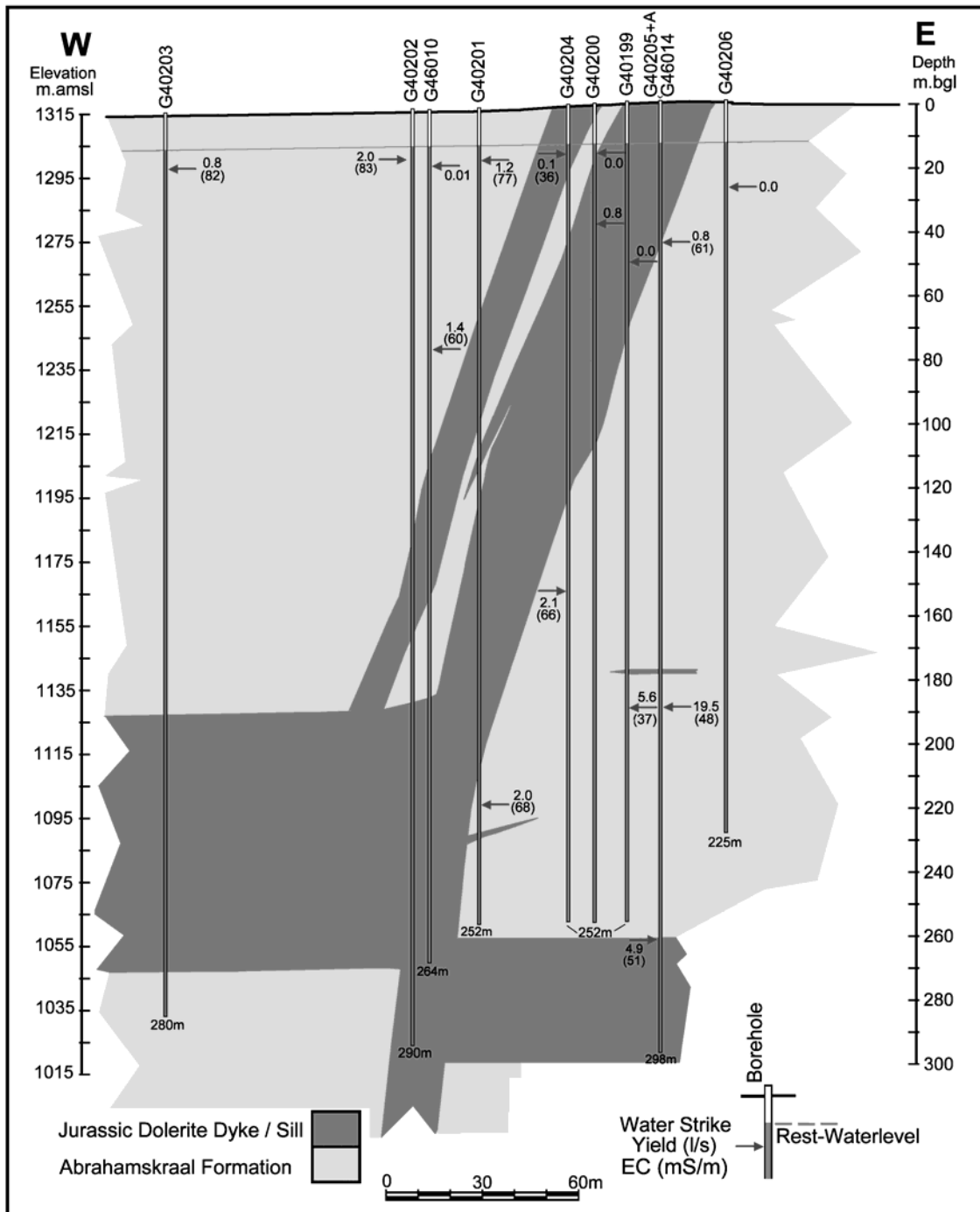


Figure 2.47: Victoria West sill- and ring-complex - Exploration Drill Site 7

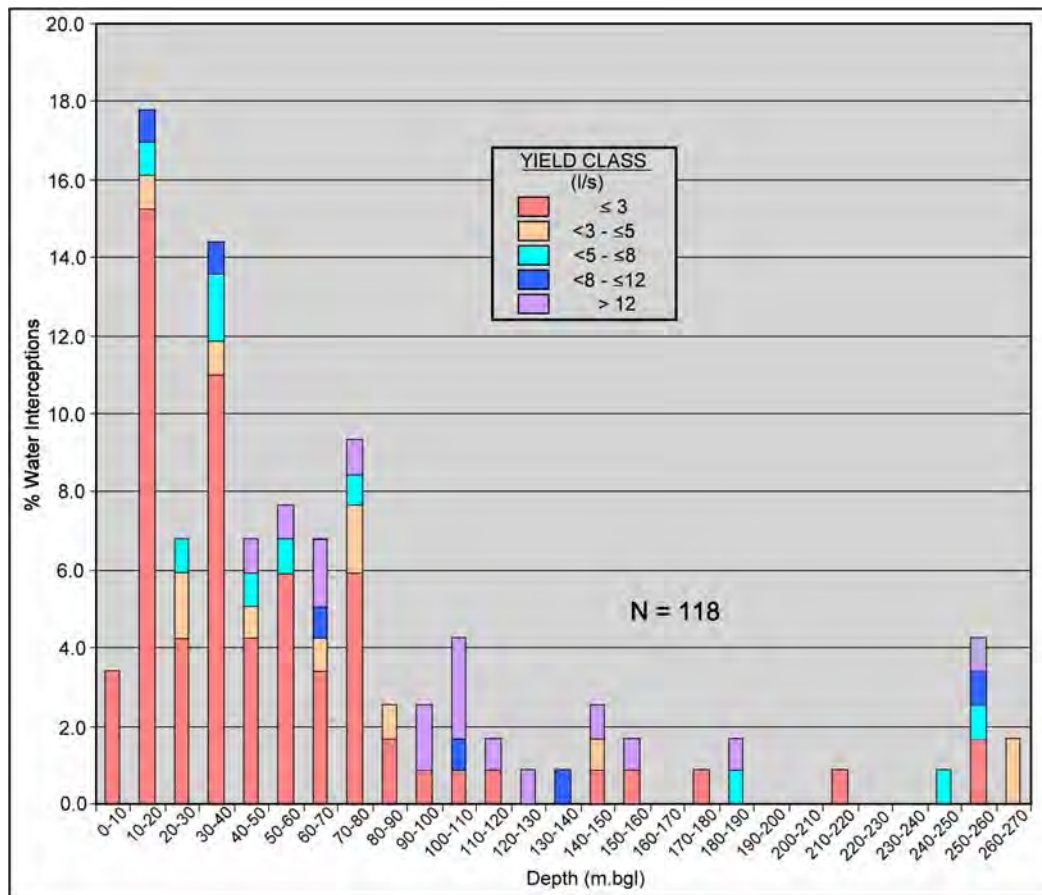


Figure 2.48: Histogram showing percentages of water-interceptions and relative percentages of drillstem yields per 10 m drilling depth intervals below ground surface

Philippolis Complex

The Philippolis dolerite sill and ring system (Colesberg 1:250 000 geological sheet, Free State) was investigated by Burger et al., (1981) and Botha et al., (1996). Different parts of the ring-dyke and sill system were targeted for exploration drilling (**Figure 2.49**).

The exploration drilling concentrated mostly upon the shallow weathered sections of the inclined sheet at Site A of the Philippolis complex. A total of sixteen boreholes were drilled to depths of between 25 and 70 m (**Figure 2.50**). The dolerite inclined sheet is some 50 m thick and is negatively weathered.

The geohydrological information obtained from the drilling programme are indicated in **Figure 2.51**. The inclined sheet is highly decomposed to a depth of 13.5 m and weathered to a depth of 15 m. Numerous water strikes were encountered between 20 and 40 m below surface. The highest water yields were intercepted along the outer contact of structure and in

the sediments away from the inner contact of the ring. No deep boreholes were drilled to test for fracturing within or below the dolerite sheet. The drilling does not exclude the possibility of a steeply dipping ring-dyke extending below inclined-sheet. Similar water-strike depths below surface were encountered at the Campus Test Site, University of the Orange Free State, and at Dewetsdorp (Botha et al., 1998), both of which are also underlain by the Adelaide Formation (mudrock and subordinate sandstone). However, it must be pointed that while the exploration boreholes at Dewetsdorp are sited along linear dykes, no dolerite dykes are present in the vicinity of the Campus Test Site. It would thus seem that this zone of frequent water interceptions is more related to the characteristic depth of weathering / erosional unloading of the Adelaide Formation in this part of the Karoo Basin, than the actual type of dolerite intrusion.

Other boreholes penetrating the Philippolis inclined dolerite sheet are 12, 13 and 14 (**Figure 2.51**). The drillstem blow-yields of boreholes 12 and 13 were considerably lower than the 4.4 ℓ/s reported by Burger et al., (1981). Borehole 14 yielded 11.9 ℓ/s, with the highest water interceptions occurring at 43, 45 and 50 m below surface. The drilling of boreholes 12 and 13 into the sheet had no influence on the waterlevels in boreholes 1, 5 and 9. However, the waterlevels in all three boreholes (1, 5 and 9) immediately responded when the first water was struck at a depth of 37 m below the sheet in borehole 14. One can thus conclude that the sheet is solid and highly impermeable, but that fractures in the baked contact zone can extend for considerable distances (± 1 km) along strike.

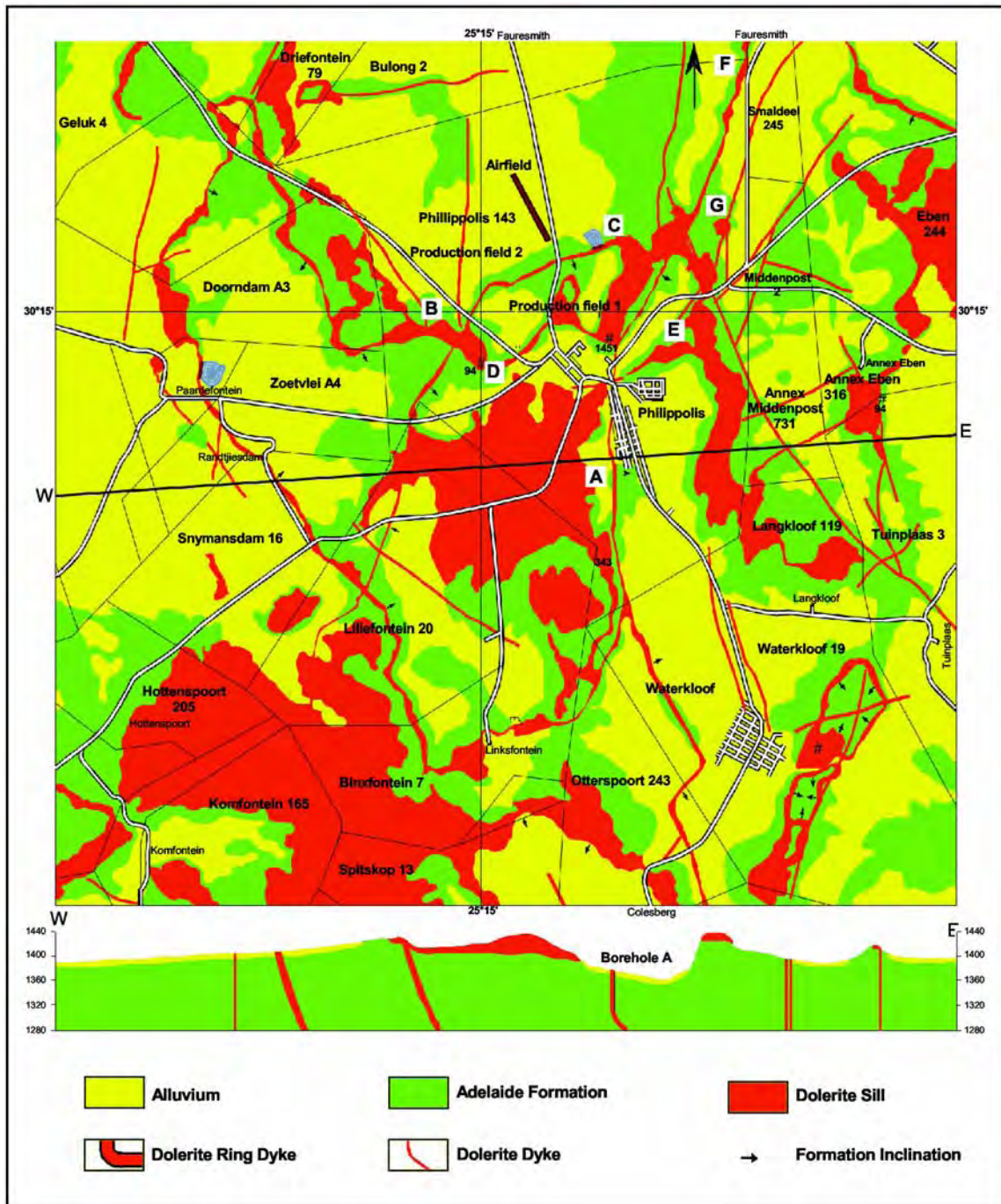


Figure 2.49: Geological map and cross-section of the Philippolis Area, Free State (after Burger et al., 1980)

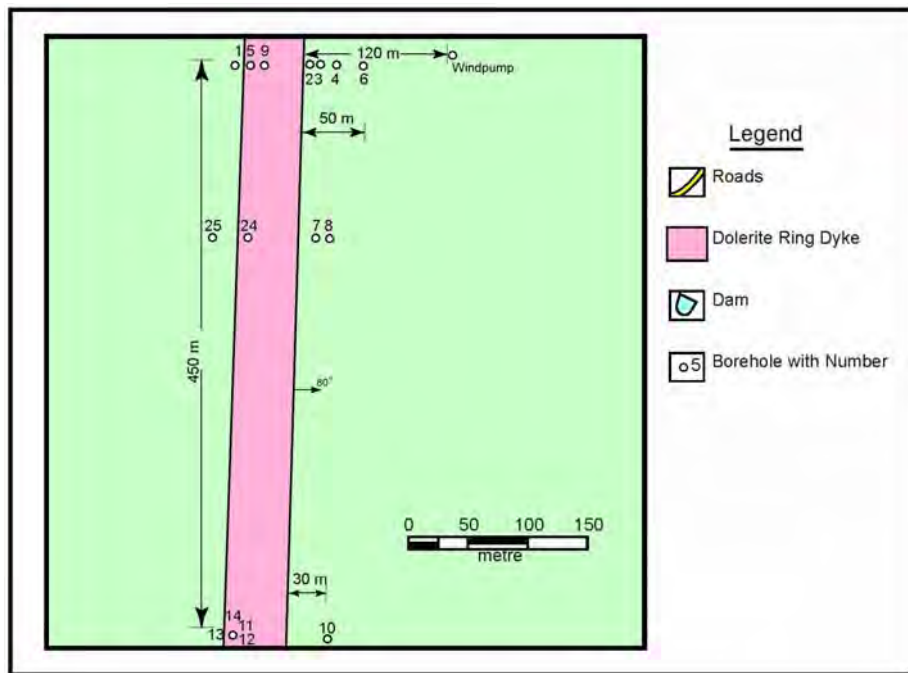


Figure 2.50: Detailed locality map of exploration drilling site A, Philippolis (after Botha et al., 1996)

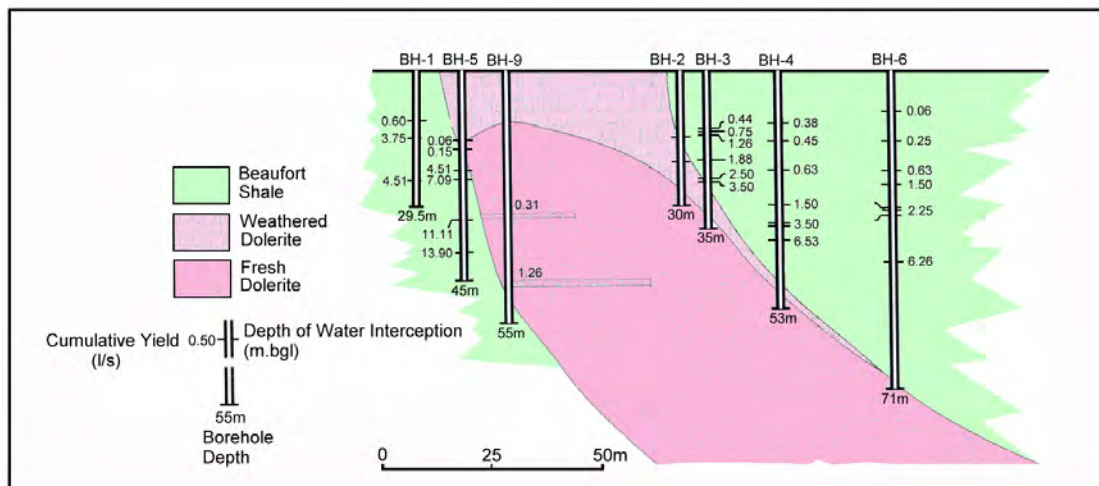


Figure 2.51: Geohydrological cross-section through the Philippolis inclined-sheet (after Botha et al., 1996)

Williston Complex

A large number of boreholes have been drilled into the Williston ring-complex (**Figure 2.52**). The boreholes penetrated the inner- and outer-sill, but missed the geohydrologically significant inclined-sheet. A second deeper, 100 m thick sill was also encountered in the northern portion of the ring system. Large differences in yield are observed between the inner-sill (low yield along the upper- and lower-contacts, as well as within the sill) and the outer-sill (high yields constrained between the upper and the lower sill contacts). This could be because the outer-sills are more intensely fractured.

Vanwyksvlei Complex

An inclined sheet on the farm Smouskolk, 18 km south of Vanwyksvlei, is controlled by dyking and regional tectonics (**Figure 2.53**). Several high-yielding boreholes were drilled into this structure (Woodford, 1992). The two boreholes drilled in the inner-sill gave poor results, whereas the six boreholes in the inclined sheet showed a higher number of individual water-strikes and relatively higher yields. Two of these boreholes, the highest yielding “freshwater” resources in the area, have since been commissioned to supply Vanwyksvlei with water. Seward (1982) drilled a number of boreholes alongside a major E-W en-echelon dolerite dyke, of which two were successful and yielded more than 2.0 ℓ/s.

Calvinia Complex

The Calvinia area is characterised by a succession of extensive, flat-lying sills. Directly north of Calvinia, the Kareedam sill shows a ‘step-up’ and this change in stratigraphic level is accompanied by a thinning out of the structure (**Figure 2.54**). A number of the boreholes are drilled into the lower contact of the structure and delivered moderate blow-out yields (Seward, 1983). Most of the boreholes were not drilled deep enough to test the upper-contact of an extensive, thick underlying sill. Borehole CT59 yielded 5.6 ℓ/s on this contact, while G32626 and G32635 yielded variable results. This illustrates the point that has been made by many authors (Van Wyk, 1963; Vegter, 1951), that high-yields are occasionally intercepted at certain localities on sills - both in the upper- and lower-contact, and especially near the sill edge. The authors state that the action of weathering played a major role in locally enhancing the permeability of incipient joints.

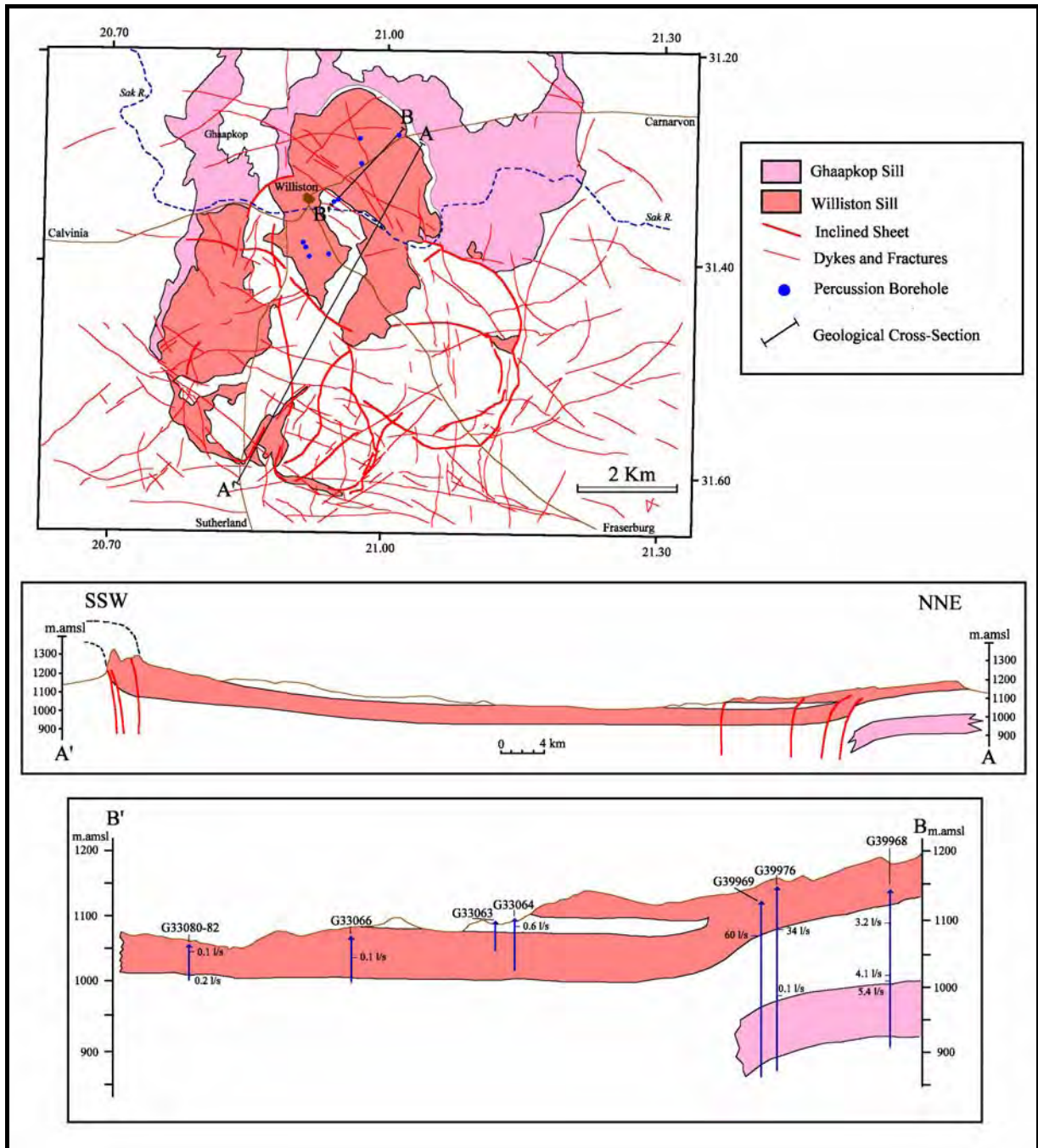


Figure 2.52: Hydrogeology of the Williston Dolerite Ring-Complex (Chevallier and Woodford, 1999)

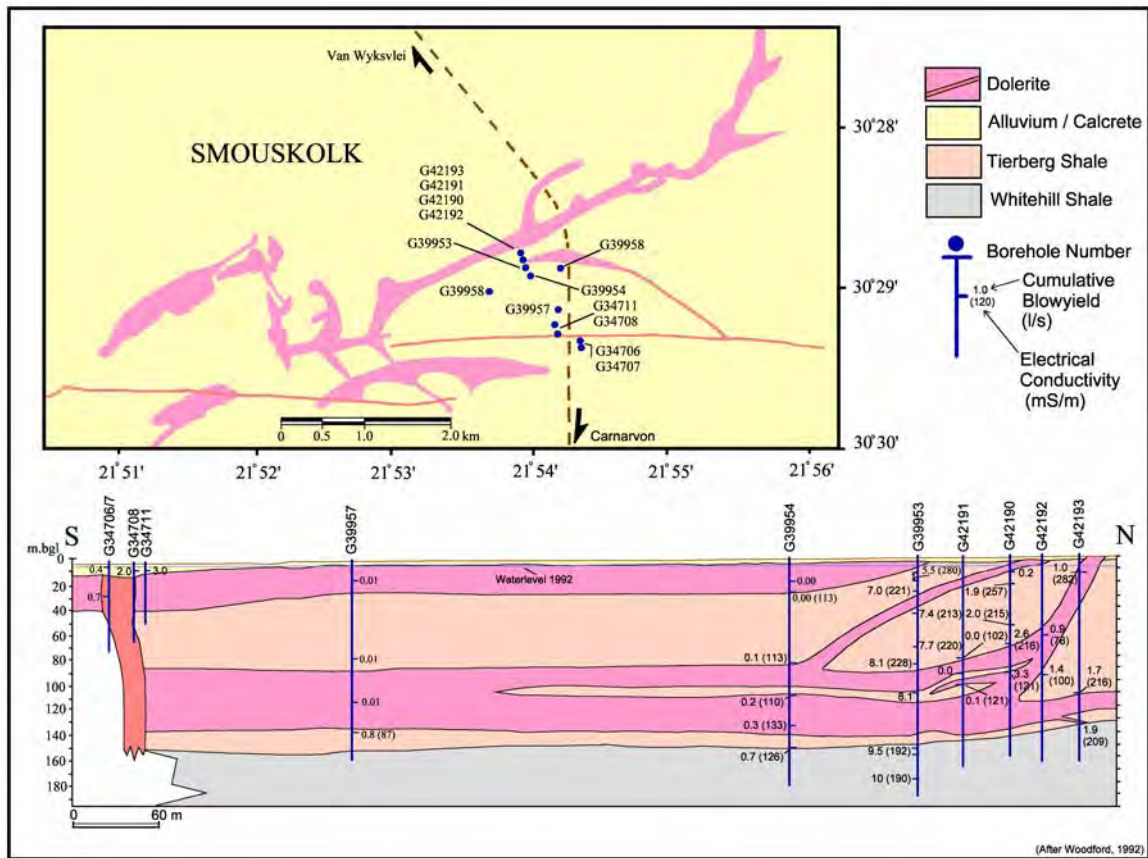


Figure 2.53: *Geohydrology of the Inclined Sheet of the Vanwyksvlei Dolerite Ring-Complex (Woodford, 1992)*

Queenstown Complex

The Hopefield boreholes (Vandoolaeghe, 1980), west of Queenstown, were drilled into the transition zone between an *inclined-sheet* and the *outer-sill* of a ring-complex (Figures 2.26(b), 2.35 and 2.38(a)). The regular depth and yield of individual water-strikes suggest the presence of three sub-horizontal fractures that transgress the structure and extend into the host sediment. High borehole yields were struck within the dolerite in this transition zone, as well as in the often highly-fractured hinge zone between the outer-sill and the inclined-sheet at the base of the dolerite body.

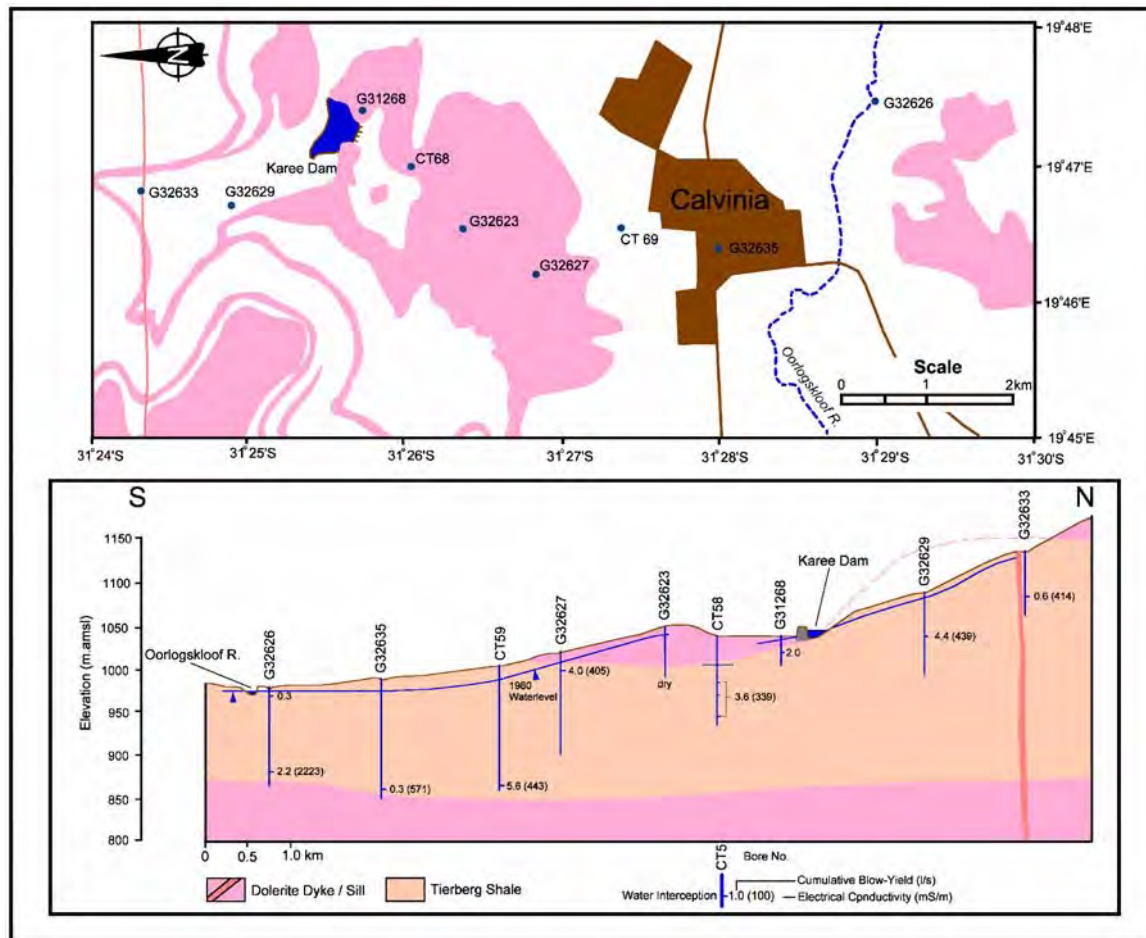


Figure 2.54: Geohydrology of an extensive, undulating sill, not related to a dolerite sill- and ring-complex (Chevallier et al., 2001)

Other Complexes

Similarly high yields were intercepted in the upper- and lower-contacts of the Dalham *outer-sill* and *inclined-sheet* intersection, north of Graaff-Reinet (**Figure 2.24(a)**), after Woodford, 1983). Vandoolaeghe (1979) obtained high-yields in the lower contact of an inclined-sheet, which forms part of the Matjieskloof ring-complex, near Middelburg (**Figure 2.55**). The influence of weathering on fracturing in the near surface zone is clearly evident, although no boreholes penetrated the potentially fractured lower contact of the sheet. The *inner-sill* / *inclined-sheet* intersection zone of the Roodekraal ring-complex, southeast of De Aar (**Figure 2.56**), contains high-yielding open fractures (Woodford, unpublished data).

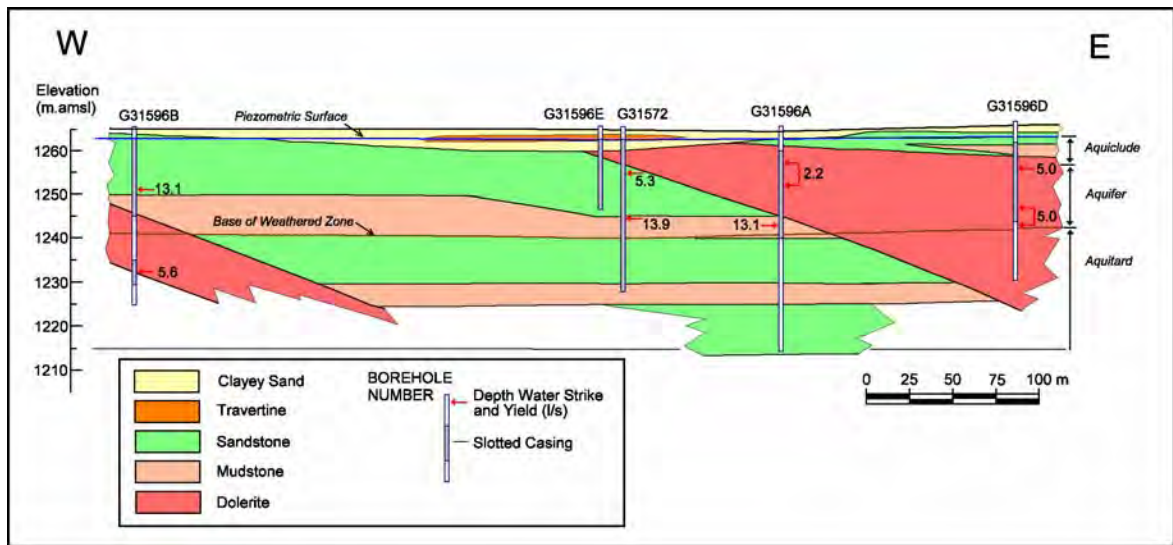


Figure 2.55: *The occurrence of groundwater on the weathered lower contact of an inclined-sheet, Middelburg (Vandoolaeghe, 1979)*

Summary

At the scale of the Karoo Basin, it is not presently possible to associate the occurrence of groundwater in ring-complexes with any particular stratigraphic level of intrusion, but they do not occur above the Molteno Formation (**Figure 2.1**).

The hydro-morpho-tectonic model (**Figure 2.57**) represents a synthesis of a WRC research project on the dolerite sill- and ring-complexes (Chevallier et al., 2001) of the western Karoo. A mechanism of emplacement of these saucer-shape intrusions has been proposed by Chevallier and Woodford (1999) and Chevallier et al., (2001), wherein the inclined-sheet that forms the ‘back-bone’ of the system is fed by regional vertical dykes (**Figure 2.38(a)**). Inclined-sheets feed both the inner- and the outer- sills. Some rings are not linked to a feeder-dyke system and can be the result of simple uplifting and up-stepping at the ‘tips’ of sills, as proposed in the laccolith model of Burger et al., (1981) (**Figure 2.38(b)**).

Exploration drilling has shown that water-bearing open fractures develop at specific locations within the dolerite and surrounding host rock, i.e. at the junction between a feeder dyke / inclined sheet and a sill (**Figure 2.37**), in the sediment above an up-stepping sill or at the base of an inner-sill (**Figure 2.57**). In the first case fracturing is very localised, whilst in the second and third cases shear and ‘open’ fractures can extend some distance away from the dolerite contact into the country rock. These zones represent challenging exploration target that requires drilling of deeper (200-350 m) boreholes.

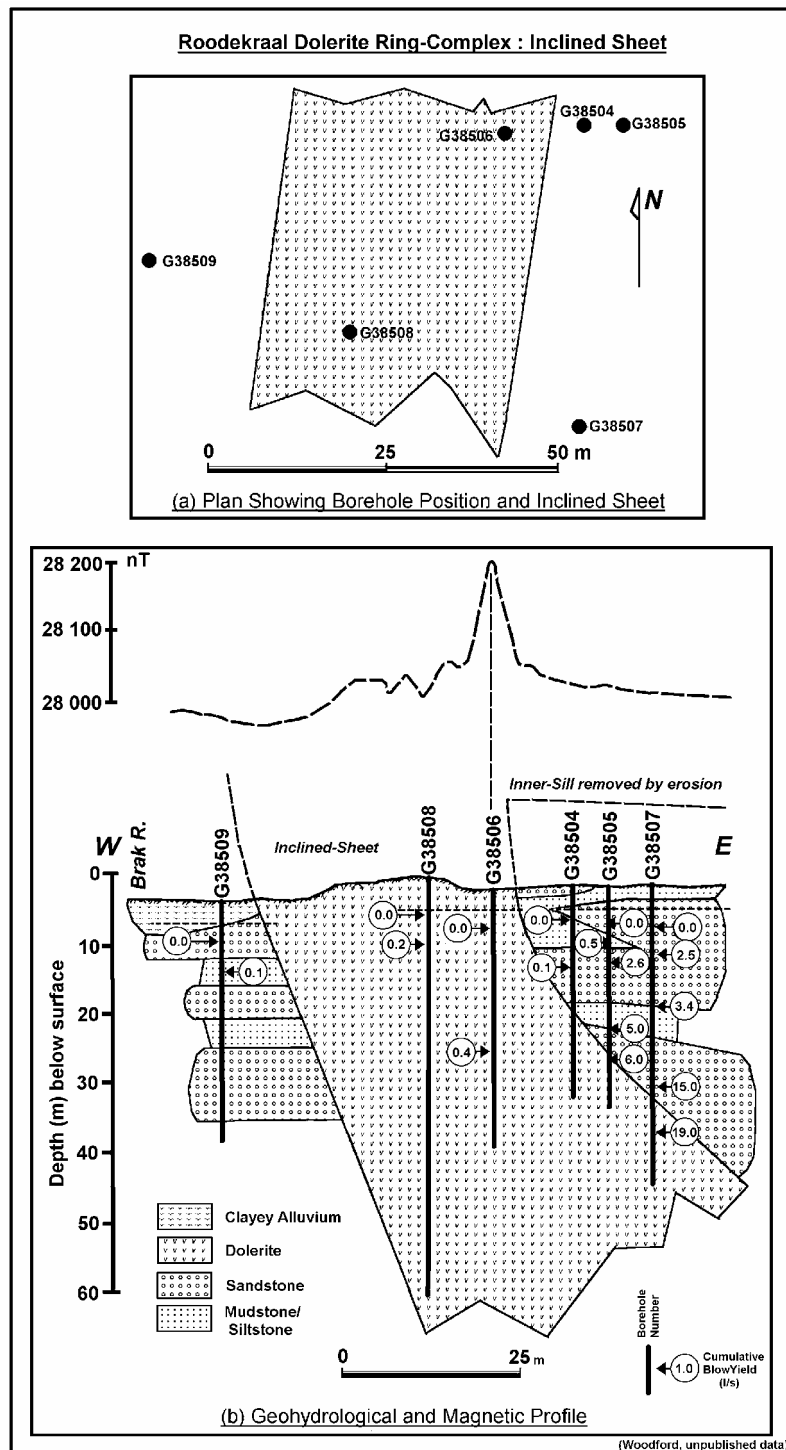


Figure 2.56: Geohydrology of the Roodekraal Inclined-Sheet, De Aar (Woodford, unpublished data)

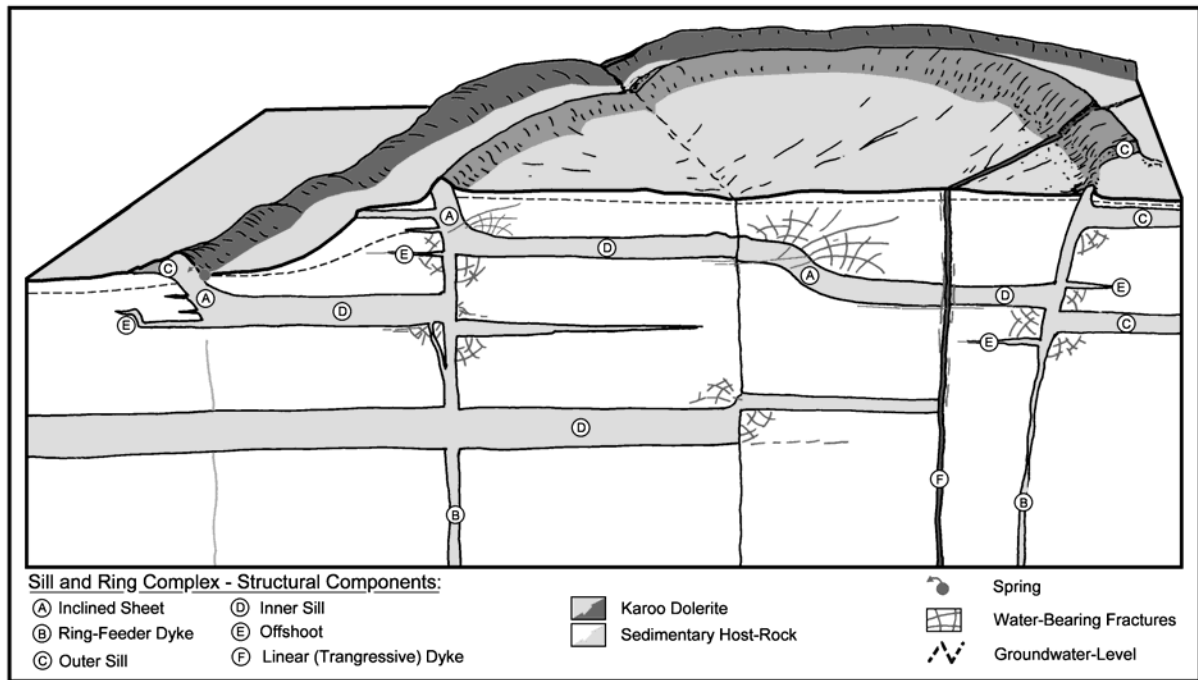


Figure 2.57: *Hydro-morphotectonic model of a dolerite sill- and ring-complex, detailed fracture pattern for inclined sheet indicated in Figure 2.37 (after Chevallier et al., 2001)*

2.3.2.2 Breccia Plugs and Volcanic Vents

Although breccia plugs and volcanic vents occur in different geographic areas and at different stratigraphic levels, they display similarities in their size, shape, texture and hydrological properties.

Dolerite Breccia Plugs

Few Karoo breccia plugs or pipes have been reported in the literature. The breccia plugs were thought to be of Cretaceous age, because of their proximity to the Salpeterkop Volcanic Suite (diatremes, olivine melilitite, kimberlite, etc.) and their apparent association with swarms of kimberlite fissures in the western Karoo. Until recently virtually no such research has been conducted on these features. From 1993 to 1996 the Department of Water Affairs and the Council for Geoscience conducted research into their distribution, constitution and geohydrology in the Western Karoo (Woodford and Chevallier, in prep.).

Distribution

Clusters of breccia-plugs occur along the western and northern edges of the Karoo Basin. They are mostly restricted to the Ecca Formation (**Figure 2.58**). Only the Skurkop plugs on the edge of the western escarpment and the isolated Muldersfontein plug, east of Middelpos, are known to have penetrated the base of the Beaufort Group. Breccia plugs are certainly not restricted to the western Karoo and therefore many probably occur further to the northeast within the same geological formations. Clusters are variable in size from a few hundred metres (Williston with only two plugs) to 50 km in diameter (Loeriesfontein with more than 80 plugs).

Description

Breccia plugs commonly form small, low-relief, circular hills, averaging 50 to 80 metres in diameter. They also occur as circular, negative-relief depressions of a similar dimension with characteristic calcrete development. On aerial-photographs they are easily recognisable by the presence of a white alteration halo around them, while only the larger breccia plugs are visible on Landsat TM imagery.

Two main facies are recognised (Woodford and Chevallier, in prep.):

- (a) *Molten Facies* - domed, baked, molten, re-crystallised and highly contorted sediment containing xenoliths from the underlying strata. Melting is often accompanied by gas-vugs, which are commonly filled with secondary calcite, quartz and to a lesser extent grossular and vesuvianite.
- (b) Breccia Facies – a true breccia with fractured, broken, shattered, displaced and re-cemented blocks of sediment. This facies is often accompanied by mineralization of quartz, calcite, gypsum, chlorite, apophyllite, baryte, siderite, fluorite, pyrite, pyrrohotite, sphalerite, galena, chalcopyrite, marcassite, bornite and traces of gold.

The (a)-type is the most frequently encountered in the field, whereas the (b)-type is much less common. This is probably because the (a)-type plug is more resistant to erosion and produces more easily detectable features of positive relief (**Plate 2.5**). The (b)-type erodes more easily, resulting in the less conspicuous features of negative relief. The degree of mineralisation of the plug is not always evident from outcrop.

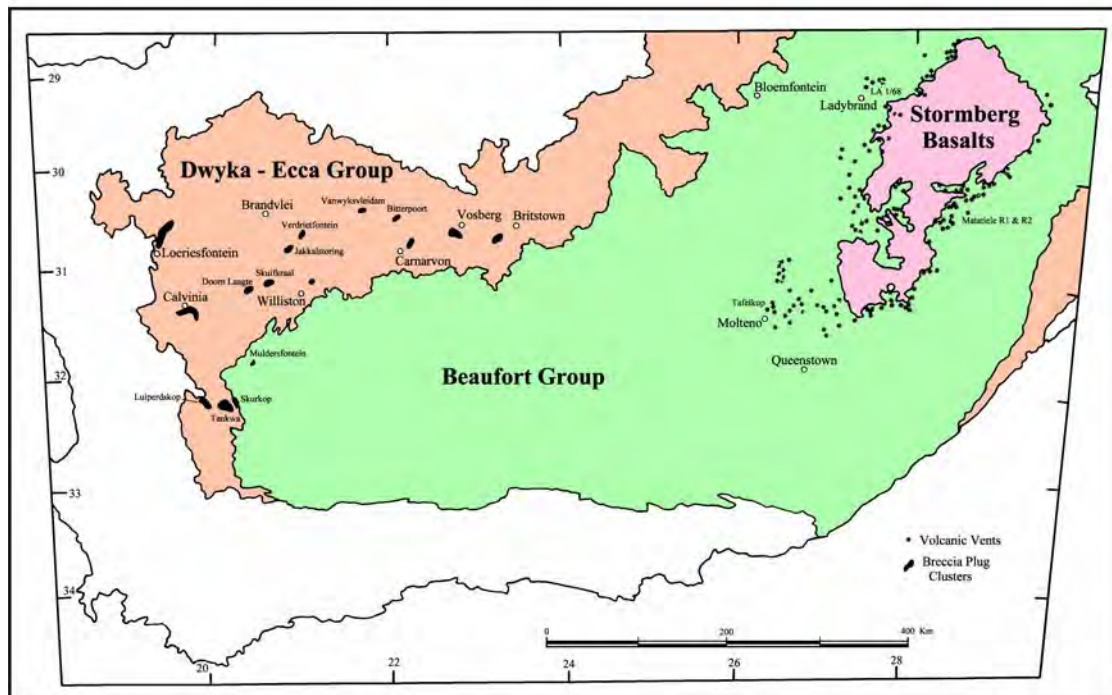


Figure 2.58: Distribution of mapped Breccia Plugs and Volcanic Vents in the Karoo Basin

A large number of boreholes were drilled into the breccia plugs using air-rotary percussion rigs. The nature of drill-chips recovered made it impossible to accurately distinguish between the two facies types. However, two breccia plugs of the Calvinia cluster (Kopoasfontein and Platberg) were drilled using a wire-line core-rig by the Department of Water Affairs and the full sequence of facies was thus recorded (**Figure 2.59**). A third borehole (G39974) was sunk at Kopoasfontein, some 500 m away from borehole G39856, in order to obtain an undisturbed stratigraphic sequence. The core-logs show that the lithological units are locally highly disrupted, but that no major stratigraphic dislocation occurred as a result of the hydrothermal activity.

The Whitehill Formation is highly baked and leached in the vicinity of the breccia plugs. It is transformed from a pitch-black, finely bedded, pyrite-rich, carbonaceous shale to a white contorted and dislocated meta-sediment. The true breccia facies, in both cases located in the upper sections of the plugs, contain numerous openings and large cavities (up to 9 m in depth) with extensive mineralisation. Borehole G39856 encountered highly-pressurised methane gas at 109 m.bgl in such a cavity.

The breccia plugs at Calvinia are linked to the intrusion of two dolerite sills at the Dwyka-Prince Albert and Prince Albert-Whitehill Formation contacts. Several features indicating molten fusion occur at the interface between the dolerite and the sediment, i.e. injection of doleritic magma within the sediment and digestion of sediment by the dolerite. The mineralisation in the Prince Albert Formation is zoned with grossular and vesuvianite, and with sulphides in the overlying Whitehill Formation. This was confirmed by drilling into breccia plugs outcropping in the Prince Albert Formation at Loeriesfontein, where large amounts of large grossular crystals occur. Sulphide mineralisation only occurs in breccia plugs that outcrop within the Tierberg Formation (i.e. above the Whitehill Formation).

Mode of Emplacement

Woodford and Chevallier (in prep.) propose that localised hydrothermal activity (often explosive), occurred when the early (lowermost) dolerite sills intruded into the partially indurated, “wet” Karoo Supergroup sediments. This resulted in the brecciation and melting of the host sediments, as well as the mobilisation and upward transport of elements from the Whitehill and Prince Albert Formations.

The breccia plugs do not contain any economical sulphide mineral deposits due to the absence of a suitable lithological trap, such as a thick carbonate-rich unit, for the concentration of relevant elements. However, lime-rich concretions found in the vicinity of certain plugs (Koffieklip) often contain a mineral-enriched weathered crust. These concretions vary in size from a few centimetres to a metre in diameter. The most spectacular example of this occurs in the vicinity of the Vosburg plugs, where malachite staining is found.

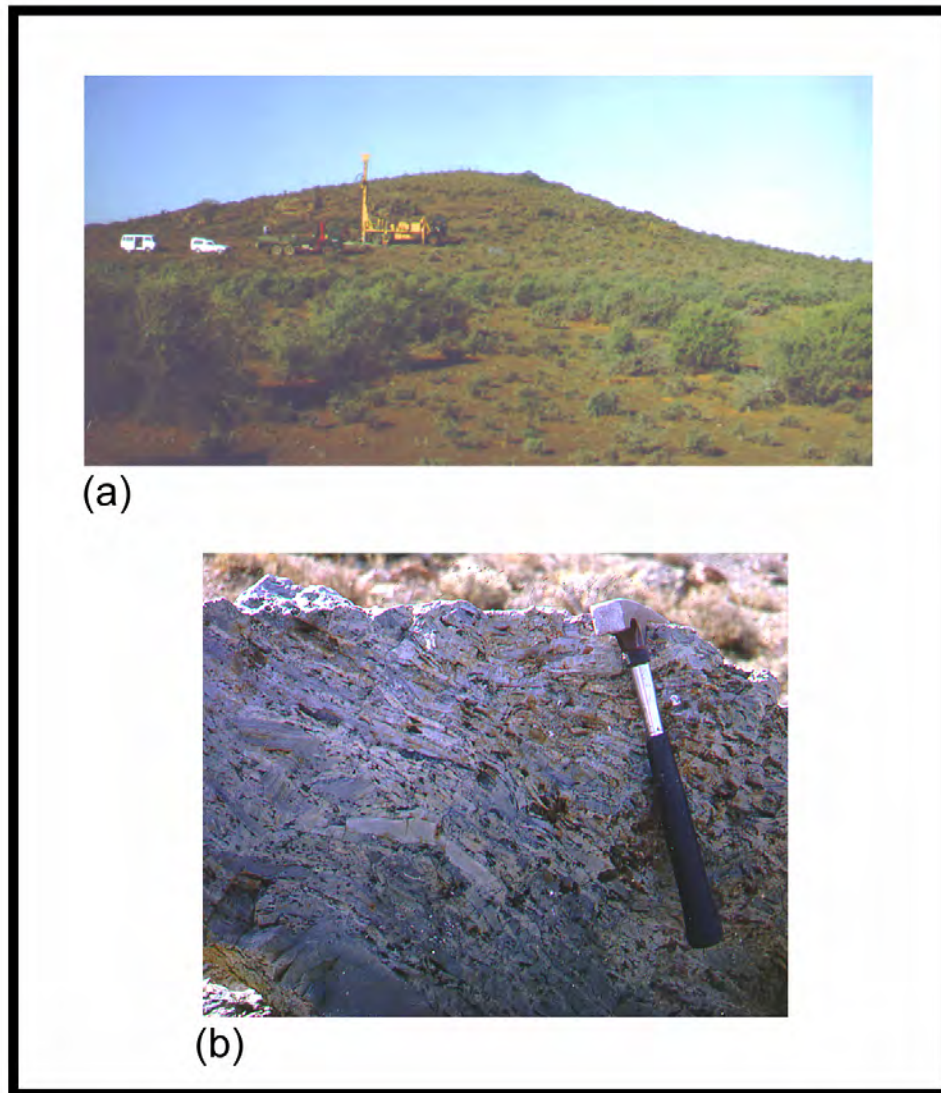


Plate 2.5: *Breccia Plugs (a) the positive-relief Jagkop plug on the Farm Lower Zwartrand in the Carnarvon district (3022CD), (b) tourmaline-rich breccia, showing flow alignment of sediment blocks, on the Farm Bo-Downes in the Calvinia area*

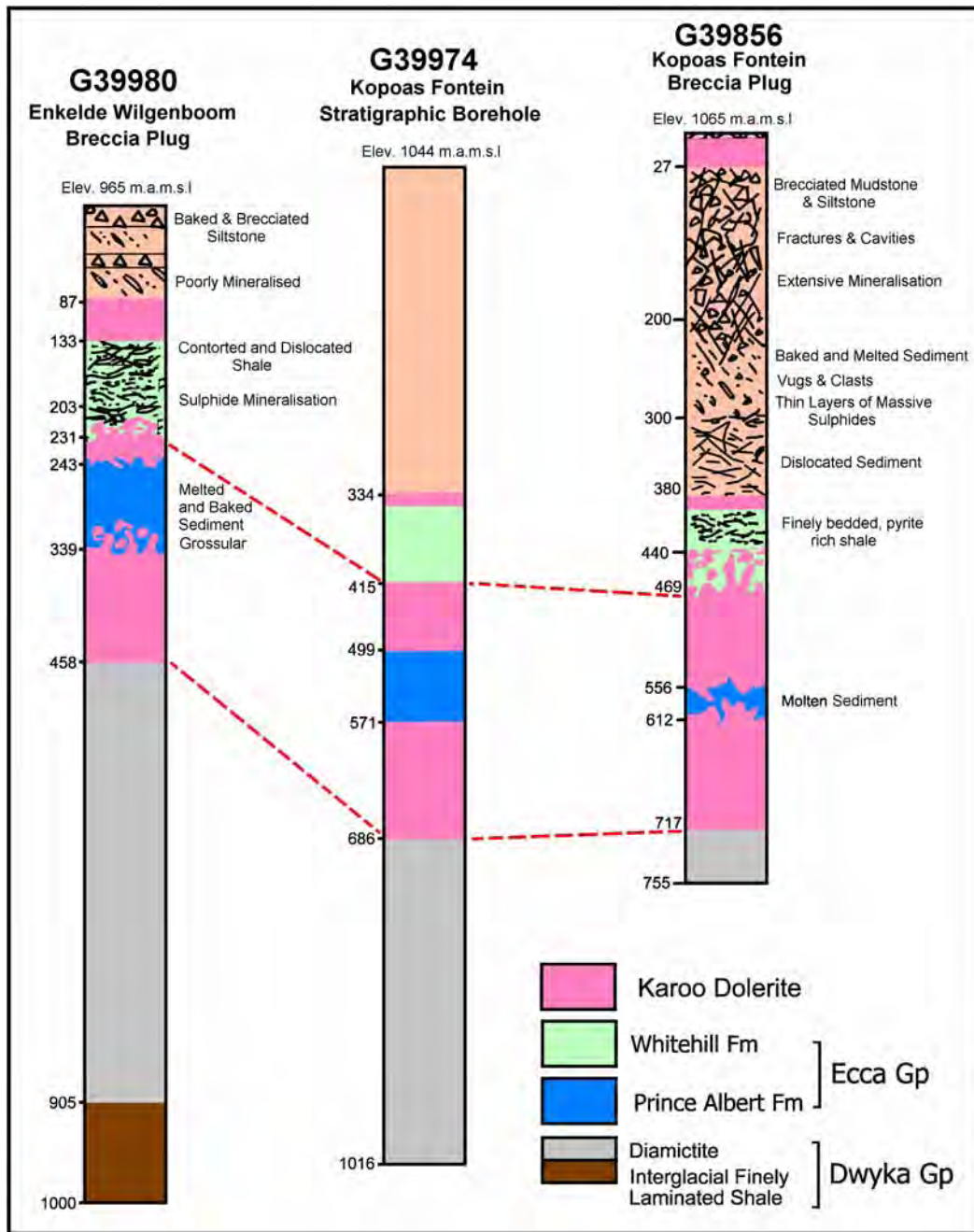


Figure 2.59: Geological logs of core-boreholes drilled into breccia plugs and a stratigraphic borehole

Volcanic vents

Distribution

Many volcanic vents (also referred to as “necks” or diatremes by various authors) have been located at the foothills of the Drakensberg Mountains, since their first discovery and description in East Griqualand by Du Toit in 1929 (**Figure 2.58**). They are restricted to the Clarens Formation and occasionally occur in the Drakensberg basalts. They represent the first volcanic outbursts that preceded the outpouring of the lava flows.

Description

The shape and size of the vents vary in diameter from few metres to a couple of kilometres at Tafelkop. In the literature, Du Toit (1929) described a typical vent as “a mixture of agglomerate and yellowish tuffs made up of shattered and pulverized sandstone from the Clarens Formation, and containing clasts of dolerite and amygdoidal basalt”.

A core-borehole (LA 1/68) was drilled by SOEKOR in 1968 just north of Ladybrand (**Figure 2.58**). The log reveals a relatively deep structure of 170 m, filled with a layered succession of block- and matrix-supported breccia, as well as tuffs (**Figure 2.60**). The blocks are angular, varying in diameter from a few centimetres to 2 m and are composed of dolerite, vesicular basalt and sandstone. The matrix consists of shattered and rounded sandstone pebbles set in a finer remobilised quartzitic and feldspar-rich groundmass. The basal section of the vent contains mostly tuff and layered-brecciated sandstone. Extensive calcite cementation has occurred throughout the breccia. Sorting is evident within each unit. No juvenile magma (bombs, accretionary lapilli, glass chards or expanded scoria) was found. Brecciated and fractured Clarens Formation sandstone occurs directly below the vent.

Another possible brecciated volcanic vent was drilled for groundwater near Matatiele in the Eastern Cape (**Figure 2.58**). The borehole was drilled to a depth of 42 m and the geological log indicated the presence of weathered breccia, clay-rich breccia, and chloritized breccia (Murray, 1996).

The upper-portion of the volcanic vents has commonly been removed by erosion. However, the Tafelkop (**Figure 2.13**) vent displays the volcanic features characteristic of aerial surge and fall deposits, viz. aerodynamically shaped bombs, lamination, cross-bedding, dunes and lenses of coarse material (Marsh, 1991).

Mechanism of Emplacement

The volcanic vents or diatremes were probably formed by phreatic-explosive activity, where excessive water and steam pressures overcome that of the magma, resulting in fragmentation of the country rock and poor participation of the magma (Marsh, 1991). Phreatic-explosions occur when an intruding magma encounters a groundwater body – causing shattering, fluidisation and mobilisation of the host sediments and/or the surrounding basalt. Layering, floating and sorting of clasts commonly occurs inside the slurry that fills the diatreme during eruption (Kokelaar, 1983).

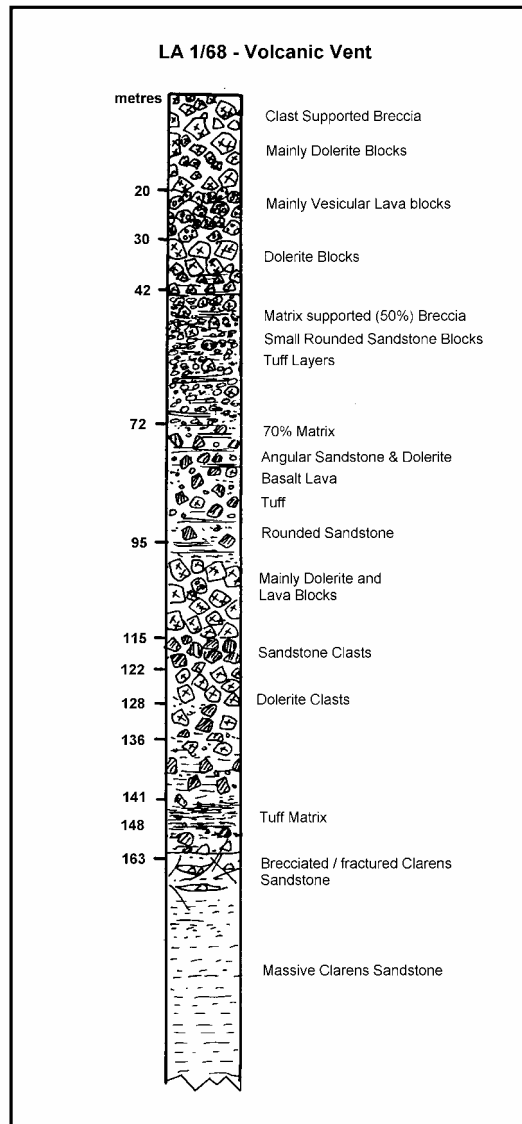


Figure 2.60: Geological log of stratigraphic borehole LA1/68, near Ladybrand

Hydrological Properties

Breccia plugs and volcanic vents are both pipe-like structures filled with brecciated and fractured material. They constitute highly permeable targets for groundwater exploration because of their geometry and large vertical extent of uniformly fractured / brecciated material (**Figures 2.59** and **2.60**), but because of their limited size are only of significance as conduits for rapidly extracting water from the subsurface. The sustainable yield of a borehole penetrating such a structure is therefore determined by the local recharge conditions and storativity of the host rocks.

The Department of Water Affairs and Forestry explored several breccia plugs from various clusters over the period 1992 to 1996, at Luiperdskop, Calvinia, Doorn-Laagte, Bitter Poort and Carnarvon (Woodford and Chevallier, in press) and by Toens & Partners Groundwater Consultants at Loeriesfontein. To date some 26 boreholes have been drilled into or alongside these plugs. The high success rate of boreholes, 70% yield in excess of 3 ℓ /s, sited on these plugs is clearly evident from **Table 2.7**; especially considering the low-yields generally encountered in Ecca shale in the Western Karoo.

Table 2.7: Yield of boreholes drilled into breccia plugs

Final borehole blow-yield range (ℓ/s)	Number of boreholes within range	% Boreholes within yield range
Dry	1	3.8
> 0 and ≤ 1	2	7.7
> 1 and ≤ 3	5	19.2
> 3 and ≤ 5	7	26.9
> 5 and ≤ 10	7	26.9
> 10	4	15.5
Total	26	100

Two deep boreholes core-boreholes were drilled into the plugs at Enkelde Wilgenboom and Kopoasfontein, which form part of the Calvinia cluster (**Figures 2.58** and **2.59**). Within each of the plugs the major stratigraphic units are preserved despite strong brecciation, fracturing, melting and remobilization of the host rock. The following aspects of groundwater occurrence would appear to be characteristic (Woodford and Chevallier, in prep.):

- Towards the top of the stratigraphic section in which they are confined, i.e. within the Tierberg Formation siltstones, the brecciation and fracturing are poorly developed. Fewer individual water strikes are recorded and yields are generally low (i.e. the breccia plugs in the Carnarvon cluster).

- Thick zones of true breccia and fracturing, cavities and mineralisation are mainly developed Tierberg Formation shales, below the above siltstone horizons. Boreholes intercept numerous high-yielding zones. The plugs of the Calvinia cluster are a good example. Borehole blow-yields of 3 to 80 ℓ/s were recorded on these features.
- Brecciation is less well developed within the White Hill and Prince Albert Formation shale, although intense fracturing and dislocation can occur at places. Only a few boreholes drilled into the plugs have actually tested this stratigraphic horizon, but it would appear that borehole yields improve towards the north (Loeriesfontein) and east (Bitter Poort) of Calvinia.
- The majority of the high-yielding water strikes occur at a depth of 60 to 150 below surface, while three of the boreholes intercepted individual water strikes in excess of 15 ℓ/s at depths of 150-200 m. In borehole G39856 at Kopoasfontein the upper 70 m, although highly brecciated, only yielded seepage inflows as the open-cavities were completely sealed by secondary calcite.
- Groundwater struck below 100m commonly has elevated fluoride concentrations (3-12 mg/ ℓ). In Calvinia, Vanwyksvlei and Bitter Poort the electrical conductivity (EC) of the “deeper” water interceptions (>150 m) is often considerably fresher than the groundwater in the “upper” aquifer (30-60 m). For example, shallow water-strikes in borehole G39859 at the golf-course in Calvinia had EC values around 300 mS/m, while the EC of the high-yielding (> 15 ℓ/s), deeper water is about 120 mS/m.
- The younger dolerite sills transgress these features and may remove the important water-bearing zone(s).
- The size and geometry of the target feature makes it possible to easily locate and site successful boreholes, without the added costs of geophysical surveys often required in locating discrete fracture zones. For example, at borehole G39856, the drilling target is an oval-shaped highly permeable body of 100 m in diameter and 270 m in vertical thickness.

In conclusion, high-yields in excess of 8 ℓ/s are almost always encountered in the intensely brecciated sections of a plug. However, the plug itself is only a highly permeable conduit for groundwater flow, similar to a dyke, and it is the rate of recharge from and storativity of the country-rock “reservoir” that will ultimately determine the sustainable yield of boreholes tapping these features. The breccia plugs, because of they originate at the base of the Karoo, present an excellent opportunity to investigate the occurrence of deeper groundwater in the Karoo.

Very little information has been published on the occurrence of groundwater in volcanic vents. SOEKOR’s borehole LA1/68 (**Figures 2.58** and **2.60**), near

Ladybrand yielded 38 ℓ/s between 35 and 80 m below the surface. A borehole drilled by the Rural Support Services (Murray, 1996) into a presumed brecciated volcanic vent near Matatiele (**Figure 2.58**) yielded 20 ℓ/s at 40 m.

The occurrence of groundwater in volcanic vents would appear to be similar to that in the breccia plugs and thus they represent easily located drilling targets for high-yielding boreholes because of their shape, size and degree of brecciation. These features have to date been largely overlooked by geohydrologists – but they may prove to be the most important groundwater exploration targets in the Clarens Formation, where the sandstone are poorly fractured and have a low permeability (**Chapter 2.2.4**).

2.3.2.3 Kimberlite and Associated Alkaline Intrusive Complexes

Distribution

Kimberlites occur as clusters of linear or arcuate swarms of dykes and fissures associated with several enlargements, blows or pipes. **Figure 2.61** indicates the geographical extent of kimberlite dykes and associated fractures in the Karoo. This map was compiled from research conducted by Chevallier (1997) in the Western Karoo, Greef (1968) in the Kimberley area, Nixon et al. (1983) in East Griqualand, Norman et al. (1977), Dawson (1962) and Bennie and Partners (1971) in Lesotho, Nixon and Kresten (1973) at Butha-Buthe, and from the Free State geological maps.

Several swarms or tectonic provinces can be distinguished, namely; the Sutherland, Victoria West, Postmasburg – Prieska - Britstown, Hanover, Kimberley, East Griqualand - West Free State, Butha-Buthe - North Lesotho, Winburg, and Kroonstad swarms.

At *Sutherland* two swarms of fractures are developed around the Salpeterkop carbonatite-olivine Melelitite Complex. The E-W swarm contains kimberlitic material. The N-S swarm is essentially carbonatitic.

At *Victoria West* three structural domains have been identified based upon the orientation of kimberlite fissures; NNE, NW and NS swarms. *The Postmasburg-Prieska-Britstown* swarm is a very extensive, arcuate feature that appears to follow the margin of the Kaapvaal-Namaqua craton.

The *Hanover* swarm could be linked to the Postmasburg swarm of kimberlites. The *Kimberley* cluster consists of four separate swarms, namely; the Kimberley, Jagersfontein, Bellsbank and Robert Victor swarms. The *Butha-Buthe-Lesotho* and *East Griqualand-Western Free State* swarms have a consistent WNW direction. The *Free State* cluster includes the Winburg and the Kroonstad swarms.

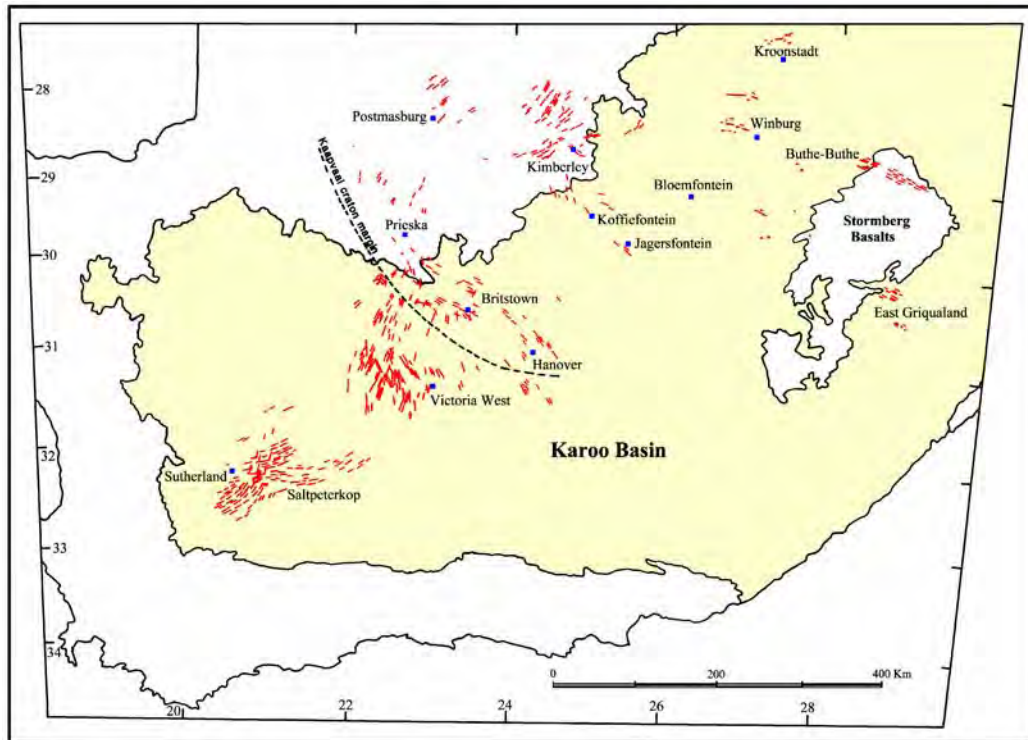


Figure 2.61: *Distribution of Cretaceous Kimberlites and Carbonatites in the Karoo Basin (after Chevallier, 1997, modified)*

Description

Kimberlite fracture swarms consist of parallel fissures and associated joints or fractures. Each swarm can be divided into sub-swarms of smaller size (**Figure 2.62**). Within each sub-swarm the fissures are always closely spaced (approximately 10 to 50 m apart). This tectonic style is often reported for kimberlite and was described by Nixon and Kresten (1973) for the Lesotho kimberlite swarm. The fissures are 0.5 to 4 m wide and often show strong upwarping of the surrounding Karoo beds (**Plate 2.6**). In outcrop the kimberlite intrusion is often inconspicuous and only visible as stringers of highly decomposed kimberlite (green-ground) or micaceous calcrete (yellow ground). Fresh hypabyssal kimberlite is usually encountered after drilling through 12 to 60 m of weathered zone. Parallel regional jointing often accompanies the fissures. They do not contain any igneous material, except for a few indicator minerals or traces of mica.

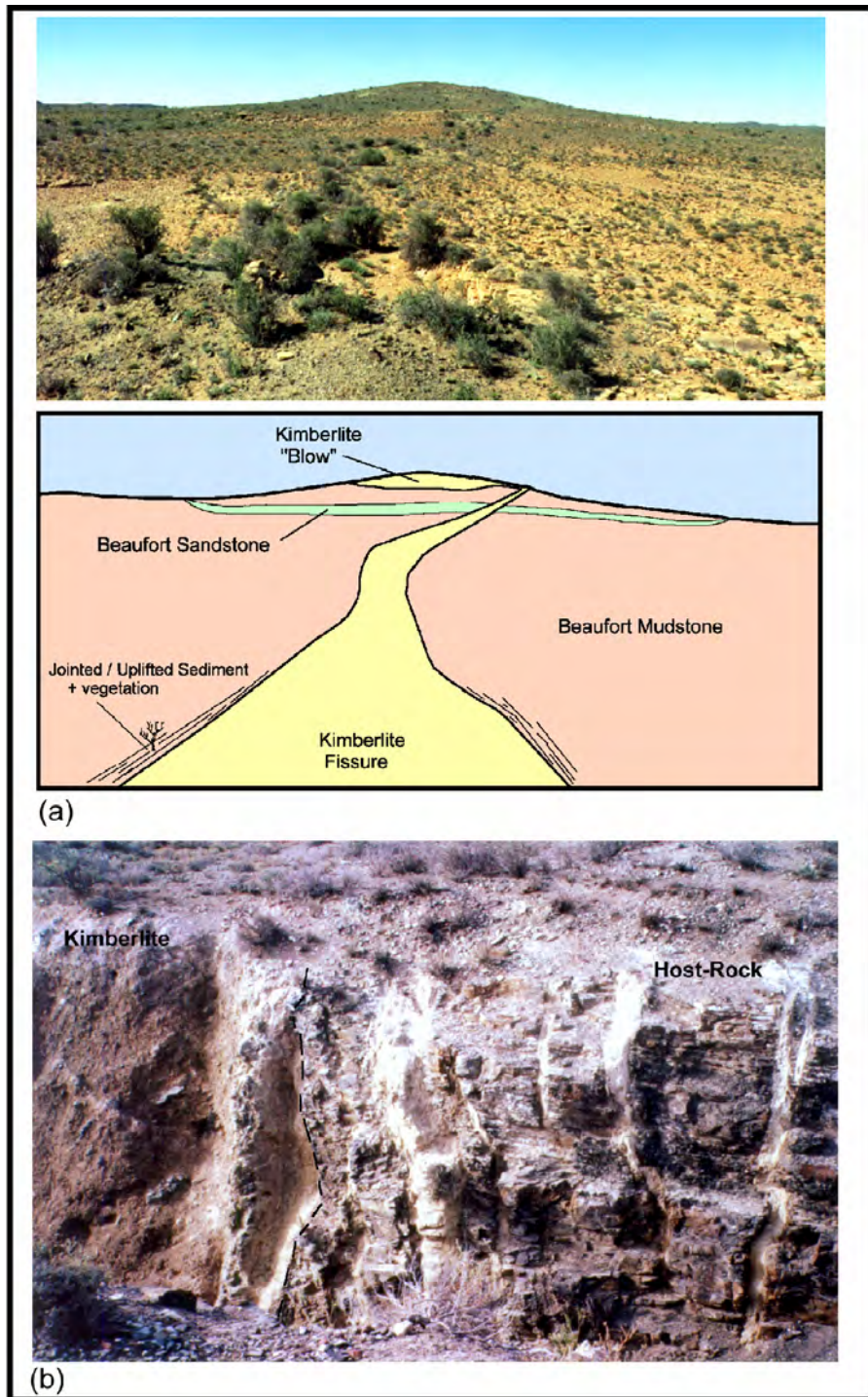


Plate 2.6: (a) Kimberlite fissure and pipe on the farm Nuweland (Loxton) and (b) Cross-section of kimberlite body on the farm Meltonwold (Victoria West) – note thin kimberlite, calcite and calcrete stringers parallel to the main body

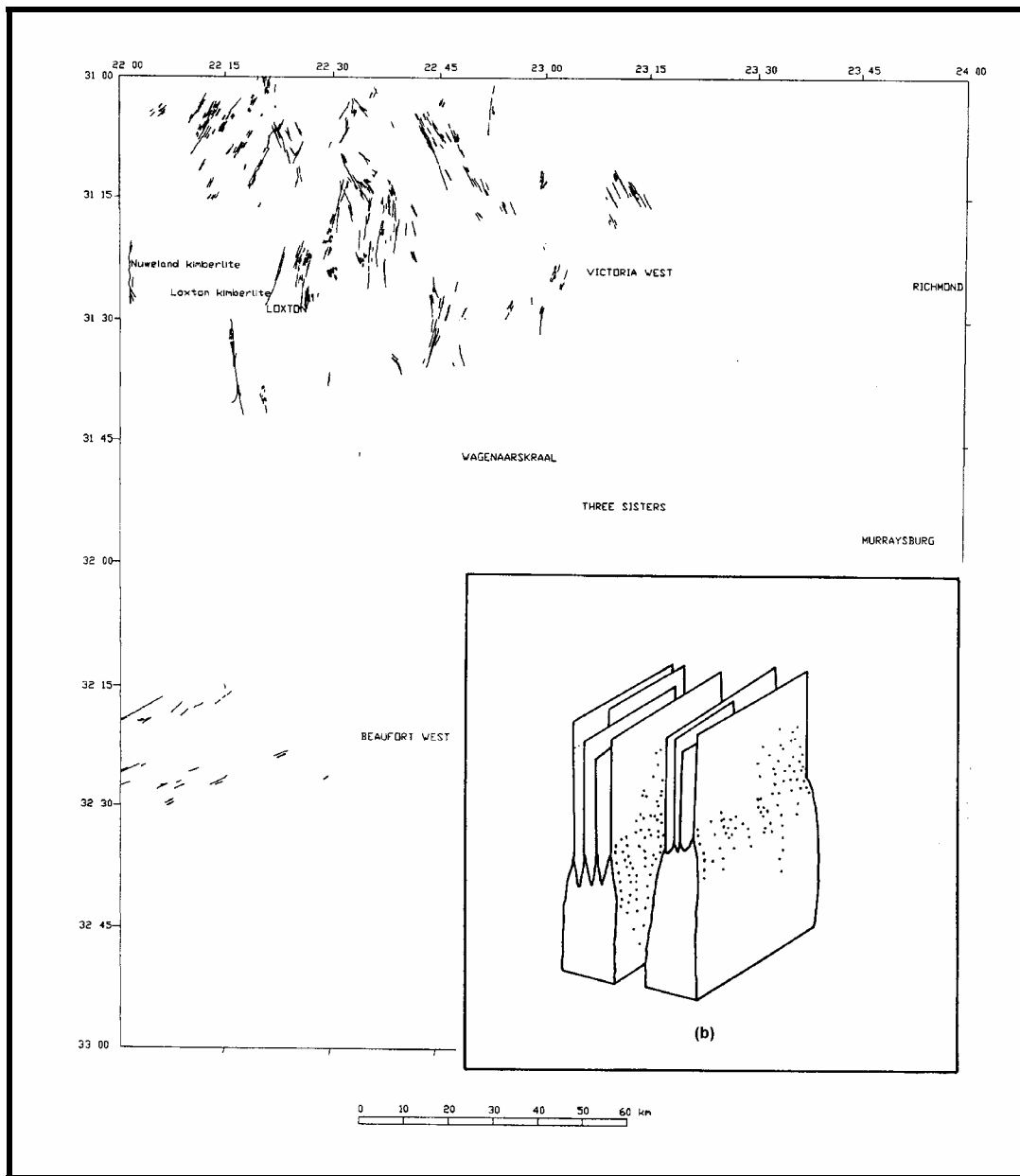


Figure 2.62: Kimberlite Swarms and Sub-Swarms of
 (a) the Victoria West – Beaufort West area
 (b) Proposed Vertical Geometry of a swarm (Woodford and Chevallier, 2001)

Blows and enlargements frequently occur along the fissure and can be easily recognized on aerial photographs due to the presence of well-developed calcrete. They are commonly 4 to 10 m wide and consist of decomposed igneous material. They often contain a fair amount of crustal or mantle xenoliths and megacrysts.

Kimberlite fissures are discerned from dolerite dykes on aerial-photographs as regularly spaced, narrow, co-linear features with relatively denser vegetation growth along the fissure.

Kimberlite diatremes are unevenly distributed. They are not very common and vary in diameter from only 10 to 400 m in the western Karoo, Sutherland, Victoria West, Britstown, Prieska and East Griqualand areas. They are more numerous and extensive (200 to 1 000 m in diameter) on the Kaapvaal craton. Both the fresh and weathered hypabyssal kimberlite can form positive-relief hills or negative-relief, calcrete-rich depressions. They contain a large amount and a wide variety of mantle and crustal xenoliths as well as megacrysts.

Factors Controlling Kimberlite Emplacement

The emplacement of clusters on a *regional scale* was guided by upwelling within the mantle. Their location has been a matter of debate for many years and several theories have been put forward, i.e. hot-spot tracks, crustal tectonics, dynamics of the mantle, etc.

On a *local scale*, a common tectonic process guided the emplacement of the kimberlite swarms. The fact that swarms can be subdivided into sub-swarms points to a vertical hierarchy within the fracturing system at depth, i.e. fissures, dykes, parental dykes, larger bodies etc (**Figure 2.62**). Deep mantle processes controlled the larger bodies, whilst individual fractures and sub-swarms were controlled by very localised pre-existing fractures, such as dolerite dykes, master joints or faults.

Hydrological Properties

The intrusion of the kimberlites did not result in the intensive thermal metamorphism of the Karoo sediments, as did the dolerites, and thus they did not significantly alter the hydrological properties of the sediments. On a regional scale, however, clusters of kimberlites may represent important fractured domains.

On a local scale, the thin kimberlite dykes (< 3 m) are generally only weakly jointed and thus have a very low permeability, especially within the highly decomposed upper section of the dyke. However, the strong regional jointing and reactivation of existing structures that accompanies the emplacement of kimberlite swarms may be important for the occurrence and movement of groundwater. Kimberlite blows or enlargements (diameter of 4 to 10 m) may represent more permeable zones along the dykes, as they are always more heterogeneous in texture, more deeply weathered and marked by dense bush growth.

Large kimberlite pipes or *diatremes* are more heterogeneous and brecciated. There is thus a possibility that high-yielding boreholes can be sited alongside or within these features, similar to the breccia plugs (**Chapter 2.3.2.2**), i.e. both the Free State towns of Jagersfontein and Fauresmith obtain their water from the abandoned Jagersfontein diamond mine.

The Department of Water Affairs and Forestry have drilled five exploration boreholes into and alongside kimberlite dykes in the Loxton area (Woodford and Chevallier, 2001) and one borehole into a diatreme at Carnarvon.

The NNE trending *Loxton kimberlite dyke* is situated 1 km north of Loxton (**Figure 2.62**). The dyke is 3 m wide and has a vertical attitude. Three 150 m deep boreholes were drilled on this structure in the vicinity of its intersection with a NW trending dolerite dyke, as follows:

- (a) in the middle of the dyke,
- (b) in the kimberlite dyke at the intersection zone, and
- (c) approximately 1m from the dyke contact (150 m north of the kimberlite / dolerite dyke intersection).

Boreholes (a) and (b) intercepted highly decomposed kimberlite (yellow-ground) to a depth of 11–12 m and weathered kimberlite (green-ground) from 12 to 14 m, whereafter the kimberlite was fresh (blue-ground). Only seepage was recorded at the transition zone between the weathered and fresh kimberlite.

The *Nuweland kimberlite dyke* forms part of narrow, N-S trending corridor of intense fracturing and kimberlite intrusion, some 12 km south-west of Loxton (**Figure 2.62**). Two diatremes and a number of blow-pipes have been mapped. The fissures and blow-pipes contain kimberlitic material (mainly yellow-ground) and the diatremes contain fresher kimberlite and breccia. Most of the other fissures and parallel joints are barren or contain micaceous, calcretized material. Two exploration boreholes were drilled as follows:

- (a) in the centre of the main kimberlite fissure to a depth of 162 m, and
- (b) into a parallel, but ‘barren’ fissure to a depth of 150 m, some 22 m east of borehole (a).

Borehole (a) only intercepted seepage inflow at 47 m, despite the heterogeneity, textural and structural complexity of the dyke. Borehole (b) drilled into the open or ‘barren’ fissure struck a water-bearing fracture at 65 m that yielded 4 ℓ/s (Woodford and Chevallier, 2001).

The *Middelfontein diatreme* is situated on the cadastral farm Blauuw Krantz 485, 10 km east of Carnarvon. It is intruded along a system of north trending fissures. It is oval-shaped with a diameter of 300 m. A borehole was drilled into the centre of the

structure to a depth of 240 m and showed that the kimberlite was highly decomposed (yellow-ground) to 16 m below surface, weathered (green-ground) from 17 to 83 m and fresh from 84 to 140 m. The borehole intercepted water in the weathered kimberlite at 26m (1.5 ℓ/s, 49 mS/m) and the jointed/weathered-fresh kimberlite transition zone at 83m (1.5 ℓ/s, 141 mS/m) (Woodford, unpublished data).

The diamond-mining operation on *Jagersfontein kimberlite diatreme* in the southwestern Free State extended to a depth of 750 m below the surface. In order to keep the waterlevel below this depth some 64 000 m³/month of groundwater had to be abstracted continuously at a rate of 25 ℓ/s (**Figure 2.63**).

In 1971, De Beers Consolidated Mines (Ltd.) ceased mining and gave the Jagersfontein Municipality permission to abstract groundwater from the mine in 1980. During this time the piezometric level in open-pit and shafts recovered from 750 m to 183 m below ground-level (bgl). Over the period January 1980 to February 1982, the Municipality abstracted a total of 497 308 m³ of groundwater via a pump installed in an abandoned shaft (Kok, 1982), with a maximum waterlevel drawdown of 0.66 m. The pump inlet was installed at 220 m and the pump rate was set at 17.5 ℓ/s. The waterlevel and chemical information point to the existence of two separate aquifers, namely:

1. a shallow, more 'typical' Karoo fractured-rock aquifer (**Figure 2.63** – Well 1, showing a waterlevel of 4.8 m.bgl), containing recently recharged water (**Table 2.8**) and,
2. a deeper aquifer (intercepted in the mine, piezometric level 183 m.bgl) containing older water (**Table 2.8**).

Table 2.8: *Groundwater chemistry from the Jagersfontein aquifer systems*

Water Quality (mg/l)	Mine Shaft (29/09/81)	Spring (29/09/81)	Dairy Borehole (29/09/81)
NH ₄	0.02	0.03	0.02
Na	236.9	41.4	36.4
K	9.15	1.57	1.38
Mg	13.3	50.81	52.46
Ca	37.6	84.9	92.7
Cl	42.9	35.3	73.1
SO ₄	408.5	112.0	77.7
HCO ₃	170.9	302.8	293.4
F	0.93	0.45	0.63
NO ₃	0.67	1.25	4.16
SiO ₂	12.03	23.2	18.4
P	0.02	0.01	0.00
pH	7.5	7.6	7.7

The occurrence of groundwater associated with *kimberlite dykes* in the Loxton – Victoria West area, was also investigated using yield information from privately drilled boreholes and field measurements of distance drilled from the dyke contact (**Table 2.9**). Only three boreholes of the 71 visited were drilled into the dyke, because farmers tend to avoid drilling into the centre of these structures due to experience of low yields and problems of borehole collapse.

Table 2.9: Groundwater occurrence on kimberlite dykes in the Loxton - Victoria West Area

Yield Range (ℓ/s)	In dyke	Distance from Kimberlite Dyke Contact (m)						Total
		>0 - ≤ 1	>1 - ≤ 2	>2 - ≤ 5	>5 - ≤ 10	>10 - ≤ 20	>20	
Dry	-		1	2	-	-	-	3 (4%)
>0 - ≤ 1.0	1	2	4	6	8	6	4	31 (44%)
>1.0 - ≤ 2.0	-	1	-	2	3	-	5	11 (16%)
>2.0 - ≤ 3.0	1	-	-	1	1	3	3	9 (13%)
>3.0 - ≤ 5.0	-	1	-	1	-	1	-	3 (4%)
>5.0 - ≤ 10.0	-	-	1	1	2	2	2	8 (11%)
>10.0	1	-	-	1	-	1	3	6 (8%)
Total	3 (4%)	4 (6%)	6 (8%)	14 (20%)	14 (20%)	13 (18%)	17 (24%)	71

Note: Mean Borehole Yield = 3.0 ℓ/s, Standard Deviation = 4.5 ℓ/s,
 Median = 1.2 ℓ/s.
 Mean Borehole Depth = 32 m
 Mean Dyke Width = 3.6 m.

Almost half (48%) of the boreholes targeting kimberlite dykes yield 1 ℓ/s or less, while 14 or 20% of the boreholes yielding more than 5 ℓ/s are located further than 2 m from the dyke contact. The ‘background’ or median borehole yield for the area is 1.3 ℓ/s (N = 827, Mean = 2.9 ℓ/s, standard deviation = 4.3 ℓ/s), which would account for the distribution within the yield classes of up to 2 ℓ/s. The “abnormally” higher yielding boreholes appear to be located away from the dyke, where the probability (0.12) of intercepting greater than 5 ℓ/s is highest at distances in excess of 5 m from the contact.

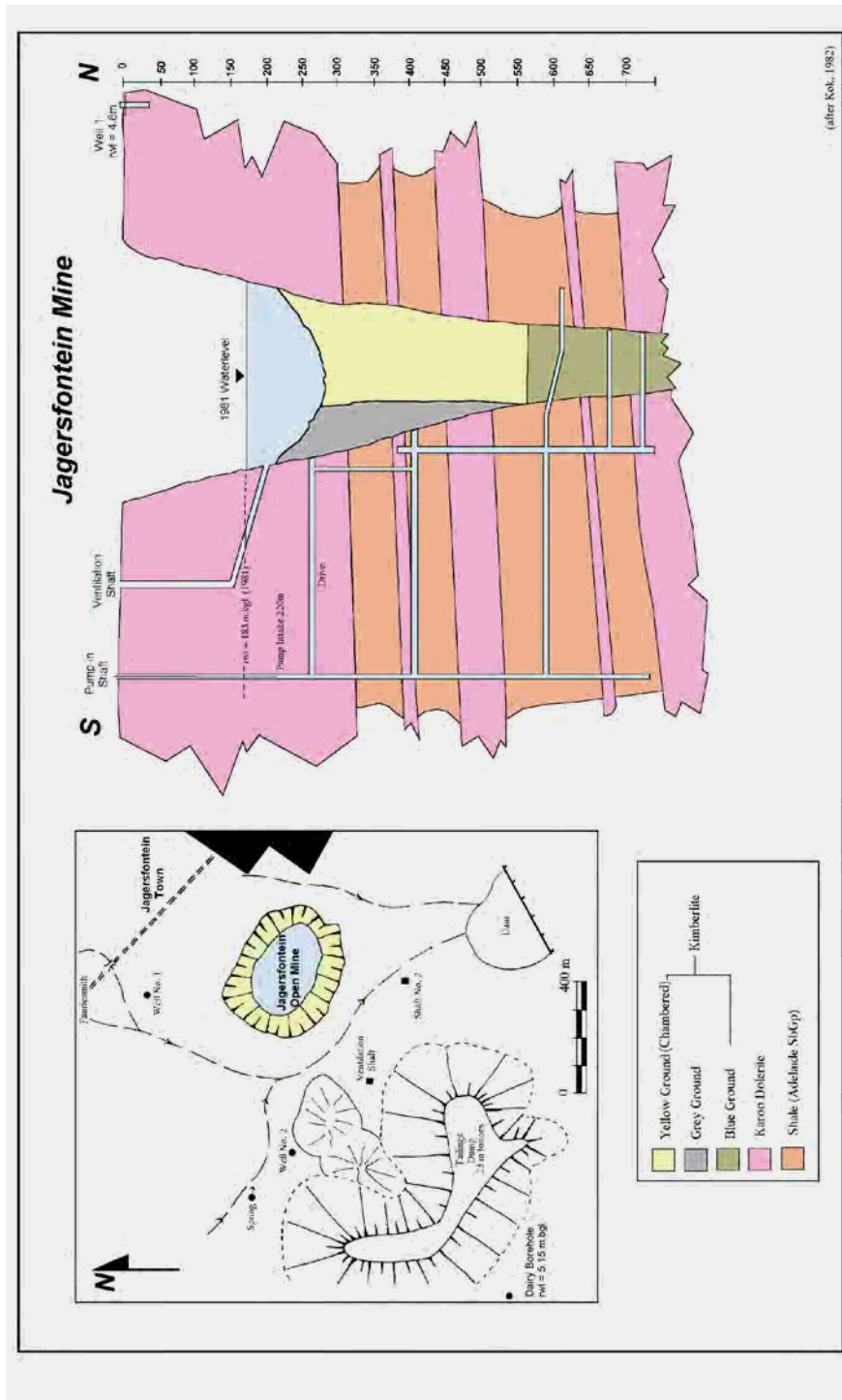


Figure 2.63: *Geohydrology of the Jagersfontein kimberlite diatreme (after Kok, 1982)*

In conclusion, boreholes sited into kimberlite fissures commonly yield very small amounts of groundwater, mainly due clogging of near-surface joints by clays produced by the weathering and decomposition of the kimberlite. The transgressive, water-bearing fractures often observed on dykes (**Chapter 2.3.2.1, Transgressive Fracturing**), do not appear to have been developed along kimberlite fissures. Seepage is only found in the weakly jointed transition zone between the weathered and fresh kimberlite. However, the local and regional fracturing that accompanied the emplacement of the kimberlite, mainly mega-joints, can deliver appreciable amounts of groundwater. Kimberlite diatremes pipes and fissures have not been fully investigated and should be reassessed as potential exploration targets.

2.4 NON-INTRUSIVE TECTONIC FEATURES

Non-intrusive tectonic features include regional lineaments, folding, vertical jointing and faulting, bedding-plane fracturing and seismotectonic / neotectonic / unloading features.

2.4.1 REGIONAL LINEAMENTS

2.4.1.1 Description

Deep crustal and hidden geophysical features of the basement include the Beattie, Williston and Mbashe magnetic anomalies, the Kaapvaal Craton margin, the megafabric of the Namaqua-Natal belt (Thomas et al., 1992) and a magnetic high below Northern Lesotho (**Figure 2.64**). Shallow crustal mega-faults that intersect the Karoo Supergroup include the Tugela (Natal), Matatiele (Transkei) and Helspoort (Lesotho-Free State) faults.

Although no regional remote sensing studies has been done to specifically identify lineaments in the Main Karoo Basin, the Digital Elevation Model of the Main Karoo Basin shows the following major morphological features that are apparently unrelated to dolerite intrusions:

1. The ENE-trending Transkei lineament seems to link the Williston anomaly to the Melville shear.
2. The NE-trending lineament-corridor of Western Lesotho links into the Tugela fault and the Lesotho fault. The Tugela fault brings the Vryheid Formation (Ecca Group) into contact with the Adelaide Subgroup (Beaufort Group). The Western Lesotho lineament is well defined on satellite imagery, but has no field expression - it probably comprises a zone of dense jointing not readily visible at the field-scale.
3. The Matatiele fault forms an extension of a curvi-linear morphological feature that cuts across southern Lesotho. It is down-thrown some 240 m to the north. Nixon et al. (1983) suggested that faulting in the Quaternary was responsible for the alluvium-filled trough in the Cedarville flats.
4. Two additional major N-S trending morphological lineaments that appear unrelated to the Karoo dolerite magmatism occur in the eastern Karoo.

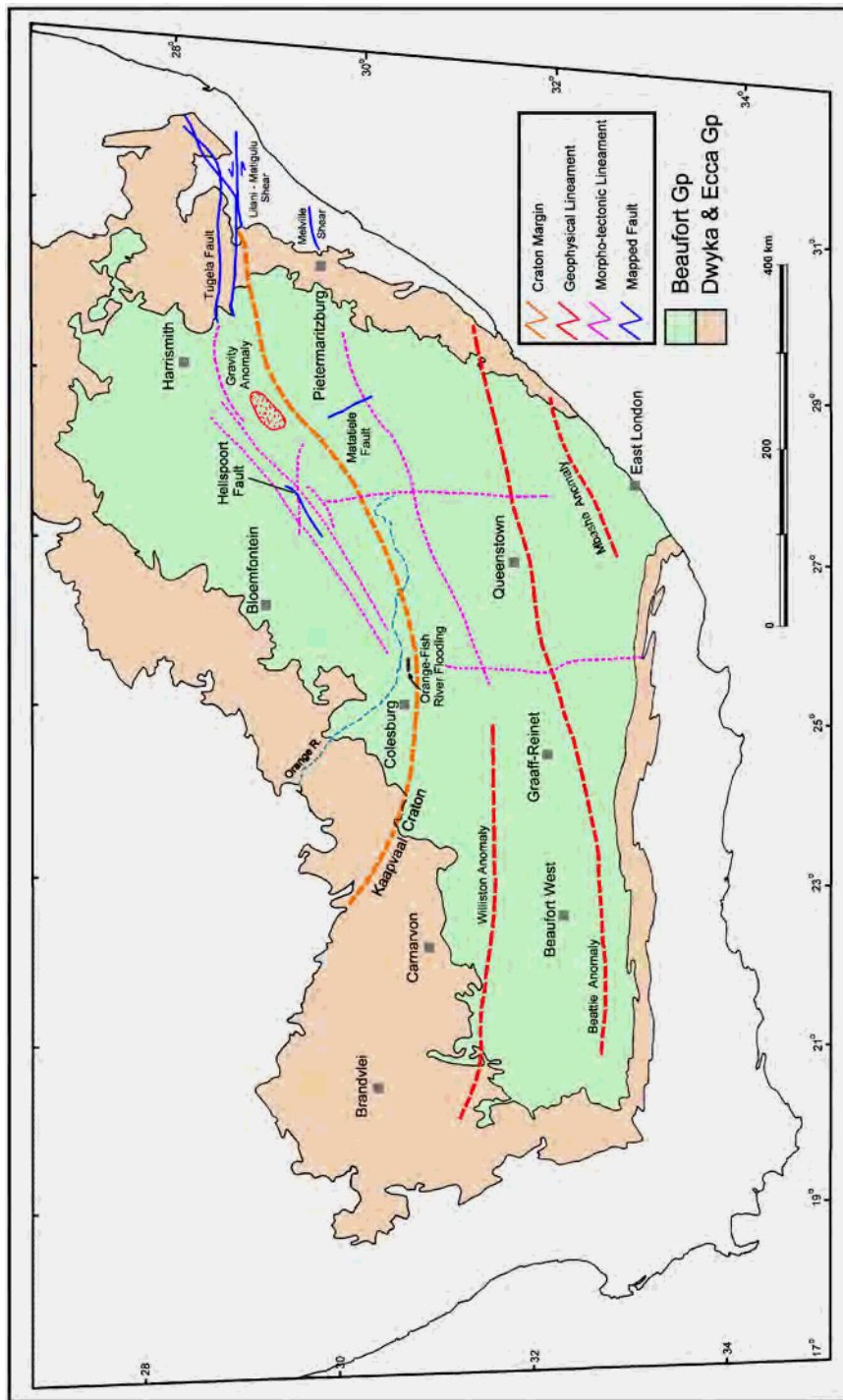


Figure 2.64: Deep-seated Pre-Karoo structures (geophysical anomalies), major faults (Thomas et al., 1992) and morphological lineaments (this study).

2.4.1.2 Hydrological Properties

None of the lineaments discussed above have been described from a hydrological point of view. The Tugela fault may be of particular interest because it resulted in the juxtaposition of two different formations of different geohydrological character.

The direct influence of deep-seated pre-Karoo structures on the hydrology of the Karoo is unknown. However, the Orange-Fish River tunnel project indicated the tremendous yield potential of these deep-seated structures, when a discrete, open east-west orientated fissure-zone was intersected and caused flooding of the tunnel (Meyer and Van Zijl, 1980). Detailed geophysical and field-mapping were not able to conclusively trace the fissure-zone on surface. From **Figure 2.64** it would appear that the fracturing responsible for this flooding may related to the intersection of a number of major deep-seated lineaments, which include the Kaapvaal craton margin, the Lesotho fault and lineament, and a further north-south orientated lineament.

2.4.2 FOLDING

2.4.2.1 Description

The east-west-trending Cape Fold Belt developed during Permo-Triassic times (278 to 230 Ma) as a result of the closure of the Cape Basin. The uplifted mountain belt became a source for large volumes of sediment that was deposited in the Karoo foreland basin. The Cape Orogeny resulted in fairly regular E-W-trending fold axes, although arcuation commonly occurs. It has been divided into six zones with differing degrees of structural deformation (Hälbich and Swart, 1983). The variable style and intensity of folding that affected the Karoo Supergroup were studied in detail along two N-S cross-sections in the vicinity of Beaufort West (Coetzee, 1983; Hälbich and Swart, 1983; summarized by Cole et al., 1991 and Woodford and Chevallier, 1998 – **Figure 2.65**).

North of latitude 32°30', i.e. above the Great Escarpment, the Karoo beds are virtually undeformed and display a gentle northerly dip of 3° or less. The rocks show no cleavage development, re-crystallisation of quartz grains or any other sign of compression.

The northernmost folded sediments of the Karoo Supergroup (**Zone 1** of Hälbich and Swart, 1983) occur between 32°30' and 32°45', and are characteristically sinusoidal, upright mega-folds with horizontal axes, interlimb angles of about 170° and wavelengths of 2 to 3 km. The sandstone beds are cut by many E-W-trending listric thrusts (fractures oblique to the bedding) filled with quartz, conjugate joints and quartz-filled shears and tension gashes. Bedding plane slip appears to have been insignificant. Cleavage development is restricted to the shale units that have been affected by thrusting. Drill-core samples from the farm Kaffirsfontein, approximately

30 km southeast of Beaufort West, indicated a total absence of bedding-plane or other horizontally disposed joints in depth. In contrast, the vertical joint component is strongly developed with joint apertures of “fissure-size”, lined with calcite or quartz (Campbell, 1975), occurring commonly. Campbell estimated an average joint-density of 3-15 joints per m² in sandstone outcrops surveyed within a 30 km radius of Beaufort West. He also noted that the joint apertures varied between 1 to 2 mm.

Zone 2 extends from 32°45' to the contact between the Beaufort and Ecca Groups. It is characterised by symmetric, up-right, rounded folds with interlimb angles of 130°. Small monoclines are sometimes associated with listric thrusts in the sandstone. They are asymmetric with respect to the fold-axial planes and are probably older. Conjugate joints, shears and tension gashes are found, similar to those in Zone 1.

Zone 3 includes the Ecca and Dwyka Groups. It corresponds to an abrupt transition to northward facing, asymmetric mega-folds with interlimb angles of less than 90° (**Figure 2.66**). Intense folding and well develop listric thrusting accounts for an estimated 30% of shortening in this zone. Well develop thrusting has been described near Laingsburg (Newton, 1993). Fracturing, in the form of tension gashes and bedding plane slip, occurs commonly. Cleavage is very well developed in the shale and mudstones.

In addition to the E-W parallel folds described above, a number of oblique lineaments, fracture-sets and master-joints, trending NNW and NNE, occur in the Beaufort West area (Stear, 1980; Woodford and Chevallier, 2001). They also occur further to the north in the Western Karoo Basin and have been related to dolerite and kimberlite intrusion and neotectonic events.

2.4.2.2 Hydrological Properties

The tightly folded Karoo strata should have well-developed secondary permeability, because of the dense network of open fractures of different geometry, size and attitude. The development of vertical fractures is controlled by lithological boundaries with the result that the vertical hydraulic conductivities are relatively low. In addition, the high degree of connectivity between fractures should result in more extensive aquifers, when compared to the intrusive-controlled aquifers. Farmers in the southern Karoo, below the Great Escarpment, commonly site successful boreholes on the fold-axes and antithetic fracture systems (**Figure 2.67**). A hydrocensus carried out by the Department of Water Affairs and Forestry in the Beaufort West and Rietbron areas indicates that E-W jointing along anticlinal fold-axes are the most successful exploration targets for groundwater.

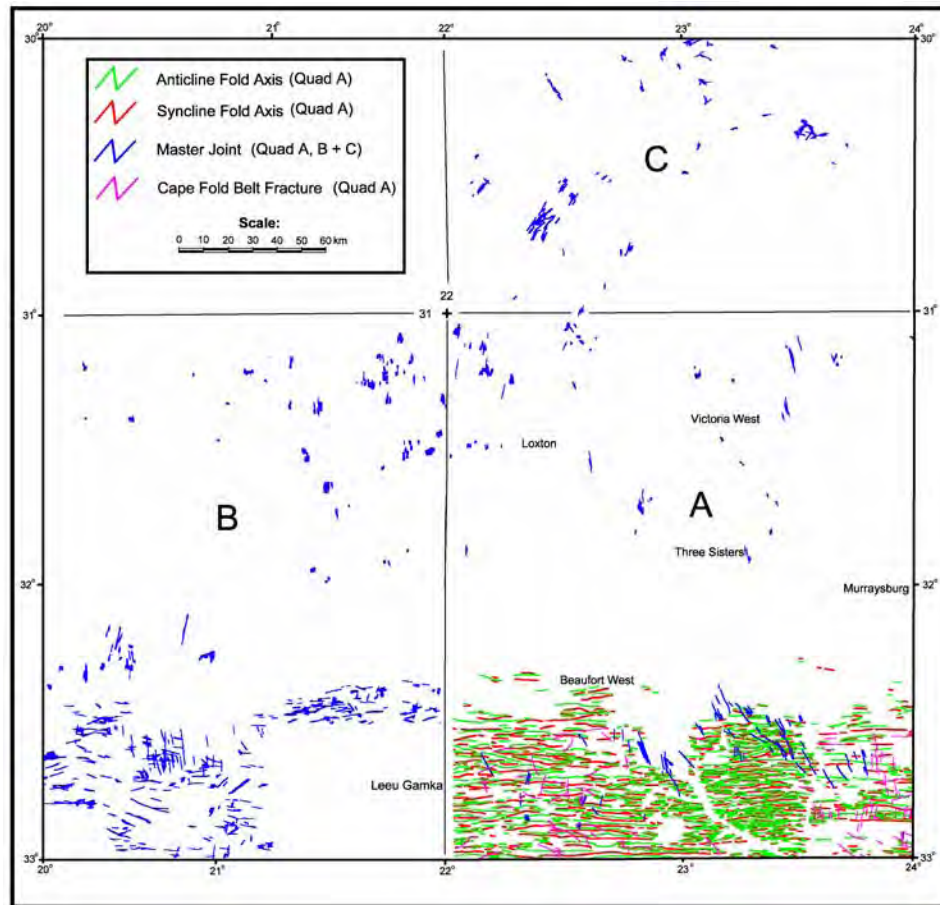


Figure 2.65: *Fold axes and master joints of the southwestern Karoo (after Woodford and Chevallier, 2001 and Chevallier, unpublished data). Fold axes are only shown for Quadrant*

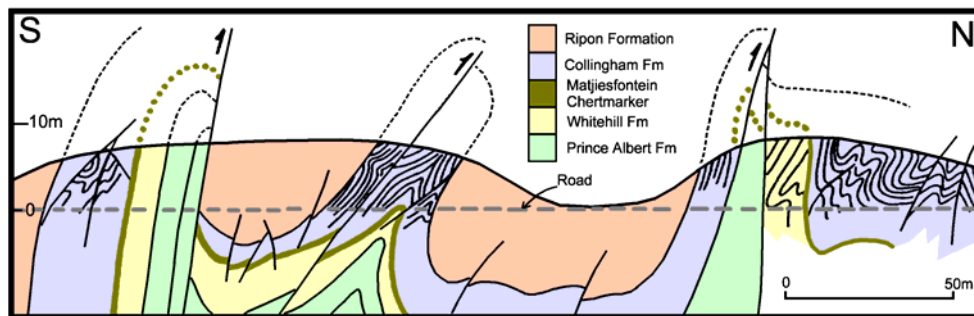


Figure 2.66: *Schematic structural profile along the Rhemhoogte road across units of the Ecca Group (taken from Coetzee, 1983)*

Parsons (1986) drilled high yielding boreholes (maximum of 39 l/s) into localised, steeply dipping, asymmetrical, E-W orientated fold structures to the south of Graaff-Reinet (**Figure 2.66**). These features are generally between 3 to 9 km in length. Parsons states that a sub-vertical fault or shear zone is often developed along the fold-axis. These structures may represent incipient thrust faults, which are common between latitude $31^{\circ}30'S$ and $30^{\circ}00'S$ (i.e. within Structural Zone 1 of the Cape Fold Belt).

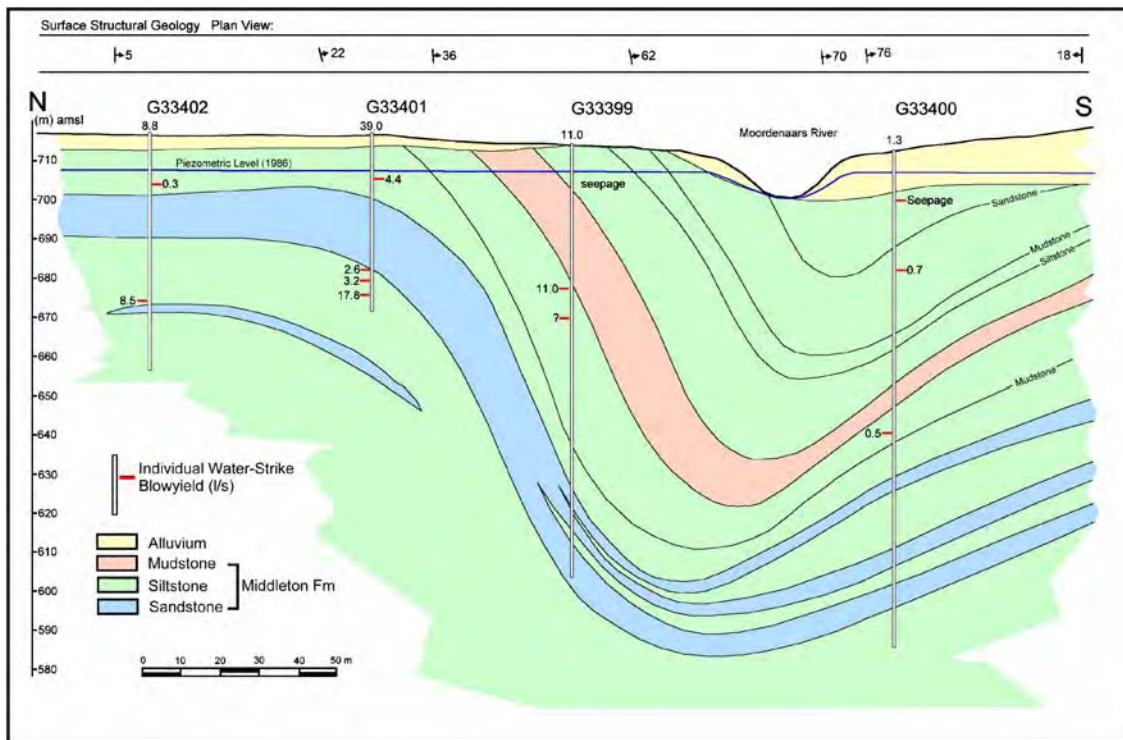


Figure 2.67: Geological cross-section of the Vorster Syncline, Graaff-Reinet

Case Study: Leeu-Gamka - Conflict between users of a limited Groundwater Resource

During 1985, the Leeu-Gamka Municipality requested that the Department of Water Affairs (Seward, 1987) investigate the “drying-up” of the town’s groundwater supplies. Inhabitants of Leeu-Gamka stated that such problems only started to occur after 1983 when Eskom electrical power was laid on to farmers irrigating along the Gamka River.

The area is arid and only receives approximately 117 mm of rainfall per annum (Station 68/857 on the farm Welgemoed measured over the period 1911-1986). Intensive irrigation takes place along the Gamka River. During 1985 it was estimated that 638 ha of lucerne and 67 ha of wheat were irrigated and the water usage was as follows:

Surface Water (Leeu Gamka Dam)	$0.85 \times 10^6 \text{ m}^3$
Groundwater	$12.50 \times 10^6 \text{ m}^3$
TOTAL	$13.35 \times 10^6 \text{ m}^3$

The Department of Agriculture at Beaufort West in collaboration with the Grootfontein Agricultural College at Middelburg estimate the irrigation requirements at $10.65 \times 10^6 \text{ m}^3$ (i.e. 25% over-irrigation).

The study area is underlain by E-W folded sandstone and mudstone of the Abrahamskraal Formation. The folds are discontinuous and asymmetrical, with dips generally less $< 10^\circ$, but may reach up to 30° (**Figure 2.68**). A narrow strip of sandy alluvium, averaging 7 m in thickness, occurs along the Gamka River. High yielding boreholes occur in the alluvial valley of Leeu and Gamka Rivers. The higher yielding irrigation boreholes are often deeper than 60 m and obtain their water from zones of enhanced fracturing in the fold-axis of synclines and anticlines. Boreholes in the town of Leeu Gamka are on average only 40 m deep.

In 1985, a DWAF ground-waterlevel survey indicated that a 20 m trough of drawdown had developed along the Gamka River in the vicinity of the intensive irrigation, also extending beneath the town (**Figure 2.69**: Sep-Nov 1985 waterlevel contours). The waterlevels beneath Leeu Gamka had dropped below that base of most of the boreholes situated in the town, while waterlevels away from the alluvial valley showed no effect of the abstraction. Heavy rainfall in December 1985 resulted in riverflow and the aquifer was fully recharged (**Figure 2.69**: Jan 1986 waterlevel contours). A third survey in 1987, however, indicated that the waterlevels in the area had again declined to the 1985 levels due to over-abstraction.

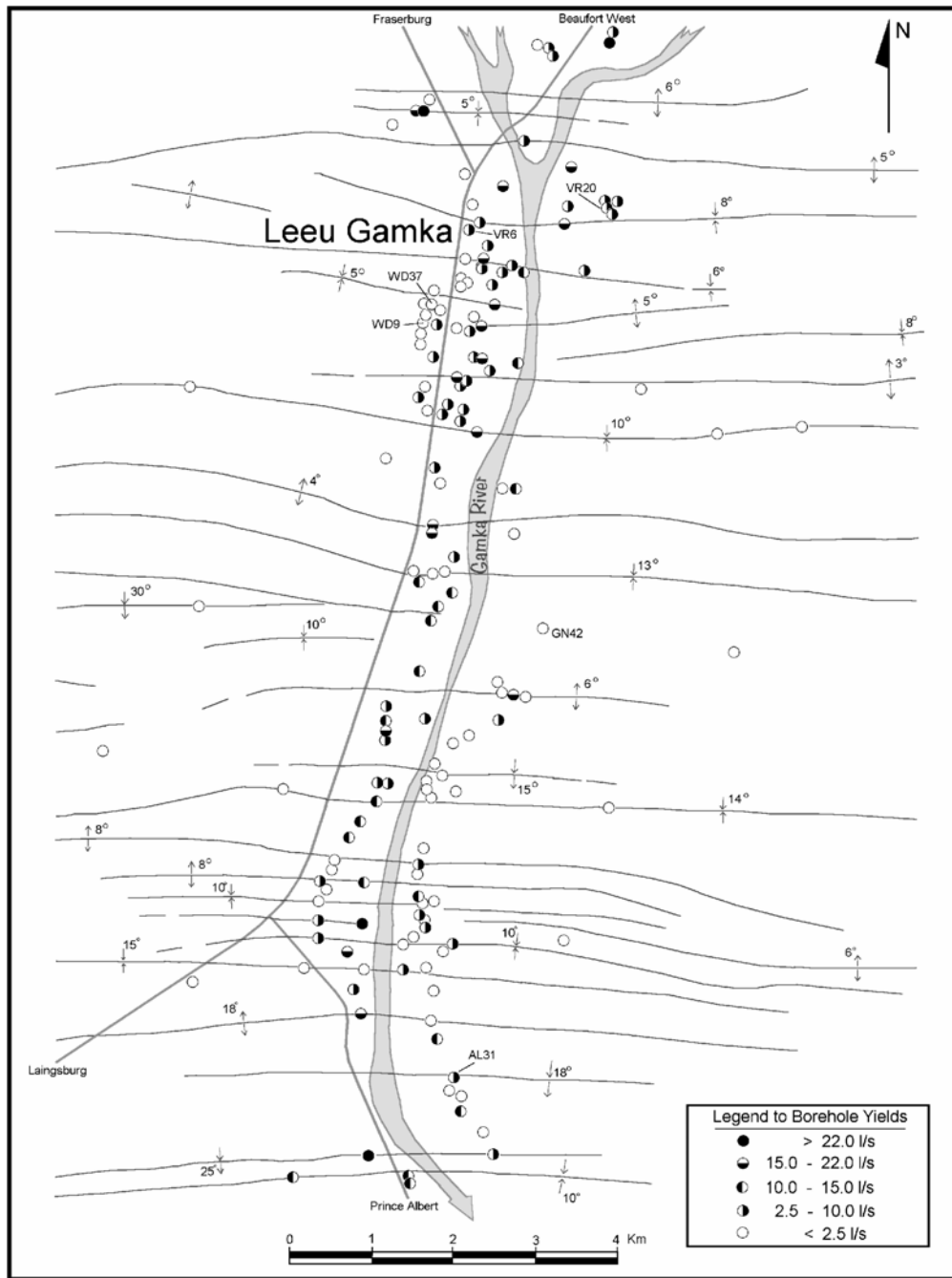


Figure 2.68: Leeu-Gamka – Borehole productivity and associated structural features

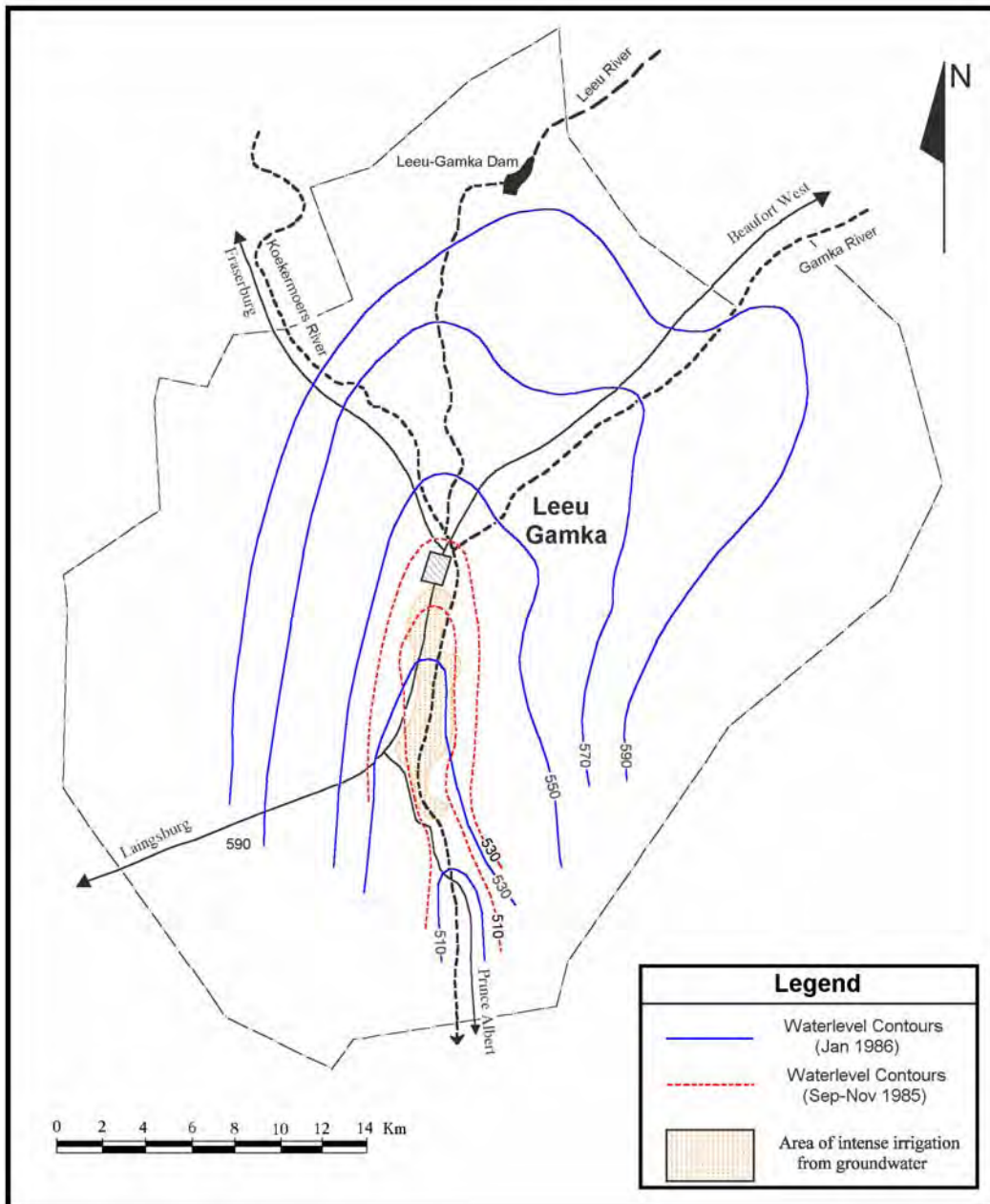


Figure 2.69: Leeu-Gamka – Groundwater level fluctuations during 1985-86

The heavy rainfalls in December 1985 resulted in a general decrease in the groundwater quality, probably due to leaching of salts accumulated in the vadose zone – particularly as a result of irrigation practices. By 1987 the groundwater quality had improved markedly (Table 2.10)

Table 2.10: Leeu-Gamka - Groundwater level and quality fluctuations

Borehole No.	Sep-Nov 1985		Jan 1986		1987	
	EC (mS/m)	Waterlevel (m.bgl)	EC (mS/m)	Waterlevel (m.bgl)	EC (mS/m)	Waterlevel (m.bgl)
AL31 *	157	14.840	198	5.170	102	11.940
AL37 **	214	9.185	227	7.490	202	11.725
BY10 **	110	19.920	99	9.910	133	11.780
GN42 *	73	16.750	58	5.360	73	10.000
SN7 **	311	8.435	200	8.610	286	13.835
SN16 **	67	20.130	67	19.890	69	20.695
VR6 *	137	35.850	214	13.500	101	29.725
VR20 *	100	22.700	112	18.080	112	20.470
WD9 *	156	33.465	314	13.690	154	18.500
WD37 *	118	35.770	106	14.950	73	24.000
Average	144	21.70	160	11.67	131	17.22

Note : * - Borehole position depicted in Figure X.

** - Borehole position depicted in Figure Y.

This phenomenon was also noted in quality of groundwater abstracted from a shallow alluvial/bedrock aquifer, south-west of De Aar, following 245 mm of rainfall (MAP 280 mm) during Jan-Feb 1988 (**Figure 2.70**). The bulk water quality from the South-Western Area deteriorated from an EC of 180 to 202 mS/m directly after the flood event and riverflow, probably due to the flushing of accumulated salts in the vadose into the aquifer by direct recharge. Thereafter the groundwater quality gradually improved to an EC of 150 mS/m by May 1988, as freshwater recharged into the surrounding hardrock formations became temporarily influent into the alluvial aquifer. The groundwater quality slowly began to decline back to its ambient levels, without significant additional recharge and the resumption of the normal rates of abstraction.

By the early 1990s, after many cycles of aquifer over-abstraction and recharge, the local farmers have by a process of attrition scaled-down the area under irrigation according to the available groundwater. Some farmers have abandoned irrigation from groundwater for economic reasons, while others continue to irrigate within these cycles of plenty and paucity.

This somewhat typical scenario has a significant bearing on the basic strategies required to manage large-scale groundwater abstraction from the *shallow* Karoo aquifers in the light of the New Water Act of 1998. The user who over-exploits a groundwater resource is always the first to feel the negative environmental and economic impacts of declining waterlevels and borehole yields, borehole collapse, the need for deeper drilling, soil and groundwater salinization etc. These localised effects can, however, impact on other users of the same groundwater resource, as in the case of the Leeu-Gamka residents. A more serious and longer-term issue is the use of groundwater of a quality that is unsuitable for irrigation purposes – thereby gradually increasing salinity of the topsoil and groundwater over time. This negative impact

may first be felt by other users (drinking water requirements) of the groundwater resource before that of the actual ‘abusers’ (irrigation / industrial water requirements).

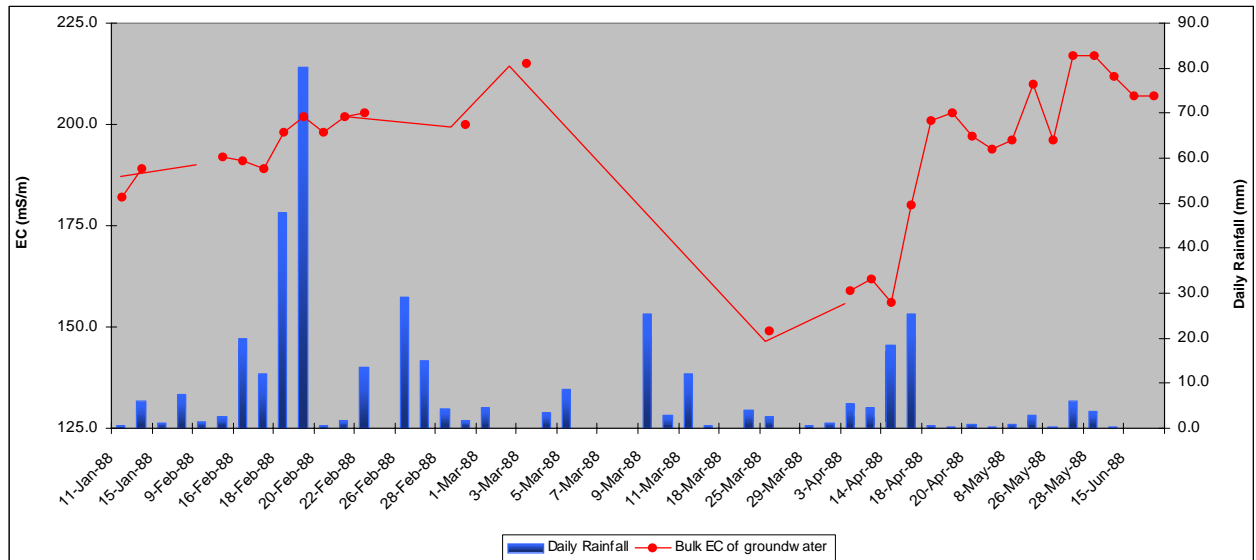


Figure 2.70: De Aar – Groundwater quality variations in an alluvial/bedrock aquifer following abnormally high rainfall in 1988 (Woodford, unpublished data)

2.4.3 VERTICAL FAULTING AND MASTER-JOINTING

The distribution of master joints and their role in the geological and structural framework of Southern Africa is not well documented. The Western Karoo has been investigated in detail (Woodford and Chevallier, 2001; Chevallier, unpublished data) (Figure 2.65).

2.4.3.1 Description

Master joints occur as orthogonal sets of fracturing, consisting of one orientation of systematic joints and another of non-systematic joints – **Plate 2.7** (Hancock and Engelder, 1989).

The *systematic joint-set* are dominant in the Karoo and often form extensive features (>1 km), that are detectable with remote sensing. In general, the spacing between joints is proportional to their length. Kilometre-long mega-joints are meters apart, whereas master joints with a length of tens of metres are spaced at half a meter or less.

Non-systematic orthogonal-joints are less extensive features, forming a link between the prominent joints without intersecting them, resulting in a “ladder-like” pattern. Non-systematic joints are not visible on the conventional remote sensing imagery.

Extensive mega-joints and faults have considerable vertical extension and therefore cut through different lithological units. Short joints, especially the non - systematic orthogonal joints, only affect individual competent layers (sandstone).

2.4.3.2 Distribution

The systematic master-joints are regionally extensive features that occur throughout the Western Karoo Basin, and extend into the Cape Fold Belt. Two sets of systematic joints are commonly encountered in the Western Karoo (**Figure 2.65**):

1. Master-joints with a predominant NNW-trend, fluctuating between NS and N 150°, and
2. those with a predominant NNE-trend, fluctuating between N 10° and N 40°.

The NNW-trending master-joint and fracture sets appear to be more extensively developed in the area between Loxton and Middelburg, where extensive NNW-trending dolerite dykes occur (**Figure 2.14**). This fracture-system has been described in other parts of the Karoo by Campbell (1975), Parsons (1986) and Woodford (1989). Tordiffe (1978) and Vandoolaeghe (1980) also found a similar joint-pattern in the Great Fish River Basin and Queenstown area in the Eastern Cape, respectively. A comparative statistical study of jointing in the Graaff-Reinet and Beaufort West areas indicates that the non-systematic orthogonal joints are not as well developed at Beaufort West as they are at Graaff-Reinet (**Figure 2.71**).

The NNE-trending master-joints and fractures appear to be more pronounced in the area between Calvinia and Loxton, where they parallel the major kimberlite /carbonatite fracture-system. Campbell (1975) noted such a joint-set (\pm N25°E) that commonly occurred in outcrops along the piedmont of the Nuweveld escarpment. The

emplacement of the Cretaceous Salpeterkop carbonatite complex had a strong influence on the regional distribution of NNE-trending master-joints (compare **Figure 2.61** and **B.65**).

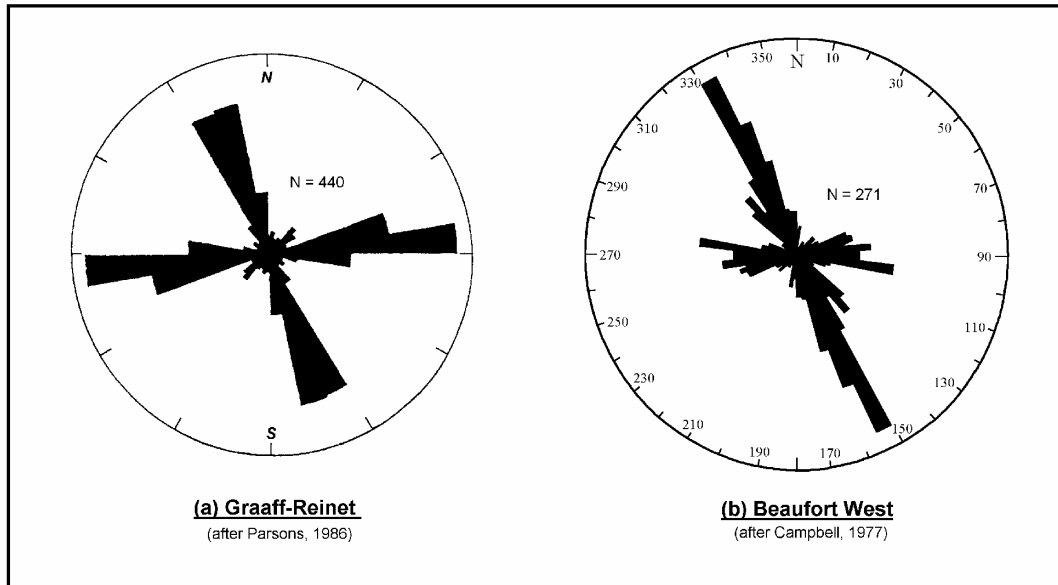


Figure 2.71: Rose diagram of joint orientations at Graaff-Reinet and Beaufort West

2.4.3.3 Jointing Mechanisms

Regional jointing is often related to neotectonics and erosional unloading (Hancock and Engelder, 1989). However, Woodford and Chevallier (2001) showed that prominent systematic master-joints and faults of the Western Karoo often show signs of reactivation and are much older than recent episodes of erosional unloading. The NNW orientated joints for instance, reflect a major stress system within the Western Karoo that has been active since the early phases of the break-up of Gondwana, until recent times. The NNE trending joint-set may be younger and linked to emplacement of the kimberlites. Both joint directions are therefore the result of regional crustal tectonics.

The less well-developed, orthogonal non-systematic joint system may be the result of uplift and thermal cooling after erosional unloading (**Figure 2.72**).

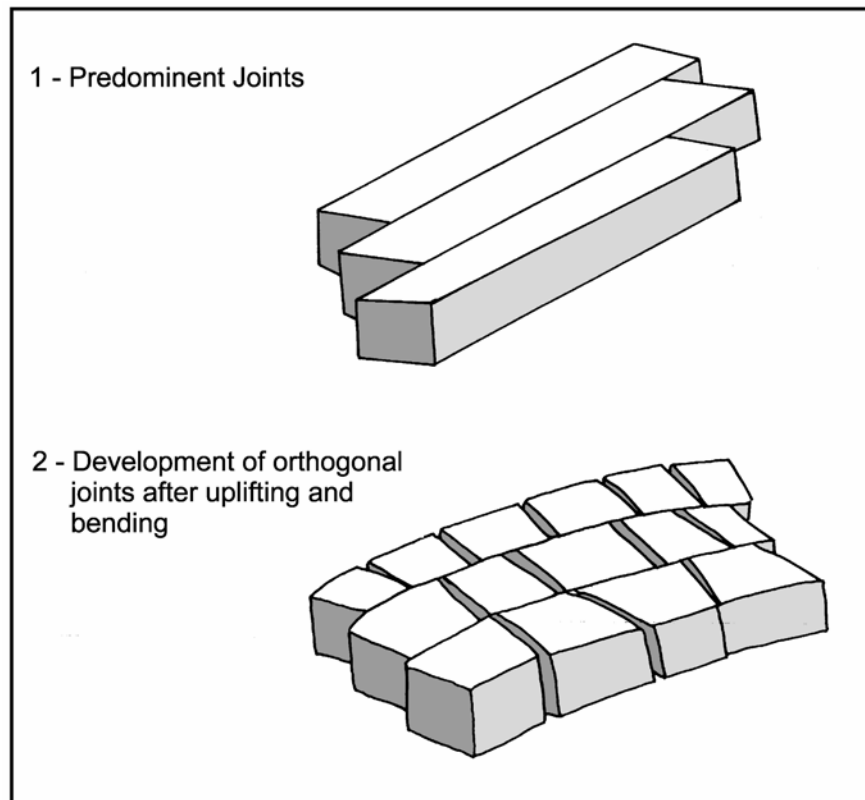


Figure 2.72: *Development of systematic and non-systematic joints of the Western Karoo (after Woodford and Chevallier, 2001)*

2.4.3.4 Hydrological Properties

Vertical jointing is largely developed in the sandstone of the Beaufort Group. With the exception of the extensive mega-joints and faults, master-joints generally have limited vertical extension and poor interconnectivity. Fracture connectivity may be enhanced where two orientations of systematic joints, together with their orthogonal systems, are present which leads to a 4-fold fractured network. Field verification by one of the authors (L. Chevallier) revealed that such areas are not evenly distributed.

The regional jointing plays a major role in determining the directional permeability (Wending, 1994) in fractured-rock aquifers, which generally at a maximum in the direction of the principal systematic joints. On a regional scale the Beaufort Group sandstones of the Western Karoo should thus exhibit a north-south orientated tensor of maximum permeability.

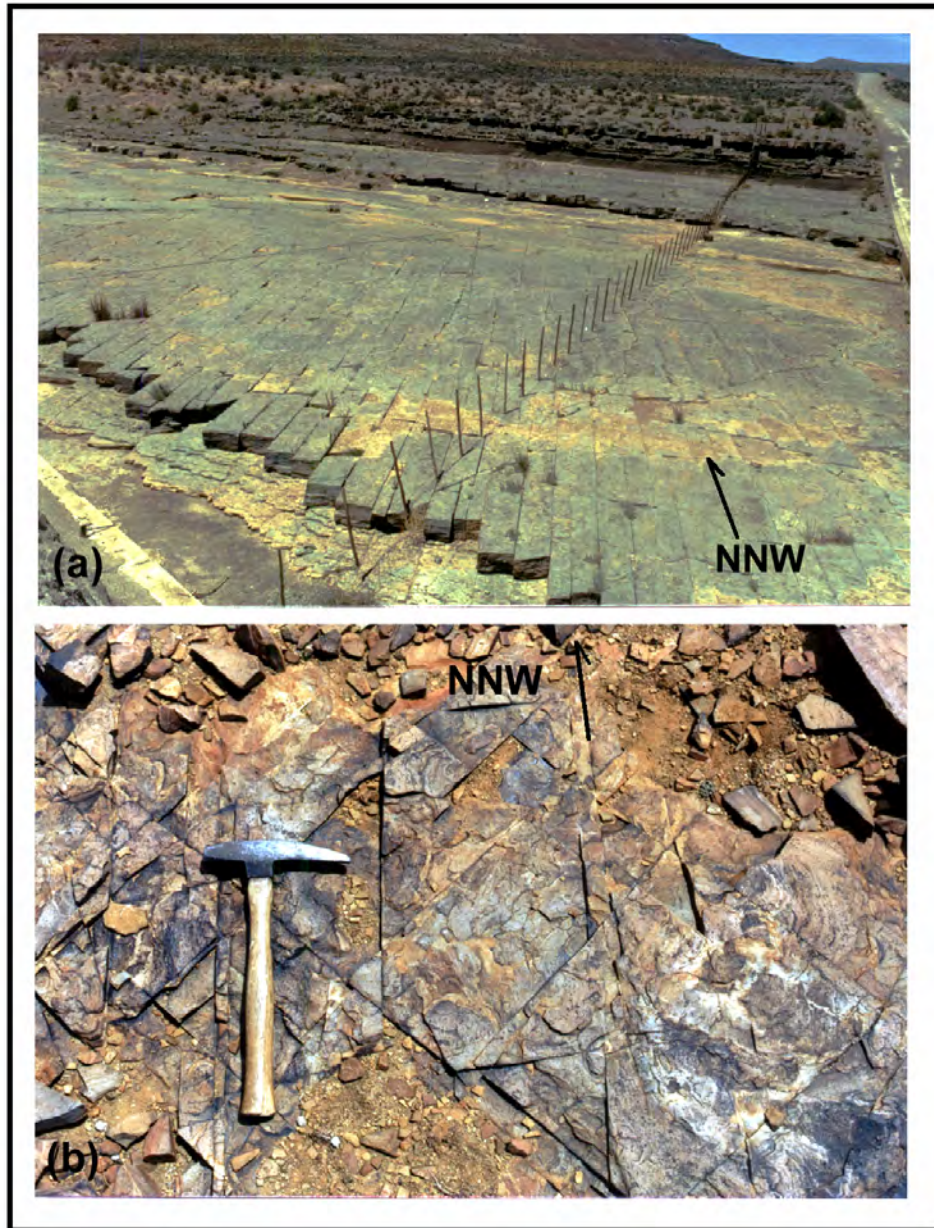


Plate 2.7: (a) *Prominent systematic NNW master joints with orthogonal a non-systematic set responsible for the 'ladder' effect, Hillcrest, Sheet 3122DC*
(b) *Superimposition of two orientations of master jointing, namely NNW and NNE at Loxton, Sheet 3122CB*

Very little information has been published on the occurrence of groundwater in discrete fracture or fissure zones *per se*, i.e. those not directly related to magma intrusion or folding in the Karoo Basin. This is probably because these structures are not easily detected on aerial-photographs, by geophysical methods or by field mapping, as well as a poor understanding of their tectonic origin. A typical example of such a fissure is the widely publicized, yet poorly understood, occurrence in Shaft 2 of the Orange-Fish River Tunnel (see Case Study, p 39).

In general, the ubiquitous and often regularly spaced joints visible in outcrop do not in themselves represent zones of higher permeability, where successful boreholes can be regularly sited. Well-jointed channel-sandstone of the Beaufort Group may be permeable and reportedly high-yielding boreholes have been drilled into these bodies, i.e. south of Beaufort West in the Poortjie Member of Abrahamskraal Formation (Andersen, pers. comm.).

Woodford and Chevallier (2001) reported higher yields in boreholes drilled within 15 m of master-joints and fracture zones (**Figure 2.73**) in the Loxton-Victoria West area, but found that the overall productivity of these boreholes (Mean = 2.4 l/s, Standard Deviation = 4.1 l/s, Median = 1.0 l/s) were on average lower than the ambient borehole yields (Mean = 2.9 l/s, Standard Deviation = 4.3 l/s, Median = 1.3 l/s), of the area.

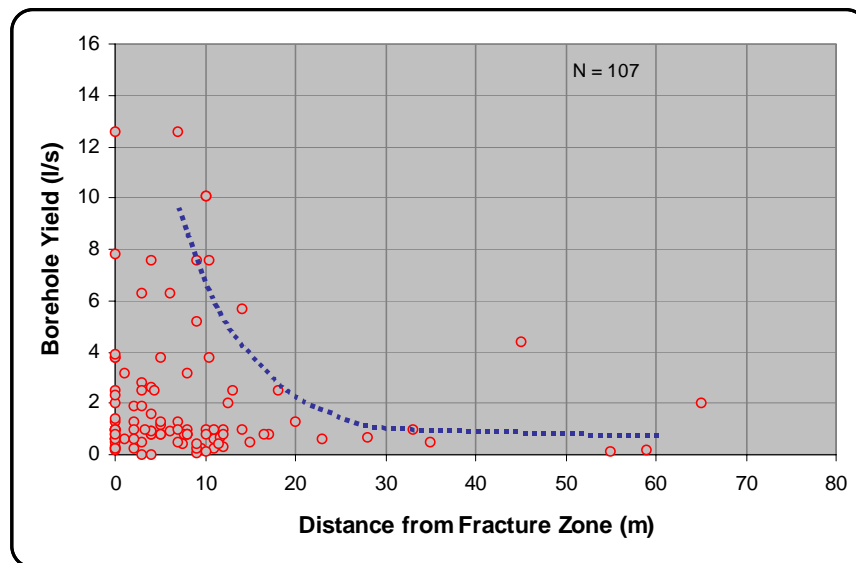


Figure 2.73: Borehole yield distribution with distance from fracture zone

Mega-joints and -faults showing signs of reactivation are more important from a geohydrological perspective as they are more deep-seated features and can act as conduits for groundwater flow. Unfortunately, only a few boreholes have been drilled into these structures, mostly by farmers.

Case Study: Flooding of the Orange-Fish River Tunnel

The Orange River Project was designed to regulate the flow of the River by means of a number of major reservoirs. Water from the Hendrik Verwoerd Dam passes through the Orange-Fish Tunnel in order to irrigate the valleys of the Great Fish and Sundays Rivers. The tunnel is 83 km long and is 5.3 m in diameter.

The tunnel was excavated in two different geohydrological zones, namely a weathered-jointed upper zone and an unweathered lower zone. By June 1971, 43.5 km of excavation had been completed, 16 km of which occurred at shallow depths of between 40 and 110 m below ground level (bgl). Groundwater was commonly intersected in pilot-boreholes at depths of 9 to 40 m.bgl.

In August 1969, an unforeseen fissure zone, not directly related to any dolerite intrusive, was intersected while tunneling some 550 m south of Shaft 2 (**Figure 2.74**). The fissure zone was intersected in the sediments of the Beaufort Group, at a depth of 110 m below the land-surface. The main inflow occurred through three 75°S dipping open fractures of 3.2, 3.2 and 7.6 cm wide, over a zone of 2.8 m. The initial inflow was estimated at 860 ℓ/s and the temperature of the water varied between 23-24°C. The waterlevel in the shaft stabilised at 18 m below the ground surface.

The area in the vicinity of Shaft 2 is cut by numerous dykes, which vary in thickness from 1 to 9 m and are mostly steeply dipping. The preferred orientation is N80W (more prominent) and N45E. The closest dyke intersecting the tunnel is some 490m away from the fissure zone.

No open, water-bearing, *bedding-plane joints* along lithological contacts or horizontal fissures were encountered in the tunnel. In the vicinity of shaft 2, however, the upper 6 to 15 m.bgl of sedimentary rock contain open water-bearing, bedding-planes joints between rock layers of different lithological character (Olivier, 1972).

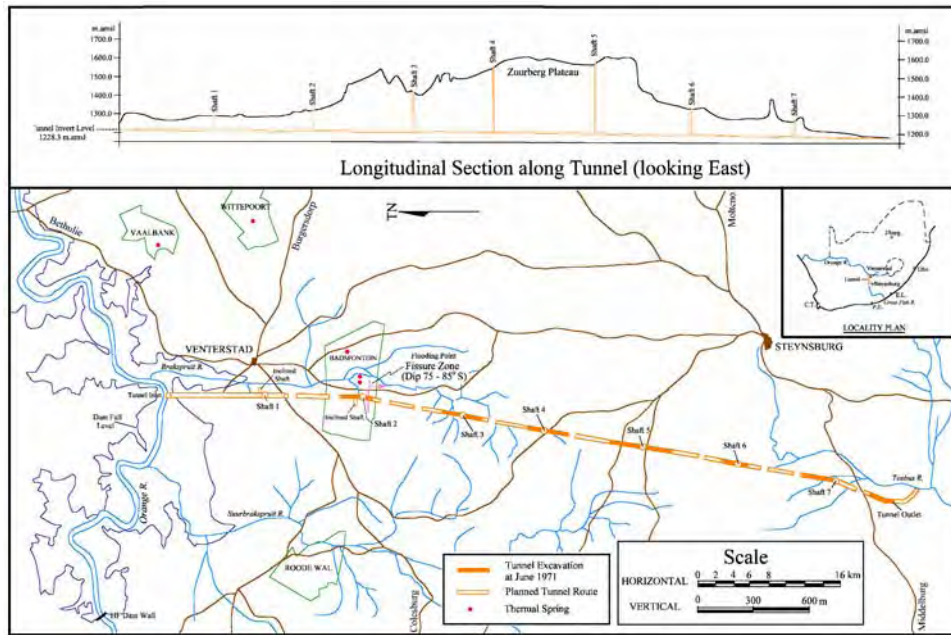


Figure 2.74: The Orange-Fish River Tunnel Scheme showing the flooding zone near Shaft 2 (after Olivier, 1972)

Numerous steep or *vertical joints* not associated with dolerite dykes, occur at various localities in the tunnel. They exhibit a preferred orientation of N50E, N75E and EW. The widths of the fractures vary from hairline to 0.95 cm. The majority of joints are dry or yield very little water, as they are either closed or sealed with secondary calcite or zeolites. In the vicinity of Shaft 2, highly permeable joints with widths of up to 7.6 cm were encountered. Two boreholes, NL13A and NL13F (**Figure 2.75**), illustrate the discrete nature of these vertical fractures – both boreholes were ‘dry’ down to tunnel-level, although they were drilled into the broader zone of fracturing within 40 m of the flooding point (Olivier, 1972).

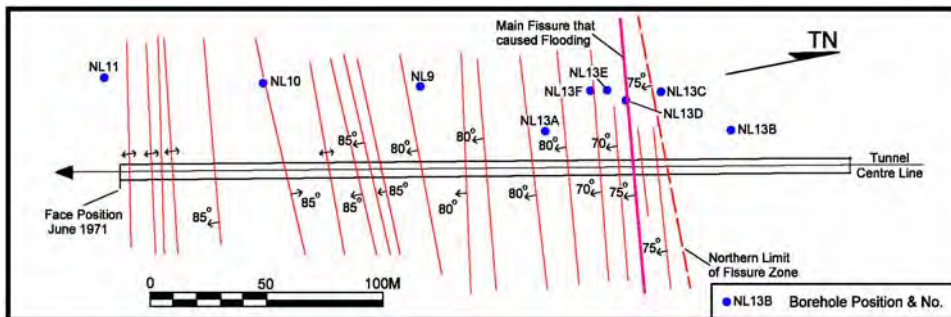


Figure 2.75: Plan showing boreholes and fractures at the point of flooding (after Olivier, 1972)

It is important to note that the majority of the dykes encountered in the 43 km of tunneling were dry or yielded flows of less than 0.1 ℓ/s at tunnel-level. Of the 55 steeply-dipping dykes encountered only 6 were fairly permeable at tunnel-level and yielded flows varying between 2.8 to 75 ℓ/s . These were all intersected in the tunnel where the rock cover was less than 110 m in thickness. Boreholes drilled into a 6m wide, east-west trending (N80W) dolerite dyke (Dyke A) yielded up to 75 ℓ/s in open fractures of up to 10 cm in width occurring along its southern contact and in the centre of the intrusion. It has been established that the high-yielding boreholes NL4 and NL5, pumped by a farmer at rates of up to 25 ℓ/s , as well as the 'western' and 'central' thermal springs on the farm Badsfontein (**Figure 2.74**) are associated with this dyke. Borehole S2/3, drilled during the site investigation, was tested for 32 hours at 28 ℓ/s , whilst borehole NL25 delivered similar results (Olivier, 1972).

An inflow of 18 ℓ/s was intercepted in the tunnel on the southern contact of Dyke B, which gradually decreased to 8 ℓ/s . Dyke C yielded similar results to Dyke B, but was dry at tunnel-level.

The majority of dykes encountered in the tunnel display prominent sheared margins and contact-zones, which cannot be regarded as mere planes of weakness. There is evidence for the development of shearing during and after the intrusion of the dolerite. The latter type of shearing is indicated by minor slick-n-slides, dark green chloritic material and secondary calcite. Prominent gravity faults, which post-date the dolerite intrusions, were also encountered in the tunnel.

Prior to the flooding event, the intersection of the high-yielding Dyke A resulted in a minor lowering of the *waterlevels* in the nearby Badsfontein boreholes, located 1 800 m east of the tunnel route. This indicated a direct hydraulic connection between the tunnel and the thermal springs along the highly permeable contact zone of the Dyke A.

The flooding of the tunnel drained an estimated volume of $6.6 \times 10^4 \text{ m}^3$ from the fissure-source within 24 h. Waterlevels in high-yielding boreholes, NL5 and S2/3, declined by 1.8 m after 3-4 days and thereafter fully recovered to that prior to the flooding. This apparent surge effect could not be observed in other existing, low yielding boreholes such as NL1, NL3 and NL7, which are not connected to Dyke A.

Porosity determinations on core obtained from exploratory boreholes drilled from the surface and petroscope boreholes in the tunnel itself yielded values varying from 2.2 to 8.2% for the various types of mudstone and 3.0 to 7.8 % for siltstones and fine-grained sandstones (Olivier, 1972).

Permeability tests performed on unweathered, non-indurated core rock samples obtained from the tunnel range from 0 to $4 \times 10^{-11} \text{ cm/s}$ for mudstones and 6.8×10^{-10} to $2.1 \times 10^{-9} \text{ cm/sec}$ for sandstones (National Building Research Institute, CSIR, 1965).

The *chemistry* of the groundwater, collected from various geohydrological environments, indicated that different water bodies are present in the area. The water quality varied from slightly saline, chloride to alkaline, soda-carbonate. Carbon-14 and tritium age determinations vary from 0 to 4 000 years (Olivier, 1992).

Figure 2.76 contains a plot of the total dissolved solids (TDS) of the groundwater against the corrected source depth. Samples obtained from Dyke A and the thermal springs indicate a vague relationship between the two parameters. Groundwater originating from source depths shallower than 180 m show a higher TDS than that of the main fissure zone (estimated source depth 90 to 460 m).

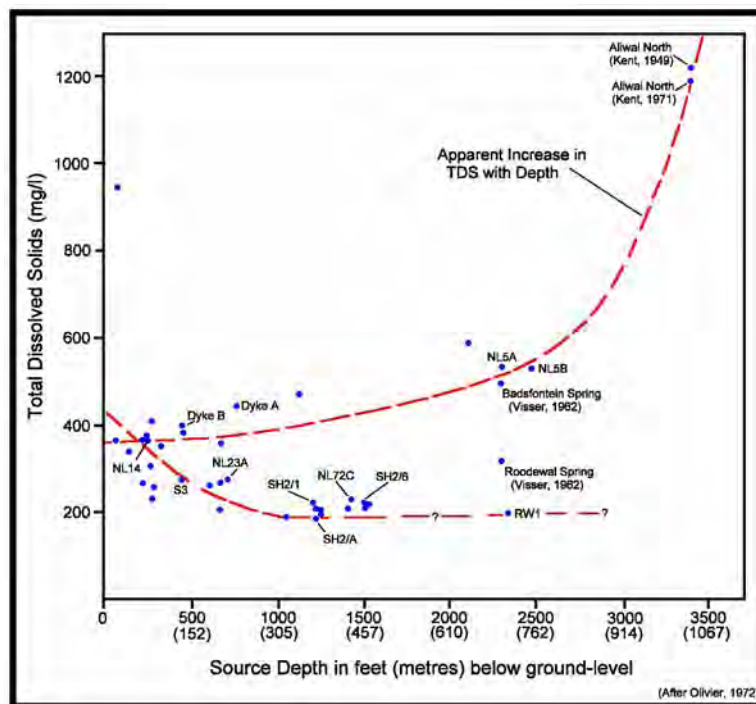


Figure 2.76: Relationship between total dissolved solids and source depth of the groundwater

A total volume of groundwater of $1.6 \times 10^6 \text{ m}^3$ was withdrawn from the area during the de-watering process over a period of 15 months, which only resulted in a relatively low drawdown in the waterlevels in some of the boreholes. The waterlevels recovered fully within 7 months, indicating the large storage capacity of the aquifer system.

It was concluded that the fissure zone is of post-Karoo age and linked to an extensive zone of crustal weakness extending from the Doringberg Fault near Prieska to the post-Karoo faults in Lesotho, and that the groundwater is of a deep-seated origin, based on the following:

- minimal decline in borehole waterlevels tapping the “near-surface” aquifer in the vicinity of Shaft 2 in relation to the large volumes of water removed during the de-watering process,
- the temperature and chemistry of the groundwater,
- the large earth-tidal fluctuations of up to 37 cm observed in some of the monitoring boreholes,
- the existence of an arcuate belt of Bouguer gravity highs between Noupoort and Aliwal North, and
- the abnormally large response of the waterlevels to the Ceres-Tulbach earthquakes.

2.4.4 BEDDING-PLANE FRACTURING

2.4.4.1 Description

Except for the southern folded regions, there is no geological record of regional horizontal fractures in the Main Karoo Basin.

Botha et al. (1998) proposed that the Karoo sediments were ubiquitously fractured along bedding-planes during episodes of isostatic rebound and erosional unloading, as a result of the difference in elasticity between the various rock units. They also concluded that increasing overburden pressures with depth have resulted in the closure of most of the deeper-seated, bedding-parallel fractures.

Differential gravity-loading in areas of extreme topographic contrast, i.e. along the margin of the Great Escarpment, may also result in the localised development of horizontal fracturing. Slope-creep along steep-sided valleys will result in the development of increased tensile stresses at the foot of the slope. Slope-creep usually causing existing joints on the slope to rotate and horizontal joints below the valley-floor to open and shear.

Smaller scale horizontal fractures are fairly common in the Main Karoo Basin. Bedding-plane, listric fractures occur within the overlying sedimentary rocks entrapped within dolerite ring-structures. They result from uplift and drag of the host rocks above the inclined dolerite sheet or ring-dyke. Single joints commonly extend for some 10 to 20 m and exhibit a horizontal-shear pattern. The thickness of the zone affected by this shear deformation is usually in the order of 0.5 m.

Drill-core from the Kopoasfontein stratigraphic borehole near Calvinia (G39974, **Figure 2.59**) showed that horizontal cleavage is well developed within the Eccca shales of the Tierberg, Whitehill and Prince Albert Formations. Horizontal cleavage is most prominently developed within the Tierberg shales. No major horizontal fractures were intercepted.

2.4.4.2 Hydrological Properties

Horizontal fractures play an important role in the lateral connectivity and groundwater circulation between vertical fractures in the near-surface, especially within the weathered zone. However, they are discontinuous features that do not form regional, laterally extensive aquifers.

Hydraulic tests on 24 shallow boreholes drilled into the Eccca shale on the Free State University Campus Test Site, by the Institute for Groundwater Studies, showed that the main water-strikes were associated with bedding-planes (Botha et al., 1998). Ten of the boreholes intersected a horizontal fracture some 100 m x 10 m in extent. The presence of this water-bearing fracture was clearly indicated using radiowave tomography (**Chapter 5.1.3**).

The existence and hydrological properties of shallow, sub-horizontal to horizontal fractures linked to areas of topographic-uplift alongside steep-sided valleys has yet to be ascertained.

2.5 SEISMICITY, NEOTECTONICS AND UNLOADING

2.5.1 SEISMO-NEOTECTONIC PROVINCES

A 'stress province' (Zoback and Zoback, 1980) is formally defined as a region of '... relatively uniform upper-crustal stress field ... with consistent stress orientations and relative magnitudes ... (having) linear dimensions that range from 100 to 2 000 km' (*op. cit.*, p. 6149).

Within the upper continental crust of Southern Africa, the ambient neotectonic stress regimes differ markedly between the southwestern and northeastern portions of the subcontinent (Zoback, 1992), such that distinct stress provinces are recognisable. The stress province boundaries coincide with an emergent belt of earthquake activity, which in turn forms part of a larger system of relatively aseismic blocks and seismically active belts between the Nubian and Somalian plates (Hartnady, 1990; Gordon and Stein, 1992; Gordon, 1995).

A distribution map of recent earthquake epicentres of South Africa shows three major seismo-tectonic provinces (**Figure 2.77**), namely:

1. The *Senqu Seismic Province* is a seismically active belt, trending E-W across the subcontinent from the Natal coast to the West coast. Two discrete zones of higher seismicity presently occur in the southern part of Lesotho and in the southern Free State. The belt forms a proposed juvenile extension of the East African Rift System, propagating southwards from other belts of earthquake activity in Mpumalanga and southern Mozambique (Hartnady, 1990; Hartnady, 1998; Du Plessis *et al.*, 1997). In **Figure 2.77** the nature of the East African Rift System is obscured by the Witwatersrand mining-induced seismicity, and also by serious deficiencies in and incompleteness of the international seismological catalogues for the western part of the southern African subcontinent. To the best of our knowledge no neotectonic activity has been described along the Senqu belt. However Andreoli *et al.* (1996) report a fault in a recent deposit on the farm Bultfontein in the Free State, which they attribute to a NNW extensional regime.
2. The *Cape Seismic Province* extends between the Tulbagh-Ceres area and the Koffiefontein region in the southern Orange Free State where, on one interpretation (Shudofsky, 1985), the dominantly strike-slip focal mechanism of the 01 July 1976 event is characterised by an E/W-trending S_{Hmax} . There is further evidence of the northward extent of this strike-slip regime to latitude 30°S in the Namaqualand-Bushmanland-Gordonia regions of the Northern Cape. Evidence for the eastward extent of the Cape stress province comes from the Orange-Fish tunnel in the Eastern Cape, where an 'open' E/W-striking joint system was intercepted (Olivier, 1972), and where in-situ measured stresses

showed a high magnitude for the horizontal component (Van Heerden, 1976). Crustal seismic activity in the Southern Karoo Basin is very limited and scattered. Woodford and Chevallier (2001) suggest that the earthquakes could be linked to the reactivation of NNW fractures (calcrete-fill mega-joints) under a WNW compressional tectonic stress regime.

3. The *Transgariep Seismic Province* is part of a large block encompassing most of southern and eastern Africa. It is dominated by a normal faulting regime in which $S_v > S_{Hmax} > S_{Hmin}$, and in which S_{Hmax} has an orientation which ranges between NW/SE and N/S. Fan and Wallace (1995) provide supporting evidence for this pattern from focal mechanism solutions for M5+ earthquakes in the South African goldfields. No neotectonic activity has been reported in this seismic province.

A recent overview of natural seismicity over Southern Africa was carried out to assess the seismo-tectonic setting of the Lesotho dam sites (Mohale Consultants Group, 2000). It was concluded that the clusters of higher activity scattered throughout the country were likely to be the result of the geomorphological dynamics of the sub-continent.

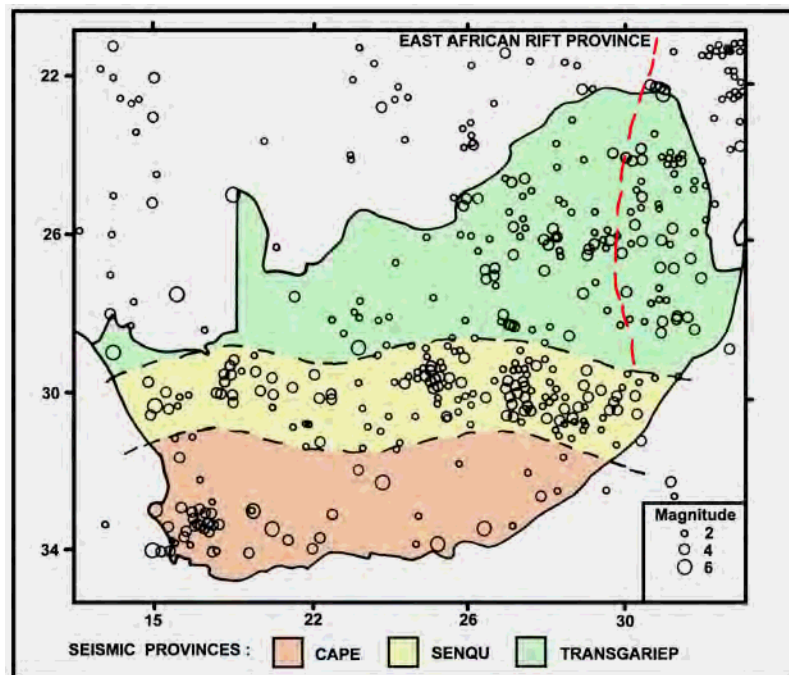


Figure 2.77: Map of seismic epicentres (Fernandez & Du Plessis, 1992) and seismotectonic provinces (Hartnady, 1998; Du Plessis et al., 1997) of South Africa

2.5.2 UPLIFTING AND EROSIONAL UNLOADING

Erosional unloading is a source of shallow neotectonic activity and important in near-surface stress fields (within the first 0.5 km of the crust). Unloading causes isostatic rebound and thermal cooling (Haxby and Turcotte, 1976), and usually creates surface extension that results in a series of recent joint systems.

After the Oligo Miocene uplift of the Lesotho region, erosion occurred to form the present course of the Orange River and the Great Escarpment. The amount of overburden that was removed in the Western Karoo over the last 30 Ma is difficult to estimate, but was relatively minor (maximum of 1 500 m). Initial crustal heat flow could therefore play a more important role in the distribution of surface stresses (Haxby and Turcotte, 1976). A tensional surface stress regime should therefore be expected above the “warmer” proterozoic Namaqua-Natal Belt and a less extensive or even compressive surface stress regime may be expected above the “colder” Kaapvaal Craton. The surface stress trajectory would therefore adopt a radial pattern all over the Main Karoo Basin, changing from tensile in the southwest to less tensional or compressive towards the northern parts of the Main Karoo Basin.

2.5.3 HYDROLOGICAL IMPLICATIONS

No direct relationship has thus far been made between seismo-tectonic provinces and the occurrence of groundwater in the Karoo Basin. However, the fact that groundwater flow within Karoo aquifers are fracture dominated makes it plausible to hypothesise that fracturing created under the prevailing crustal-stress regime will significantly effect the occurrence of groundwater - but this has not yet been definitively demonstrated nor critically tested (Hartnady and Woodford, 1996).

Bodmer (1994) and Sibson (1990) show that orientation of reactivated faults are not only a function of the external principal stress, but also of the gradual build up of pore-fluid pressure. The greater the angle between the external stress and the fault, the greater the hydrostatic pressure must be to permit for reactivation. The build up of hydrostatic pressure will result in seismic-valving, a mechanism responsible for many earthquakes. Bodmer (1994) suggested that the focal mechanism could be used for predicting hydraulic overpressures and that seismicity is expected to concentrate in areas where groundwater is trapped.

In the transition zones between one stress province and another, or along particular seismogenic structures within a stress province, the stress regime probably also displays temporal variations that depends upon the local state of strain buildup during an earthquake cycle. That the local earthquake cycle may have hydrogeological significance is illustrated by the (transient) groundwater phenomena encountered during and after the 29th September 1969 Tulbagh-Ceres earthquake (Olivier, 1972, Gordon-Welsh, 1974, Maclear and Woodford, 1995).

2.6 GEOMORPHOLOGY, FLUVIAL TERRACES AND PEDOCRETES

2.6.1 GEOMORPHOLOGY

2.6.1.1 First Order Features

The first order morphology of the Main Karoo Basin is a result of reduced crustal tectonics, uplifting and erosion (Partridge and Maud, 1987; Burke, 1996) and consists of the African surface and the post-African surface (**Figure 2.78**).

The *African surface* is dated from around 40 Ma before the African Plate came to rest over the mantle and is mainly reflected in the topography of the central part of the basin. The Great Escarpment that was formed during the Jurassic continental break-up was still a prominent feature. The general course of the Orange River was established.

The *post-African I surface* (± 30 Ma) and resulted from uplift centred below Lesotho. It was responsible for the reactivation of the Great Escarpment and controlled the present-day course of the Orange River. Uplift occurred in two phases, initially a phase of modest uplift of 150-300 m was followed by strong uplift that raised the eastern interior of the sub-continent by 900 m. The resultant surface is mainly reflected in the peripheral topography of the Karoo Basin. The lower sections of the Orange River shifted further northwards, leaving the Brandvlei palaeo-terraces.

2.6.1.2 Second Order Features

The second order features are mainly reflected by terrain variations, chiefly created by weathering and erosion of the dolerite ring-complexes. Large dolerite sill and ring-complexes, such as the Middelburg Basin (see **Figure 2.34**), may produce strong regional topographic anomalies (**Figure 2.79**). The smaller ring-complexes (50 to 5 km in diameter) form most of the more prominent topographic features in the Karoo. They are also reflected in the 3rd order drainage system (**Figure 2.80**).

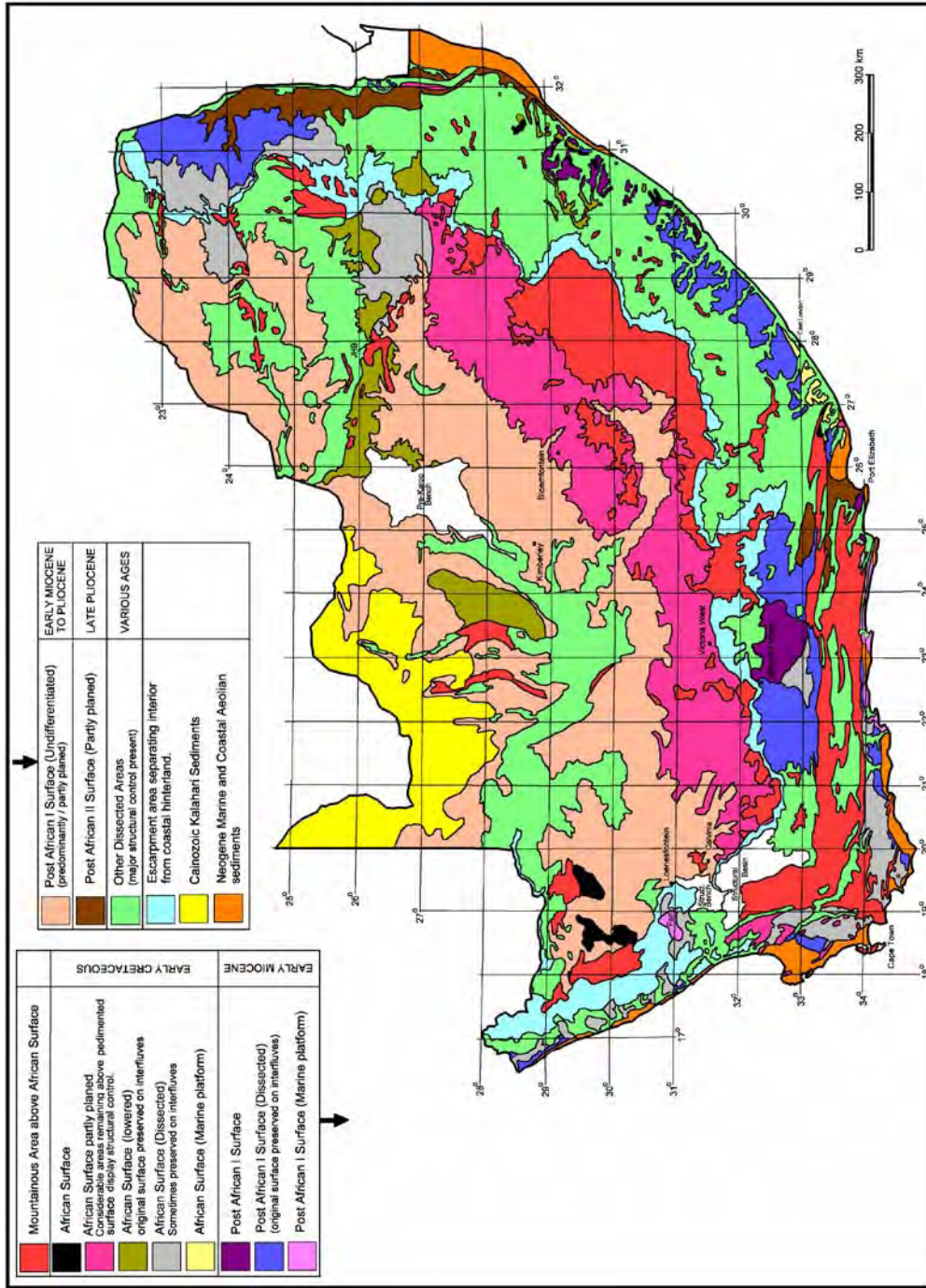


Figure 2.78: The African and Post-African land surfaces in South Africa (after Partridge and Maud, 1987)

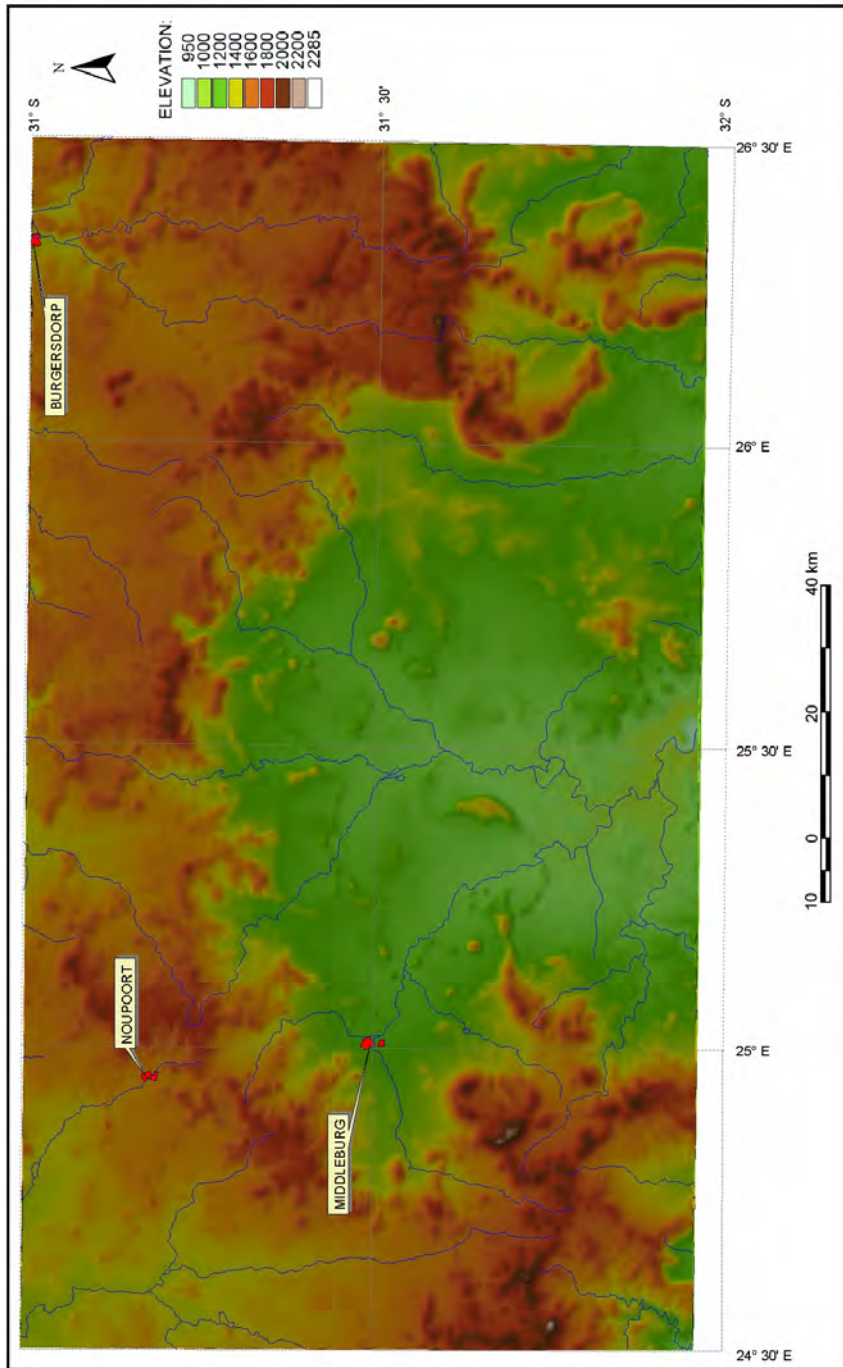


Figure 2.79: Digital elevation model indicating the regional topographic anomaly associated with the Middelburg Dolerite ring-complex

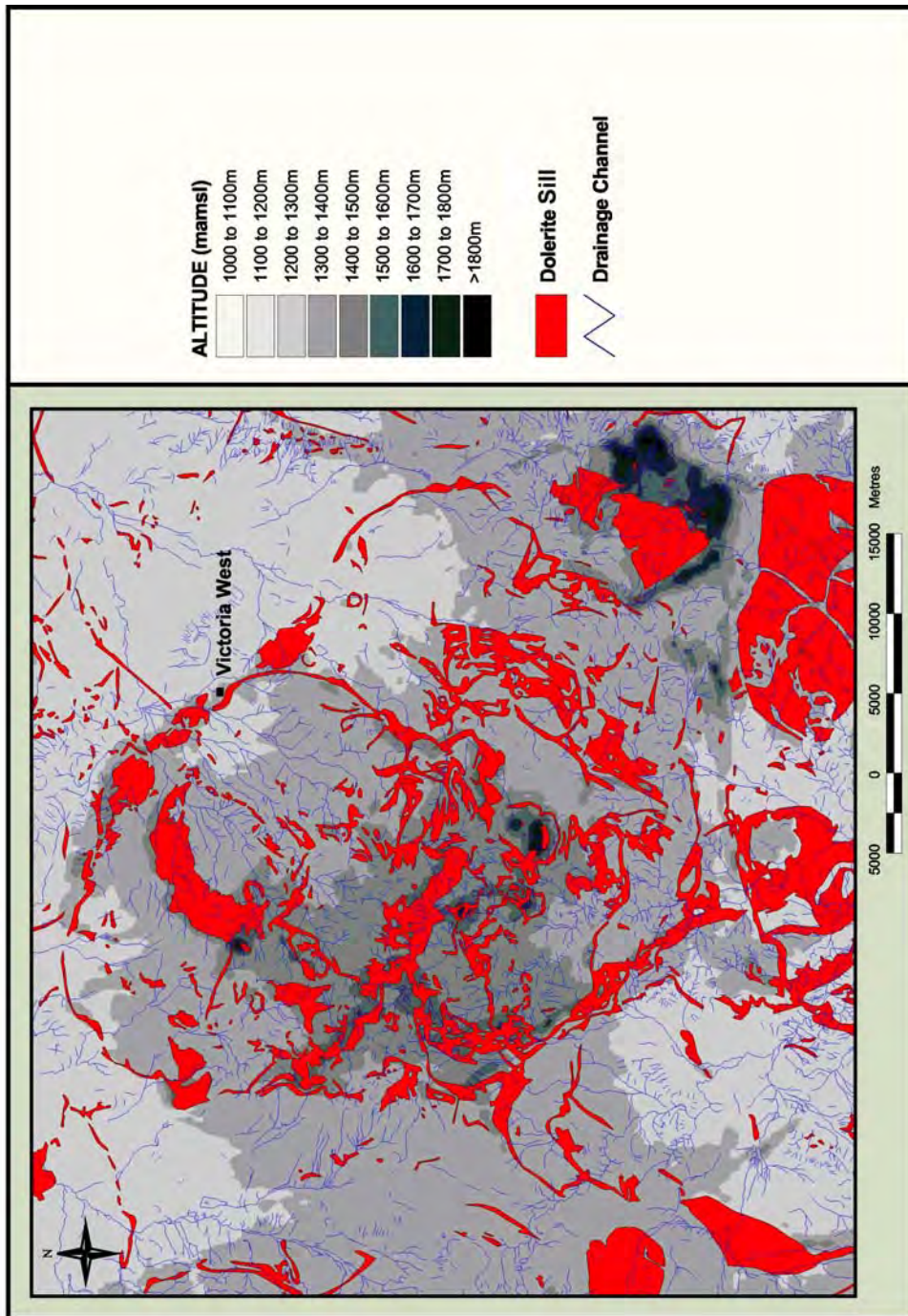


Figure 2.80: The influence of dolerite sill-ring complexes on the drainage system near Victoria West

2.6.1.3 Hydrological Significance

The hydrological significance of the *first-order geomorphological features* (African and Post-African surfaces) are difficult to assess. The margins of the Karoo Basin were most affected by the Post-African cycle, where a greater degree of erosional unloading took place. This resulted in surface stress relaxation and the development of a tensional regime, which coupled with isostatic uplift, may have resulted in the development of horizontal fractures in the near surface. These events may have positively enhanced the hydraulic properties of the shallow, fractured-rock aquifers along the edges of the Basin, i.e. the Tierberg Formation in the north and the Beaufort Group to the south of the Great Escarpment. Vegter (1992) states that the Karoo fractured-rock aquifers are formed by permeable fractures which are largely restricted to the shallow zone of weathering. In the De Aar area, Vegter states that this zone does not generally extend any deeper than 10-15 m below the watertable.

Second-order geomorphological features, mainly related to the dolerite sill and ring complexes, exhibit an orderly structure, viz. stratigraphically bounded 'rings-within-rings'. These features may influence the more regional geohydrological character of Karoo fractured-rock aquifers, due to variations in the stratigraphic-level and density of the intrusion.

2.6.2 FLUVIAL TERRACES AND FLOODPLAINS

2.6.2.1 Description

River terraces are present along most of the major rivers in the Karoo Basin (**Plate 2.8**). The main fluvial deposits are shown on **Figure 2.81**. They are Miocene or Plio-Pleistocene in age (Late Tertiary - Early Quaternary) and occur up to 60 m above the elevation of the present river channel. They mainly consist of gravels, comprising well-rounded cobbles and boulders, sometimes cemented by calcrete.

The large Plio-Pleistocene aged terrace to the south of Beaufort West lies some 10m above the general land surface and was deposited by sheet-wash action.

The Sak River terraces around Brandvlei consist of an Upper (60 m) Miocene and a Lower (30 m) Plio-Pleistocene terrace and result from channelling and meandering of the proto- and meso-Orange River. They are covered by windblown sand and are diamond-bearing (De Wit, 1996).

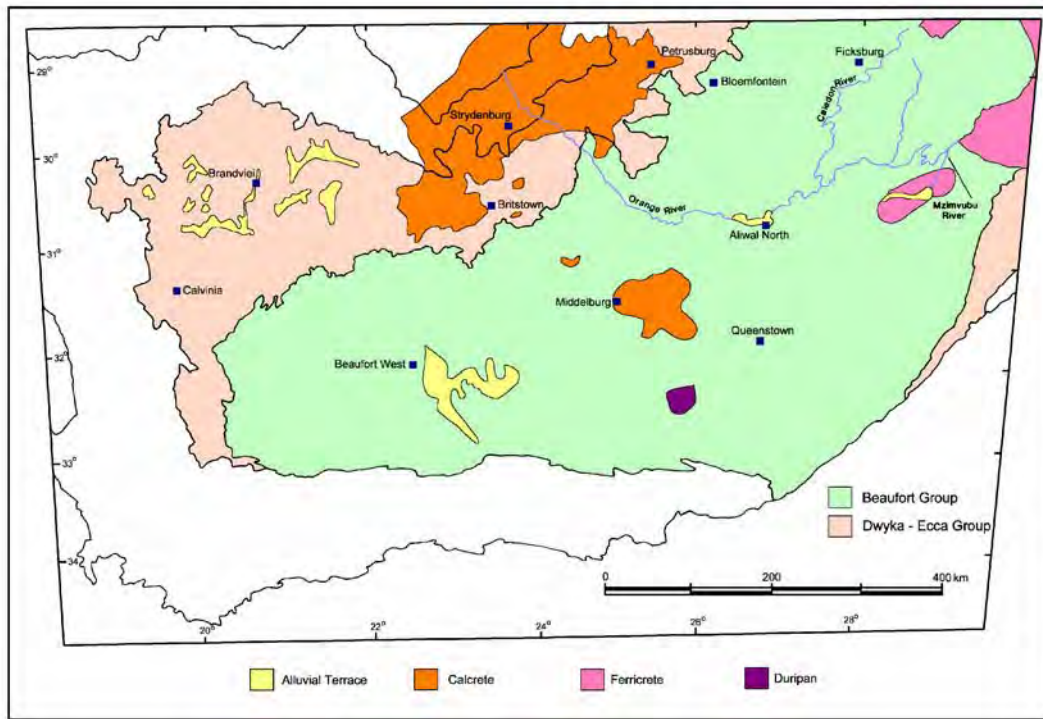


Figure 2.81: Schematic distribution of major Late Tertiary - Early Quaternary fluvial terrace and pedocrete (excluding gypsum) deposits of the Main Karoo Basin



Plate 2.8: Calcitized river-terrace overlying mudstone of the Middleton Formation, Graaff-Reinet

The Aliwal North terrace also lies between 15 and 70 m above the present river and could represent different cycles of deposition (Holmes and Reynhardt, 1989). Diamonds have been recovered from a trap-sited in the bedrock where a dolerite dyke cut at right angles across the river (De Wit, 1991).

The terraces of the Mzimvubu River (the Cedarville flats) are covered by dark clayey-humic sands and sometimes by lateritic soils. The deposit may reach 52 m in thickness and are composed of alternating thin lenses of variable grain-size sand and clay.

2.6.2.2 Hydrological Properties

Saturated alluvial deposits often form an important component of composite bedrock aquifers, which are limited in extent to a thin strip along the main river courses. These aquifers supply large volumes of groundwater to many towns in the Karoo, i.e. Ficksburg obtains approximately 50% of its water from alluvial beds in the Caledon River, De Aar extracts some 3.0×10^6 m³ per annum from deposits along the Brak River and its tributaries (Kirchner et al, 1991, Vegter 1992, Woodford, 1990). Composite alluvial-bedrock aquifers containing significant volumes of groundwater have been proven along the Salt River at Beaufort West (BRGM, 1979), the Salt River at Nelspoort (Leskiewicz, 1979), the Carnarvonleegte River north of Carnarvon (Smart, 1993), the Oorlogskloof River at Calvinia (Seward, 1983, Woodford, unpublished data), the Sundays River at Graaff-Reinet (Woodford, 1989) and Middelburg (Vandoolaeghe, 1979). The Masotcheni sediments that occur as isolated deposits along the valleys of the major rivers of KwaZulu-Natal are capable of storing significant quantities of groundwater (KwaZulu-Natal Project, 1995).

Productive alluvial-bedrock aquifers, such as the Caroluspoort aquifer near De Aar (**Figure 2.82**), commonly exhibit the following characteristics:

- The thickness of the alluvium varies between 5 and 40 m, with 10 to 15 m being more common.
- The upper section of the alluvium is commonly fine grained (silts and clays), which acts as a confining or leaky layer.
- The basal section is generally coarse grained, consisting mainly of fine-grained sand to coarse gravel. This zone is typically 1 to 5 m thick and represents the most transmissive portion of the aquifer.
- The bedrock is weathered and/or jointed and also acts as a conductive layer, although to a lesser extent. The depth and degree of weathering of the rock decreases from eastern to the western Karoo, i.e. at Calvinia in the western Karoo this zone is approximately a metre in thickness, while in Graaff-Reinet it varies between 2-5 m.
- The waterlevel is normally very shallow (i.e. less than 5 m bgl.).
- The groundwater quality is typically more saline than that in the adjoining fractured-rock aquifers.

Vandoolaeghe (1979) conducted granulometric analysis on samples of alluvium collected during exploration drilling in the Middelburg area. A typical analysis of these deposits is presented in **Table 2.11**. The results indicate the heterogeneity and general fining-upward nature of these deposits.

Table 2.11: Borehole G31579A - Granulometric analysis of alluvium

Depth Interval (m)	% of Fraction > 2 mm				% of Total Sample
	Clay	Silt	Fine Sand	Coarse Sand	Gravel (> 2mm)
0 - 1	55.4	18.4	18.6	2.9	6.7
- 2	40.3	39.1	18.4	1.0	14.3
- 3	45.7	31.6	17.2	1.3	1.7
- 4	32.2	31.3	29.9	5.7	1.9
- 5	22.5	17.3	51.6	6.9	1.8
- 6	17.1	6.5	59.5	15.1	1.4
- 7	15.4	10.7	57.7	14.5	2.6
- 8	13.9	14.0	47.8	20.9	38.2
- 9	17.3	13.0	32.8	37.6	32.0
- 10	18.4	17.3	24.5	38.8	38.5
- 11	17.7	17.4	27.2	37.7	31.3
- 12	20.3	18.8	26.2	38.0	25.1
- 13	19.4	14.1	36.0	30.3	17.6
- 14	19.3	19.9	34.6	24.9	66.8
- 15	17.3	17.0	33.0	34.9	56.9
- 16	23.3	21.9	28.6	26.6	68.3
- 17	22.0	18.0	21.2	38.8	50.5
- 18	26.0	8.5	23.8	44.6	73.5
- 19	20.7	8.2	28.6	41.5	83.1
- 20	22.2	7.4	24.7	50.0	70.0
- 21	21.7	9.0	28.7	40.6	55.1

Alluvial aquifers capable of sustaining long-term, large-scale production rarely occur east of longitude 23° in the southern Karoo Basin. This is probably because the deposits are not as well developed and are finer grained, as well as due to continued aggradation of the river systems as a result of more recent uplift along the eastern margin of the Basin. Vandoolaeghe (1980) found that the alluvial deposits in the Queenstown area were confined to thin strips along the major river courses, but were commonly clayey and unsaturated.

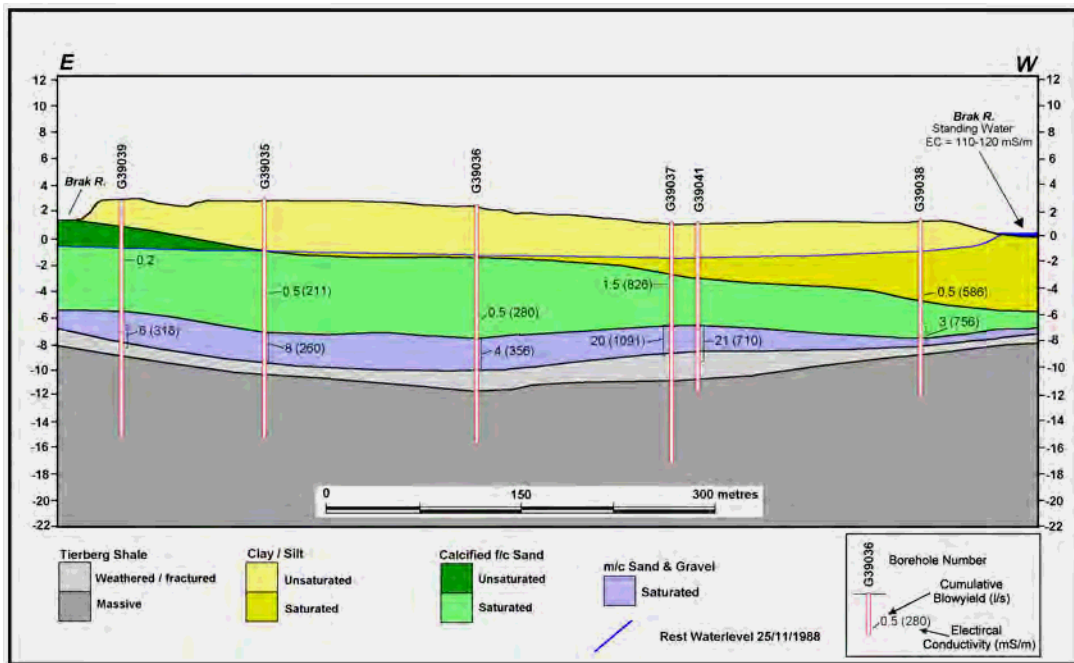


Figure 2.82: Geohydrological section across the Caroluspoort alluvial-bedrock aquifer, De Aar (Woodford, unpublished data)

Similarly, the majority of the boreholes drilled into the alluvial deposits along the course of the Mzimvubu River on the Cedarville Flats yielded poor results, although reasonable yields were intercepted in the underlying fractured Beaufort bedrock.

2.6.3 PEDOCRETE

2.6.3.1 Description

Pedocretes are soils that have been to a greater or lesser extent cemented or replaced by carbonates (*calcrete*), iron-oxides (*ferricrete*, *plinthite* or *laterite*), silica (*silcrete*), manganese-oxides (*manganocrete*), phosphate (*phoscrete*), gypsum (*gypcrete*) or magnesite (*magnesicrete*). Pedocretes appear to deposit at average rates of between about 20 and 200 mm per thousand years (Brink, 1985).

Calcrete deposits may attain a thickness in excess of 30 m, but are rarely homogeneous over depths exceeding 1 to 5 m. They are thought to be of two basic origins; (1) groundwater and (2) pedogenic. In the *groundwater type*, carbonate is precipitated above a fluctuating, shallow water-table or by lateral seepage of groundwater. In the *pedogenic type* the carbonate is transported downwards through the soil by infiltrating rainwater. The carbonate may originate from the soil or it may

be transported on dust particles or within the rainwater itself. Calcrete is usually formed in arid and semi-arid areas or as a weathering product of dolerite. The distribution map (**Figure 2.81**) shows two main areas of calcrete deposition in the Main Karoo Basin. The northern domain can be linked to the aridity of the region, whereas the Middelburg domain is geographically bounded by the Middelburg dolerite mega-ring complex (see **Figure 2.34**).

The term '*ferricrete*' or 'ouklip' has been widely used in South Africa to denote indurated, iron-rich deposits. Ferruginous pedocretes are formed by absolute accumulation, in which sesquioxides are added, or by relative accumulation in which sesquioxides are concentrated by the removal of the more soluble constituents under conditions of intense weathering and free drainage (D'Hoore, 1954). Ferricrete appear to need at least a sub-humid climate and chemical decomposition to release the necessary iron from the parent material. Ferricrete are well developed in two main areas of the Main Karoo Basin, namely Kwa-Zulu Natal and the terrain below the eastern Drakensberg escarpment (**Figure 2.81**).

According to Ellis and Schloms (1984) duripans or 'dorbanks' are indurated, usually reddish brown, massive or platy horizons of up to about 1.2 m thick, which are cemented by silica, and sometimes by calcium carbonate or iron oxides, to produce a consistency similar to that of hard rock. Duripans (Ellis and Schloms, 1984) are most common in the drier parts of the Cape and Namibia where the rainfall is less than 300 mm. Brink's (1985) map of the distribution of duripan shows deposits in the Graaff-Reinet area (**Figure 2.81**).

The *gypcrete* or gypsum deposits of the Karoo Basin were formed by chemical reaction between sulphuric acid and calcareous material (Visser et al., 1963) (**Figure 2.83**). The sulphuric acid is formed during the oxidation and decomposition of pyrite contained either in the White Hill Formation or in the dolerite intrusions. The gypcrete is present in the Ecca and Upper Dwyka rocks as either lenticular layers or nodules. An arid climate with a long-dry season is favourable for the development of gypsum deposits. Evaporation of groundwater during the long, dry seasons results in the concentration of calcium sulphate, which is then precipitated at the fluctuating groundwater-table interface.

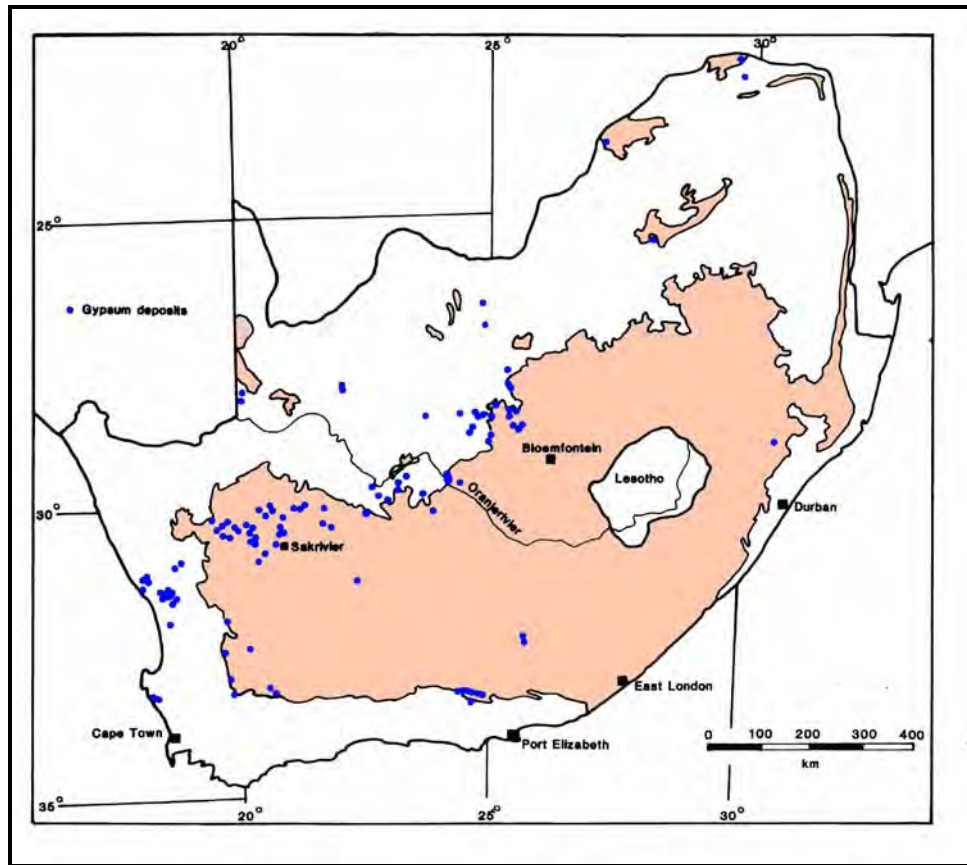


Figure 2.83: *Distribution of gypcrete in Southern Africa (after Visser et al., 1963)*

2.6.3.2 Hydrological Significance

Calcrete deposits often form excellent, albeit localised, sources of groundwater due to:

- a higher rate of recharge from rainfall than the average of 2-5% for Karoo aquifers (Kirchner et al., 1991), and
- dissolution of the calcrete results in highly permeable zones within the deposits, as well as enhancing their storage capacity.

Farmers in the central Free State district of Petrusburg often tap calcrete aquifers of up to 30 m thick for irrigation purposes. Weaver et al. (1993) explored valley calcretes situated within a dolerite ring-complex near Strydenburg in the Northern Cape Province and delineated an extensive, thin aquifer using electrical-resistivity geophysical techniques (see **Chapter 5.1.3.3**).

2.7 DIAGENESIS, PALEO-FLUID MOVEMENTS AND THERMO-METAMORPHISM

2.7.1 DESCRIPTION

Diagenetic studies of the sediments were carried out during the SOEKOR exploration for oil and gas in the Karoo Basin (Rowse and De Swart, 1976). All the physical properties of the sediments, i.e. shale density and porosity, sonic velocity, vitrinite reflectance, sandstone porosity and permeability, proportion of chloroform extract, indicate a general trend of diagenesis increasing from north to south (see **Chapter 2.2.5**). This is related to the depth of burial, i.e. the greater the depth of burial the greater the degree of compaction and cementation.

The migration of hydrothermal fluids from the Cape Fold Belt in the south during the orogeny was responsible for the uranium mineralisation in the Karoo Basin. Most of the uranium occurrences are located in the fluvial channel sandstone of the Adelaide Subgroup (Beaufort Group) and are mainly located in the Western Karoo (Fraserburg, Laingsburg, Aberdeen) (Cole, 1991). Low temperature groundwater formed the mineralising solutions, which migrated northwards along geological structures and the more permeable sandstone layers.

In addition to contact metamorphism that occurs adjacent to the major dolerite intrusions, Duane and Brown (1992) demonstrated a thermal overprint in the Karoo sediments dated at around 190 Ma, i.e. during the intrusion of the Jurassic dolerites. The authors suggest that the break-up of Gondwanaland may have resulted in the total rejuvenation of the Karoo aquifers. Regional hydrothermal systems were generated, the most striking results of which are the breccia plugs (**Chapter 2.3.2.2**).

The thermal influence of the later intrusion of the kimberlite fissures and diatremes was negligible and there is no evidence for any regional scale metamorphism of the Karoo sediments. The uplifting and fracturing that accompanied the intrusion of the kimberlite may have provided a mechanism whereby the entrapped, deeper-seated groundwater could have risen to the surface and deposited secondary minerals containing carbonate and silica into the open voids, thereby reducing the porosity and permeability of the sediments even further.

2.7.2 HYDROLOGICAL IMPLICATIONS

A decrease in the degree of diagenesis of the Karoo sediments from south to north corresponds to an increase in porosity and permeability of the shale and sandstone towards the north portion of the Main Karoo Basin (**Figure 2.9 and 2.10**).

The influence of the uranium province on hydrological properties of the Karoo sediments has as yet not been determined. The rejuvenation of the Karoo aquifers

during the break-up of Gondwana raises the possibility that palaeo-aquifers may occur within the deeper portions of the Basin.

2.8 **WEATHERING**

The primary factors controlling the weathering of rocks in the Karoo Basin are (1) climate and (2) the second order drainage.

1. Brink (1983) subdivided South Africa into two major climatic and weathering zones, separated by a north-south line extending from Port Elizabeth to Bloemfontein. The Karoo Basin is subdivided into an arid western zone where mechanical disintegration dominates and a humid eastern zone where chemical decomposition is the dominant mode of weathering (**Figure 2.84**).
2. The second order drainage density is higher in the eastern half of the Basin when compared to the western areas (**Figure 1.1**). This further enhances the differences in the nature and processes of weathering between the two areas.

There is a clear correlation between the mean annual precipitation and evaporation (**Figure 1.3**) and the dominant mode of weathering in the Karoo Basin (**Figure 2.84**). Weinert (1974) used this basis and field evidence to further subdivide the country into zones where the weathering processes are similar, according to a so-called N-value climatic index, where:

- $N < 2$: rocks are deeply weathered often to depth of several tens of meters and decomposition is pronounced. Montmorillonite is the dominant product of decomposition of dolerite.
- $N \geq 2$ and $N < 5$: the thickness of the cover soil decreases gradually. Smectite is the dominant product of decomposition of dolerite.
- $N \geq 5$ and $N < 10$: mechanical disintegration is the dominant weathering process. The decomposition of dolerite is less pronounced.
- $N \geq 10$: all rock types weather by mechanical disintegration. Shallow residual soils are developed, which are gravely and granular.

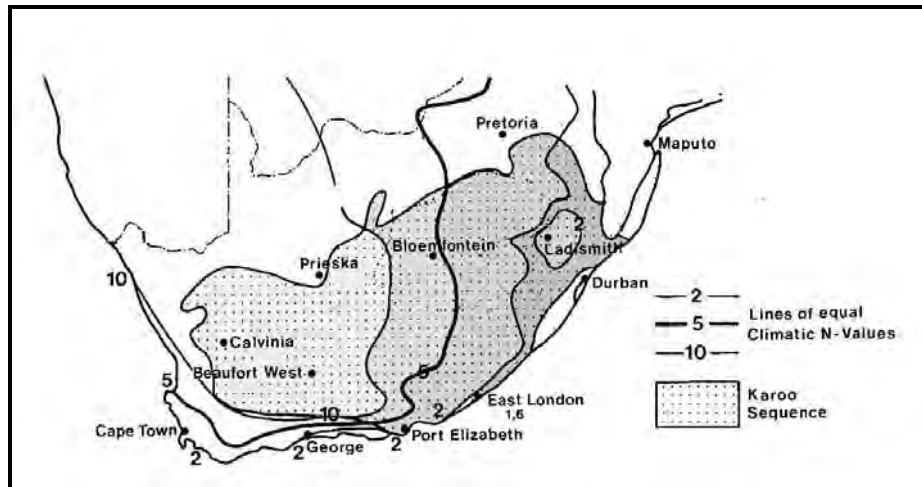


Figure 2.84: Climatic N-values of 2, 5 and 10 in Southern Africa (Weinert, 1974)

2.8.1 SEDIMENT WEATHERING

The Karoo rocks can, from a weathering and engineering viewpoint, be grouped into three major categories of rock masses, namely diamictite tillite, mudrock and sandstone (Brink, 1983).

2.8.1.1 Dwyka Diamictite

Chemical weathering of the fine matrix usually results in a clay-rich decomposition product. The diamictite of the Karoo Basin can be divided into three distinctive regions (Brink, 1983):

- **KwaZulu-Natal:** the diamictite is fresh in valleys incised during Pleistocene times. At higher elevations the diamictite decomposes to weathered, blocky rockmass covered by up to several meters of gravely residual soil.
- **South-western Karoo:** mechanical disintegration dominates and ‘tombstone weathering’ along cleavage characterises these outcrops. Virtually no residual soil is developed.
- **North-Eastern Cape:** the Dwyka rocks are highly weathered due to the large percentage of shale units compared to diamictite.

2.8.1.2 Mudrock

It includes a range of fine grain sediments: siltstone (more silt than clay), mudstone and shale (more clay than silt). On weathering shale and mudstone become very friable and decomposes to produce dark brown cohesive soils that can reach a few meters in thickness in the eastern weathering-zone of the Karoo Basin (Brink, 1983). At depth the weathering of mudrock results in clay seams along joints, fractures and bedding-plane partings. These clay seams result from preferential leaching in the vadose zone. Weathering weakens the intergranular bonding of the mudrock and leads to the removal of a large proportion of the cementing material.

2.8.1.3 Sandstone

Because of the large percentage of quartz in such rocks (>50%), sandstone weathers by mechanical disintegration. Thin sandy topsoils are produced from the decomposition of feldspar cemented sandstone, whilst virtually no weathering or soil development occurs on silica-bond sandstones.

2.8.2 DOLERITE WEATHERING

Dolerite weathers in a manner similar to many crystalline rocks. In addition to climatic and geomorphological factors, the weathering of Karoo dolerite intrusions are determined by the degree of fracturing, the width of the intrusion, the cooling rate and the grain size.

- The degree of fracturing is controlled by thermal jointing and tectonic reactivation (**Figure 2.16**). If only thermal jointing is present the dolerite intrusion remains relatively solid and intact. However, if tectonic (hydrothermal) reactivation of the dolerite has taken place the rockmass appears 'shattered' and consists of small boulders usually less than 0.5 m in diameter set in a friable, fine-grained matrix (**Plate 2.9**).
- The influence of dyke width, cooling rate and grain size are inter-related:

Wide dykes (>8 m) generally exhibit a prominent chill-margin containing a fine grained, porphyritic, melanocratic dolerite that weathers to produce well-rounded, small, white-speckled boulders (i.e. spheroidal weathering). This zone is normally only 0.5 to 1.5 m wide and exhibits well-developed thermal-shrinkage joints. The central portion of such dykes consist of medium- to coarse-grained, mesocratic and occasionally leucocratic dolerite that decomposes to a uniform 'gravely' material, which exhibits a typical exfoliation weathering pattern. Sporadic fractures or meta-sedimentary veins are encountered in this zone and they often do not extend into the

country rock. Magnetic traverses across these features normally produce two distinctive peaks.

Narrow dykes (<3 m) commonly consist of fine-grained, porphyritic, melanocratic dolerite (Vandoolaeghe, 1979). These tend to be more resistant to weathering than the thicker dykes and in outcrop exhibit a uniform pattern of shrinkage-joints. The dyke weathers to produce small rounded, white-speckled boulders set in a finer angular groundmass.



Plate 2.9: *Fractured and weathered dolerite dyke, north of Victoria West*

The weathered appearance of a dolerite intrusion will therefore be determined by a combination of all of the above factors (climate, drainage, fracturing, width, cooling, grain-size) and Brink (1983) proposed the following classification scheme for engineering purposes (**Table 2.12**):

Table 2.12: Classification of weathered Karoo dolerite rocks (adapted from Brink, 1983)







Type	Appearance	Description
1		<u>Solid dolerite</u> : thermal jointing, <15% weathered material in the rockmass.
2		<u>Fractured dolerite</u> : boulders of <0.5 m in diameter, moderately thick zones of weathered material within joint spaces.
3		<u>Boulder dolerite</u> : boulders of >0.5 m in diameter with rounded edges, up to 1m thick zone of weathered material between boulders (Plate 2.9).
4		<u>Gravel dolerite</u> : friable, gravel with solid particles <10 cm in diameter, variable weathering of the particles.
5		<u>Granular dolerite</u> : fine 'gravely' to occasionally clayey, remnant of boulders with onion structure, may include calcrete or ferricrete (Plate 2.10).
6		<u>Residual dolerite</u> : soft homogeneous sandy to clayey soil.



Plate 2.10: *Fractured and decomposed dolerite sheet, Victoria West*

2.8.3 HYDROLOGICAL IMPLICATIONS

Sediments

Van Wyk (1963) and Vegter (1992) state that the porosity and permeability of the Karoo sediments appears to be highest in the near-surface (i.e. the upper 30 m), which generally corresponds to the weathered zone. There is no clear relation, however, between the occurrence of groundwater and the weathering of the different Karoo lithologies. In this regard, the following generalisation may be stated:

- Dwyka diamictite may represent potential ‘weathered’ aquifers due to their low resistance to weathering.
- Weathering of Karoo shale and mudrock produces clays, which often reduces the permeability of the sediments.
- Karoo sandstone is highly resistant to weathering and thus these processes are unlikely to directly affect the hydraulic properties of these rocks.

Composite alluvial-weathered bedrock aquifers are commonly developed along the major drainage systems (see **Chapter 2.6.2.2**).

Dolerite Intrusions

Extensive weathered zones often develop in dolerite sills that are situated in low lying and well drained areas - similar to 'weathered basins' described in other crystalline basement rocks (Enslin, 1943; Wright and Burgess, 1992). These localised, shallow intergranular aquifers are capable of storing large volumes of groundwater.

Dolerite ring-dykes and inclined sheets seldom form negative features of the landscape, as they are more resistant to weathering. The hydrological properties of weathered dolerite rings and inclined sheets seem very variable. Vegter (1995) states that the upper or lower contact of dolerite sills located within the weathered zone, i.e. 20 to 50 m.bgl, are favourable zones for striking groundwater. Recent extensive exploration drilling along dolerite inclined sheets and ring dykes in the Victoria West area (Chevallier et al, 2001), shows that the contact between the sediment and the dolerite within the first 50 m below surface did not yield significant volumes of groundwater.

The contact between dolerite dykes and the host rock, within the weathered zone, remains the favourite target for groundwater exploration (Vegter, 1995; Smart, 1998).

Chapter 3

PHYSICAL AND CHEMICAL DESCRIPTION OF KAROO AQUIFERS

3.1 GROUNDWATER FLOW AND BEHAVIOUR OF KAROO FRACTURED-AQUIFERS

3.1.1 INTRODUCTION

The simplest approach to study the physical behaviour of an aquifer is probably to perform a hydraulic test on the aquifer. Although there are quite a number of these tests that one can perform (Botha et al., 1998; Kruseman and De Ridder, 1991), the discussion in this section will be restricted to the results obtained from the analysis of approximately 50 constant rate tests from various places underlain by the Karoo Supergroup. These include places such as: Beaufort West, Bloemfontein, Calvinia, De Aar, Dewetsdorp, Graaff-Reinet, Kestell, Kokstad, Philippolis, and Rouxville (Botha et al., 1998).

The physical behaviour of an aquifer system is determined, ultimately, by the interactions between the water and the rock matrix in which the aquifer occurs. Although there exist other interactions, there is no doubt that the adhesive force, between the water molecules and the boundaries of the voids in the rock matrix, is the most basic interaction. This force can be described mathematically by Laplace's equation (Bear, 1972)

$$(p_0 - p_i) = s \left(\frac{1}{r_1} + \frac{1}{r_2} \right) \quad \text{Eq. 3.1}$$

where, s is the surface tension of water, p_n and p_i the outer and inner pressure on the water surface, and r_1 and r_2 the radii of curvature of the water surface, which is determined by the void's geometry. The flow of water through an aquifer is thus in the first instance determined by the geometry of the voids, in the rock matrix of the aquifer. This dependence is so basic, that it is rarely mentioned in the groundwater literature. The most common approach is simply to assume that the rock matrix can be represented as a porous medium (Black, 1993). It is only when the observations cannot be reconciled with the behaviour of a porous medium, that other media are considered. However, such a change in the representation of the rock matrix should be made, not merely because the observations cannot be reconciled, but rather on sound physical evidence. The first step to be taken, in the study of any aquifer, therefore should be to determine the geometry of its voids.

The geometry of the voids, at any point in the earth's subsurface, is ultimately determined by the geological formation present at that point. The present geological and geophysical methods commonly employed for this purpose, unfortunately, are not very efficient. The void geometry of the formations is consequently mostly neglected in studies of aquifer systems.

One approach that can contribute significantly towards a better, albeit qualitative, knowledge of an aquifer's geometry, is through an understanding of the origin and evolution of the formations that contain the aquifer. Although this approach is rarely applied, or mentioned, in existing groundwater literature, Botha et al., (1998) were able to trace many properties of Karoo aquifers to their historical evolution. This chapter will therefore be devoted to a brief review of how the present geometry of the Karoo Supergroup influences the behaviour of Karoo aquifers.

The typical water-level drawdown responses observed during the above constant-discharge tests are near 'textbook' examples of the model, proposed by (Gringarten and Ramey, 1974) for the drawdown in a borehole that penetrates a horizontal fracture in a confined aquifer. This correlation suggests that one could expect to observe four flow periods in the drawdown curves of boreholes tapping Karoo aquifers – initially (i) a storage-type flow, followed by a period of (ii) vertical linear flow from the rock matrix to the fracture, (iii) a transitional period, and finally (iv) pseudo-radial flow, provided that the fracture has a significant aperture and areal extent. Otherwise, only the last three flow periods will be observed.

Botha et al. (1998) found that the water-level drawdowns in the majority of constant-rate tests investigated began to deviate from the Gringarten-Ramey model at some stage. Botha et al. states that this may be caused by two factors, namely: (i) the inability of the surrounding rock matrix to supply enough water to the fracture to satisfy the discharge demand, and (ii) the possible deformation of the fracture and/or aquifer.

3.1.2 NATURE OF GROUNDWATER FLOW IN FRACTURED AQUIFERS

3.1.2.1 General

The aperture and areal extent of water-yielding fractures in Karoo formations are limited, and therefore unable to store large quantities of water (Botha et al., 1998). The formation - not the fractures - must therefore act as the main storage units of water in Karoo aquifers. This conclusion of course contradicts the conventional view that these formations as dense and relatively impermeable, at least when compared with formations such as unconsolidated sands and dolomite.

Detailed geological assessment of Karoo formations has indicated two very important consequences for the behaviour of Karoo aquifer systems, namely:

- (a) Flow in the Karoo formations very much resembles flow in a porous medium and therefore must obey Darcy's Law.
- (b) The formations may contain large quantities of water, but are not able to release it readily over small areas, such as the circumference of a borehole.

To discuss these consequences further, consider the section of a hypothetical aquifer depicted in **Figure 3.1**. Since the Karoo formations are dense, the borehole will receive almost all its water from the water-yielding fracture, the moment the pump is switched on. However, this will create a drop in the piezometric pressure within the fracture, and consequently an imbalance in the flux of water across its interface with the rock matrix. According to Darcy's law, $q = -K=j$ - this imbalance will cause a flux of water (q) from the matrix to the fracture, for as long as the piezometric pressure gradient ($=j$) in the rock matrix exists. Although this flux may be small, the flow over a large water-yielding fracture can be considerable. To illustrate this, consider the case of the aquifer system on the *Campus Test Site*, where the main water-bearing fracture is horizontal (**Figures 3.1** and **3.2**) that has been intersected by a number of boreholes.

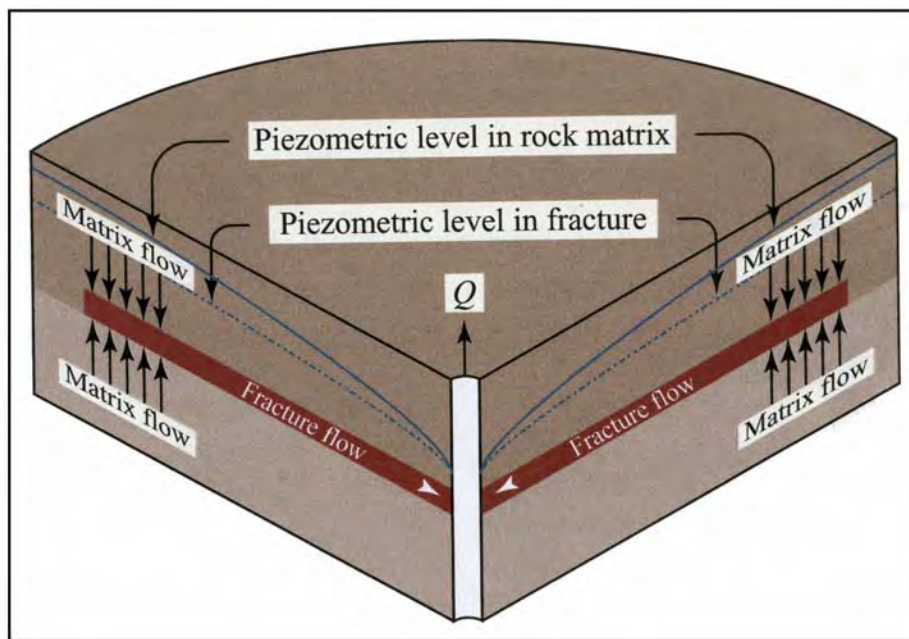


Figure 3.1: Schematic illustration of groundwater flow, towards a borehole in a Karoo aquifer

The exact extent of the fracture in **Figure 3.2** is not known, but it certainly does not exceed an area with a radius of greater than 100 m and core-drilling has indicated the fracture aperture to be no larger than 1 mm. The fracture can therefore store at most 7.854 m³ of groundwater, which means that it can only supply Borehole UO5 with its immediate yield of 8.3 l/s, with water for approximately 16 minutes. The fracture

therefore cannot serve as the main storage unit of groundwater on the Campus Test Site. Since the sandstone and shale surrounding the fracture are the only other storage units available on the site, they must be the main suppliers of water to these boreholes. To test this hypothesis, assume that the vertical hydraulic conductivity of the sandstone is 10^{-6} m/s and that the hydraulic gradient between the sandstone and fracture is unity, i.e. no pressure difference exists between the fracture and sandstone, and that the water flows towards the fracture under gravity. In this case, water can percolate into the fracture at a rate of 56.549 m³/h. Groundwater in Karoo aquifers must therefore be stored mainly in the sedimentary rocks and not in the fractures. Fractures in Karoo aquifers are therefore not the main storage units for water, but serve only as conduits for the water to move from the sedimentary rock matrix towards the pumping borehole. Since this interpretation is also valid for a vertical fracture, matrix flow will be the predominant type of flow in stressed Karoo aquifers, unless the fracture has an unusually large aperture and areal extent.

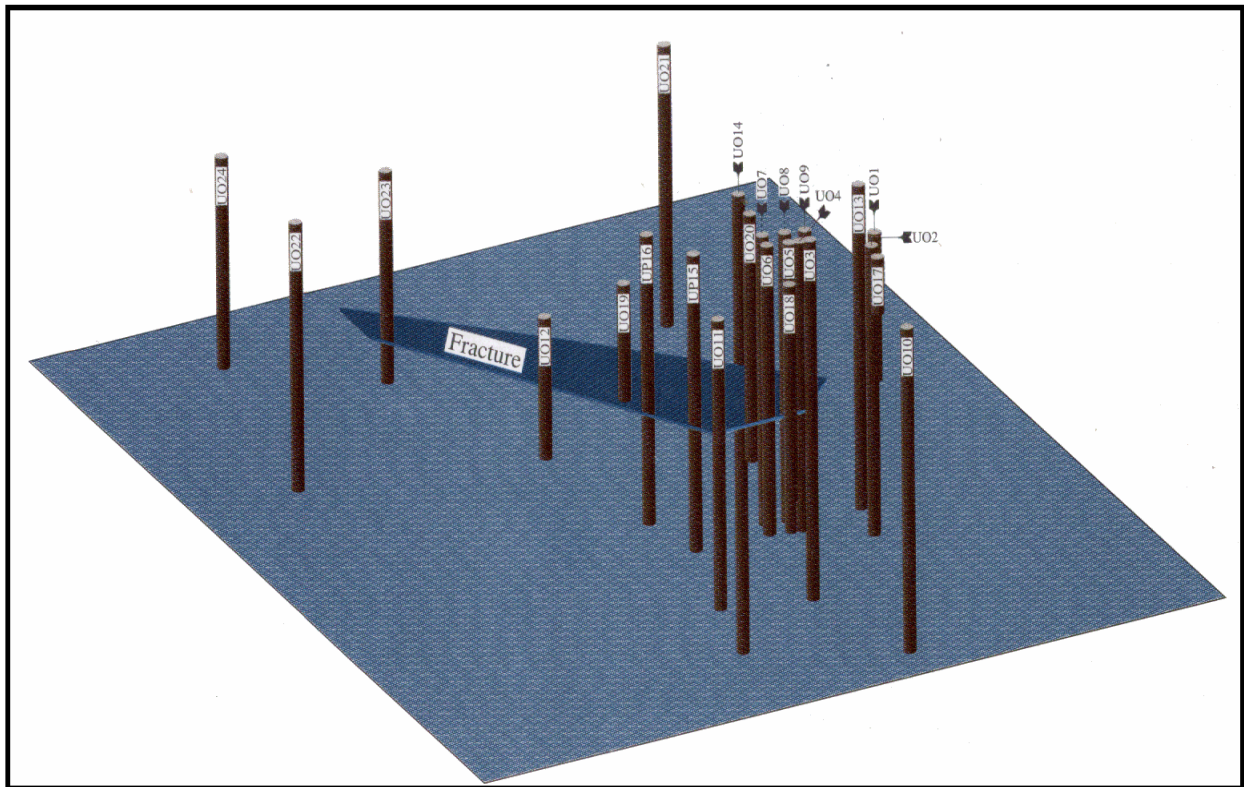


Figure 3.2: *Approximate areal extent of the horizontal water-bearing fracture in the campus test site aquifer (Botha et al., 1998)*

3.1.2.2 Fracture Hydraulics

Botha et al. (1998) states that the main water-bearing fractures in Karoo aquifers are almost horizontal and they pose the question: ‘*why are there boreholes that intersect a horizontal fractures, but with drawdowns that deviate from the Gringarten-Ramey model?*’ In other words, how does one explain the fracture-controlled response of boreholes tapping Karoo aquifers?

The first question is relatively simple to answer, if one keeps in mind that the Gringarten-Ramey model is essentially a horizontal-flow model. The model therefore cannot account for variations in the vertical flow field, particularly variations in the flow from the rock matrix to the fracture. This can only be achieved by using a full three-dimensional model as discussed by (Botha et al., 1998). . Nevertheless, there is another way to explain this behaviour physically, albeit qualitatively.

The flow in a fully fractured medium is largely controlled by the fracture dimension, orientation and connectivity (Odling, 1993). However, the water-yielding fractures in Karoo aquifers are too sparsely distributed to satisfy the connectivity requirements of such percolation models. Nevertheless, it is clear that the flux through a water-yielding fracture in a Karoo aquifer must also depend upon the aperture of the fracture, as well as the flux within the rock matrix. Consider therefore the simple parallel-plate fracture model illustrated in **Figure 3.3**. It is not difficult to show (De Marsily, 1986) that the discharge rate through such a fracture, with width (a) and aperture (b), can be expressed as:

$$Q = -\frac{ab^3rg}{12m} = j \quad \text{Eq. 3.2}$$

where, r is the fluid density, g the acceleration of gravity, m the dynamic viscosity of the fluid and $=j$ the gradient of the piezometric head in the fracture. The flux of a fluid through the fracture is:

$$q = \frac{Q}{ab} = -\frac{b^2rg}{12m} = j \quad \text{Eq. 3.3}$$

Therefore the flux depends on two factors: (i) the square of the fracture’s aperture, b , and (ii) the piezometric gradient within the fracture. Although the apertures of water-yielding fractures in Karoo aquifers are wider than those present in the more conventional fractured-aquifers, they are still not very greater than ~ 1 mm (Botha et al., 1998). A borehole in a Karoo aquifer may therefore not be able to sustain a specific discharge rate, even if the leakage from the surrounding rock-matrix is sufficient to sustain the piezometric gradient within the fracture. On the other hand, a fracture with a very large aperture will also not be able to sustain a specific discharge rate if its piezometric level declines continuously.

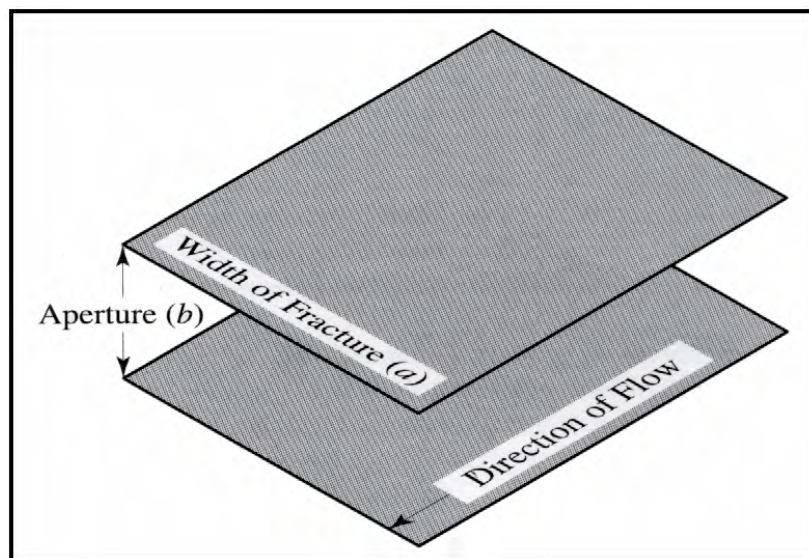


Figure 3.3: *Schematic illustration of the parallel plate model for a fracture*

The water-level borehole may stop declining and temporarily stabilise, if a second fracture exists with an aperture that is large enough, and the piezometric pressures in the layers immediately above and below the fracture are great enough to supply the water demand. This conjecture is supported by the behaviour of the piezometric levels in the three-layered aquifer system on the Campus Test Site. This was clearly indicated in the observation borehole UO18 during a constant-rate test on borehole UP16 of the 15th May 1995 (**Figure 3.4**). Aquifer unit 2 entered a pseudo steady-state after 12 hours of pumping; which is same time it took the water-level in borehole UP16 to stabilize. The piezometric level in aquifer unit 1 continued to decline throughout the test, whilst that in unit 3 also stabilized after a small but rapid decline at the beginning, probably caused by the slight difference in the initial piezometric level between itself and that of unit 2. These test results suggest that there may be fractures in a borehole that are not able to retard or stop a declining water level. This behaviour is even more clearly illustrated by water-level drawdown during a constant-rate test on a borehole at Kokstad (**Figure 3.5**). Although the water-level in this borehole did not experience any sharp decline, the short duration stabilizing patterns are clearly visible at each the level of each fracture.

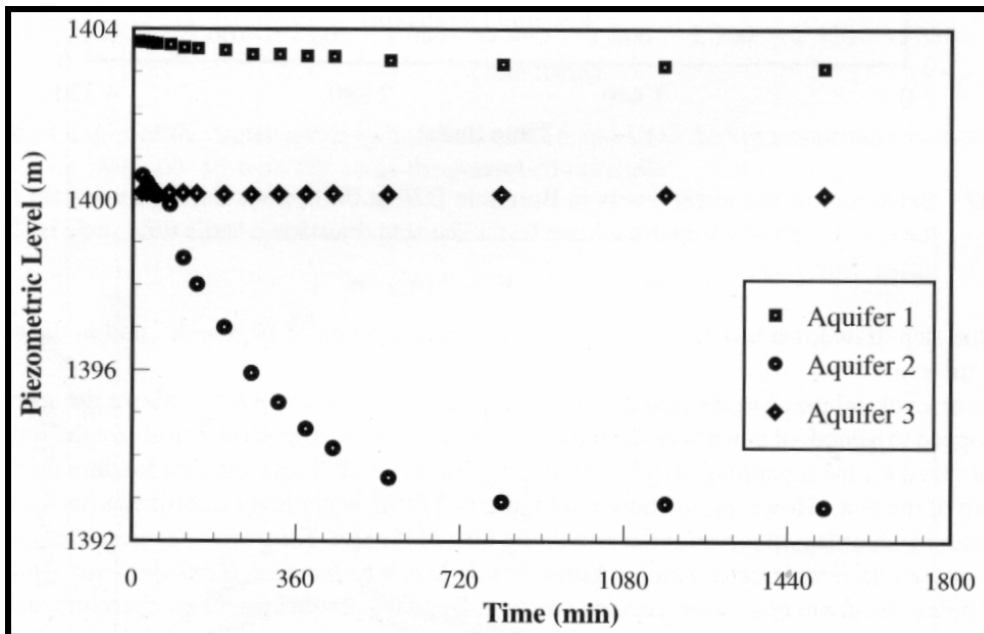


Figure 3.4: Response of the piezometric heads in the three-layered aquifer system on the Campus Test Site, as measured in Piezometer UO18 during the constant-rate test on Borehole UP16

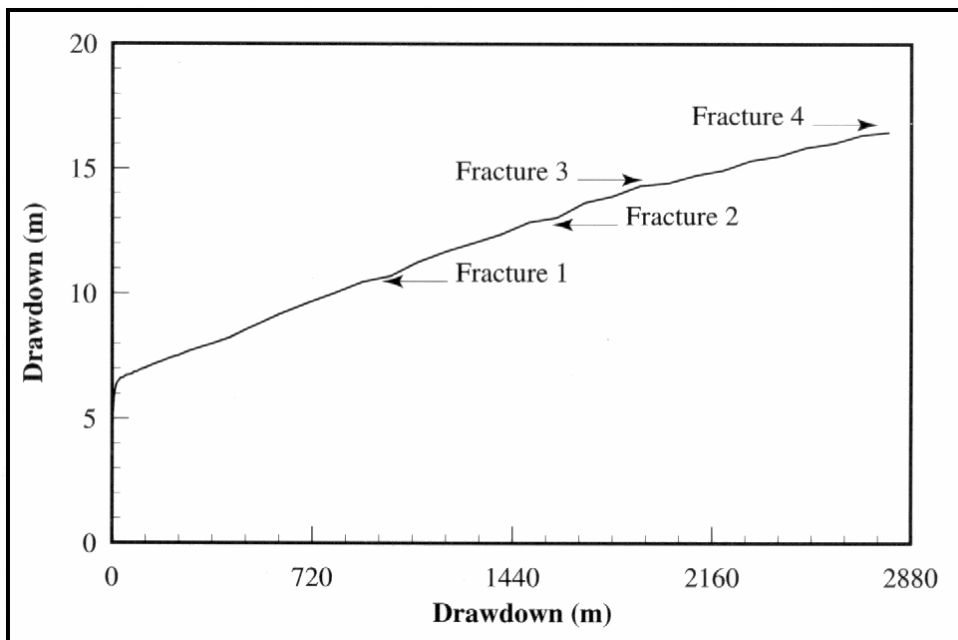


Figure 3.5: Drawdowns observed during a constant-rate test on a high-yielding borehole at Kokstad ($Q = 13 \text{ l/s}$)

An interesting consequence of this type of flow in Karoo aquifers is that the fracture-controlled behaviour of production boreholes should not be observed in a single-layered aquifer. However, such an aquifer may be very rare in Karoo formations, judging from the discussion of their general structure and the geology.

A more common explanation for the fracture-controlled behaviour of water-levels in Karoo boreholes would be that the drawdown reached a classical impermeable boundary during the test (i.e. a dolerite dyke or the fracture boundary). This phenomenon occurs in boreholes on the Campus Test Site, where no dykes are present, thus a dyke related boundary is not the cause for this behaviour. The fracture boundary are also not responsible for the phenomenon, for one would then expect this response in the water-levels of all boreholes connected to the fracture, which is clearly not the case with the water levels of boreholes UO5 and UO20 in **Figure 3.6**. The phenomenon is thus a hydraulic characteristic of the production borehole itself, and not *boundary effects*.

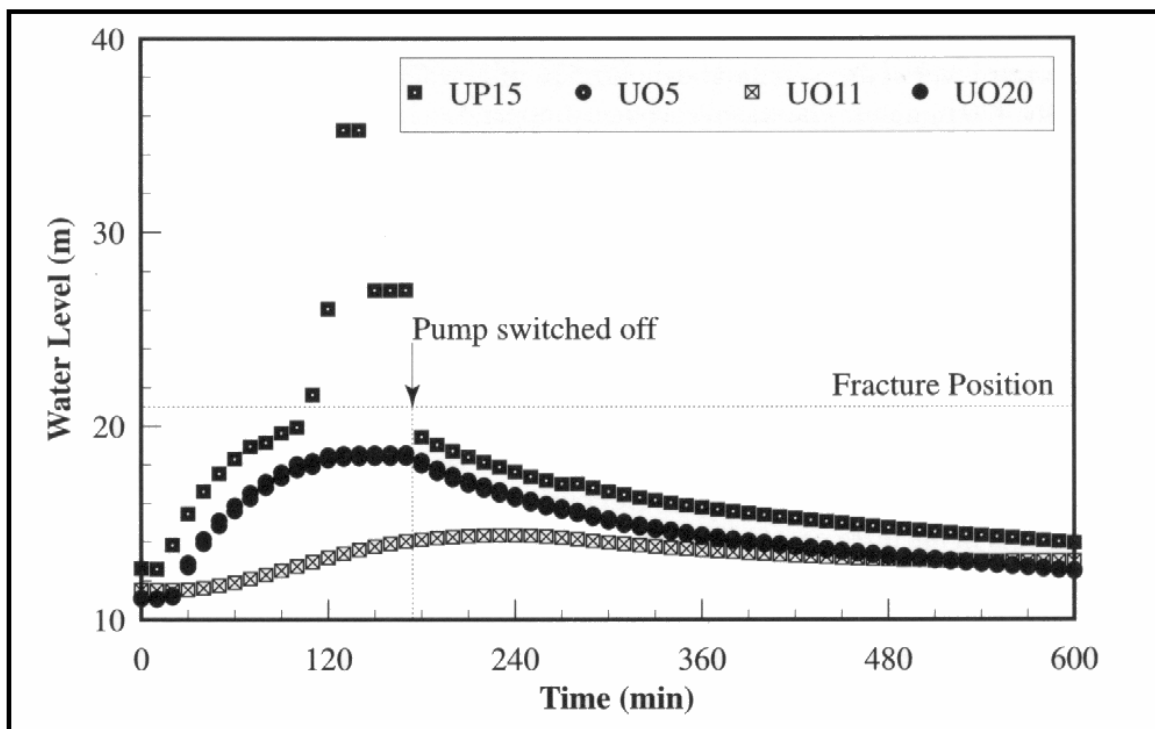


Figure 3.6: Water-level response in boreholes UO5, UO11, UP15 and UO20 during a constant-discharge test on pumped borehole UP15

3.1.2.3 Fracture Mechanics

Horizontal fractures can be readily deformed by a number of forces, which may pose a serious problem when water is pumped from them, unless special precautions are taken (Botha et al., 1998). Such a deformation, even if limited, can influence the rate of flow through the fracture dramatically, as can be seen from **Equation 3.3**. For example, a 20% decrease in the fracture aperture during pumping, will cause a yield decrease of almost 50%. A deformation of this nature will obviously be disastrous for production boreholes that depend on horizontal fractures for their water supply.

The first, and obvious, force that may cause the deformation of a fracture is the weight of the overburden. The effect of this force can be considerably enhanced in a fracture dewatered by excessive pumping. Indeed, there is a possibility that such a fracture may even collapse completely. If true, then this postulation may provide a natural explanation as to why it is often possible to drill a new successful borehole within a short distance from the one that has ‘dried up’ in Karoo aquifers.

The problem of a borehole whose yield steadily decreases with time (climatological and recharge factors remaining constant) can also possibly be related to the permanent deformation of near well water-bearing fractures. This phenomenon has never been discussed in the literature, as far as could be ascertained, but discussions with farmers indicated that it is quite common in Karoo boreholes that are older than 10 years (Botha et al., 1998).

The above phenomena can also be caused by other factors, and cannot therefore be considered as proof that fracture deformations do actually take place in Karoo aquifers. The only direct information that such deformations do occur comes from the acoustic scanner image of Borehole UO5, on the Campus Test Site in **Figure 3.7**. Of particular interest is the ‘fracture’ zone at a depth of 23.8 m and the sub-vertical fracture between 22.5 and 22.9 m, that was not present in the original BPB caliper-trace and dip-meter survey of the borehole on the 1st February 1993. These features must therefore have developed after December 1993, and probably after 1994, if the decreasing transmissivities noted in **Table 3.1** can be ascribed to such fracture deformation. Nonetheless, there can be little doubt that Karoo aquifers, and boreholes in particular, are subject to deformations (Botha et al., 1998).

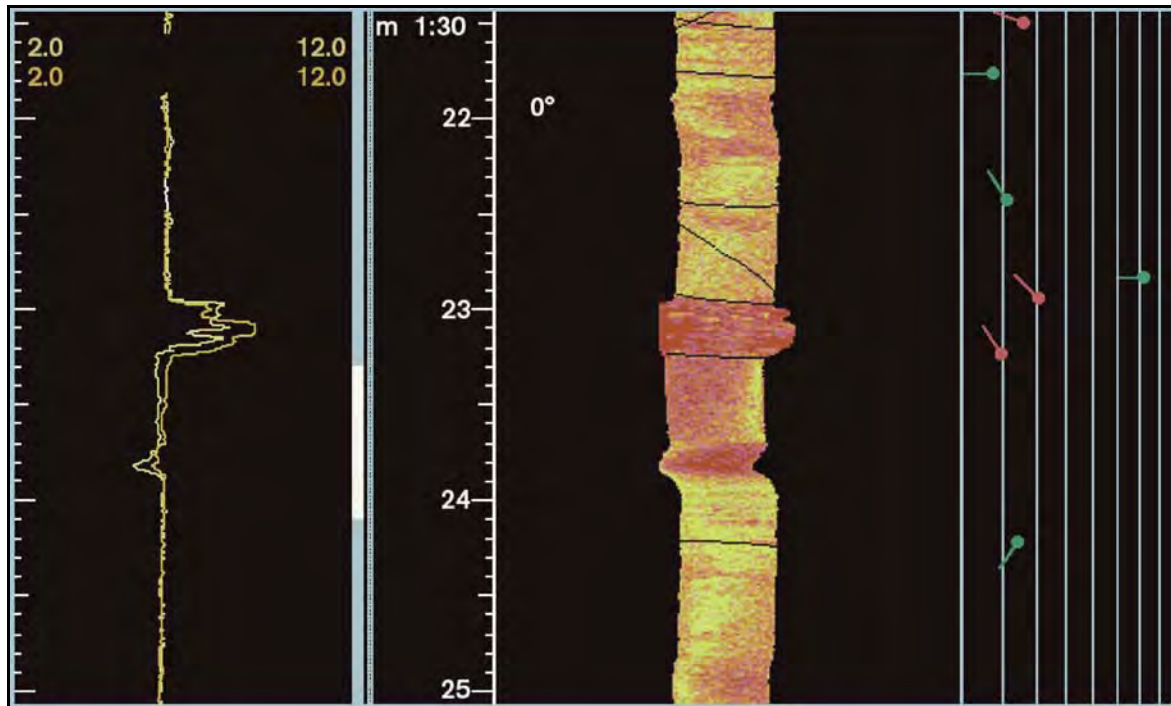


Figure 3.7: Acoustic scanner image Borehole UO5 on the campus test site. The orientation of the oblique fracture above 23 m in UO5 is 085 65

Table 3.1: Temporal changes in the Transmissivity of Borehole UO5 on the campus test site, as derived from slug-tests

Year	T (m ² /day)
1992	33.0
1994	28.5
1996	8.0

Another indication that elastic deformation of fractures may play a prominent role in the behaviour of Karoo aquifer systems is illustrated in the behaviour of the water-level in Borehole UO11 during the constant rate test on Borehole UP15 (**Figure 3.6**). The water-level in this borehole did not decline for approximately 30 min after the test was started, although it is roughly the same distance from UP15 than UO5 and UO20, and it continued to decline for at least an hour after the pump was switched off.

One mechanism that can explain this behaviour is that the fracture in the immediate vicinity of Borehole UP15 contracted when the pumping started, thereby creating a pressure pulse that increased the water pressure in the adjacent formations. Since borehole UO11 does not intersect the fracture, it took sometime before this increase in

pressure dissipated. The exact opposite happened when the pump was switched off. The fracture then expanded with a corresponding drop in its piezometric pressure that had to recover before the piezometric-level in the rock matrix could be recharged. This observation, incidentally, clearly demonstrates that boreholes in Karoo aquifers not only withdraw water from fractures, but also the Karoo rock matrix itself. The commonly held view, that Karoo formations do not contain significant quantities of groundwater, is thus wrong.

Dewatering and re-watering are not the only phenomena that can affect the aperture of a fracture. It is known that fractures are often kept open by asperities associated with the fracture walls, sand grains or other particles. The horizontal fracture on the Campus Test Site (**Figure 3.2**), for example was filled with mud, silt and fine-grained particles at the time the drill-cores were recovered. The flow velocities in bedding-parallel fractures can be very high, judging from the force with which water enters a borehole when such a fracture is intercepted. Abstracted groundwater could thus easily remove particles from the fracture, thereby causing the fracture to collapse or clogging of the pump. Friction between the fracture surface and water could also change the flow from laminar to turbulent, thereby reducing the flux through the fracture substantially (Gilbrech, 1966).

It is difficult to delineate all the effects that deformations may have on the behaviour of boreholes tapping Karoo fractured-aquifers, because they have not been considered in previous investigations.

3.1.2.4 Summary

The main conclusion that can be drawn from the above discussion is that the behaviour of Karoo aquifers is ultimately determined by their *unusual geometry*, particularly where horizontal, bedding-parallel fractures are present. These features provide not only the conduits for water to boreholes in Karoo aquifers, but also play a prominent role in the interactions responsible for the behaviour of these aquifers. One very important consequence of these interactions is that flow in Karoo aquifers is *not radial and horizontal, but linear and vertical*. This property differs so much from that of the theoretical media usually presented in the literature on aquifer mechanics, that the existing conceptual models are useless for the analysis of hydraulic tests performed on Karoo aquifers. Investigations by Botha et al. (1998) have shown that the horizontal Gringarten and Ramey (1974) fracture-model may be the only analytical model that can be applied to Karoo aquifers. However, the mathematics of the model is rather complex, and it cannot account for vertical variations in the flow field. It is thus doubtful if it will require less effort to implement than a numerical model.

Another result that emerged from Botha et al. (1998) study is that Karoo formations, and thus aquifers, may be readily deformed by pumping water from them. This will

not only affect the ability of these aquifers to store and yield water, but can also have a considerable impact on mass transport in such aquifers. Unfortunately very little is known about these deformations. It is thus imperative that more attention should be given to this aspect, if the aquifers are to be used for water-supply schemes and protected from pollution.

It is generally accepted that boreholes are the most cost-effective method of withdrawing water from an aquifer. The dependence of a borehole's yield on the presence and properties of a fracture, however, again raises the question if boreholes are actually the best method whereby water should be withdrawn from Karoo fractured-aquifers? Botha et al. (1998) concluded that, although some of the negative impacts can be restricted by adopting optimal pumping regimes and correct spacing of production boreholes, it would be better to withdraw water from Karoo fractured aquifers by methods other than boreholes.

3.1.3 THEORETICAL MODELS OF FRACTURED AQUIFERS

Various theoretical models can explain the flow of groundwater in fractured-aquifers. Muskat (1937) was one of the first who analyzed the flow in fractured media. Gringarten (1982) reviewed the extensive literature and found that three main types of approaches to the problem are used:

- the deterministic approach, which is based on an accurate and detailed description of individual fracture systems, and is mainly used for small-scale problems in geotechnical engineering;
- the double-porosity medium approach, which assumes a uniform distribution of matrix blocks and fissures throughout the aquifer (including single-fractured models and multi-porosity/multi-permeability models);
- the equivalent homogeneous aquifer approach, which considers only main trends of the pressure behaviour of the fissured aquifer and tries to relate them to a known model of lower complexity.

These theoretical models form the basis of the type-curve methods derived by various researchers for the analysis of pumping test data in fractured aquifers. For a complete description of all the different models, the reader is referred to Kotze (1993) and Kruseman and De Ridder (1991).

Barenblatt et al. (1960) introduced the *dual-porosity* concept that has been used extensively in the petroleum industry. Two approaches that differ in the way that flow occurs from the matrix block to a fissure have been considered, namely: (i) that flow occurs under pseudo-steady state conditions (Warren and Root, 1963); and (ii) the flow occurs under transient conditions from the block to the fracture (Kazemi, 1969).

Although the pseudo-steady state approach simplifies the mathematical computations, it ignores some of the physics of the problem. This implies that the transient approach is clearly superior from a theoretical standpoint. Moench (1984) incorporated the idea of *fracture skin*, which is a thin skin of low-permeability material deposited on the surfaces of the blocks that serves to impede the free exchange of fluid between the blocks and the fracture. The effect of fracture skin in dual-porosity systems is to delay flow from the blocks to the fractures and thereby give rise to a pressure responses that is similar to that predicted under conditions of pseudo-steady state flow (Moench, 1984). According to Moench, by reducing gradient of hydraulic head in the compressible matrix-blocks, the fracture skin provides theoretical justification for the pseudo-steady state flow approximations used in the Warren and Root (1963) model. Bourdet and Gringarten (1980) showed that the dual-porosity behaviour of a fractured aquifer only occurs in a restricted area around the pumped borehole. Outside of that area (i.e. for λ -values greater than 1.78), the drawdown behaviour is similar to that of an equivalent porous medium.

The unrealistic hydraulic parameters derived from pumping-tests in Karoo fractured-aquifers have been addressed in previous works (Kirchner et al., 1991). A particular problem was in the estimated value for the storativity. Pumping-test analysis in the Dewetsdorp and De Aar regions has pointed to S-values as low as 10^{-6} , whilst water-balance studies, specifically the SVF method (Kirchner et al., 1991), produced S-values in the order of 10^{-3} .

The S-values obtained from pumping-tests using common radial-flow based techniques, as well as fracture analysis procedures (i.e. Moench, 1984) show a distance-dependency as first observed by Bredenkamp (1992) and Bredenkamp et al., (1994). The reason for this distance dependency of the S-value (if analyzed using these incorrect aquifer models) is very easy to explain. At one end of the spectrum, a few large, permeable fractures occupy a relatively small rock volume that therefore has a small porosity and storativity. On the other end, numerous small, low-permeable fractures occupy a relatively large rock volume, which therefore has a large porosity and storativity. Close to the pumping well, the pressure in the large fracture declines rapidly relative to its rate of decline in the small fractures. The latter, therefore release a relatively large amount of water into the large conductive fractures due to a sizeable local pressure gradient between the small and large fracture reservoirs – and hence S is large. At some distance from the pumping well, the pressure gradient between the small and large fractures is relatively small. Therefore, water release from the small to the large fractures occurs very slowly. Most of the initial observed drawdown in the large fractures at a great distance is associated with water release from storage in the large fractures – and hence S is small.

With time, local pressure differentials between the reservoirs stabilize and flow everywhere within a given radius approaches a steady radial pattern. Therefore, it would be expected that the storativity could approach a uniform value representing both reservoirs. However, as the flow pattern has now essentially stabilized and

pseudo steady state conditions prevail (even though absolute pressures may continue to decline), standard pumping-tests may not reveal the fact that the flow is sensitive to S only at early times. If there were only two reservoirs with very different S values, log-log time-drawdown-curve close to the pumping well would exhibit a familiar dual-porosity time inflection, similar to that analysed by Neuman in unconfined aquifers. However, if a continuous hierarchy of such reservoirs exists each with a more or less a continuous range of T - and S -values, such sharp inflections will not be evident. The early log-log time-drawdown behaviour would then take the form of a Theis curve. During a WRC project (Botha et al., 1998) derived a numerical two-layered radial model (**RPTSOLV**) to overcome the problem of finding correct S values from pumping-test analyses.

The effective management of an aquifer system is primarily dependent on how well the aquifer hydraulic parameters are known. Most of the pump-test interpretation methods applied to boreholes in Karoo aquifers are based on analytical solutions of the porous flow equation, which is dependent on a number of simplifying assumptions, including aquifer homogeneity. However, in a fractured porous medium, especially on the scale of a pumping-test, this assumption is violated. The combined effect of horizontal flow in the fractures and vertical leakage in the surrounding rock-matrix cannot be accounted for using such analytical solutions.

Case Study: Meadhurst Site

The borehole layout at the Meadhurst test terrain is shown on **Figure 3.8**. Boreholes FP1, F4 and F5 are drilled alongside a dolerite dyke whilst the other boreholes are situated on a dolerite sill. A sandstone layer intercepted between 20 and 28 m is the main aquifer and the water was struck at a depth of 27 m below surface in FP1 and 21 m in F4 and F5. **Figure 3.9** shows the water-level drawdown curves at borehole FP1 and F4. It is interesting to note, that at FP1 an early T -value $35 \text{ m}^2/\text{d}$ was obtained whilst the T -value at F4 is $75 \text{ m}^2/\text{d}$, although the blow-yields of the two boreholes were both 2 l/s . The question now is which T value is the typical value for the fractured sandstone layer - is it 35 or $75 \text{ m}^2/\text{d}$? The T -value in FP1 decreased to about $8 \text{ m}^2/\text{d}$ after 500 minutes of pumping indicating that some kind of boundary condition was reached (zone with lower T – similar to that of the matrix). Naturally, the effective T -value to be used for management purposes is the lower T . If the drawdown in FP1 is corrected for borehole losses using the Hantush or Hurr methods (see **Figure 3.10**), the estimated early time T -value is $73 \text{ m}^2/\text{d}$, which clearly shows that borehole losses cause a decreased calculated T -value in the abstraction borehole. The two-layered model RPTSOLV also yielded a early time T -value of about $40 \text{ m}^2/\text{d}$.

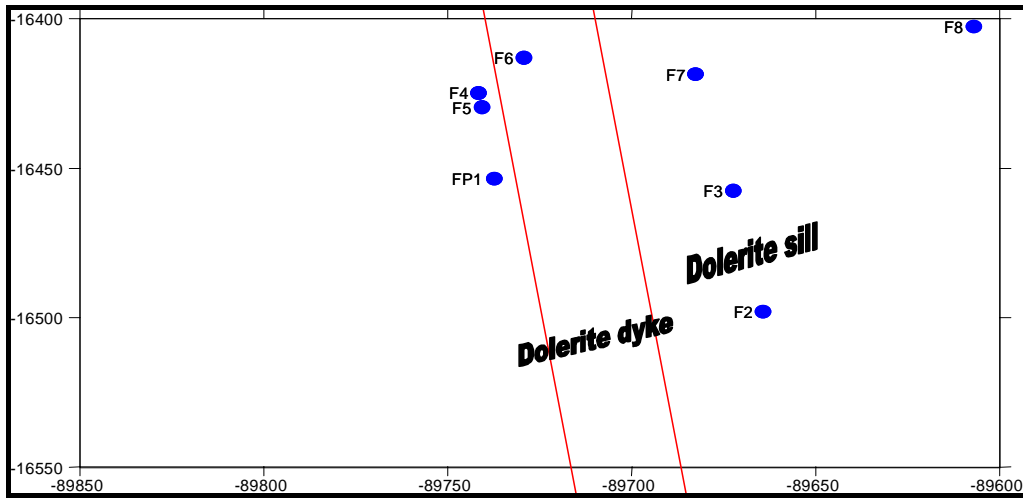


Figure 3.8: Plan indicating position of boreholes at the Meadhurst site

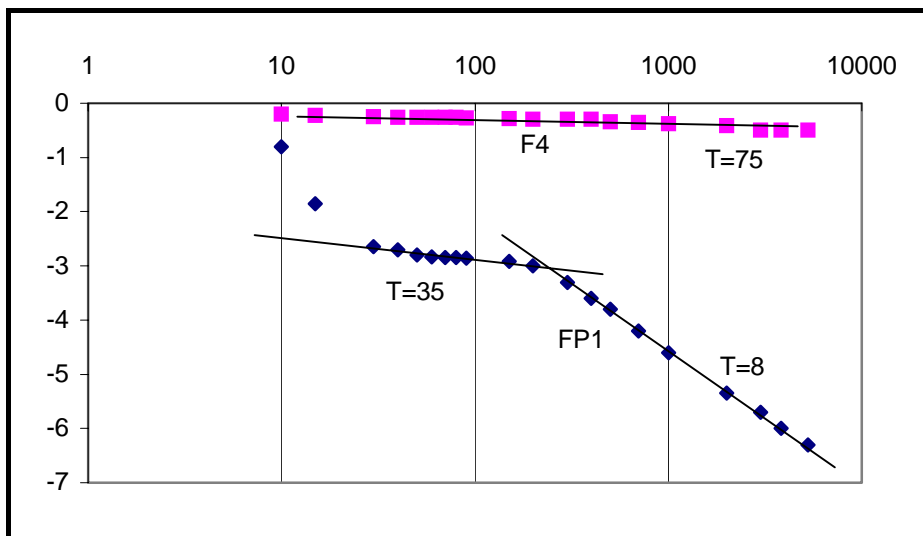


Figure 3.9: Pump test results at the Meadhurst site

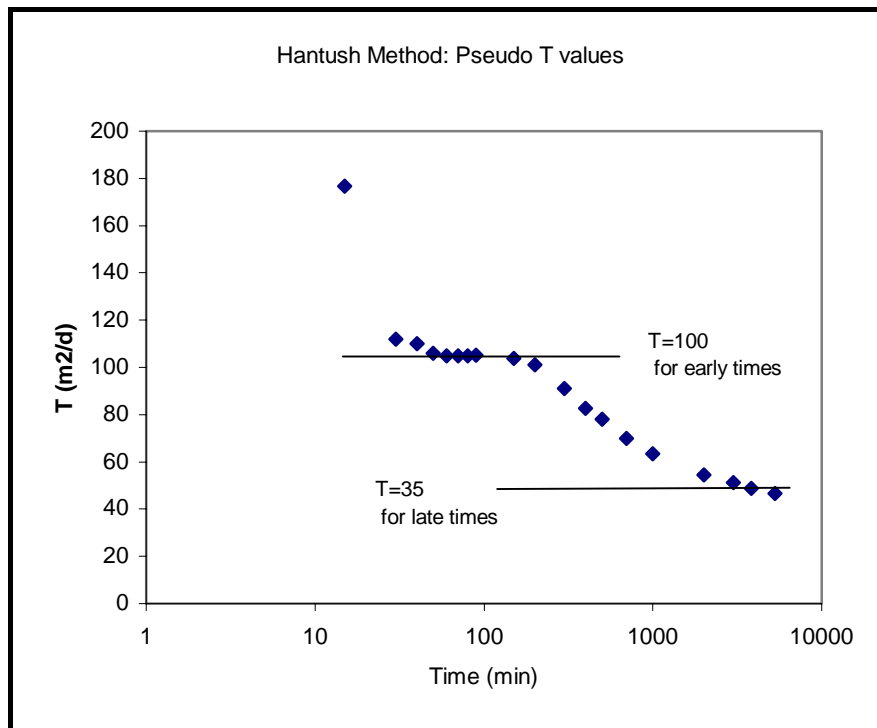


Figure 3.10: Hantush pseudo T -value estimation for production borehole at Meadhurst site

3.1.4 Flow Regime Characteristics

During a typical pumping test, the production borehole is pumped at a constant rate (i.e. the input signal) in an aquifer with unknown parameters and only the output signal (i.e. water-levels in the abstraction or observation boreholes) is measured. The purpose of such a test is to identify the aquifer parameters and this is known as the *inverse problem* – where the response of a theoretical aquifer model, as computed using a specific set of inner and outer boundary conditions, is compared to the actual behavior of the aquifer system. The actual aquifer model will not be correct if an incorrect conceptual theoretical model is selected. On the other hand, the inverse solution is not unique and it is always possible to find several aquifer configurations that would produce the same output signal as that measured during the pumping test.

It is crucial that the appropriate *theoretical model* is selected when analyzing data from pumping tests. It is thus important to correctly identify the *aquifer characteristics* from the pumping test information and geological logs of the borehole.

In general, a theoretical model consists of (i) a basic model, (ii) inner boundary conditions and (iii) outer boundary conditions.

The basic model is of infinite lateral extent, may be homogeneous or heterogeneous (i.e. dual porosity, multi-layered, etc.), and contains initial hydrological conditions (i.e. uniform water-levels). This model is, however, only applicable to *observation boreholes*.

To apply this basic model to a *production borehole*, the inner boundary conditions (i.e. well bore storage, skin effects and geometry of the water-bearing fracture) must be known. The *effective radius* must also be used in place of the actual radius of the borehole if the drawdown curve is to be analyzed using a logarithmic analytical model (e.g. Theis model). Finally, outer boundary conditions may have to be added if necessary (e.g. no-flow or constant head boundaries).

3.1.4.1 Inner Boundary Conditions

The aquifer characteristics can be best identified on a *log-log plot* of drawdown versus time. The following inner boundary conditions can only be identified from the early water-level drawdown data in the abstraction borehole:

- *Well bore storage* (WBS) yields a straight line of unit slope on the log-log plot at early time.
- A highly conductive fracture (vertical or horizontal) yields a straight line with slope = 0.5 at early time (i.e. *linear flow* is dominant).
- A finite conductive fracture yields a straight line with slope = 0.25 at early time (*bi-linear flow* is dominant). Occasionally, a line with a slope of 0.5 is developed prior to a line with a slope of 0.25.
- At early times, *radial flow* dominates if drawdown is proportional to log time.

The various types of inner boundary conditions are indicated in the time-drawdown graph of production borehole U16 on the University Campus Site at Bloemfontein (**Figure 3.11**).

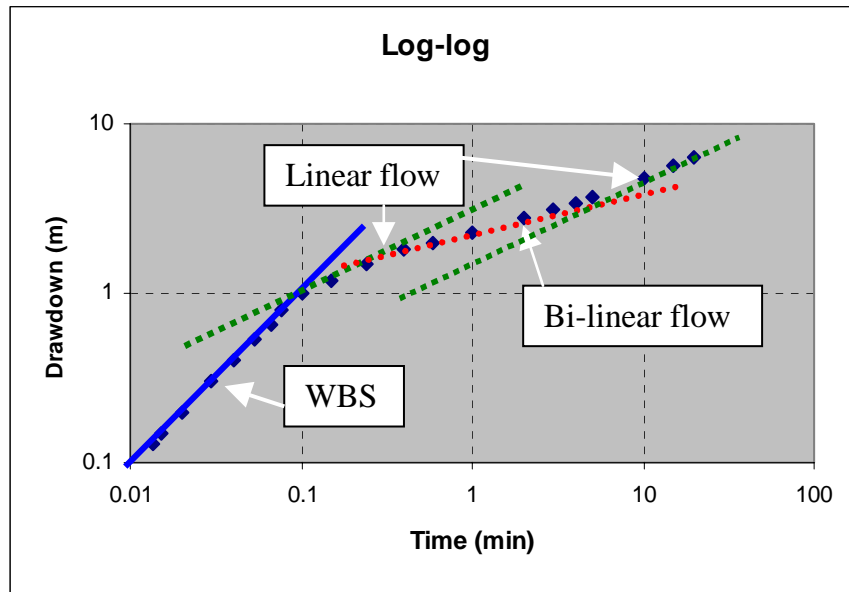


Figure 3.11: Early time-drawdown curve of borehole UP16 at the campus site showing inner-boundary conditions

The following inner boundary conditions are identified on **Figure 3.11**:

- *Well Bore Storage (WBS)* continuing up until 0.1 minutes.
- *Linear flow* from 0.1 – 0.4 minutes (all water pumped is coming from the fracture).
- *Bi-linear flow* from 0.4 – 5 minutes (water is coming from the fracture and rock matrix).
- *Linear flow* again from 5 minutes onwards (all the water is coming from rock matrix).

The hydraulic characteristics determined from a pumping test will thus depend upon the time period being analyzed, because the inner boundary, the basic model and the outer boundary conditions will dominate the aquifer's water-level response at different times during the test. Usually the early time drawdown data is used to determine which basic model to apply in the analysis of the test data.

3.1.4.2 Outer Boundary Conditions

The outer boundary conditions (as well as the inner boundary conditions) can be identified from a *derivative plot* of water-level drawdown with respect to log time is taken and plotted on log-log scale.

Some other specialized water-level time-drawdown plots associated with the aquifer flow characteristics, which should produce a straight line through the points of interest, are:

- (a) *Linear Flow* - drawdown versus square root of time.
- (b) *Bi-Linear Flow* - drawdown versus cube root of time.
- (c) *Pseudo Steady State Flow* - cartesian plot of drawdown versus time.
- (d) *Spherical Flow* - drawdown versus 1/square root time.

A specific flow regime has a characteristic pump test curve. The use of the *derivative* of piezometric head has been in use for many years in the oil well industry to evaluate the flow regime characteristics (Bourdet et al., 1984; Horne, R.N; 1997). Use of the derivative of piezometric-head versus time is mathematically satisfying as it forms an integral part of the *diffusivity equations*, which in turn govern all models of transient pressure behaviour currently in use to analyse well tests. Consequently, the derivative of drawdown is far more sensitive to subtle phenomena of interest in the data, which are all integrated and, hence, diminished by the piezometric-head versus time solutions presently in use for well test interpretations. However, good field measurements are required to use the piezometric-head derivative in groundwater, which is estimated as follows:

$$d(H)/d(\log t) = (n\sum x_i y_i - \sum x_i \sum y_i) / (n\sum x_i^2 - (\sum x_i)^2) \quad \text{Eq. 3.4}$$

where

the summation is from 1 to n, and

n = number of points to be average, usually n = 5 or n = 7 is suitable.

$x_i = \log(t_i)$ at point i, (t = time)

$y_i = h_i$, i.e. head H or (drawdown) at t_i

The derivative of drawdown with respect to log t is simply the gradient of the data plotted on semi-log paper (i.e. a typical Cooper-Jacob plot). The derivative head d(H) in Eq. 3.4 represents the least-square linear-regression fit through n number of points, i.e. if n=3 then the derivative head is the least square fit of a straight line though the data point to the left, the point itself and the point to the right.

It is also possible to use the log-derivative (i.e. the gradient of the Theis plot) and the second derivative (i.e. the derivative of the derivative of the Cooper-Jacob plot) to derive flow characteristics for an aquifer.

The following types of time-drawdown plots can be used to obtain important information on the character of groundwater flow in an aquifer:

3.1.4.3 Typical Water-level Drawdown Plots

Semi-log (i.e. typical Cooper-Jacob plot)

A semi-log plot, with drawdown on linear scale and time on logarithmic scale, is useful to show the semi-log straight line that is characteristic of infinite acting *radial flow*. This plot is also useful to recognize certain *boundary types* and positions of *fractures*.

Log-log (i.e. typical Theis plot)

The log-log plot is the most generally useful plot, in that almost all of the common aquifer responses are easily identified as long as the derivative is also used.

Linear

This cartesian-plot is useful to estimate *drainage area* during pseudo steady state flow conditions, but cannot be used to diagnose pseudo steady state conditions.

Square Root of Time (i.e. $t^{0.5}$)

Linear flow, i.e. parallel flow in a single fracture, observed in some fractured aquifers and dominance of horizontal fractures can be discerned from the early time portions of these graphs. In this case, most of the groundwater is coming from the fracture itself and not from the aquifer matrix.

Cube Root of Time (i.e. $t^{0.25}$)

Bi-linear flow, observed at early times in finite conductive fractures, can be seen on these graphs, where groundwater is leaking from the aquifer matrix into the fracture.

Inverse Square Root of Time (i.e. $1/t^{0.5}$)

Spherical and *hemispherical flow* can be identified on these graphs.

In general, it is always possible to fit a straight-line through a small number of the data points - but meaningful deductions can only be made if a sufficient number of observation points are available to clearly indicate a trend.

3.1.4.4 Derivative Plots of Water-level Drawdown

Log-Log

Many responses, which cannot be discerned from drawdown log-log graphs, can be observed on the derivative of drawdown graphs. For example, dual porosity behaviour is usually recognized by a characteristic ‘dip’ or depression in the derivative curve, after cessation of the WBS response and before the onset of radial flow. Note that this dip is not restricted to this position on such graphs.

3.1.4.5 Summary of Drawdown Graph Characteristics

Tables 3.2 to 3.7 summarize the various flow characteristics that may be observed on the various types of water-level drawdown graphs.

Table 3.2: *Semi-log (typical Cooper-Jacob) graphs*

Feature	Characteristic
Straight line segment	Indication of radial flow
Two parallel lines	Dual porosity
Horizontal line	Recharge boundary or period where leakage from matrix = abstraction rate or water level has reach position of a fracture
Steepening segment during late times	Boundary reached or matrix flow becomes dominant

Table 3.3: Log-log (typical Theis) graph

Feature	Characteristic
Slope =1 at early time	Well bore storage
Slope = 0,5 at early time	Linear flow in fracture, water derived from fracture only. If difference between drawdown and derivative = factor 2, the fracture has a large areal extent
Slope = 0,25 at early time	Bi-linear flow dominant, where water is leaking from the matrix into the fracture. If difference between drawdown and derivative = factor 4, the fracture has a limited areal extent.
Horizontal line	recharge boundary or leakage from matrix = abstraction rate or position of fracture is reached

Table 3.4: Cartesian graph

Feature	Characteristic
Steep Straight line at late time	Impermeable boundary
Horizontal line	Recharge boundary or position of fracture is reached

Table 3.5: Square root of time ($t^{0.5}$) graph

Feature	Characteristic
Straight line	Linear flow in fracture, water derived fracture only

Table 3.6: Fourth root of time ($t^{0.25}$) graph

Feature	Characteristic
Straight line	Finite fracture, water leaking from matrix into the fracture

Table 3.7: Inverse square root of time ($1/t^{0.5}$) graph

Feature	Characteristic
Straight line	Spherical flow

3.1.4.6 Characteristics of Derivative Drawdown Graphs

The characteristic features of derivative water-level drawdown-graphs are summarized in **Table 3.8**.

Table 3.8: *Characteristics of derivative drawdown graphs*

Feature	Characteristic
Slope = 1 at early time	Well bore storage
Slope = 0.5 at early time	Long fracture (usually factor 2 difference between drawdown and derivative. Limited fracture network.
Slope = 0.25	Finite fracture with factor 4 difference between drawdown and CJ- derivative. Well connected fracture network.
Slope = 1 at late time (upwards)	Closed boundary.
Slope = downward and then upward.	Position of fracture reached, whereafter the fracture is dewatered.
Strong downward trend	Recharge boundary.
Dip in derivative	Dual porosity aquifer response.

Tables 3.9 and **3.10** provide useful insights into how to ascertain the dominant flow-regimes and aquifer characteristics from various time-drawdown graphs.

Table 3.9: Methods of recognizing commonly observed aquifer characteristics from pumping test data

Characteristic	Derivative graph (log-log)	Log-log graph	Log-linear graph	Square root of time graph	Cube root of time graph
Well bore storage	Slope =1 line at early time with a hump	Slope = 1 line fit at early time			
Radial flow	Horizontal line (slope=0) with intercept of say d_0 . Usually about 1.5 log/cycles after well bore storage. The T-value could be estimated from this value.		Straight line		
Linear flow : Limited fracture network	Slope=0.5 line fit on derivative. Usually factor 2 difference between drawdown and derivative.	Slope = 0.5 line fit		Straight line	
Bilinear flow: Good fracture network	Slope=0.25 line fit on derivative. Usually factor 4 difference between drawdown and derivative.	Slope = 0.25 line fit			Straight line
Position of water-bearing fractures	Hump in the derivative	Flattening of curve at fracture position	Flattening of curve at fracture position		
Dual porosity	Characteristic dip				
Single no-flow boundary	Horizontal line with derivative value = $2d_0$		Doubling of slope		
Double no-flow boundary	Horizontal line with derivative value = $3d_0$		Tripling of slope at most		
Closed no-flow boundary	Slope = 1 line at late time and derivative value $> 4d_0$		More than tripling of slope		
Recharge boundary	Strong downward trend in derivative, i.e. derivative $< d_0$		Decrease in slope		

Table 3.10: Porosity systems and boundary conditions

No Boundaries			Boundaries			
System	Model	Drawdown-time relation	Single no-flow	Dual no-flow	Closed no-flow	Recharge
Single porosity (T and S)	Porous: Infinite acting radial flow	$s \sim \log t$	$s \sim 2\log t$	$s \sim 3\log t$	$s > 4\log t$	$s < \log t$
	Purely fractured: Infinite acting radial flow	$s \sim \log t$	$s \sim 2\log t$	$s \sim 3\log t$	$s > 4\log t$	$s < \log t$
	Single fracture in an otherwise impermeable matrix	$s \sim (t)^{0.5}$ (i.e. square root t)	$s \sim 2(t)^{0.5}$	$s \sim 3(t)^{0.5}$	$s > 4(t)^{0.5}$	$s < (t)^{0.5}$
Dual porosity T_f, T_m, S_f, S_m	Good fracture network	Early time $s \sim (t)^{0.25}$ (i.e. cube root t)	-	-	-	-
	(Bi-linear flow at early times): Water is coming from fracture and matrix.	Late time $s \sim \log t$	$s \sim 2\log t$	$s \sim 3\log t$	$s > 4\log t$	$s < \log t$
	Limited fracture network	Early time $s \sim (t)^{0.5}$	-	-	-	-
	(Parallel flow inside fracture at early time). Water is coming from just the fracture or just the matrix (tending to single porosity system).	If T of matrix is small and the fracture is elongated this parallel flow period may last relatively long Late time $s \sim \log t$	$s \sim 2\log t$	$s \sim 3\log t$	$s > 4\log t$	$s < \log t$

Note: The symbol \sim stands for proportional

The following can be deduced from the *early time log-derivative graph*:

- A value of the log derivative = 0.5 implies that the fracture network is limited (i.e. *linear flow* usually dominates during early time)
- A value of the log derivative = 0.25 implies a good fracture network (i.e. *bi-linear flow* dominates during early time)
- A value of the log derivative < 0.1 implies a very good fracture network and aquifer (i.e. *radial flow* dominates)

If the *second derivative* (i.e. s') of drawdown is taken, the following important characteristics could be obtained:

- Closed no-flow boundary - value of s' reaches a value of exactly 1.
- Homogeneous infinite aquifer (Theis model) - value of s' is equal to zero.

3.1.4.7 Example of drawdown and derivative graphs

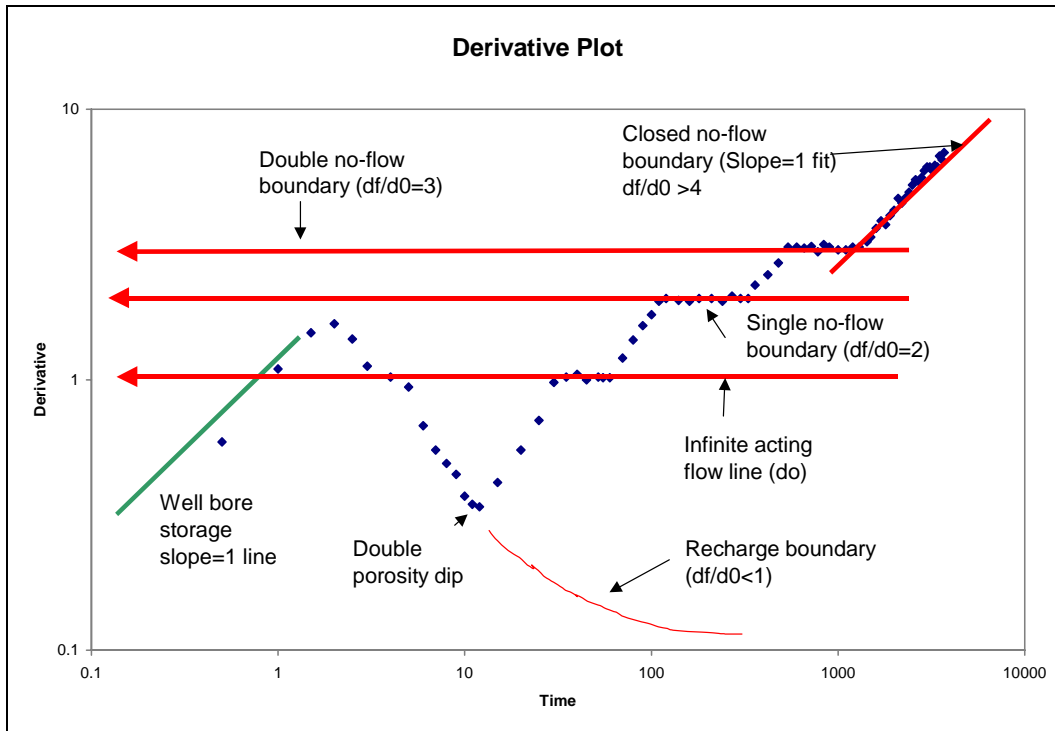


Figure 3.12: Typical derivative graph for various boundary conditions

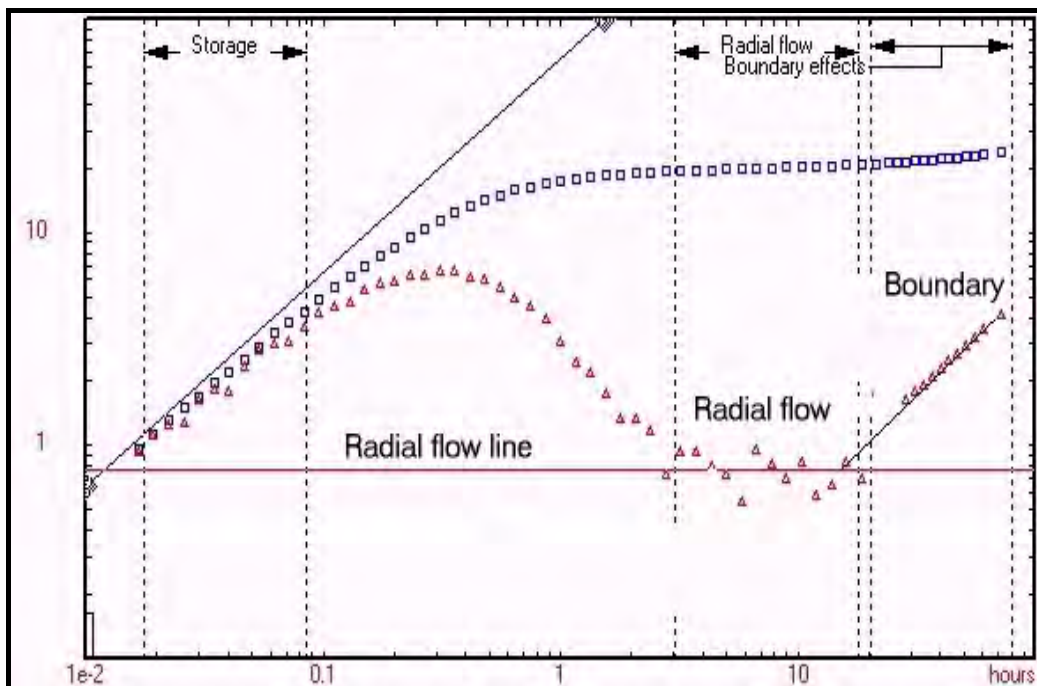


Figure 3.13: Water-level drawdown and derivative graph indicating borehole storage, radial flow and boundary effects

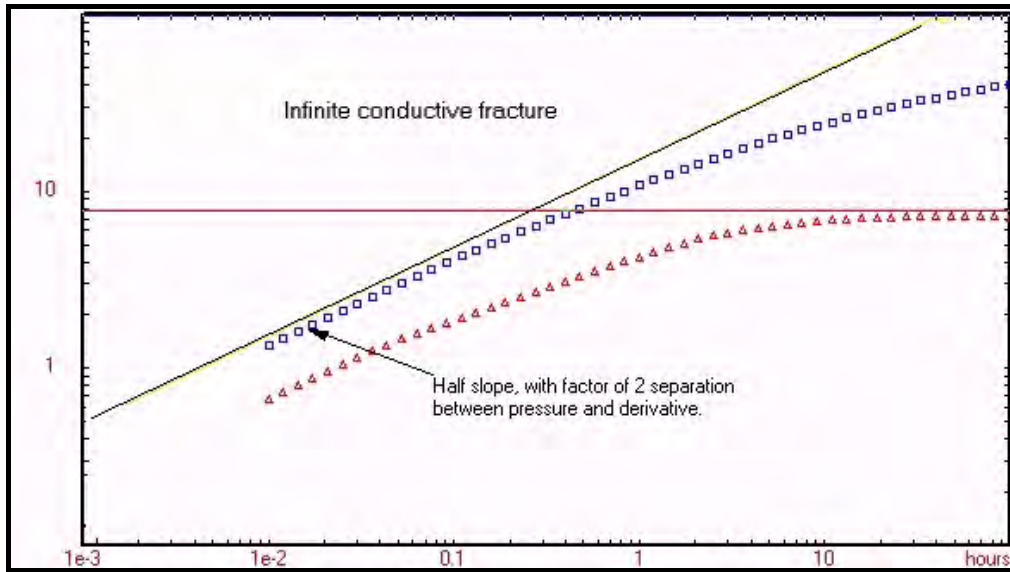


Figure 3.14: Water-level drawdown and derivative plot showing flow to an infinite conductive fracture

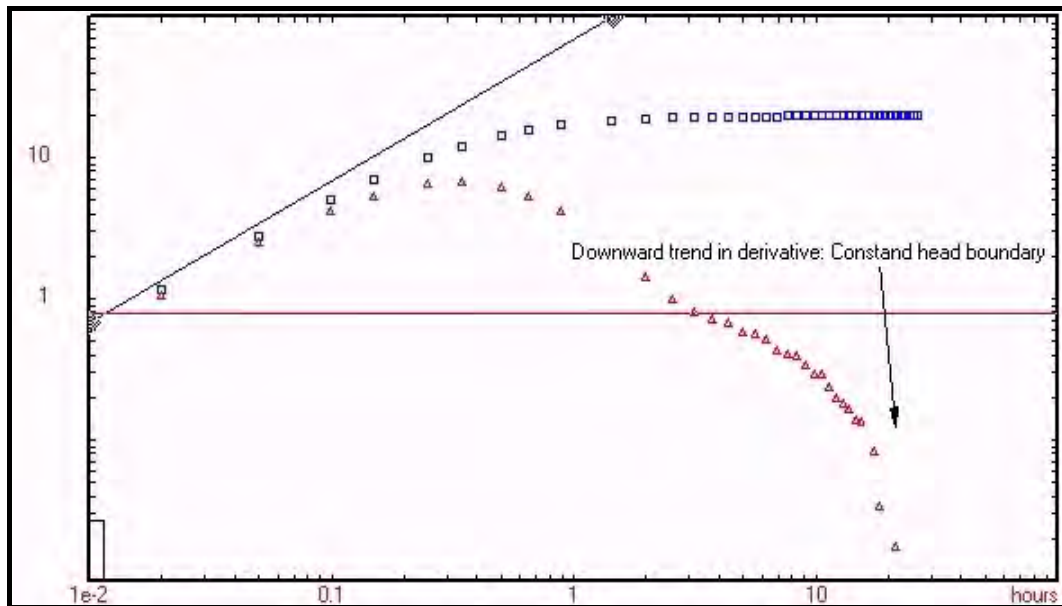


Figure 3.15: Water-level drawdown and derivative plot showing a constant head -type boundary

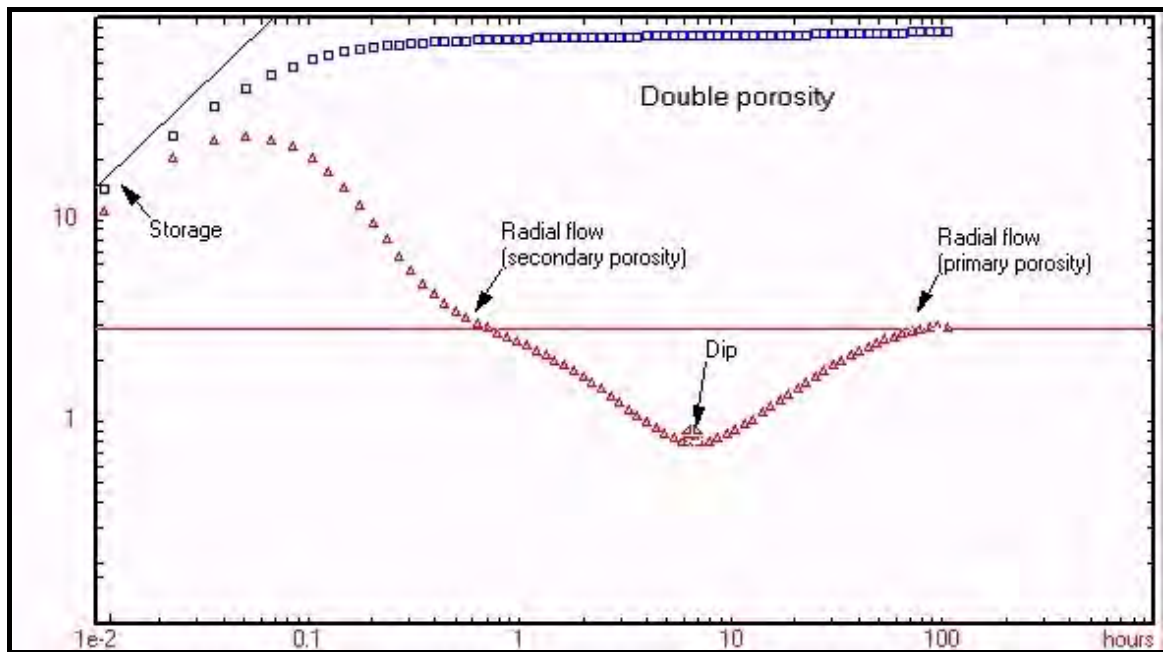


Figure 3.16: *Water-level and derivative plot showing dual porous flow*

Case Study: Borehole GR2 at Graaff-Reinet

The constant discharge test data from borehole GR2 in Graaff-Reinet will be used to illustrate some of the diagnostic plots that could be used to identify certain flow characteristics in an aquifer. The following **Figures 3.17 to 3.25** show diagnostic plots for production borehole GR2 at the Mimosadale Wellfield, Graaff-Reinet.

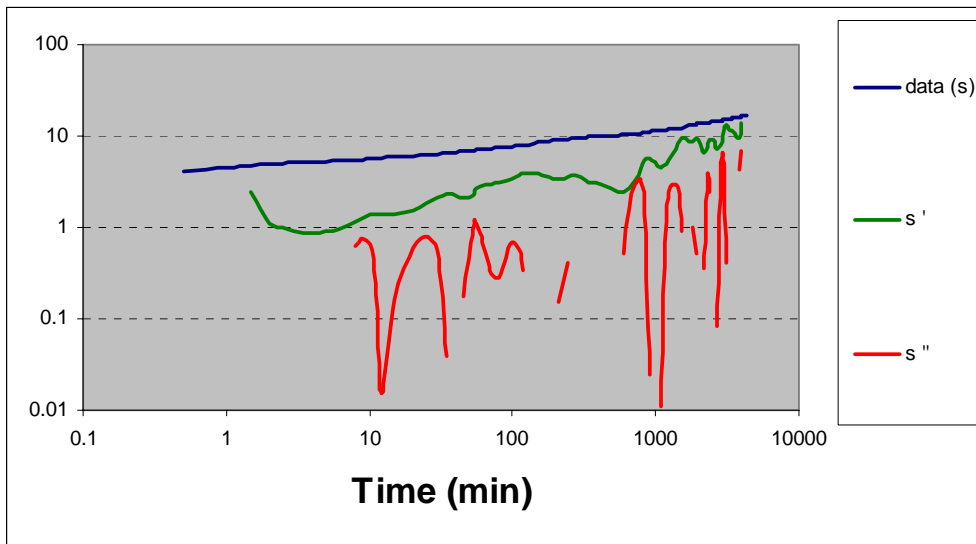


Figure 3.17: *Water-level Drawdown, and the different derivative plots for borehole GR2*

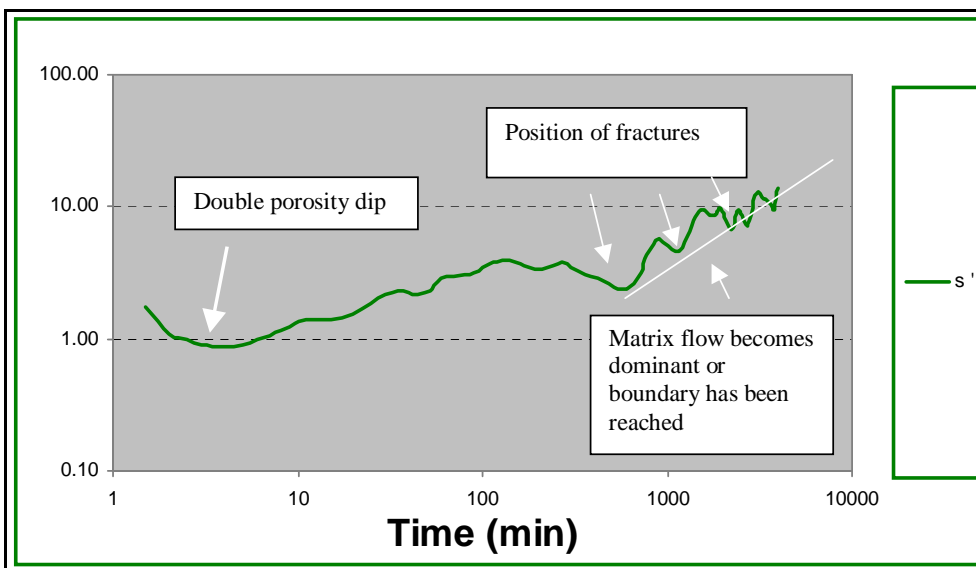


Figure 3.18: *Flow characteristic analysis of drawdown Derivative Plot for borehole GR2*

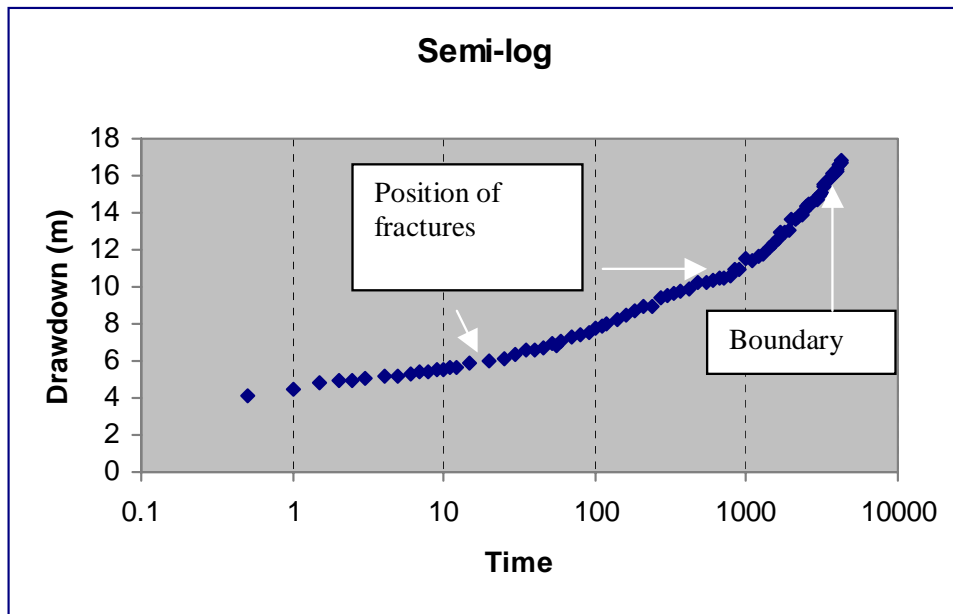


Figure 3.19: Cooper-Jacob plot of borehole GR2 showing position of fractures and boundary

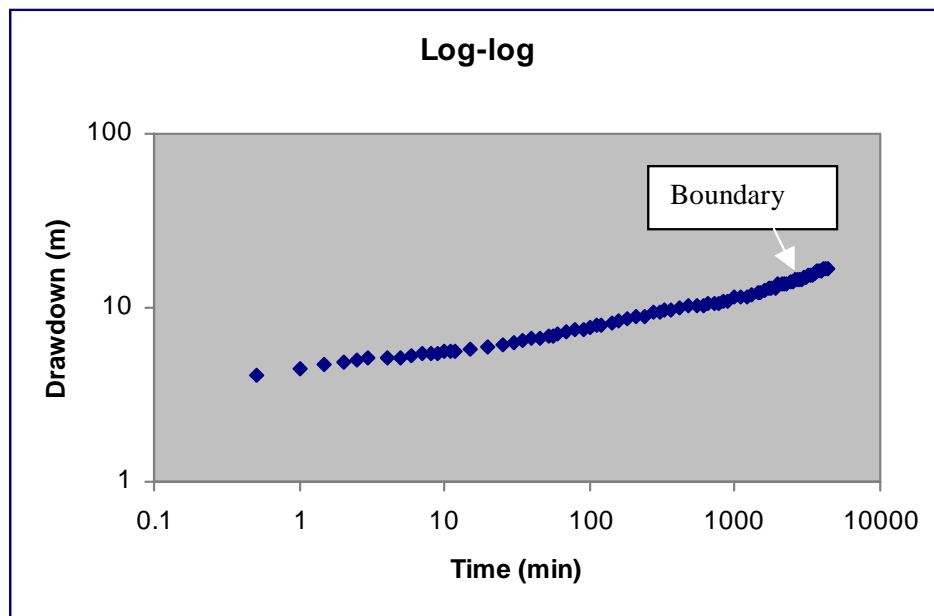


Figure 3.20: Log-log Theis plot of borehole GR2

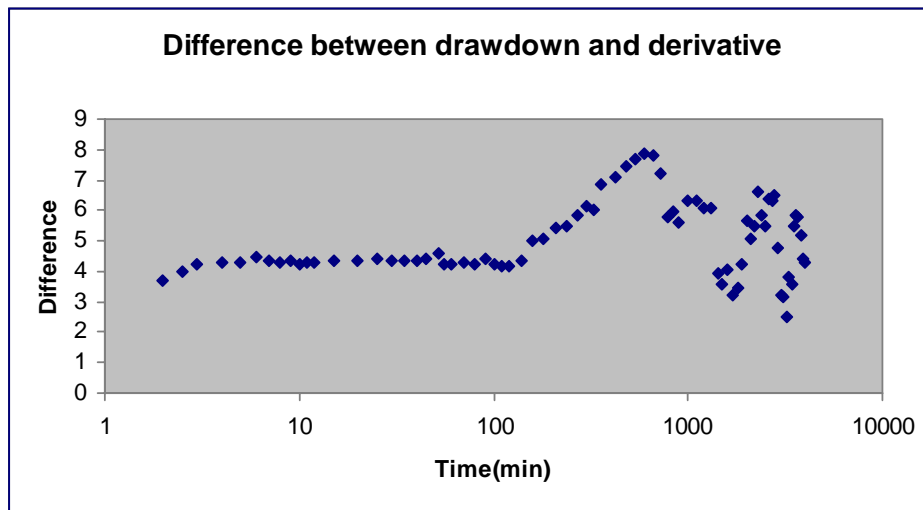


Figure 3.21: *Difference between drawdown and derivative is equal to 4 until 140 min, indicating a good fracture network (i.e. bilinear flow, water is derived from fracture and matrix)*

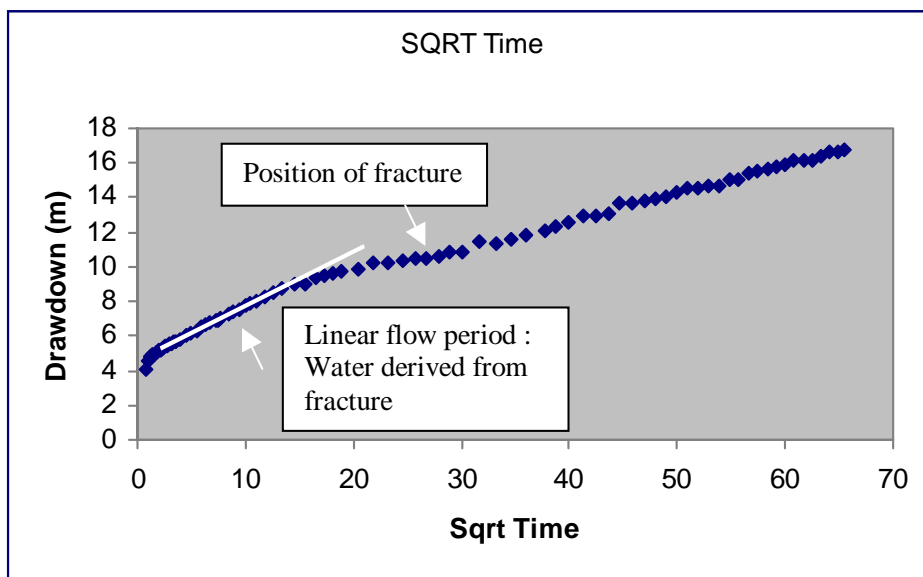


Figure 3.22: *Square root of time plot. After the linear flow period (water is coming from fracture), a flow period is evident where water is derived from the matrix (i.e. flow from matrix to fracture)*

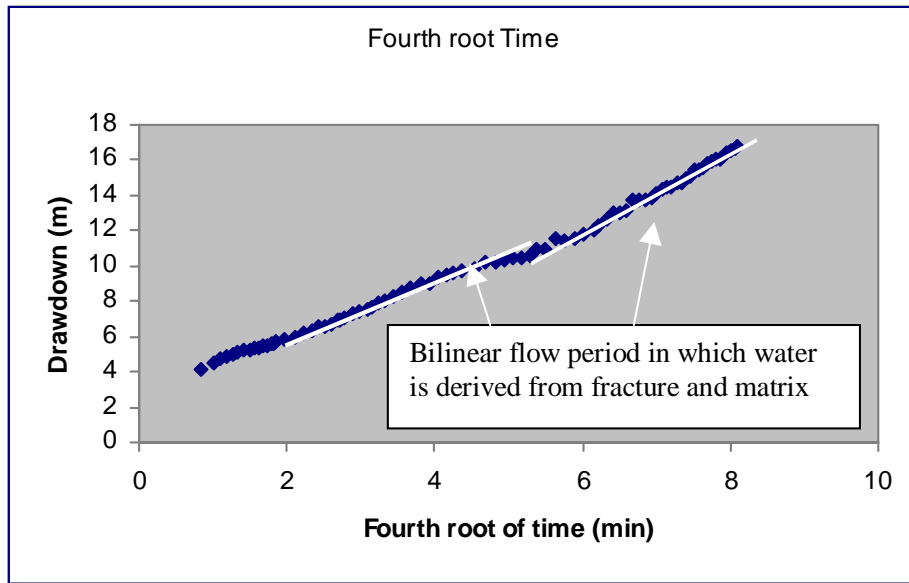


Figure 3.23. After well bore storage, a period of bilinear flow is occurs, where water is derived from both the fracture and the matrix (good fracture network). Last segment - matrix flow becomes dominant (water derived from matrix)

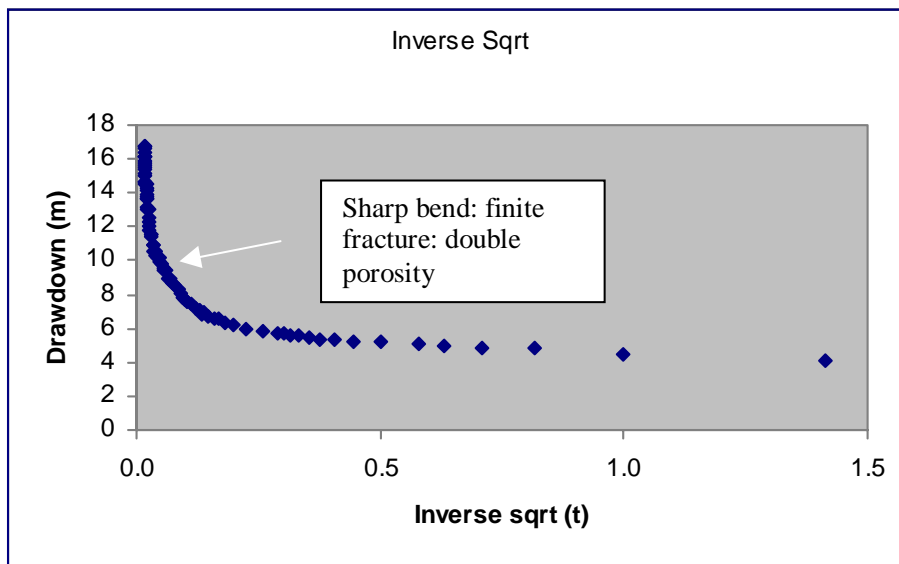


Figure 3.24: Inverse square root time graph showing 'sharp bend' indicating that the fracture is finite. Note that the graph plots from right to left (i.e. early time is plotted at large inverse square-root of time)

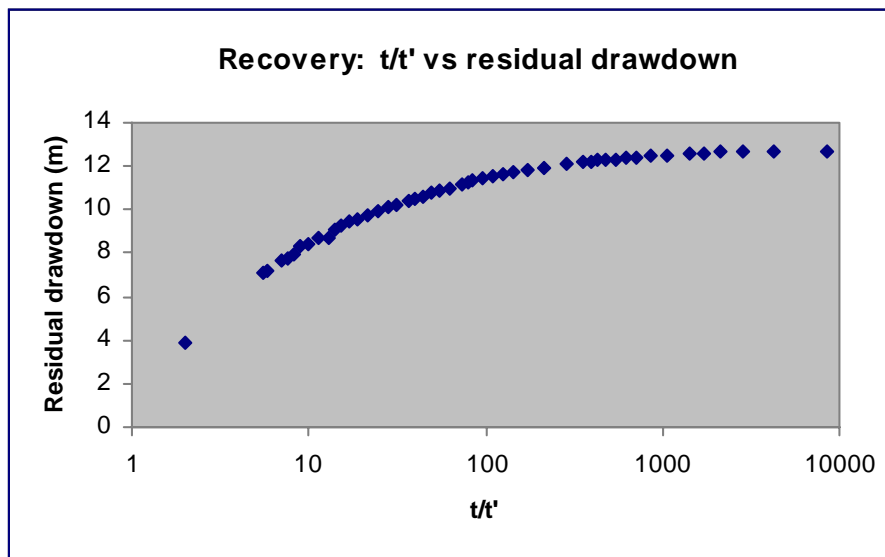


Figure 3.25: *Graph of residual recovery indicating that recovery was incomplete*

The use of the different forms of derivative graphs can thus be used with great effect to identify certain flow regime characteristics of fractured-rock aquifers.

3.2 MACRO-CHEMICAL CONSTITUENTS AND WATER QUALITY

3.2.1 INTRODUCTION

Karoo formations due to their ubiquity throughout Southern Africa display variable water quality properties. Lateral changes in climatic patterns seem to be the main factor controlling the diversity of the mineralization and water types occurring in Karoo rocks. This variability is caused by differences in rainfall, recharge, evaporation, topography, soil type and thickness, vegetation cover and human activities.

Due to the nature of groundwater flow, which varies significantly from area to area, local groundwater quality variations are significant and anomalies to the large-scale generalisations are prevalent. Micro-scale differences occur due to the nature of groundwater flow in Karoo rocks, namely the resulting variations within matrix and 'fracture' components of the groundwater flux. The residence times are often different for these two main components and give rise to the differences in mineralization and solute proportion in passing groundwater.

3.2.2 SOLUTE-FORMING PROCESSES

Numerous hydro-geochemical processes have major or minor effects on the quality of groundwater in aquifers in the Karoo Basin. Different processes dominate the quality of water in the parts of the aquifers deposited within different sedimentary environments.

The major hydro-geochemical processes and their interrelations are discussed in this section. The processes that occur in aquifers, the effect of these processes on the quality of groundwater and the relations of the processes to the sedimentary environment will be discussed.

3.2.2.1 Physical Weathering

Apart from mineralogical composition of the parent rock, hydraulic and hydrological factors greatly influence groundwater quality. Dolerite dykes and sills on one hand and fracture / fault sets on the other often control the mode of groundwater flow, availability of rainfall recharge and groundwater velocity and hence the residence time of water in the subsurface. Openness of groundwater systems is important in terms of availability of electron acceptors and carbon dioxide.

Mechanical processes close to the surface also influence the weathering patterns. Ice expansion, experienced on freezing of water, growth of the plant roots, animal holes etc. are activities that contribute to the development of the weathering process.

Interestingly enough termite mounds were reported in Australia as being responsible for elevated nitrate concentrations on regional basis (Barnes et al., 1992).

Changes in dynamic equilibrium – be it hydrological or hydrochemical reflect themselves in changes in groundwater quality. The minerals become unstable and react in a way that thermodynamically allows for a development of a new equilibrium.

Certain minerals and rocks are more vulnerable to the chemical reaction than the others – this is reflected morphologically where more resistant rocks form the more elevated areas, while the less resistant rocks are eroded away. Most of the boreholes in Karoo are sited on dolerite dykes, either on a contact between the dyke and other rocks or directly into the dyke. Weathering of these extrusive rocks will therefore have definite impact on groundwater chemistry.

3.2.2.2 Weathering of Dolerite

Weathering of main Karoo rock types was described by Tordiffe (1980). The weathering sequence for igneous rocks is as follows:

anorthite → augite, hornblende, biotite or albite → K-feldspar, muscovite → quartz.

The minerals that form dolerite are susceptible to chemical weathering. In this process certain amounts of calcium, magnesium and sodium are released into passing groundwater. Major anions are most probably not derived from the parent rock (with exception of fluoride). Bicarbonate, chloride and sulphate are derived from processes that will be discussed below.

3.2.2.3 Weathering of Sedimentary Rocks

The Karoo sedimentary sequence is composed of sandstone, mudstone and shale as main representatives of the sedimentary rock types. Mudstone is by far the most ubiquitous rock in the Karoo. This is the reason why parent sedimentary rocks are prone to contain high concentrations of salts when compared to groundwater associated with dolerite structures.

In addition to silicates the sedimentary sequence contains important groundwater chemistry minerals such as calcite and pyrite, largely in the form of incrustations between detrital grains. Calcite is a common secondary mineral in basin sediments of dry climates. Sandstone in particular contains K-feldspar in addition to quartz and also minor amounts of Na-plagioclase. The important fact is that most of the intergranular cement material is calcite, although silica is not uncommon.

Gypsum is also commonly found in arid soils. **Figure 3.83** illustrates the correlation between known gypsum deposits in the Karoo Basin and the high sulphate content of groundwater in the western part of the Karoo.

3.2.2.4 Role of Carbon Dioxide

Karoo aquifers are known for their relatively poor soil cover, especially in the western parts of the Karoo Basin. Although this encourages the free flux of oxygen into the subsurface, the important weathering agent - carbon dioxide - is in low supply. Weathering of the sedimentary sequence by carbon dioxide is the most important decomposition process in unconfined aquifers and in the recharge zone of the confined aquifers.

Both, the availability of carbon dioxide (and dissolved oxygen), together with distinctive climatic patterns are responsible for the groundwater quality variations between the rainfall-rich eastern portion and the rainfall-deficient western portion of the Karoo basin. These variations even affect the hydraulic properties of the aquifer matrix - decomposed residues as a result of soil-generated carbon-dioxide in the eastern part of the Karoo Basin provide material for a soil cover and may completely or partially fill in fracture sets in the parent rock.

Silicate weathering results in appreciable bicarbonate concentrations, which is typical for the eastern part of the Karoo Basin. Weathering of plagioclase results in the release of cations such as calcium and sodium

When the availability of carbon dioxide is greatly reduced, hydrolytic decomposition of the silicates takes over and adds solutes into passing groundwater. Major ions are subsequently slowly removed leaving clay minerals and amorphous iron oxides. The general rainfall conditions and residence times determine what type of clay mineral is formed. Montmorillonite should be formed under relatively dry conditions (western Karoo) and kaolinite in the wetter environments (eastern Karoo).

3.2.2.5 Ion Exchange and Sorption

Ion exchange and sorption are processes that change the proportions of ions in the solution. The better known reaction is the exchange of calcium for sodium on the exchange sites of sodium-rich minerals. This reaction depends on the concentrations of exchangeable ions in solution.

If availability of carbon dioxide is limited, hydrolysis of calcite (and silicates) occurs and the resulting hydroxyl ion may be involved in further reactions. In this way iron present in clay minerals may be leached out to form ferric hydroxide. This mineral commonly forms a coating on Karoo rocks.

The exchange capacity of clay minerals allows for the dissolution of more calcite than would otherwise dissolve. The process also mobilizes significant amounts of sodium into solution and can lead to excessively alkaline solutions, i.e. at some coal-mines in the northern part of the Karoo.

3.2.2.6 Evapotranspiration

It is not surprising that recharge and evaporation patterns have a solute-shaping influence on the groundwater chemistry of the Karoo rocks when considering the highly variable climatic conditions within the Basin (**Chapter 1.4**). The contrast in groundwater concentration and type between the eastern and western Karoo Basin is most significant. The global climatic effects are very different along the edges of the Karoo Basin. The regular and relatively high rainfall in the eastern Karoo results in continuous dilution, leaching and further transport of leached constituents - thereby maintaining a relatively low overall concentration of constituents. Groundwater is under-saturated with respect to most of the minerals, which do not attain their solubility limits.

On the other hand, erratic and sparse rainfall, combined with high evaporation rates in the Western Karoo induces a continuous concentration of solutes as the flushing-effect is at a minimum. The combination of a long groundwater residence times and evapotranspiration results in the reported high salt concentrations of groundwater in the Western Karoo.

The high concentration of anions in groundwater is often the result of rainfall-originated constituents being concentrated many times over by evaporated water leaving its salt content behind.

The concentration effect is further exacerbated by the lack of organic-matter due to the thin soil cover. Unfavourable denitrification conditions thus may result in elevated nitrate concentrations. As some minerals reach their solubility limits they tend to precipitate forming rejuvenated calcite and ferric incrustations.

3.2.2.7 Redox Controlled Reactions

Chemical reduction and oxidation induced by various factors can lead to dissolution of certain oxides, oxidation of sulphides and conversion of nitrogen forms. A commonly described sequence involving the presence of sedimentary organic matter from a more oxidized to a more reduced state is:

- Consumption of dissolved oxygen.
- Reduction of nitrate to nitrogen gas (denitrification).
- Dissolution of manganese.
- Dissolution of iron.
- Reduction of sulphate to sulphide.
- Conversion of dissolved nitrogen gas to ammonia.

These reactions can occur in the reverse sequence depending on the redox state of the aquifer system and how “open” or “closed” the system is towards influencing environmental impacts.

One of the more important reactions to occur in Karoo rocks is oxidation of pyrite. When oxygen-enriched water reaches these pyrite-mineralized rocks the sulphate concentrations increase and a low pH (acidic) water is produced if there is insufficient buffering capacity present in the aquifer – which may mobilize an array of trace metals into solution. The oxidation of pyrite causes a major environmental problem in mines operating in the Karoo environment. Coal and gold mines in the northern part of the Karoo Basin can produce effluents with sulphate concentrations measured in thousands of mg/ℓ.

Redox controlled reactions also influence the status of nitrates in groundwater. The rates of nitrification and denitrification are affected by the prevailing redox conditions, and more specifically any changes in these conditions. Spatial analysis of observed nitrate concentrations often shows poor correlation with other chemical constituents due to redox conditions that vary rapidly over short distances within the aquifer.

3.2.3 SPATIAL DISTRIBUTION OF MAJOR CONSTITUENTS

3.2.3.1 Approach

The spatial distribution of the major chemical constituents of groundwater in the Karoo was evaluated on a regional basis. Although small-scale variations may be of importance for a local development of groundwater resources, the emphasis was placed on identifying broad, macro-scale trends in groundwater quality.

No special groundwater study was ever conducted to identify groundwater quality trends on such a basin-wide scale. There were, however, two attempts to describe the groundwater quality in Karoo aquifers:

- Bond in 1946 presented a national account of groundwater quality in South Africa. This pioneer work is however outdated and is based on very few sampling points with a limited scope of analyzed constituents.
- The regional characterization programme conducted by DWAF. This is a relatively new initiative that is focused on the description of groundwater resources of South Africa, on map-sheet (1/500 000) basis. The groundwater quality section is however not described in any depth, authors limit their description to electrical conductivity and identification of the most salient problems. Only one sheet has thusfar been completed (Queenstown). The characterization programme generates a valuable database of boreholes, springs and groundwater quality, which should not be left without a detailed analysis as soon as the database is updated.

The groundwater quality database used in this analysis is based on the available dataset housed at the QualDB (DWAF). This database is the most representative source of groundwater quality nation-wide.

The main Karoo Basin was evaluated using analyses from over 11000 sites. At sites where more than one analysis was available the most recent analysis was considered for further evaluation. No consideration was given to vertical variations in groundwater quality within the aquifers – the available dataset does not really allow for such an examination. It goes without saying that it may be of importance to examine vertical variations of groundwater quality when installing a groundwater abstraction system under site-specific circumstances.

The data records do not reflect a snapshot of a single representative period. All available data have to be used in order to obtain acceptable coverage of the entire study area. The temporal changes in groundwater quality could thus not be screened out and units are compared using data records from different time periods. All records fall within the 1970-1997 period. A map (**Figure 3.26**) was compiled

showing the percentage of data records for the period 1990-1997 out of the total number of records used for this analysis.

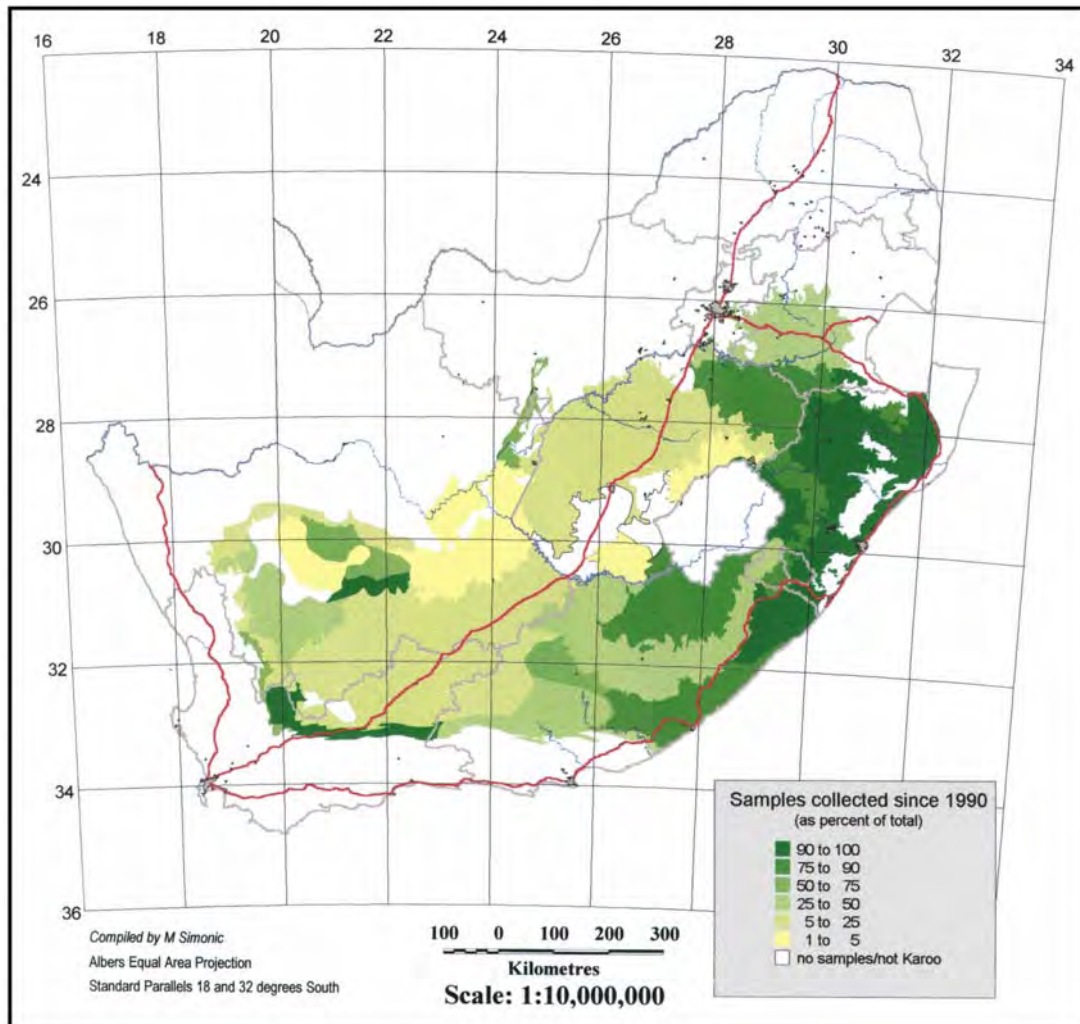


Figure 3.26: *Samples collected since 1990 as percent of total sample count.*

The groundwater quality data were evaluated statistically using the approach that was applied for mapping of Groundwater Resources of South Africa (1995). The major lithological units within the Karoo Basin were subdivided into smaller domains by considering their hydraulic properties. The groundwater chemistry within each of the domains was characterized using the water chemistry data falling within the geographic area of the domain. This approach inherently assumes that aquifers can be defined on the basis of geological units. The log-transformed groundwater quality data (to improve statistical distribution properties) of a specific domain was

summarized using the geometric mean. The variability of the data was portrayed as a range defined by standard deviation space. The standard deviation was also determined from the log-transformed data.

This approach therefore gives a probability range of values of solute concentrations that may be expected within a certain domain. Hence all anomalies are more or less smoothed-out. As with any other method the evaluation is biased, the main sources include the following:

- Temporal variation – groundwater quality in the borehole may change with time.
- Uncertainty resulting from different sampling methods.
- Uneven spatial distribution of sampled boreholes.
- Uncertain information on the status of the sampled borehole – whether it reflects “ambient” or “polluted” conditions.
- Vertical variations in groundwater quality along the borehole profile are not taken into account.

Virtually all the chemical parameters were analyzed for in the laboratory. The sensitive parameters such as pH and alkalinity are thus not always representative of the field conditions. Other parameters such as dissolved oxygen, redox potential and temperature have only been recently added to the National Groundwater Quality Monitoring Program’s protocol and their regional analysis is not as yet feasible.

Trace element and data other than the major constituents are not available for the entire Basin. Only very few analyses exist where trace elements were determined and these do not allow for any regional generalizations. Trace element data – which include iron and manganese – have mainly been collected for pollution studies and thus do not represent natural conditions.

Groundwater domains with similar chemistry (statistical parameters) were grouped together according to the ranges defined by the DWAF drinking water quality standards (DWAF, 2000). The colour scheme representing drinking quality classes was used whenever appropriate.

The information was analysed on a national-scale and are discussed below.

3.2.3.2 Summary of Chemical Parameters

Water is often judged on its ‘salt content’, i.e. the amount of total dissolved solids (TDS) within a unit volume (mg/l). In South Africa another indirect parameter for water mineralization is often used – electrical conductivity (EC) measured in mS/m. The effect of dissolved solids is not, however, only affected by concentration alone. In highly mineralized waters the concentration has to be replaced by *ion activity*,

which is a transformed portion of concentration that is active in chemical processes. The equivalent of the 'activity' characterized to TDS is *ionic strength*.

Ionic strength is an important parameter for more sophisticated hydro-geochemical analysis and it is used for the determination of saturation indices and hydrogeochemical modelling. The assumptions for Davies equation and/or Debye-Huckel equation are applicable to solutions with ionic strength of 0.1 - 0.5 and less. Approximate activity coefficients for typical groundwater constituents were provided by Hem (1989). At an ionic strength of 0.01 the activity coefficients for the monovalent species are near 0.91, for divalent species 0.67 and for trivalent species 0.45. This means that only 91, 67 and 45 % of total concentration is "active" in speciation. Ionic strength is therefore an important chemical parameter as it affects inhibition of chemical reactions and prevents them from taking place. If the ionic shielding effect limits the effective concentration of a solute more mineral containing the solute can be dissolved and the overall mineralization of water increases. This mechanism plays a great role in arid zones where evaporites mobilized by groundwater increase dissolution of other minerals

Concentrations of dissolved constituents increase from the east to the west following a similar decrease in precipitation (**Figure 3.27**). The geometric mean concentration of dissolved solids range from less than 100 mg/l at the base of the NE slopes of the Drakensberg Mountains to more than 3 400 mg/l in the Western Karoo – representing a concentration factor in excess of 30 fold due to an increasing 'rainfall deficit' (rainfall – evapotranspiration) towards the Western Karoo (**Figure 1.3(c)**).

Most of the Karoo Basin has TDS in the range of 450-1 000 mg/l, which is not excessive by any standards. High concentrations are limited to westernmost and southernmost edges of the Basin, especially to groundwater in the Dwyka Formation. This water is partly of a connate origin. As mentioned earlier, the relatively well-defined picture of TDS may be skewed by the fact that fresh water related to dolerite structures was sampled most often. The groundwater quality in the sedimentary sequence is regarded as poorer due to longer residence time.

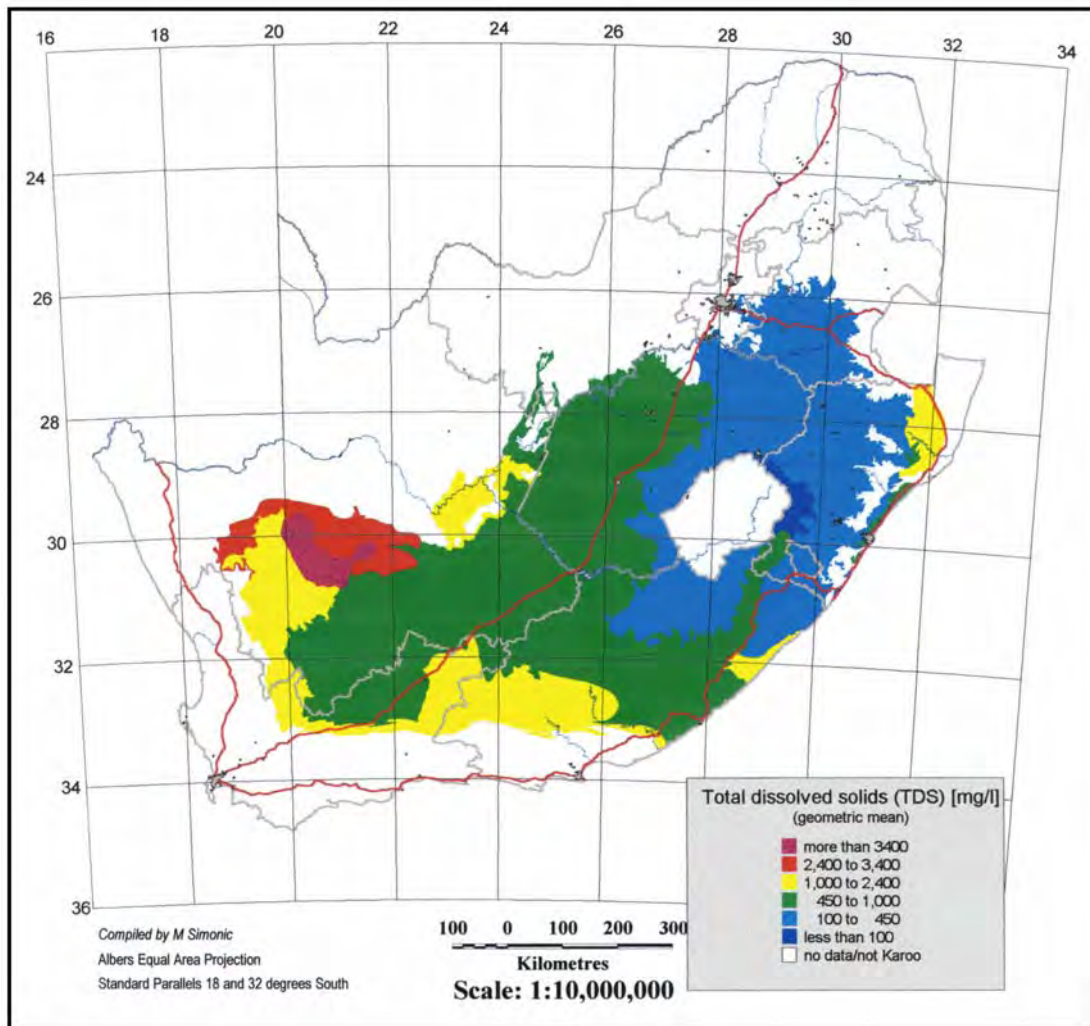


Figure 3.27: Ranges of total dissolved solids (TDS) expressed as geometric means over representative lithological units

pH is the most important parameter to consider when studying the quality of groundwater. Unfortunately, one has to rely on pH measurements made in the laboratory. According to these measurements Karoo aquifers have in general a rather high pH, in the range of 8.0-8.5. Only a relatively small part of the Karoo Basin has pH less than 7.5 (Figure 3.28), limited to the east and north where rainfall (and carbonic acid activity) is comparatively higher than in the other parts of the Karoo.

High pH values are rather typical for dry desert-like climates. Occurrences of pH greater than 7.5 are however not limited to dry area only. In the northern and north-eastern part of the basin the high and “low” pH zones are next to each other. The pH variations in those territories most probably reflect differences in groundwater

residence times. The pH values go from low in high-lying territories around Lesotho to higher in flat-lying domains where the groundwater circulation should be comparatively lower.

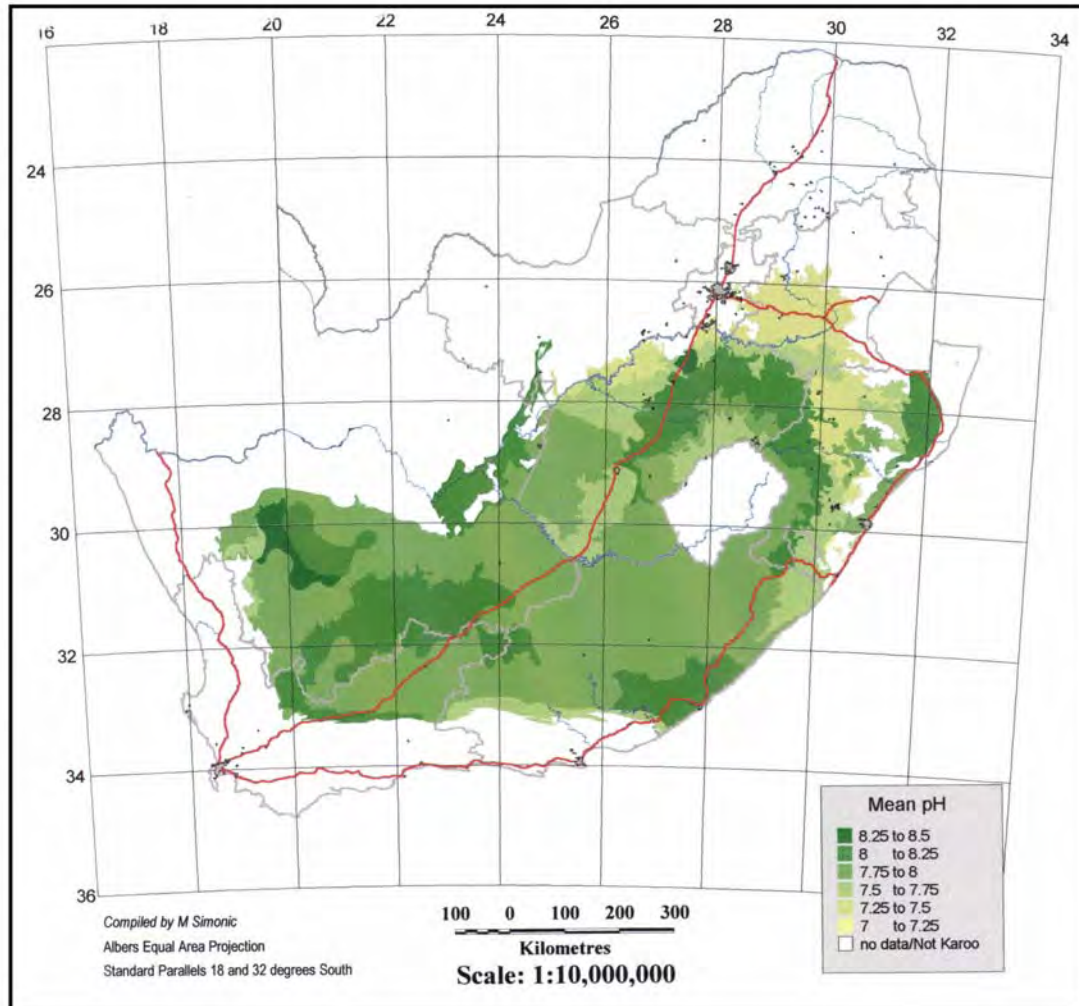


Figure 3.28: Mean pH for representative lithological units

Low-pH values broadly encountered in the Witbank and Newcastle areas are probably influenced by measurement obtained from the numerous coalmines in the area.

This section describes the concentrations of major constituents found in Karoo aquifers. All constituents, except of nitrate, show an east-west trending increase in concentration.

3.2.3.3 Major Cations

Calcium and bicarbonate are usually the dominant ions in recharge water, at the beginning of groundwater cycle. For most parts of the Karoo calcium occurs in relatively low mean concentrations – commonly between 30-80 mg/ℓ (Figure 3.29). Lower Ca ranges of between 10-30 mg/ℓ occur in the eastern Karoo and around Lesotho. Calcium is balanced by alkalinity in the central and eastern Karoo, and by sulphate in the western Karoo. Elevated calcium concentrations occur in the extreme west, mainly in the Dwyka Formation, and in the high evaporation/low recharge area around Rietbron.

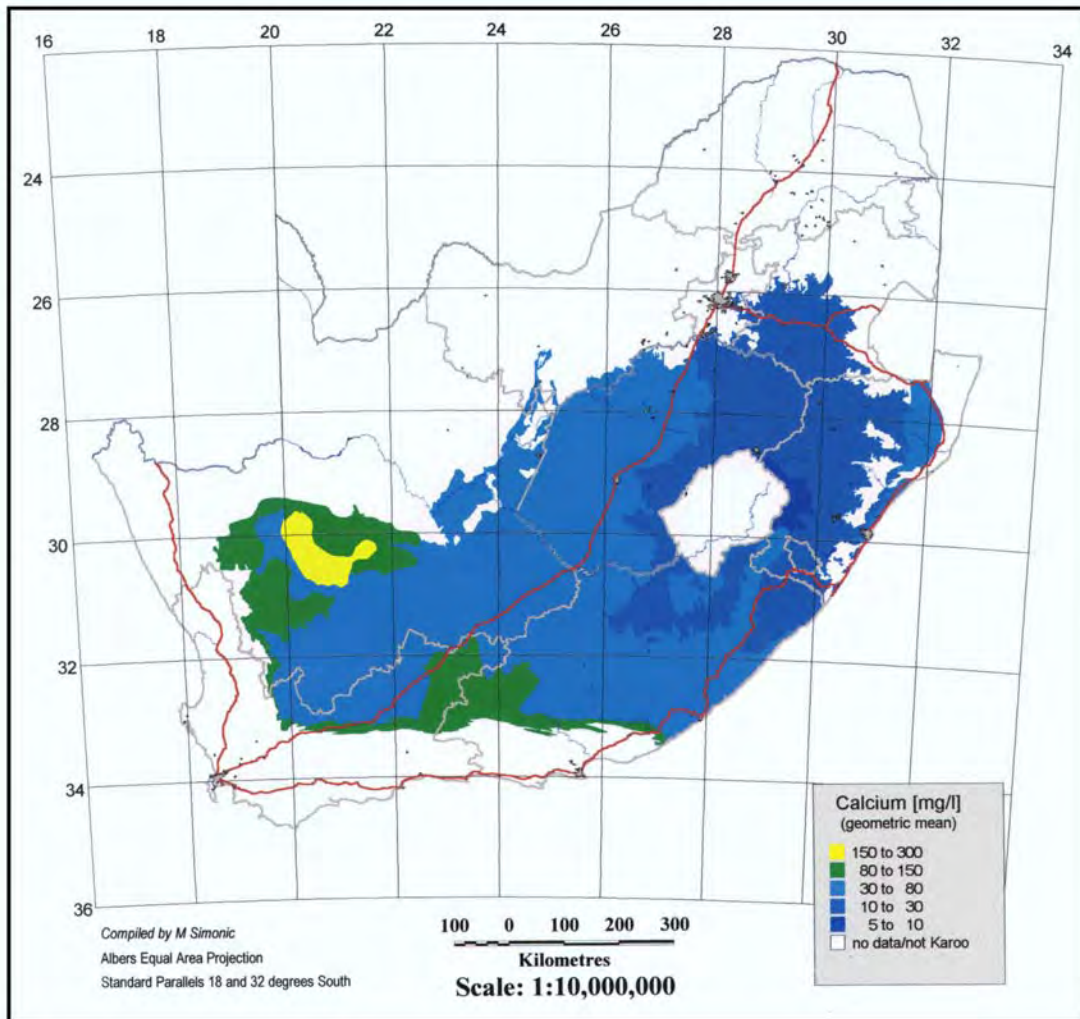


Figure 3.29: Calcium concentrations expressed as a geometric mean within each lithological unit.

Magnesium reveals a similar distribution pattern to calcium (**Figure 3.30**), but does not occur at the same concentration levels as calcium. Rather low ranges are encountered in the south-western portion of the Basin. Magnesium seldom more abundant than calcium, suggesting that magnesium minerals are not as readily soluble as calcium. The Ca/Mg ratio for most parts of Karoo is between 1.1 and 4.0. Groundwater from the Dwyka Formation in the area between Sodium and Barkly West has Ca/Mg values slightly below 1.0.

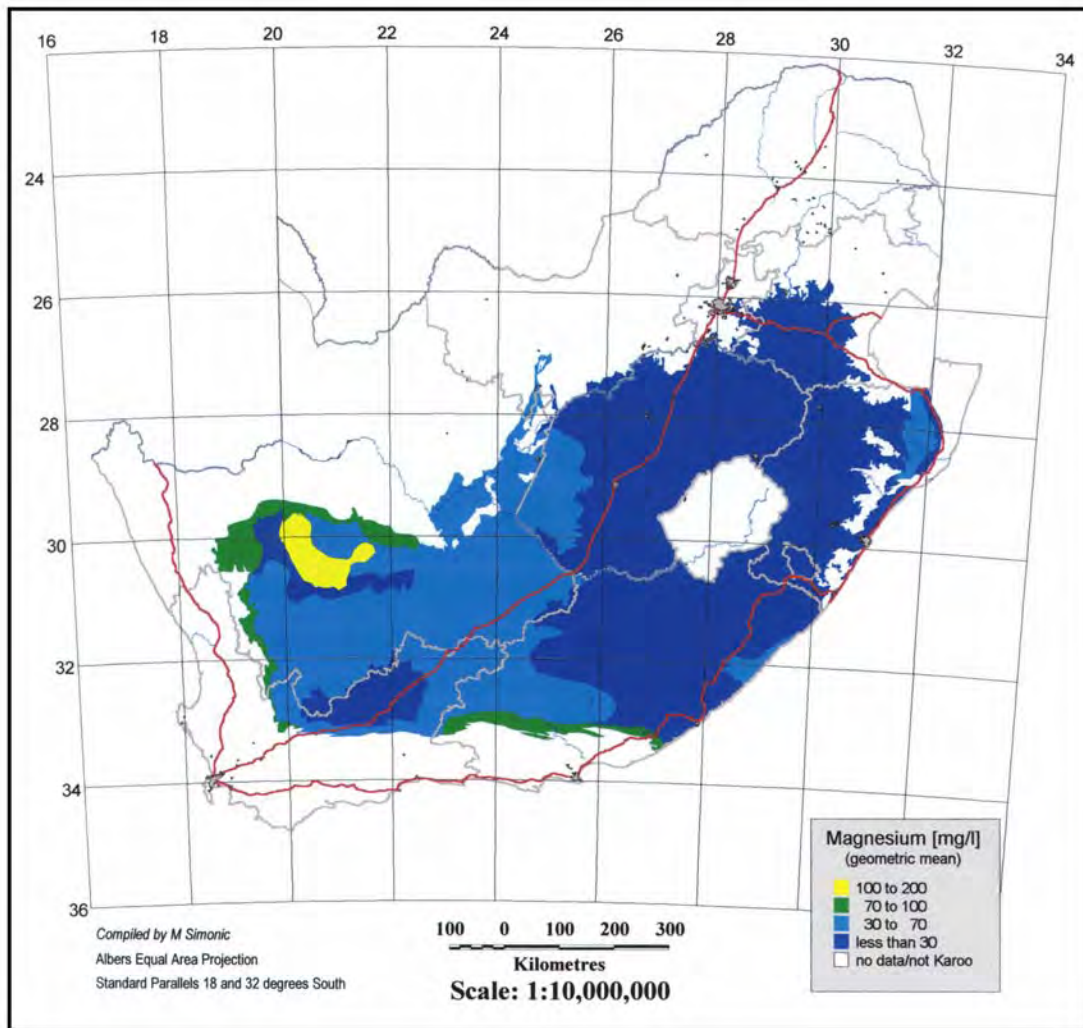


Figure 3.30: *Magnesium concentrations expressed as geometric mean over elementary lithological units*

Calcium and magnesium ions participate in a property that is known as *total hardness*. Based on this property groundwater in Karoo is regarded as hard in most parts (Figure 3.31). Very soft to soft groundwater is found in the eastern and northern part of the Karoo. The western edge of the Karoo Basin contains groundwater that is very hard to extremely hard.

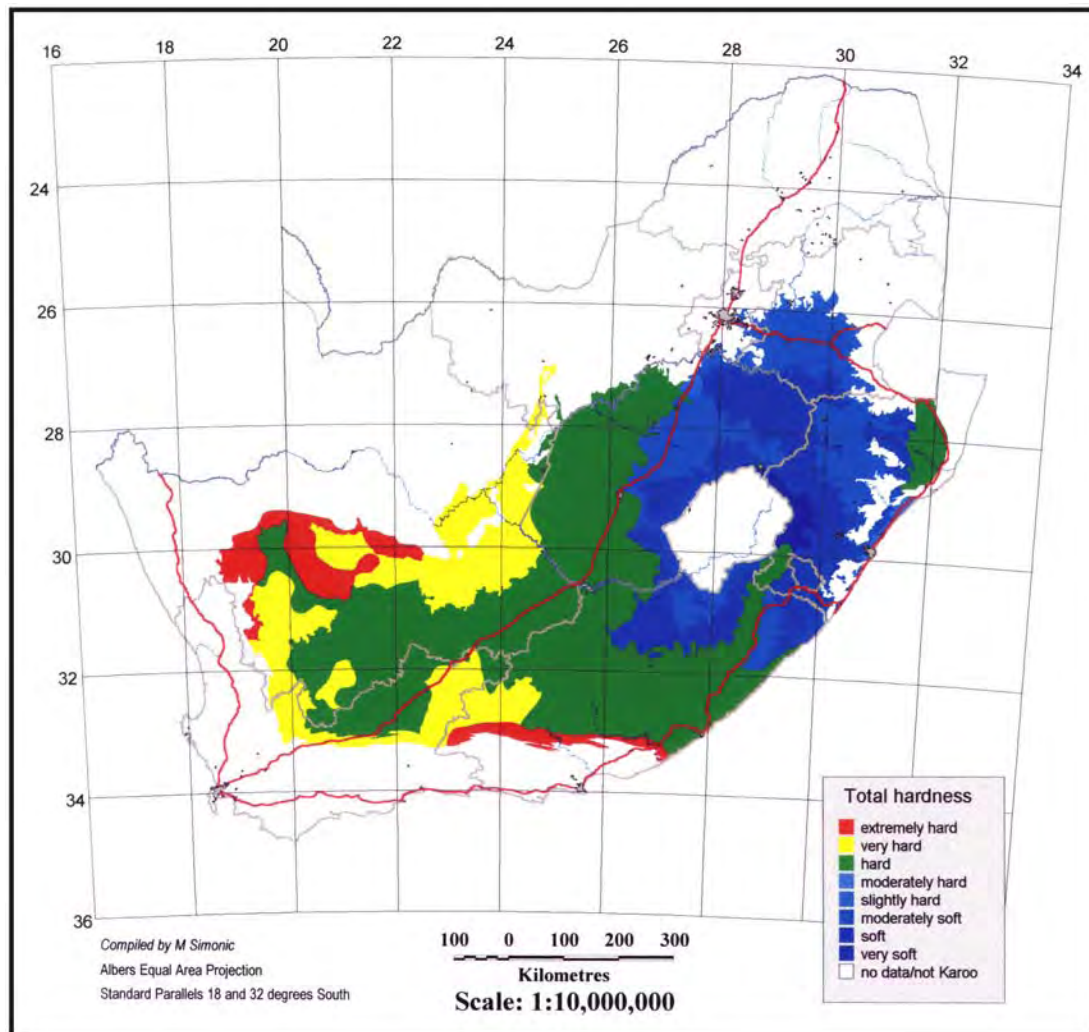


Figure 3.31: Total hardness of groundwater in the Karoo Basin

The concentration of Sodium is more variable than that of calcium and magnesium (**Figure 3.32**). Most of the Karoo has sodium concentrations within acceptable drinking limits, i.e. below 100 mg/l. The coastal sections of Karoo rocks in Kwazulu-Natal and the Eastern Cape show elevated sodium concentrations, that on average exceeding 100 mg/l. This is most likely the impact of the sea-born salts in which sodium dominates as the main cation. Sodium almost exactly mirrors the distribution of chloride, suggesting the two ions are closely associated. It also suggests that the process of Ca-Na exchange is not significant on a regional basis. If the exchange model is not dominant, then most of the sodium chloride concentration is of meteoric origin, i.e. coming from rainfall and subsequently concentrating due to evaporation.

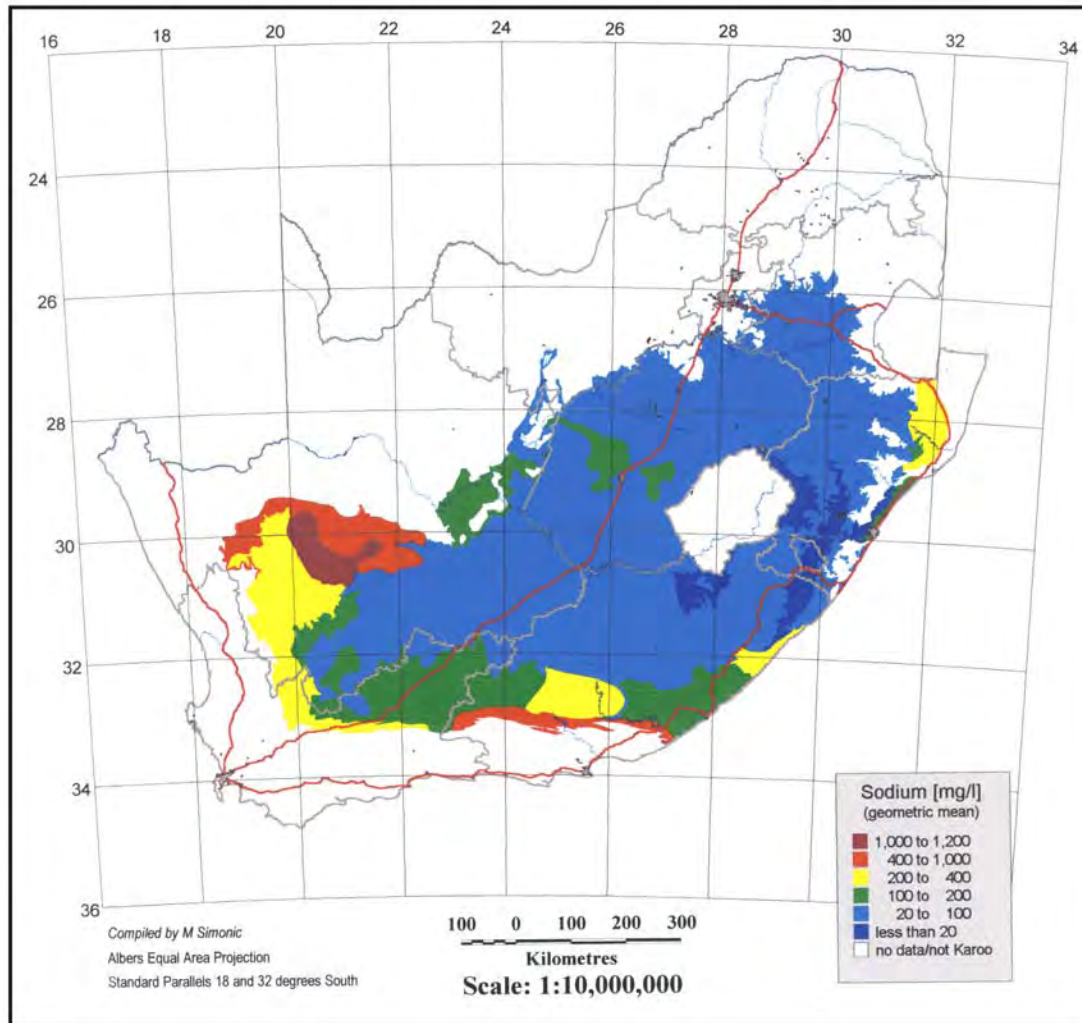


Figure 3.32: Sodium concentrations expressed as geometric mean over elementary lithological units

If the meteoric origin theory is true then the Na/Cl ratio should be approximately equal to 1. However when inspecting Na/Cl ratio map (**Figure 3.33**) the values close to 1 cover only a small area of the Basin, i.e. a narrow strip along the Indian Ocean, the western and south-western edges of the Karoo Basin.

In addition to rainfall there is therefore an additional source of sodium. This is especially the case in the eastern half of Karoo where sodium ions are correlated with alkalinity rather than by chloride.

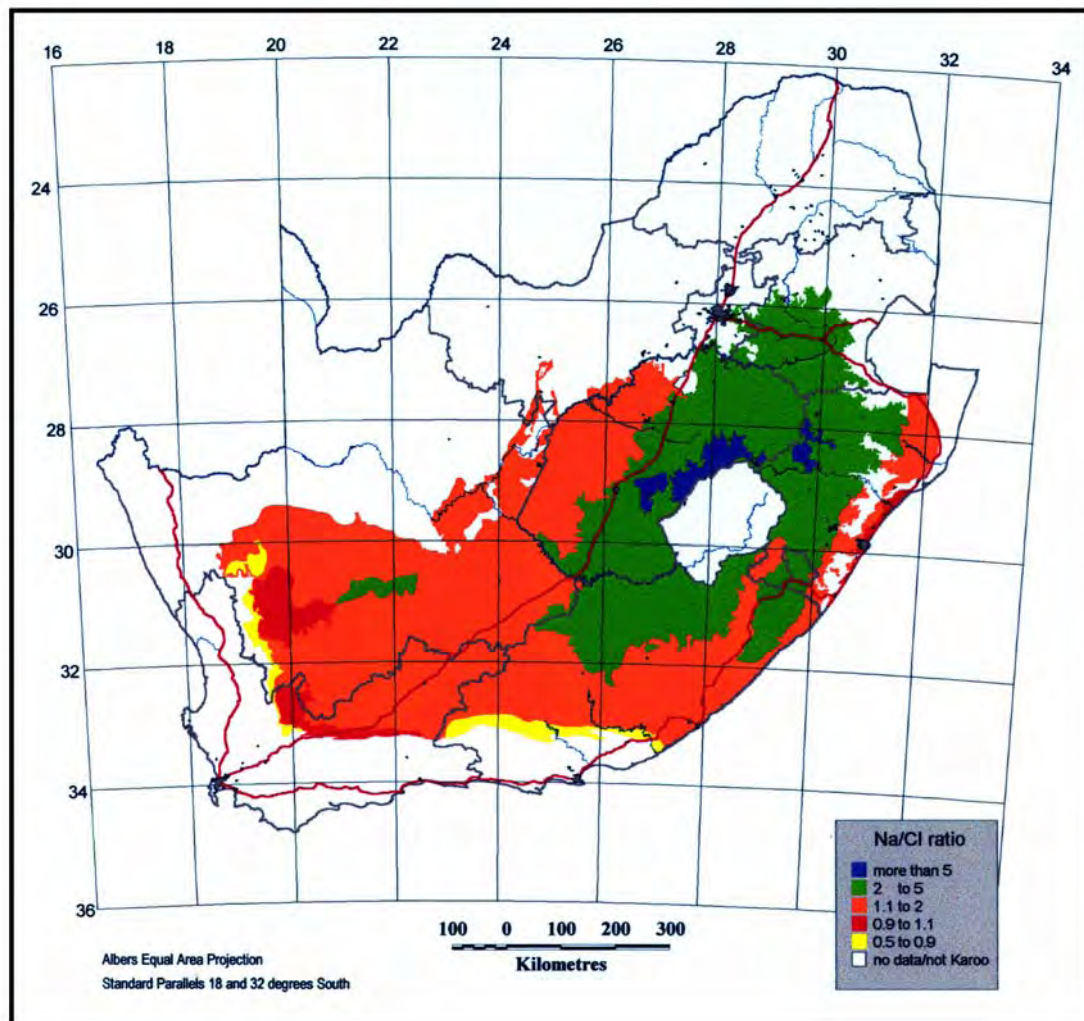


Figure 3.33: *Spatial Distribution of the Na/Cl ratio in the Karoo Basin*

Potassium concentrations seldom exceed 10-20 mg/l. Potassium ions are easily adsorbed by the aquifer material and therefore can seldom reach significant concentrations in groundwater.

3.2.3.4 Major Anions

Bicarbonate and carbonate are represented by the total alkalinity. In the dynamic systems they are formed by introduction of carbon dioxide with rainfall and by the biological activities in the soil. Further dissolution of carbonates in the aquifer material introduces additional alkalinity into solution until the solubility limit is reached. This is the most probable fate mechanism that is shown by the regional distribution (**Figure 3.34**). Relatively low total alkalinity concentrations occur in groundwaters of low ionic strength in the eastern portion of the Karoo Basin. The exception is the most eastern segment of Karoo rocks around Nongoma where groundwater quality is affected by relatively high mineralization.

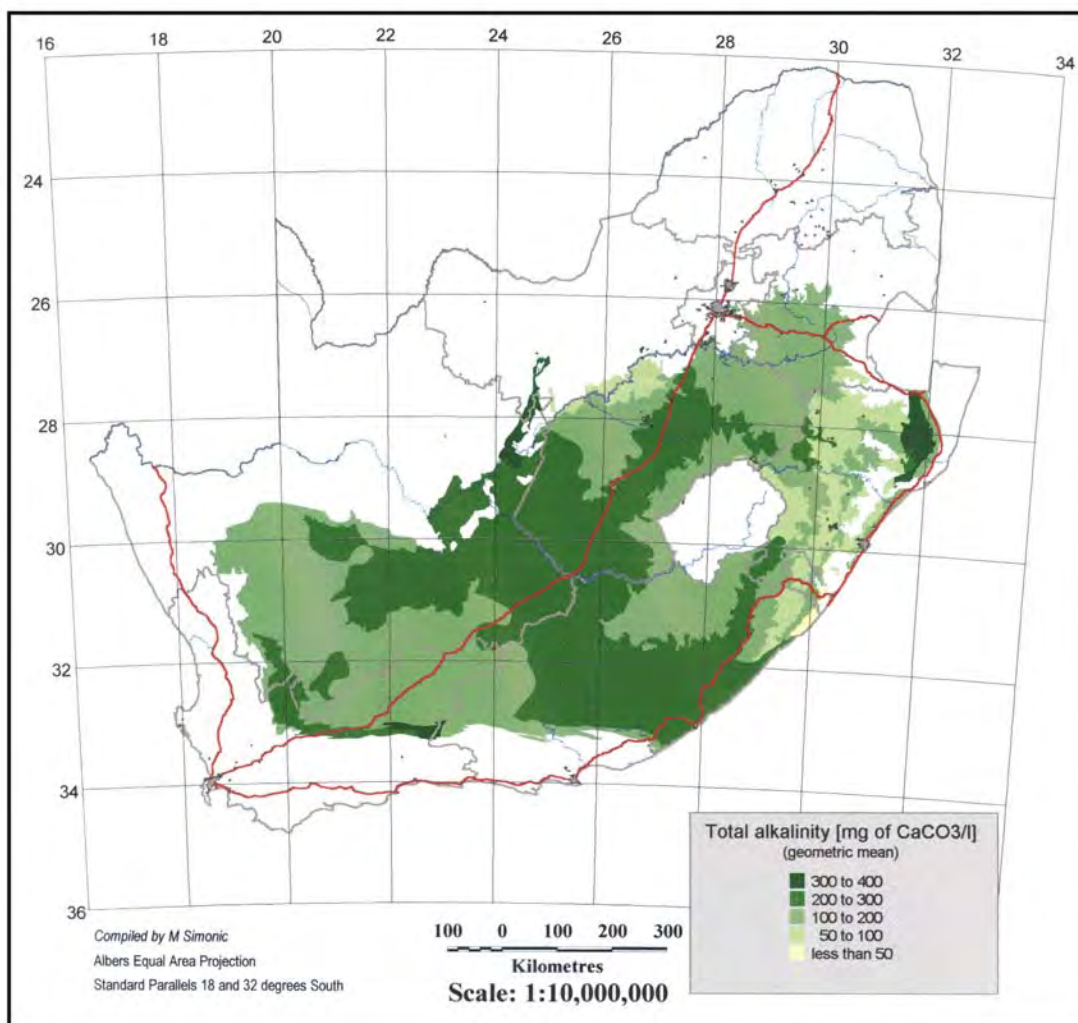


Figure 3.34: Total alkalinity expressed as geometric mean over elementary lithological units

The total alkalinity increases towards the centre of the basin and averages between 200-300 mg/l. In the south-western section of the Basin the alkalinity decreases, probably due to solubility limits of CaCO_3 and part of alkalinity may be lost to precipitation of carbonate minerals. Calcite fracture incrustations are common in the Western Karoo.

In order to understand the development of alkalinity it useful to know the partial pressures of carbon dioxide in groundwater. The accurate computation of carbon dioxide requires accurate field measurements of pH and alkalinity. Although these field measurements are not available for establishing accurate CO₂ partial pressures, the spatial distribution of pCO_2 (expressed as $\log \text{pCO}_2$) do illustrate the major differences in CO_2 activity in various parts of the Karoo (**Figure 3.35**). Relatively high pressures are documented in the central part of the Basin where alkalinity is also high. High pCO_2 values are also encountered the Dwyka sediments in the Eastern Cape, where the partial pressures are some 10 fold higher than the atmospheric pressure.

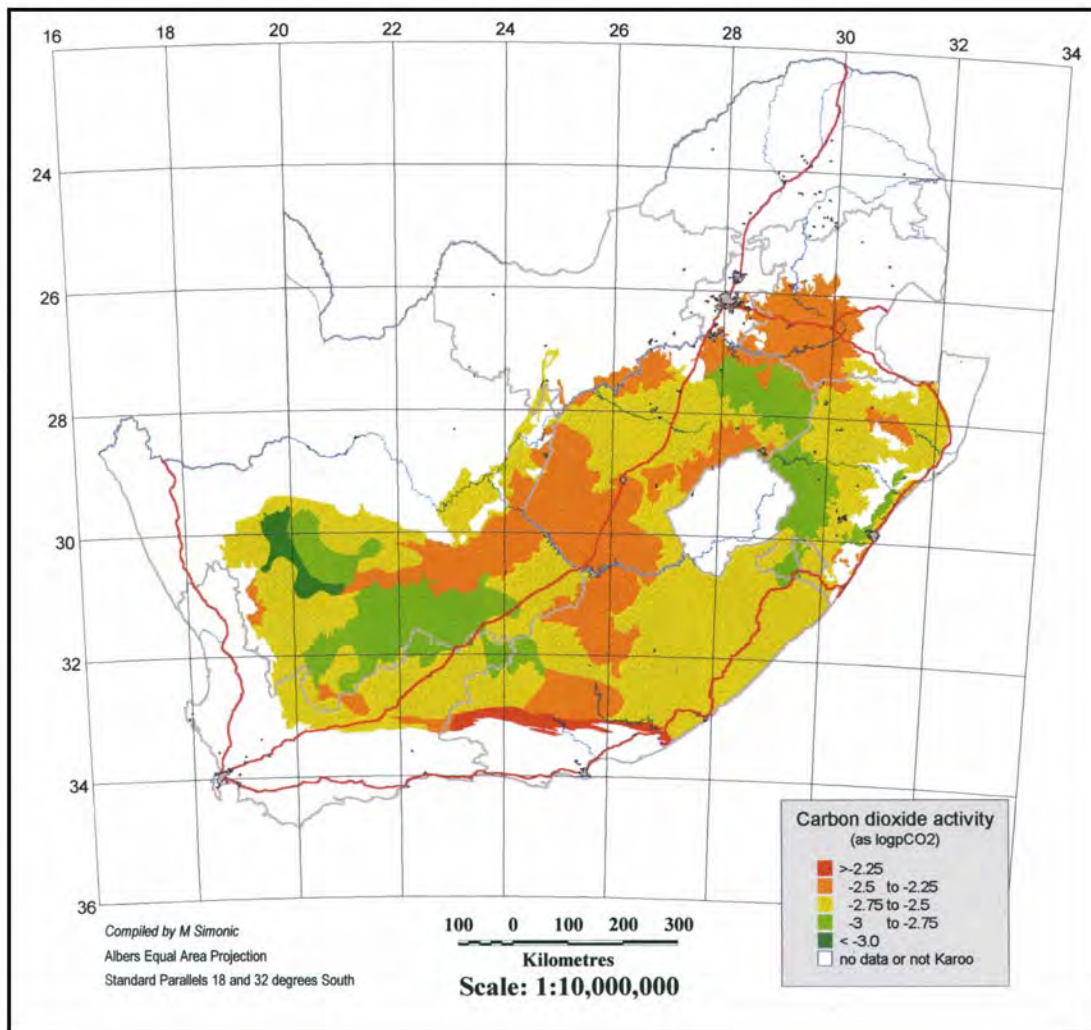


Figure 3.35: Carbon dioxide activity expressed as mean log pCO_2 over representative lithological units

On the other hand, pCO_2 close to that of atmospheric pressure are found in the central part of the Western Karoo, on southern Highveld and east of Lesotho in Kwazulu-Natal. Low partial pressures develop within an environment where there is either insufficient CO_2 as a result of low organic carbon content in soil, or where most of CO_2 was depleted by reactions occurring in the aquifer.

Alkalinity is not the only process requiring the presence of CO_2 . Dissolution of silicate minerals is also a process where CO_2 is consumed. Availability of CO_2 is therefore the factor limiting to some extent the weathering and dissolution processes.

Chloride and sulphate concentrations seem to be well correlated (**Figures 3.36** and **3.37**). Chloride however dominates over sulphate in most areas of the Karoo Basin, a

fact already mentioned by Bond (1946). Chloride shows obvious enrichment in the coastal strips along the Indian Ocean and is also profuse along the western margins of the Basin. In the north-western section both ions show relatively high concentrations exceeding 1 000 mg/l. The low-recharge area around Rietbron shows elevated concentrations of chloride, as well as sulphate. Long groundwater residence times, poor irrigation practices and saline influxes via rivers are noted as the probable causes for these high concentrations.

High nitrate concentrations do not pose any regional health-risk problems, but do occur locally in excessive concentrations. High concentrations occur in the Dwyka rocks of the northern portion of the western Karoo (**Figure 3.38**). This however does not mean that the nitrate problem can be completely disregarded. Numerous locally elevated nitrate concentrations have been reported from different parts of the Karoo – most of which are related to point source contamination of the groundwater from the surface.

Fluoride concentrations are usually elevated in acid igneous rocks. These rocks do not occur in the Karoo Basin. The fluoride concentrations often correlate with pH. However, inspection of pH values and mean fluoride concentration maps (**Figure 3.39**) do not show any apparent correlation either. Evaporation and long-residence time processes seem to be the most viable processes responsible for fluoride concentrations in the Karoo aquifers.

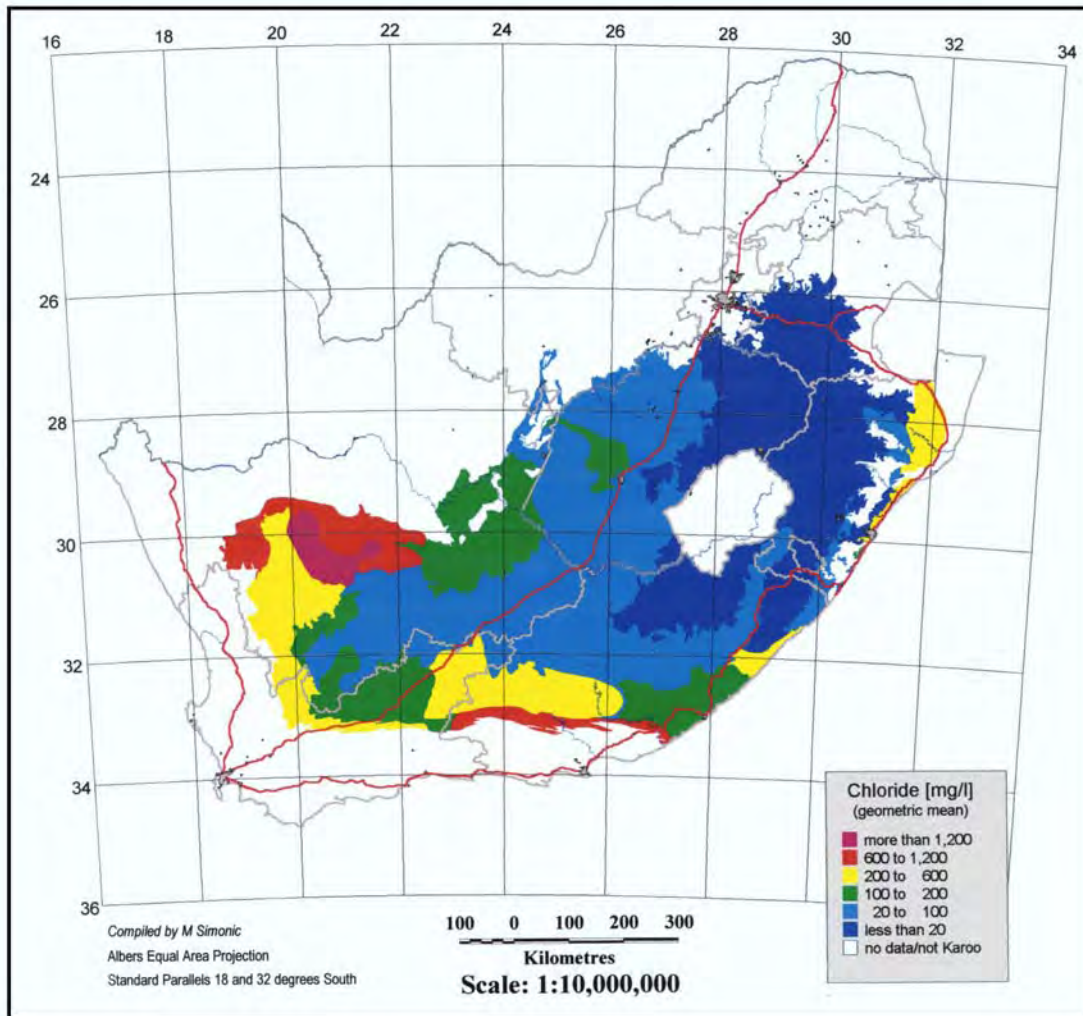


Figure 3.36: Chloride concentrations expressed as geometric means over representative lithological units

Silica: the concentration ranges of silica (as SiO_2) in groundwater are a measure of the silicate weathering processes. The bulk of matrix of Karoo aquifers is composed of silicate minerals. Silicates are much more resistant to weathering than for example the carbonates and the rates of dissolution rates are slower. The dissolution of silicates is irreversible and the products of dissolution usually form secondary minerals or quartz. The sources of silica in Karoo aquifers are mainly minerals like feldspar, albite and anorthite.

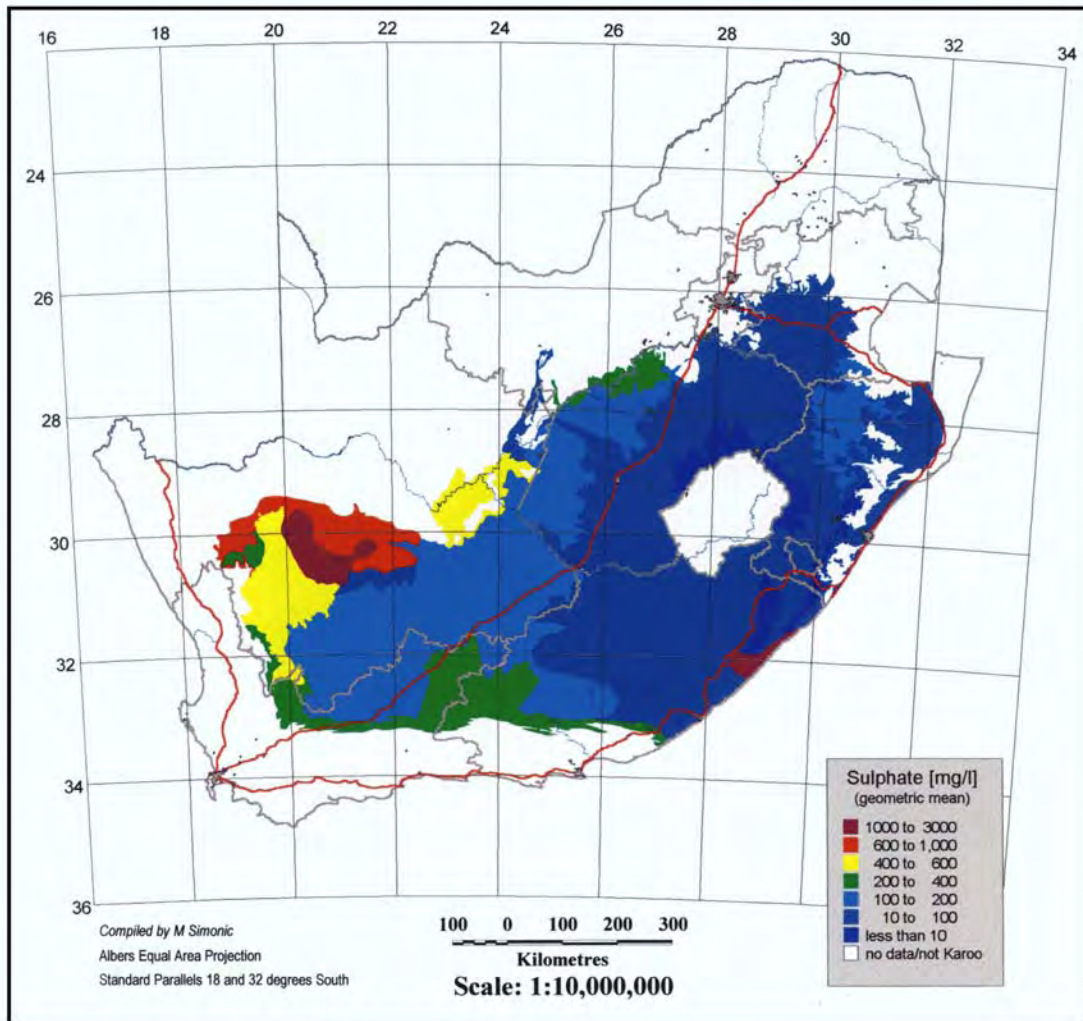


Figure 3.37: *Sulphate concentrations expressed as geometric means over representative lithological units*

The highest mean concentrations of silica in groundwater occur in the northern half of the central Basin. The mean concentrations are 15-25 mg/l. Other regions have lower mean concentrations, controlled by solubility of the silicate minerals.

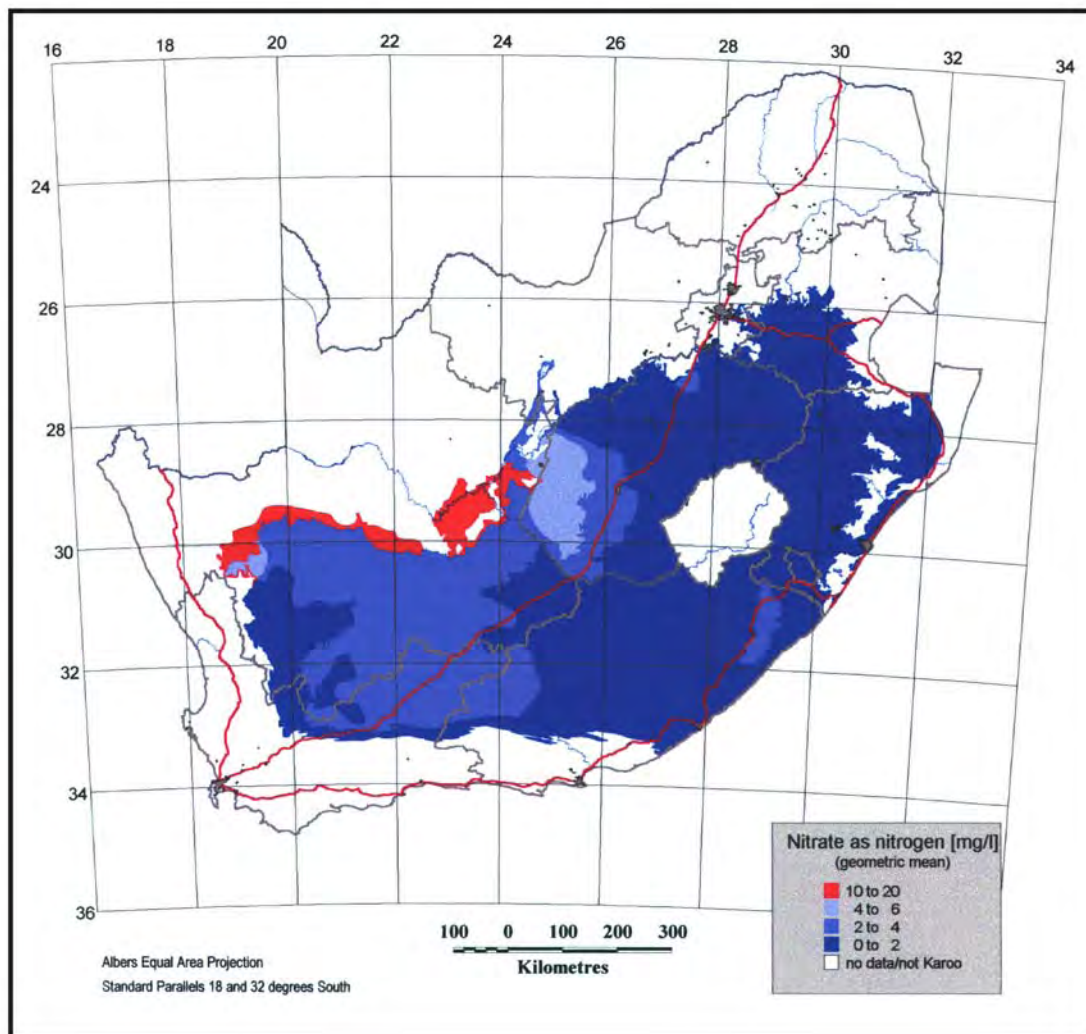


Figure 3.38: Nitrate (as nitrogen) concentrations expressed as geometric means over representative lithological units

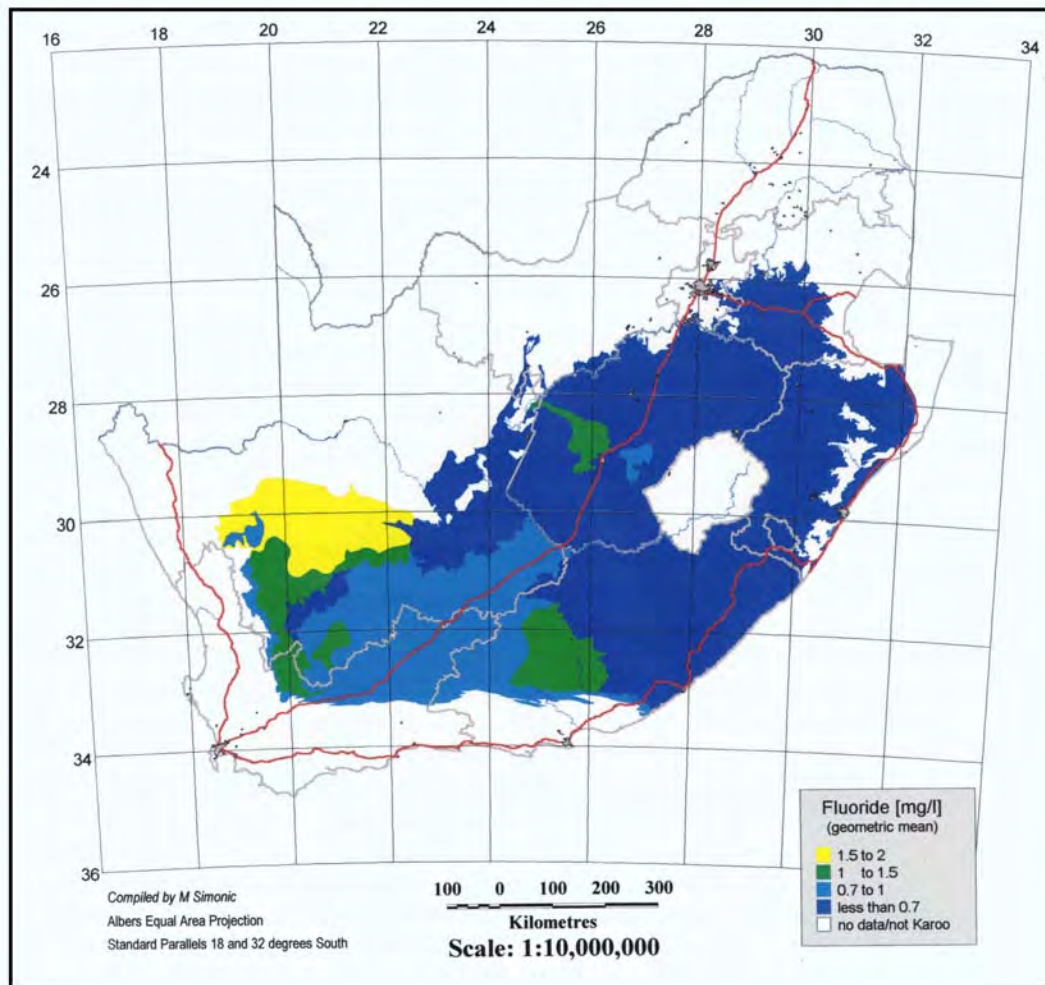


Figure 3.39: Fluoride concentrations expressed as geometric means over representative lithological units

3.2.4 VARIABILITY OF THE MAJOR CONSTITUENTS

The presented maps do not give a complete picture on the groundwater quality as they provide *only mean concentrations assigned to representative lithological units*. No information is provided on how variable the concentrations for the particular units are. In order to provide the reader with an estimate on variability of assessed concentrations the following measure of variability was computed:

The standard deviations (SD) from selected log-transformed constituents (Ca, Mg, Na, TAL, SO₄, Cl) were normalized using the Lilliefors transformation (the transformation factor is the mean). The normalized SD were summed up and mapped (**Figure 3.40**). It must be remembered that variability is directly proportional to the mean. Higher

relative variability in the eastern part of the Karoo does not necessarily mean that the concentration ranges in the eastern part are higher.

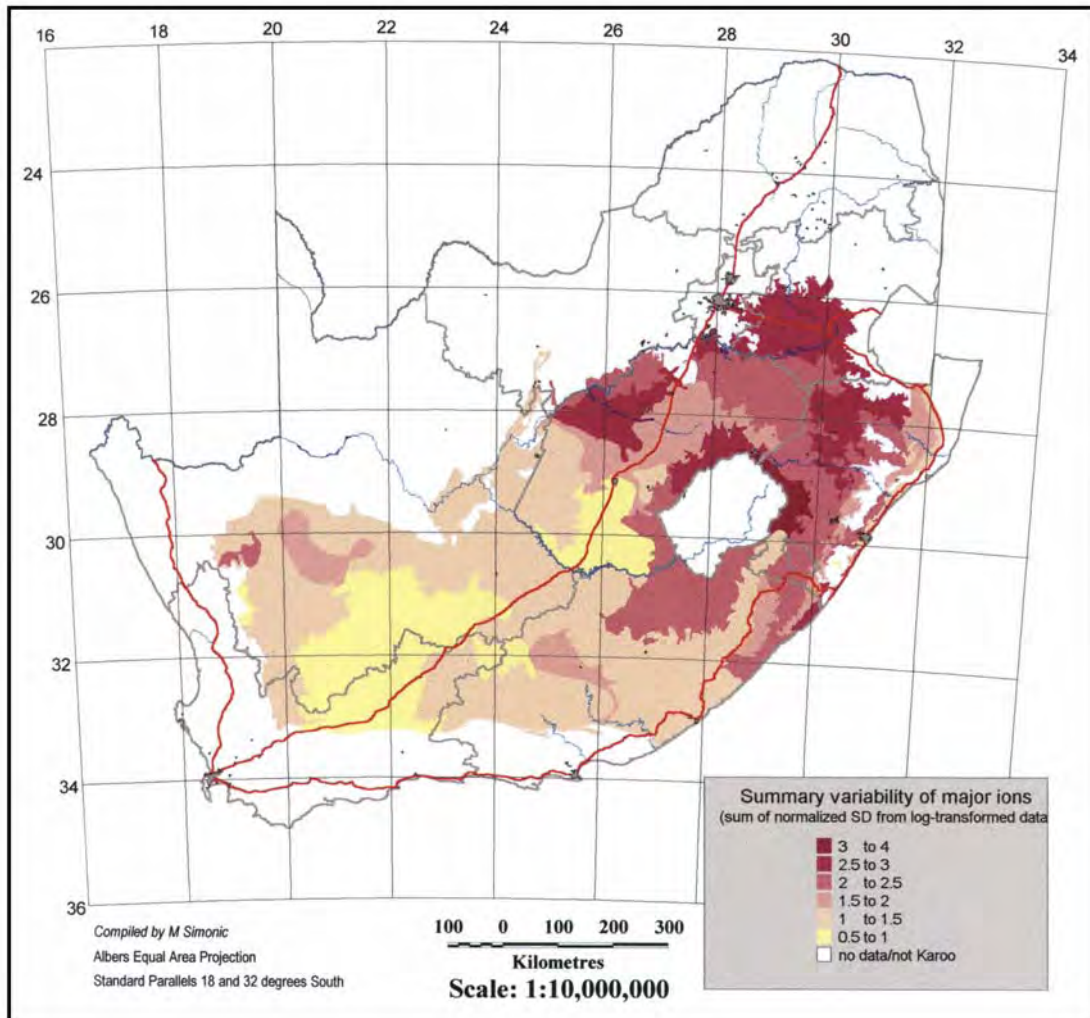


Figure 3.40: *Variability of Major Ions*

3.2.5 GROUNDWATER QUALITY WITH RESPECT TO DRINKING WATER GUIDELINES

The groundwater quality in the Karoo aquifers varies considerably. This is not surprising bearing in mind the areal extent of the Karoo Basin and variety of different hydrological regimes represented. After inspection of the spatial distribution of all the ions presented it is obvious that most groundwater quality problems occur the western half of the Karoo Basin, especially along the edges – as well as portions of the eastern

Karoo, i.e. in the vicinity of Nongoma. Local pollution sources may negatively effect groundwater in area which are generally mapped as favourable for drinking purposes, and thus all groundwater intended for drinking purposes should be assessed by a professional hydrogeologist or water quality scientist.

Constituents that most typically exceed drinking water quality guidelines are sulphate, nitrate and fluoride. In the western Karoo, especially within the Dwyka rocks, this list almost includes all the major constituents. However, this does not propose that there is no potential for groundwater development in these regions. The geometric means represent values somewhere in the middle of the frequency curve of the measured values, which implies that some samples will exceed guidelines and others will not.

In future it will be necessary to focus on the development of methods to assess additional chemical parameters than those presently being monitored. The industrial development and use of chemical agents in agriculture will require the measurement of other constituents that may be harmful minute quantities.

3.2.6 FLUORIDE AND POSSIBILITIES FOR DEEP-SEATED GROUND WATER IN THE KAROO BASIN

Elevated fluoride concentrations in groundwater are often reported by geohydrologists working at various localities in the Karoo Basin (**Table 3.11**). Little is known about the origin of fluoride in Karoo groundwater and elevated concentrations have often been overlooked as problematic “anomalies” that pose a drinking-water health risk, without any explanation as to the source of the fluoride. Hergesell (1997) proposed three possible sources of fluoride in Karoo aquifers, namely:

Leaching and concentration of fluorine from rocks and soils during weathering and alteration processes.

Dissolution of secondary hydrothermal–pneumatolytic fluoride-rich minerals.
Circulation and regional-flow of a deeper-seated (thermal) groundwater.

Since fluorine is the most abundant halogen in sedimentary rocks it has to be considered as a major source of fluoride in groundwater. This does not, however, account for the marked fluoride variability on a local scale in “shallow” aquifers (upper 150 m.bgl), where the host-rocks are similar (**Figure 3.39**). This suggests that fluoride concentrations are not only controlled by the near-surface lithology (CSIR Technical Report 392, 1980 and Kent, 1949).

Table 3.11: Fluoride content of groundwater at specific localities in the Karoo Basin (Hergesell, 1997)

Location	% of boreholes with groundwater in excess of 1.5 mg/l fluoride (number of samples)	Maximum F content (mg/l)	Reference
Shannon	-	4.5	Bond (1946)
Dewetsdorp	-	4.8	
Nelspoort	28 (99)	7.5	Leskiewicz (1979)
Beaufort West – Salt River	47 (39)	2.9	BRGM (1978)
Venterstad	39 (26)	7.6	CSIR (1980)
Vanwyksvlei	39 (39)	10.1	Seward (1982)
Graaff-Reinet	19 (101)	6.7	Parsons (1986)
De Aar	33 (18)	3.8	Woodford (1989)
Loxton	28 (182)	4.2	DWAF National Groundwater Database

During recent drilling in the Loxton area, where elevated fluoride values are known to occur, typical hydrothermal F-bearing fracture mineralisation was commonly encountered - apophyllite in association with calcite (Woodford and Chevallier, unpublished data). Fluorine-bearing hydrothermal-pneumatolytic mineralisation was commonly reported in breccia-plugs in the Western Karoo (Woodford and Chevallier, in prep.), which are known for their anomalously high fluoride-bearing groundwater (**Chapter 2.3.2.2**). Drill core from the Calvinia breccia plugs showed fracture mineralisation of quartz, calcite, *fluorite*, *apophyllite*, *tourmaline*, gypsum, chlorite, siderite, baryte, pyrite, pyrrhotite, chalcopyrite, galena, marcasite, bornite and covellite (Hallbauer et al., 1995). Groundwater samples from these breccia-plugs showed fluoride concentrations of up to 12 mg/l. It is postulated that fluorine-bearing minerals were precipitated in certain fractures systems in the Karoo Basin by hydrothermal-pneumatolytic fluids during and after the emplacement of the dolerite and kimerlite intrusives.

The existence of deep-seated groundwater in the southern Karoo was demonstrated by two SOEKOR boreholes that struck thermal-artesian water (**Table 3.12**). The water was highly saline and considered to be partly connate and of marine origin – having entered the rocks during an extensive marine transgression during early Dwyka times (Upper Carboniferous) (Kent, 1969).

Table 3.12: Deep-artesian boreholes of the Southern Karoo (after Kent, 1969)

Name (Date Drilled)	Depth of water- strike (m.bgl)	Artesian Rate of Flow (l/s)	Temperature °C at the surface	Total Dissolved Solids (mg/l)	pH	Lithology
KL1/165 (1966)	1006	0.3	n.d	1390	8.9	Ecca Shale Table Mountain Sandstone
	2347+3184	1.2	76.7	10010	7.5	
SAI 66 (1966)	2975	3.7	65.5	6460	8.0	Dwyka
	3029	1.2	43.3	n.d	n.d	Tillite
	3206	3.0	46.1	n.d	n.d	“ “

Studies by Kent et al (1966) revealed that warmer, and thus deeper circulating groundwater contains more fluoride (up to 5 mg/l) than nearby ‘cold-water’ springs and shallow aquifers (0.2 mg/l). Evidence pointing to thermal deep-seated water as a source for anomalous high fluoride values in groundwater of the Karoo are:

- Many of the thermal springs which rise along dolerite dykes and faults in the Beaufort and Ecca Group contain more than 1.5 mg/l of fluoride (Table 3.13).

Table 3.13: Fluoride content of thermal springs in the Karoo Basin

Locality	Fluoride (mg/l)	Total dissolved solids (mg/l)	Temperature (°C)
Fort Beaufort	13.2	520	27.0 – 29.0
Florisbad	6.0	2189	28.3
Stinkfontein	6.0	806	28.7
Cradock	5.8	181	29.0 – 31.3
Badsfontein	5.3	412	27.1
Aliwal North	4.8	1214	36.9
Roodewal	2.3	224	30.2

- The fluoride distribution of the area southeast of Beaufort West (32.0 – 33.0°S, 22.0 – 26.0°E) is displayed in **Figure 3.41**, as perspective topographic view. The fluoride values range from 0 to 10.4 mg/l. The highest fluoride values are observed in the Grasrand area between latitude 32.30–32.32°S and longitude 24.43 – 24.45°E, which can be clearly seen as the highest peak in the fluoride distribution plot – central to which occurs the Grasrand thermal spring.

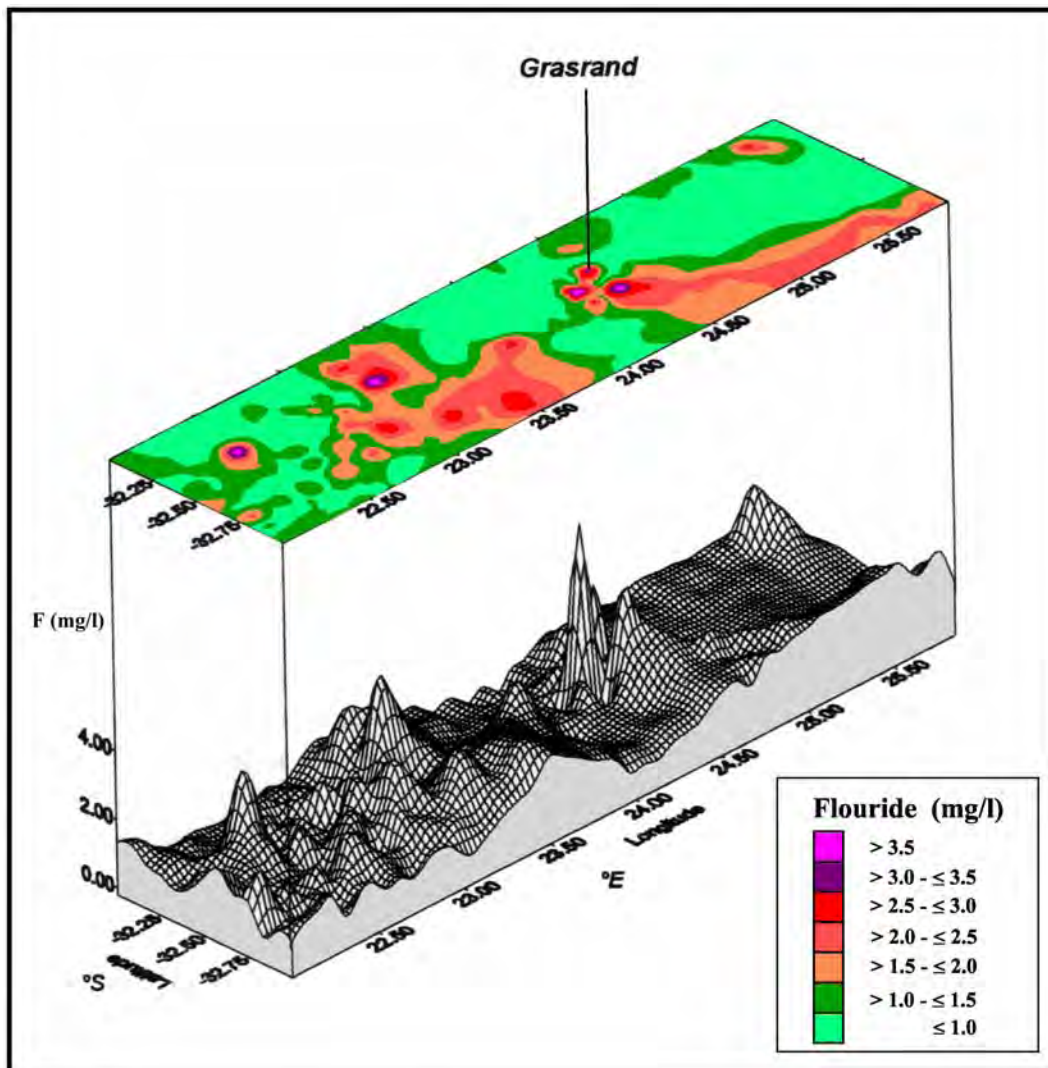


Figure 3.41: *Flouride distribution in the Southern Karoo Basin (after Hergesell, 1997)*

Investigation of the flooding the Orange-Fish River tunnel near Venterstad (**Chapter 2.4.3.4**) indicated that thermal springs are located along the presumed extension of the fissure, including the well-known Badsfontein spring. The CSIR (1977) conducted an isotopic and chemical study of the water from 27 boreholes and springs within a 120 km radius of Venterstad. Three genetically unrelated water types of different origin were defined:

- I. Recently recharged (<20 years old), shallow Ca-Mg-HCO₃ water of local origin.
- II. Older Na-Cl-HCO₃ water, and

III. Old Na-Cl water.

The waters of types II and III are characterised by low ^{14}C , tritium and oxygen values, and high fluoride concentrations. All the type I and II water samples exceed 1.5 mg/ℓ of fluoride, ranging from 1.9 to 7.6 mg/ℓ – while only one water of type-I exceeded 1.5 mg/ℓ. The radiocarbon ages estimates varied from 800 to 4 750 years. These waters are often associated with “warm”, high yielding boreholes and springs. Elevated helium gas concentrations were also associated with these waters in association with methane – suggesting the gas is derived from depth.

This evidence points to a relationship between age, origin, temperature and fluoride content of groundwater in certain areas of the Karoo Basin. It therefore seems likely that deep-seated thermal waters may rapidly transport fluoride upwards from greater depths as a constituent of connate or palaeo-meteoric water and/or dissolve fluorine-bearing minerals along its flow-path to the surface along discrete fracture zones due to an increase in solubility with temperature. This water will normally mixed in the near-surface with the recent, shallow, meteoric water of local recharge.

3.3 ENVIRONMENTAL ISOTOPE HYDROLOGY

3.3.1 PRINCIPLES AND APPLICATION TO THE GEOHYDROLOGY OF THE KAROO BASIN

Environmental isotopes have found a firm place amongst the large variety of techniques with which ground water can be studied and resources can be assessed (e.g. IAEA (1983), Fontes (1980), Mazor (1991), Verhagen et al., (1991)). Initially confined largely to academic studies, isotope techniques are now firmly established as practical, even indispensable, tools in groundwater investigations. Although environmental isotope facilities and expertise have been available in South Africa for many years, there was until recently little awareness of the potential of isotope hydrology amongst groundwater practitioners. As a result, relatively little work in isotope hydrology has been performed in the main Karoo basin. The published studies are presented as brief case-study resumes below (**Chapter 3.3.3**). In addition, a few studies from outside the main basin are presented (**Chapter 3.3.4**), in order to highlight the potential of these techniques in Karoo aquifers in general.

Environmental isotope tracers constantly "label" groundwater, principally during recharge from the surface. At any one time, a groundwater body reflects its isotopic history, or the cumulative input of the isotopic tracers. The basic approach in their application is that of the "isotope snapshot"; i.e. the analysis of isotope, chemical and other environmental tracers of groundwater samples from a particular area reflects the origins and mobility of the different groundwater occurrences. These need to be interpreted in terms of other meaningful information, using various concepts and models. Some of these are enumerated briefly below.

Isotope techniques can be employed at various phases of a groundwater investigation. If little else is known on the local geohydrology, the results are efficient in suggesting a conceptual model. In cases where an a priori conceptual model exists, isotope data can set boundary conditions to these concepts. When the isotope data has been interpreted quantitatively in terms of known aquifer parameters, it can be used to calibrate, or at least set limits to conclusions from, numerical groundwater management models.

3.3.2 ENVIRONMENTAL ISOTOPES USED IN HYDROLOGY

The principal environmental isotope species discussed in this chapter are listed in **Table 3.14**. The radioactive isotope ^3H and the non-radioactive or stable isotopes ^{18}O and ^2H label the water molecule itself. The radioactive isotope ^{14}C and stable isotope ^{13}C label the total dissolved inorganic carbon (TDIC). Other isotopes label other dissolved compounds such as the stable species ^{15}N in dissolved nitrate. Dissolved gases act as environmental tracers of ground water, and some will be discussed below.

3.3.2.1 Definitions

Radioactivity

The process through which unstable atoms (nuclides) spontaneously emit one or more particles or quanta to reach stability. This process is random, the emission rate being proportional to the number of radioactive atoms:

$$dN/dt = -\lambda N$$

where N is the number of radioactive atoms,
 t is the time, and
 λ is the decay constant or probability.

Integrated over a time period t , this equation becomes:

$$N = N_0 e^{-\lambda t} \quad \text{Eq. 3.5}$$

where N_0 is the number of radioactive atoms at time $t = 0$.
 When $N/N_0 = 1/2$, the time elapsed is called the half-life $t_{1/2}$

Table 3.14: *Summary of isotopes commonly used in hydrological studies*

Element	Isotope	Average abundance	Comments
Hydrogen	^1H	0.9984	Radioactive; $t_{1/2} = 12.43$ a
	^2H	0.0015	
	^3H	$10^{-17} - 10^{-19}$	
Carbon	^{12}C	0.9989	Radioactive; $t_{1/2} = 5730$ a
	^{13}C	0.0111	
	^{14}C	10^{-12}	
Oxygen	^{16}O	0.9976	
	^{18}O	0.0020	
Nitrogen	^{14}N	0.9934	
	^{15}N	0.0037	
Radon	^{222}Rn		Radioactive; $t_{1/2} = 3.82$ a

The half life and decay constant are related by:

$$t_{1/2} = 0.693 / \lambda \quad \text{Eq. 3.6}$$

Equation 3.6 governs the concept of radioactive dating. When the initial and final concentration of radioactive atoms is known, the time t since the initial condition can be determined. Groundwater cannot strictly be "dated", as a fluid undergoes processes such as mixing, hydrodynamic dispersion and diffusion.

Fractionation

Molecules of a compound have different masses as do the isotopes of the elements making up molecules differ in mass. These mass differences influence factors such as vapour pressure, diffusivity etc. During phase processes, such as evaporation, condensation and exchange reactions the abundance of the isotopes of individual elements change, or undergo fractionation. Such processes are usually operative at the interface of different phases or compounds containing the same elements, such as vapour in contact with a liquid, a liquid in contact with a solid etc. These changes in abundance can be traced through natural and other systems.

The unit fractionation factor (α) is defined as:

$$\alpha = R_A/R_B,$$

where R_A and R_B are the ratios of the abundance of the rare (heavier) isotope to the more abundant (light) isotope in phases A and B respectively, and α is temperature dependent.

As isotopic abundances and changes in these abundances are generally small, it is customary to express these changes as fractional differences δ in per mille with respect to the value of a reference standard

$$\delta = [(R_S/R_R) - 1] \times 1\,000 \text{ (‰)} \quad \text{Eq. 3.7}$$

where the measured ratios for the heavy to the light isotope are R_S for the sample and R_R for the reference standard, respectively.

3.3.2.2 Radioactive Isotopes

Tritium (^3H)

This hydrogen isotope is formed in the upper atmosphere through cosmic ray reactions. Oxidised to $^3\text{H}^1\text{HO}$ it reaches the surface of the earth as part of rainwater, in which it is essentially a conservative tracer. The isotopic ratio $^3\text{H}/^1\text{H}$ established by this natural source in continental environments and is approximately 5×10^{-18} , or 5 TU (tritium units). The half-life of tritium is 12.43 years. When rainwater is isolated from the atmospheric source, i.e. during groundwater recharge, no new tritium is added and the tritium concentration will decrease with this characteristic half-life.

The useful range of measurement of environmental tritium in geohydrological applications spans four to five half-lives. It is therefore measurable only in and can act as an indicator of recently recharged ground water. From the mid 1950s the atmospheric input increased due to nuclear weapons fallout (IAEA 1992: **Figure 3.42**). Since the middle sixties, rainwater tritium levels have declined from the "bomb peak" to reach about pre-bomb levels in non-industrialised areas at present.

Tritium levels in ground water with a mean residence time (MRT) in excess of about 200 years, lie at or below the limit of detectability (routinely 0.2 ± 0.2 TU). At present, a TU value of greater than 1 unequivocally indicates that groundwater body received significant recharge during the thermonuclear era (the past 35 years).

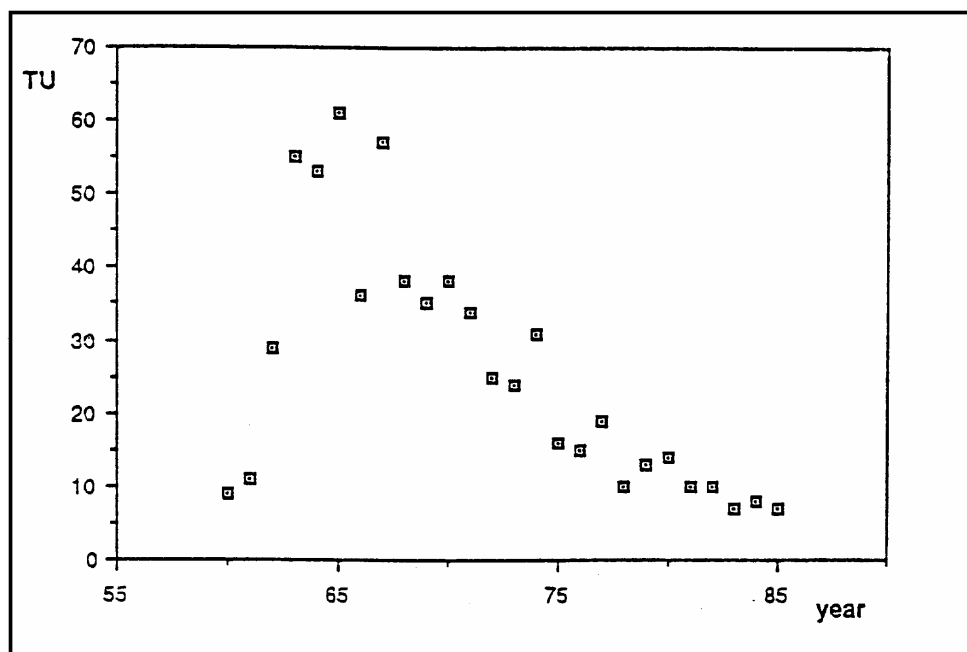


Figure 3.42: Tritium in Southern African rainfall showing the thermonuclear “peak”

Sampling: A 1-litre sample of water is required for determination of low-level tritium. The sample bottle is rinsed with the sample-water, completely filled and tightly stoppered. The water should not be treated in any way before sampling. Samples can be taken by field technical personnel, under guidance from the participating laboratory.

Radiocarbon (^{14}C)

Formed in the upper atmosphere by processes similar to tritium, radiocarbon is oxidised to $^{14}\text{CO}_2$ and becomes part of atmospheric carbon dioxide, in which the natural isotopic ratio $^{14}\text{C}/^{12}\text{C} \sim 10^{-12}$, is called 100 pMC (100% modern carbon). The ^{14}C half-life is 5730 years. As with tritium, thermonuclear tests increased the atmospheric level of radiocarbon to peak in the early 1960s. Plants assimilate atmospheric carbon dioxide through photosynthesis. Humus and roots liberate CO_2 labelled with environmental ^{14}C , which dissolves in infiltrating groundwater, rendering the water chemically aggressive, which leads to the various species of ^{14}C -labelled total dissolved inorganic carbon (TDIC). Thus, radiocarbon (a) becomes a time dependent radioactive tracer of ground water, and (b) allows for the estimation of ground water residence times.

In contrast to tritium, radiocarbon it is not strictly a conservative tracer of water, as numerous chemical processes can alter the $^{14}\text{C}/^{12}\text{C}$ ratio. Attempts have been made by several authors (Verhagen et al., 1991) to develop correction models, based upon hydrochemistry and $\delta^{13}\text{C}$ values. These models all assume that the hydrochemical processes occur principally during the initial development phases of, and therefore affect the initial isotopic ratio established in, the TDIC of ground water (e.g. during recharge). Once the hydrochemistry has been stabilised, the $^{14}\text{C}/^{12}\text{C}$ ratio is taken to effectively alter only through radioactive decay. Vogel (1970) suggested a rule-of-thumb initial (recharge) value of about 85% of atmospheric CO_2 for many aquifers. In principle however, this initial value may be as low as 50% in carbonate aquifers, approach 100% in purely crystalline terrain and has to be assessed for each individual terrain. Subsequent water/rock interactions in the saturated zone of established aquifers are usually regarded as negligible.

In spite of its potentially complex hydrochemistry, radiocarbon is the principal radioactive environmental tracer of deeper-seated groundwater, its useful range of measurement in geohydrological applications spanning five to six half-lives.

During the early sixties, atmospheric ^{14}C concentrations rose due to thermonuclear fallout, and have since declined (**Figure 3.43**). In qualitative terms therefore, ground water radiocarbon values of > 100 pMC can be interpreted as falling in the thermonuclear era, i.e. substantially recharged over the past three and a half decades. Within this time-span, interpretations can be further constrained by tritium data.

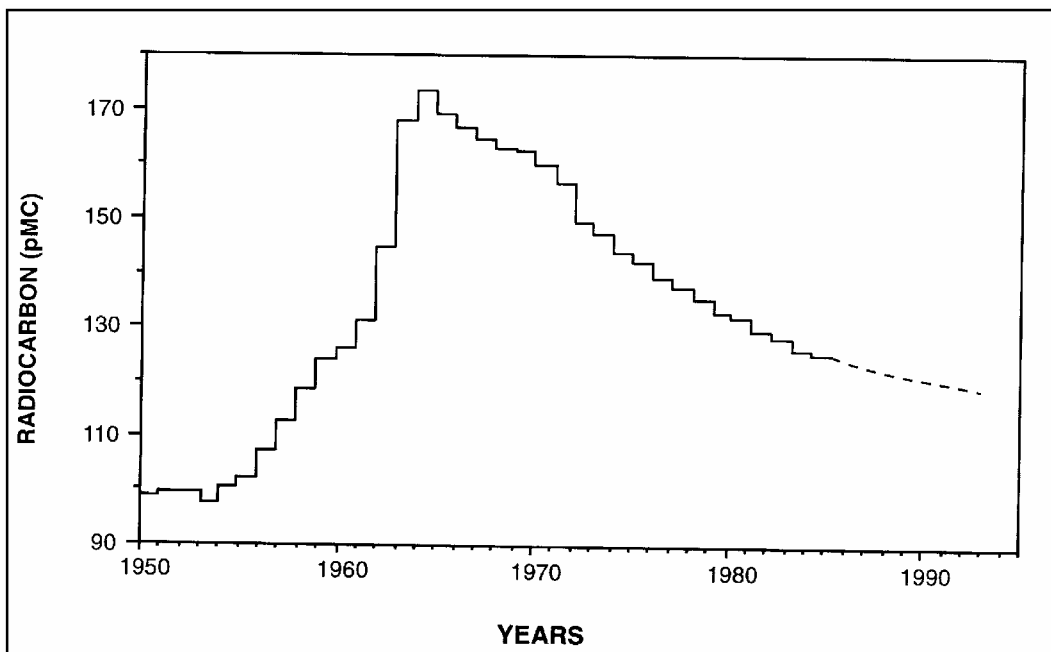


Figure 3.43: Radiocarbon in southern hemisphere atmospheric CO_2 (after Zuber, 1986)

Sampling: About 1-2 g of carbon is needed for measurement. The most common field procedure is to collect and treat about 50 l of water at a TDIC of 200 mg/l in a suitable closed container. The water is rendered alkaline and the carbonate precipitated by e.g. barium or strontium chloride. The supernatant is decanted and the precipitate transferred to a sample bottle for transport to the laboratory. The procedures can be performed by technical field personnel, under guidance from the collaborating laboratory.

Approaches to Interpretation

Radiocarbon and tritium can be employed as:

- (a) Long-lived and short-lived radioactive tracers, respectively, of the infiltrating rainwater. In this way, their isotopic ratio is employed as a qualitative, or semi-quantitative, indicator of actively "turned-over" or dynamic groundwater. As such, they can be used to delineate recharge areas and in tracking hydrochemical processes. The isotopic ratio of radiocarbon defines the concentration in the TDIC. When the ratio is multiplied by the TDIC concentration (usually closely approximated by the alkalinity), a factor is obtained which is proportional to the radiocarbon concentration *in the water*. It then becomes a tracer akin to tritium (Verhagen et al., 1996).
- (b) Through suitable models to interpret groundwater residence times, which can give information on groundwater dynamics and estimates of recharge rates.

Groundwater Flow Models

Models of groundwater movement are required in order to interpret radioactive environmental tracer data in terms of parameters useful for practical geohydrology. Amongst these are the piston-flow, dispersion and exponential models. For a more complete discussion of models see e.g. Zuber (1986) and Verhagen et al. (1991). In these models, it is assumed that at recharge small volume elements or "parcels" of water enter the ground from the surface and then move unaltered through the sub-surface along smooth flow paths (i.e. isotropic, homogeneous aquifer) to a discharge point.

The convolution integral governing the concentration of the tracer $A(t)$ at time t is

$$A(t) = \int_0^{\infty} A_0(t - \tau) e^{-\lambda\tau} f(\tau) d\tau \quad \text{Eq. 3.8}$$

where A_0 is the tracer concentrations at recharge;
 τ the individual parcel transit time;
 $A_0(t - \tau)$ the input function;
 $e^{-\lambda\tau}$ the radioactive decay function; and
 $f(\tau)$ the transit time function or "model" of the movement of ground water through the aquifer.

There are two extreme idealised groundwater regimes.

- (a) A confined, flowing system, in which water moves from a defined recharge area and is then isolated from further contact with the surface (**Figure 3.44**). At the point of extraction (borehole) all flow lines are of equal length and all parcels will have travelled for the same time τ . This is known as the *piston flow model*. Here, the transit time function = 1, and for a constant tracer input concentration, the ground water residence time is (cf. **Eq. 3.5**):

$$A(t) = A_0 e^{-\lambda\tau}$$

which is the equivalent of "dating" the groundwater.

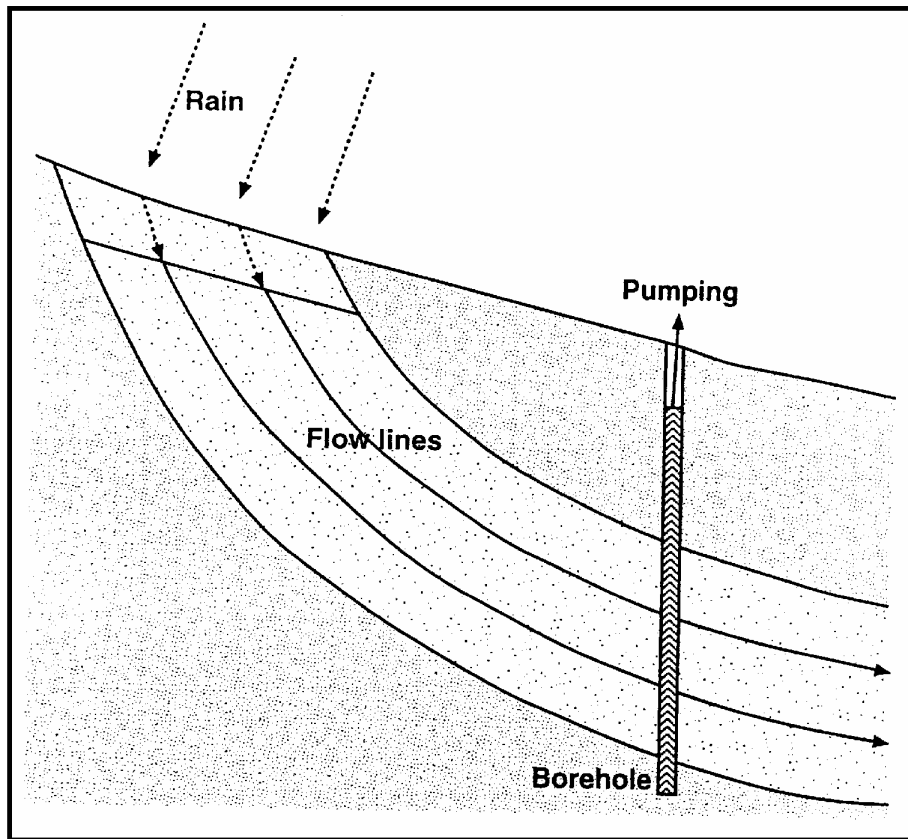


Figure 3.44: *Idealised flow-lines for a confined aquifer receiving recharge only in the outcrop area*

- (b) An isotropic, phreatic aquifer, receiving uniform diffuse recharge (**Figure 3.45**). At the point of extraction, the deeper flow lines have a longer transit time than the shallower ones. The water pumped from the borehole will contain a well-mixed sample of components of different transit times or ages. Therefore a mean residence time (MRT) T is introduced. The transit time function is here taken to be:

$$f(\tau) = \frac{e^{-\tau/T}}{T}$$

known as the exponential model.

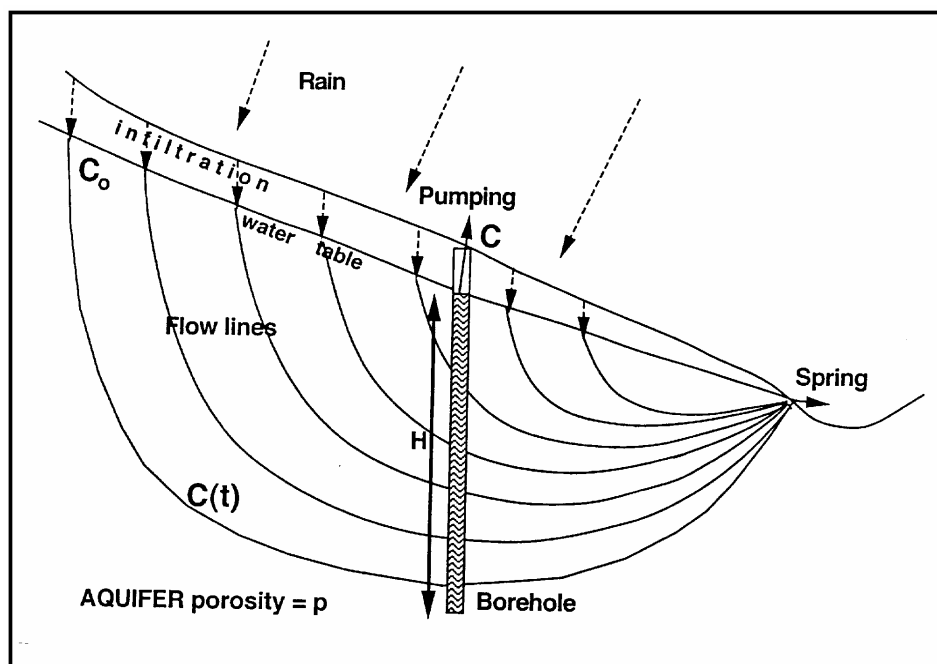


Figure 3.45: *Idealised flow-lines for an isotropic, unconfined, phreatic aquifer receiving uniform diffuse recharge*

These are "lumped-parameter" or "black-box" models, in which spatial variations are ignored (they are usually not, or only poorly, known) and the various properties are considered homogenous throughout the system .

Both ^{14}C and ^3H input concentrations underwent considerable changes over the past 40 years and therefore are functions of time or $A_0(t - \tau)$. These values are input into the convolution integral. The integral is then evaluated for increasing mean residence times T from the present (time of observation) for each isotope, using the exponential transit time function. Typical results for Southern Africa are shown in **Figures 3.46** and **3.47**. These curves can now be used to estimate MRT values for either the observed ^3H or ^{14}C concentrations. With the bomb peak still measurable in the environment, ambiguous MRT values in the range 10 - 60 years are produced at values > 2 TU and > 100 pMC. This can often be overcome by considering both ^3H and ^{14}C in evaluating the most likely value of MRT, as well as the geohydrological conditions. **Figure 3.48** shows a plot of ^{14}C against ^3H for different MRT values calculated by the exponential-mixing model. When observed values plot on or close to this line, it implies that conditions conform reasonably to the assumption of an isotropic, diffusely recharged, aquifer.

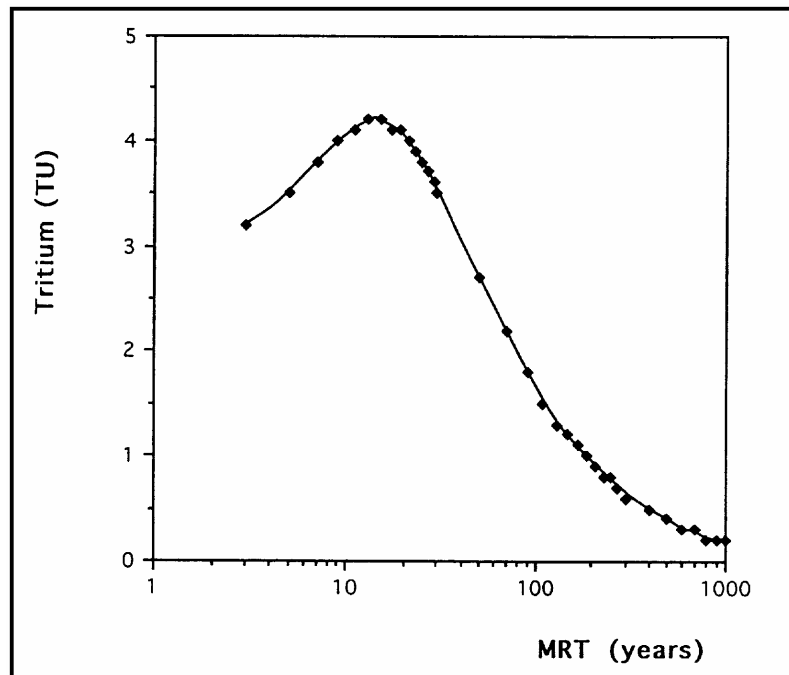


Figure 3.46: *Expected tritium values calculated with the exponential model for an idealised Southern African phreatic aquifer as a function of a mean residence time (MRT) for 1998. Note ambiguous MRT values for tritium > 2 TU*

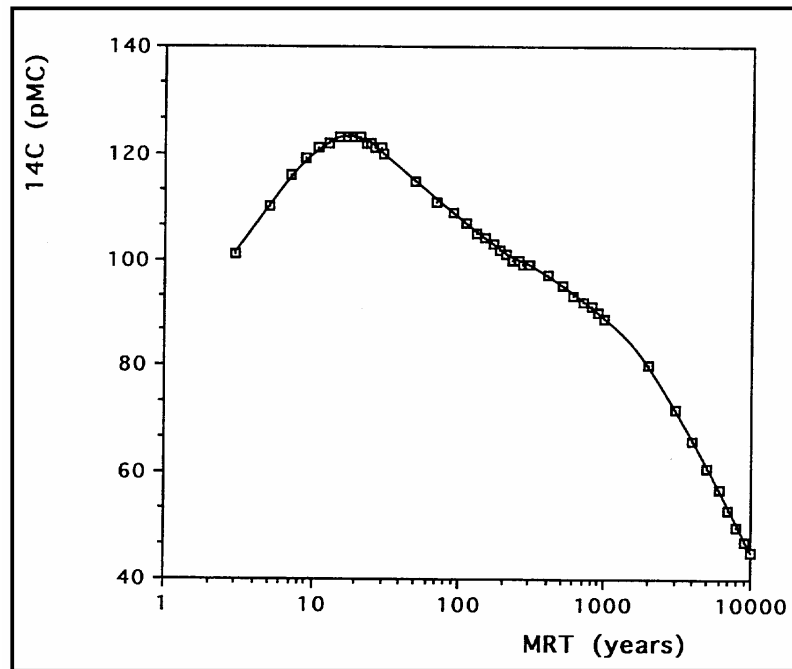


Figure 3.47: Radiocarbon values expected at present calculated with the exponential model for an idealised Southern African phreatic aquifer as a function of the mean residence time (MRT) for 1998 and 100 % atmospheric. Note ambiguous MRT values for radiocarbon > 100 pMC

In addition, CFC (chlorofluorocarbon) measurements potentially can assist to remove ambiguity in this MRT range, as the atmospheric concentration of these dissolved gas tracers have not undergone a transient, but are monotonously increasing or are levelling off.

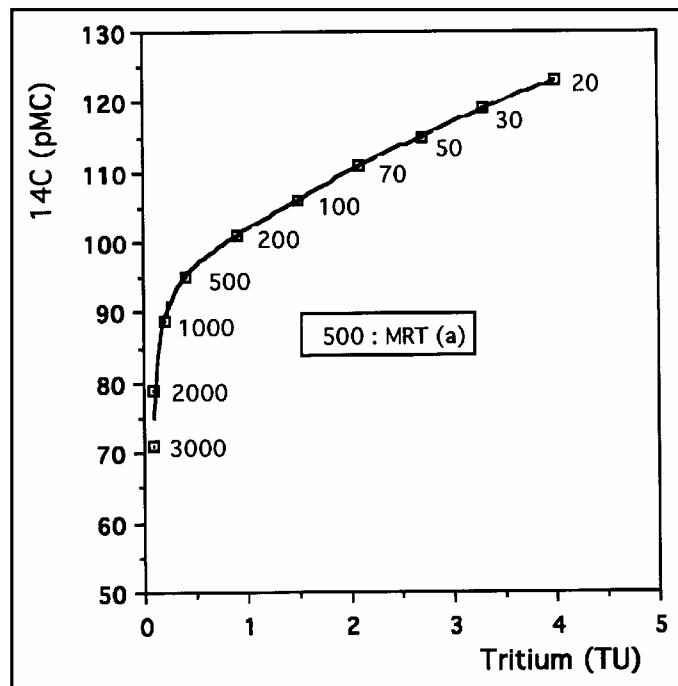


Figure 3.48: Radiocarbon values plotted against tritium values calculated with the exponential model for different MRTs. The line forms the locus of values expected for an idealised phreatic aquifer in 1998

Estimating Recharge

The recharge rate (R) can be estimated from the mean residence time by assuming that a pumped borehole produces a well-mixed sample of all the water flowing into it:

$$R = \frac{\sum_i H_i \cdot p_i}{T} \quad \text{Eq. 3.9}$$

where H_i is the thickness of individual saturated aquifer zones intersected by the borehole, and p_i their porosity.

For radiocarbon values less than 80 pMC and tritium at less than 0.5 TU it can be assumed to a good approximation that there is no bomb-produced input. A_0 is therefore essentially constant and

$$R = \frac{\sum_i p_i H_i}{8270[(A_0/A) - 1]} \quad \text{Eq. 3.10}$$

Aquifer porosity is a critical parameter in these calculations. Values may be measured directly from drill cores. In many cases, such information is not available. At best the porosity can then be estimated. This implies at least a good knowledge of the borehole log and the nature of the local rock formations. In addition, borehole depth and rest-waterlevel should be known.

Note:

- Given enough time, an environmental tracer will “label” by advection and diffusion all the water held within interconnected aquifer openings, in a manner similar to other chemical species.
- Porosity is the relevant parameter for all aquifer types. Storativity is a hydraulic parameter sometimes orders of magnitude lower than the porosity.
- Effective porosity may be assessed using artificial tracers. This factor is time-scale dependent and relevant to short-lived tracer or transient responses. The time scales assessed with environmental tritium and even more so radiocarbon are such that they effectively label the entire water body (Bredenkamp et al., 1998).
- In one of the case studies presented below (**Chapter 3.3.3**), reasonable correspondence has been achieved between recharge assessment using the above approach and other independent methods. Although most aquifers deviate substantially from the idealised phreatic case, the exponential mixing concept gives a fair approximation.

3.3.2.3 Non-Radioactive or Stable Isotopes

Oxygen-18 and Deuterium

Oxygen-18 (^{18}O) and deuterium (^2H) are present in water in isotopic abundances (or ratios, R) of about $^{18}\text{O}/^{16}\text{O} = 0.20\%$ and $^2\text{H}/^1\text{H} = 0.015\%$. In various combinations, these isotopes make up water molecules, principally of masses 18, 19 and 20. In phase processes such as evaporation and condensation, the different vapour pressures of these molecules produce isotope fractionation, the heavier isotopes tending to concentrate in the denser phase. These small changes can be expressed as a fractional deviation δ from a standard called SMOW (standard mean ocean water).

Values of δ can be diagnostic of water from different origins. Water vapour rising from the ocean is depleted in the heavy isotopes. Vapour masses moving inland are subject to equilibrium (or Rayleigh) isotopic exchange processes, the depletion of the heavy isotopes continuing on the vapour trajectories inland due to rainout. Consequently, the stable isotopic content of meteoric water lies on a regression line

$$\delta^2\text{H} = s \delta^{18}\text{O} + d \quad \text{Eq. 3.11}$$

where s is the slope, and d the intercept d on the $\delta^2\text{H}$ axis the deuterium excess.

The line with $s = 8$ and $d = +10$ is called the world meteoric water line (WMWL; **Figure 3.49**). The position of any pair of $\delta^2\text{H}$ and $\delta^{18}\text{O}$ values on this line for rainwater worldwide will depend on local climatological conditions (temperature, latitude, altitude, rainfall effects).

Surface water bodies, such as dams, lakes and pans will develop an enrichment in their heavy isotope content when undergoing significant kinetic (non-equilibrium) evaporation. Light isotopes are preferentially transferred to the vapour phase. The surficial layer of the water body is thus enriched in the heavy isotopes and is then readily mixed into the bulk of the water body through convective processes. This evolutionary enrichment produces $\delta^2\text{H}$ and $\delta^{18}\text{O}$ values which lie to the right of the meteoric water line, and plot on an evaporation line of lesser slope (s of usually 4 - 5) and lower d than the WMWL (**Figure 3.49**). Groundwater derived through infiltration from such water bodies will carry this distinctive evaporative isotopic signal.

Evapotranspiration losses from soil and groundwater system generally occur under isotopic equilibrium, i.e. without fractionation. In semi-arid environments such as the Karoo, isotopic values of groundwater derived directly from rain will therefore lie on or close to, the WMWL. They will tend however to be displaced to δ -values more negative (or "lighter") than the weighted mean in rain, due to the process of rainfall selectivity (Vogel and Van Urk 1975; Verhagen, 1984). Major rainfall events, which produce isotopically lighter precipitation, with more negative δ -values, may contribute proportionately more to recharge. Different processes of rainfall recharge (viz. diffuse, channelled, bank infiltration) can be distinguished by different stable isotope ranges on the WMWL.

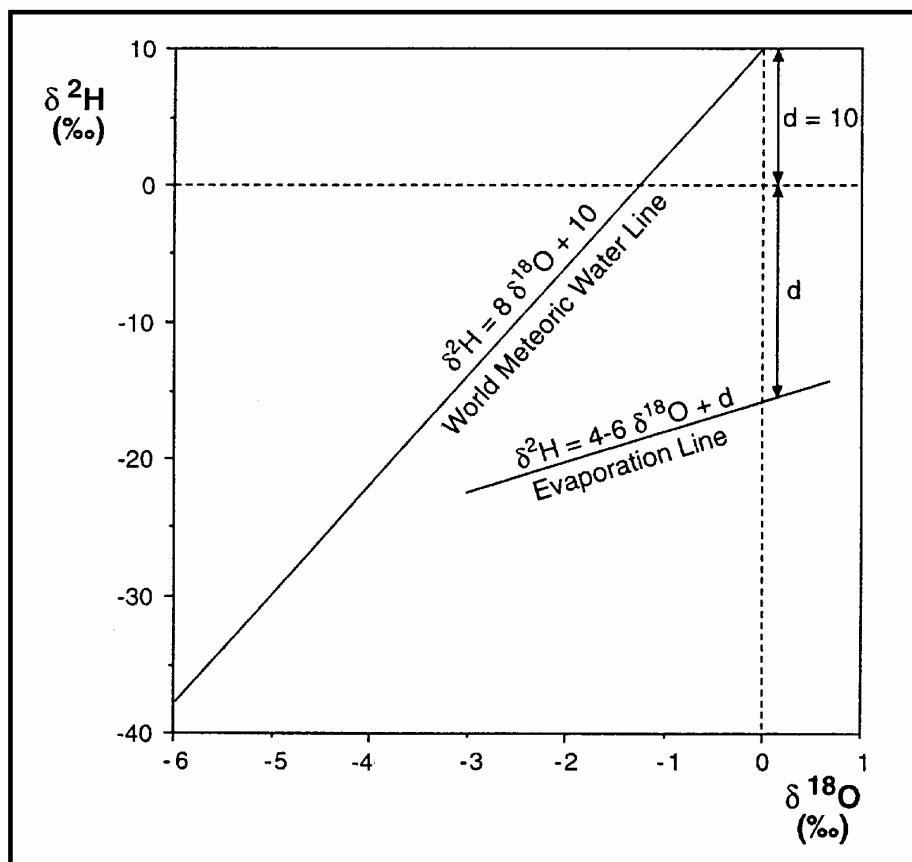


Figure 3.49: $\delta^2\text{H}$ vs $\delta^{18}\text{O}$ plot, showing the world meteoric water line (WMWL) and a typical evaporation line

Sampling: A 20 ml sample suffices for the measurement both of $\delta^2\text{H}$ and $\delta^{18}\text{O}$. The bottle should be rinsed with the untreated sample water, completely filled and securely stoppered, preventing any leaks. Sampling can be performed by technical field personnel, under guidance from the collaborating laboratory.

Carbon-13

The isotopic abundance $^{13}\text{C}/^{12}\text{C}$ of atmospheric carbon dioxide, when expressed as in **Equation 3.2**, is about $\delta^{13}\text{C} = -7$ ‰ with respect to a marine limestone isotopic standard PDB (PeeDee belemnite). During photosynthesis, this abundance is modified through biological isotope fractionation, which establishes organic values of about $\delta^{13}\text{C} = -25$ ‰ in C3 plants (e.g. trees) and -12 ‰ in C4 plants (e.g. grasses). The soil CO_2 produced by such plants will have similar isotopic ratios. These ratios can be modified through isotopic exchange and dilution processes, such as the dissolution of soil or rock carbonate of differing carbon isotopic abundance, resulting in isotopic ratios in the different TDIC species in groundwater, governed by appropriate

fractionation factors. The $\delta^{13}\text{C}$ is therefore diagnostic of some of the chemical processes which groundwater has undergone, and can give information of the provenance of the TDIC, and thus of the water itself. It is also useful in assessing the $^{14}\text{C}/^{12}\text{C}$ ratio, as this is likewise modified by such processes, and forms the basis of ^{14}C correction models (**Chapter 3.3.2.2**).

Sampling: For hydrological purposes, $\delta^{13}\text{C}$ usually is measured on the same precipitate sample taken for radiocarbon, and requires no separate sampling.

Nitrogen-15

The study of nitrogen isotopes provides a method of monitoring the migration of nitrogenous compounds in groundwater. As nitrogen compounds are altered chemically within a system, the stable isotopes ^{14}N and ^{15}N may undergo isotopic fractionation. If such fractionation is unique, then nitrogen isotopes can be used to determine major sources of nitrate.

The isotope ratio $^{15}\text{N}/^{14}\text{N}$ in the atmosphere is 0.3663 %. Small deviations from this value as standard are given as $\delta^{15}\text{N}$ ‰, as defined in equation 2. $\delta^{15}\text{N}$ values in terrestrial nitrogen compounds generally fall in the range -15‰ to +20‰ (Hübner, 1986)

As with the isotopes of hydrogen and oxygen, fractionation occurs through either equilibrium (reversible) or kinetic (unidirectional) reactions. The equilibrium processes occur mainly in the atmosphere. More important in the hydrosphere are kinetic reactions, facilitated by bacteria, producing dissolved nitrate with depleted values of $\delta^{15}\text{N}$. Nitrogen isotope variations in groundwater therefore allow at best semi-quantitative interpretation (Heaton, 1986).

Typical values of $\delta^{15}\text{N}$ in nitrate derived from different sources are given in **Figure 3.50**. A considerable range is covered by each of the main source categories, which sometimes overlap. For most practical purposes, the only source which can potentially be clearly distinguished in groundwater nitrate is animal and human waste. Walton et al., (1993) could assign nitrate occurrences in groundwater pumped from numerous boreholes to respectively agricultural lands and sewage disposal in Northern Province villages. Extreme positive values of $\delta^{15}\text{N}$ were found accompanying high nitrate and coliform bacteria. Heaton (1986) was able to show a marked positive correlation between bacterial content and $\delta^{15}\text{N}$ in four boreholes near Pretoria.

Very positive values of $\delta^{15}\text{N}$ in groundwater nitrate may also result from denitrification through anaerobic bacterial reactions, which proceed under anoxic conditions in the aquifer. One is reasonably assured that the original (recharge) $\delta^{15}\text{N}$ values are being conserved only if oxic conditions can be shown to prevail throughout the system being studied.

As yet, no applications of nitrogen isotopes in the main Karoo basin have been reported. However, the usefulness of this method is likely to increase as urban and agricultural activities develop in the region.

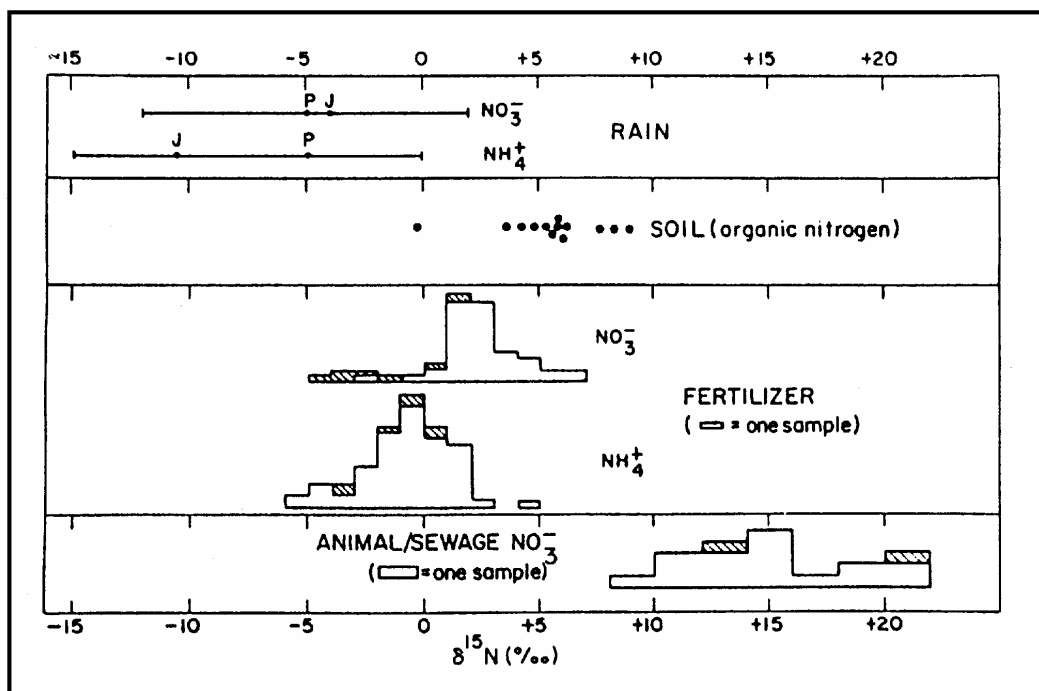


Figure 3.50: Values of $\delta^{15}\text{N}$ for different dissolved nitrogenous species derived from different sources (Heaton 1986)

Sampling: A sample of about 1 ℓ of water is required, depending on NO_3^- concentration. The water should be filtered and HgCl_2 added in order to arrest any biological activity in the sample. These procedures can be performed by technical field personnel, under guidance from the collaborating laboratory.

3.3.2.4 Dissolved Gases

Gases dissolved in rainwater during the process of infiltration can be used as tracers of groundwater and reflect conditions at the time of infiltration (Vogel et al., 1980 (a),(b); Mazor and Verhagen, 1983). The concentration of gases in water is dependent on their atmospheric gas partial pressure and solubility, which is temperature dependent, at equilibration before the water is removed from effective atmospheric contact. If there is reasonable assurance that the water has been held under closed-system conditions, the relative concentrations of gases such as N₂ and the noble gases He, Ne, Ar, Kr, Xe give information about the conditions at infiltration, such as temperature.

Radon-222 is a daughter product in the radioactive decay chain of uranium. It is short lived ($t_{1/2} = 3.82$ days) and emits high-energy α rays. It therefore has a high specific activity. Being a noble gas, it is very mobile and can easily diffuse from the aquifer rock, which contains the parent uranium, into the groundwater (Andrews, 1972). Aquifer porosity is a critical parameter in this diffusive process and faults and fractures conduct radon rapidly. ²²²Rn in groundwater therefore reflects aquifer conditions and can be a sensitive indicator of deep-seated highly conductive zones.

Of particular interest are chlorofluorocarbons (CFCs). These gases have been released into the atmosphere since the 1950s, their concentrations steadily increasing, with new compounds being added over the past few decades (**Figure 3.51**). When carefully sampled and measured, the concentrations of the different CFCs give a measure of the time since infiltration of groundwater (Busenberg and Plummer 1992). The water can therefore be "dated" in principle over a span of some 4 decades, a very useful range covered also by thermonuclear tritium. The latter exhibits a peak in its input concentration, rendering its interpretation terms of short residence times ambiguous. Measurements of radiocarbon values can assist in removing this ambiguity. A similar function may be fulfilled by CFCs in that the concentrations in the atmosphere have been steadily rising, or levelling off.

As the source of the dissolved CFCs is the atmosphere itself, extreme care has to be exercised in obtaining samples. Contact with the atmosphere has to be rigorously avoided, requiring elaborate equipment to obtain sealed samples. Rigorous conditions also have to apply to extracting water from a borehole, avoiding any atmospheric contact. Several parallel samples have to be collected and the lowest of the results usually taken as the most reliable. Busenberg and Plummer (1992) recommend simultaneous tritium measurements in order to assess the degree of atmospheric contamination.

Sampling

Special procedures are required in sampling for dissolved gases and in particular for CFCs where extreme care has to be taken in avoiding atmospheric contact, both in extracting water from the borehole and in producing the sealed samples. These field operations require special equipment and are usually performed by the personnel of the collaborating laboratory.

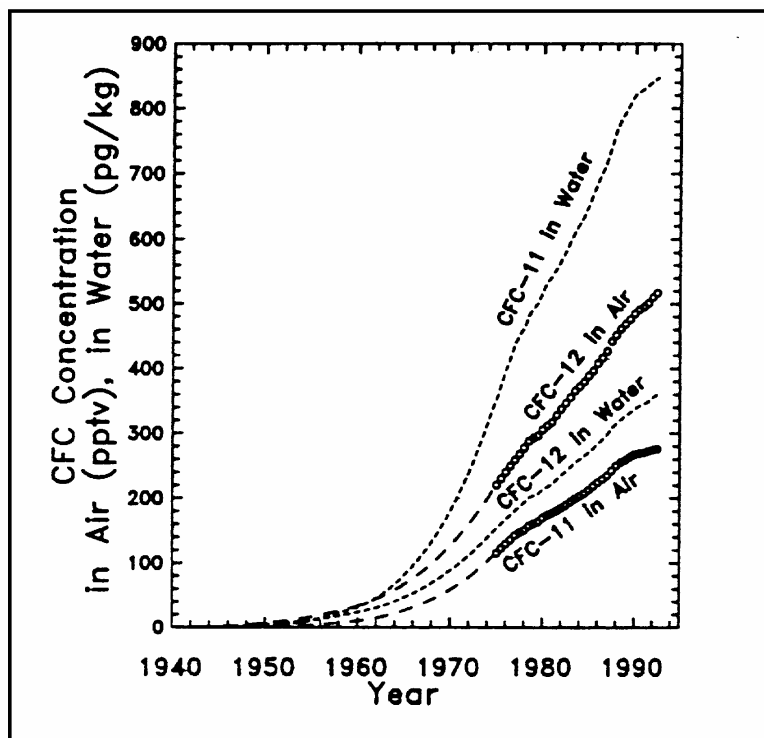


Figure 3.51: Atmospheric concentrations of a number of different chlorofluorocarbons (CFCs) as a function of time (Dunkle et al., 1993)

3.3.2.5 Unsaturated or Vadose Zone

The most important recharge mechanism to groundwater is by diffuse infiltration of rainwater through the vadose. Piston-like or plug intergranular-flow of moisture is usually assumed, modified by various processes of dispersion. To study this flow requires ideally a thick (tens of metres) and reasonably uniform sand/soil cover, from which samples can be taken at various depths. The column of moisture at any one moment contains components of various rainfall events with variable isotopic characteristics (oxygen-18 and deuterium) over a period of time, which may be employed to assess the transport of water towards the water table. Evaporative

moisture losses from just below the ground surface may be reflected in the enrichment of the stable isotopes near the top of the profile.

The depth of penetration of the tritium thermonuclear bomb peak of tritium gives a measure of the amount of water retained in the zone since the mid-sixties. Another approach is comparing the total amount of tritium in the profile containing the peak with the total amount of tritium in the rainfall over the same period. The latter method is akin to the chloride balance method. Although in principle much simpler than the tritium method, the chloride method suffers from the difficulty of estimating adequately the input concentration (Beekman et al., 1996), a factor much better known and widely monitored for tritium.

Although tritium concentrations in present-day rainfall have returned to near-natural values and the bomb tritium peak has been flushed out of all but very thick (tens of metres) vadose zones, bomb tritium can still be identified in certain instances. Thus Beekman et al. (1996) concluded from a recent study of Kalahari sand profiles that by-pass flow through root-holes, and animal and insect burrows, probably constitutes the bulk of the downward transport of moisture, rather than intergranular flow. The study highlighted the limitations, and local nature, of the conclusions drawn from such profiles.

As soils are generally poorly developed in the Karoo, it is therefore clear that the use of isotopic tracers in vadose zone investigations holds out little potential in assessing recharge in this environment.

3.3.3 ISOTOPE STUDIES OF GROUNDWATER IN THE MAIN KAROO BASIN

3.3.3.1 Irrigation Return Flow in the Fish River Valley, Eastern Cape Province

A pilot study was conducted of groundwater and riverwater in the Cradock area during 1978 in order to assess:

the applicability of environmental isotope techniques to the problem of salinisation of groundwater, and of the Fish River through irrigation return flow, and whether turnover times would be sufficiently short for the origins of irrigation return flow to be established by using artificial groundwater tracers.

A series of samples were analysed for tritium in order to assess relative ground water residence times (Verhagen and Smith, 1978). In a few cases, carbon-14 samples were taken to refine the interpreted MRT values. In particular, the question to be addressed was the influence of H₂S smelling water on the seepage into the river.

It could be established that the older water in the area, such as the "kruitwater" encountered in the Cradock hot-spring, had the lowest mineralisation. On various farms in the Fish River valley, very recent (MRT a few decades) groundwater is encountered with a high mineralisation. On the farm Sarnia, boreholes tap "kruitwaters", which show MRT values of a few hundred years. Nearby seepage into the river, show chloride and conductivity values some 10x that of the local groundwater, with mean residence time of about a decade. It is therefore clear that the seepage water and its concomitant mineralisation constitutes a system effectively separate from that of the local groundwater system. The generally argillaceous condition of soils and underlying rock formations tends to isolate the different sub-surface water regime. It is concluded that the shallow drainage system is principally responsible for the mineralisation of the river and would be amenable to detailed artificial tracer investigations.

3.3.3.2 Phillipolis Study, Southern Free State

During 1976, a study was undertaken of the hydrochemistry and isotopic composition of Karoo formations in the Phillipolis area of the southern Free State (Hodgson et al., 1977). The aquifer system is comprised of shale with interbedded lenses of sandstone and dolerite intrusions. The ionic ratios of the various water samples lie in a range between end members; (1) Ca,Mg,Na-HCO₃, SO₄, Cl type and (2) Na,Ca,Mg-HCO₃, Cl,SO₄ type. The total mineralisation of the samples varies widely within each of the two generalised hydrochemical facies. The results of radiocarbon and tritium analyses showed a considerable range of between 50 to 133 pMC and 1.1 to 12.1 TU, respectively. At present, this variability of isotope values would be reduced due to radioactive decay and atmospheric washout.

As was to be expected, the two isotopes were positively correlated, suggesting MRT values ranging from a few decades to some several thousands of years. The relationship however is almost linear, rather than would have been expected from the exponential model (**Figure 3.52**) for an isotropic phreatic aquifer. In particular, the tritium values accompanying radiocarbon values below 80 pMC are considerably higher than predicted by the model. This suggests mixing of groundwater with differing MRT, rather than a single, continuous, phreatic groundwater body. The most recent ground water has the highest mineralisation, whilst the hydrochemical types 1 and 2 clearly belong to the lowest and highest MRT values, respectively.

Within the constraints of a limited number of samples, a clear evolution from Ca,Mg dominance to Na dominance was observed, which may be time related and/or controlled by the aquifer material. The study did not inquire about the detailed hydrogeological relationships giving rise to the particular hydrochemical and isotopic groupings. What is clear, however, is that the isotopic parameter opens a completely new approach to our understanding of the chemical evolution of ground water in the

Karoo, as it has done in other environments, and provides a rich field of applications and further research.

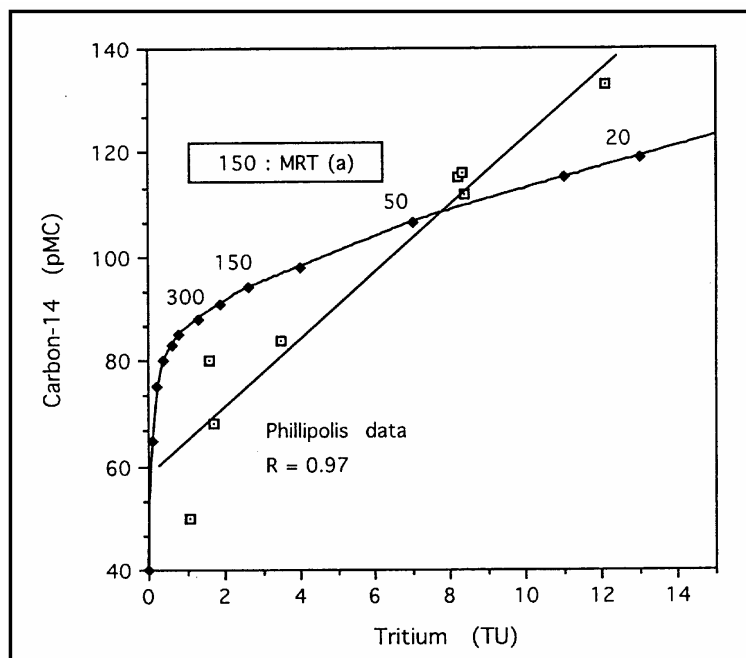


Figure 3.52: *Plot of radiocarbon vs. tritium for ground water in the Phillipolis area showing a near-linear relationship. Also shown is the expected relationship (cf. Figure 3.47) calculated with the exponential model for the time of sampling (1977)*

3.3.3.3 De Aar – Dewetsdorp Study

In cooperation with the Schonland Research Centre, University of the Witwatersrand, the Institute for Groundwater Studies, University of the Free State undertook an isotope study of groundwater and rainwater in the framework of a Water Research Commission project entitled: Exploitation potential of Karoo aquifers (Kirchner et al., 1991). The areas studied during 1985/86 were Dewetsdorp in the Orange Free State and De Aar in the Northern Cape Province. Sequential samples were obtained from different rainstorms with a device specially developed for the purpose. The $\delta^2\text{H}$ and $\delta^{18}\text{O}$ plotted as a function of time in **Figure 3.53**, show more negative values as the storms progress. This is the well-known "rain-out effect" and demonstrates how sensitive isotopic values can be to modes and rates of recharge.

Rainfall and groundwater $\delta^2\text{H}$ and $\delta^{18}\text{O}$ values are plotted in **Figure 3.54**. Rainfall values for both De Aar and Dewetsdorp fall between the WMWL and the regression line $\delta^2\text{H} = 8 \delta^{18}\text{O} + 20$ and cover wide and overlapping ranges. Dewetsdorp groundwater is more closely grouped and plots on the WMWL. Groundwater from De Aar trends towards the right of the WMWL and shows evidence of considerable evaporation before infiltration. This data therefore contain information on the contrast in physiography and drainage between the two locations.

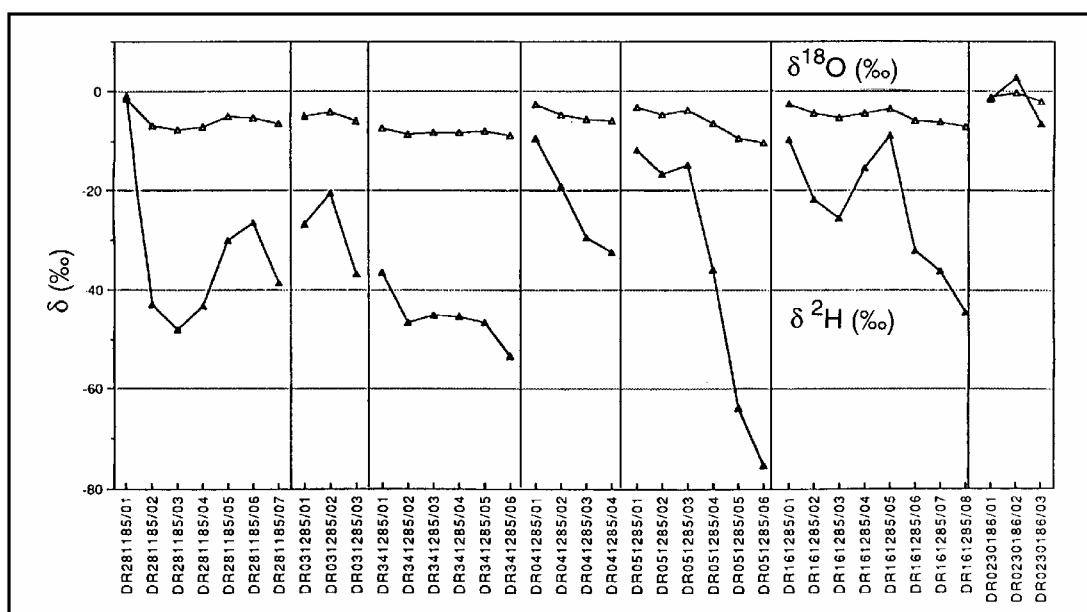


Figure 3.53: $\delta^2\text{H}$ and $\delta^{18}\text{O}$ values as a function of time for a number of rainfall events at Dewetsdorp (Kirchner et al., 1991). Note negative rainout trends

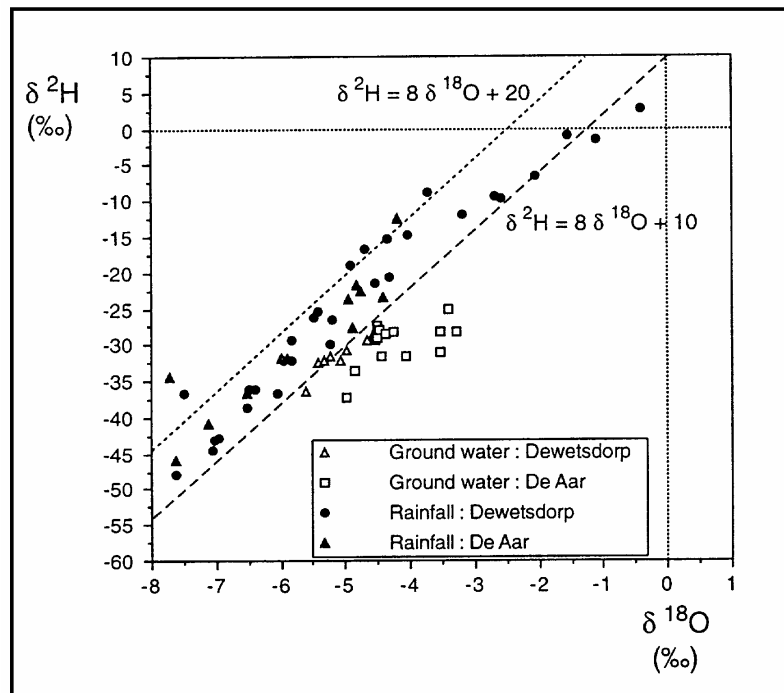


Figure 3.54: $\delta^2\text{H}$ vs. $\delta^{18}\text{O}$ plot for rain water and ground water at De Aar and Dewetsdorp. Note rainwater trends between regression lines $\delta^2\text{H} = 8 \delta^{18}\text{O} + 10$ (WMWL) and $\delta^2\text{H} = 8 \delta^{18}\text{O} + 20$. Dewetsdorp groundwater clusters close to the WMWL, whilst De Aar groundwater shows the effect of evaporation

The interpretation of the data, limited at the time, needs to be revisited and extended in the light of all other information available. The project furthermore needs to be resurrected in the two study areas, which will allow for useful comparisons of isotope levels over more than a decade.

3.3.3.4 Beaufort West Study

A brief survey using a variety of isotopic and other environmental tracers of ground water at Beaufort West was conducted by the CSIR (Vogel et al., 1980(b)) as an adjunct to major development of groundwater resources in the area. The town itself is situated on a fairly featureless plain. To the north, the Nuweveld mountain range of the Great Escarpment rises some 400 m above the town. Some 15 boreholes over an area of 500 km², ranging in collar elevation from less than 900 to 1 200 m.amsl were sampled with a special depth-sampling device. The area is underlain by a variable sequence of Beaufort Group siltstone, mudstone and intercalated sandstone.

Radiocarbon and tritium values (**Figure 3.55**) generally plot along the locus of values expected from the exponential model, indicating that the more mobile ground water in the area is effectively phreatic. Boreholes at higher elevation all show high ^{14}C and ^3H values, indicating rapid groundwater fluxes. Much slower moving (older) groundwater and higher mineralisation is found in the plain, albeit that more rapid turnover and fresher water (local recharge) is found at various locations.

Although only relatively small variations in measured parameters are observed with increasing depth in the six boreholes profiled, the authors do discern some increase in the helium concentration which they ascribe to deep degassing. Dissolved oxygen tends to decrease with depth but shows little variation with inferred "age", or residence time.

No differentiation in $\delta^{18}\text{O}$ values were found, which is somewhat surprising in view of the range of altitudes. An altitude dependence of $\delta^{13}\text{C}$ is however observed. The authors propose some vegetation control. More significant may be the greater groundwater mobility on the high ground, and mineralisation processes in the plain. $\text{N}_2\text{-Ar}$ concentrations and $^{234}\text{U}/^{238}\text{U}$ ratios in groundwater also show differentiation at higher and lower altitudes. The authors conclude that recharge in the area occurs predominantly at higher elevation, but that localised recharge also occurs on the plain. They speculate that the lower $\delta^{13}\text{C}$ values seen in the high altitude samples should be seen deeper in the aquifers of the plain.

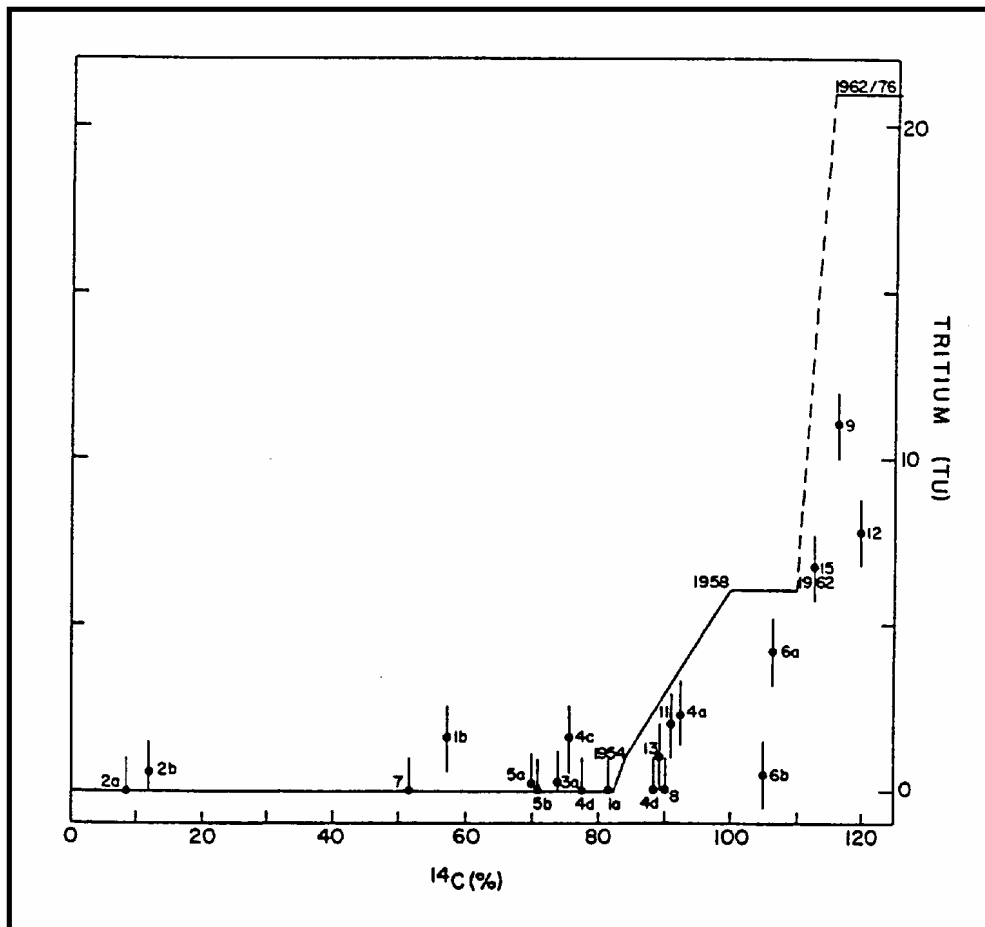


Figure 3.55: Plot of tritium vs. radiocarbon for ground water at Beaufort West (Vogel et al., 1980 (a)). The relationship is similar to that expected for an idealised phreatic aquifer (Figure 3.48).

More recently, a groundwater study involving some isotopic measurements (SRK, 1997) was conducted in the same general area of Beaufort West. All the samples were collected in the plain and to the south-east of those of the previous study. Most $\delta^2\text{H}$ and $\delta^{18}\text{O}$ values lie on the WMWL and cover a much wider range than those observed by Vogel et al. (1980(b)). At least one point lies well to the right of the WMWL and reflects water from a nearby farm dam. As in the earlier study, the tritium and radiocarbon values show active recharge and MRT values of a few decades. Very little correlation is seen between groundwater mineralisation and radioactive and stable isotope content.

The results from these two investigations show that a more in-depth study is warranted in order to obtain a better understanding of the chemical behaviour, and isotopic relationships, of the groundwater in the aquifers at Beaufort West and in other Karoo environments.

3.3.3.5 Doornberg Fault Zone Study

As part of a larger investigation of the Doornberg fault zone and the inflow of large volumes of ground water into the Orange-Fish tunnel during 1969, various samples for isotope analysis were taken from shafts in the tunnel and from springs (Bredenkamp, 1978). A general increase of deduced radiocarbon ages was observed with water temperature, which ranged from 19°C to 35°C. These values were interpreted in terms of depth from the known geothermal gradient for the area. Recharge for the area was calculated at some 6 mm/annum, using a method akin to the well-mixed approach (**Equation. 3.9**) and assuming a porosity of 0.035.

A groundwater survey was conducted in the Venterstad area, also in connection with the Orange-Fish tunnel flooding, using isotopes and other environmental tracers (Vogel et al., 1980(a)).

Most of the groundwater in the area was found to be of short residence time, and therefore superficial and of local origin. As in the Beaufort west area, ^{14}C and ^3H value pairs for more recent water conform to the exponential model predictions. Three groundwater types are discerned, with ionic ratio dominance:

- Ca,Mg- HCO_3 (Type I);
- NaHCO_3 (Type II), and
- NaCl (Type III).

The Type III water reflects longer residence times and elevated water temperatures, while the $\delta^{18}\text{O}$ values clearly separate this groundwater from Types I and II. A similar difference is seen in the ionic concentrations.

Dissolved oxygen was found to be highest in recently recharged water, a potential recharge zone indicator. *Helium* concentrations were unexpectedly high, but could not be related to specific rock features. The older water types have 2-3 orders of magnitude higher He, which might allow mixtures of water types pumped from boreholes to be identified. It would appear as though the deeper, more productive, and shallower ground water systems are largely unrelated, and could be exploited without mutual interference.

Water which flooded the Orange-Fish tunnel from fissures was essentially Type II, whilst water from a dyke intersecting the tunnel was of Type III. Although dewatering hydraulically affected the dyke, the chemical composition of the pumped water never changed. This suggests that the contribution of groundwater from the dyke was relatively small.

3.3.3.6 Waste Disposal Impact on Groundwater, Bloemfontein

The landfill sites to the north and south of Bloemfontein were studied using environmental isotopes (Verhagen et al., 1996). Both sites have been developed on Karoo shales, and both are associated with dolerite intrusions. The northern site lies close to the drainage channel and farm dam in a rather narrow valley. The southern site lies on open, slightly sloping terrain. A small number of monitoring boreholes were drilled at each of the sites.

Neither site produces visible leachate on surface. One of the boreholes, drilled within the northern site, produces highly polluted groundwater, which could be classed as leachate. In both this borehole, and in a borehole on the south-western corner of the southern site, tritium levels were measured well above expected ambient values. This first drew attention to the fact that waste containing artificial tritium was finding its way onto general and domestic waste disposal sites. Tritium readily exchanges with infiltrating rainwater. Such *in situ* tritium is an excellent tracer of leachate as:

- the site can be regarded as the sole source of the tracer;
- tritium is a conservative tracer of water, independent of changing chemical load;
- environmental tritium levels in Southern Africa are low, leading to high contrast, and
- the tracing is ongoing, requiring only the "isotopic snapshot" approach.

Slightly raised tritium values were observed in boreholes further away from the sites. This, along with chemistry, stable isotope and radiocarbon measurements allows for a detailed analysis of the pathways through which actual and potential contamination moves. At the northern site, the probable route of contaminants is via the stream, which then infiltrates near the boreholes. Such surface-ground water interaction was also observed at a landfill site in Johannesburg (Verhagen et al., 1996). At the southern landfill site, boreholes some 500 m away were found to be affected by leachate on account of the observed tritium values and chemistry. However, groundwater transport considerations showed that the subsurface transport would be too slow. It is therefore postulated that the contamination is transported by overland flow from the site, which has been observed during heavy rains.

3.3.3.7 Study of Groundwater at Dewetsdorp Using Environmental CFCs

Several pilot studies were undertaken in the past few years by the CSIR in which CFCs were employed to "date" groundwater. These were conducted in Table Mountain sandstone aquifers as well as in the Karoo aquifers of Dewetsdorp (Weaver and Talma, 1997). In the latter study, five boreholes were selected in the presumed groundwater flow direction towards an ephemeral drainage under a surface gradient of some 2%. The two upstream boreholes were sunk into Karoo shales whilst the next two intersected dolerite at some depth and are high yielding. The depressed waterlevel

of the borehole at the streambed is ascribed to pumping from a nearby wellfield. Radiocarbon values from 92 to 113 pMC suggest water recharged in the past few decades, whilst the chemical character changed from more stagnant to more dynamic between 1985 and 1997. This change of chemistry is ascribed to recharge produced during the flood event of 1988.

The three CFCs analysed for were interpreted in terms of recharge dates. The dates for the three upstream boreholes lie around 1980, which is explained in terms of mixing of 1988 and older water. The chemically different borehole with lower ^{14}C gave dates around 1952. The results for the borehole at the stream, with high ^{14}C but CFC date of about 1972, could not be easily explained.

3.3.4 ISOTOPE STUDIES OF KAROO AQUIFERS IN THE KALAHARI BASIN

The case studies presented in **Chapter 3.3**, although limited in number and often in scope, have suggested the power of isotope and other environmental tracers in providing information on groundwater origin, recharge and mobility in the Karoo basin. However, the full potential of such environmental tracer techniques may be achieved only when they can be integrated into well-conducted geohydrological investigations or groundwater development programmes.

Numerous and extensive isotope hydrology studies have been conducted over the past 15 years in the Karoo aquifers of the Kalahari basin. Three of these, conducted by the Schonland Research Centre (then NPRU) are reviewed briefly in this section in order to highlight aspects not explicitly dealt with in the main Karoo basin. The first addresses the influence of ephemeral surface drainage on regional groundwater systems, an important question still to be addressed in the Karoo basin. The second is an illustration of detailed evaluation of a groundwater flow regime at the hand of integrating isotope and other data. The third concerns the determination of recharge by isotopes and by independent means in a project specifically designed as a model for fractured Karoo aquifers in South Africa.

3.3.4.1 Surface Water and Groundwater Interaction in Gordonia

The question addressed was the regional significance in the groundwater balance of bank infiltration during flooding of the Kuruman River as a linear recharge source (Verhagen, 1984). Shallow groundwater along and close to the riverbanks generally was found to have radiocarbon values of 80-90 pMC, occasionally with measurable tritium, implying rapid recharge. If, as was assumed at the time, diffuse rain recharge could be ignored in this sand-covered environment, a more or less systematic increase in groundwater residence time and chemical evolution should be seen with increasing distance from the river-bed. Samples were taken from boreholes along a sand-filled

paleo-valley extending some 30km from the south bank of the river. No systematic spatial variation was seen in either the hydrochemistry or the radiocarbon values, ranging from 30-75 pMC, evidence of low but finite diffuse recharge. There are two quite distinct clusters of stable isotope values $\delta^2\text{H}$ and $\delta^{18}\text{O}$ for groundwater – those nearby and further away from the river (**Figure 3.56**). The one reflects the stable isotope signal of Kuruman flood-water and the second approximates the weighted mean value for Pretoria rainfall (IAEA, 1992). There is therefore no basis for the assumption that recharge from the river bed has regional significance and can support sustained groundwater abstraction well away from the river.

The river flows every 10-15 years following successive seasons of monsoon-type rains, when bank infiltration occurs and the region's vegetation flourishes. The distinct stable isotope signal occurring away from the river proves that in such years, there is very little diffuse recharge. It is postulated that the signal is more characteristic of intense localised convective thunderstorms, often producing ponding, which can produce diffuse recharge during periods of vegetal dormancy. Similar conclusions were arrived at by totally independent means for a different area of the Kalahari.

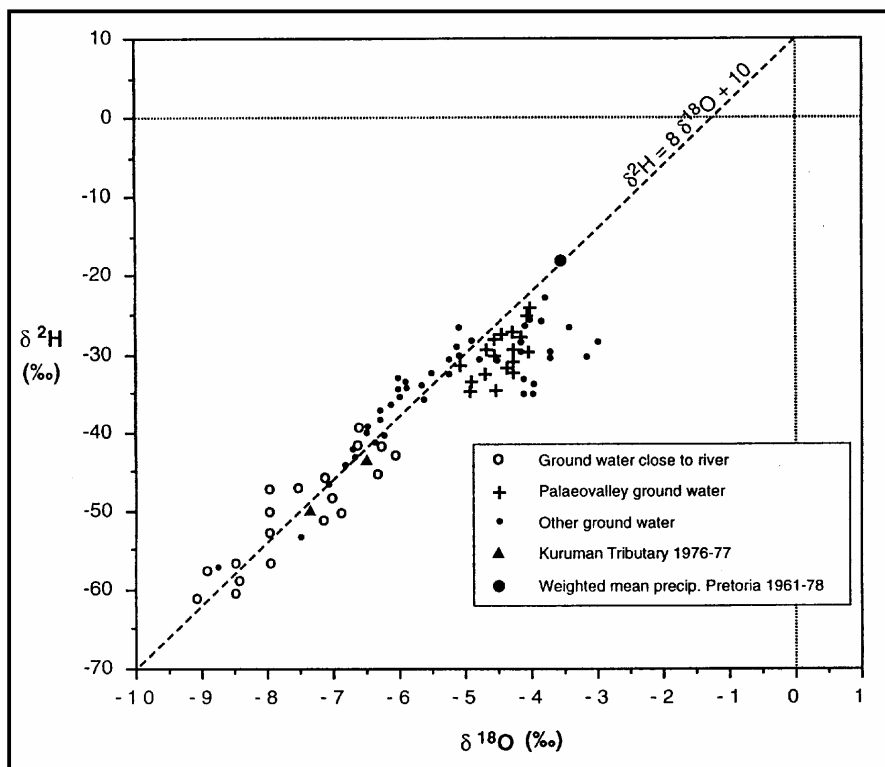


Figure 3.56: $\delta^2\text{H}$ vs $\delta^{18}\text{O}$ plot for Gordonia groundwater, showing the WMWL and the two groups of values for groundwater near to, and further away from, the Kuruman River bed, respectively

3.3.4.2 Jwaneng Mine, Botswana

The Jwaneng diamond mine in southern Botswana extracts more than 10×10^6 m³/annum of groundwater from an Ecca sandstone aquifer, an alluvial fan or delta, which dips below increasing thicknesses of a mudstone aquitard. Soon after abstraction commenced from a wellfield of 14 boreholes, individually yielding up to 28 l/s, it became obvious that drawdown was much lower than had been predicted from evaluation of aquifer test data. Over a number of years several updates of the wellfield model were necessary, invoking a substantial leakage factor. The source of the leakage remained uncertain, however. Although the groundwater chemistry suggests active recharge to the aquifer, recharge through the Kalahari cover was not considered, and the source was assumed to lie some 50 km to the south, the water moving through fractures in the basement rocks.

An ongoing isotope study undertaken in 1983 (Verhagen, 1993) produced radiocarbon values ranging from around 50 pMC where the sandstone aquifer sub-outcrops below the semi-consolidated Kalahari cover and up to 75 pMC, paradoxically where the aquifer is more confined. Much deeper village boreholes a few kilometres further north gave near-zero radiocarbon, showing stagnant water. A conceptual flow model (**Figure 3.57**), assuming recharge at the aquifer sub-outcrop, shows that the boreholes penetrating the entire range of flow lines in the SE may be expected to produce water at about 50 pMC. Those boreholes penetrating increasing thicknesses of aquitard tap only the more recent flow lines in the aquifer, evidenced by higher ¹⁴C values. The model requires a “sink” for the ground water. It is postulated that diffuse leakage occurs from the aquifer into the wide contact area of the aquitard. The isotope conceptual model is consistent and clearly shows that recharge to the aquifer cannot come from below. It furthermore identifies the source of the leakage sought in the management model - with pressure reduction due to exploitation, the diffuse leakage into the aquitard is being reversed. Quantitatively, the isotope model allows for recharge to be calculated on the basis of ¹⁴C derived MRT values (**Equation. 3.10**) at 3-8 mm per annum. This amounts to a fraction of abstraction, but is significant and draws attention to the long-term vulnerability of the resource to pollution with changing land use in the recharge area. It also illustrates that the aquitard can represent a significant groundwater resource when it presents a large contact area with the exploited aquifer

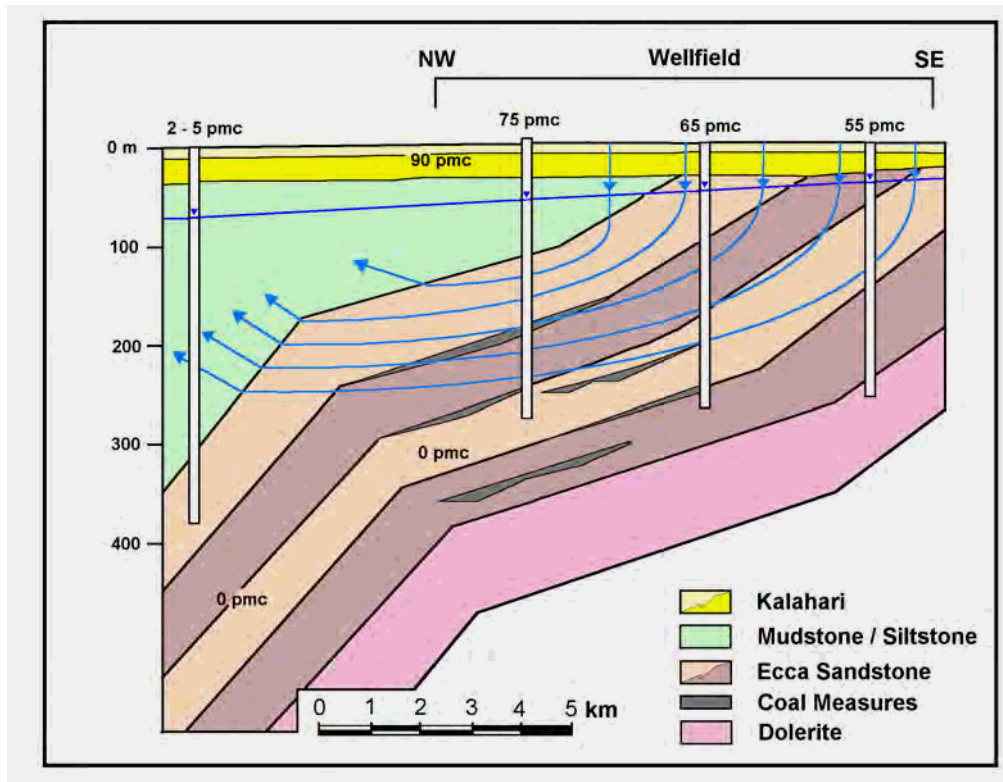


Figure 3.56: Schematic section of the alluvial-fan aquifer at Jwaneng, showing radiocarbon values at different wells and inferred groundwater flow paths from recharge at the aquifer sub-outcrop to leakage into the aquitard

3.3.4.3 Karoo Aquifers at Orapa, Botswana

The applicability of the isotope approach to recharge assessment was assessed during a study conducted on a fractured Karoo sandstone aquifer in Botswana. This study, undertaken for the Water Research Commission (Bredenkamp et al., 1998) was seen as a model project for Karoo aquifers in South and Southern Africa in general. Several wellfields had been established over three decades to supply the Orapa and Lethlakane diamond mines that constitute a unique groundwater abstraction scheme amounting to a large-scale, long-term pumping test. From the extensive data-base built up over many years, it was possible to assess groundwater recharge and aquifer storativity, using the SVF method, as well as the method of cumulative rainfall departures. An interesting conclusion reached was that in the period following on above-average rainfall years, groundwater recharge appears to be lower than during normal years. This is ascribed to the vegetation cover, which develops during wet periods, and for some time maintains its increased water demand. Similar conclusions had been reached by Verhagen (1984) on the basis of isotopic studies in Gordonia.

The results confirmed the qualitative conclusions reached on the basis of isotope data by Verhagen et al., (1974) that active recharge was occurring in the area, and allowed for an estimate of groundwater recharge rate at a few mm per annum. Earlier radiocarbon measurements of groundwater were re-examined in terms of mean residence time, based on the exponential mixing model (**Chapter 3.3.2.2**). Coupled to extensive information on the aquifer's porosity obtained from numerous exploration drill-cores, recharge values quite compatible with those of the other, completely independent, methods could be calculated. This exercise was unique in that conclusions based on isotopic data can rarely be compared with such a detailed and independent quantitative assessment of a groundwater system.

3.3.5 CONCLUDING REMARKS

The Karoo basin is characterised by fractured rock aquifers that are bisected by numerous dolerite intrusions. These conditions produce a complex hydrogeological system, which complicates the study and development of groundwater. Universal models of groundwater flow hardly apply to these conditions, and the geohydrologist needs additional tools with which to understand the movement and chemical evolution of groundwater. This brief exposé of environmental isotope techniques and their use in Karoo aquifers is intended to draw attention to one set of such tools which, when properly integrated with the other means at the geohydrologist's disposal, are powerful and efficient. One of the most important of these is hydrochemistry, and programs such as FLOWPATH, with which evolutionary trends in the data may be followed. As mentioned above, the potential of environmental isotopes has not properly been exploited in the main Karoo Basin, and their use in groundwater investigations is encouraged.

Chapter 4

RESOURCE DEVELOPMENT AND EVALUATION

4.1 GROUNDWATER EXPLORATION AND DEVELOPMENT

4.1.1 REMOTE-SENSING

4.1.1.1 Introduction

Air-photogrammetry has been widely applied in the earth sciences since the 1950s. In the last two decades, satellite imagery and computer-based digital-processing techniques have been used as an aid to groundwater exploration in arid to semi-arid areas, especially in areas where hydrogeological information is sparse. The site-specific occurrence of groundwater in hardrock areas is often difficult to predict and limited knowledge of the hydrogeological conditions that collectively control the water-bearing capacity of various fracture systems is a major constraint to the cost-effective exploration and development of these groundwater resources.

Geohydrological analysis of remotely-sensed imagery is one of the most difficult hydrological applications of remote-sensing, because groundwater by nature is not available for direct observation. Siegal and Gillespie (1980) regard groundwater exploration using satellite imagery to be a hydrogeologic 'inference' task, which makes use of indirect physiographic indicators such as:

- Distribution of lithologies.
- Geologic structures and intrusions.
- Geomorphology.
- Drainage patterns.
- Hydrophile / hygrophile vegetation density and health status.
- Seasonal variations in soil moisture conditions.

Satellite imagery has been successfully applied to a number of geohydrological projects, mainly as an exploratory tool during the reconnaissance phase of groundwater investigations (Salman, 1983; Finch, 1990). The main emphasis of this work has involved the mapping of geological lineaments.

Other potential geohydrological applications of digital airborne and satellite imagery, both direct and indirect, include:

- Location of springs and seeps.
- Mapping of shallow aquifers.
- Delineation of shallow saline water bodies and contaminant plumes.

- Monitoring the long-term effects of groundwater abstraction on the natural vegetation.
- Monitoring of groundwater abstracted for irrigation purposes, by mapping of areas under irrigation and crop type.

4.1.1.2 Commonly Used Satellite Imagery

The following satellite imagery are commonly used by scientists in their study of the earth's surface:

LANDSAT

The first LANDSAT satellite was launched in 1972 and was initially called the Earth Resources Technology Satellite (ERTS). The early LANDSAT satellites 1, 2 and 3 are no longer operational and gathered Multi-Spectral Scanner (MSS) data. LANDSAT 4 and 5 gather MSS and Thematic Mapper (TM) data, although LANDSAT 4 is no longer operational. The spatial resolution (i.e. 'pixel' size) of the MSS data is 79 x 79 m, while the radiometric resolution of the data is 6-bit, although it is archived as 8-bit data. The TM scanner is a multi-spectral scanning system, similar to the MSS, except that the TM sensor records reflected/emitted electromagnetic energy from the visible, reflective infra-red, middle infra-red and thermal infra-red regions (**Figure 4.1**). TM has a spatial resolution of 28.5 x 28.5m, except for Band 6 that has a spatial resolution of 120 x 120 m. The radiometric resolution of the TM data is 8-bit. The LANDSAT World-Wide-Reference System (WRS) catalogues the earth's landmass into 57 784 standard scenes, each 183 km wide (swath width) by 170 km long.

In April 1999, after the failure of LANDSAT 6, LANDSAT 7 was launched into orbit and is equipped with the 'Enhanced Thematic Mapper Plus' (ETM+) instrument. The ETM+ instrument is an eight-band multi-spectral scanning radiometer capable of providing high-resolution imaging information of the Earth's surface. The spectral resolution of the ETM+ is similar to that of LANDSAT 5 (**Figure 4.1**), but it provides an additional panchromatic band in the 0.50 – 0.90 μm range. The panchromatic band has a spatial resolution of 15 x 15 m, whilst the 6 visible, near and short-wave infrared bands are 30 m; and the thermal infrared band is 60 x 60 m. The satellites orbit is sun-synchronous with a 16-day repeat cycle. This enhanced LANDSAT information has not, as yet, been widely used in South Africa, as the Satellite Applications Centre (CSIR), do not have a contract to receive and distribute the imagery.

The LANDSAT TM imagery is useful for vegetation type and health assessment, soil moisture, lithological and water discrimination. The spatial and spectral resolution of the LANDSAT TM data makes it the most commonly applied satellite imagery in both geological and geohydrological investigations.

SPOT

The first Systeme Pour l'observation de la Terre (SPOT) satellite was developed by the French and was launched in early 1986. A second and third satellite was launched in 1990 and 1993, respectively. The sensors operate in two modes, namely, a multi-spectral and panchromatic mode. The satellite can observe the same area of the globe once every 26 days and normally produces 'nadir' or perpendicular views of the earth's surface, although it does have off-nadir viewing capabilities. The off-nadir or 'side-looking' capability allows the same portion of the earth to be viewed every 3 days. The swath width varies between 60km for nadir views to 80km for off-nadir views.

The SPOT panchromatic imagery consists of a single band, which is sensitive to the visible light spectrum (i.e. similar to a black and white aerial photograph), and has a spatial resolution of 10 x 10 m (**Figure 4.1**).

The SPOT XS or multi-spectral imagery has a spatial resolution of 20 x 20 m and contains three bands with a radiometric resolution of 8-bits (**Figure 4.1**). The multi-spectral imagery is useful for discriminating between plant species, vegetation biomass, landuse identification, soil and geological mapping.

NOAA

The NOAA (National Oceanic and Atmospheric Administration) AVHRR (Advanced Very High-Resolution Radiometer) satellite provides coverage of large areas of the earth, with an image swath width of 2 700 km. These satellites were originally designed for meteorological applications, but have been applied in many fields from agronomy to oceanography, including regional geological mapping. AVHRR is available in 3 formats, where the Local Area Coverage (LAC) has the highest spatial resolution of 1.1 x 1.1 km per pixel. There are 4 to 5 bands of data available depending upon when the data was acquired. The radiometric resolution of the data is 10-bit in a packed format or 16-bit in an unpacked format. This satellite views the entire globe every 14.5 days.

IKONOS

In September 1999, the sun-synchronous IKONOS satellite was launched and it captures the following information:

1. A single panchromatic band with a spectral resolution of 0.45 – 0.90 μm and a spatial resolution of 1 x 1 m.
2. Four multi-spectral bands, 0.45-0.52 (blue), 0.52-0.62 (green), 0.63-0.69 (red) and 0.76-0.90 μm (near infra-red), and a spatial resolution of 4 x 4 m (i.e. similar to LANDSAT 5 TM bands 1 to 4).

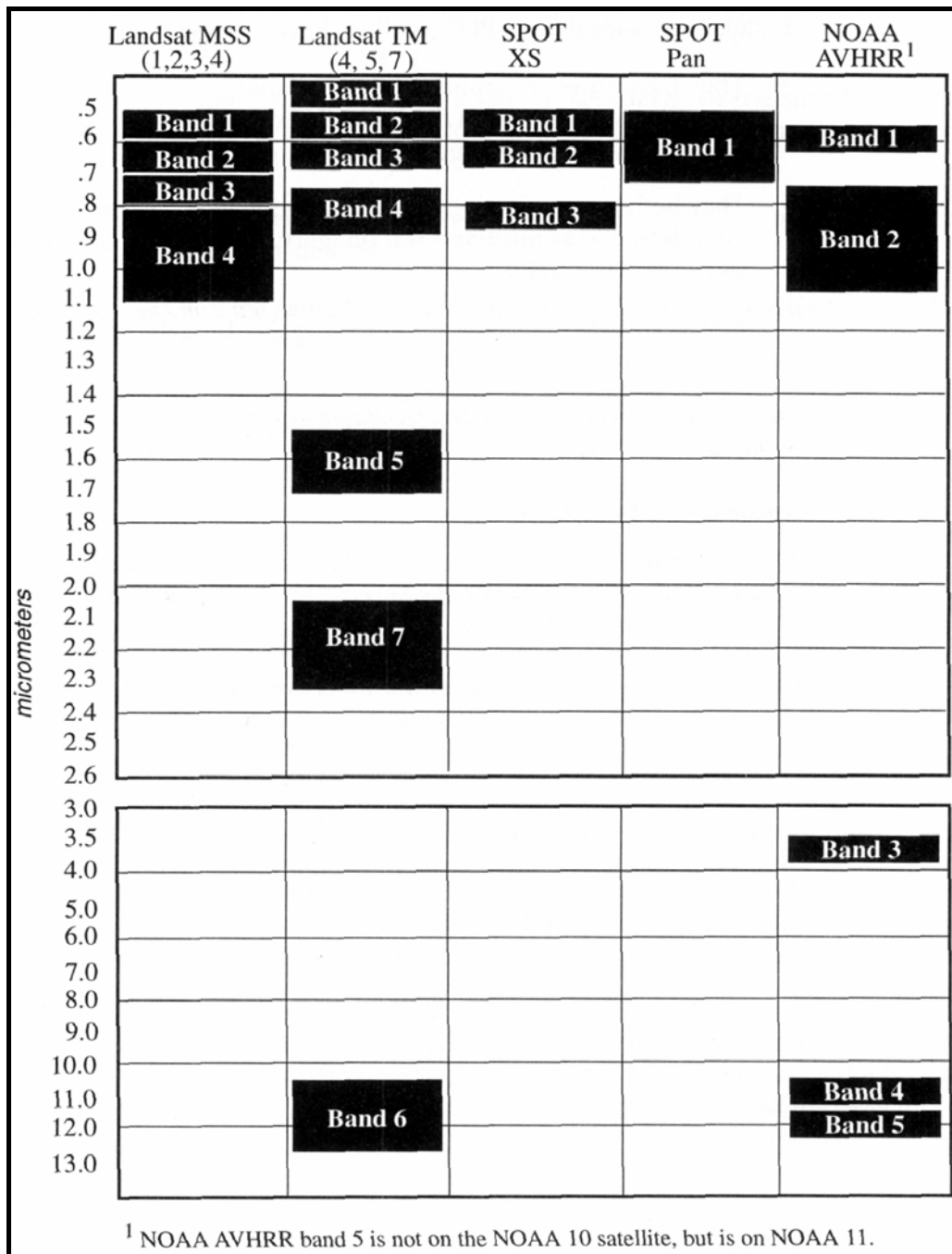


Figure 4.1: Comparison of the spectral resolution of commonly used satellite imagery (after ERDAS, 1997)

RADAR

Radar systems can be airborne, space-borne or ground-based. Researchers have found that a combination of the characteristics of radar data and visible/infrared data (i.e. LANDSAT TM) provides a more complete picture of the earth. In the last decade the importance and application of radar imaging has grown rapidly. One of the main advantages of radar is its capability of recording data, both day and night, and in all weather conditions. Radar's ability to partially penetrate the ground surface, especially in arid areas, and its sensitivity to surface moisture and micro-relief makes it useful for geohydrological mapping, mineral exploration etc. Radar imagery can aid in the mapping of structural features reflected by topography only, due to its sensitivity to surface roughness. **Table 4.1** summarizes the characteristics of the most commonly used radar satellites.

Table 4.1: Characteristics of commonly used radar satellites

	ERS-1, 2	JERS-1	SIR-A, B	SIR-C	RADARSAT
Availability	Operational	Operational	1981, 1984	1994	Operational
Resolution (m)	12.5	18	25	25	10-100
Revisit time (days)	35	44	NA	NA	3
Scene area (km)	100 x 100	75 x 100	30 x 60	variable	50 x 50 to 100 x 100
Bands	C	L	L	L,C,X	C
Frequency range (GHZ)	3.9-6.2	0.39-1.55	0.39-1.55	0.39-1.55 3.9-6.2 5.77-2.75	3.9-6.2
Wavelength range (cm)	3.8-7.6	76.9-19.3	76.9-19.3	76.9-19.3 3.8-7.6 5.77-2.75	3.8-7.6

The usefulness of various types of remotely-sensed imagery, namely air-photographs, LANDSAT TM, SPOT and ERS, to Karoo fractured-rock investigations were assessed during a Water Research Commission funded project (Woodford and Chevallier, 2001), aimed at investigating the relationship between groundwater occurrence and geological lineaments (**Chapter 4.1.2**). Various LANDSAT TM and ERS satellite images of the Loxton area are presented in **Figure 4.2** to illustrate the following:

- Image **A** is a natural or *true colour composite* image created using LANDSAT TM bands 1,2 and 3 in the visible portion of the electromagnetic (EM) spectrum (WRS Scene No. 173-82). Note that the dolerite dykes and sills have their natural 'reddish-brown' colours, the mudrock is a bluish hue and the alluvium is white.
- Image **B** is a *false colour composite* image created from LANDSAT TM bands 3, 4 and 5 in the reflective- to mid-infrared portion of the EM spectrum. Notice that the dolerite intrusions are a bright green colour and that the healthy green-

leaved vegetation, mainly along the drainage courses, are a bright red to reddish orange colour.

- Panchromatic LANDSAT TM images **C** and **D** represent diurnal and nocturnal scenes, respectively, of emitted / reflected energy in the thermal infra-red portion of the EM spectrum. The high-relief dolerite intrusions are clearly evident on the diurnal image (C), where the contrast between the light 'warmer' tones of the sunlit northerly slopes and the darker 'cool' tones of the shadow covered slopes help to enhance these features. Note also the dark 'cooler' tones of the vegetated areas along the drainage courses. In contrast, the major dolerite intrusions are reflected as light 'warmer' tones in the nocturnal image (D), where the dolerite emits more energy retained from the diurnal sun heating-cycle due to its relatively higher thermal conductance. Note that the nocturnal imagery is more 'blurred' as the only source of energy is that emitted by the earth's surface, which is influenced by factors such as air temperature, wind etc.

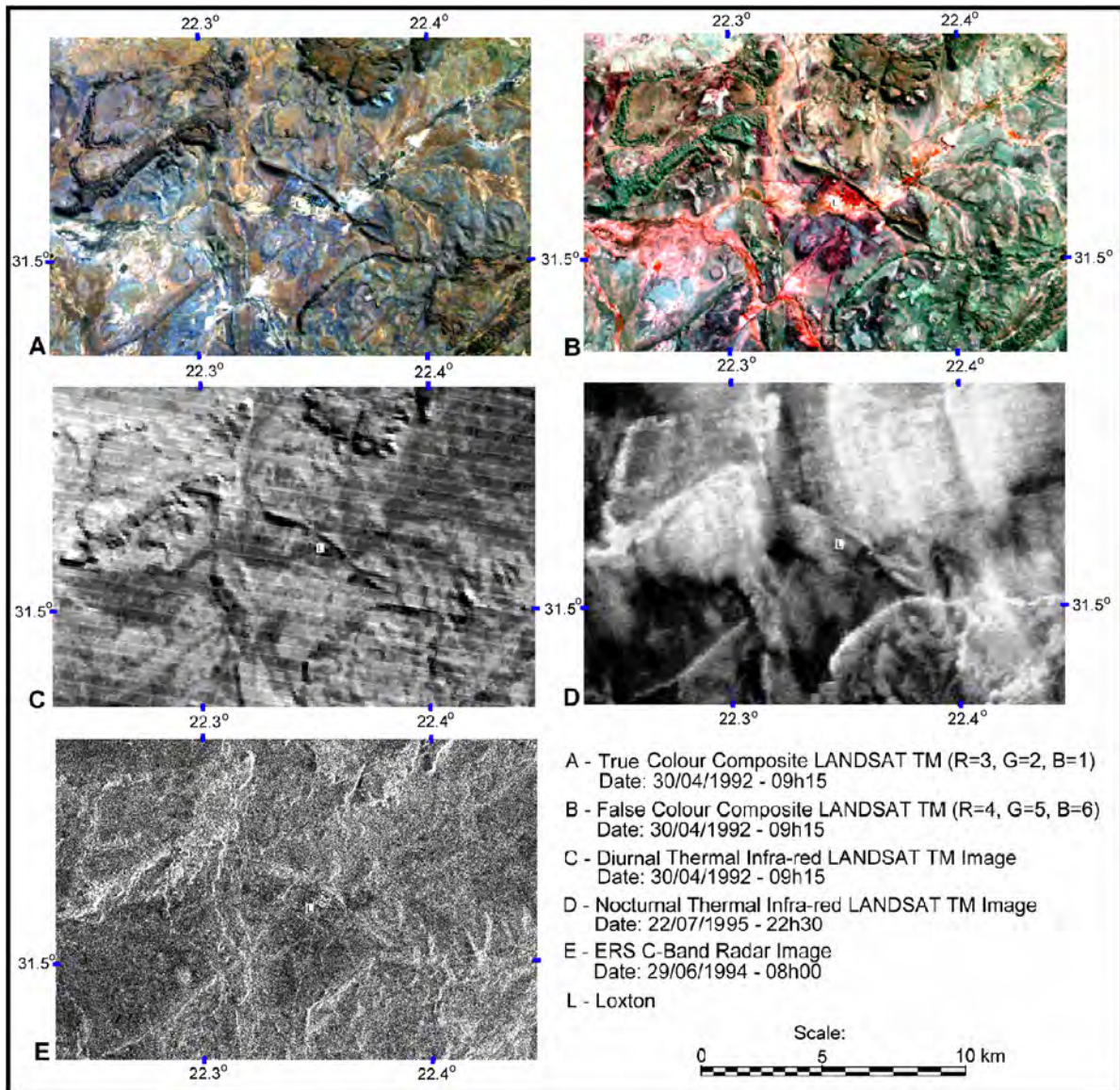


Figure 4.2: *LANDSAT TM and ERS satellite imagery of the Loxton area in the Western Karoo Basin*

- The Panchromatic ERS image (E) clearly shows clearly major dolerite intrusions due to its sensitivity to relief, whilst the more ‘moist’ zones along the drainage courses are reflected as darker tones in the image (e.g. the dry Loxton and drainage system, to northeast of Loxton).

4.1.1.3 Geological Lineament Mapping and Structural Analysis in Groundwater Exploration

Theoretically, lineament studies should be most applicable in hard-rock areas where the *primary* permeability is negligible and where groundwater occurs mainly in zones of fracture-induced *secondary* permeability. In these areas, groundwater exploration is therefore directed towards finding the ‘open’ or dilated fracture zones and it is expected that boreholes located on or at the intersection of such structures should have relatively higher yields than those drilled away from these features.

The attitude of a lineament is generally governed by simple mechanical laws, which relate to the orientation of the maximum, minimum and intermediate stress-axes prevalent in the crust, the strength of the rock and the resultant potential surfaces of failure. The synoptic view provided by remotely-sensed imagery is ideal for evaluating fracture patterns and other reflections of brittle tectonics over large areas. In satellite imagery, the small, regionally insignificant features are suppressed and often very large, subtle lineaments become apparent when viewing various false colour composite (FCC) images made up from bands outside of the visible spectrum.

The hydrogeological significance of a particular lineament will depend upon its deformational history and the present state of stress in the host-rock. Under normal deformation conditions in the upper crust, rocks fracture in a brittle manner by a pure shear mechanism during which failure occurs along one or two sets of conjugate shears (*S*). These fracture systems are essentially compressional features (**Figure 4.3**). Tension (*T*) or extensional fractures may form as an early response to the applied stress, but do not normally continue to propagate once shearing commences (Waters et al., 1990).

Larson (1984) classified fractures in hard-rocks into three categories based upon hydrogeological considerations, namely:

1. *Tensile Joints* related to plastic deformation:

The joints exhibit a characteristic ‘en-echelon’ pattern. The hydraulic interconnectivity between individual joints is often poor and this results in a fractured media of low storage capacity. Later brittle deformation may re-activate these zones of weakness and create a highly permeable fracture system.

2. *Tensile Fractures* related to brittle deformation:

This type of fracture system generally has a high storage capacity because of a high degree of hydraulic interconnectivity and their tensile origin. Such fractures also act as highly transmissive conduits into which water drains from minor fractures belonging to the same fracture-system.

3. *Shear Fractures* related to brittle deformation:

The storage capacity of fracture systems resulting from the complex phenomenon of shearing is variable. It seems that most, if not all shear fractures are tightly compressed by residual stresses. Larson (1984) states that extensive permeable, brecciated zones are more commonly observed in low-angle thrust faults than in vertical or sub-vertical shears.

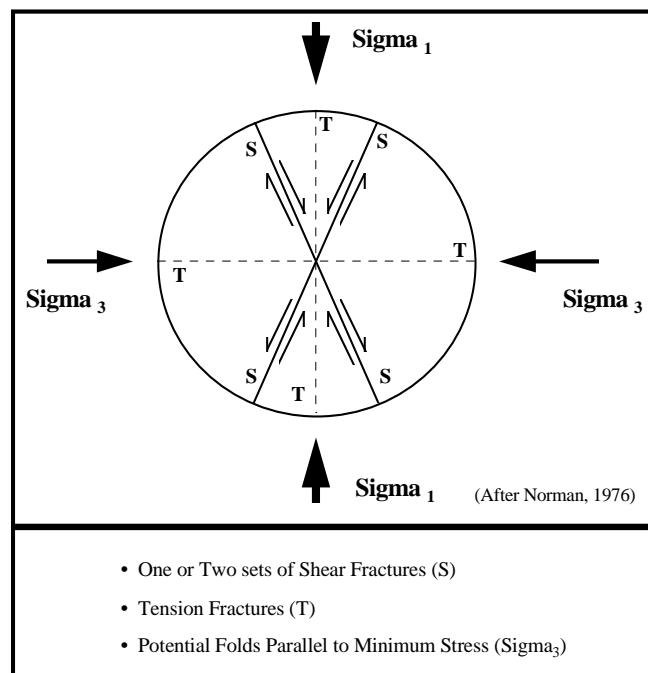


Figure 4.3: *Fracture patterns caused by a major compressive horizontal force*

Note that it is common to find that structures have undergone reactivation during later stages of deformation so that their geometry may not always provide information relating to the current stress environment. Abundant steep joints and surface-parallel sheeting is often of recent origin and indicates that the near-surface zone, 50 – 150 m bgl, is under decompression and tension caused by erosional unloading and/or tectonic uplift (Waters et al., 1990). Under these conditions, many pre-existing fractures regardless of their origin could be under tension and ‘open’ to the movement of groundwater. Furthermore, the extensive fracturing of rocks is often followed by intensive weathering, which may either enhance or degrade the hydraulic properties of the fracture system.

Based mainly upon investigations in the United States, the frequency of occurrence of fractures in crystalline rocks has generally been found to decrease with depth (Lachenbruch, 1961, Davis and De Wiest, 1966; Davis and Turk, 1964; Landers and Turk, 1973; Legrand, 1967). However, underground mines have encountered vast inflows of groundwater hundreds of metres beneath the surface, indicating that some fractures do extend to great depths (Hurr and Richards, 1966; Snow, 1968a, 1968b; Wahlstrom and Horback, 1962). Robinson (1976) suggested that two geohydrological zones of fracturing are generally present, namely:

- an 'active' upper-zone wherein the majority of the fractures are related to local weathering and unloading processes, and
- a 'passive' underlying zone where the fractures are related to regional tectonics.

A number of researchers have attempted to quantify the occurrence of groundwater in fractured-rock environments based upon lineaments mapped from various forms of remotely-sensed imagery. The key assumption that underlies all these lineament studies is that the identified linear features are "real" and not artifacts of either the observers imagination and/or the result of anthropogenic activities. The mapped lineaments are assumed to represent the surface manifestations of transmissive fracture systems within a low permeability rock-mass.

The results of remote-sensing studies aimed at assessing the influence of linear structures on borehole productivity have been varied and the findings of a number of these investigations are summarised in **Table 4.2** and **4.3**. A similar study in Karoo fractured-rock aquifers is presented in **Chapter 4.1.2**.

The results have not always been very conclusive, although most workers agree that a better understanding of mapped lineaments is needed for successful siting of boreholes. Borehole yields are affected by factors other than the permeability of the fractures and they should also be taken into account during such analyses, e.g. borehole diameter and construction, depth to the water-table, recharge, host rock type, dip of bedrock, topographic setting etc. Many of these factors are complexly inter-related and their individual influences cannot easily be determined.

Table 4.2: Air-photograph lineament studies in groundwater exploration

Photo-lineament analysis in geohydrological investigations	
Successful	Unsuccessful
<i>Lattman and Parizek</i> (1964) found that boreholes drilled on or near air-photograph fracture traces in dolomites of Central Pennsylvania, USA; had yields of between 10 and 100 times greater than those drilled into zones between these fractures.	<i>Meisler</i> in 1963 (in <i>Waters et al.</i> , 1990) failed to find any significant relationship between borehole yield and lineaments in carbonate rocks in the Lebanon Valley near Harrisburg, USA.
<i>Setzer</i> (1966) sited high-yielding (> 14 l/s) boreholes on fault and fracture traces in crystalline rocks in São Paulo, Brazil; mainly by analyzing drainage patterns mapped from air-photographs	In Ghana, <i>Teeuw</i> (1995) found that only 5 boreholes out of 38 drilled into the sandstones and mudstones of the Volta River Valley were successful (0.02 l/s). These boreholes were sited on air-photograph mapped fractures and electromagnetic surveys. A review of the aerial-photograph lineament mapping carried out for this project showed that only 2 out of the 5 successful boreholes were within 30 m of the lineaments targeted.
<i>Wobber</i> (1967) investigated the usefulness of air-photograph mapping of bedrock fractures obscured by unconsolidated glacial till in Illinois. He found that bedrock fractures could be effectively mapped with up to 50 m of overburden. <i>Wobber</i> concluded that these lineaments reflected jointing in the dolomitic bedrock, similar to the earlier findings of <i>Lattman and Nickelson</i> (1958) and <i>Lattman and Matzke</i> (1961).	
<i>Waters et al.</i> (1990) cites the following researchers as having found a positive relationship between photo-lineaments and borehole productivity, albeit rather qualitative - <i>Akers</i> (1964) in Arizona and <i>Woodruff et al.</i> (1964) in Delaware.	
<i>LaRiccia and Rauch</i> (1976), examined borehole productivity in relation to photo-lineaments in two carbonate aquifers in Maryland. Non-parametric statistical tests were performed on the specific capacity data from 15 boreholes located within 30 m of photo-lineaments and 50 boreholes considered to be sited in the inter-lineament areas. The results showed that boreholes sited on lineaments had greater yields.	

Table 4.3: Satellite lineament analysis in groundwater exploration

<i>Satellite-lineament analysis in geohydrological investigations</i>	
<i>Successful</i>	<i>Unsuccessful</i>
<i>Parizek</i> (1976) found a positive relationship between borehole productivity and satellite lineaments in Pennsylvania using LANDSAT and SKYLAB imagery.	
<i>Salman</i> (1983) used LANDSAT imagery to select promising areas for groundwater exploration in Egypt based upon lineament and drainage density analysis. Drainage density analysis was conducted to define areas of potentially higher bedrock permeability and therefore recharge - the assumption being that, given all factors to be equal, the lower the drainage density the higher the bedrock permeability.	
<i>Rauch and LaRiccía</i> (1978) found that boreholes sited within 200 m of <u>strongly</u> expressed photo- and satellite-lineaments in the Hagerston Valley, Maryland, showed a two-fold increase in yield.	<i>Rauch and LaRiccía</i> (1978) found no relation between <u>weakly</u> expressed air-photograph lineaments and borehole yield in the Hagerston Valley, Maryland.
Later <i>Rauch</i> (1984) and <i>Rauch et al.</i> (1984), concluded that air-photo lineaments related best to borehole yield, with two thirds of boreholes near such lineaments having higher yields.	<i>Rauch</i> (1984) concluded that satellite lineaments related poorly to borehole productivity and that certain areas give inconsistent results.
<i>Moore and Holliday</i> (in <i>Waters et al.</i> , 1990) found that yields of boreholes near mega-lineaments detected using SKYLAB photographs were generally higher than those near to lineaments mapped from LANDSAT imagery or aerial photographs. They postulated that fewer lineaments would be detected from satellite imagery, but that they would represent the more extensive features and would thus be more significant for occurrence of groundwater.	In Botswana, <i>Buckley and Zeil</i> (1984) found that the most obvious and more extensive linear features represented shear zones and that the more productive boreholes were commonly located on a system of less obvious tensional fractures.
<i>Schowerngerdt et al.</i> (1979) found a strong positive correlation between lineaments and aquifer transmissivity, borehole specific capacity and water temperature at various localities in the north Arizona sandstone aquifer.	<i>Dietvorst et al.</i> (1991) found that the regional variations in borehole productivity were strongly correlated with the occurrence of tectonic basins in the Precambrian rocks of southeast Botswana. Lithology and major fracture systems had no significant effect on the formation of regional aquifers, although individual high-yielding boreholes were commonly associated with these features
In Ghana, <i>Sander</i> (1996) found that higher yielding boreholes are associated with LANDSAT TM lineaments. About 93 percentage of wet ($> 0.2 \ell/s$) boreholes were located within 250 m of such a lineament. <i>Sander</i> also noted that SPOT and air-photo lineaments were less correlated with wet boreholes than the LANDSAT lineaments	In the Arizona Sandstone Aquifer, <i>Schowerngerdt et al.</i> (1979) found a negative correlation between LANDSAT lineaments and aquifer transmissivity / borehole specific capacity. They ascribed this anomalous result to (1) poor bedrock exposure due to a thick overburden, (2) inadequate mapping of the small-scale fractures which may locally influence the productivity of a borehole, and (3) the relative positional errors between boreholes and lineaments that could effect the correlation significantly, especially where lineament density is low.
	<i>Greenbaum</i> (1992) investigated the relation between borehole yield and linear structures in south-eastern Zimbabwe. He could not find any significant correlation between the two and proposed that this was due to the predominance of horizontal tensile stresses in the near-surface zone as a result of gravitational unloading.

4.1.1.4 Exploration of Karoo Aquifers

The application of remote-sensing techniques in the exploration of Karoo fractured-rock aquifers has been restricted mainly to the localized mapping of dolerite intrusions, faults and fractures from panchromatic aerial photograph stereo-prints. Recently, a number of geohydrologists have made use of small-scale LANDSAT TM satellite photo-prints to identify regional geological lineaments. The usefulness of such satellite lineament studies is severely limited due mainly to the fixed, small scale of the contact print, as well as the inability to process and interactively view all seven bands of information. Processing of the digital satellite imagery on computers using specialized software allows the user to overcome these restrictions and thereby utilise the information to its full potential.

Conditions in the Main Karoo Basin are ideally suited to the application of remote-sensing techniques in groundwater exploration, due to:

- The relatively simple geology consisting mainly of undeformed sediments, which have been intruded by dolerite dykes and sills.
- The relatively well-known relationship between groundwater occurrence and geology (i.e. dolerite intrusions).
- The generally weak ‘masking’ effects commonly associated with areas of high relief, dense vegetation, excessive surface and/or soil moisture. Where natural, healthy ‘green-leaf’ vegetation does occur it is normally associated with a shallow groundwater occurrence.

Woodford and Chevallier (2001) conducted a detailed remote-sensing study of the area between Beaufort West and Loxton, using panchromatic aerial photo-prints, digital aeromagnetic, panchromatic SPOT and LANDSAT TM imagery. The aim of the study being to map all geological lineaments (i.e. dykes, master-joints, faults etc.), evaluate the usefulness of the various forms of remotely-sensed imagery and to assess the influence of these structures on borehole productivity.

4.1.2 STRUCTURAL, STRESS AND SPATIAL ANALYSIS

The Water Research Commission funded a detailed structural geological and geohydrological investigation of the areas covered by Victoria West and Beaufort West 1/250 000 scale mapsheets (Woodford and Chevallier, 2001). The first phase of the research programme involved:

1. An assessment of the usefulness of the various sources of remotely-sensed imagery and different techniques of lineament mapping,
2. Structural analysis of the geological lineaments and determination of the palaeo-stress regimes, and
3. Spatial analysis of the lineament dataset.

The second phase of the research programme was to assess the relationship between the structural information and the occurrence of groundwater (i.e. borehole productivity). The third phase of the project, given this relationship, was to compile a groundwater productivity (yield) map of the study area using the structural information to extrapolate between borehole information, using a GIS. Exploration drilling was conducted in Loxton area to scientifically assess the structural evaluation of the lineaments in terms of groundwater occurrence.

4.1.2.1 Lineament Mapping

Geological lineaments were mapped from four different but complementary sources of remotely-sensed data, namely:

- 1/50 000 scale, panchromatic air-photograph prints, combined with existing 1/50 000 geological maps and field checking.
- computer enhanced LANDSAT TM satellite imagery,
- panchromatic (XS) SPOT imagery, and
- aeromagnetic imagery.

A detailed lineament database (LINAIR) was compiled from aerial photographs and existing 48 1/50 000 scale geological mapsheets (**Figure 4.4**). The majority of the lineaments were classified either as dolerite dykes, kimberlite fissures, master- joints or faults. Limited field checks were conducted and modifications were subsequently made to the database. A second lineament database (LINCAMP) was compiled by integrating the LINAIR dataset with lineaments mapped from the LANDSAT TM and aeromagnetic digital imagery (**Figure 4.5**).

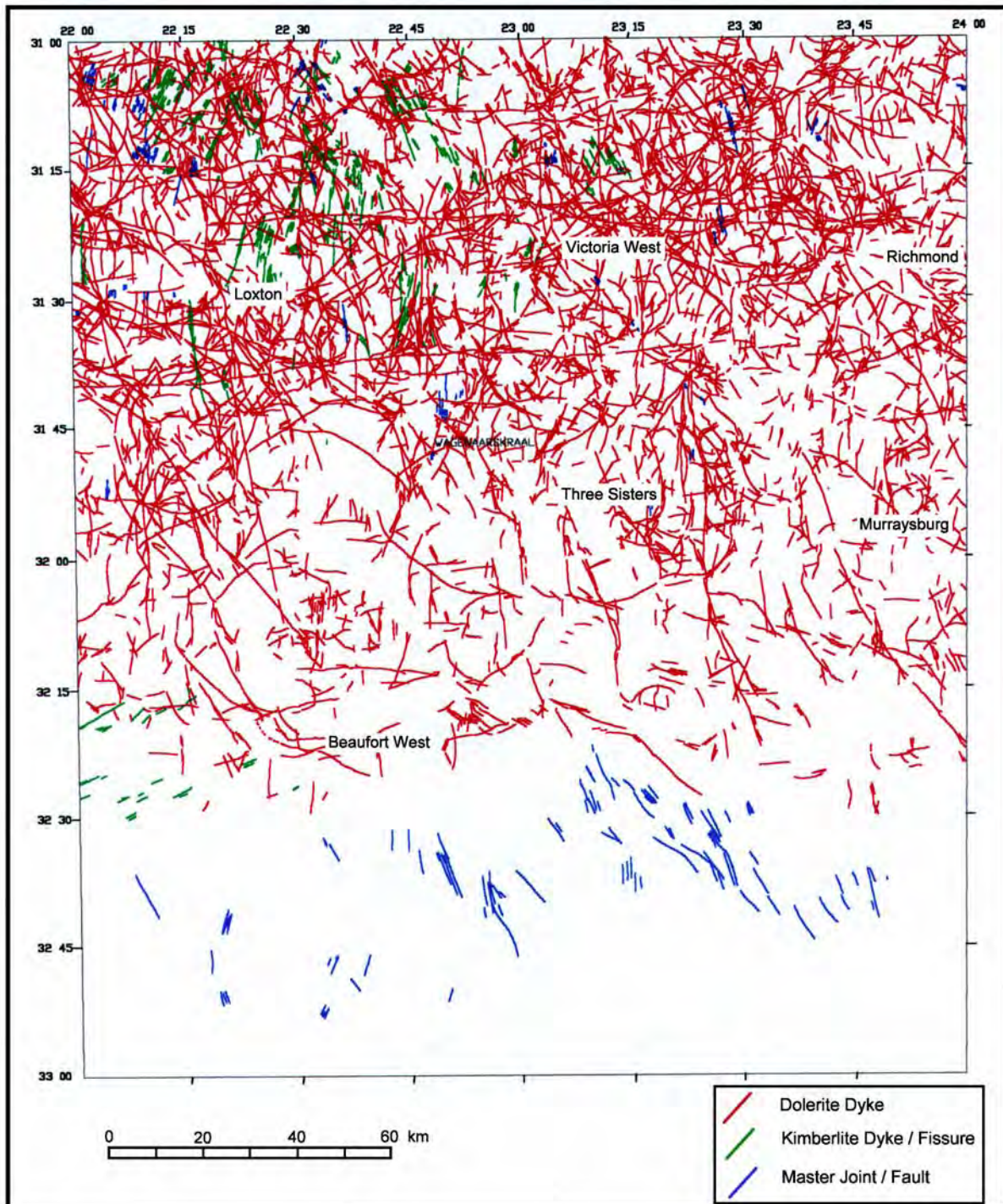


Figure 4.4: *LINAIR - Lineaments captured from aerial-photographs, existing geological maps and field mapping*

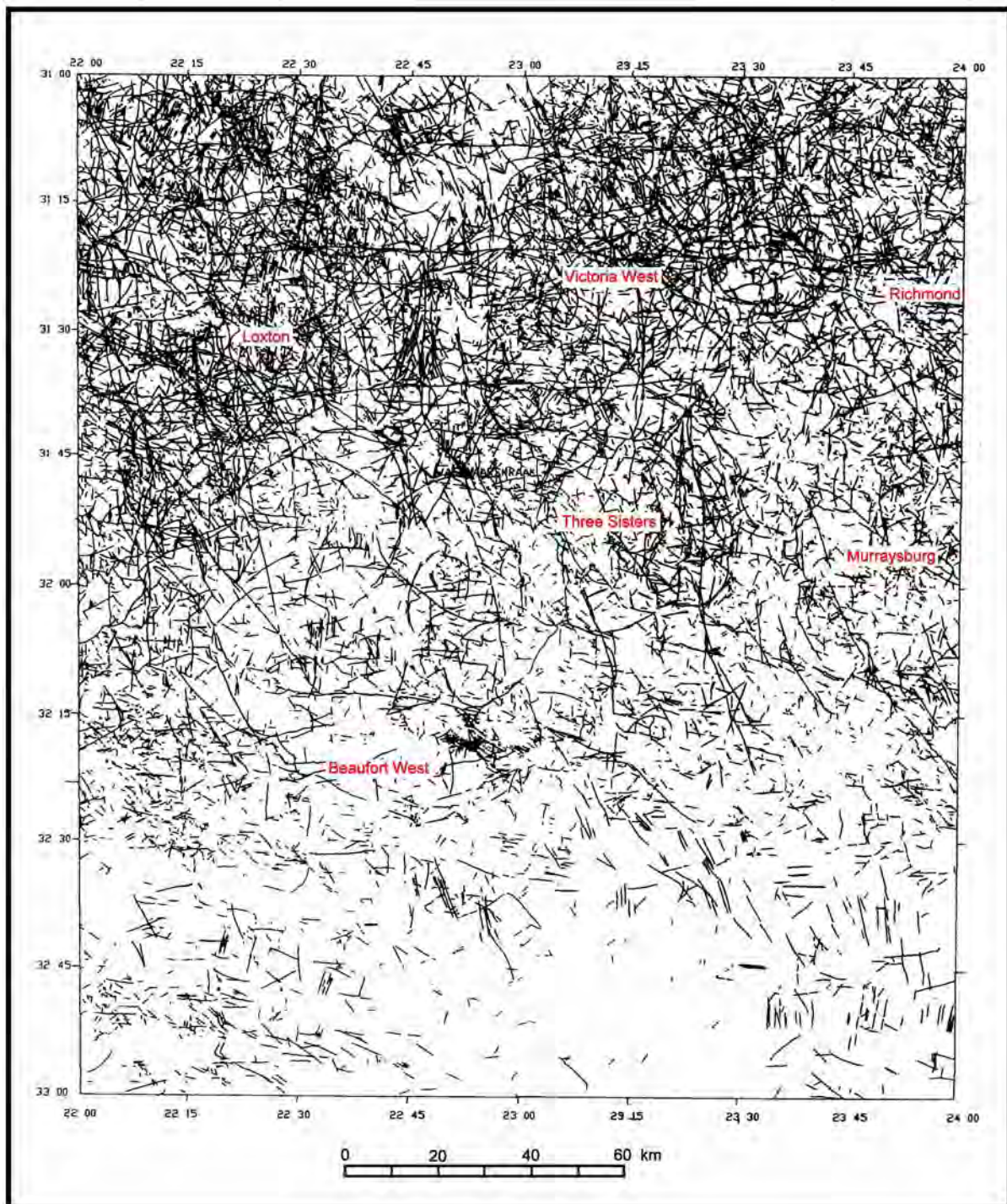


Figure 4.5: *LINCOMP* – Integrated map containing lineaments from *LINAIR*, *LANDSAT TM* and aeromagnetic imagery

Geological lineaments were also mapped onscreen from a 60 x 60 km, digital SPOT image of the Loxton area, where the exploration borehole drilling was conducted. Two separate interpretations were conducted done by two different operators (Figure 4.6(c) and (d))

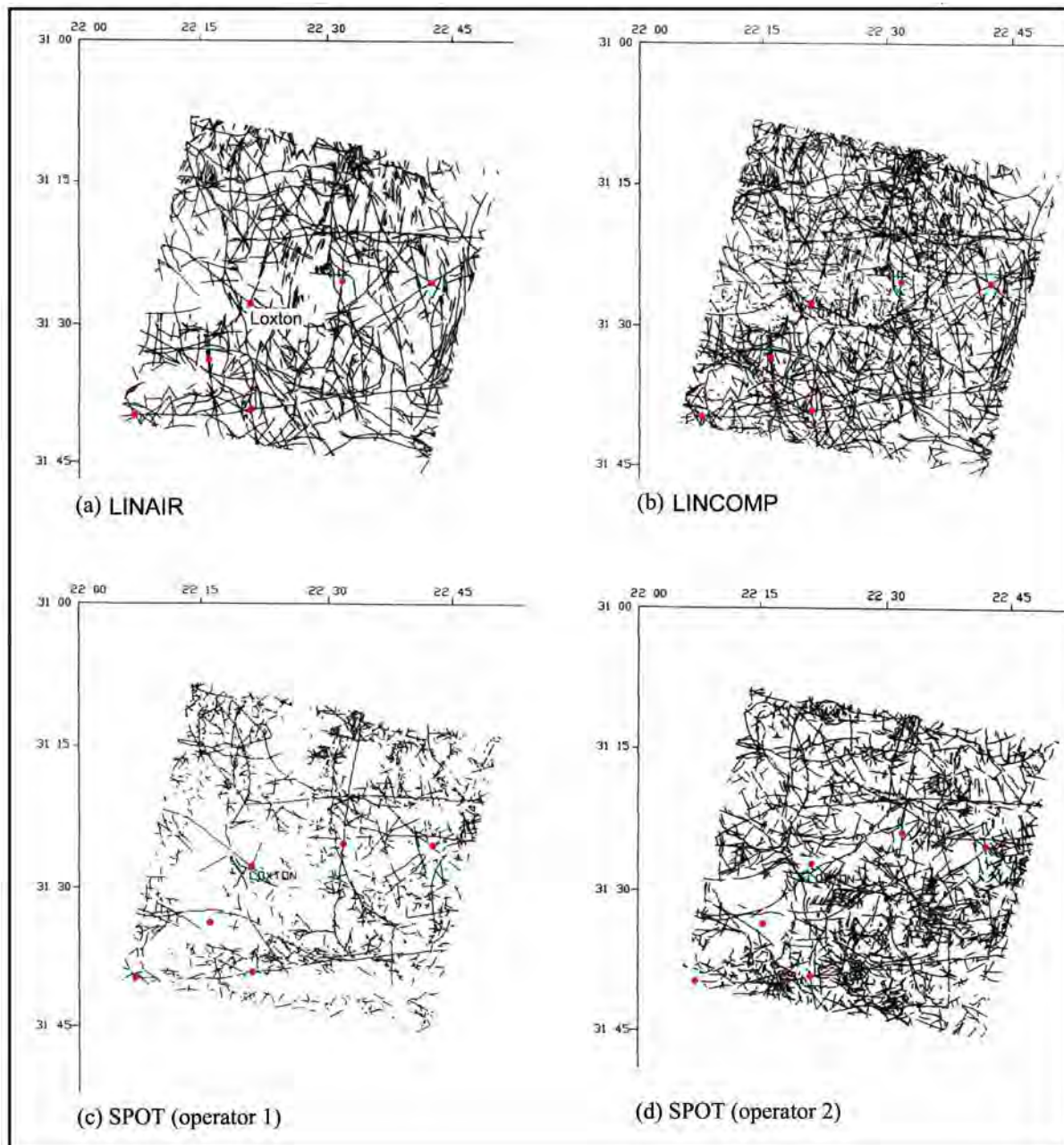


Figure 4.6: A comparison of lineament datasets from the Loxton area (a) LINAIR, (b) LINCOMP, (c) SPOT-1 and (d) SPOT-2. The exploration drilling sites are shown in red.

LINCOMP displays a much greater density of lineaments than LINAIR and contains numerous short ‘fractures’, which are associated with the main directional trends. Major lineaments are also enhanced and ring-like patterns are more prominent. The two SPOT interpretations differ substantially from one another (i.e. two operators) indicating the subjective nature of the mapping process, as well as from LINCOMP and LINAIR. The SPOT imagery enhances structural “knots” and high density fracturing (master-joints).

4.1.2.2 Structural and Stress Analysis

Three different tectonic styles and patterns of lineaments characterise the study area, namely: dolerite dykes, kimberlite fissures and master-joints. Note that the research project excluded the folded terrain to the south of latitude 30°S, as well as the dolerite sills. Many examples of tectonic reactivation were observed in the field (**Plate 2.1**).

The network of dolerite dykes in the study area shows two distinct tectonic patterns:

- a right-lateral E-W shear-dislocation zone, and
- a series of NNW intrusions.

The master-joints form two regional systems, trending NNW and NNE. The later emplacement of the kimberlite fissures was controlled by these dolerite and/or master-joint trends. The NNW fractures appear to be the oldest and most prominent structural features in the study area. They exhibit many signs of tectonic reactivation, as well as recent tectonic movements.

A NW orientated, horizontal crustal compressional system prevailed during and directly after the break-up of Gondwanaland, which accounts for the E-W shear zone and the reactivation of the NNW trending structures. The modern regional tectonic stress regime appears to be characterised by a WNW compressional system (**Chapter 2.5**).

A near-surface stress system is likely to play a dominant role in the reactivation of fractures. Near-surface stresses are created during uplifting and thermal cooling as a result of erosional unloading. Analysis of the surface stresses in the study area shows that a general NE tensional stress can be expected.

Following the structural and stress analysis of geological lineaments in the study area, it is estimated that the N 90° and 150° trending structures are the most likely to have been reactivated and dilated during recent times.

4.1.2.3 Spatial Analysis of Lineaments and Borehole Productivity

Borehole Database

The borehole database of the study area was compiled from DWAF’s National Groundwater Database, geohydrological reports and hydrocensus work (**Figure 4.7**). The borehole data was subdivided according to its positional accuracy.

The boreholes with yield information are most important to this study and the results thereof are presented in **Table 4.4**. The median and average yield of the 3951 ‘wet’ borehole records is 1.50 and 3.84 ℓ/s, respectively. The class II yield statistics are skewed by the inclusion of the relatively high-yielding, scientifically sited boreholes to the north, northeast and south of Beaufort West. This area is indicated by a stippled grey boundary-line in **Figure 4.7**, which contains 1 023 ‘wet’ boreholes indicating the following yield statistics: median 2.220, mean 5.066 ℓ/s, standard deviation 7.482, maximum 94.7 and minimum 0.003 ℓ/s. The yield information of accuracy class I are therefore taken to represent the ‘ambient’ yield statistics for the study area. Only 82 or 1.2% of the boreholes were reported to be ‘dry’.

Table 4.4: *Yield statistics for boreholes within the various accuracy classes*

Borehole dataset	Number	Borehole yield (ℓ/s)				
		Average	Standard deviation	Median	Max	Minimum
No Data	2790	-	-	-	-	-
All ‘Wet’	3951	3.836	6.079	1.500	94.7	0.001
Dry	82	-	-	-	-	-
Total	6823					
Accuracy Class						
I	1917	3.076	4.886	1.300	69.0	0.001
II	1603	4.944	7.405	2.000	94.7	0.005
III	431	3.090	4.598	1.260	40.0	0.003
Total	3951					

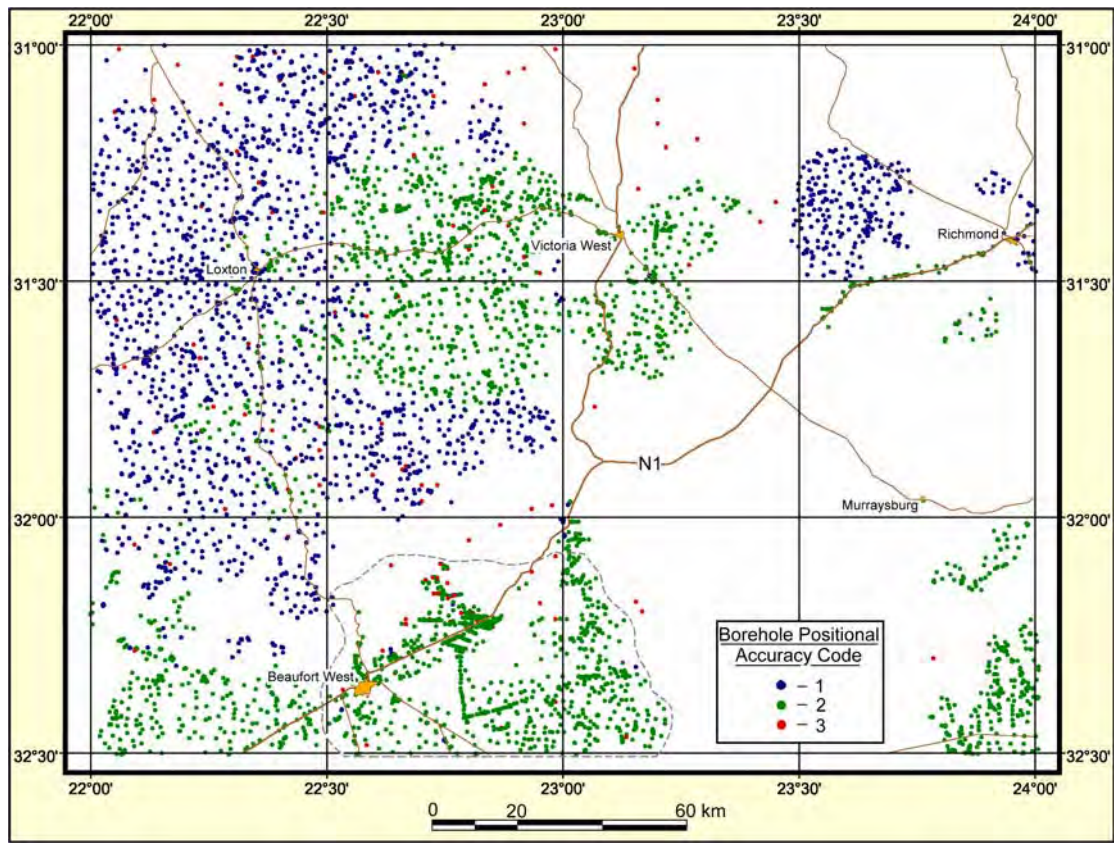


Figure 4.7: Borehole GIS indicating positional accuracy of data

Spatial Analysis

Arc/Info was used to analyse the relationship between borehole productivity and geological lineaments (LINCOMP) in the study area. The influence of the following structural controls was analysed:

- Lineament Zone of Influence
- Lineament Type and Orientation
- Major Lineament Corridors
- Lineament Intersection
- Structural Domains
- Dolerite Sill and Ring-complexes
- Drainage System
- Terrain Slope
- Fracture Spatial Density

The results of the spatial analyses indicated that the following four structural factors control the productivity of boreholes in the study area, namely:

1. Orientation of dolerite dykes trending in 10-30° and 90-150° (**Figure 4.8**), as well as satellite lineaments trending 70-90°.
2. Corridors of major lineaments (**Figure 4.9**).
3. Fracture Spatial Density (FSD) ratio (**Figure 4.10**).
4. Proximity of dolerite sills and ring-complexes (**Figure 4.11**).

The spatial analyses showed that the kimberlite fissures, master-joints, structural domains, drainage system and terrain slope did not significantly influence variations in borehole productivity. Analysis of borehole productivity and lineament intersections yielded similar results to that of the FSD analysis.

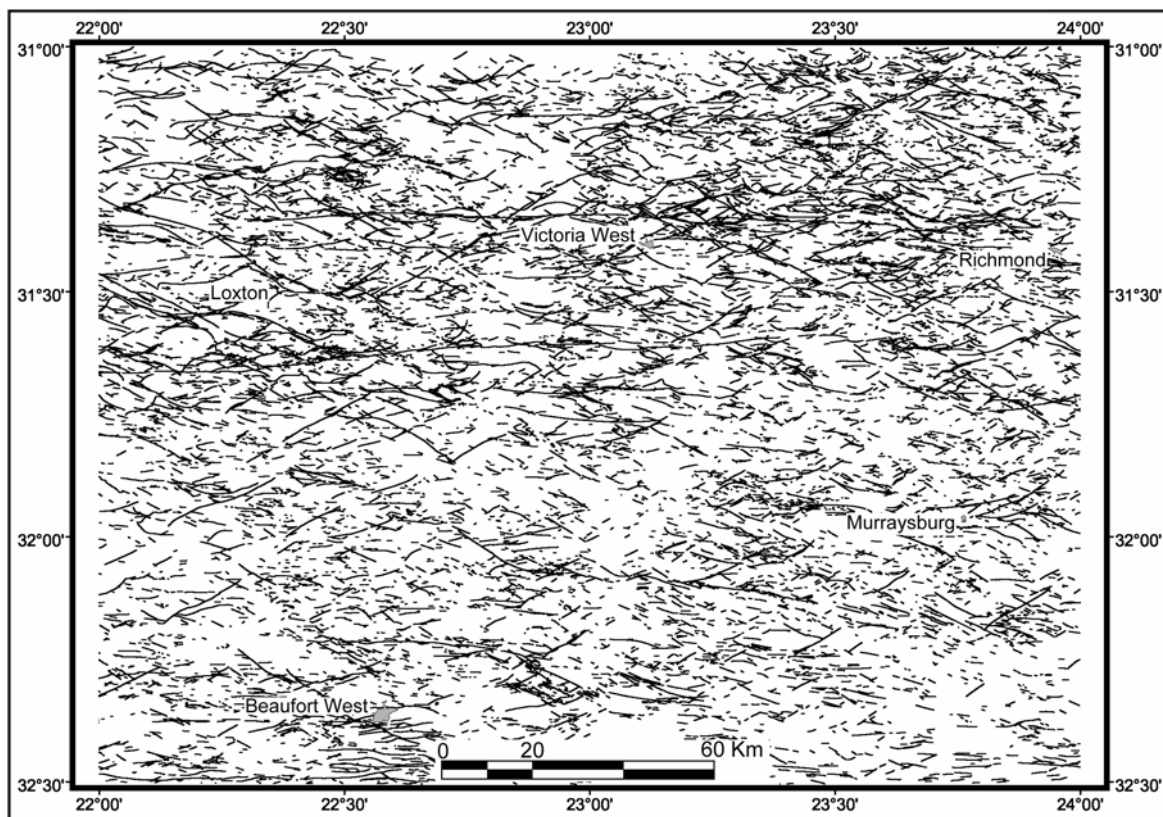


Figure 4.8: *Lineaments with orientations ranging between N70° and N130° (from LINCOMP), correlated with higher than average yielding boreholes*

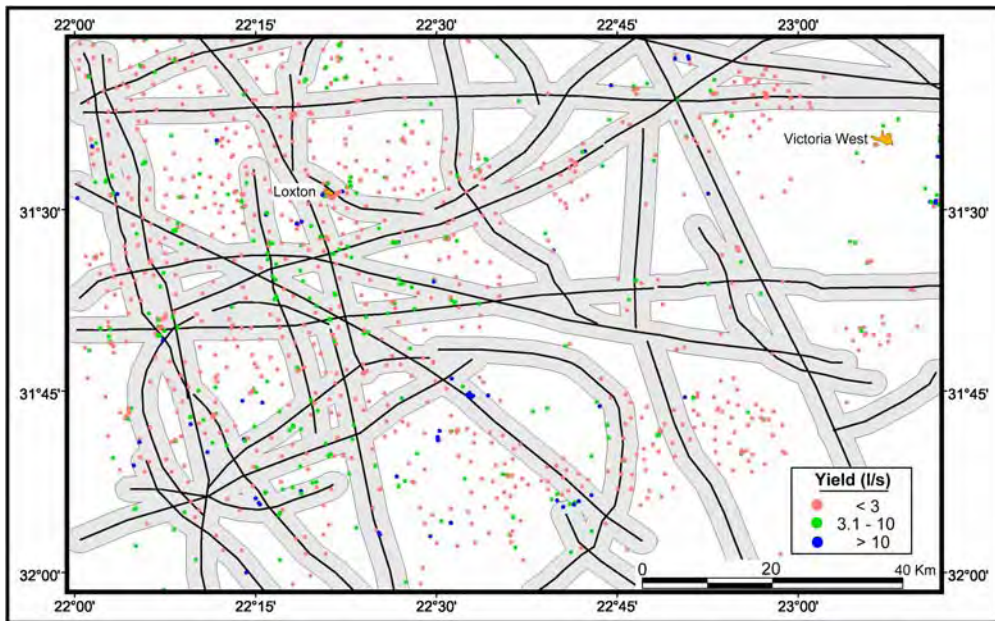


Figure 4.9: 'Wet' borehole yield variations associated with 2 km wide corridors of major lineaments in the Loxton-Victoria West area

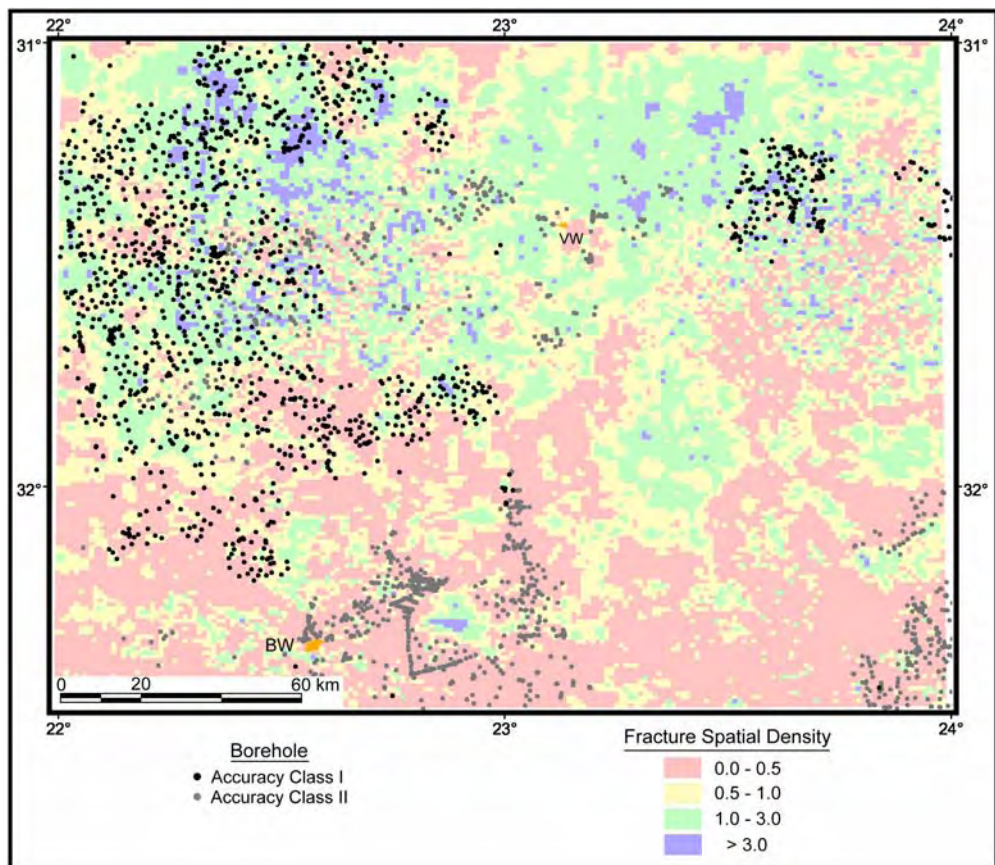


Figure 4.10: Fracture spatial density map showing positions of accuracy classes I and II boreholes

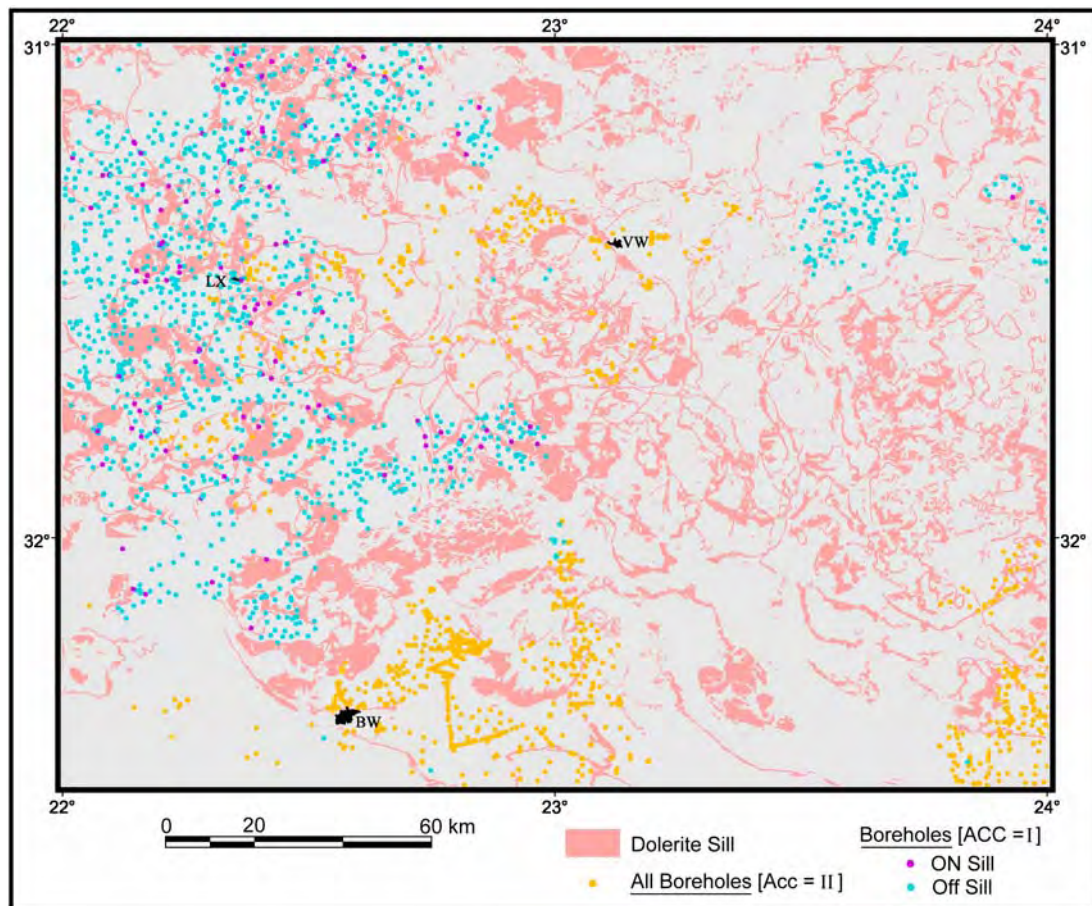


Figure 4.11: *Dolerite sill and ring-complexes of the study area showing the position of ON- and OFF-Sill ‘wet’ boreholes in Positional Accuracy Class I, as well ‘wet’ Boreholes in Accuracy Class II*

Development of a Hydro-tectonic Groundwater Map

The four identified structural controls (**Figures 4.8 – 4.11**) were weighted to produce hydro-tectonic groundwater yield maps using the following procedures:

1. Three 1 000 x 1 000 m cell-size ‘base’-grids indicating the ambient yield conditions of the study area were created, namely a mean-base grid of 3.84 ℓ/s , a median base-grid of 1.50 ℓ/s and a standard deviation (SD) base-grid of 6.08 ℓ/s .
2. A set of ratios were calculated for the mean, median and SD yields of each structural control by dividing each yield by the ambient yield value.
3. Individual 1 000 x 1 000 m SD, mean and median yield ratio grids were created for each of the structural controls.

4. Derivative grids of mean and median yield for the study area were calculated by multiplying the relevant yield 'base'-grids by the mean and median yield grids for each of the structural controls.
5. An upper and lower mean yield grid was also generated by adding and subtracting the SD grid, respectively, from the mean yield grid for the study area.
6. The circular-based 'smoothing' or mean-filter (radius 8 km) was applied to the yield derivative grid.

The mean and median yield maps are presented in **Figures 4.12** and **4.13**. The validity of the mean and median groundwater yield maps of the study area was assessed by comparing the yield zones on the map with the yield statistics of accuracy class I boreholes situated within each zone. Good correlations are found.

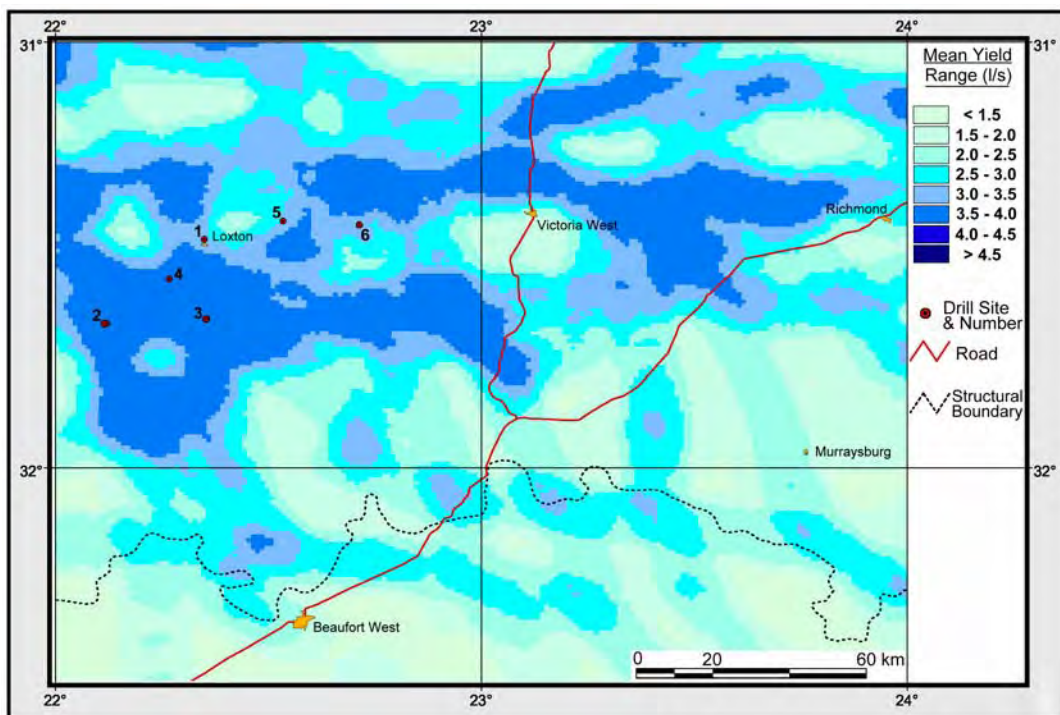


Figure 4.12: *Hydro-tectonic map showing mean groundwater yield showing exploration boreholes used in the case study (Chapter 4.1.2.3)*

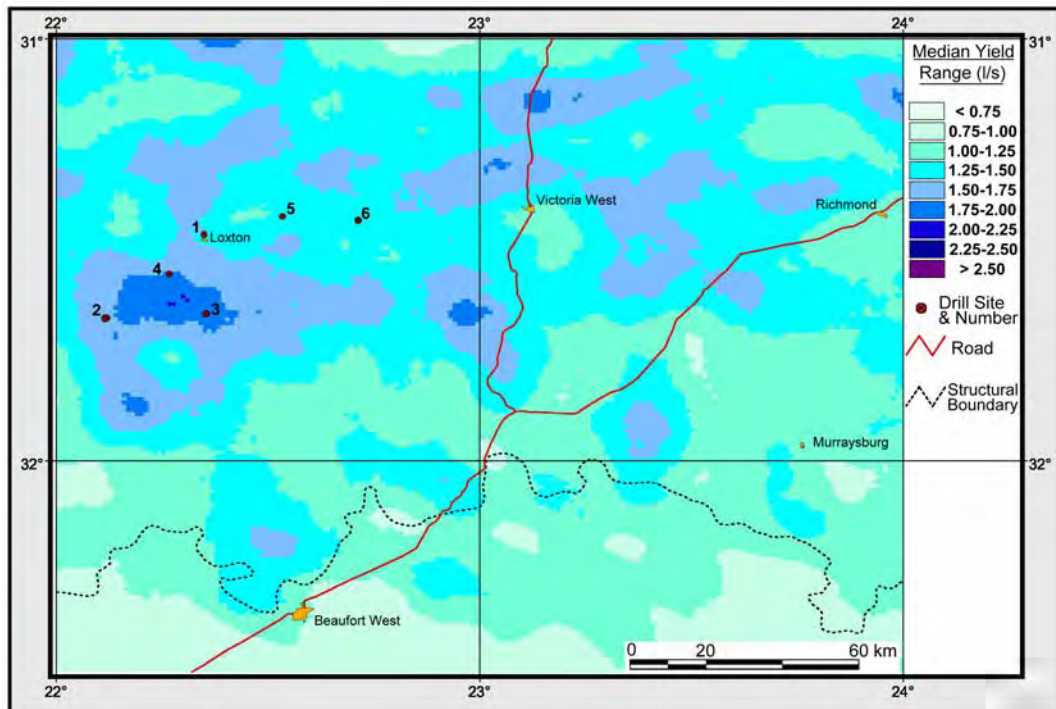


Figure 4.13: Hydro-tectonic map showing median groundwater yield, showing exploration boreholes used in the case study (Chapter 4.1.2.3)

4.1.2.4 Loxton Case Study - Exploration Drilling of Lineaments

Six sites were selected for exploration drilling by the Department of Water Affairs and Forestry (**Figure 4.14**). A number of different structural parameters were used to select each site, namely: type of fracture, major lineaments, orientation, stress-field, reactivation, structural domain and roughness, density of fracturing. The results of the drilling at each exploration site are discussed separately below and summarised in **Table 4.5**.

Site 1: Loxton Allotment

Two boreholes were drilled into the dolerite dyke and three in the kimberlite dyke (**Figure 4.15**). All three boreholes in the kimberlite fissure were ‘dry’, including that drilled at its intersection with a dolerite dyke. The boreholes in the dolerite dyke produced moderate blow-yields of between 3 and 4 l/s (**Table 4.5**).

Site 2: De Wilg

A total of eleven boreholes were drilled (**Figure 4.15**). The E-W dyke produced high blow-yields (up to 15 l/s) and the majority of water strikes occurred at depths of between 100 and 230 m.bgl (**Table 4.5**), where the dyke displays a very complex offset pattern (**Figure 2.25**). The boreholes on the NNW dyke were ‘dry’.

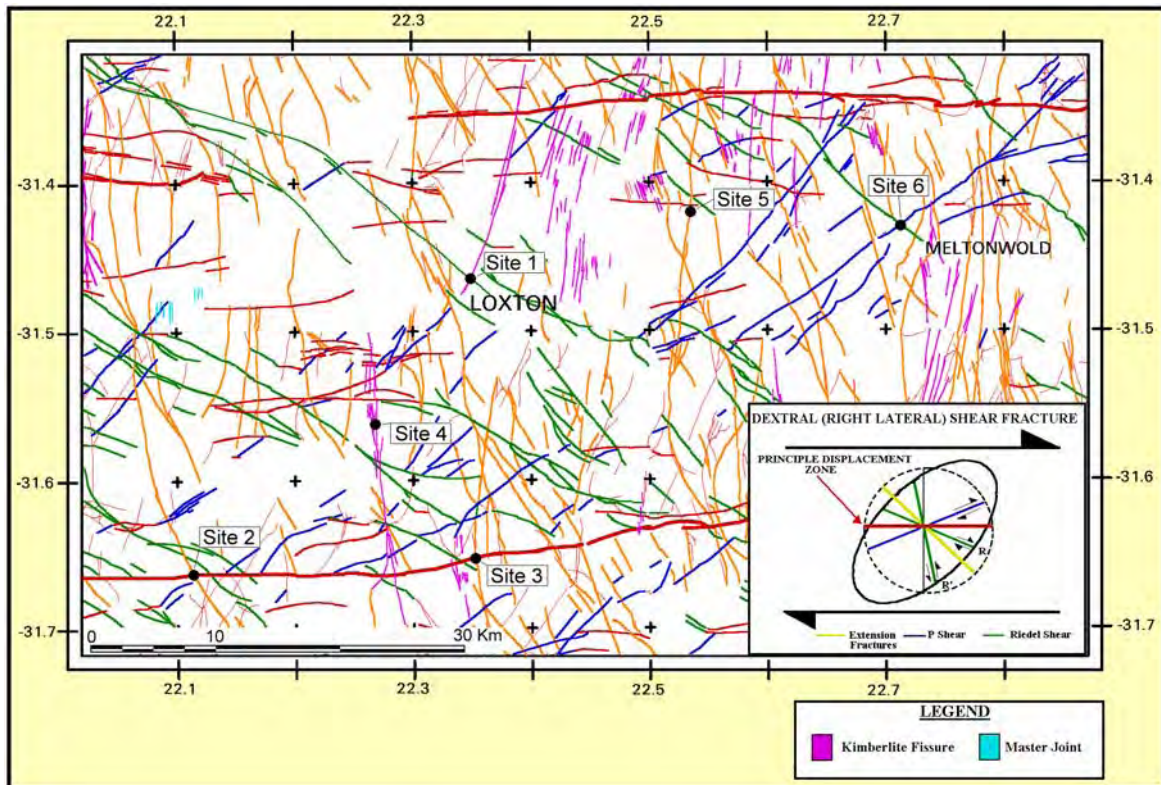


Figure 4.14: Lineament map indicating exploration drill-sites in the Loxton Area. Inset map indicates various structural types of dolerite dykes that developed along the Jurassic E-W dextral shear zone: **Red** - E-W strike-slip fractures, **Green** - riedel-type fractures, **Blue** - P-type fractures. Orange lineaments - NNW dolerite dykes. Other lineaments are: **purple** - kimberlite fissures and **turquoise** - master-joints. Under the modern WNW compressive regional stress regime lineaments trending between $N90^\circ$ and $N150^\circ$ are supposed have been reactivated.

Site 3: Midlands

A total of ten boreholes were drilled (**Figure 4.15**). All of the boreholes were successful and delivered moderate to high blow-yields (**Table 4.5**). The borehole drilled at the intersection of the two features delivered the highest blow-yield (32 l/s)

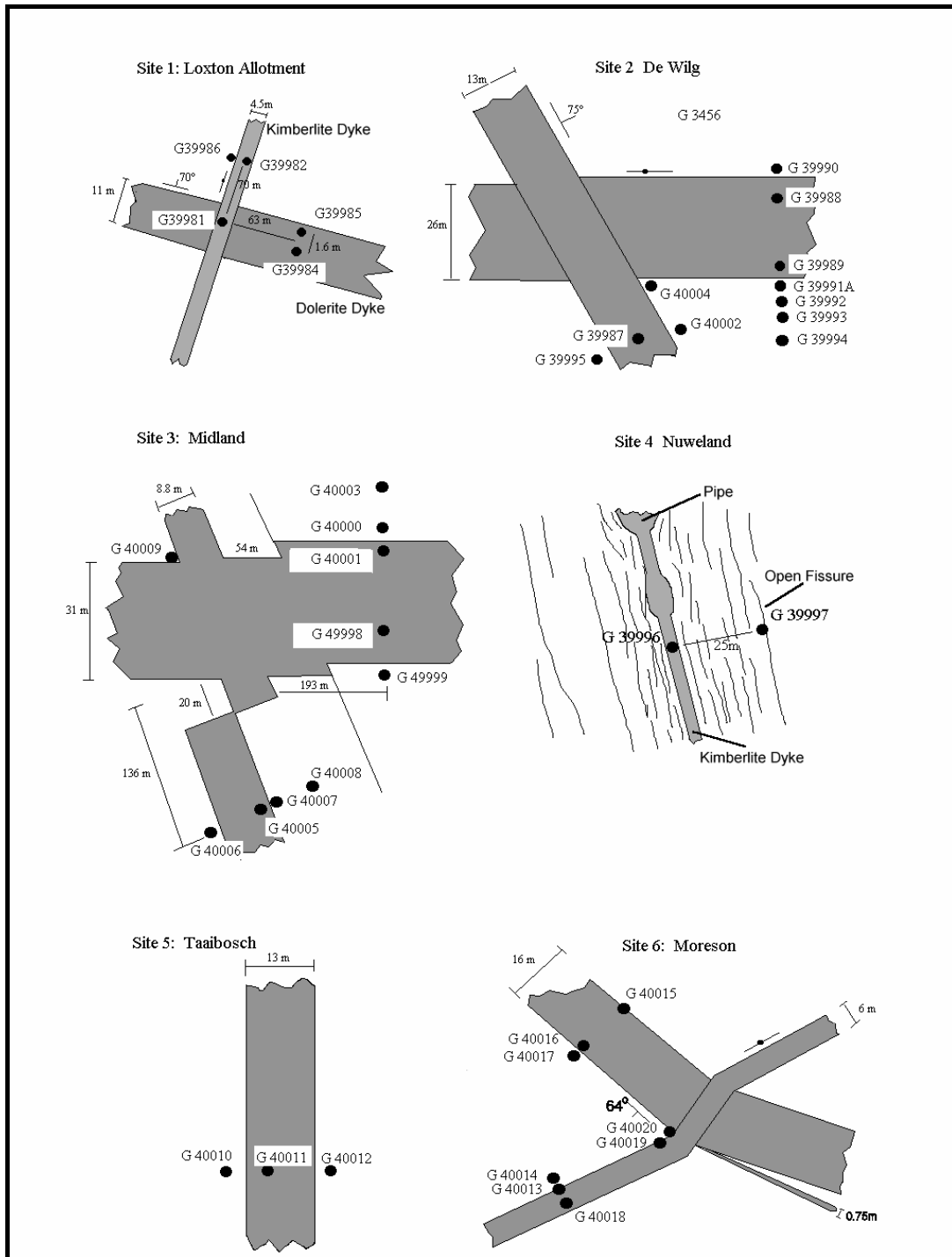


Figure 4.15: Detail plans of exploration drilling sites at Loxton

Table 4.5: Summary of Loxton exploration drilling results

Site No.	Borehole number	Depth (m)	Blow-yield (ℓ/s)	Water level (m.bgl)	Final EC (mS/m)	Depth of water strike(s) (m.bgl)
1	G39981	151	0.05	10.62	77	14
	G39982	151	dry	-	-	-
	G39984	109	3.40	10.18	44	54,61,69,72,101
	G39985	61	3.40	10.08	-	61,69,72,101
	G39986	151	dry	11.44	-	-
2	G39987	157	0.05	9.90	-	97
	G39988	201	2.00	6.61	250	108,121
	G39989	175	3.60	6.70	299	73,108,124
	G39990	211	0.20	6.67	304	99,148
	G39991A	250	15.10	6.74	230	113,170,177,180,202,213,221.5
	G39992	253	2.80	6.82	273	95,106,111,159,170,214
	G39993	251	10.90	6.67	246	105.5,118,142-145,156,162,172,178,194,215
	G39994	254	0.10	6.52	-	194
	G39995	251	dry	8.95	-	-
	G40002	250	1.85	10.00	136	145,164.5,187,226
	G40004	250	10.30	8.94	93	10,19,31,90,103,123,144,165,223,225
3	G39998	250	6.00	5.15	163	12,24,50,149,162
	G39999	250	12.70	5.10	163	20,22,61,204
	G40000	250	23.80	4.35	166	17,20,57
	G40001C	144	13.50	3.19	191	20
	G40003	250	1.85	4.45	127	46
	G40005	252	5.00	8.93	139	60,110-112
	G40006	216	25.30	6.84	103	9,21,41,82
	G40007	240	16.50	8.53	142	17,20,27,35,40,50,54
	G40008	186	28.00	8.26	144	24,40,58,68.5,119,184,186
	G40009	208	31.70	4.69	146	14,15,18,19,21,23,25,29,32,33,36,60,62
4	G39996	162	0.01	16.09	90	16,59
	G39997	150	4.00	17.08	87	59,128
5	G40010	249	1.10	9.35	68	13, 95
	G40011	255	1.10	11.03	66	(39-41m Calcite fill fissure), 68, 144
	G40012	246	4.42	12.58	56	17, 67
6	G40013	252	0.15	16.90	67	21
	G40014	204	0.53	17.00	80	32
	G40015	100	0.01	12.47	82	23
	G40016	252	1.50	11.92	75	27
	G40017	252	2.55	11.60	79	19
	G40018	252	0.05	17.05	78	97
	G40019	132	0.55	17.05	73	25
	G40020	252	0.75	17.24	143	27, 47
Notes: <ul style="list-style-type: none"> G40004 (Green) – Borehole drilled at intersection of two structural features. 1.00 – Depth (m.bgl) of main water strike. 1.00 – Depth (m.bgl) of individual water strike in excess of 3 ℓ/s. 1.00 – Yield (ℓ/s) greater than median borehole yield for study area of 1.3 ℓ/s. 						

Site 4: Nuweland

The drilling target is a 3 m wide, N-S trending kimberlite dyke, with a ‘blow’ and a pipe, as well as a series of parallel mega-joints and fissures (**Figure 4.15**). The dyke was not detected on the SPOT imagery by either of the interpreters. The borehole in the kimberlite was ‘dry’, whilst the borehole in one of the parallel fracture systems away from the dyke yielded 4.0 ℓ/s (**Table 4.5**).

Site 5: Taaiboschfontein

A NS-NNE trending dolerite dyke was targeted that was reactivated during the emplacement of the kimberlite. Many kimberlite fissures follow the same trend in the area (**Figure 2.61**). The dyke represents a mega-lineament, which falls within the theoretical N90°-N150° trend of possible modern reactivation. In outcrop, the dyke is highly fractured and sheared, with most of the fractures being filled with calcite or calcrete (**Plate 2.1**). Three boreholes were drilled at this site (**Figure 4.15**), with only one moderate yielding (4.4 ℓ/s) borehole (**Table 4.5**).

Site 6: Moreson

A thin NE-trending dolerite dyke did not, as anticipated, yield any significant amounts of groundwater (**Table 4.5, Figure 4.15**). Boreholes drilled into the NW-orientated structure showed it to be an inclined sheet (a dipping 64°SE, curvilinear body), rather than a dyke. Moderate yields of 1.5 - 2.6 ℓ/s were struck at shallow depths within and along the upper contact of the inclined sheet.

Discussion

The exploratory drilling programme in the vicinity of Loxton showed that:

- The E-W mega-lineaments (Shear Zone) produced high-yielding boreholes. The overall borehole yield improving if the site is located close to a structural 'knot'.
- The NNW lineaments form a second strong structural overprint in the Western Karoo. However, boreholes drilled on these features at Site 2 produced low yields, whilst high borehole yields were intercepted at Site 4 located close to a structural 'knot'.
- The NW dolerite dykes (possibly recently reactivated) delivered moderate yields at Site 1 and Site 6, although the structure at Site 6 proved to be an inclined sheet.
- Boreholes drilled on the N-S and NNE lineaments, which represent kimberlite dykes, master-joints or kimberlite-reactivated dolerite dykes, were moderate to low yielding. This could be ascribed to the poor hydrological properties of the kimberlitic material and/or to the unfavourable orientation of the lineaments.
- The NE-trending lineaments are supposedly 'closed' under the modern WNW compressional stress regime. Only one of these lineaments were drilled at Site 6 and the boreholes were 'dry'.

The six drilling sites are all located within zones of medium to high yield potential. The most productive boreholes occur at Sites 2 and 3 located within or in the proximity of a zone of high mean (**Figure 4.12**) and median (**Figure 4.13**) yield potential. Drill site 4 also falls within this high yield potential zone even though the kimberlite fissures and master-joints targeted were found to be associated with low-yielding boreholes. It is, however, anticipated that higher yields would have been obtained if a more favourable type and orientation of lineament had been selected for drilling (i.e. E-W trending dolerite dyke). The least productive Sites, 1, 5 and 6, are situated in zones of medium to low potential on the mean and median yield maps, respectively.

Two important conclusions relating to the occurrence of groundwater can thus be drawn:

1. The E-W and NW trending lineaments are within the N90° - N150° range of possible modern reactivation. They were more productive than the NNW, NS, NNE and NE lineaments, which lie outside this orientation range.
2. It appears that structural 'knots' could play a significant role in siting of successful production boreholes in Karoo fractured-rock aquifers. Panchromatic SPOT or merged SPOT / LANDSAT TM imagery is preferred for lineament and structural mapping in the Karoo Basin, when compared to LANDSAT TM or aerial-photographs alone.

4.1.3 GEOPHYSICS

4.1.3.1 Introduction

The application of geophysical techniques to the study of the Karoo Basin can be grouped in five categories, namely:

- geophysics applied to shallow targets that have a direct bearing on groundwater occurrence and geohydrology in general,
- applied geophysical research aimed at studying the geometry of aquifers in detail, the tracing of dolerite dykes in the coal industry (airborne, surface and underground techniques) and to investigate the nature of dolerite ring-structures,
- geophysics applied in studies of groundwater pollution and other environmental investigations,
- geophysics applied to deep-seated targets such as oil exploration and in unravelling the structural complexities of the basement to the Karoo Basin, the occurrence of the dolerite intrusions in the Karoo, and the inter-relationship between the Karoo and the Cape Fold Belt, and
- geophysics in the search of economic mineral deposits (coal, diamonds, uranium, gold under a cover of Karoo sediments, etc.).

The objective of this section is twofold. The first objective is to describe, by way of examples, those techniques that have over the years proven to be most successful in identifying groundwater drilling-targets. As part of this objective, the correct use of the techniques and potential for further development of these techniques will be addressed. Secondly, to identify and describe those techniques which have potential, whether from a practical or research viewpoint, to become a tool that can and should be used in future to enhance our knowledge on the occurrence and behaviour of Karoo fractured-rock aquifers.

In terms of these objectives, only the first four categories mentioned above are relevant in the context of this book. In order to address these objectives, however, the primary focus will be on the practical application of the different geophysical techniques to the exploration for groundwater resources. A wide variety of geophysical techniques are applicable, but not necessarily currently employed, to the Karoo environment and therefore warrant discussion.

The **Sections 4.1.3.2 - 4.1.3.3** are of an introductory nature and are followed by a brief description of the different geophysical techniques available to the practitioner and researcher in the exploration for groundwater, as well as to increase our understanding of the complexities of the Karoo fractured-rock aquifers.

Information for this section was mainly obtained from publications in journals, unpublished technical reports of the Directorate of Geohydrology (DWAF), unpublished internal reports of the Geological Survey of South Africa, Memoirs and Bulletins of the Geological Survey, reports of the Water Research Commission, consultants reports and the authors experience.

4.1.3.2 Description of Commonly Applied Techniques

Ground Magnetic Surveys

Magnetic techniques are one of the oldest methods of geophysical exploration and measure variations in the earth's magnetic field. Magnetic anomalies in the earth's field are caused by two types of magnetism, namely (i) induced and (ii) remnant or permanent magnetism. The induced magnetism of a body is in the same direction as the present day earth's field, whereas remnant magnetism need not be in the same direction and could even oppose the earth's field. Modern magnetometers, referred to as proton magnetometers record the total magnetic field, while the earlier instruments measured either the horizontal or vertical components of the earth's magnetic field. Some of the pioneering geophysical groundwater exploration in South Africa, and in particular in the Karoo Basin, was carried out using magnetometers measuring the vertical component of the earth's field, to trace the position and orientation of dolerite intrusions (Enslin, 1950). Magnetic surveys are relatively inexpensive, the instrumentation is easy to operate and interpretation of signatures from dyke intrusions or dolerite/sediment contacts are relatively easy to perform using either standard anomaly curves or with the appropriate and readily available PC software.

Aeromagnetic Imagery

Airborne magnetic surveys can cover large areas in a relatively short period of time, using helicopters or low-flying aircraft trailing a magnetometer (referred to as the 'bird'). Although these surveys do not have the same spatial resolution of ground surveys, they are invaluable for tracing larger structural features, and especially major dyke intrusions into the Karoo sediments. The entire Karoo Basin has been covered by aeromagnetic surveys carried out on behalf of the Council for Geoscience and are available in digital format (re-sampled to a 400 x 400 m grid cell-size) or as printed maps at scales of 1:50 000 and 1:250 000.

High-resolution airborne magnetic surveys are commonly used to produce detailed maps of dolerite structures in the Karoo. The technique employs a low-flying microlight with the following specifications:

- Survey flying height: 50 m (as low as possible)
- Line Spacing: 200 m
- Sample Spacing Magnetics: 3 m
- Sample Spacing Radiometrics: 30 m
- Calculated Magnetic Grid Spacing at a quarter of the line spacing
- The 200 m survey consisted of 278 lines.
- Traverses are numbered 20 to 2 880.
- Tie lines are numbered 9 010 to 9 100.
- A total of 7 510 km was flown on line.

The survey is undertaken using the following equipment:

- A Jabiru ultralight aircraft
- Geometrics G822A cesium vapour magnetometer
- A Bicron 4l NaI(Tl) detector with ancillary equipment, in an onboard PC.
- A SATLOC real-time differential GPS recording once a second to an accuracy of less than 3 m in x and y and 5 m in Z is utilized.
- The SATLOC GPS controls the navigation.
- A highly focused Riegl laser altimeter is utilized.
- A Geometrics G856AG or Geotron G5 is utilized for sunspot monitoring and for diurnal correction.

Radiometric

Radiometric surveys are conducted to assess the presence of radioactive minerals located at relatively shallow depths in the subsurface. It is mainly used for aerial reconnaissance purposes and is generally not used in groundwater exploration. During the 1970s, this technique was extensively applied in the exploration for uranium deposits in the Main Karoo Basin and some of this information is available in map format from the Council for Geoscience. High-resolution radiometric information is also simultaneously gathered during high-resolution aeromagnetic surveys (see above).

Electrical and Electromagnetic Techniques

Apart from the magnetic technique, electrical and electromagnetic techniques are the most commonly and widely used techniques in groundwater exploration of Karoo aquifers. The immediate purpose of the electrical method is to determine the resistivity of various rock types, as well as the resistivity variation with depth and lateral extent. In general, the resistivities of the Karoo sediments are significantly lower than that of the crystalline rocks. The Karoo sediments therefore seldom have

resistivities of greater than a thousand ohm-metres, and are generally in the order of a few tens to a few hundreds of ohm-metres. In this regard the shale and mudstone successions are more conductive (less resistive) than the sandstone units. On the other hand, dolerite is highly resistive, which results in a high contrast between itself and the surrounding host rocks and it is therefore a good target for electrical techniques.

Electrical surveys are primarily applied in two modes: (1) depth soundings and (2) horizontal profiling. Depth soundings are mainly used to determine the thicknesses of layers, depth of weathering and the depth to the first thick dolerite sill. On the other hand, profiling techniques are used to trace lateral variations in resistivity at a constant depth, which could indicate the presence of intrusive structures, faults and fracture zones, as well as the degree of weathering associated with these structures. For soundings, the best results are achieved using the Schlumberger array, whilst during profiling both the Wenner and Schlumberger arrays are commonly used. However, lateral effects are reduced when using the Schlumberger technique for profiling.

Electromagnetic (EM) techniques, as the name implies, is a combination of the magnetic and electrical method and is primarily employed for profiling. This technique involves placing a transmitter coil (Tx) on the ground surface and energising it with an alternating current at audio frequency. The time-varying magnetic field arising from the alternating current in the transmitter coil induces very small currents into the earth. These generate a secondary magnetic field, which, together with the primary field, are sensed by the receiver coil (Rx), usually placed a short distance away. The ratio of the secondary to the primary magnetic field is linearly proportional to the ground conductivity.

The Geonics EM-34 instrument is most commonly used in groundwater exploration and it is best used in profiling mode, although it can also be used to do qualitative depth soundings (Botha et al., 1992). The more sophisticated and expensive EM-37 and EM-47 units, primarily designed for depth soundings, are seldom applied in groundwater studies. However, their application in Karoo environments is often restricted because of the generally conductive nature of the Karoo formations, which limits the depth penetration unless relatively large transmitter coils are employed.

Gravity Techniques

The gravity method involves measuring the natural variations in the force of gravity. Such variations are primarily caused by density differences within different formations. In South African hydrogeological investigations, gravity prospecting is mainly used for locating zones of karst development, fractured dolomite or determination of the bedrock geometry beneath extensive alluvial-filled basins, where a large density contrasts often exist between the unconsolidated sediments and the basement rocks. Its application to Karoo aquifers is limited.

Seismic Techniques

Seismic prospecting is based upon the analysis of propagation times of elastic waves within the earth. Seismic waves are generated by an artificial source that is either located on the surface or underground. The travel time of these waves to reach a series of receivers or ‘geophones’, depends upon the travel path. Information on the nature of the overlying formations and depth to various geological layers can be determined by analysing these travel time records. The most commonly used technique in groundwater applications is seismic refraction. It is a fairly time consuming and expensive technique, and although it has potential applications in a Karoo environment, but it is seldom used.

Radar Techniques

Ground Penetrating Radar (GPR)

Ground Penetrating Radar (GPR) operates on the principle that electromagnetic waves emitted from a transmitter antenna are reflected from buried objects and detected at another antenna, called the receiver. The signals recorded at the receiver provide an image or cross-section of the subsurface that is similar in appearance to that obtained from seismic reflection instruments, which are widely used in the oil industry. GPR is a high-resolution geophysical technique that is similar to normal radar, with the exception that the electromagnetic pulses are transmitted through the ground rather than through air.

Borehole Radar

Similar to GPR, borehole radar operates on the principle that electromagnetic waves emitted from a transmitter antenna are reflected from surfaces and objects in the rockmass, and are detected by the receiver antenna. The differences are, however, mainly in the instrument design where one of the challenges is to construct a suitable antenna that can fit into the relatively narrow diameter of a borehole. Using radar tomography, the presence of subsurface fresh-water bodies can be mapped. Here radar travel times are measured in transmission mode, and images of radiowave velocity, instead of attenuation rates, are produced. The system can be used in two modes; either single-hole reflection or cross-hole measurements.

Geophysical Borehole Logging

A wide variety of geophysical borehole-logging techniques are available to the practising geohydrologist, as well as to researchers. Most of the techniques have been developed for the oil exploration industry and adapted for geohydrological applications. The most common techniques applied in the ground water industry, with their field application, are listed in **Table 4.6**.

The reader is referred to the texts of Repsold (1989) and Keys (1989), where detailed descriptions of geohydrological applications of the different techniques are illustrated with many practical examples.

Table 4.6: Geophysical borehole logging tools and their fields of application

Technique	Types of log	Field of application
Radioactivity	Natural gamma Gamma-gamma Neutron	Clay content; rock structure and lithology Rock density; porosity; fracturing Porosity
Resistivity	Normal (multiple array). Focussed Induction	Rock or formation resistivity; lithology; detection of thin (clay) layers
Caliper	Caliper log	Borehole or casing diameter
Temperature (water)	Temperature	Ground water temperature; fracture location; geothermal gradient
Conductivity (water)	Conductivity	Ground water conductivity; water quality stratification (pollution investigations)
Sonic	Accusti-log	
Groundwater flow	Flowmeter	Ground water flow velocity; inflow points (water bearing fractures)
Borehole orientation	Dipmeter Deviation	Dip and strike of penetrated layers, fractures and fissures. Spatial course of borehole
Optical	Borehole or TV camera	Casing attributes (Damage, clogging); fracture position; visual inspection of borehole sides

Tomography Techniques

Radiowave Tomography

Radiowave tomography (RT) is a novel geophysical technique that utilises radiowaves to extrapolate geological information between boreholes by producing attenuation images of the intervening rockmass. Since radiowave attenuation rate is primarily a function of conductivity, geological features correlating to changes in conductivity are thus mapped.

The RT equipment comprises the following components:

- a down-hole radiowave transmitter (Tx),
- receiver (Rx) probes,
- a radiowave receiver unit located at the borehole collar,
- cabling and winches for lowering the two probes down the boreholes,
- a PC-based control unit,
- fibre-optic links for recording the data and controlling the transmitter and receiver units, and
- data processing software.

RT is usually applied at frequencies of between 1 and 30 MHz, but frequencies as high as 90 MHz have been used in studies of the Karoo formations. There is a trade-off between resolution, depth of penetration and the frequencies used.

The different scanning modes include:

1. *Reconnaissance parallel scans*: used to determine operating ranges and frequencies,
2. *Background imaging* used for lithology characterization,
3. *Differential tomography* to produce images of the gradient of the attenuation of the rockmass with respect to frequency, and
4. *Alterant tomography* that is used to track tracer flow directly thereby giving an indication of flow paths and the porosity of the medium.

In general, the technique is most applicable to the mapping of conductive features within resistive country rocks. Features that fall into this category are weathered zones, fissures filled with saline water, base-metal mineralization, and electrically distinct lithologies, such as clays and sandstone.

Seismic Tomography

The principles of seismic tomography (ST) are similar to that of RT. The variation in seismic velocity is mapped in ST, whereas the variations in electrical conductivity are mapped in RT. Similar to the RT method, a seismic source (Tx) is lowered into one borehole, whilst geophones (Rx) are lowered into another borehole. Seismic borehole tomography provides a propagation seismic velocity profile in the borehole plane, which can ultimately be used to produce a respective geological cross-section between the two boreholes, using all other available information.

Resistivity Tomography

Resistivity tomography is also a new and exiting technique available to the researchers and practitioners in geohydrology. Two boreholes are required for the source field electrodes, while potential field measurements are made on surface. By lowering the source field electrodes progressively down the boreholes, the area between boreholes can be imaged at increasing depths. The technique has been developed at the CSIR and has thus far been applied mainly in the coal industry to locate structural features such as dolerite dykes and faults. The advantage of the technique is its ability to trace very thin structures that are not normally detectable with other ground or aeromagnetic techniques, unless a very detailed and high-resolution survey is conducted. The method has great potential in the assessment of groundwater pollution, although it has only been tested to a limited extent.

4.1.3.3 Examples of Groundwater Exploration Techniques Routinely Applied To Karoo Aquifers

Target Features

Groundwater is known to occur in several ways in the Karoo environment. The more important ones are:

- groundwater associated with dolerite intrusions;
- groundwater associated with structural features other than those associated with dolerite intrusions;
- horizontal or near horizontal fractures along bedding planes and formation interfaces;
- other fracture and joint systems;
- within more porous sedimentary successions (e.g. Cave sandstone);
- shallow groundwater associated with near surface calcrete layers; and
- in alluvial deposits associated with ephemeral rivers and streams.

From this it is clear that the geophysical target is varied and therefore no one technique will be successful for all the different modes of groundwater occurrence. In the following sections these different situations and how geophysical techniques can be employed most efficiently, will be addressed.

Magnetic Techniques

Dolerite intrusions, particularly the dykes, are one of the more important targets for high-yielding boreholes in the Karoo rocks (**Chapter 2.3.2.1**). Groundwater is associated in different ways with dolerite dykes, it is most often associated with the contact zone between the sediments and the dolerite, but there are also cases where the most successes are achieved by drilling into the centre of the dyke. The contact

zone ring-dykes and the surrounding sedimentary units, as well as the basin formed by inner-sill are also known for their water-bearing properties.

Magnetic surveys have proven themselves over the years to be the most efficient way to trace dolerite intrusions and these have been applied successfully in South Africa for more than 50 years (Frommurze, 1937; Maree, 1943; Van Eeden and Enslin, 1948; Enslin, 1950; Enslin, 1955; de Villiers, 1961; Campbell, 1975; Gombar, 1977; Vandoolaeghe, 1980; Vandoolaeghe, 1979; Potgieter, 1981, Woodford, 1984 and others).

The introduction of large-scale aeromagnetic surveys during the 1960s and 1970s, allowed for the identification of the larger dolerite structures in the Karoo. This data is commonly used during the initial reconnaissance phase of an investigation – prior to any more detailed ground magnetic surveys. An example taken from the newly produced Magnetic Fabric map (Council for Geoscience, 1998) at a scale of 1:1 000 000, shows the magnetic signature of the dolerite ring-complexes and large dolerite dykes (**Figure 4.16**).

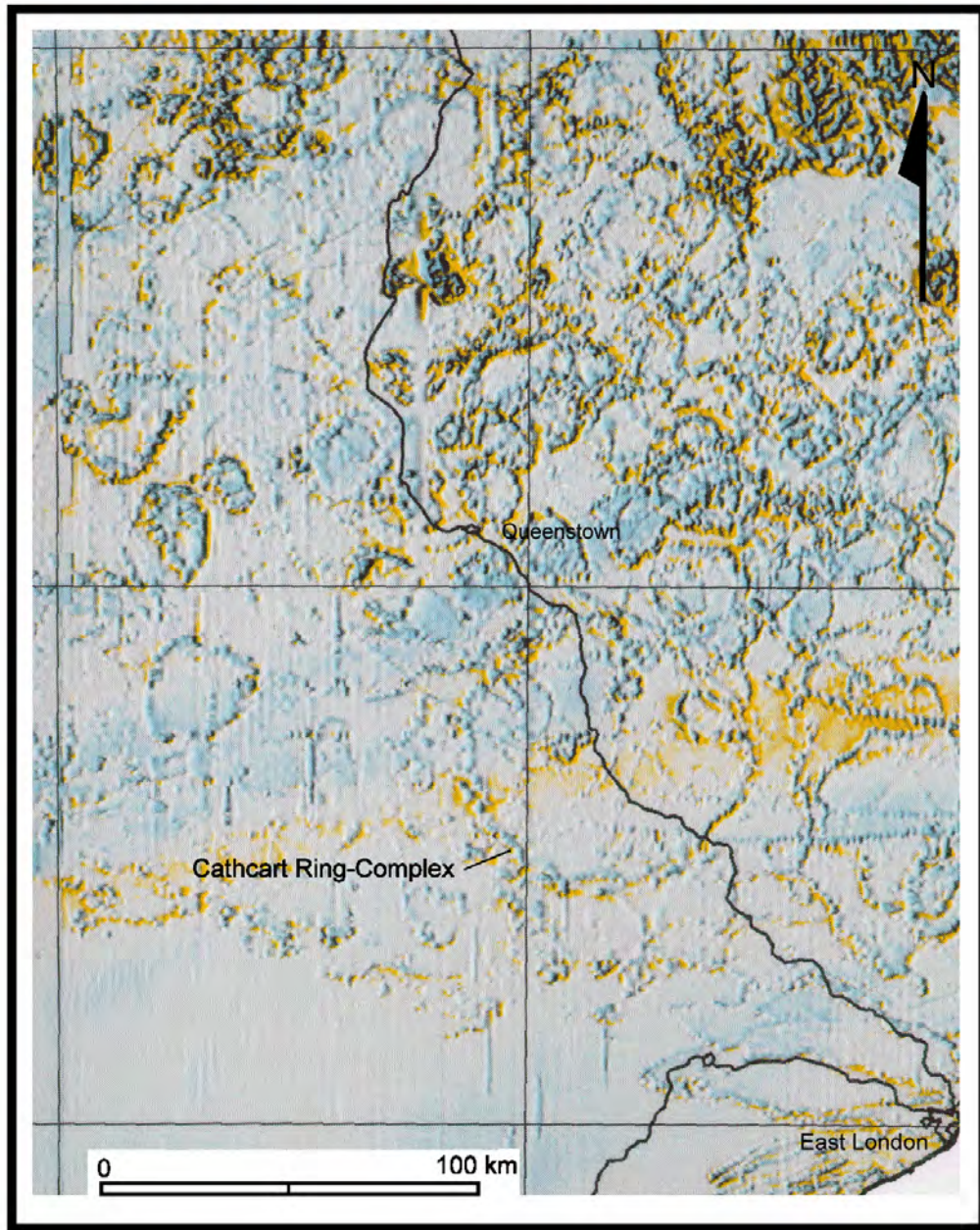


Figure 4.16: *Magnetic fabric map of the Queenstown-East London area, clearly showing the dolerite ring-complexes and mega-dykes*

The Council for Geoscience performed a high-resolution airborne radiometric and magnetic survey over an area covering the two 1/50 000 scale maps of Melton Wold (3122BD) and Victoria West (3123AC), and corresponding to the local study where drilling was performed (**Section 2.3.2.1** – Victoria West Complex).

The results of the survey are shown in **Figure 4.17**, where the dolerite structures are clearly visible. A very interesting feature is the circular structure of low magnetic intensity in the SE part of the area (blue tones to the southwest of Victoria West). It is known from drilling that this corresponds to a flat inner-sill some located 120 m below the surface. Its western rim is particularly important since it seems to correspond to a hidden ring fed by a dyke branching in from the NE.

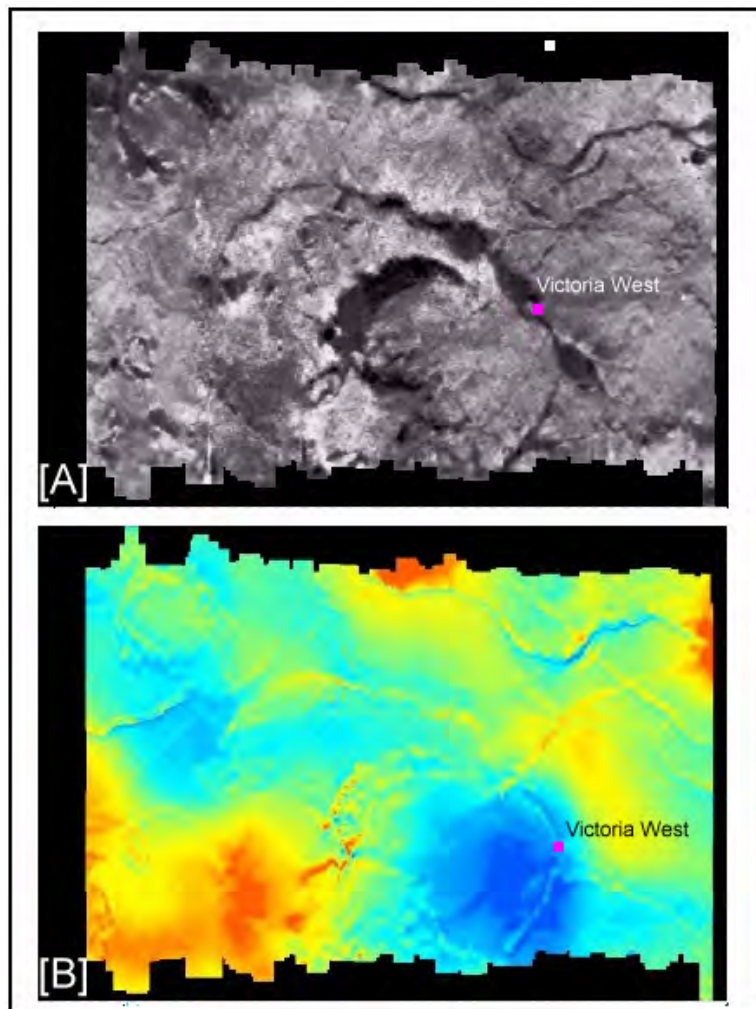


Figure 4.17: High-resolution [A] radiometric and [B] aeromagnetic surveys of the Victoria West area showing prominent dolerite dykes and sills (see Figures 2.39 and 2.41)

Ground magnetic profiling is probably the most widely used geophysical technique to identify the position, edges, strike direction and dip of dolerite dykes and probably the most widely used technique, and when used correctly results in a high degree of success.

The earlier South African literature on the location of dolerite dykes (approximately pre-1970) almost exclusively refers to vertical magnetic field magnetometer surveys, whereas the later reports refer mostly to total field surveys. The earliest well documented record of the application of the ground magnetic technique is by Maree (1943). He realised that the groundwater is often associated with the dyke contact zones, and therefore it was important to determine the width of the dyke. In addition, Enslin (1950) published statistics on the borehole yield versus the distance from a dolerite intrusion, which showed that the highest yields are normally found within 1 metre of the contact zone (**Figure 2.17**). In an attempt to determine the width of the dyke from an anomaly, he made the interesting observation that there is a relationship between the half-width of the anomaly and the width of the dyke. In later years this observation became a standard, quick and accepted technique for the interpretation of magnetic anomalies of thin vertical and steeply inclined structures (Roux, 1980). Examples are shown in **Figures 4.18, 4.19** and **4.20** (Maree, 1943; Enslin, 1955). He also noted that in the case of a vertical or near vertical dyke, the dyke edges are reflected by the steepest part of the anomaly. If the thickness of the overburden approaches the width of the dyke, and if both parameters are unknown, the width of the dyke cannot be accurately resolved.

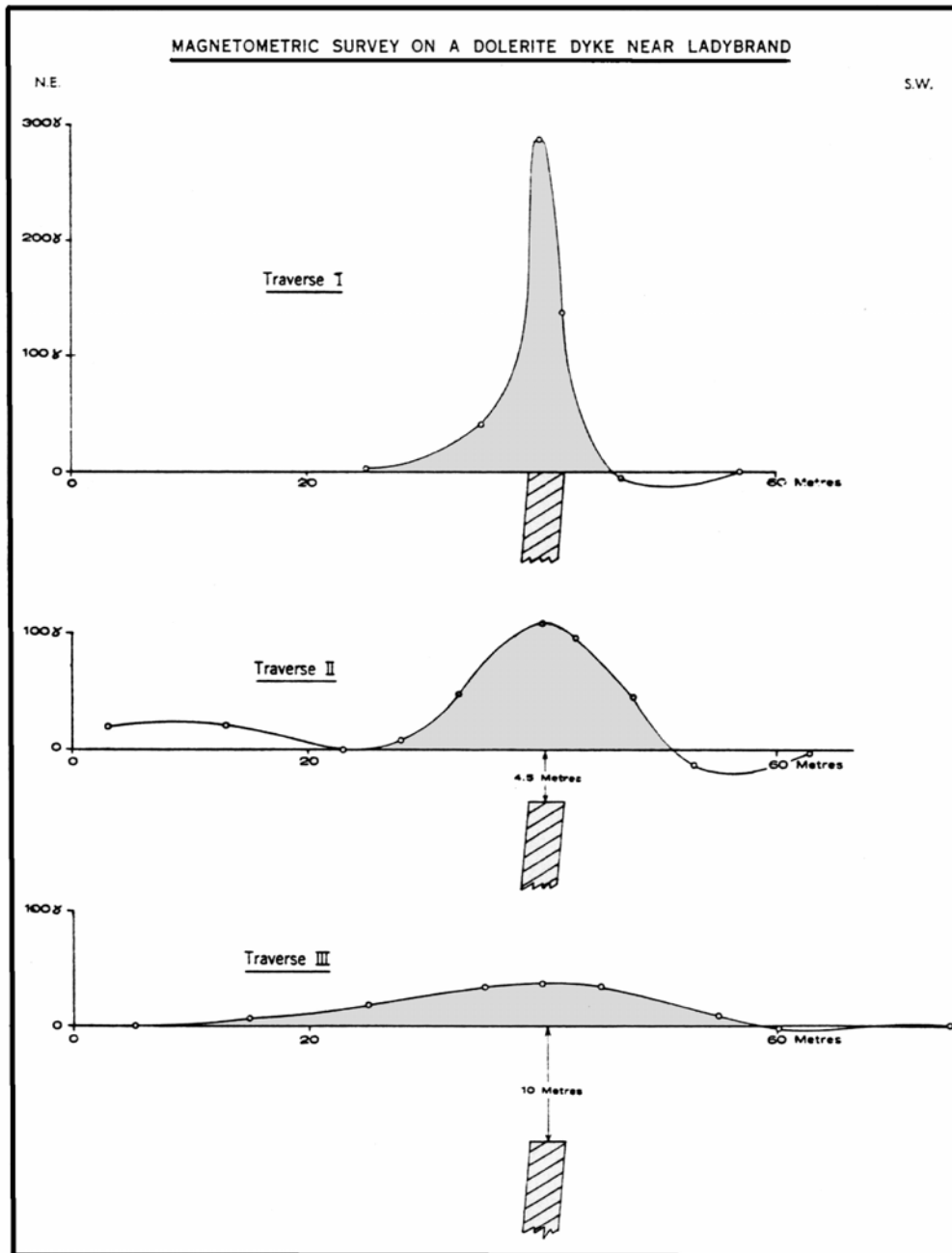


Figure 4.18: *The effect of the depth of burial on a dyke anomaly*

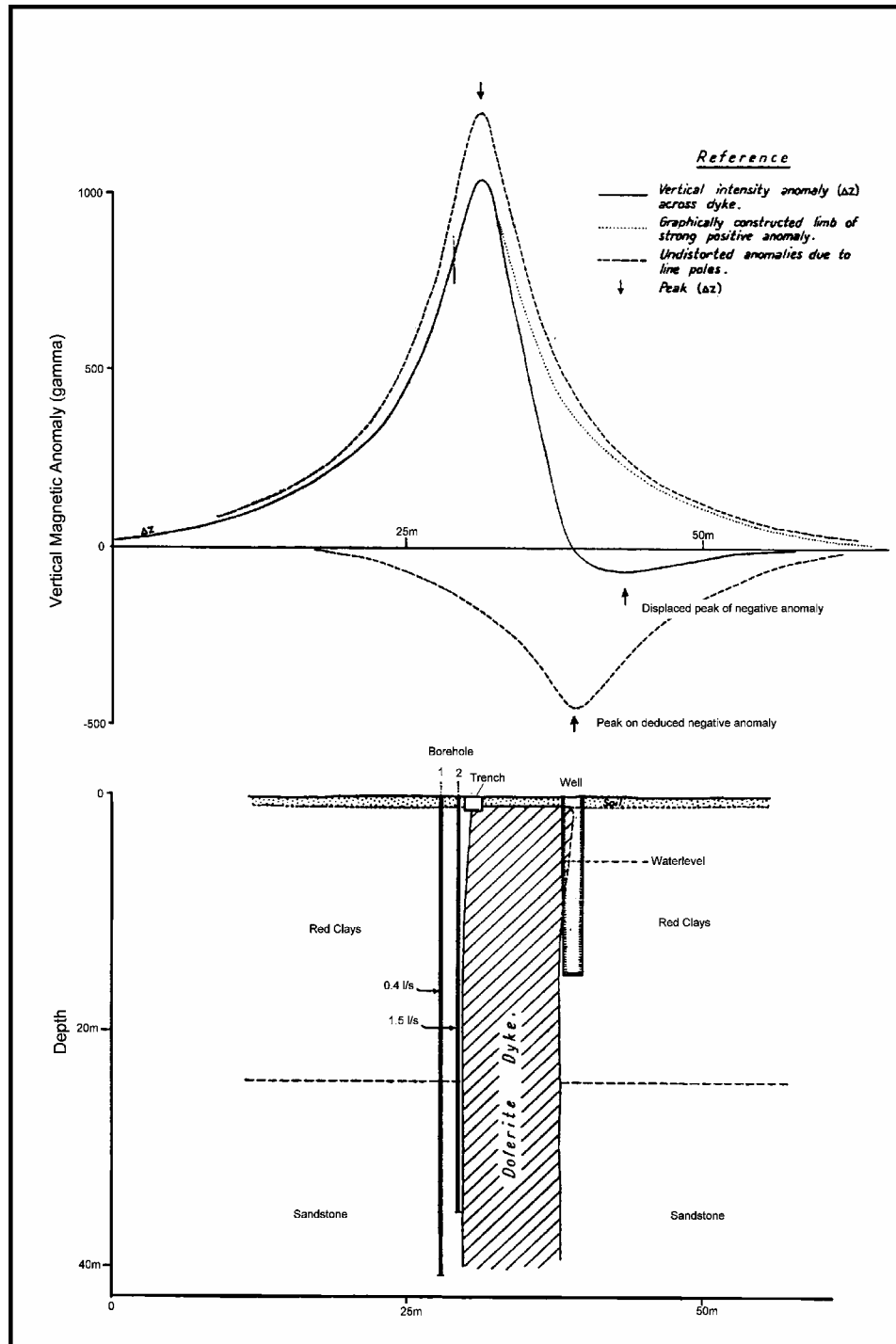


Figure 4.19: Interpretation of contacts of a dolerite dyke from the vertical intensity magnetic anomaly, Loch Lamind N0.157, Bethlehem

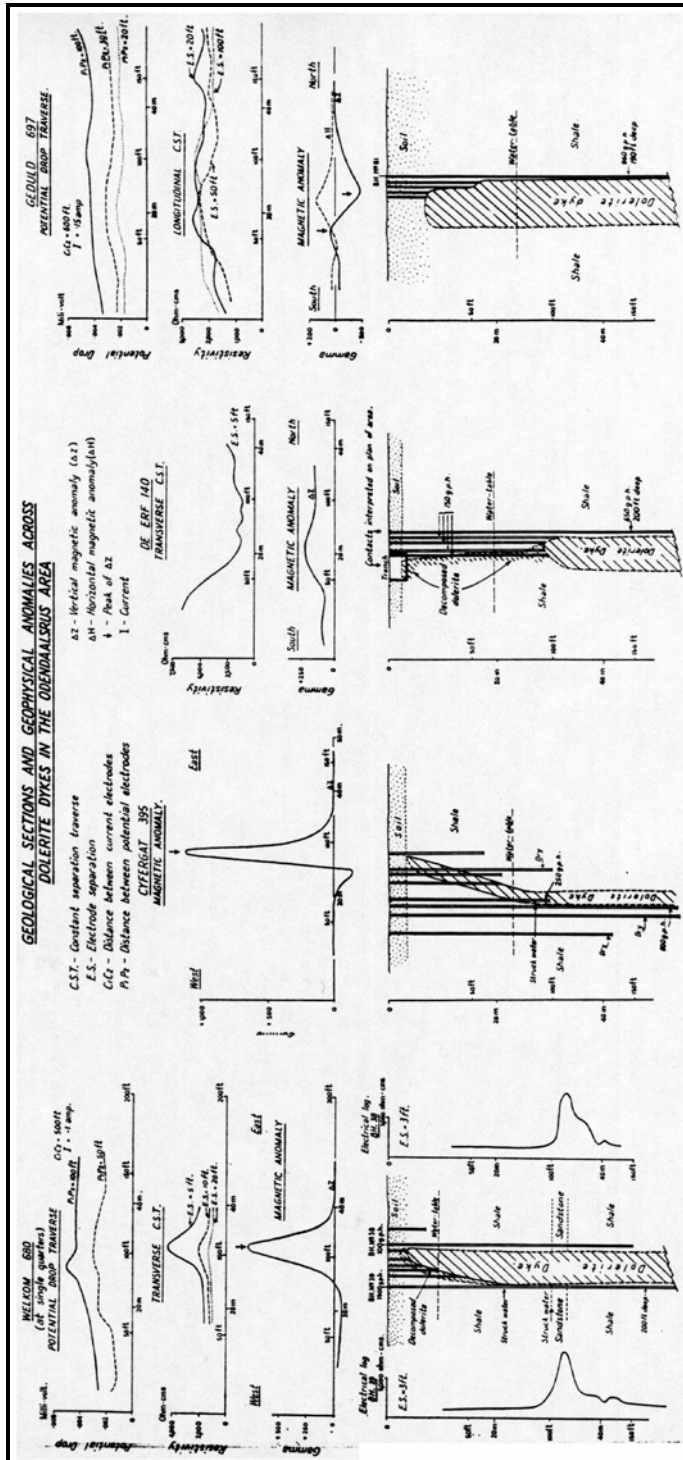


Figure 4.20: Geological sections and geophysical anomalies across dolerite dykes in the Odendaalsurs area

According to Maree (1943) the dip direction of a dyke can be obtained from the shape of the anomaly. A positive anomaly is usually flanked by two negative anomalies and the smaller one of the two indicates the dip direction (Maree, 1943). However, in later reports (Enslin, 1950; Vegter and Ellis, 1968; Gombar, 1977), examples are shown that do not support this theory of Maree. The dip direction can also be determined from the slope of the sides of the anomaly. The dip direction is towards the side with the less steep slope (De Villiers, 1961). These techniques, however, do not always lead to the correct interpretation. Magnetic interpretation is complicated by the fact that the magnitude and shape of the magnetic anomaly are not only related to the magnetic mineral content (or susceptibility), depth of burial and attitude of the intrusive body, but also to its attitude or orientation in relation to the earth's magnetic field. The amplitude of an anomaly is determined by the depth of burial and/or weathering, magnetic susceptibility of the body, magnitude of the earth's field and to a lesser extent the attitude of the body. Roux (1980) provides an excellent account of the theoretical aspects affecting the anomaly patterns. **Figure 4.21** is taken from Roux (1980) and shows clearly the strike of the profile line on anomaly shape, and dip of the dyke for a magnetic inclination of 60° in the southern hemisphere.

Numerous examples can be cited from DWAf reports where the nature of the dolerite dykes have been well defined through drilling. The variations in the anomaly patterns that can occur across a single dyke are well illustrated in a paper by Enslin (1950) where he describes numerous magnetic traverses across dolerite dykes in the Odendaalsrus area (**Figure 4.22**). Other examples are from a report by Gombar (1977) on geophysical work in the Lindley District (**Figure 4.23 and 4.24**).

More recent studies across dolerite intrusions into Karoo sedimentary sequences, where the modern proton magnetometers, which measure the total magnetic field, were used, are reported by Campbell (1975), Vandoolaeghe (1980); Vandoolaeghe, (1979); Potgieter (1981) and Woodford (1984). Potgieter (1981) used the magnetic method to trace the shape and position of dolerite ring-structures, whereas Woodford (1984) used the technique to trace the position and dip of dolerite dykes. Woodford (pers. comm.) routinely analyses total magnetic field anomalies across dyke structures using a simple PC-based 2-dimensional forward modelling approach, where remnant is ignored. This approach has been very successful in locating high production boreholes along the edges of dolerite dyke intrusions.

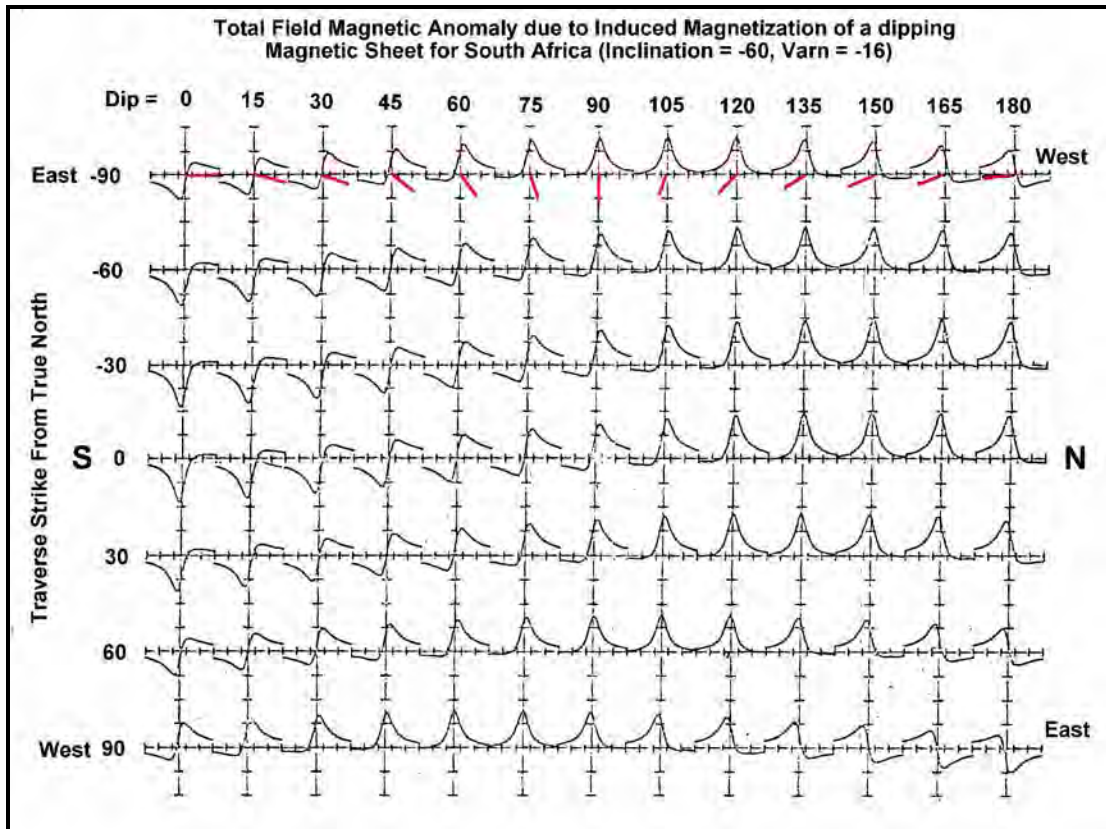


Figure 4.21: Type curves for magnetic anomalies over dipping dolerite dykes in South Africa

Campbell (1975) made the important observation that in the Beaufort West area, magnetic anomalies across dolerite dykes are almost without exception, positive, with subsidiary negative anomalies to the south. Vandoolaeghe also reports similar conditions for the Middelburg (Cape Province) area (Vandoolaeghe, 1979). This is in sharp contrast to the conditions experienced in the Karoo rocks around De Aar, where non-magnetic dolerite intrusions are frequently observed.

Station spacing during ground magnetic traverses varies and depends largely upon the width of the intrusion. A spacing of 20 m is commonly used during reconnaissance surveys, but siting the actual drilling position, often requires very detailed surveys with 1 m station spacings across the contact zone (Campbell, 1975). Campbell (1975) reports that drilling targets near dyke intrusions were usually selected on the peak of the positive magnetic anomaly or within 1-2 m from the maximum. In the case of inclined dolerite sheets, boreholes need to be placed not to intersect the dolerite at shallow depth. Therefore, in the case of sheet intrusions in the Beaufort West area, drilling targets were selected to coincide with the first positive deviation from the background magnetic signature, taken from the upstream side of the body.

Electrical and electromagnetic techniques

Dr. J.F. Enslin was instrumental in the implementation of geo-electrical methods in groundwater exploration in South Africa and promoted the use of Wenner depth soundings and Constant Separation Traverses (CST). Enslin applied these techniques during Karoo hydrogeological investigations (Enslin, 1950; 1963). According to Enslin (1950) electrical methods do not compare favourably with the magnetic method in respect of speed, cost of survey or accuracy.

During the late 1960s and 1970s the Geophysics Division at the CSIR, under the leadership of Dr. J.S.V. van Zijl, advocated the use of the Schlumberger electrode configuration rather than the Wenner configuration, which was until then, the more commonly used technique used in South Africa. One of the major advantages of the Schlumberger configuration, compared to other configurations, is that the measurements are less prone to electrode effects, and thus result in less distortion of the sounding curves. Van Zijl (1977) published a practical manual on the resistivity method. This together with numerous short courses where field and interpretation techniques were explained with practical examples, resulted in the wide acceptance of the method under South African conditions. Today the Schlumberger technique is widely used in groundwater exploration projects by DWAF and many consulting firms. The technique was used extensively during the large-scale groundwater exploration investigations conducted by DWAF in the Karoo basin, to study both the groundwater potential of the sedimentary rocks, as well as alluvial deposits in the Karoo basin (Campbell, 1975; Vandoolaeghe, 1980, Vandoolaeghe, 1979; Potgieter, 1981; Woodford, 1984).

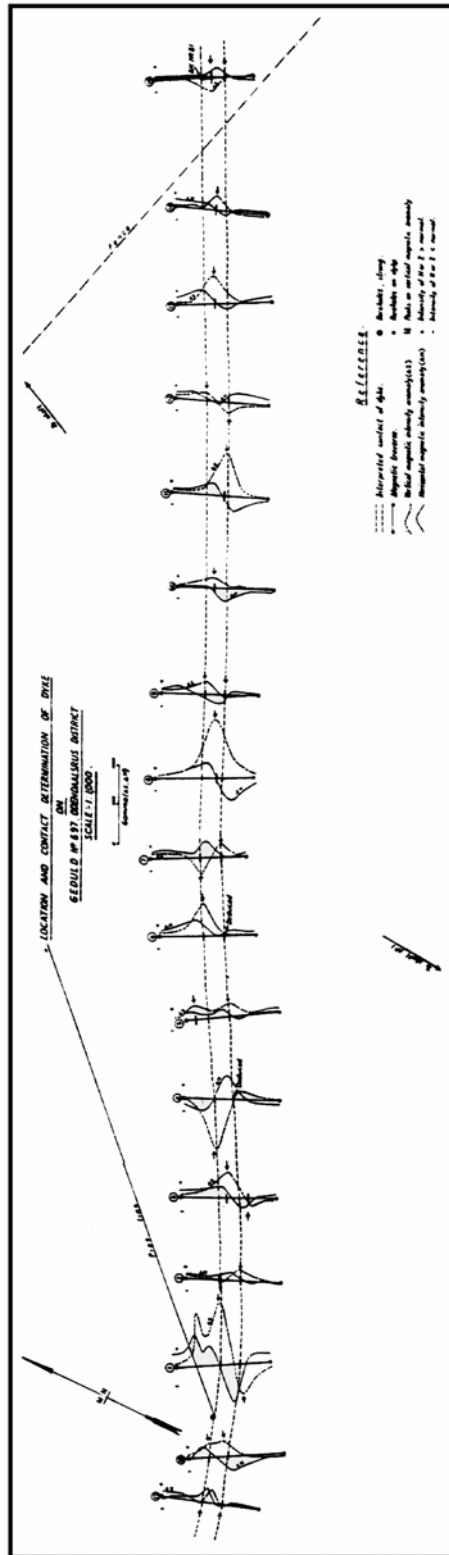


Figure 4-22: Variation in magnetic anomalies along strike of a dolerite dyke at Odendaalsrus

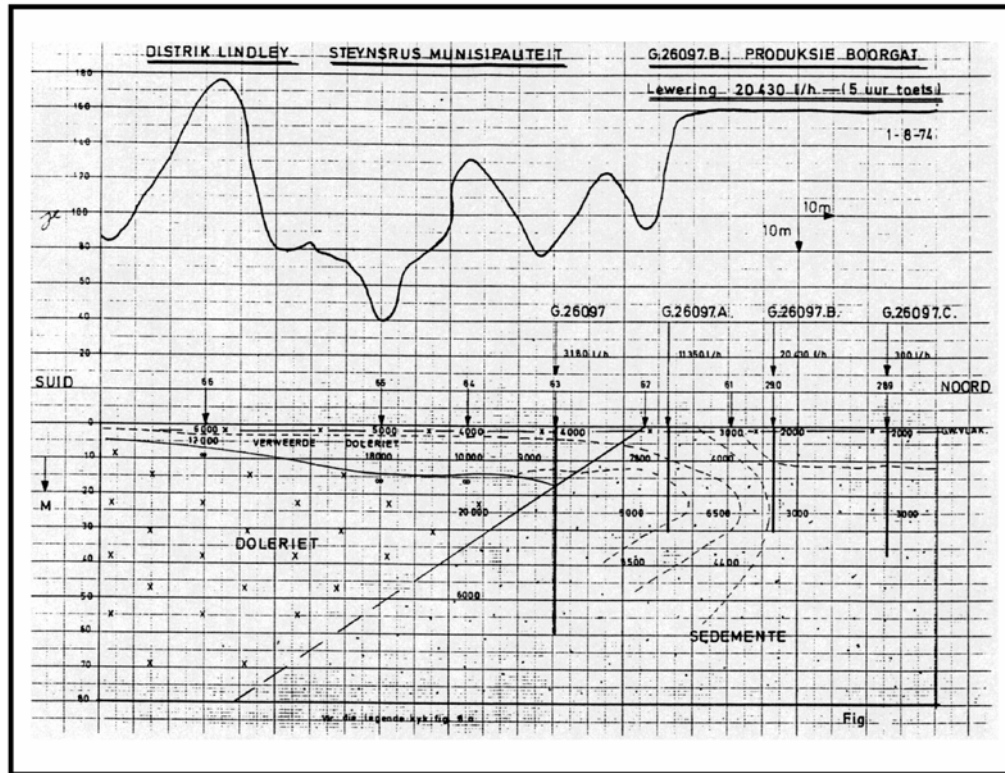


Figure 4.23: Magnetic anomaly across an inclined-sheet, showing exploration drilling results, Steynsrus area (Lindley District)

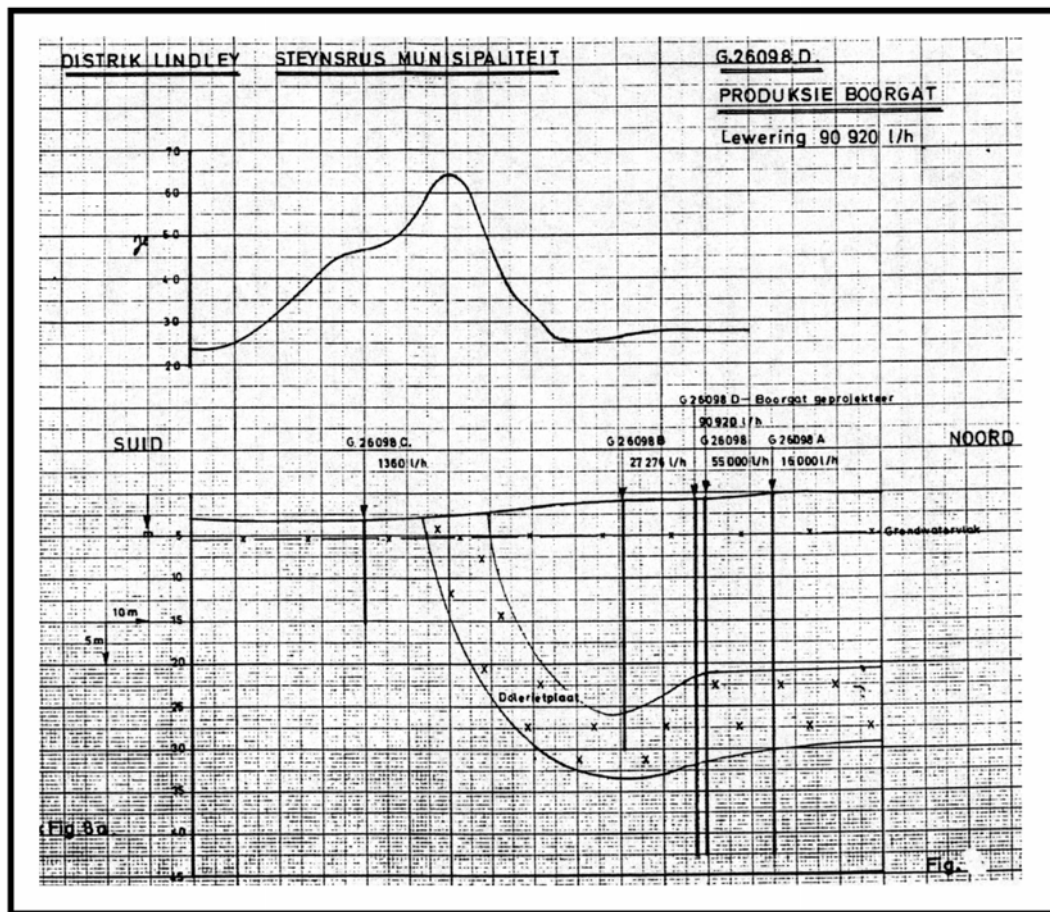


Figure 4.24: Magnetic anomaly across the intersection of an inclined-sheet and an inner-sill, showing exploration drilling results, Steynsrus area (Lindley District)

Resistivity techniques have been used to study various aspects of Karoo hydrogeology, for example:

- the thickness and distribution of sedimentary units and weathering in the Karoo;
- locating the position of dolerite intrusions;
- determining the depth to the first thick dolerite sheet;
- determining the distribution and nature of alluvial aquifers; and
- correlating hydraulic and geo-electrical parameters.

As is generally the case in the application of geophysical methods to various forms of exploration, the choice of the technique to be employed depends to a large extent on the local geological conditions. Integrating the results of more than one technique improves the overall results substantially. In this respect, the Karoo formations are not an exception to this rule and this has been demonstrated in several cases.

Enslin (1950) and Vegter and Ellis (1968) have attempted to relate Karoo formation resistivity obtained from resistivity depth soundings with borehole yield. According to Enslin a formation resistivity of 50 to 100 ohm.m correlates with the higher yielding boreholes in the Karoo. Vegter and Ellis (1968) calculated the range to be between 35 and 75 ohm.m based on the analysis of 436 sets of borehole and sounding information. Both these surveys are based on Karoo sediments in KwaZulu-Natal and southern Mpumalanga areas. Some examples of their work are shown in **Figure 4.25**.

Examples of the application of resistivity techniques in Karoo hydrogeology are numerous. Some of the most extensive applications of the technique have been reported by Campbell (1975, Beaufort West area, 1056 soundings), Vandoolaeghe (1979, Middelburg survey, 430 soundings) and Vandoolaeghe (1980, Queenstown survey, 396 soundings) and Woodford (1984, Graaff-Reinet Survey 180 soundings). However, most of these were to study alluvial deposits in the Karoo.

The resistivity values for the different sedimentary vary greatly. For examples weathered Beaufort sediments (in the Beaufort West and Queenstown areas) vary between 20 and 300 ohm.m., whereas fresh Beaufort sediments range between 200 and 600 ohm.m (Vandoolaeghe, 1980; 1979). Vandoolaeghe (1980) highlighted the complexity of geo-electrical sounding curves obtained in Karoo environments. Despite the difficulties in interpreting Karoo sounding curves, he states “*The application of the (resistivity) method as an exploration tool is sometimes doubtful. Still, a better and more profitable method in such conditions is not available.*” Often more than 70% of the sounding curves measured in Karoo environments represent 4- or more layer situations.

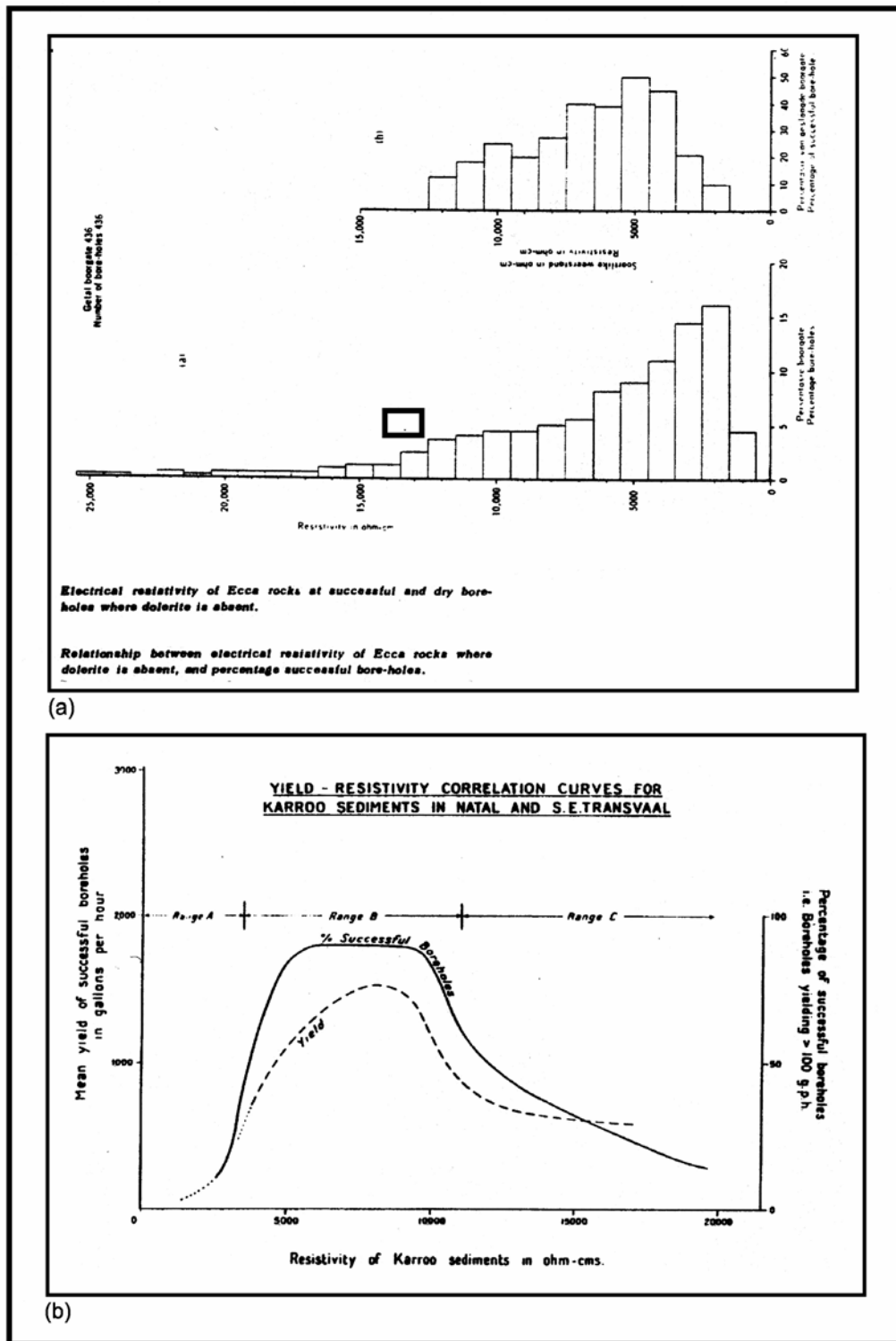


Figure 4.25: Relationship between electrical resistivity and borehole yield

Potgieter (1981) used the Schlumberger array exclusively in an investigation of the groundwater potential of the Karoo sediments in the Petrus Steyn area. He made extensive use of geological borehole information for calibration of the sounding curves, as well as cross-soundings to study lateral effects caused by geological variations. The resistivity parameters observed in this way were then used to interpret the rest of the 41 sounding curves measured.

Potgieter came to the conclusion that the resistivity technique can be used with a large degree of success to investigate the structure of dolerite ring-structures as well as the depth to dolerite sheets. He did, however, caution that in areas of heterogeneity of the Karoo sediments and the dolerite, the sounding curves become complex and difficult to interpret. Some examples from his work at Petrus Steyn are shown in **Figure 4.26**.

Woodford (1984) reported on the results of 180 Schlumberger soundings performed in the Graaff-Reinet area to determine the geometry of a composite alluvial weathered/jointed bedrock aquifer. The resistivity method was able to define the base of the composite aquifer (i.e. thickness of the alluvium and weathered bedrock), but failed to identify the presence of a gravel horizon (the prominent water-bearing zone) at the base of the alluvium. The reason given for the poor results are attributed to:

- (1) the principle of *suppression*, which states that unless this layer has a substantial thickness, this layer will be difficult to interpret from the curves, and
- (2) the “masking” effect of the poor quality groundwater in the aquifer.

Woodford, in contrast to the observations of Vegter and Ellis (1968), was not able to distinguish the dolerite sheet from the overlying alluvium and underlying sediments of the Beaufort Group. He further warned that the results of the survey should be used with caution due to the complex geohydrology.

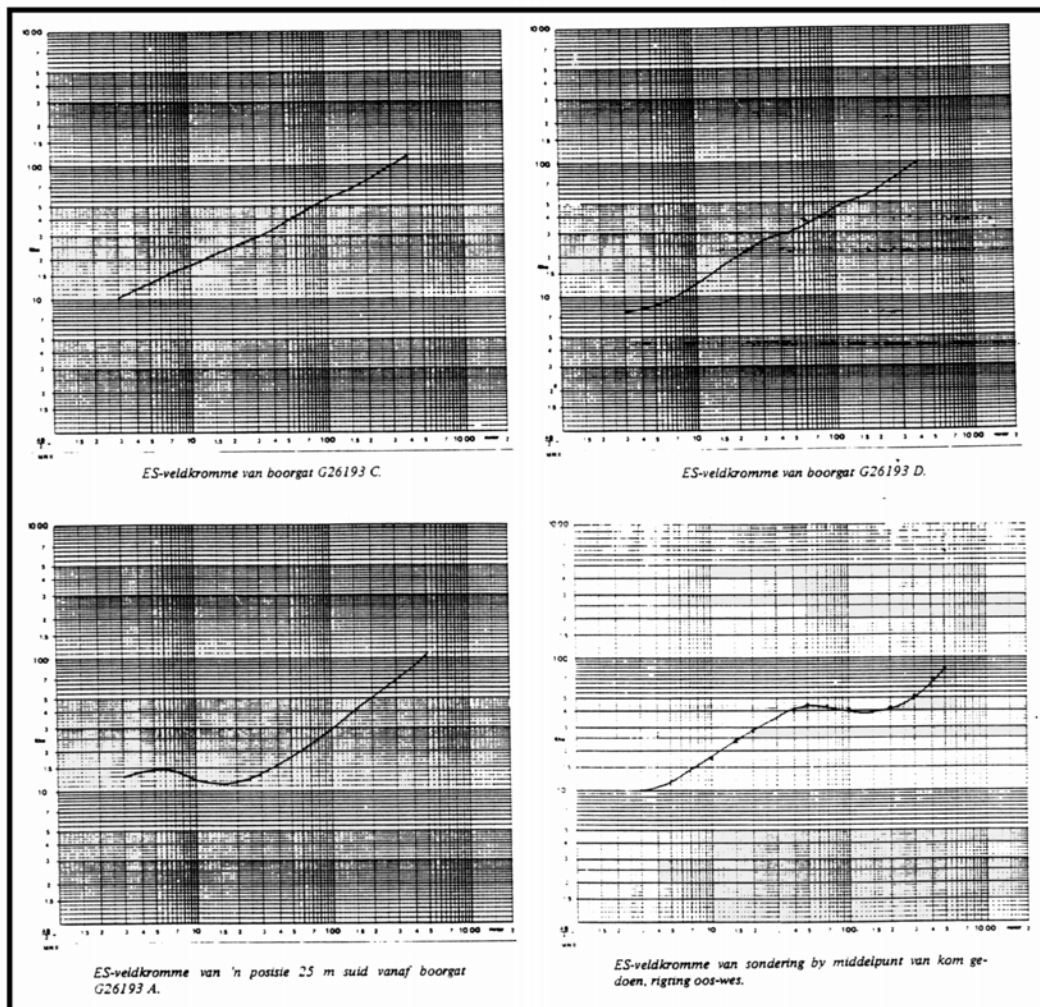


Figure 4.26: Resistivity method used to site boreholes on dolerite ring-structures, Petrus Steyn

During a survey to locate additional water resources for Strydenburg, Weaver (1991); Weaver et al., (1993) identified a high-yielding aquifer associated with a calcrete layer overlying Karoo sediments, situated within a dolerite ring-structure. Traditionally the drilling target is the contact zone between dolerite and Karoo sediments (Vegter, 1957; Schumann, 1966; Erasmus, 1984; Dziembowski, 1984; Venables, 1985; Woodford, 1988). In total some 116 boreholes were drilled in the area of which the majority exploit the dolerite/shale contact or the weathered/fresh dolerite contact. Weaver (1991) targeted the shallow alluvium overlying the black shales of the Prince Albert Formation. A presumably extensive alluvial aquifer was delineated using Schlumberger resistivity soundings. Drilling, however, indicated

the presence of up to 8 m of calcrete, the lower part of which often contains solution cavities and forms an ideal aquifer. Yields of up to 3.5 ℓ/s have been recorded from some of these boreholes. Examples of the sounding curves are shown in **Figure 4.27**.

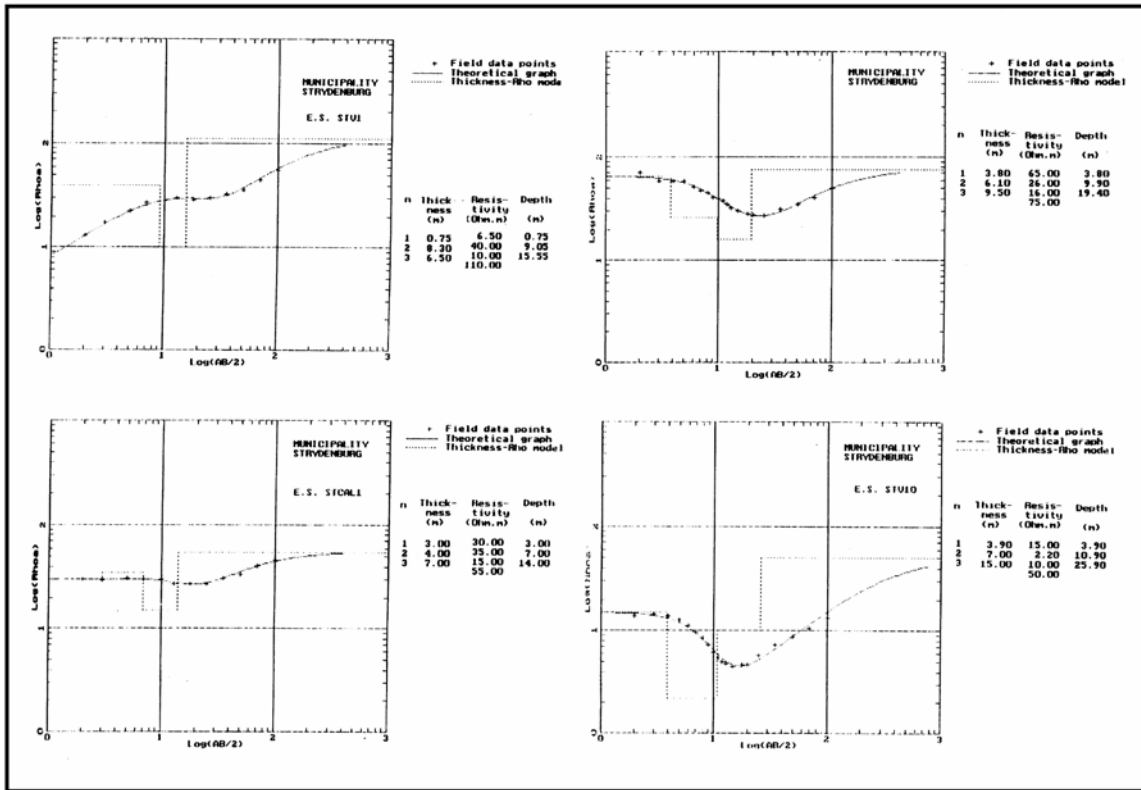


Figure 4.27: Schlumberger depth-sounding curves used to delineate an alluvial aquifer overlying the Prince Albert Formation shale, Strydenburg

The modern electromagnetic instrumentation (EM-34, EM-37 and EM 47) has to the author's knowledge, been used only occasionally. These applications have mainly been alluvial valleys and alluvium in river courses. Enslin (1955) described a new electromagnetic technique for groundwater exploration, but no examples of its field application in a Karoo environment could be traced.

Geophysical Borehole Logging

Geophysical borehole logging techniques have had limited application in the Karoo environments. Although frequently used, the value added by the results has generally been limited. Resistivity logs (normal) have been used with good results in assisting with the calibration of sounding curves, whereas natural gamma logs were in the case of the Beaufort West surveys, invaluable in the construction of complex geohydrological models (Vandoolaeghe, 1978).

4.1.3.4 Examples of Techniques Primarily Applied in Research Environments

Although the material presented in this section is perhaps not that relevant to the typical geohydrological investigations, it does contain information that is relevant to the overall geohydrology of the Karoo basin, and for that reason is included.

Deep Resistivity-Soundings and -Profiling

During the construction of the Orange Fish River tunnel in the late 1960s, flooding of the tunnel workings occurred at Shaft 2 of the tunnel some 10 km south of Venterstad (see **Chapter 2.4.3 – Case Study**). As a direct result of this, a WRC project was initiated in 1975 to investigate the origin of the 830 l/s inflow that occurred at this point. Pumping tests that were done indicated that the aquifer was associated with a steeply dipping, east-west striking, open fissure system and with an enormous storage reservoir. Support for the model that linked the water inflow with some major linear feature was to be found in the presence of the large positive east-west striking Bouguer gravity anomaly with an associated series of parallel magnetic anomalies, as well as the presence of numerous hot springs along the line of geophysical anomalies stretching over a few hundred kilometres. Several theories were proposed. One of the most favoured models predicted a zone of tension in the Karoo rocks in the tunnel area, but this was discarded as a result of the in-situ stress field measurements done in the tunnel (van Heerden, 1972; Orr, 1975). These measurements showed that the area is subjected to compressional stress, which would rule out the presence of open tensional fractures. Another explanation for the groundwater inflow was that the intense fracturing may be associated with the south-easterly extension of the Doornberg fault zone, i.e. along the postulated boundary of the younger Namakwa-Natal Belt (~1 000 Ma) and the older Kaapvaal craton (~2 600 Ma).

An extensive geophysical and geological mapping programme was initiated during which detailed studies were carried out at the site of the inflow point, as well as regional-scale investigations into determining the position of the boundary between the two cratons. This programme consisted of gravity and ground magnetic surveys covering several 1:250 000 map sheets, a few hundred deep electrical Schlumberger resistivity soundings and detailed resistivity profiling, self potential and induced

potential measurements at the inflow point. The summarised results are contained in a series of WRC reports by Meyer et al., (1980a), Meyer and Van Zijl (1980), Hodgson and Van der Linde (1980), Vogel et al., (1980a), Potgieter et al., (1980), Meyer et al., (1980), Meyer et al., (1980c), and Vogel et al., (1980b).

Detailed geological mapping, linked to an extensive geohydrological investigation, showed the presence of two dolerite ring-structures and a single prominent dolerite sheet to be present in the area. Geophysical work centred around the inflow point where resistivity profiling, using a 6 km current electrode spacing, was done over an area of 3 x 11 km. In addition, the area was covered by 49 deep resistivity soundings (AB electrode spacing ~ 10 km).

The researchers concluded that the large groundwater inflow was most probably caused by a combination of the following:

- the depth to the top of the first thick dolerite sheet increases from about 250 m and less on either side of the inflow point, to more than 800 m just north of the 1.2 km wide inflow zone (**Figure 4.28**),
- east-west orientated linear structures were delineated by the resistivity work in the vicinity of the inflow area;
- the strike direction of all large pre-Karoo structures as determined from the gravity and magnetic anomaly patterns, are also east west, strengthening the argument for a link between the proposed east-west fracture zone and the inflow; and
- the hot spring is also associated with an east-west dyke structure.

An important result that became evident from the deep resistivity soundings in the Karoo, is that depth penetration is confined to the depth of the top of the first thick dolerite sheet. Due to the contrast in resistivity between the Karoo sediments and dolerite, very large current electrode separations (>10 km) are required to see through a dolerite sheet with a thickness of a 100 m or more. These results form an important contribution to the understanding of the role of dolerite structures in the occurrence of ground water in the Karoo formation and need to be incorporated into new models to explain the relation between ring-structures, dolerite dykes, fracture patterns and groundwater occurrence.

Tomographic Techniques

Two new and novel geophysical techniques have over the last few years been developed at the CSIR. Both can be employed to investigate the rock mass between two boreholes, or alternatively, only one borehole can be used with the rest of the monitoring occurring on surface. The two techniques are referred to as *Radiowave Tomography* (RT) and borehole-to-borehole resistivity tomography. The first technique is a high resolution and relatively short distance technique capable of

investigating features associated with fractures, whereas the second technique is ideally suited to study the occurrence of dolerite dykes between boreholes.

The CSIR applied the new high resolution RT technique, originally developed to map conductive ore bodies in the mineral exploration, to study fractures associated with the Karoo formations at the test site of the IGS on the campus of the University of the Free State. Several different configurations of the technique were tested, as it was the first time the technique was being applied to a groundwater study.

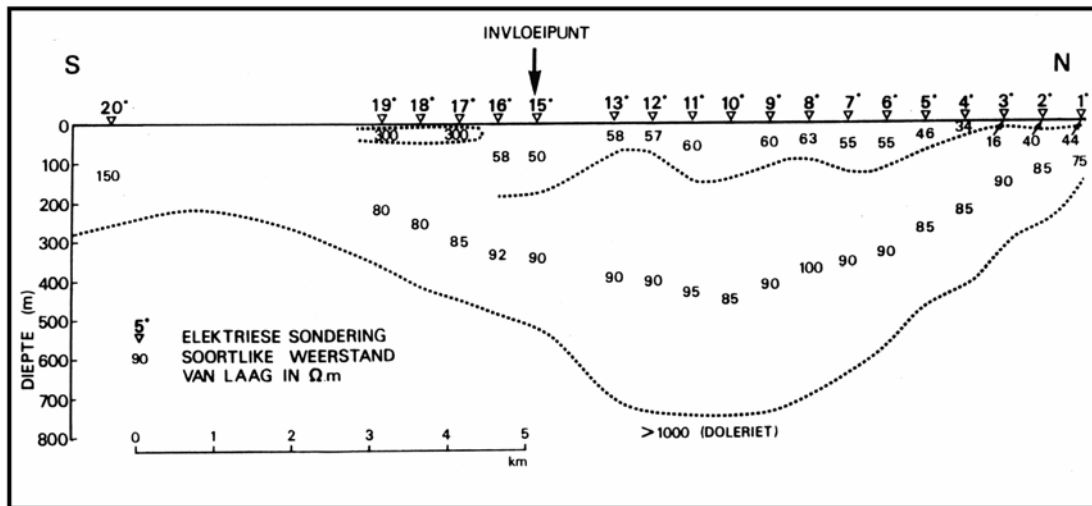


Figure 4.28: Schlumberger deep resistivity sounding at the Shaft No2 inflow point, showing depth to dolerite sill

Some of the most interesting results obtained will be discussed briefly. A more extensive account of the project is documented in a WRC report (Meyer et al., in press). Scans were done between different boreholes and at over different distances between boreholes (Figure 4.29), in order to build up a 3-D picture of an electrically conductive structure between boreholes (Figure 4.30). The scans were then repeated during the injection of salt-water in an attempt to determine the flow paths of the water. The results clearly indicate zone of higher conductivity associated with fluid in the fractures (Figures 4.31 and 4.32). This feature makes it an ideal tool to study fractures in an electrically resistive environment like granite or quartzite. Despite the relatively low conductivity of the Karoo sediments, the results obtained at the IGS test-site are very promising. The technique is, however, very expensive and it is time consuming to conduct the field-work and data analysis. This aspect makes it a tool that is almost exclusively for research purposes, and it will rarely be used in the development of water resources.

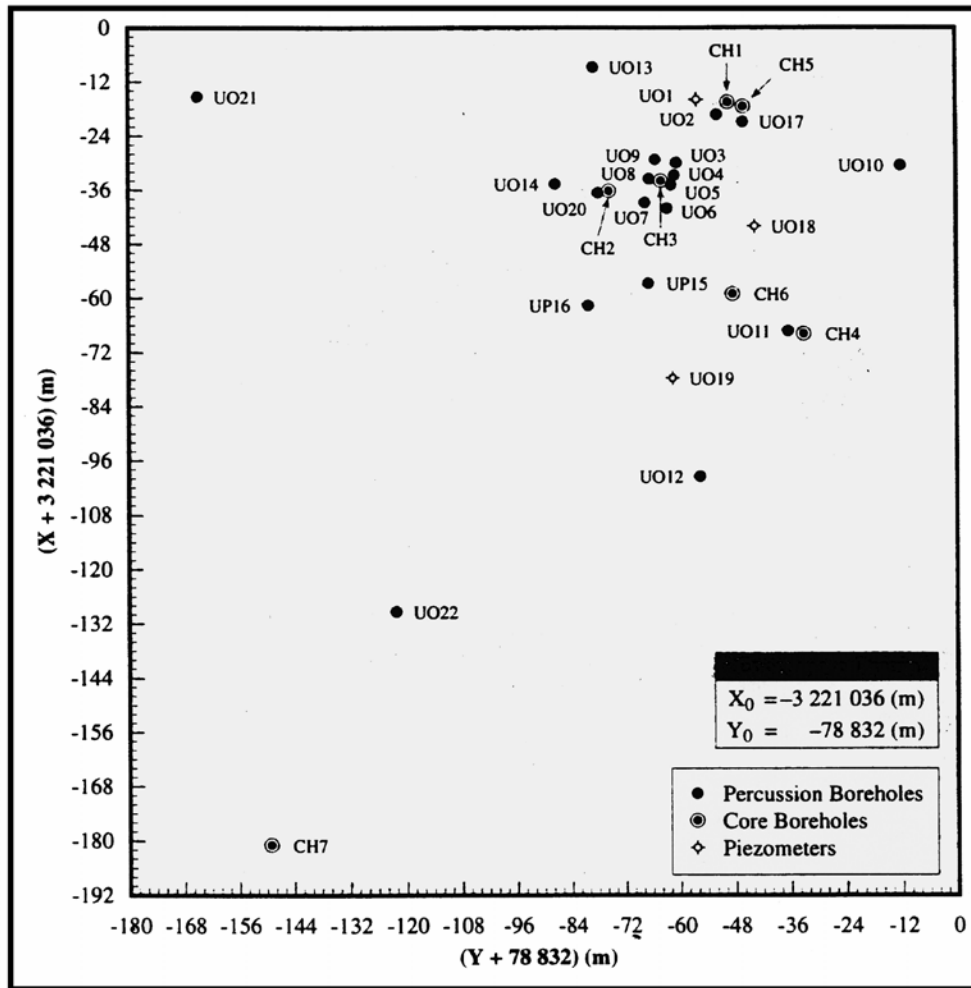


Figure 4.29: Plan showing borehole positions on the Institute for groundwater Studies campus test-site

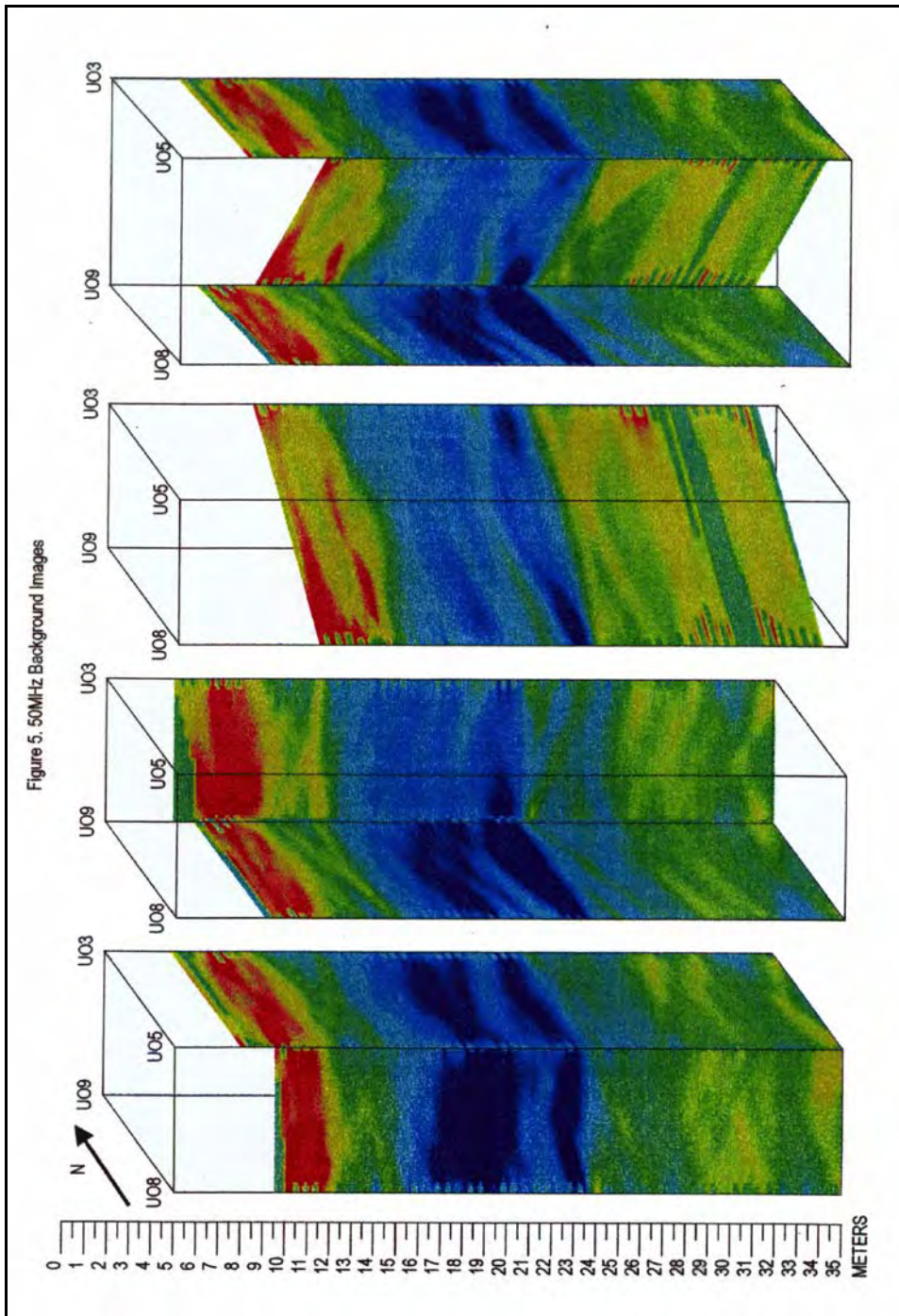


Figure 4.30: Radio-tomograph between boreholes on the campus test site, showing position of main fractures

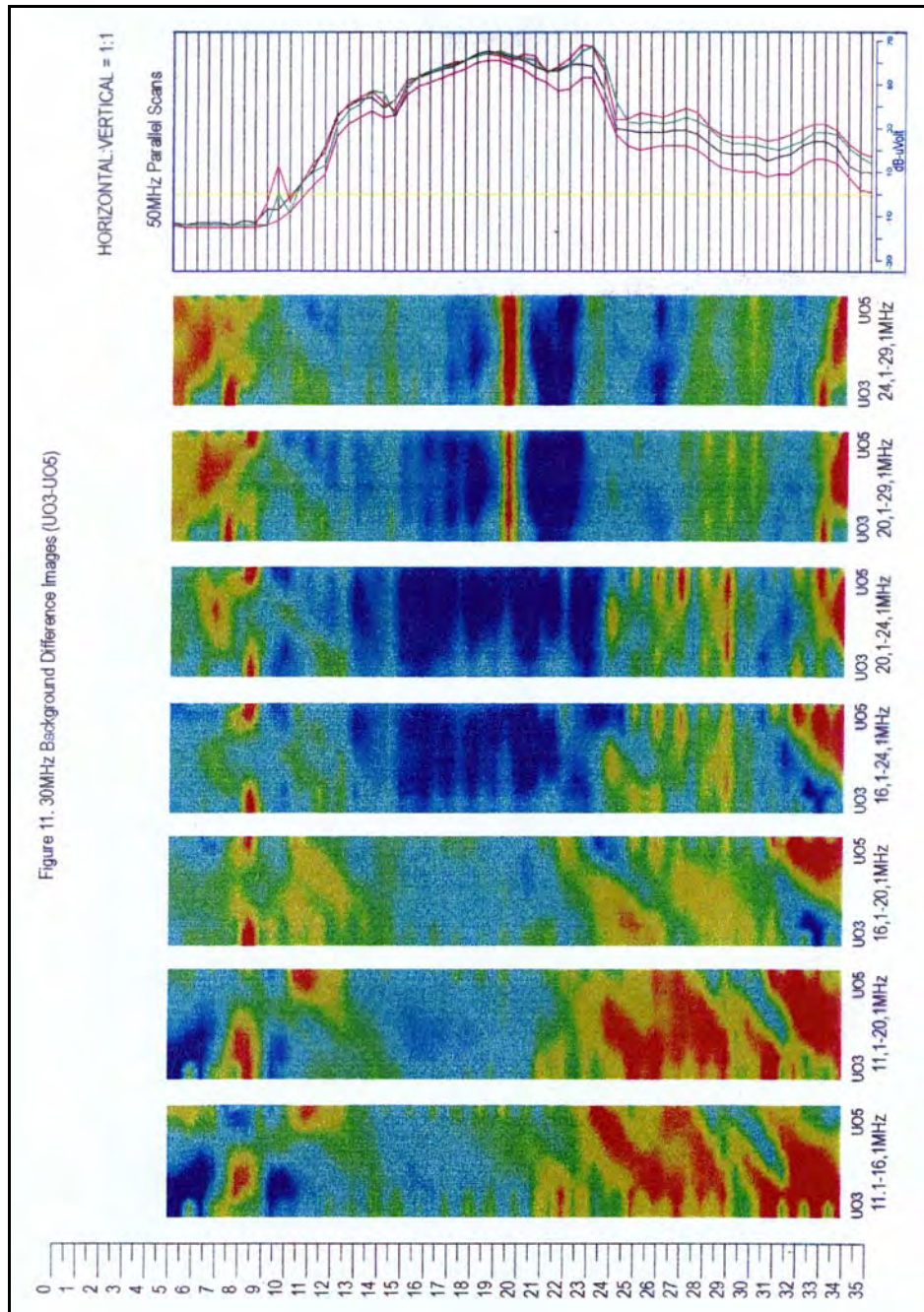


Figure 11. 30MHz Background Difference Images (U03-U06)

Figure 4.31: Campus test site – 30 MHz background difference images between boreholes U03 and U05, showing zone of horizontal jointing

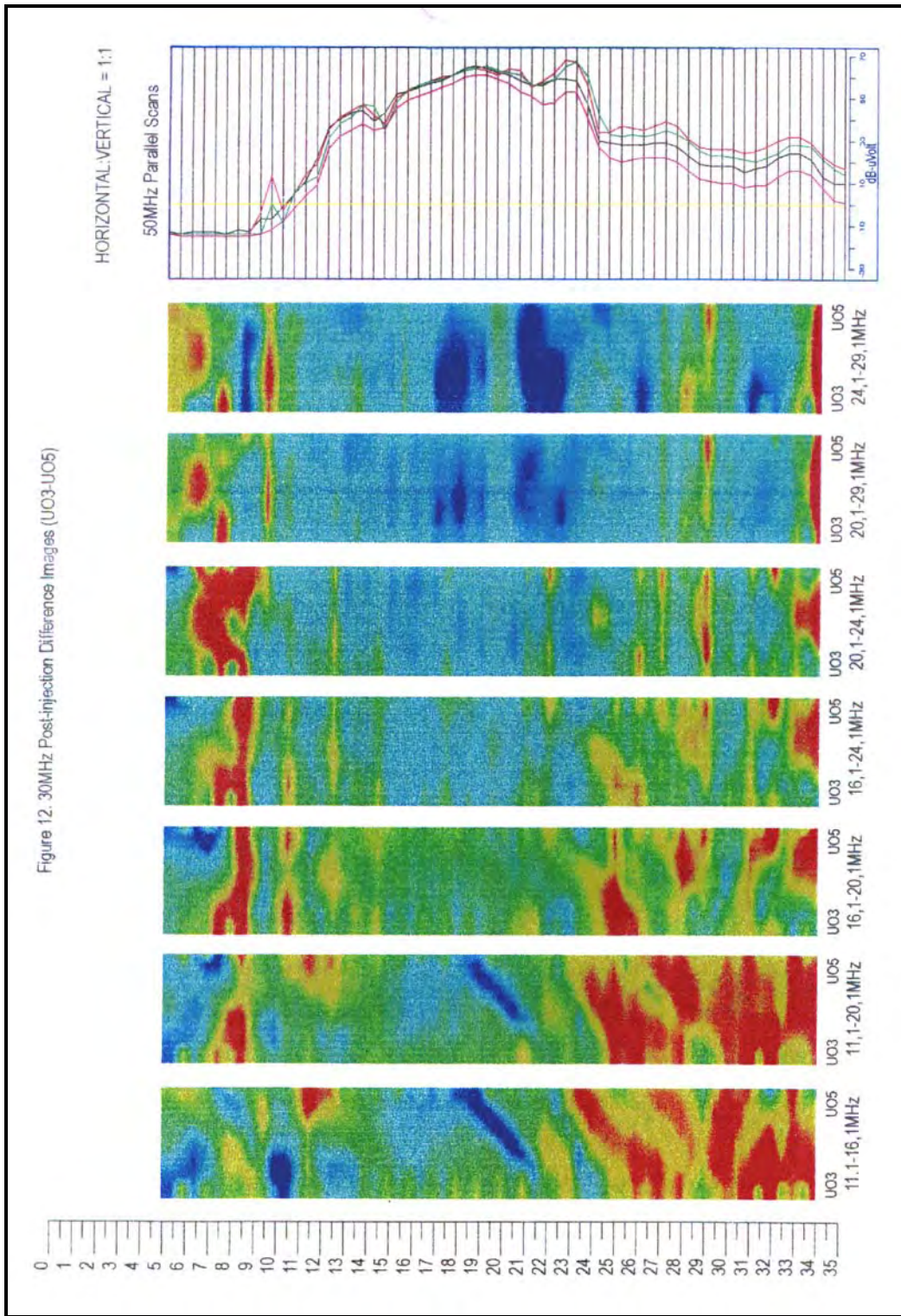


Figure 4.32: *Campus test site – 12MHz background difference images between boreholes U03 and U05, showing zone of horizontal jointing*

SOEKOR Deep Seismic Reflection

SOEKOR (Southern Oil Exploration Corporation (Pty) Ltd) was established in 1965 with the mandate to prove or disprove the existence of economic accumulations of oil or gas in the Republic of South Africa. In the course of their exploration programme, many hundreds of line kilometres of seismic reflection surveys were conducted by mainly foreign geophysical consultants. The surveys covered large parts of the main Karoo basin, as well as parts of the eastern Karoo. As far as could be established, none of the results of these surveys have unfortunately ever been published or released.

Although it may be argued that the depth of oil exploration targets usually far exceed those of the groundwater fraternity - it does, however, provide a wealth of information on the thickness of the different stratigraphic units in the Karoo, the petrophysical character of particular horizons, the occurrence, thickness and type of dolerite intrusions, structural information such as the presence and frequency of fractures, etc. All this information can be of assistance to geohydrologists when trying to understand the regional geometry and character of Karoo aquifers.

Another aspect of the oil exploration project was the many deep (>1 500 m) boreholes, as well as some shallow (<1 000 m) boreholes that were drilled. These provided invaluable information on for example the dolerite:sediment ratios over the Karoo basin, and porosity and permeability variation with depth (Winter and Venter, 1970; Rowsell and De Swart, 1976). In addition, most of these boreholes have been geophysically logged. The results of the logging could prove to be a potentially valuable source of information for geohydrological research on the deeper Karoo formations. As none of this information has ever been released by SOEKOR, it is not known in what format this information is available, or what the resolution of these logs are and which types of logs were routinely measured in the boreholes.

A further spin off of the oil search, was a series of north-south striking deep resistivity sounding profile lines in the southern Karoo which were measured by the CSIR in the late 1960s and early 1970s. All these profiles were recorded south of the so-called "dolerite line". The results of these were mainly used to explore the Beatty magnetic anomaly in the southern Cape and its relation to the Karoo and Cape Fold Belt tectonism (Van Zijl, 1979; De Beer, 1983).

Radiometric Surveys

The discovery of uranium in the main Karoo basin during 1970 triggered intensive exploration by private companies. Most of the uraniferous occurrences are situated in the fluvial-channel sandstone of the Adelaide Subgroup of the Beaufort Group, and the core of the Karoo Uranium Province is located between Fraserburg, Laingsburg and Aberdeen (Cole et al., 1991). Extensive drilling, most of it shallow was done during this exploration phase, but unfortunately very little attention has been given to

the groundwater occurrences and no records were kept as part of the geological logging of the boreholes.

Geophysical borehole logging

During the Soekor oil exploration in the Karoo all the deep boreholes were geophysically logged. However, as the upper 100 m or more of the boreholes were usually cased, the logs are of little use in the groundwater field. When studying deeper groundwater targets, these may become important sources of information. Apart from the limited use of modern geophysical borehole logging tools at the IGS Test Site (Botha, 1998), no other published information on the use of geophysical logging is available.

Radar techniques

Ground Penetrating Radar (GPR) has only been tested on a few occasions in the Karoo environment. To the authors' knowledge the results have been disappointing – where the widely acclaimed resolution of this revolutionary technique was not able to significantly contribute to our understanding of the shallow Karoo successions. Borehole radar has been tested at the IGS test site, but yielded disappointing results.

4.1.3.5 Concluding Remarks

The *Magnetic method* has proven over the years to be a cost efficient and rapid tool for groundwater exploration of dolerite intrusions in the Karoo, with which a high success rate can be achieved if applied correctly. *Resistivity techniques* are the second most commonly used technique. These can be, and have been, used to identify dolerite intrusions, weathering depth of the sedimentary succession, depth to the top of the first thick dolerite sill and for the determination of unsaturated / saturated thickness of alluvium.

If the recently proposed theories on the occurrence of groundwater in Karoo formations are correct, i.e. associated with mainly horizontal bedding-plane fractures - then none of the standard geophysical techniques will be capable of providing meaningful and cost effective results. The contrasts between the physical parameters in this instance are not great enough to produce significant and detectable geophysical variations.

In general, the other geophysical techniques, including the new tomographic techniques, are of only limited use under most Karoo aquifer conditions - often due to the high costs involved. However, when applied in research studies, the results can be very rewarding.

4.1.4 DRILLING TECHNIQUES AND BOREHOLE CONSTRUCTION

4.1.4.1 Historical Perspective of the Influence of Drilling Technology on the Utilisation of Karoo Aquifers

Groundwater has played a crucial role in the development of the many areas in South Africa – the scale and rate of development these resources was to a great extent linked to the available drilling technology.

The indigenous peoples and later the early colonial farmers obtained their water from numerous springs and ephemeral seeps scattered throughout the Karoo Basin. Conflict soon developed over access to these scarce sources of water. Many wells or “pits” were excavated at the location of the springs to increase the supply, as the demand for water increased or to maintain the groundwater outflow during periods of drought.

In the 1870s interest in the Cape Colony had been stirred up by the excellent results that had been obtained by water drillers in Australia and America, and a request was made to the Commissioner for Crown Lands and Public Works to acquire this drilling technology. At this time, towns, villages and farms in Colony were dependant on streams, surface impoundments, springs and shallow dug-wells (Brown in Vegter, 1984). In 1880, John Gamble, the Hydraulic Engineer of the Cape of Good Hope reported that a driller and “boring-tools” had arrived from England and that drilling had been undertaken for the Graaff-Reinet Municipality. The first drilling-rigs to be used were hand-operated rotary machines with diamond-tipped crowns, capable of making a 50mm diameter hole. The small diameter of these boreholes only allowed the abstraction of very limited quantities of groundwater and was undoubtedly to a large extent responsible for the initial lack of interest shown by farmers in drilling and for their insistence on artesian boreholes. A modification enabled the hand-machine to be powered by draught animals and by 1890 steam-power was introduced (Vegter, 1984).

The use of windpumps by Cape Colony farmers for abstracting groundwater only started to take root in 1885, after demonstration and testing of the various makes of equipment was carried out at Willowmore. It was not until 1893 that drilling on farms really got into stride in the Cape Colony, while in the Transvaal and Natal, very little or no drilling for water took place until the end of the 19th century. Drilling of water boreholes in the Free State commenced in about 1892 (Vegter, 1984).

In 1901, the Engineer-in-Chief of Public Works of the Cape Colony reported that, after studying trends in water drilling in Australia and the United States, drilling for water with diamond-rigs was outdated. The introduction of an American-built percussion cable-tool or “jumper” drilling-rig in the first decade of the century provided a boost to water drilling in South Africa. In 1904, the newly established Boring Branch of the Transvaal Colony Irrigation Department started using rotary-drills with chilled steel-shot as a cutting agent (commonly referred to as a “haël-boor”

or “shot-drill”) in the harder rock formations, where the steel chisel-bits of the cable-tool rigs failed to progress. Although the shot-drill was used in conjunction with the cable-tool rig until the 1950’s, its use was rather restricted because of the considerable volumes of water required in the process (Vegter, 1984).

The boreholes were normally drilled fairly shallow (< 30 m) and were stopped when resistant dolerite was encountered. In order to avoid striking the dolerite at too shallow a depth, many of the older boreholes were sited well away from the main water-bearing dolerite features, especially the more complex sheet / sill structures. Drilling was a slow affair with a typical 20 m borehole taking approximately 2-4 days to complete.

After 1921, petrol, kerosene and diesel engine-driven machinery began to gradually replace the steam-powered rigs. The wooden-framed drilling-rigs were replaced by locally designed and built steel-framed rigs after World War II. Since 1950, the cable-tool drilling-rigs were gradually replaced by pneumatic down-the-hole-hammer machines (Vegter, 1984). These air-rotary-percussion drilling-machines were capable of drilling deeper and more rapidly (i.e. a 20 m borehole could be completed in a few hours). The penetration of the more resistant dolerite became feasible and thus boreholes could be sited closer to the target features, resulting in a greater number of higher yielding boreholes. The depth of drilling, however, did not increase dramatically due to the ubiquitous occurrence of shallow groundwater in the more fractured upper 5 – 30 m of the Karoo strata and the low yields required to meet domestic and stock water requirements.

4.1.4.2 Drilling Methods

The drilling methods employed in the development of groundwater supplies are many and varied. Only those methods commonly employed in Karoo aquifers will be briefly discussed below.

Cable-Tool or Percussion Drilling

This is one of the oldest methods of drilling (see above). It basically involves continuously lifting and dropping a sharp-ended solid-steel drill-bit, suspended from a wire cable, onto the bottom of the hole. This process drives the cutting bit deeper and deeper by fracturing and pulverising the rock. The bit rotates and strikes a different section of the bottom with each successive blow. The crushed material forms a slurry on mixing with water that is either artificially added or that flows naturally into the borehole. When the bit can no longer fall freely through the slurry/cuttings, the drill tools are withdrawn from the borehole. A tubular bailer is then used to remove debris from the hole before drilling is resumed. The casing is driven down the hole as the drilling proceeds.

Because of the relatively low cost of purchase and simplicity of the equipment the cost per metre drilled is relatively low. However, the technique is tedious and when the increased cost of labour is taken into account, there is no real cost benefits over faster rotary drilling methods in the drilling of new boreholes.

Rotary-Percussion Air Drilling

This method is the most economical way of rapidly drilling boreholes into hardrock and semi-consolidated formations, which are self-supporting. The method basically involves the fracturing and shattering of the formation via the rotary and pneumatic percussion action of a down-the-hole hammer and drill-bit. The cuttings produced by this process are removed from the borehole via the annulus between the drill-stem and the wall of the hole by circulating air at high-pressure. The continuous cleaning of the hole exposes new formation to the bit and thus energy is not expended re-drilling old cuttings. Foaming additives are sometimes used to increase the up-hole carrying capacity of the return air.

A major advantage of air drilling is that water is blown to the surface as soon as a water-bearing zone is encountered. This allows the geohydrologist to obtain a progressive indication of the available supply and to monitor any changes in the quality and quantity of water as drilling progresses. This cumulative measurement of increasing quantities of water expelled from the borehole is commonly referred to as the *blow-yield*. This cumulative blow-yield only provides a qualitative indication of the water yield from an individual fracture. Many other factors may either positively or negatively effect the measured blow-yield, such as the capacity of the compressor, depth of the water-strike below the waterlevel, annulus between the drill-stem and wall of the hole, emplacement of casing and screens, fracture permeability etc. For example, Von Hoyer (1974) reported 100-300% increases in the blow-yields from shallow boreholes (<20 m) drilled in the De Aar area, as a result of enlarging the diameter of the hole from 165 mm to 250 mm.

The *reverse-circulation or dual-tube drilling method* is a modification of the standard air-drilling technique described above, in that air is continuously passed down to the drill-bit via one tube in the drill-stem, and returned to the surface (including drill cuttings and any to water intercepted) through a second tube within the stem. This method is not commonly used in groundwater development, but is useful for obtaining uncontaminated lithological and water samples, especially where the lithology and/or water quality varies over short depth intervals.

Mud Rotary Drilling

This method of drilling was developed to handle unconsolidated formations and operates in a similar manner to rotary-percussion air drilling, except that the circulation system is a high density and/or viscosity fluid rather than air. The mud forms a membrane on the wall of the hole, thereby providing structural support to and inhibiting flow through it.

The drilling fluid is continuously circulated down the drill-stem, through the drill-bit nozzles and upwards within the annular space around the drill-stem to the surface. At the surface, the fluid is passed into a settling-pit, where most of the drill-cuttings are deposited, and thereafter to a storage-pit, where a mud-pump re-circulates the fluid to the drill-rig.

The method is useful for drilling deep boreholes that are beyond the capacity of the air-compressors of the rotary-percussion drill-rig.

4.1.4.3 Borehole Construction

The design and construction considerations of individual boreholes will depend of the intended purpose of the hole, drilling depth, the physical character of the aquifer, chemical quality of the groundwater and drilling method to be employed.

The natural flow regime of an aquifer may be negatively affected by the drilling of a borehole, namely:

- Poorly designed boreholes provide direct and rapid access of pollutants to the aquifer,
- Boreholes penetrating multi-layered aquifers can provide vertical connection between aquifers of different piezometric head and/or water quality, and
- uncontrolled artesian boreholes cause wastage of the resource and loss of hydrostatic pressure in the aquifer.

Production Boreholes

The design and construction of a production borehole will depend on the criteria discussed above, as well as economical considerations related to its intended use (i.e. life span of the borehole, expected production yield, risk of pump loss). It is important to select the correct casing diameter in relation to the anticipated yield of the borehole and the required size of the pump (**Table 4.7**)

Table 4.7: Recommended diameter of production boreholes in Karoo Aquifers

Expected production yield of borehole (ℓ/s)	Recommended minimum internal diameter of Borehole (mm)	Use
< 5 ℓs	100 – 165	Stock Water / Domestic – Localised.
5 – 15	165 – 210	Irrigation / Municipal Bulk Supply.
> 15	> 210	Irrigation / Municipal Bulk Supply.

Fractured Hardrock Aquifers

Most of the groundwater in the Karoo Basin is abstracted from shallow fractured-rock aquifers via shallow (< 60 m deep) boreholes. These boreholes are normally open holes that are only equipped with a short length of solid steel casing, which extends from the surface to the base of the unconsolidated overburden. This simple borehole construction often results in borehole collapse and loss of pump equipment, especially in high-yielding holes, where blocks of highly fractured rock are dislodged from the wall of the borehole. This process is facilitated by the continual depressurization / pressurization of fractures in the vicinity of the borehole during cycles of over-pumping/recovery, as well as turbulent flow into the borehole during pumping at excessively high rates.

A simple, but more appropriate, production borehole design is presented in **Figure 4.33**, which includes the use of both solid and slotted casing. The slotted casing is more for *formation stabilization*, than for restricting the inflow of fine aquifer material into the borehole. The selection of a slot width is therefore aimed at providing the maximum amount of open-area (widths of 10-15 mm are normally adequate), particularly where the fracture zones are thin and discrete. Slotted casing is commonly inserted from the rest-waterlevel to a depth just below the last unstable fracture zone, to the main water-bearing fracture or to a depth below the waterlevel that allows sufficient available drawdown for the intended purpose of the borehole. The basic principle is to always *protect the pump* by inserting sufficient casing to ensure that the pump inlet can be installed within the casing.

Cement / grout plugs or seals are strategically placed to provide effective isolation of the productive aquifer from aquifer(s) of poorer quality, (i.e. shallow alluvial/bedrock-aquifers), and from contamination via surface runoff and/or seepage.

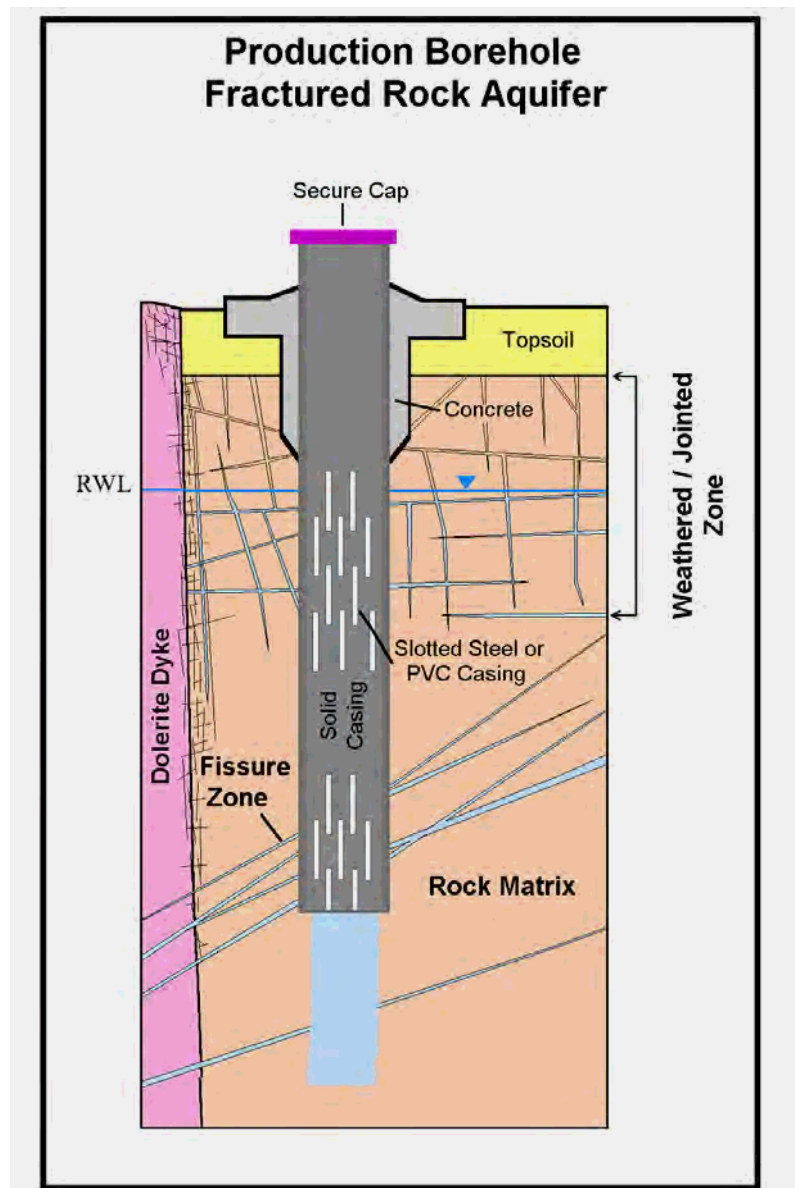


Figure 4.33: *Typical production borehole design for a fractured hardrock aquifer.*

Intergranular Semi- to Unconsolidated Aquifers

Composite alluvial/jointed-bedrock aquifers (**Chapter 2.6.2**) are an important exploitable groundwater resource in the central and western Karoo Basin, although they are not extensive in area. They form shallow aquifers that do not require drilling deeper than 30m. Production boreholes in these aquifers are designed to ensure that the formation remains stable and that abstraction takes place at a maximum efficiency without influx of fine aquifer material into the hole.

In these aquifers the important design considerations are:

- The diameter of the borehole must be large enough to allow for a 50 to 150 mm annulus about the casing for a gravel-pack.
- Selection of the screen length, diameter and slot aperture that will allow water to enter the borehole at the required yield, without resulting in turbulent entrance velocities. The screen slot aperture is normally selected to be 20% smaller than the modal size of the gravel-pack.
- Selection of the gravel pack should be based on grain-size analysis of the water-bearing formation. Ideally, the gravel pack should consist of well-rounded and clean material. In the Karoo this type of material may not always be readily available and, although not optimal, a crushed quarry- aggregate is commonly used. A sandstone aggregate should be used rather than a coarse grained, dolerite aggregate because of its susceptibility to weathering.
- Typically the basal 1-3 m of these Karoo aquifers are comprised of moderately rounded, medium- to coarse-grained sand and gravel, with minor amounts of finer material. In this case the aquifer material may be developed as a natural gravel-pack. Care must, however, be taken during the drilling and construction of these boreholes to ensure that the screened portion of the hole is not contaminated by finer material falling from above.
- A cement seal is placed around the top of the borehole to provide effective isolation of the aquifer from contamination via surface runoff and/or seepage.

A typical design for such a production borehole is illustrated in **Figure 3.34**. These boreholes are generally more costly to develop than similar boreholes located in the fractured-rock aquifer. The long-term stability and optimal production capacity of these boreholes should not be compromised by short-term cost savings in the borehole construction.

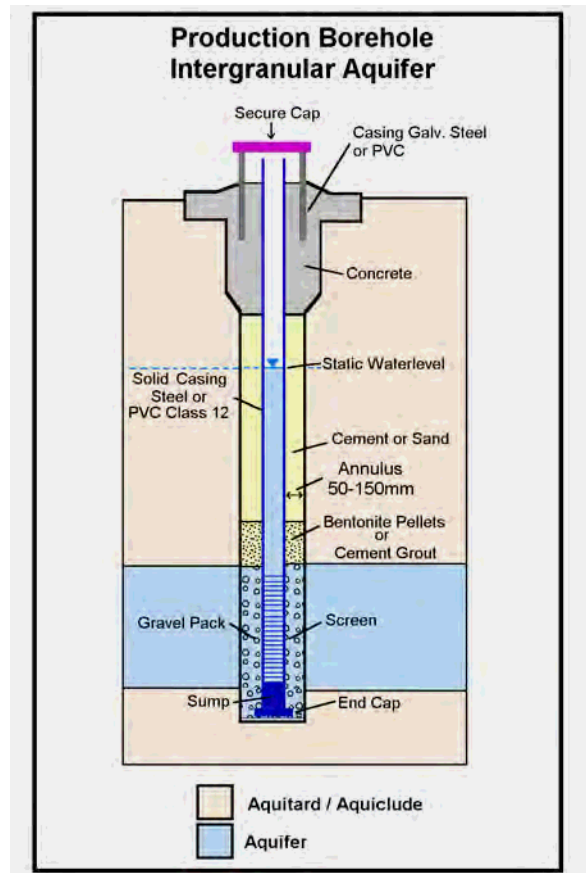


Figure 4.34: Typical production borehole design for an intergranular aquifer

The pump inlet is placed directly above the screens and not within the screened portion of the borehole, which will prevent excessive drawdown of the waterlevel and the influx of fine aquifer material into the borehole due turbulent flow within the screen / gravel-pack. An electrical pump cut-off switch is normally placed at this level of maximum permissible waterlevel drawdown. Significant volumes of groundwater can be extracted from fine-grained unconsolidated aquifers, where individual borehole yields are low using the following techniques:

- (1) a system of narrow diameter wellpoints (**Figure 4.35**), and/or
- (2) horizontal collector wells (**Figure 4.36**).

The collector well system is only suited to areas that are underlain by a reasonable thickness of saturated, permeable, unconsolidated material and where the watertable is less 2 m.bgl. This system consists of a single or a number of horizontal screen(s) that are connected to a central caisson or collector well. The horizontal screen is placed within the most permeable portion of the aquifer and perpendicular to the direction of groundwater flow (i.e. across the valley floor). The pump is installed in the caisson.

Note that a riser-pipe is placed on the opposite end of the system to allow for cleaning of the screens using a ‘pull-through’ brush mechanism. The selection of the correct screen placement depth below the watertable, screen slot-width and grain size of the gravel pack are crucial to the success of the system.

The wellpoint system can also be developed under similar geohydrological conditions, as well as where the weathered bedrock is the most permeable section of the aquifer and/or where the watertable lies below 2 m.bgl. This system allows for more flexibility and may be expanded incrementally with time as the water demand increases. The single line of boreholes indicated in **Figure 4.35**, can be repeated so as to produce a regular grid of wells. The optimum spacing required between the boreholes is determined by the physical properties of the aquifer. The boreholes are connected via a header-pipe to a single pump.

Both of these systems are installed perpendicular to the regional groundwater flow direction and to span the entire valley floor so as to increase the ‘capture-zone’ during pumping and thereby reduce ‘losses’ of water passing downstream of the system. A number of these systems can be placed at regular intervals along the floor of suitable valleys.

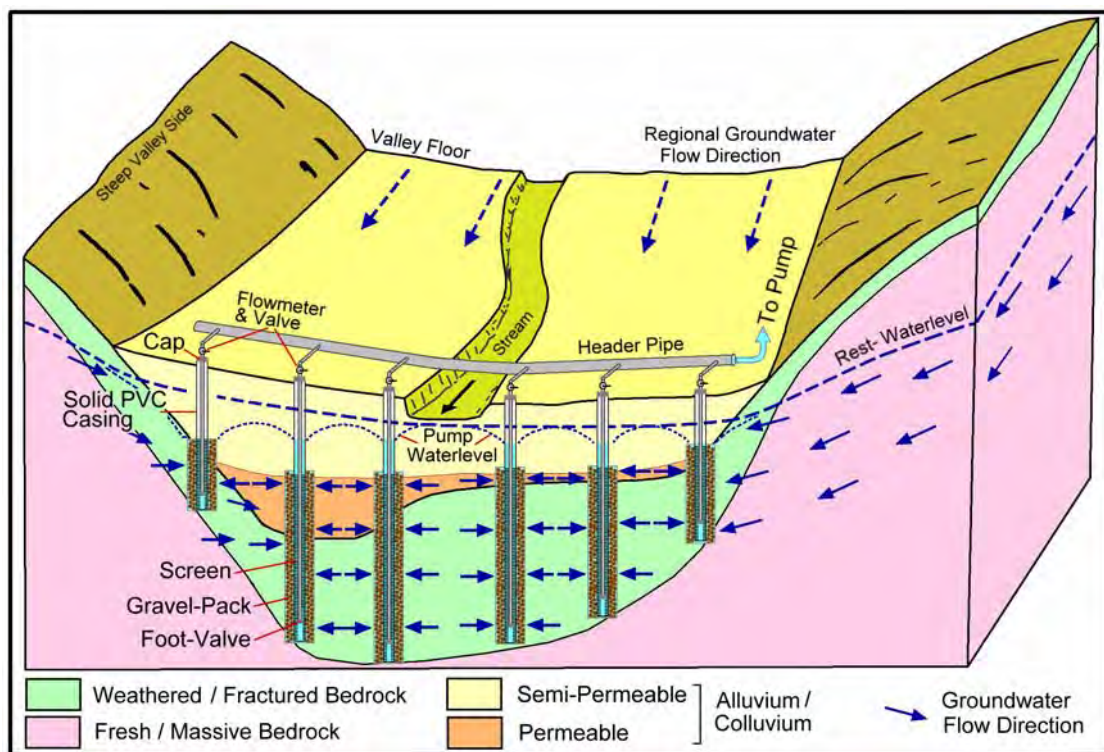


Figure 4.35: Schematic plan of well-point system (Woodford, 2000)

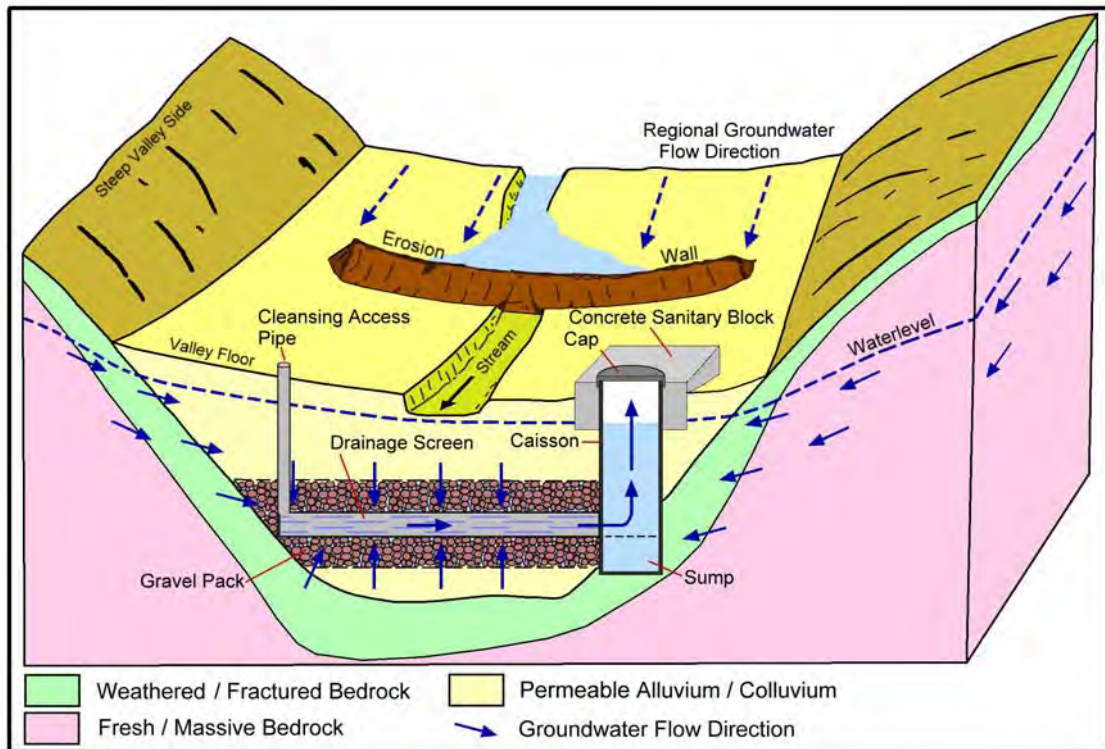


Figure 4.36: Schematic plan of a collector well system (Woodford, 2000)

In the case of stock-water boreholes, where high yields are not required, the alluvium may be cased-off and the water is drawn from the weathered/jointed bedrock directly below the alluvium. The groundwater in the alluvial material is thus allowed to drain into the jointed bedrock (**Figure 4.37**).

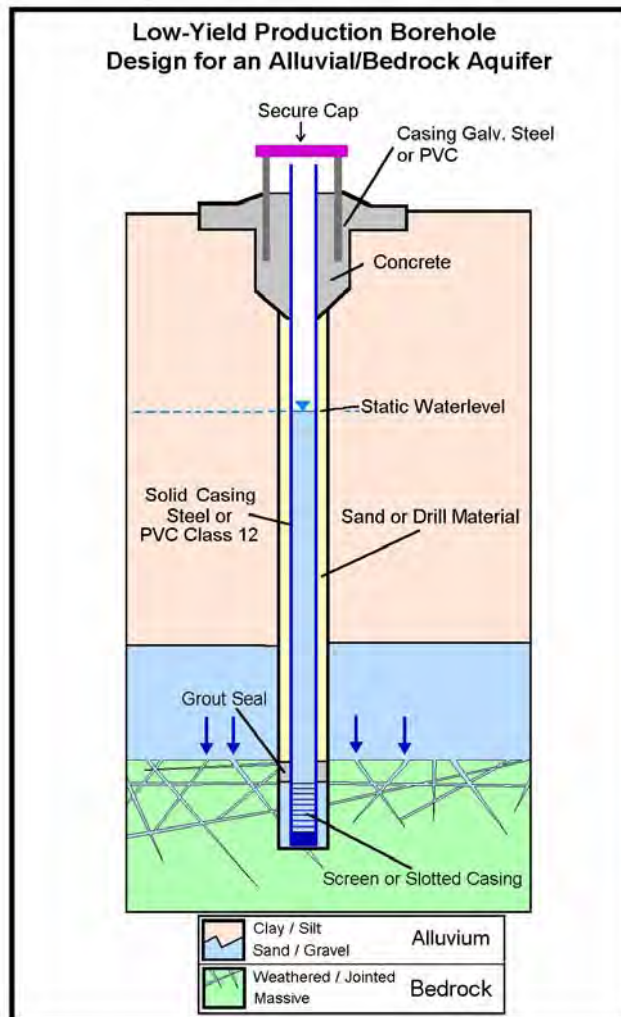


Figure 4.37: Typical low-yield production borehole design for an alluvial-bedrock aquifer

Production boreholes in highly weathered / decomposed hardrock, especially coarse-grained dolerite bodies, and the so-called ‘calcrete’ aquifers (**Chapter 2.6.3**) often require similar a design.

Monitoring Boreholes

Monitoring boreholes are used for the sole purpose collecting temporal information on waterlevel and / or groundwater quality changes within an aquifer. In shallow aquifers, such as those in the Karoo, these boreholes are commonly drilled to provide a completed hole diameter of 90-150 mm and are equipped with PVC Class 12 casing and screens.

In multi-layered aquifer the monitoring piezometers may be clustered in a single borehole (Figure 4.38), by selective placing of piezometer screens and annulus sealing.

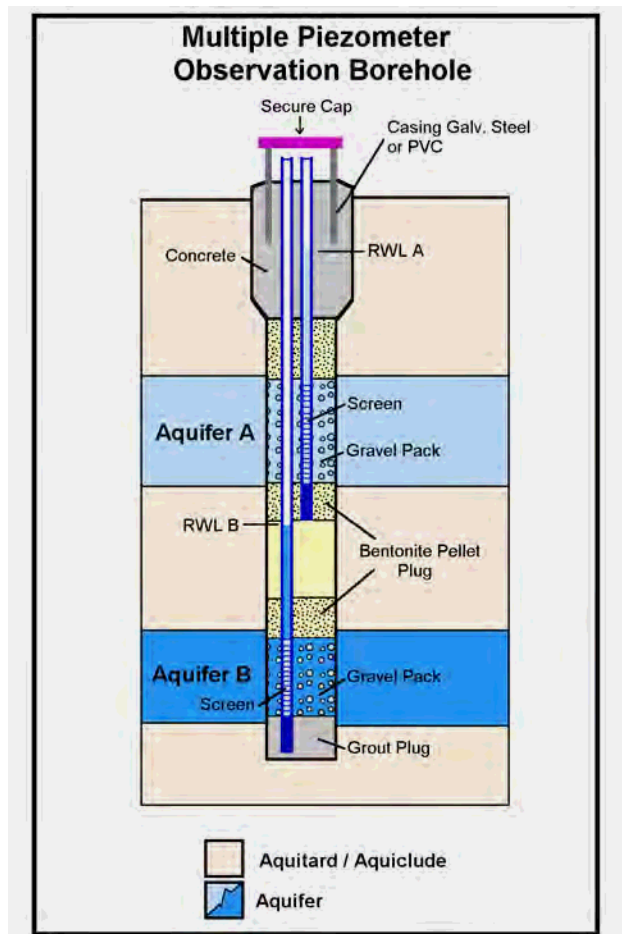


Figure 4.38: Multi-piezometer monitoring borehole

The usual method of construction is to drill and sample the hole to its full depth and then insert the deepest piezometer first, ensuring the correct placement of the screens. A gravel-pack is then placed around the screened section of the piezometer and a grout or bentonite annular seal placed directly above the gravel-pack. The borehole is then back-filled with fine sand to a level just below the next higher aquifer requiring monitoring and a second piezometer is similarly installed.

Installation of a multi-piezometer monitoring borehole is a specialised drilling operation and unless carefully constructed by an experienced driller the system may fail resulting in hydraulic connection between the aquifers via the borehole. The alternative is to install the individual monitoring piezometers in separate boreholes.

Artesian Boreholes

Strongly flowing artesian boreholes are uncommon in Karoo aquifers. The design objective of such boreholes is to control the artesian pressure and flow. At this stage it is not necessary to elaborate on the specialised construction techniques required to properly equip such boreholes. These issues will have to be addressed when and if deep production boreholes (> 300 m) are drilled into the multi-layered Karoo aquifer system, with variable potentiometric pressures and water quality.

4.2 GROUNDWATER RESOURCE EVALUATION AND MANAGEMENT

4.2.1 AQUIFER PUMP-TESTING

In this section, the following important points are illustrated:

- The use of an appropriate pumping test analysis technique is very important, and it is very easy to obtain incorrect estimates of T and S, if a wrong conceptual model is used;
- The T-value estimated in an abstraction borehole by using a porous flow model like Theis, is usually quite accurate, but a far too high T-value could be obtained by fitting a porous flow model to data of an observation borehole which is drilled into the matrix (no fracture intersection, i.e. a so-called “dry borehole”);
- The calculated S-value in a fractured rock aquifer will show distance dependency if analysed with a porous flow model or analytical fracture model like Moench (the further the observation borehole from the abstraction borehole, the smaller the calculated S value);
- The duration of a pumping test is very important (if this duration is too small and the last steep part of the pump test curve is not obtained, a too high T-value will be calculated which will lead to an incorrect calculated sustainable abstraction rate);
- Vertical and sub-vertical fractures will display a linear relationship between drawdown and the square root of time (i.e. a slope of 0.5 on double logarithmic paper) at early times. This is an indication that flow from the fracture to the matrix is perpendicular at early times. If the aquifer has a low T-value and the fracture is elongated, the parallel-flow period may last relatively long. During longer times the flow becomes pseudo radial (log t relationship) from the matrix to the fracture. In the case of horizontal fractures, the curve will display the following characteristic drawdown features: at early times: linear in $t^{0.5}$, then linear in $\log t^{0.5}$ then linear in $\log t$ as time goes on;
- The calculated T-value in an abstraction borehole is usually less than the actual T-value if borehole losses are not accounted for;
- Slug tests provide a quick technique to obtain a first estimate of the yield of a borehole;
- If slug tests are to be analysed, the Cooper method (which gives a T-value) must be used and not the Bouwer and Rice or Hvorslev method (which only gives a K-value – this K-value is scale dependent);

- To obtain reliable parameters for S (and also T), at least a two-layered model must be used and correct boundary conditions must be assigned to this model;
- Short duration step drawdown and multi rate tests must not be used for the estimation of aquifer parameters but only to estimate borehole losses;
- The Karoo Sequence can be viewed as a multi-layered aquifer. The top layer usually displays water table conditions while the other layers are confined or semi-confined;
- A minimum of two piezometric levels exists in a borehole, namely, a piezometric level due to the pressure in the fracture and a piezometric level (or water level) of the matrix. The fracture displays confined (or semi-confined) conditions while the level in the matrix could be either confined or a water table depending on the lithology;
- During pumping the drawdown in the abstraction borehole will display confined characteristics (i.e. drawdown will be according to the storage coefficient) until the position of the fracture is reached. At this position the characteristics change from confined to unconfined conditions (i.e. drawdown will be according to the specific yield and not the storage coefficient), with a consequent flattening of the drawdown curve. The T-value, however, still remains the same until the water level drops below the fracture, which then results in a much lower T-value.

Most of the pumping tests in South Africa are conducted for a short duration of less than 48 h, often because of the expenses associated with longer tests. The behaviour of the water levels with time in boreholes, drilled in Karoo aquifers during short duration pumping tests, differed significantly from long duration tests. After longer pumping times, the true behaviour of the aquifer matrix and the transition between the fracture- and matrix dominant flow periods can be distinguished. In some of the fractured aquifers, borehole yields are controlled by meso-fractures and the yield might drop suddenly once the fracture is dewatered. The sudden drop in yield occurs when the cone of depression reaches a boundary and the yield becomes dependent on the flow from the matrix.

Although the term water level is used in the following description of the behaviour of the aquifers during constant discharge pumping tests, most of the water levels are actually piezometric levels, representing the pressure in the fracture. The water level in a borehole is more representative of the piezometric pressure in the fracture than that of the aquifer matrix (Van der Voort, 1996).

Several examples of pumping tests in Karoo aquifers are given in **Figures 4.39** to **4.42**. The four tests display the same characteristic time-drawdown curves. On all the curves, two distinct slopes are present that represent different flow regimes. This behaviour is not restricted to Karoo aquifers only. Some pumping tests in other

fractured aquifers also exhibit the same behaviour. All of these boreholes are located on large-scale fractures, like faults or dykes. The tests are constant discharge tests that lasted for 48 h and longer.

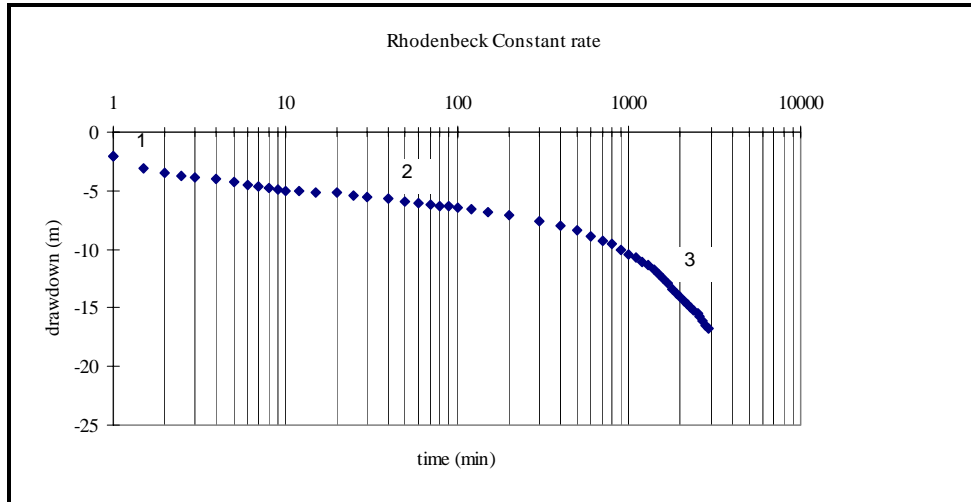


Figure 4.39: Constant discharge test at Rhodenbeck, Bloemfontein (Karoo aquifer $Q = 15.4 \text{ l/s}$)

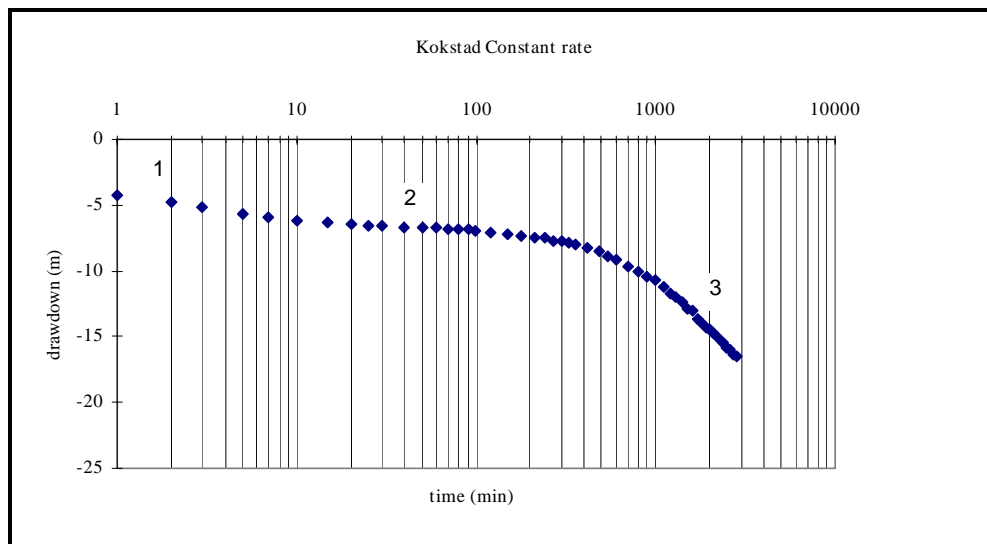


Figure 4.40: Constant discharge test at Kokstad (Karoo aquifer $Q = 13.0 \text{ l/s}$)

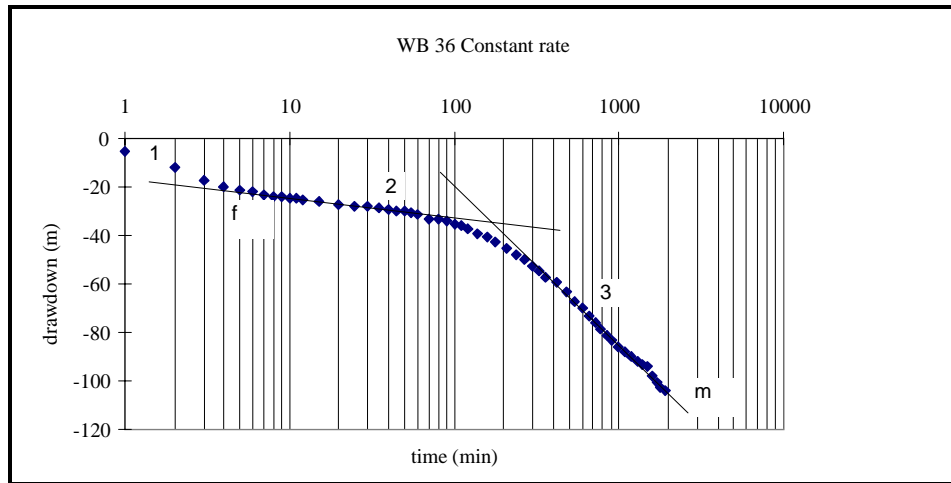


Figure 4.41: Constant discharge test at Grootegeluk, Ellisras (Karoo aquifer $Q = 18.4 \text{ l/s}$), f = fracture fit and m = matrix fit.

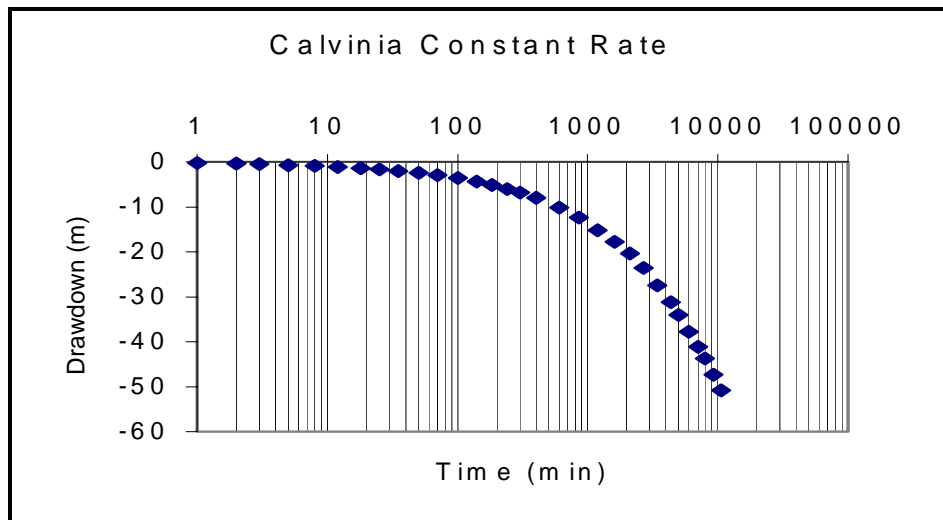


Figure 4.42: Constant discharge test on borehole G39973, Calvinia (Karoo aquifer $Q = 24.0 \text{ l/s}$)

The semi-log drawdown curves of these pumping tests display three main stages or slopes. The first stage is a rapid drawdown, after which it enters the second stage. During this stage, the water level seems to stabilize. During longer pumping times, the third stage becomes evident when the slope steepens again. The first stage can be ascribed to storage effects in the borehole (well bore storage) and it only lasts for a few minutes, depending on the extraction rate. The second stage is due to the contribution of the fracture storativity and fracture transmissivity. Its contribution lasts

only for a limited time because of the limited extent of the fracture. Although the internal porosity of the fracture is high, its volume is negligible if compared to the volume of water contained in the aquifer matrix. The steepening of the slope is caused by a boundary. The contribution of the fracture lasts only until the cone of depression reaches a boundary. These boundaries can be due to geological barriers or the termination of the fracture. The last stage prevails with longer pumping times and it is representative of flow from the matrix to the fracture over the surface area of the fracture.

Case Study: Putdam Pumping Test

The following pump testing data were collected 20 km from Bloemfontein. Borehole Put 1 (abstraction borehole) has a flow yield of 3 l/s and borehole Put 2 (observation borehole situated 18 m from Put 1) has a very low yield (less than 0.2 l/s).

The drawdown curves of Put 1 and Put 2 differ a lot. The curve of the observation borehole, Put 2, differs completely from that of Put 1 and it is evident that the Put 1 and Put 2 are not situated in the same fracture system. The borehole logs of the two boreholes confirm this observation in that borehole Put 2 is drilled into rock matrix and is very low-yielding. Abstraction from Put 1 will have very little effect on Put 2 and only slow leakage to the fracture system will occur at later pumping times. This is exactly what happened with the two boreholes during the pumping test and **Figure 4.43** can be viewed for the result.

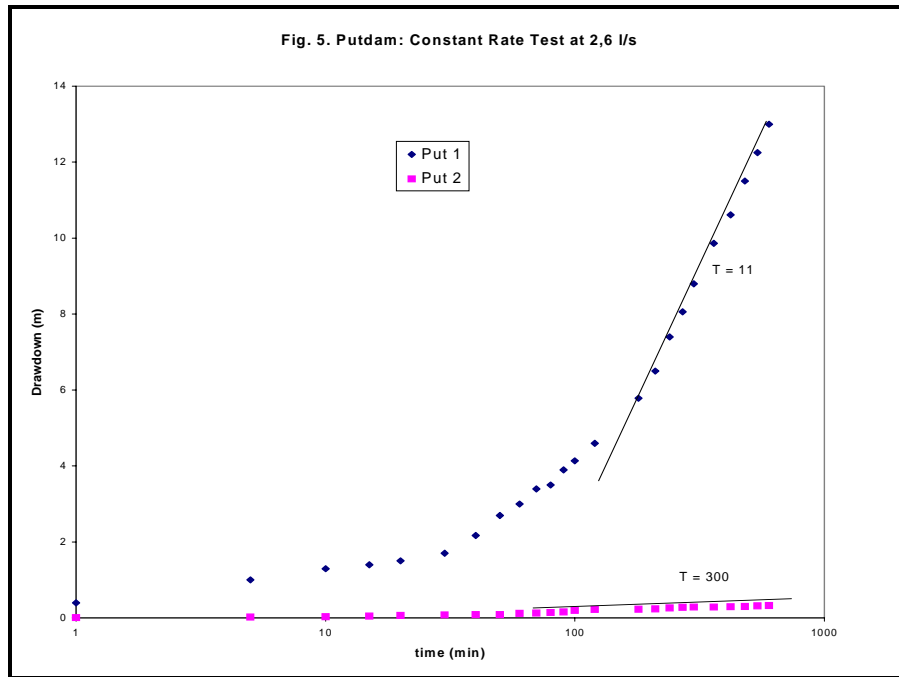


Figure 4.43: Putdam constant rate test at 2.6 l/s

It is also evident from the transmissivity and storativity values obtained from borehole Put 2 (practically a dry borehole) that a borehole situated in the matrix can and may not be used to calculate aquifer parameters for a borehole in the fracture system. The transmissivity value of 300 m²/d obtained from the fit on the Put 2 curve is ample proof that the estimated T-value is largely erroneous because a wrong conceptual model (in this case the Cooper-Jacob model) was applied.

Usually the following type of aquifer tests are performed in the Karoo Formations in South Africa:

- Slug tests
- Well performance tests (step-drawdown or multi-rate)
- Constant discharge tests
- Packer tests (only occasionally)

4.2.1.1 Test Pumping Procedures

Slug tests

In performing a slug test, the static water level in a borehole is suddenly lowered or raised. This is accomplished by lowering a closed cylinder into a borehole. The cylinder replaces its own volume of water within the borehole, thus increasing the pressure in the borehole. As the equilibrium in the water level is changed, it will recover or stabilise to its initial water level. The reaction of the water level with time could be used to:

- calculate the T or K of a borehole, and
- predict borehole yields by correlating between the recession time and yield of boreholes (empirical). The higher the T-value (and Yield), the quicker it will recover.

Vivier et al., (1995) use data obtained from 32 slug tests to obtain a correlation between the yield of a borehole and the recession time (time from input of slug until water level is again within 90% of original water level) (**Figure 4.44**)

The slug tests are quick to perform, cheap and easy to conduct and makes a handy tool to evaluate a borehole or to perform as a preliminary test for a pumping test. By performing a slug test on a borehole, it can be decided whether it is feasible to conduct a pumping test.

If the recession time is very quick (i.e. less than 10 s), it is very difficult to take the measurement without an automatic water level recorder.

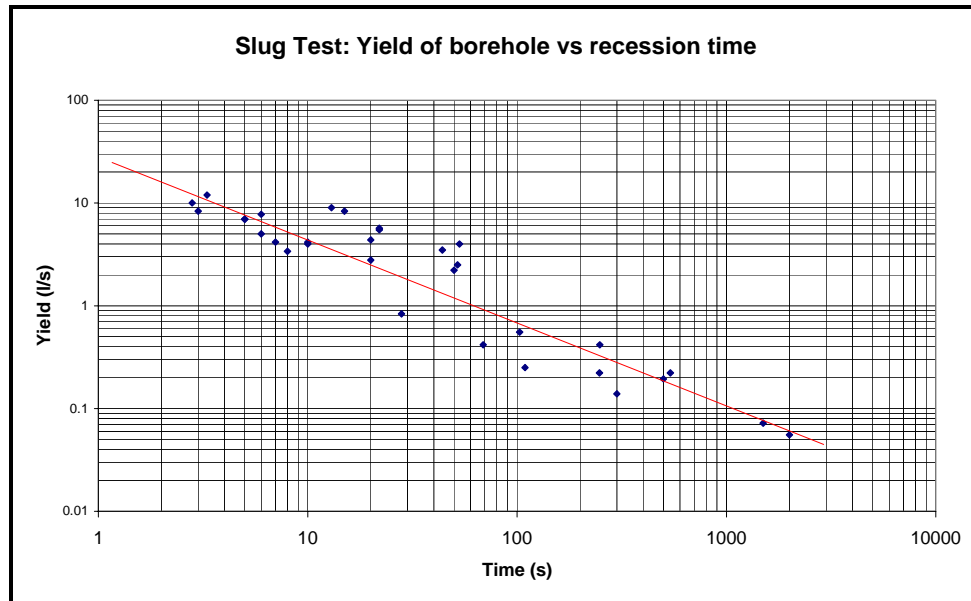


Figure 4.44: *Slug test: Recovery time versus yield of borehole*

The type of test pump procedures carried out on the borehole generally depends on the planned water usage (Weaver, 1993), but often includes a multiple discharge test (step-drawdown test), a constant discharge test and a recovery test.

Multiple-Rate Discharge Test

The multiple discharge test or step test is used to determine the hydraulic efficiency of the borehole at different pumping rates and to recommend a suitable pumping rate for the constant discharge test. The test involves monitoring the drawdown in the borehole while the discharge is increased in steps. Each step is usually carried out for no less than sixty minutes. A comprehensive description of the methods used to analyse the data obtained from multiple discharge tests is given in Kruseman and De Ridder (1991). The multiple-discharge test can also be used to establish the depths of the water strikes and the thickness of the weathered formation, so long as the initial steps are carried out for a sufficient duration at relatively low discharge rates (Woodford, pers. comm.). Information on the depth of the water strikes and the thickness of the weathered zone can be vital in the determination of daily abstraction rates. The relevance of this is discussed in **Chapter 4.2.2.2**.

Constant Rate Discharge Test

The constant discharge test is used to determine an aquifer's hydraulic parameters like transmissivity, storativity (if an observation well exists) and a conceptual model of the aquifer's hydraulic scenario, for example the presence of impermeable or recharge boundaries. The test involves monitoring the drawdown in the borehole while the discharge is kept constant. A description of the various methods used to analyse the data obtained from constant discharge tests is given in Kruseman and De Ridder (1991). The duration of the constant rate test may be determined by the information and level of reliability required (Weaver, 1993). It is common practice to run the test for about eight hours for boreholes to be equipped with hand, solar or wind driven pumps, and for forty-eight hours for boreholes to be equipped with electricity or diesel driven pumps, which are to be operated on a daily basis.

Recovery Test

The recovery test can be used to calculate an aquifer's hydraulic parameters, to establish whether recharge has taken place during or shortly after the constant discharge test and whether the storativity values vary throughout the aquifer (Driscoll, 1986). It can also give an indication of the extent of the aquifer, or the extent and connectiveness of fractures. The Geological Society of South Africa recommends this test to be continued until: the water level in the borehole recovers to its pre-pumping level; the water level recovers to less than 5% of the total drawdown experienced during the constant rate test; three readings in succession are identical; or the test is carried out for half the length of time of the constant discharge test (Weaver, 1993). In order to establish whether the aquifer has been significantly dewatered during the constant discharge test, and in order to accurately apply the recovery test data for estimating sustainable borehole yields, it may be preferable to monitor recovery water levels for at least the same duration as the constant discharge test.

In general, the conducting of these tests is well-known procedures among geohydrologists and poses no problem in the field. A serious problem, however, is that all these tests are performed in open boreholes (no piezometers installed) and that the results are analyzed with typical porous flow models like the Theis and Cooper Jacob method.

“Before one can pass judgment on the correctness of applying porous flow models to Karoo aquifers, one must construct a typical conceptual model for these aquifers”.

4.2.2 SIMPLIFIED METHODS CURRENTLY USED IN KAROO ROCKS FOR SUSTAINABLE BOREHOLE YIELD ESTIMATION

Murray (1996) gave a very comprehensive summary of available methods for sustainable borehole yield calculations in his master's thesis and the following is an abstract from his thesis.

In the previous section methods of determining aquifer parameters was discussed. The final borehole yield recommendation will depend on the interpretation of the test pump data. Presented in this section, is a review of established methods and newly developed methods for recommending borehole abstraction rates based on test pump data. The last section compares these methods and the methods based on an aquifer yield assessment to established yields from production boreholes.

In general, hydrogeologists tend to combine borehole and aquifer yield analyses. These include an assessment of test pump data, geological data, the topographic position of the borehole and climatic data. The type of test pump programmes carried out usually includes a multiple discharge test (step test), a constant discharge test and a recovery test. The geological data usually includes the type and extent of rock formations present and the degree of weathering and fracturing. The climatic data is used to obtain an indication of aquifer recharge, usually includes an estimate of the mean annual precipitation and the occurrence of droughts in the area.

Hydrogeologists differ in the degree of quantitative and qualitative analyses they use before recommending a borehole's yield. Some hydrogeologists place their emphasis on a qualitative assessment of the shape of test pump curves, while others will tend to combine qualitative test pump curve assessments with quantified borehole and aquifer parameter analyses. While the qualitative information may give an indication of the type of aquifer, and the presence and nature of hydraulic boundaries, quantitative information may include an assessment of the aquifer's transmissivity, storativity and recharge, as well as an assessment of how the borehole responds to pumping.

The importance of establishing the hydraulic properties of an aquifer and the need to understand the geological environment in which the borehole is located, is recognized by all geohydrologists. Hydraulic and geological conditions such as: transmissivity; storativity; the nature of boundaries (for example recharge, low permeability or barrier boundaries); whether the aquifer is characterised by double porosity, leaky conditions or vertical fractures, etc., all affect groundwater flow towards a pumping borehole and thus its sustainable yield. While an initial assessment of the geological environment is usually obtained from air photographs, satellite photographs, geological maps, topographical maps, geophysical surveys and drilling logs, a more comprehensive understanding of the geological environment is obtained by combining this information with test pump data.

4.2.2.1 Justification for Use of the Cooper-Jacob Approximation of the Theis Equation for Interpreting Test Pump Data

There is an on-going debate about the nature of groundwater flow in fractured media and its response to pumping. Many theoretical models have been developed to describe aquifer response to constant discharge pumping, all of which assume simplified regular fracture systems, and all of which are complex due to the complex mechanism of fluid flow in fractured rocks. Some of these methods are described by Kazemi et al., (1969), Warren-Root (1963), Gringarten-Witherspoon (1972) and Boonstra-Boehmer (1986), and most are applicable to observation wells rather than to pumped boreholes. A drawback with many of the fractured-rock test-pump analysis methods is that they may require laborious curve fitting, like the Boonstra-Boehmer method for flow in single vertical dykes and the Gringarten-Witherspoon method for flow through single vertical fractures.

Many fractured aquifers can be described by the double porosity aquifer concept. This theory regards a fractured rock formation as consisting of interconnected fractures of high permeability and low storage, which serve as conduits for flow, and matrix blocks of higher storativity and lower permeability. The effect of water abstraction from these aquifers exhibits a strong time dependency. During the early-time response, flow to the borehole comes from storage in the highly permeable fractures. The resulting drop in the piezometric head of these fractures creates a pressure gradient, which induces leakage from the surrounding blocks, leading to a temporary stabilizing of the drawdown curve. With continued pumping, the pressure gradient between the matrix and the fractures decreases and leakage occurs more slowly, causing the rate of drawdown, and thus the slope of the drawdown-curve, to increase.

The flow towards the well in double porosity systems is considered to be through the fractures, radial and in transient state. Transient or unsteady flow conditions imply a state of non-equilibrium, where flow rates and hydraulic gradients are changing over time and direction. While some of the double porosity models assume the flow from the matrix to the fractures is in pseudo-steady state, Boulton and Streltsova (1977) developed a transient matrix-to-fracture flow solution because the pseudo-steady-state inter-porosity flow models do not have a firm theoretical justification (Kruseman and De Ridder, 1991).

The analytical borehole yield assessment methods which are described later in this section, and which require the interpretation of constant discharge test data, however, are all based on the Cooper-Jacob approximation of the Theis transient-state flow equation (described in the following section). The Cooper-Jacob analysis has the advantage of being easy to apply in comparison to the methods that were developed to describe aquifer response to pumping in fractured media. Although not conceptually correct in many fractured rock environments, Phillips (1994) showed that the Cooper-Jacob analysis could provide acceptable estimates of transmissivity in a wide range of geological environments. Phillips (1994) compared transmissivity values obtained

using the Cooper-Jacob analysis which assumes radial groundwater flow in an isotropic, homogeneous aquifer, to the Boulton-Streltsova (1977) analysis which was developed for groundwater flow in fractured, double porosity aquifers. Figure 4.45 shows the similarity of the transmissivity values obtained using these two analytical methods.

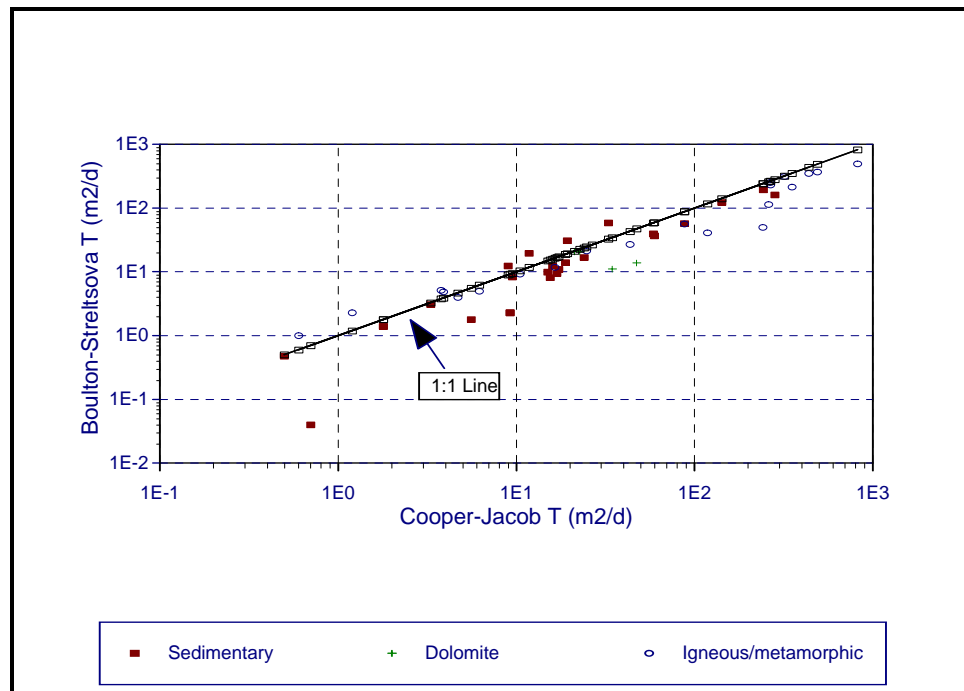


Figure 4.45: A comparison between transmissivity values obtained using the Cooper-Jacob and the Boulton-Streltsova methods in different hydro-lithologies

4.2.2.2 Estimating Sustainable Borehole Yields

The sustainable yield of a borehole is not obtained from conventional test pump interpretations. These interpretations are used to establish the hydraulic properties of the aquifer. Presented in this section are six methods for estimating the sustainable yield of a borehole, some of which require a transmissivity value and other parameters, which are obtained from test-pump curves. Two of the methods have been developed during the course of the study by Murray (1996), both of which are based upon the Cooper-Jacob approximation of the Theis equation. Although the remaining four methods have been previously described, none of them were given titles, which necessitated the naming of them by Murray (1996).

The maximum drawdown method (Enslin and Bredenkamp, 1963)

This method establishes the borehole yield from the maximum drawdown test, and is probably the most common type of pump test carried out in South Africa. Most of the test pumped boreholes in the former “homelands” and on the farms throughout South Africa have been tested using this method. The method involves placing the pump near the bottom of the borehole and pumping at a high rate until the water in the borehole is drawn down to the pump. Thereafter the abstraction rate is reduced until the water level in the borehole rises above the pump. The recommended yield for an 8 - 12 hour pumping day is usually taken as 60% of the highest yield a borehole can give without the water level in the borehole returning to the pump after 4 - 12 hours of pumping. The former Cape Provincial Administration’s pump test team in the Eastern Cape Province recommend that 65% of the borehole’s yield be taken as the production yield rather than the commonly used 60%. The duration of the test varies, but it is commonly carried out for 4 - 12 hours, and contractors seldom take a time series of water levels.

Murray (1996) evaluated this test by assessing the performance of three boreholes whose daily abstraction rates were determined by the maximum drawdown method. The boreholes are currently pumped between five to seven days a week for about 12 hours per day. They are located in a broad valley near the perennial Swart Kei River in the Queenstown area of the Eastern Cape Province, and they penetrate fractured Karoo aquifers. Although the depths of the main water strikes were not recorded, it was common practice for the relevant former “homeland” department to place the pumps near the main water strike.

Case Study - Borehole T 26325A (Figure 4.46)

Depth:	35 m
Water strikes:	Unknown
Pump intake:	14 m
	Tested yield: 11.4 ℓ/s (after a 9-hour maximum drawdown test)
Recommended yield using the maximum drawdown method:	6.8 ℓ/s
Current pumping rate:	6.3 ℓ/s (prior to the water in the borehole reaching the pump)
Percentage of tested yield:	55%
Current pumping duration:	10 - 12 hours per day Monday - Friday
Comments:	The water in the borehole reaches the pump after 20 minutes of pumping at the rate recommended by the maximum drawdown method. Without knowing the depth of the water strikes it is not possible to say whether the pump was set at the most suitable depth.

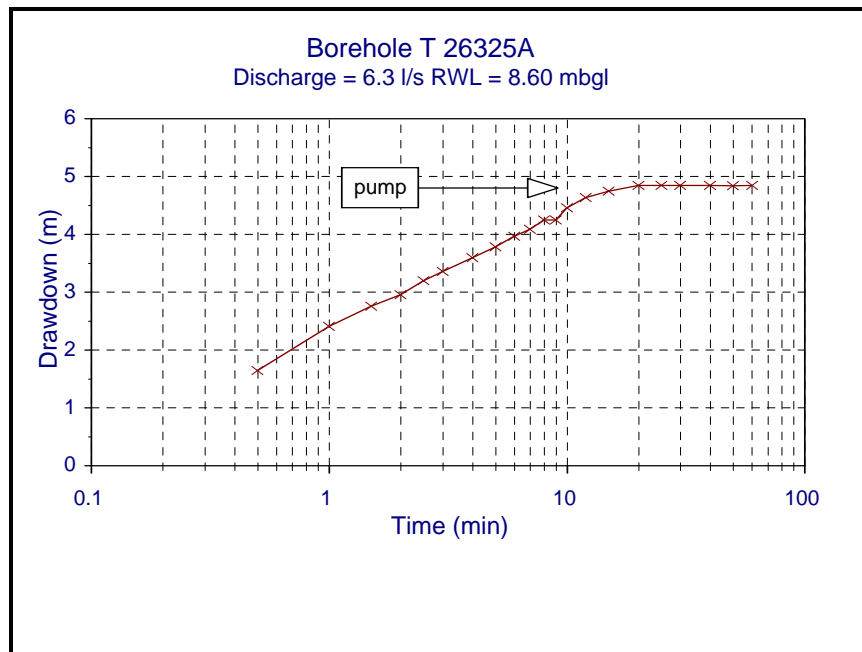


Figure 4.46: Drawdown in borehole T26325A at current production rates (the depth of the pump intake is indicated)

Case Study - Borehole CHB754B (Figure 4.47)

Depth:	54 m
Water strikes:	7 m & 24 m
Pump intake:	23.6 m
Tested yield:	5.6 ℓ/s (after a 9-hour maximum drawdown test)
Recommended yield using the maximum drawdown method:	3.4 ℓ/s
Current pumping rate:	4.2 ℓ/s (prior to the water in the borehole reaching the pump)
Percentage of tested yield:	75%
Current pumping duration:	12 hours per day Monday - Friday
Comments:	The water in the borehole reaches the pump after 40 minutes of pumping at 0.8 ℓ/s greater than is commonly recommended by the maximum drawdown method.

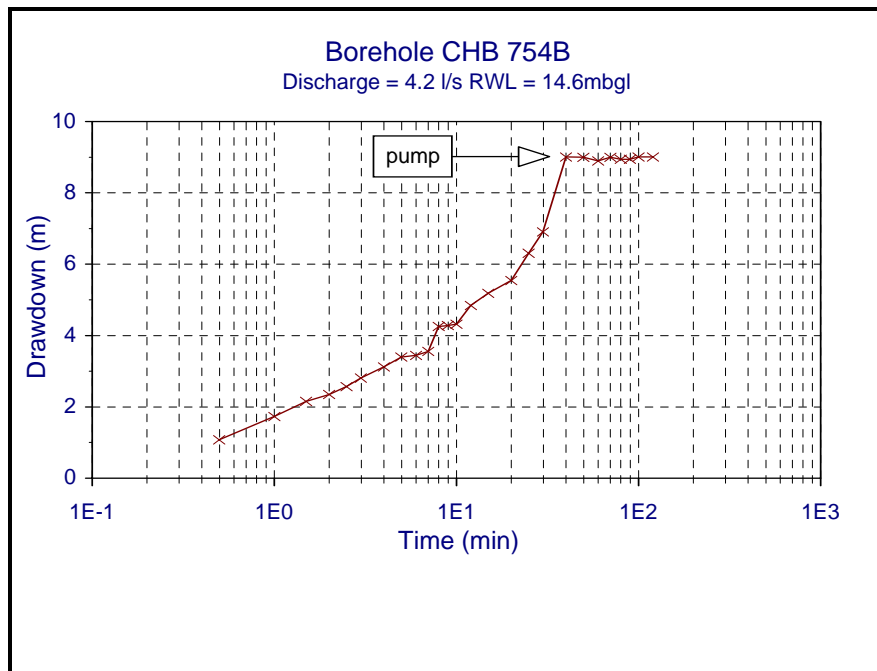


Figure 4.47: Drawdown in borehole CHB754B at a production rate of 4.2 ℓ/s (The depth of the pump intake is indicated)

In all three cases, the maximum drawdown method over-estimated the sustainable yield of the boreholes, although in the case of borehole CHB754B, the current production rate is slightly higher than what is usually recommended by this method. Enslin and Bredekamp (1963), commenting on maximum drawdown tests in secondary aquifers, state that where equilibrium (or a constant drawdown) is reached before the end of the pumping test, the yields measured are the reliable indicators of the long term potentials of those boreholes, and that these yields equal the safe yield of the borehole if storage and recharge are not the limiting factors. Because borehole water level readings are seldom taken during this test, it is usually not possible to establish whether equilibrium has been reached.

In the three examples presented, it is unlikely that recharge or storage limits the sustainable yield of these boreholes. Recharge to the aquifer in which these boreholes are located was determined through an inverse modelling exercise under steady state conditions, using the finite difference model, MODFLOW. The annual recharge was found to be in the order of 8 mm (Sami and Murray, 1995), which translates to approximately 400 000 m³ per annum for the whole basin in which these boreholes are located. Due to the size of the basin and because other, disused boreholes in the basin are water bearing, it is likely that storage is not the limiting factor either, even if the aquifer has a low average storativity.

The unsustainable high initial yields of these boreholes suggest that the aquifer is characterised by localized, high permeability fracture zones, which are supplied by a matrix with a lower permeability. It would appear that the sustainable yields of these boreholes are controlled by matrix transmissivity rather than fracture transmissivity, aquifer recharge or storage. In all three cases, the high, unsustainable discharges at the end of the nine hour pumping tests reflect the transmissivity of the fractures. For equilibrium to be reached which reflects the hydraulic characteristics of the matrix, the test should have continued for a much longer period.

The above case studies highlight the limitations of the maximum drawdown method. These limitations include:

- This test is usually not carried out for a sufficient duration to recognise the consequences of lower permeability boundaries. Such boundaries may consist of a low permeability matrix, which supplies water to the fractures, or a lower permeability formation located laterally from the fracture zone in which the borehole is located.
- There is no justification for assuming 60% or 65% of the borehole's yield after four to twelve hours of pumping will equate to the borehole's sustainable yield.
- This method considers aquifer permeability only, and therefore a borehole's sustainable yield could be over estimated if aquifer recharge or storage controlled the sustainable yield of the borehole.

Based on the conceptual limitations and failure of the maximum drawdown method in the cases studied, this method was not considered for further study.

Recovery Test Method (Kirchner, 1991)

This method involves calculating the maximum number of hours a borehole should be pumped each day at the tested rate, and it is based on the time it takes for the water level in a pumped borehole to return to the original rest water level (prior to pumping). Borehole water level measurements during the recovery period following a constant discharge pump test are plotted on semi-log graph paper against the time since pumping began (t), divided by the time since pumping was stopped (t').

The following formula is then used to determine the maximum number of hours (h) a borehole should be pumped for each day, at the pumping rate of the preceding test:

$$h = 24 - (24/x) \qquad \text{Eq. 4.1}$$

where:

x = the x-axis intercept of the residual drawdown versus recovery plot (t/t') on semi-log graph paper after a constant discharge pumping test (**Figure 4.48**). Residual drawdown is the water level in a borehole after pumping has ceased.

If, for example, the aquifer is recharged and complete recovery has occurred at e.g. $t/t' = 3$, then the pumping time was twice the recovery time. That means the borehole can be pumped for 16 h/d at the same hourly rate that the hole was pumped during the test. Whether the same quantity of water per day may be abstracted at a higher rate in a shorter period depends on the results of the step tests.

A complete recovery at e.g. $t/t' = 1.6$ indicates that the abstraction rate of the pumping test cannot be maintained for longer periods. In this case, a recovery time of $\frac{24}{1.6} = 15$ h/d and a corresponding pumping time of 9 h/d must be regarded as more adequate.

Theoretically zero residual drawdown should occur at $t/t' = 2$ if the abstraction rate equals lateral recharge (Kirchner, 1991). In this case, the recovery time for the borehole is equal to the preceding pumping time and a 12-hour pumping day can be maintained. A more rapid recovery may be observed if either vertical recharge has occurred or if storativity is different during pumping and recovery due to air entrapment or elastic deformation of the aquifer (Driscoll, 1986). A longer recovery time or incomplete recovery would indicate a limited extent of the aquifer or lower permeability boundaries.

A major problem in applying the recovery method is when incomplete or rapid recovery is experienced. Recovery readings are seldom taken for a longer period than the pumping period, that is beyond $t/t' = 2$, hence extrapolations are necessary. Extrapolations can produce non-unique t/t' intercepts, which may have serious implications for yield derivations. For example, if intercepts could fall between 1.01 and 1.1 from a pumping rate of 4 ℓ/s , which is a very plausible range given the standard error of slope extrapolations, yields of 3.4 to 31.4 m^3/day would be calculated. Extrapolations may also produce a t/t' value which is less than one, which gives a negative yield recommendation using equation 1. Under these circumstances it does not necessarily mean that the borehole cannot yield anything at all on a sustainable basis. Rather it indicates that partial dewatering of the aquifer took place during the constant discharge test, or that the aquifer is bounded by formations with relatively low permeabilities. While these may be good reasons to be cautious in recommending a long-term abstraction rate, they are not reasons to abandon the borehole altogether.

In cases where rapid recovery occurs due to leakage from overlying material or variations in storativity, relatively high t/t' values may be obtained. This results in the calculation of large yield values. Since the extent of storage in these horizons is not taken into account, the sustainability of these yields would be uncertain.

It is also necessary to examine the assumption that recovery time is related to the preceding pumping rate. Could a borehole pumped at a low rate relative to its potential require just as long to recover than if it were pumped at a higher rate? If a low rate was selected, a low pressure gradient would be induced in the fractures, which would limit their rate of replenishment from the surrounding matrix. Consequently, similar t/t' intercept values may be obtained irrespective of the preceding pumping rate.

The implication is that a much lower yield value would be calculated relative to that which would have been calculated from a high pumping rate recovery test. The application of this method should possibly be restricted to tests where the pumping rate is close to the borehole's capacity and where the recovery is complete. The implication is that a much lower yield value would be calculated relative to that which would have been calculated from a high pumping rate recovery test. The application of this method should possibly be restricted to tests where the pumping rate is close to the borehole's capacity and where the recovery is complete.

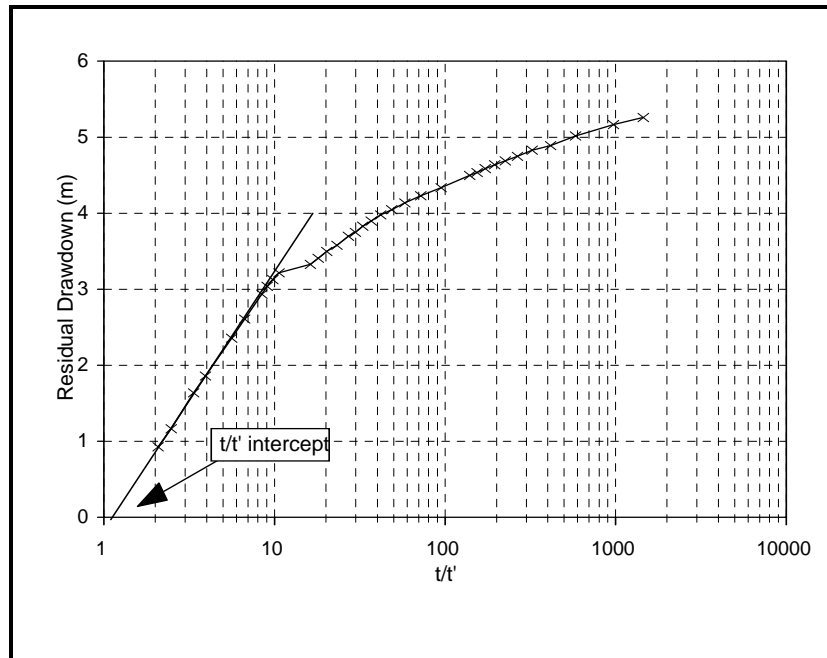


Figure 4.48: Recovery curve showing t/t' intercept

Transmissivity Method

The method is described in unpublished groundwater course notes by the Canadian International Development Agency (CIDA), and has been used by the Geological Survey in Swaziland (Ngwenya, pers. comm.). Swaziland's Geological Survey carries out twenty-four hour constant-discharge tests on boreholes to be equipped with motorized pumps and eight-hour tests on boreholes to be equipped with handpumps or windmills.

An approximate daily production yield in m^3/day (Q) is calculated using the following formula:

$$Q = 0.068 T.s$$

where:

- T = transmissivity (m^2/day)
- s = available drawdown (m)

CIDA recommend transmissivity be calculated using Jacob's straight-line recovery method (Todd, 1980) and available drawdown be taken as the distance between the rest water level and the main water strike.

After unsuccessfully trying to establish the theoretical basis of this equation, Murray (1996) felt that the only possible justification could have been that the maximum recommended drawdown in primary aquifers is commonly taken as 68% of the saturated thickness (Driscoll, 1986). Because no other theoretical basis for this equation could be established, it was not considered for further study. The hypothetical example given below illustrates the sensitivity of this method to available drawdown, and the weakness of this dependency in fractured rock aquifers.

Consider a fractured rock aquifer that is characterised by a steeply dipping, permeable fracture zone with low porosity, and a porous weathered zone, which serves as the aquifer's storage reservoir. Two closely spaced boreholes intersect the fracture zone at different depths. When test pumped, they give similar transmissivity values. The available drawdown in the two boreholes differ because the distance between their rest water levels and their water strikes differ. Because the groundwater resource available to the boreholes is much the same (similar permeability, storage and recharge), the sustainable yields of the boreholes would also be much the same. However, in applying the transmissivity method, the borehole with the deep-water strike would give a far greater yield than the borehole with the shallow water strike.

Methods Based on the Theis Equation

Three methods that are based on the Cooper-Jacob approximation of the Theis equation are presented. These methods can only be used if the constant discharge test is carried out in accordance with standard test pump procedures (Weaver, 1993).

In order to calculate the maximum pumping rate that would maintain a drawdown (s) above a specific point, after a long duration of pumping, the Cooper-Jacob equation can be defined as:

$$Q = 4 \Pi T s / [2.3 \log (2.25 T t / r^2 S)] \quad \text{Eq. 4.2}$$

where:

Q	= sustainable yield (m ³ /day)
T	= transmissivity (m ² /day)
s	= available drawdown (m)
t	= pumping time (days)
r	= radius of the borehole (m)
S	= storativity

Note that the sustainable yield (Q) obtained in **Equation 4.2** is not very sensitive to the logged variables in the equation. Errors in the S and t estimate therefore do not significantly affect the Q -value. The equation however, is sensitive to transmissivity and available drawdown, which makes the accurate determination of these parameters

critical. **Equation 2.2** is used in different ways in the following three borehole yield assessment methods.

Late-T Method

This method, described by Kirchner and Van Tonder (1995), uses the well-known Cooper-Jacob method to recommend a daily discharge, Q .

This equation is not very sensitive to S and usually a $S=0.001$ could be used in the calculations for Karoo Formations. A very convenient way to apply this equation is to estimate a unit drawdown s' for a unit abstraction rate Q and a large t (usually 365 days). The safe daily abstraction rate is then calculated from:

$$Q = s' / \text{available drawdown}$$

Where available drawdown = water above main water strike

The data of the late time-drawdown plot are used to fit a straight-line and obtain a T value. This segment of the curve reflects the rate of leakage from the matrix to the fracture, or it indicates that the radius of influence incorporates zones of lower T -values. If the last data show a flattening on semi-log paper, the method could not be used because an overestimation of T (and thus Q) will be obtained. In this method the Q value is obtained from the Cooper-Jacob equation such that the calculated drawdown in the abstraction well equals the available drawdown (distance from static water level to water strike) after a long time (usually 365 days are used). In many practical cases this method fails especially in cases where a deep water-strike occurred (available drawdown more than 30 m). For shallow water-strikes (less than 15 m available drawdown, the late T -method were found to work reasonably satisfactorily.

The matrix storativity (S_m) is used in the Cooper-Jacob equation. S_m is usually greater than S_f (fracture storativity), and therefore has greater influence on the long-term exploitation potential of the aquifer (Vegter, 1995).

Kirchner and Van Tonder (1995) recommend the available drawdown, a sensitive parameter in **Equation 4.2**, be taken as the distance from the rest water level to the main water strike in the borehole. The assumption that a borehole's sustainable yield is directly proportional to this distance, is questioned in the following two hypothetical examples.

Case Study: Example 1

Two boreholes that penetrate a fractured Karoo aquifer are located about 4 m apart, perpendicular to a steeply dipping dyke. The following hydraulic conditions prevail:

Matrix storativity:	0.001
Late-time transmissivity:	5 m ² /day
Rest water level:	10 m.bgl.
Main water strike - B/h 1:	50 m.bgl. (i.e. Available drawdown = 40 m)
B/h 2:	30 m.bgl. (i.e. Available drawdown = 20 m)

Using the late-T method, a yield of 124 m³/day is obtained for Borehole 1, and 62 m³/day for Borehole 2. The sustainable yield of the borehole may be influenced by the depth of the main water strike, because with increasing depth of the water strike the cone of depression can have a greater area of influence, it is clearly unreasonable to assume that these factors are directly proportional. If the main storage component of the aquifer was a narrow, near surface band of weathered rock, the depth of the water strikes below the base of this zone should not significantly affect the sustainable yields of the boreholes.

Case Study: Example 2

A borehole intersects a deep-water strike in an unconfined aquifer with a high storage capacity. The late-T method assumes that the entire available drawdown can be pumped in a given year, thus assuming that annual recharge will result in its complete replenishment. Should the aquifer not be fully recharged, the water table would be lower than when pumping first started, and the available drawdown would be less than the initial available drawdown. The drop in the available drawdown would be in proportion to the volume of water removed from storage. To continue pumping at year one's rate could result in the water strike being reached during, rather than at the end of year two, thereby indicating that the yield predicted by the late -T method is not sustainable. If recharge cannot replenish the water held in storage over the chosen recharge period, this method may give an exaggerated yield recommendation.

The concept of applying the transmissivity that reflects flow from the matrix to the fractures in the double porosity model has a good theoretical basis, because it is the matrix with its high storage capacity that supports the abstraction between recharge events. **Equation 4.2** is however highly sensitive to available drawdown, a parameter which should not necessarily be based on the distance between the rest water level and the main water strike.

A drawback in the application of this method is that it relies on knowing the depth of the main water strike. This is often a problem because of unreliable or non-existent borehole records.

Drawdown-to-Boundary Method

This newly developed method has been adapted from a borehole yield assessment approach used by A.C. Woodford (Directorate of Geohydrology, DWAF). It is referred to as the drawdown-to-boundary method because emphasis is on determining the maximum drawdown permitted in order to prevent the dewatering effects that may result once a low permeability boundary is encountered. As with the late-T method, **Equation 4.2** is used to recommend a daily discharge, Q .

The available drawdown, s in **Equation 4.2**, is limited to the point at which an inflection in the semi-log slope of the time-drawdown curve is identified (8 m in **Figure 4.49** and 4.5 m in **Figure 4.50**). Hence, if a sharp increase in the rate of drawdown is observed, the height of the rest water level above this point is taken as the available drawdown. The aim of this method is to determine an abstraction rate that will restrict the drawdown at the end of a pumping year to the inflection point. The modelled drawdown curve in **Figure 4.50**, which is derived from equation 2 using T_f and $s = 8$ m, reflects this pumping rate.

Woodford recommends that the s -value be taken as the thickness of the weathered formation below the piezometric level or water table in aquifers which derive most of their storage from this zone. By limiting the long-term drawdown to the base of the weathered zone, the risk of dewatering the storage component of the aquifer is reduced.

Fracture transmissivity (T_f in **Figure 4.49**) and fracture storativity values should be used in equation 2 because they control the rate of drawdown during the early, pre-boundary pumping times. Vegter (1995) suggests that storativity values for fractured rocks are at least an order of magnitude less than that of the porous, decomposed and disintegrated rock, regardless of fracture density. Thus an S_f value that is an order of magnitude less than the regional S_m values can be used in **Equation 4.2**.

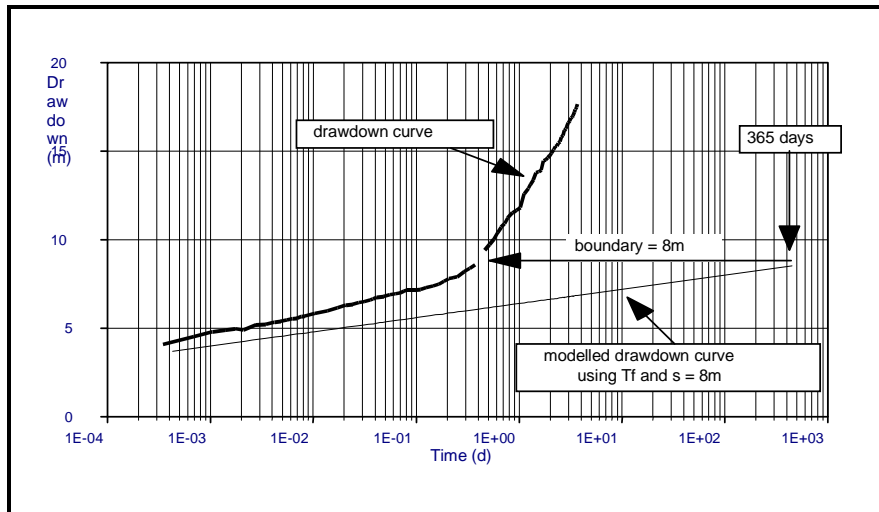


Figure 4.49: *Modelled drawdown curve based on the drawdown-to-boundary method*

An advantage of the drawdown-to-boundary method is that it aims to limit the long-term drawdown in the borehole to a level at which a hydraulic boundary is encountered. As stated earlier in this chapter, such boundaries may be caused by different geological conditions. A boundary may consist of a geological barrier that delineates the lateral extent of the aquifer; it may consist of a geological formation with lower permeability, or zones within a formation of lower permeability; and it may consist of a matrix of lower permeability than the fractured parts of the aquifer.

A possible drawback of the drawdown-to-boundary method is that it does not consider permeability of the material that forms the boundary. Limiting drawdown according to the nearest hydraulic boundary does not take into account that such a boundary may not be impermeable but may only represent reduced permeabilities or a reduced rate of vertical leakage in double porosity or semi-confined formations. These may bear additional water under higher-pressure gradients when stressed and would therefore not be utilised under drawdowns maintained by the prescribed yield. Where the aquifer is highly heterogeneous or exhibits a delayed yield response, the rapid appearance of such an apparent boundary may lead to an attempt to maintain too small a drawdown, thereby resulting in overly conservative yield estimates.

Distance-to-Boundary Method

The above name has been given to this newly developed method because it requires that the theoretical radius of influence at the hydraulic boundary be determined. The method employs a modification to the Cooper-Jacob **Equation 4.2** where r is the radius of influence in the aquifer when boundary conditions are encountered. When an

inflection in the semi-log slope of the time-drawdown curve is identified at time t , the radius of influence (r) at that time is calculated by solving for:

$$r^2 = 2.25 T t / S \quad \text{Eq. 4.3}$$

The point at which the early-time slope departs from the drawdown curve indicates the time a hydraulic boundary was encountered, and may be taken as the t -value (**Figure 4.49**). Again, it is important to note that this break in slope might not represent a true physical boundary to flow, but may represent a point in time at which the permeability of major fractures no longer controls a borehole's discharge-drawdown relationship in double porosity fractured rock systems. From this identified point in time a borehole's discharge is predominantly controlled by the rate at which water can leak into the main fractures from the surrounding rock matrix or from smaller micro-fractures.

Using this distance (r), Equation 2 is used to calculate the pumping rate (Q) that can be sustained over the long-term (e.g. $t = 365$ days) while maintaining a negligible drawdown, Δh at distance r . The Δh value, which represents the drawdown during the transition from early- to late-time conditions (**Figure 4.50**), is substituted for s in equation 2.

The value r in **Equation 4.3** should be obtained using T_f and S_f because the fracture transmissivity and storativity control the rate of drawdown during early pumping times, before the boundary is encountered. In the calculation of Q in equation 6.10, T_f and S_m should be used since long term yield is controlled by the rate at which water stored in the matrix S_m can be released to the permeable fractures T_f .

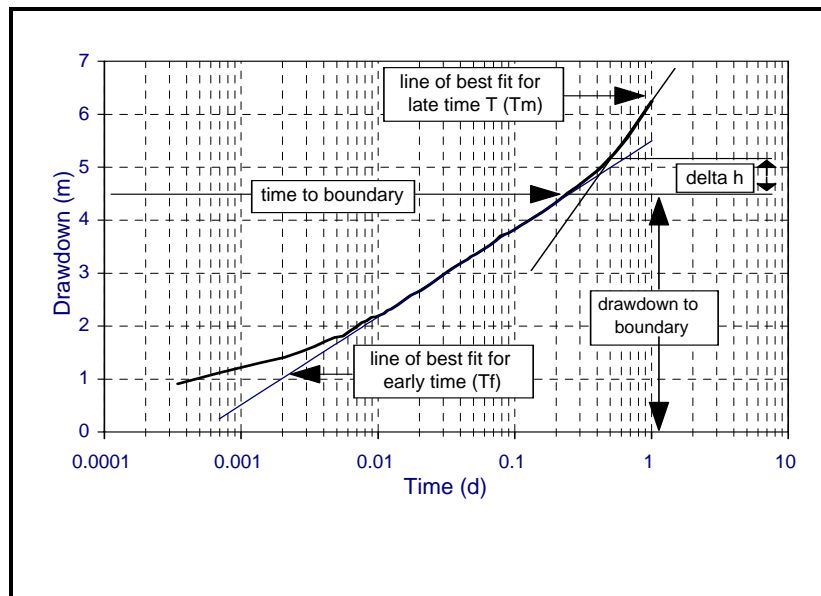


Figure 4.50: Distance to boundary values

The concept of restricting the maximum abstraction so that significant drawdown is limited in extent to the theoretical distance of an observed boundary, seems appropriate in aquifers which are characterised by boundary effects. A drawback in the application of the distance-to-boundary method is that a Δh value may not be easy to obtain, for example where delayed yield or double porosity effects are experienced (**Figure 4.49**). An acceptable Δh value is essential when applying the distance-to-boundary method because of the sensitivity of Q in **Equation 4.2** to available drawdown (Δh in this case). Examples from Karoo aquifers indicate that a maximum Δh value of 1 m should be employed.

RPTSOLV (Radial Two-Dimensional Numerical Model)

This method was first published by Verwey et al., (1995). In practice, it was found that this method usually underestimates Q , because a no-flow boundary is used at some distance from the abstraction borehole.

Case Study: Production Borehole GR2 at the Mimosadale Wellfield, Graaff-Reinet

Location: Graaff-Reinet, Eastern Cape, South Africa

Lithology: Beaufort Group, Karoo Sequence

The relevant drilling information for borehole GR2 is presented in **Table 4.8**, whilst the results of the pump-test evaluation are presented in **Table 4.9**. The pump drawdown and recovery curves are presented in **Figures 4.51** and **4.52**, respectively.

Table 4.8: Geological Log of Borehole GR2

0-2 m	Calcareous sandy alluvium
2-10 m	Siltstone and shale
10-39 m	Sandstone
39-44 m	Sandstone and shale
44-53	Sandstone
Depth	53 m
Water strikes	18 (4.4 l/s)-36 (3.4 l/s)- 38 (3.0 l/s)-42 (17.2 l/s)- 44 (11.0 l/s)
Final blow yield	39 l/s
Current use	Municipal production borehole

Comment: Borehole failed at 7.7 l/s - Current yield = 2.1 l/s

Table 4.9: Mimosadale Wellfield - Aquifer properties

T-early (m ² /d)	137
T-late (m ² /d)	47
T-recovery	83
S _f	0.0004
S _m	0.004
t/t'' intercept	0.6
RWL	8
Dist-boundary (m)	11
Time-boundary (d)	0.7
Δh	1
Catchment area (km ²)	180
Recharge (mm/a)	7
Aquifer thickness	20 m
Years without recharge	3
Hydraulic gradient	0.005

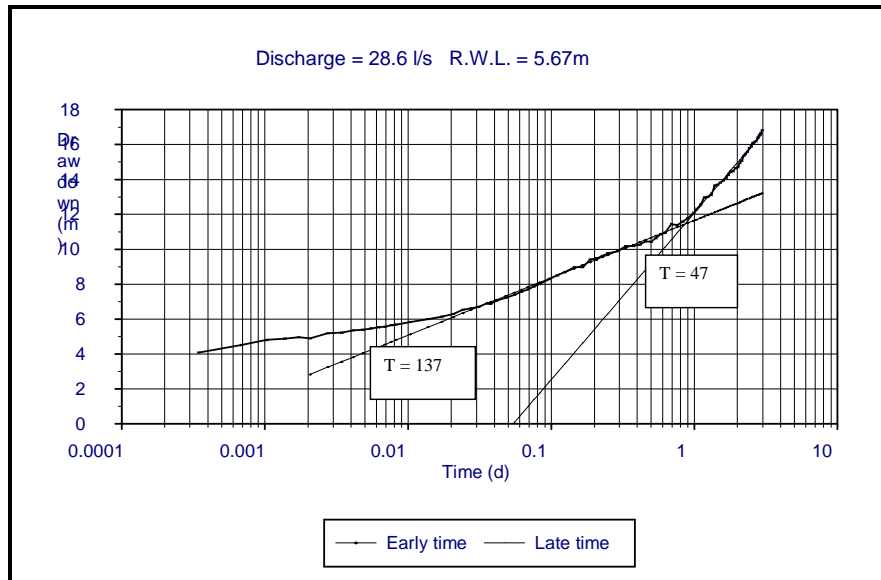


Figure 4.51: Borehole GR2 - Constant discharge test at 28.6 l/s

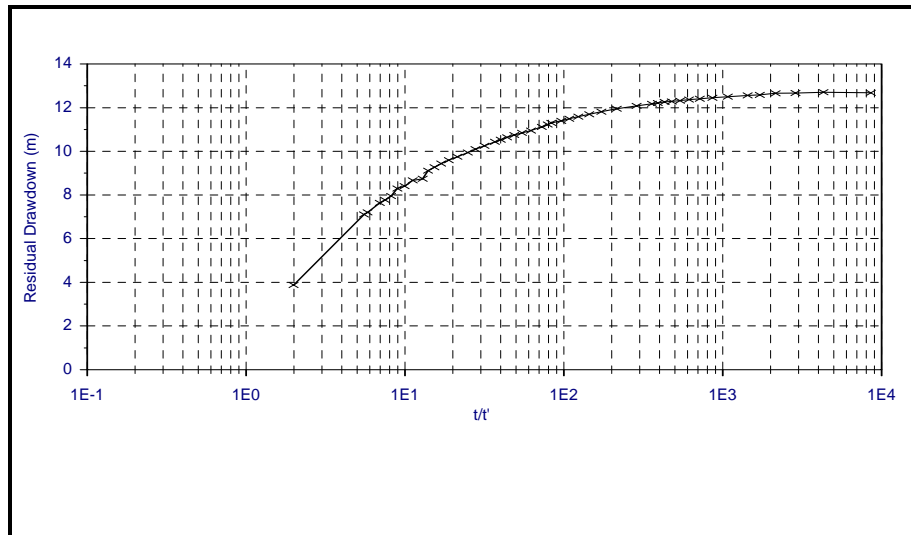


Figure 4.52: Borehole GR2 - Recovery test

Discussion

The drawdown curve deviates from a straight line at about 19 hours (**Figure 4.51**), indicating that the cone of depression encountered a hydraulic boundary of lesser permeability. The recovery test (**Figure 4.52**) gave a residual drawdown of 3.88 m three days after the constant rate test was stopped.

Boreholes GR2 and another borehole, GR1, are less than 800 m apart and penetrate a common aquifer, which is also exploited by a third, lower yielding borehole. After assessing abstraction and borehole water level data, Smart (1994) estimated the sustainable yield of the wellfield to be 288 000 m³/annum or 789 m³/day, and Woodford (1992) recommended that this borehole be pumped at 360 m³/day. Abstraction records show that borehole GR2 was pumped at an average yield of 665 m³/day for the first two years of production. The waterlevel in the borehole dropped by about 10 m (**Figure 4.53**) and the yield was reduced to an average of 181 m³/day. With two other boreholes in the wellfield being used on a regular basis, GR2 could not sustain a pumping rate of 665 m³/day. However, the rise in waterlevel after the yield reduction indicates that a yield greater than 181 m³/day could be sustained. If it was the only production borehole in the aquifer, its sustainable yield would likely be significantly greater than 181 m³/day, and possibly even more than Woodford's recommended yield of 360 m³/day. It is also likely that this borehole's sustainable yield is significantly less than Smart's aquifer's yield of 789 m³/day, as it is improbable that a single borehole can abstract the full yield that the wellfield can supply.

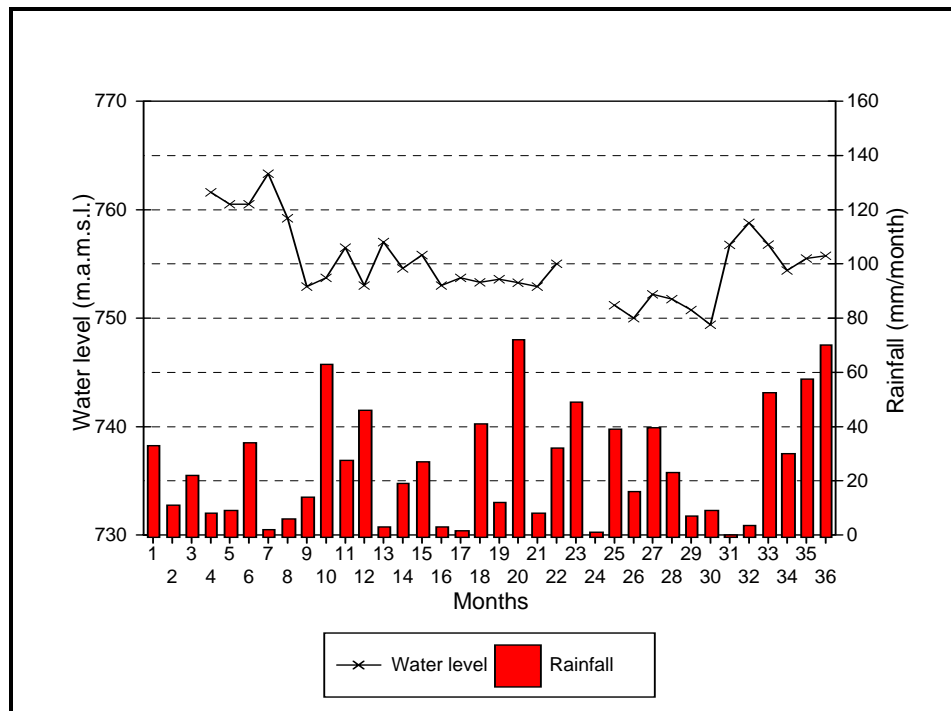


Figure 4.53: Borehole GR2 - Waterlevel and rainfall data

The late-T method's yield of $1\,010\text{ m}^3/\text{day}$ is greater than the aquifer yield (Smart, 1994), and clearly over estimates the sustainable yield of this borehole. The drawdown-to-boundary method's yield of $775\text{ m}^3/\text{day}$ also appears to be too high, that is, if the 11 m inflection point on the drawdown curve is used. If the thickness of the saturated weathered zone is used, which according to Woodford (pers. comm.) is 6 m, a yield of $423\text{ m}^3/\text{day}$ is obtained. This appears to be a reasonable figure so long as no other boreholes within the wellfield were brought into production. Interestingly, the first inflection point on the drawdown curve at 6 m, corresponds to the thickness of the saturated weathered zone. The yield obtained using the distance-to-boundary method ($436\text{ m}^3/\text{day}$), is similar to the yield obtained using the drawdown-to-boundary method with an available drawdown value of 6 m. Given that the borehole showed incomplete recovery after the constant discharge test, and that the pumping rate of $665\text{ m}^3/\text{day}$ could not be sustained, the $\pm 430\text{ m}^3/\text{day}$ yields obtained from the distance-to-boundary method and drawdown-to-boundary method (using an s-value of 6 m) seem to be reasonable.

The fit of the pump test data with RPTSOLV is given in **Figure 4.54** and yielded a sustainable yield of 1.96 l/s .

Square Root of Time Method

If the last 13 points on the drawdown curve is used, a very good correlation (99.39%) exists between drawdown and $t^{0.5}$ (i.e. square root of time):

$$\text{Drawdown} = 0.1715t^{0.5} + 5.5799$$

The abstraction rate of 28.6 ℓ/s during the constant-rate pump-test yields a drawdown of 130 m after 365 days (i.e. $t^{0.5} = 725$ min). If an available drawdown of 36 m is taken, a sustainable yield of 7.92 ℓ/s is calculated for GR2 with this method.

Table 4.10: *Summary of sustainable yield estimates from the different techniques*

Method	Estimated yield (ℓ/s)
Late T-method	11.68
Drawdown-boundary	8.96
Distance-boundary	5.05
t/t intercept from recovery	Not applicable
RPTSOLV	1.96
Square root of time method	7.92

Borehole GR2 failed at 7.7 ℓ/s and is now being operated at an abstraction rate of 2.1 ℓ/s . As can be seen from the above table, only the RPTSOLV method gives a rate lower than the current abstraction rate.

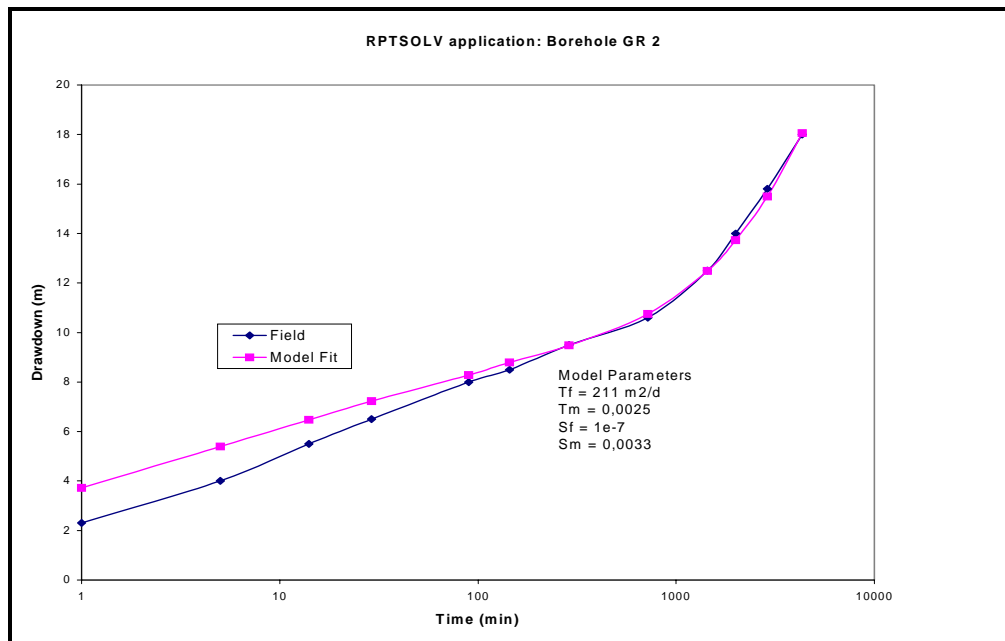


Figure 4.54: RPTSOLV's fit of borehole GR2

Flow Characteristic (FC) Method

Van Tonder et al., (1988) proposed a new and practical approach to estimating the long-term sustainable yield of a borehole from pumping tests, which includes the following important features:

- It is easy to apply.
- Is applicable to both porous and fractured-rock aquifers.
- Observation boreholes are not a necessity.
- Does not require a storativity value *a priori*.
- It incorporates the effects of well-losses.
- The rate of waterlevel recovery is taken into account.
- The Late-T (Kirchner & Van Tonder, 1995) and Drawdown-to-Boundary Methods (Murray, 1996) are special cases of the FC-Method.
- It incorporates various characteristic flow regimes (**Chapter C.1.1**).
- The influence of other production boreholes on the estimated sustainable yield is also taken into account.

The method was tested on more than 30 pumping-tests in fractured-rock formations in Southern Africa and the results are looking promising.

Theoretical Formulation of the FC-Method

The drawdown in a pumping borehole after a long period of time (i.e. 10^6 minutes for convenience of working in full log cycles or about 700 days) can be estimated as follows:

$$s = s_{10} + 5.\nabla s$$

or similarly by

$$s = s_{100} + 4.\nabla s \quad \text{Eq. 4.4}$$

where

- s = drawdown after 10^6 minutes
- ∇s = drawdown per log cycle
- s_{100} = drawdown after 100 minutes of pumping

For practical purposes, it is proposed that **Eq. 4.4** is utilised, as the early drawdown data, prior to 100 minutes, may exhibit effects of borehole storage, discharge-pipeline pressurization and pump-rate adjustments.

Considering the Cooper-Jacob equation of $\nabla s = 2.3Q/4HT$, then **Eq. 4.4** can be rewritten as:

$$s = s_{100} + 0.73Q/T \quad \text{Eq. 4.5}$$

where

- Q = abstraction rate in m^3/d , and
- T = transmissivity in m^2/d

and can then write:

$$(s_{100} + 4\nabla s)Q_s = sa.Q$$

- where Q_s = daily sustainable abstraction rate in m^3/d , and
- sa = available drawdown

Thus:

$$Q_s = \frac{sa * Q}{(s_{100} + 4\nabla s)}$$

or

$$Q_s = \frac{sa * Q}{(s_{100} + 0,73Q/T)} \text{ for a confined, homogeneous, infinite porous aquifer.}$$

These equations can now be rewritten to include various flow regimes, such as fracture-flow, and the rate of recovery by introducing two factors F1 and F2, respectively:

$$Q_s = \frac{sa * Q}{F1(s_{100} + 4\nabla s F2)} \quad \text{Eq. 4.6}$$

or

$$Q_s = \frac{sa * Q}{F1(s_{100} + 0,73 * Q * F2 / T)} \quad \text{Eq. 4.7}$$

where

- Q_s = daily sustainable abstraction in m³/day.
- Q = abstraction rate in m³/day during pumping test
- sa = Available drawdown (m)
- s_{100} = drawdown after 100 minutes of pumping (m)
- ∇s = drawdown per log cycle (m)
- $F1$ = factor relating drawdown to recovery data.
- $F2$ = factor describing type of characteristic flow regime.

Note that when factor $F1 = 1$ and $F2 = 1$ we are dealing with the classical Theis model.

Estimation of the Factor F1

The determination of F1 is straight-forward and takes into account the both the early and late stages of the drawdown and recovery in the production borehole:

$$F1 = \frac{S_{100}}{S_{100}^*} \cdot \frac{S_m}{S_m^*} \quad \text{Eq. 4.8}$$

where (Figure 4.55)

- s_{100} = Drawdown (m) after 100 minutes of pumping.
- s_{100}^* = Recovery of waterlevel (m) after 100 minutes of pump shut-down.
- s_m = Maximum drawdown at time (t_m) of pump shutdown.
- s_m^* = Recovery of waterlevel (m) after an equivalent time (t_m).

Theoretically, if water is to be abstracted continuously from a production borehole then $F1 = 1$, as no recovery will take place. By using actual drawdown after 100 minutes of pumping, well losses are included into the FC-method.

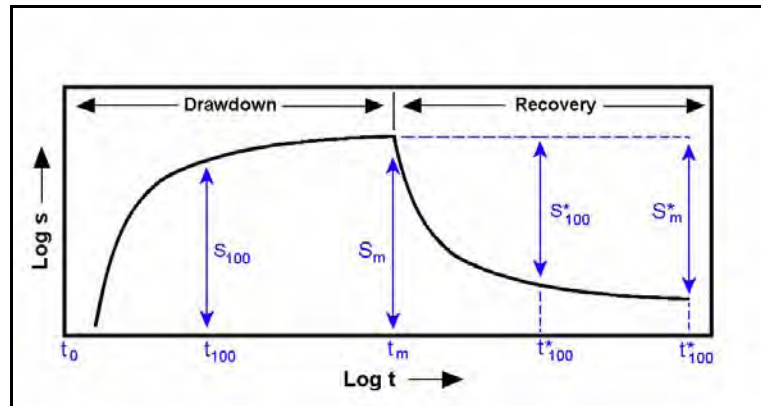


Figure 4.55: Drawdown parameters used to calculate factor F1

Estimation of Factor F2 from the Drawdown Derivative Graph

Typical F2 values were obtained by running the well-known MODFLOW-3D program for many fractured-rock scenarios, including fracture-matrix and various boundary relationships. The RPTSOLV program was also used to control these F2 estimates. The ratio of $T_{\text{fracture}}/T_{\text{matrix}}$ plays also an important role in the determination of the F2 value. When a boundary is reached, the F2-value can be estimated from the derivative of drawdown graph. The *derivative plot* is simply a graph showing the small-scale incremental changes in the gradient of the semi-log drawdown-time plot (i.e. Cooper-Jacob) (Chapter D.2.2.1).

The value of F2 can be easily determined from *derivative graph* using the following procedure:

1. The initial *infinite-acting flow* period is determined, i.e. the first horizontal straight line after cessation of borehole storage effects:
Intercept of infinite acting flow line on derivative axis = d_0
2. The late *infinite-acting flow* period is similarly determined:
Intercept of any other horizontal line on derivative axis = d_f

The Effect of Boundaries on the Derivative Graph

In an infinite porous aquifer, the following boundary effects can theoretically be discerned from the derivative drawdown plot (Figure 4.56):

(i) *Single No-Flow Boundary*

A single no-flow boundary results in the establishment of a semi-radial flow regime with an increased rate of head change. On a semi-log drawdown-time graph this produces a doubling of the slope. Consequently, after a certain transition period, the boundary appears on the derivative graph as a horizontal straight line.

Thus: $F2 = df / d0 = 2$

(ii) *Dual No-Flow Boundary*

A further boundary can double this value to 2. Thus $F2 = df / d0 = 3$ at most.

(iii) *Closed No-Flow Boundary*

A closed no-flow boundary is easily identified on the derivative plot as a straight line with unit slope at late time.

Thus: $F2 = df / d0 \geq 4$ and the exact value is dependent on the aquifer size, shape and properties.

(iv) *Recharge boundary*

The derivative plot will show a strong downward trend. In this case $F2 = df / d0 < 1$

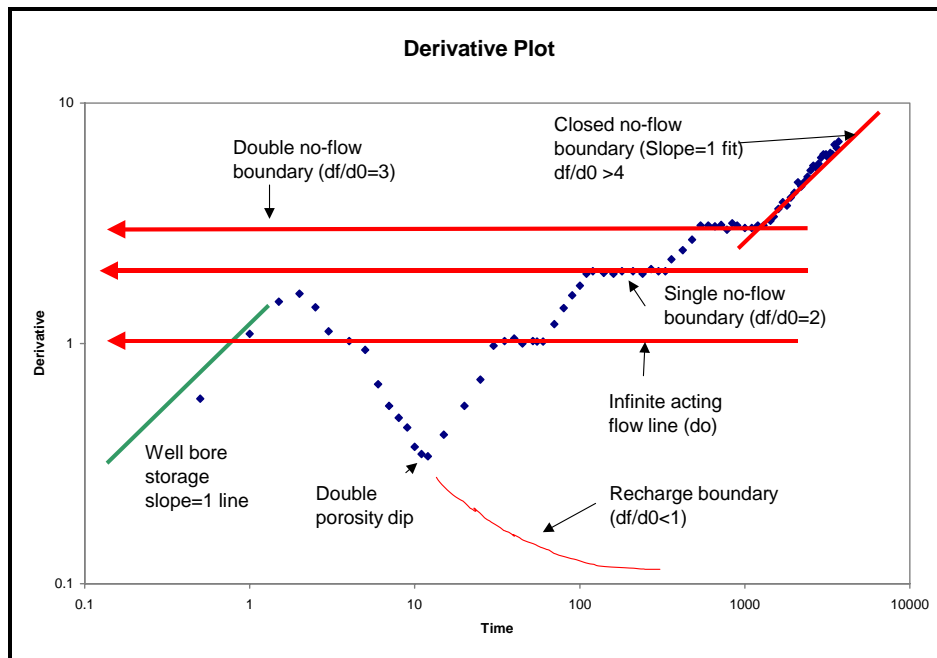


Figure 4.56: Derivative plot of drawdown showing various boundary conditions

In fractured-rock aquifers some of the boundary and inter-porous flow effects are often manifested simultaneously in the derivative plot, so that specific values of $F2$ are difficult to determine. However, the following general guidelines, based upon a large number of MODFLOW and RPTSOLV model simulations, are proposed to overcome these problems in obtaining $F2$:

- (a) $F2 \geq 4$ if closed-boundary is evident on the late-time derivative plot, i.e. it resembles a straight line with slope = 1. RPTSOLV modelling of this drawdown scenario shows that $F2$ usually falls between 4 and 6.5, the extreme value of 6.5 resulting from a closed boundary condition set at 500 m from the pump borehole.
- (b) If no late-time closed-boundary effect is detected (a), then the following procedure is proposed:
 - Determine the early infinite-acting flow line ($d0$). This early flow line may never be fully established due to boundary effects. In which case the $d0$ -line must be shifted to a position just after cessation of borehole-storage effects, which is usually about 1.5 log cycles after borehole storage ‘hump’ (Figure 4.56).
 - Determine the late time infinite-acting flow line (df -value).

- Calculate $F2 = df / d0$. This value will give the minimum value of the F2-factor
- (c) If the derivative plot shows a recharge boundary (i.e. strong downward trend and $df / d0 < 1$), then set :
 - $F2 = 1.0$ if $df / d0 \geq 0.5$
 - $F2 = 0.5$ if $df / d0 < 0.5$
- (d) Compare the calculated F2 value to the theoretical F2 values in Table 4.11. These theoretical F2 values can be used as a first-order approximation in cases where the flow regime is already known or not evident from the test data.

Table 4.11: Theoretical F2 values for typical flow regimes

F2 value	Characteristic flow regime
1.0	Infinite, homogeneous aquifer (Confined)
2.0	Fractured aquifer in general (Double Porosity)
2.0 – 3.0	Fractured aquifer showing matrix flow at late time (increase in ∇s)
4.0 – 6.5	Fractured aquifer showing a closed no-flow boundary at late time.
0.5	Recharge boundary at late time

- (e) The influence of other nearby production boreholes in the aquifer on the sustainable yield of the pump borehole must also be accounted for in the F2 factor, as follows:
 - Increase F2 by 1 if another production borehole is situated within a radius of 300 m of the pump borehole.
 - Increase F2 by 0.5 if another production borehole is situated between 300 to 1 000 m of the pump borehole.

Calculation of Transmissivity from the Drawdown Derivative Graph

The derivative of drawdown (**Chapter 4.2.2.1**) is given by:

$$d(s)/d(\ln t) = (n\sum x_i y_i - \sum x_i \sum y_i) / (n\sum x_i^2 - (\sum x_i)^2)$$

Notice that the log is used to calculate the derivative and not natural log (ln where $\ln = 2.3 \log$). From Cooper-Jacob equation:

$$s = (2.3Q/4\pi T)\log(2.25Tt/r^2S)$$

the derivative of the Cooper-Jacob equation is calculated using:

$$d(s)/d(\log t) = (2.3Q/4\pi T) = 0.183Q/T$$

Therefore, the transmissivity (T) of a porous, homogeneous aquifer can be estimated directly from the derivative graph:

$$T = 0.183Q / dn \text{ (m}^2\text{/day)}$$

Where dn = the intercept on the derivative axis.
 Q = abstraction rate in m³/day during pumping test

This equation is also valid in the case of vertical and horizontal fractures.

Case Study: Campus borehole UP15

A constant discharge test was conducted on borehole UP15 at the Institute for Groundwater Studies Campus Site in Bloemfontein. The borehole was pumped at 1 ℓ/s for 180 minutes. The borehole intercepted a single water-bearing fracture at 19 m below rest-waterlevel.

The relevant information obtained from the geohydrological log and pump testing of borehole UP15 are:

- available drawdown s_a = 10 m
- s_{100} = 2.09 m
- s_{180} = 2.51 m
- s^*_{100} = 2.07 m
- s^*_{180} = 2.16 m
- late time transmissivity = 10 m²/d
- drawdown per log cycle ∇s = 1.58 m

Thus $F1 = (2.09/2.07) \times (2.510/2.16) = 1.2$

Then by using **Eq. 4.6**:

$$Qs = \frac{sa * Q}{F1(s_{100} + 4\nabla s F 2)}$$

$$Qs = \frac{10(86,4)}{1(2,09 + 4(1,58)F 2)}$$

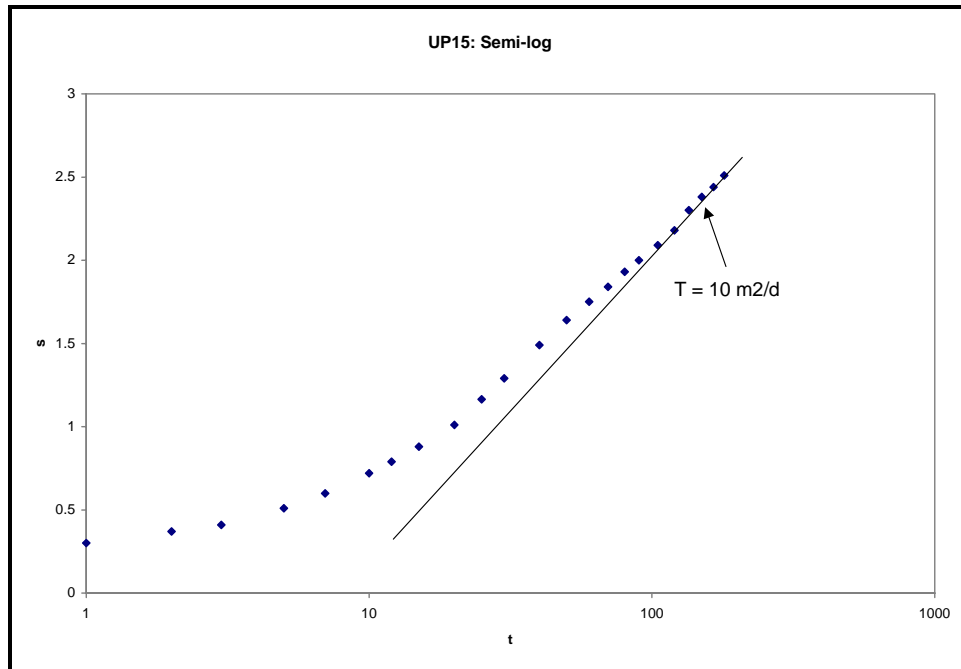


Figure 4.57: Constant discharge test on Borehole UP15 – drawdown versus time

Note that **Equation 4.5** could also be applied and will produce similar results.

Choice of factor F2:

All possible values of F2 are deduced from the derivative graph as follows:

1. The borehole taps a fractured-rock aquifer and thus $F2 \geq 2$.
2. No late-stage closed-boundary condition (i.e. slope = 1) is evident on the derivative graph, thus $F2 < 4$.
3. The daily sustainable yields are calculated for all possible F2 values (**Table 4.12**).

Table 4.12: Borehole UP15 – daily sustainable yield estimates for various F2 values

F2	Q_s (m ³ /d)	Q_s (l/s)
2	48.9	0.57
3	34.2	0.40
4	26.3	0.31

4. The most appropriate F2 value is now chosen as follows:

- Some matrix-flow is evident on the semi-log graph, as well as on the derivative plot – where an increase in gradient is observed - so $F2 = 3$.
- There are no other production boreholes within a radius of 1 km, therefore $F2 = 3$.

The most appropriate F2 value for borehole UP15 is 3, which yields a daily sustainable abstraction rate of 0.40 l/s. Note that the duration of this test was short and it is quite possible that the factor F2 could increase to a value of 4. Check that this daily yield does not exceed the mean annual recharge to the aquifer.

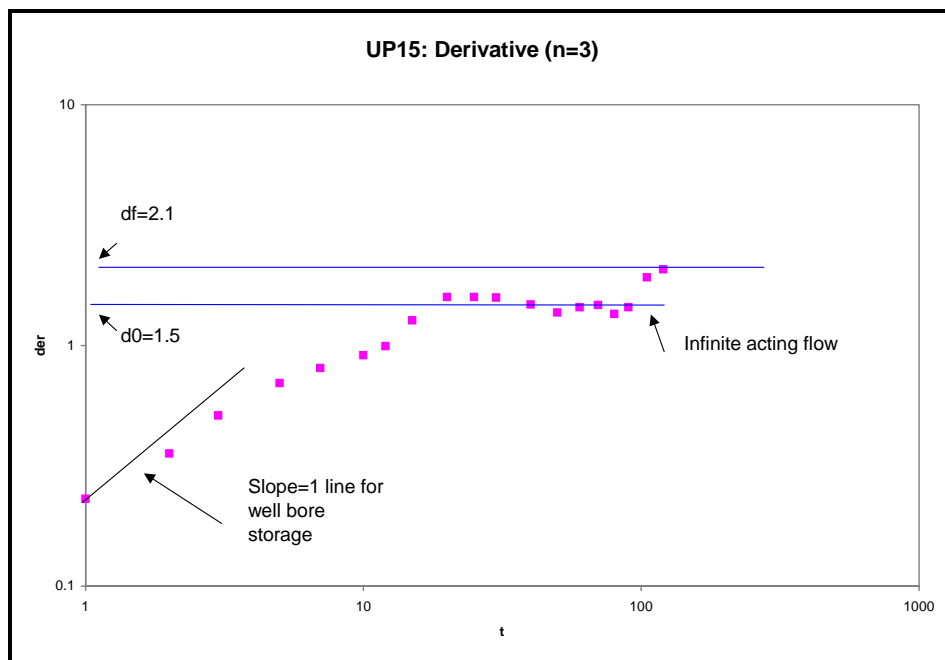


Figure 4.58: Constant discharge test on Borehole UP15 – derivative versus time

The transmissivity was calculated as follows: $T = 2.3Q/4\pi d_0 = 10.5 \text{ m}^2/\text{d}$ (Figure 4.57) and $T\text{-late}=7.5 \text{ m}^2/\text{d}$ by using $df = 2.1$ (Figure 4.58)

Case Study: GR2 at the Mimosadale Wellfield, Graaff-Reinet

A constant discharge pump-test was conducted by Steffen, Robertson & Kirsten (SRK, 1987, 1988) on borehole GR2 at a rate of 28.6 ℓ/s, aimed at assessing its potential as a production borehole for the town of Graaff-Reinet. The relevant geohydrological information is as follows:

- Constant discharge Q = 2 471 m³/d.
- s_a (main water-bearing fracture) = 36 m.
- S₁₀₀ = 7.71 m.
- S₁₀₀^{*} = 6.18 m.
- S₄₃₀₀ = 16.83 m.
- S₄₃₀₀^{*} = 12.95 m.
- S₄₃₂₀ = 12.95 m.
- Late transmissivity = 40 m²/d

Therefore F1 = 1.62

Using **Equation 4.7**:

$$Q_s = \frac{s_a * Q}{F1(s_{100} + 0,73QF2/T)}$$

$$Q_s = \frac{88956}{1,62(7,71 + 0,73 * 2471 * F2 / 40)}$$

$$Q_s = \frac{88956}{12,49 + 73 F2}$$

Choice of factor F2:

Table 4.13: Borehole GR2 – daily sustainable yield estimates for various F2 values

F2	Q _s (m ³ /d)	Q _s (ℓ/s)
2	561	6.5
3	384	4.5
4	292	3.4
5	236	2.7

The following procedure is used to select an appropriate value for F2:

- The derivative graph (**Figure 4.59**) shows a strong upward trend during late time and the influence of a closed-boundary (slope of line = 1), therefore must be $F2 \geq 4$.
- But two other production boreholes are situated between 300 and 1 000 m away from GR2 and F2 is increased to 5 ($4 + 0.5 + 0.5$)

The maximum sustainable yield of borehole GR2 is thus 2.7 ℓ/s , taking into account that it will be operated in conjunction with two further production boreholes in the same wellfield.

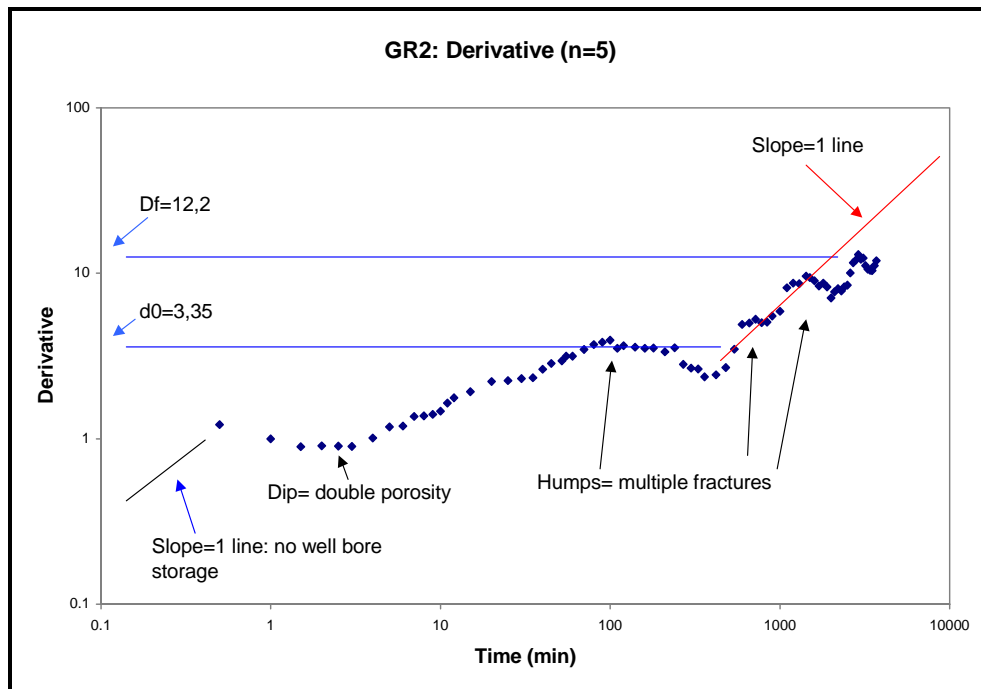


Figure 4.59: Constant discharge test of Borehole GR2 – Derivative versus time

The values of d_0 and d_f on the derivative graph yield T-early and T-late values of 135 and 37 m^2/d , respectively.

Case Study: Borehole Bacl-01 at Ramatshowe in the Northern Province

Borehole Bacl-01 was drilled into the Goudplaat Gneiss Formation, a heterogeneous rock consisting of alternating bands of amphibolite and pegmatite. A constant discharge test was conducted on the borehole at a rate of 15 l/s. The relevant parameters were estimated from the test data:

- S_{100} = 16.67 m
- S_{2880} = 26.60 m
- S_{100}^* = 26.00 m (rapid recovery)
- S_{2880}^* = not measured.

Because the waterlevel had almost fully recovered within the first 100 minutes after pump-shutdown, $F1 = (16.67 / 26.00) = 0.64$

No water-strike information is available for this borehole and therefore the step-drawdown and constant discharge test is used to identify the position of the major fractures.

Three major inflection points in the drawdown data are common to both the step-drawdown and constant discharge test (**Figures 4.60 – 4.62**), namely at 8-10 m, 15 - 16 m and 22 - 24 m – which are inferred fracture positions.

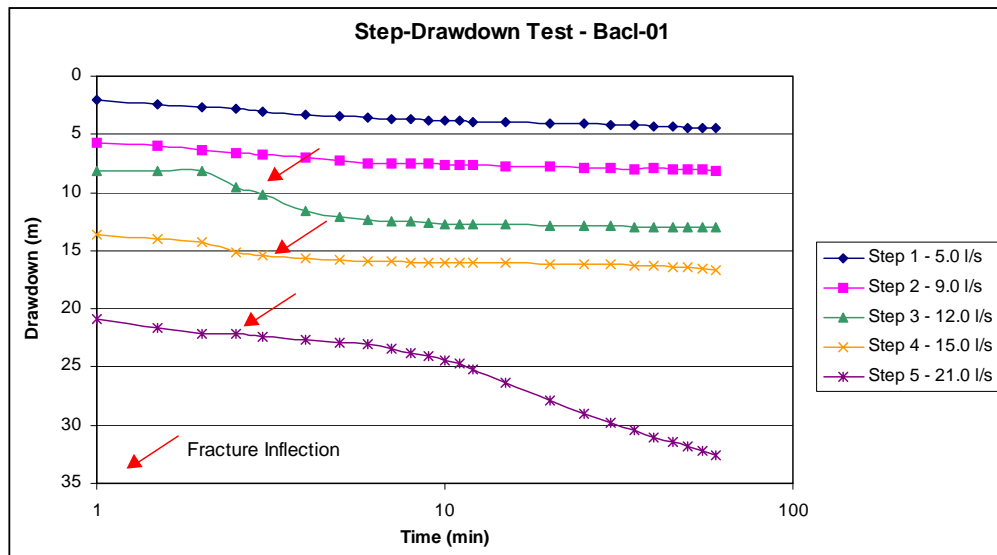


Figure 4.60: Step-drawdown test on borehole Bacl-01 – drawdown versus time

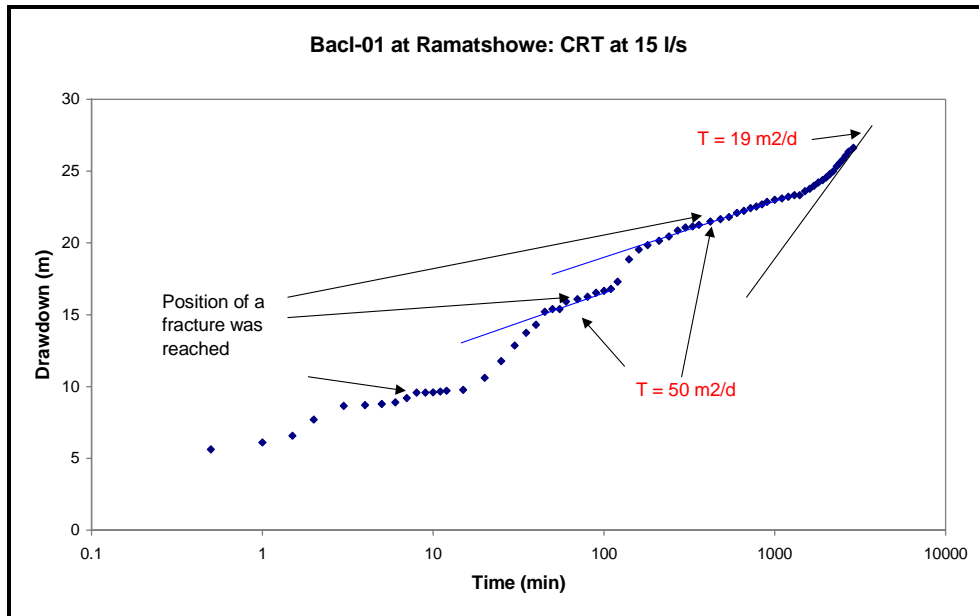


Figure 4.61: Constant discharge test on borehole Bacl-01 – drawdown versus time

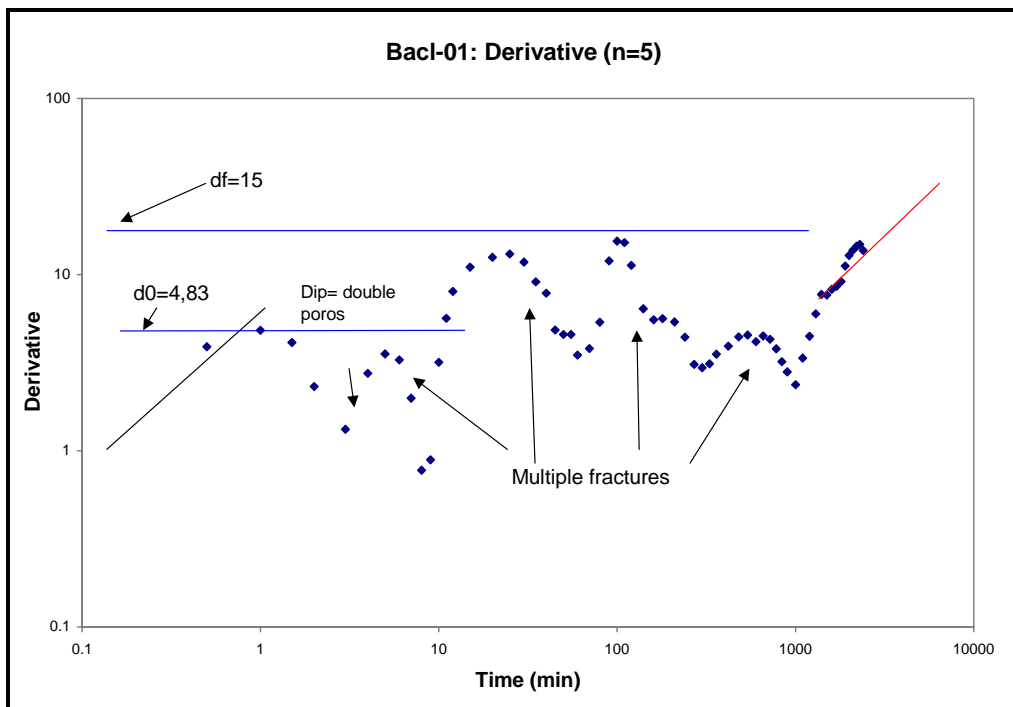


Figure 4.62: Constant rate discharge test of Bacl-01 - derivative versus time

The specific drawdown graph (**Figure 4.63**) indicates an inflection at approximately 16 m drawdown, which is accepted as the ‘available drawdown’. The abstraction management strategy is therefore to ensure that the rest-waterlevel in the production borehole never reaches this position.

The ∇s -equation (**Equation 4.6**) is used and not the T-equation (**Equation 4.7**) to obtain the daily sustainable abstraction rate:

$$Q_s = \frac{sa * Q}{F1(s100 + 4\nabla s F2)}$$

Then

$$Q_s = \frac{16(15)}{0,64(16,67 + 4(5,5)F2)}$$

$$Q_s = \frac{240}{10,66 + 14F2}$$

Notice that ℓ/s can be used directly in ∇s -equation, instead of m^3/d because the equation does not contain the transmissivity units.

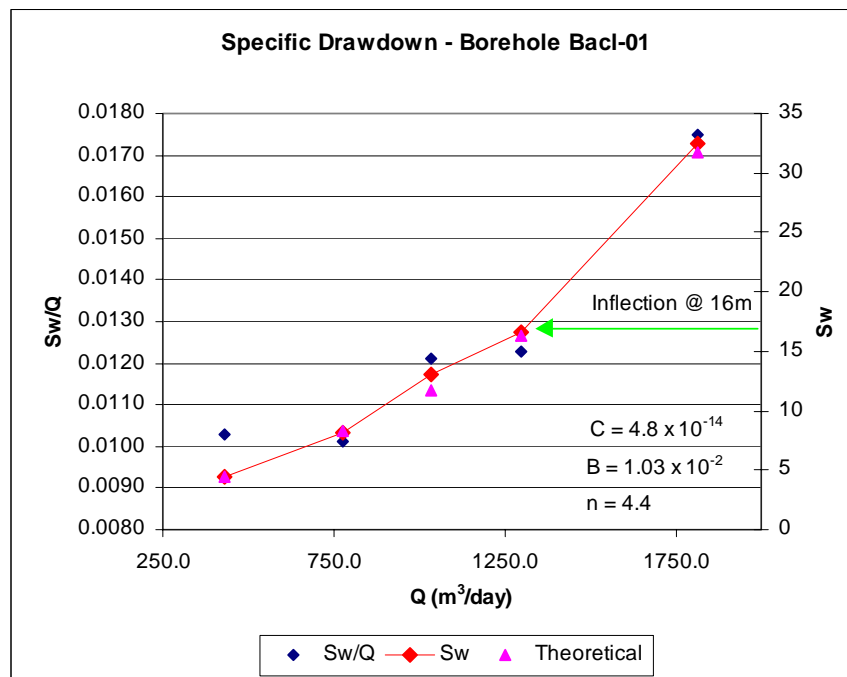


Figure 4.63: Bacl-01 step drawdown test - specific drawdown curve

Table 4.14 lists all the possible sustainable production rates for borehole Bacl-01, according to the relevant F2 values.

Table 4.14: Sustainable yield and F2 values for borehole Bacl-01

F2	Q _s (ℓ/s)
2	6.2
3	4.6
4	3.6
5	3.0

Choice of F2:

- Matrix flow is evident at late times, therefore $F2 \geq 3$
- On the derivative graph (**Figure 4.62**) shows a closed-boundary condition (fitted line slope = 1), thus $F2 \geq 4$.
- On **Figure 4.61** a further boundary is evident between 1 000 and 3 000 minutes and thus $F2 \geq 5$.
- No other production boreholes are situated within 1 km of Bacl-01 and therefore $F2 = 5$ and a daily sustainable yield of is 3.0 ℓ/s is accepted.

Note the rapid recovery of the waterlevel after pump-shutdown (**Figure 4.64**), which also reflects a significant inflection at 15-16 m drawdown.

The Recovery Test Method produces an x-axis intercept of 10 and yields a high abstraction rate of 13.5 ℓ/s per day (i.e. $24/10 = 2.4$ hours rest per day at 15 ℓ/s) - which based on past experience of such aquifers is not feasible in the long-term.

The transmissivity values are calculated from the derivative graph (**Figure 4.62**) as 49 and 16 m²/d.

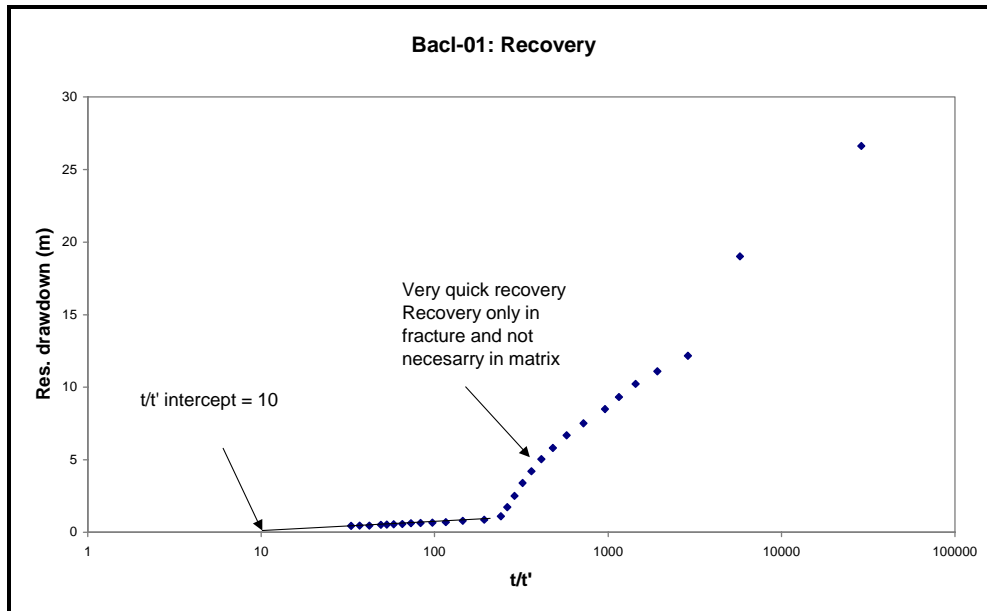


Figure 4.64: Constant rate discharge on Borehole Bacl-01 - recovery

Pseudo-Steady-State Management Method

A very easy and practical method to obtain a safe daily abstraction rate for a borehole, is by using the so-called pseudo-steady-state drawdown ('farmers') method. To perform this method in the field, the following suggestions are made:

A submersible pump with a tap fitted to the outline pipe is a prerequisite. Start abstracting water at maximum pump capacity from the borehole. After some time (usually in the order of a few minutes), start closing (or opening) the tap at regular intervals until the measured water level in the borehole stabilises more or less (pseudo-steady-state drawdown achieved).

Continue abstracting at this rate for as long as practically possible (within cost limitations) - if the drawdown still increases, decrease the rate a bit or visa versa. The final abstraction rate is the rate at which the pseudo steady state water level is obtained (i.e. water leaks at this rate from the matrix to the fracture), and this yield could usually be viewed as a very safe rate for the borehole for a long period of time.

Alternatively this method could be applied after the last step of the step-drawdown test.

This method was applied on the Meadhurst Pumping Test Site. Borehole F4 was used as pumping borehole and water levels were measured in F4 as well as F5 (5 m from F4) and FP1 (30 m from F4). The abstraction rate was changed

continuously until a pseudo steady state water level was achieved in F4. The rate which produced this pseudo steady state water level, was 0.289 ℓ/s (i.e. about 24 m^3/d). Borehole F4 was then pumped for another five days and the results are displayed in **Figure 4.65**. It is clear that this final rate is also the rate at which water leaks from the matrix to the fracture.

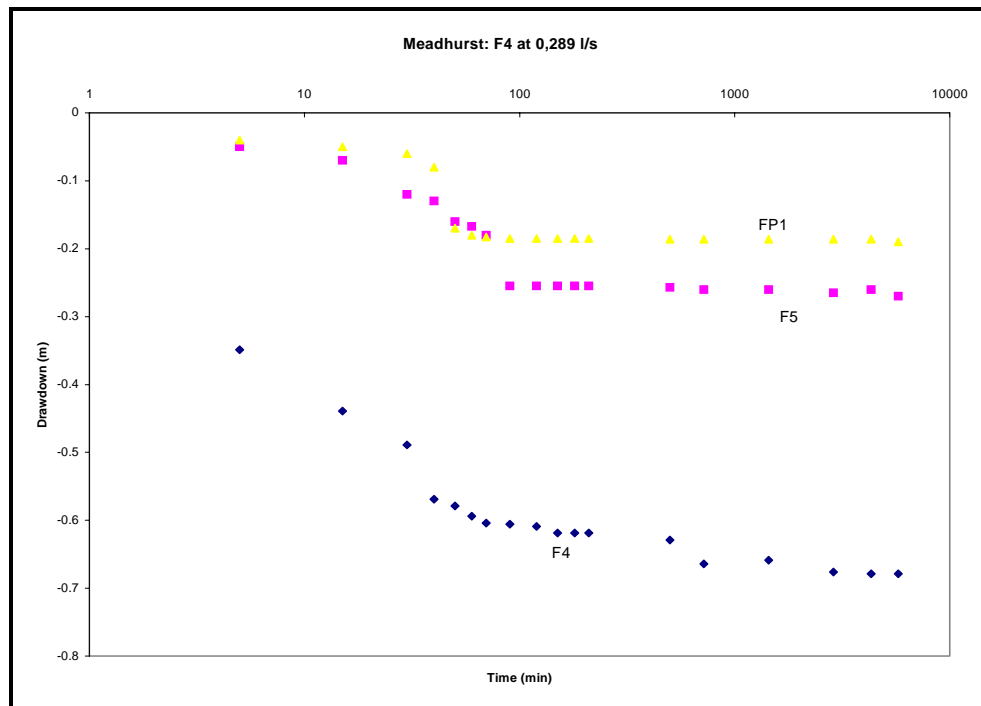


Figure 4.65: *Pseudo steady-state method applied to borehole F4 at Meadhurst*

In the pseudo-steady state drawdown method, water could be abstracted from the borehole for 24 hours per day. However, it may often happen that this method produces an unsatisfactory low abstraction rate, which is not very cost-effective and practical.

4.2.2.3 General Discussion of Methods

Late-T method

The yield obtained for GR2 using the late-T method was higher than the estimated upper sustainable yield.

The concept of using transmissivity that reflects steady-state flow from the matrix to the fractures seems reasonable when assessing borehole yields in fractured rock aquifers. However, it may not be possible to determine whether the late-time segment of the drawdown curve reflects only inter-porosity flow or other boundary conditions, as more than one hydrogeological environment can produce similar late-time drawdown curves.

Kirchner and Van Tonder (1995) state that the difference between boundary and double porosity effects can be recognised by the shape of the late-time drawdown curve: a barrier boundary in a radial flow system will cause at the most a doubling of the drawdown slope after boundary conditions have been encountered, and double porosity effects will cause a far greater increase in slope. While a single boundary may cause the drawdown slope to double, the water level in a borehole that penetrates an aquifer of limited extent could plummet to the bottom of the borehole once the cone of depression dewateres the most permeable fractures, thereby resulting in a 'steep' late-time slope. The late-T method requires the late-T value to reflect steady state flow from the matrix to the fractures. This may be difficult to establish considering the various hydraulic conditions that can cause a 'steep' late-time drawdown slope.

The main reason for the relatively high yield obtained using this method, is that it uses the distance between the rest water level and the main water strike as the available drawdown. The yield obtained using the Cooper-Jacob equation is directly proportional to the available drawdown value that is used, and in confined fractured-rock aquifers, this value can be substantial. For example, the distance between the rest water level and the main water strike in borehole GR2 is 36 m. While the sustainable yield of a borehole may be influenced by the depth of the main water strike, because the deeper the water strike, the greater the permissible drawdown and the cone of depression's area of influence, it is unlikely that these factors are directly proportional. Another drawback with the method is that it allows the entire available drawdown to be pumped in a given year, thereby unreasonably assuming that, annual recharge will result in its complete replenishment.

Although it may appear as if the method should be discarded altogether, this is not the case, as it can be modified to give lower yields in cases where a more conservative value is needed. This may be necessary where incomplete recovery is experienced after the constant rate test, or where the main water strike is very deep. In such cases, instead of using the main water strike as the reference point on which to obtain the available drawdown, the first water strike could be used. If the first water strike is

used in borehole GR2, an acceptable yield of 3.9 ℓ/s is obtained, whereas if the main water strike is used, the yield are clearly over estimated.

It would appear as if this method could be applied with a fair degree of accuracy in cases where the water strikes are not far below the rest water level (possibly within or slightly below the weathered formation in aquifers where the bulk of the storage lies within this zone), and where the late transmissivity values are not too high.

Unfortunately, no guideline as to what constitutes reasonable available drawdown and late-time transmissivity values can be given.

Drawdown-to-Boundary Method

Emphasis on this method is the determination of the maximum drawdown permitted in order to prevent the dewatering effects that may result once a low permeability boundary is encountered. If a sharp increase in drawdown is observed, the height of the rest water level above this point is taken as the available drawdown. If no sharp increase in drawdown is present, this method is the same as the late-T method.

Distance-to-Boundary Method

The concept of restricting the maximum abstraction so that significant drawdown is limited in extent to the theoretical distance of an observed boundary, seems appropriate in aquifers which are characterised by boundary effects. A drawback in the application of the distance-to-boundary method is that a Δh value not be easy to obtain, for example where delayed yield or double porosity effects are experienced. An acceptable Δh value is essential when applying the distance-to-boundary method because of the sensitivity of Q in the CJ-equation to available drawdown (Δh in this case). Examples from Karoo aquifers indicate that a maximum Δh value of 1 m should be employed.

The determination of Δh is not straightforward and this method should be applied with great care.

Recovery Method

It was found from practical experience that this method usually over-estimates the safe daily abstraction rate.

RPTSOLV Programme

If a no-flow boundary is included into this numerical model, this method yields a minimum daily abstraction value. The application of this method requires an experienced user, which is a drawback of this method for general applications by hydrogeologists. Another problem experienced with this method is that because it is a

numerical method, solutions are not very accurate when $r \rightarrow 0$ (i.e. close to the borehole). Usually if an r of between 1 and 3 m is taken as the radius of the borehole, the solution is acceptable.

4.2.3 ESTIMATION OF RECHARGE

4.2.3.1 Introduction

Estimation of recharge in the Karoo is not different from other geological formations, except that the aquifer is normally only covered by a thin layer of soil, which limits the application of methods relating to the unsaturated zone. Rock and dolerite outcrops are regarded as preferential areas of recharge. Therefore the most reliable and most practical methods entail a mass balance approach, such as:

a water quality balance using the chloride method, and

a balance between groundwater input and output based on the integrated response of groundwater levels over the delimited boundaries of the system.

4.2.3.2 Mechanisms of Recharge

Many towns in the Karoo Basin obtain their water supply from wellfields tapping the underlying Karoo aquifers and as the water demand increases, so these abstraction schemes have to be expanded and/or new ones built. The climate is arid to semi-arid (**Chapter 1.4**) and the available groundwater resources limited. The question arises how large and how reliable are these resources. These aquifers can only be optimally exploited and managed if a reliable method can be obtained to estimate their long-term sustainable yield. The sustainable yield of these aquifers is dependent upon the rate recharge from rainfall, storativity and subsurface in- and outflows to and from the aquifer system.

The results obtained from the analysis of several pumping tests and piezometric-head measurements performed in typical Karoo formations, i.e. at the Campus Test Site, as well as aquifers of Dewetsdorp and De Aar, shows that two distinguishable but interacting systems determine the large scale groundwater flow behaviour, namely:

- (i) the low permeability, *matrix system* with its high specific yield acts mainly as storage reservoir, wherein no regional flow takes place, and
- (ii) the high permeability, *fracture system* with its very low storativity, wherein regional groundwater flow takes. The simplest mathematical equation representing such an aquifer system is the dual porosity / dual permeability approach.

Rainfall recharge into the porous matrix can occur in two ways, namely:

- (a) direct, vertical infiltration via the soil layers, and
- (b) via vertical fractures (preferred pathways) exposed at the surface.

The latter method results in the water initially entering the fracture system, where after it flows from the fracture system into the matrix, due to the induced pressure gradient between the two systems. Under present state of knowledge, it is unclear as to which, if any, mechanism dominates the recharge process to Karoo fractured-rock aquifers. It is, however, likely that both mechanisms of recharge take place. Waterlevel hydrographs from open boreholes that do not intersect the main fracture system show little or no response to rainfall events, while piezometric-levels in boreholes tapping the fracture system respond rapidly to recharge following major rainfall events. These observations do not, however, shed any light on which recharge mechanism is dominant, as such a waterlevel response is also a function of low storativity of the fracture system and the high specific yield of the matrix system. Certain clayey horizons in the topsoil swell on being wetted during rainfall events, which restricts movement of the water to the deeper soil horizons. It has, however, been observed that shrinkage cracks in clays sometimes remain open for up to two weeks

In our opinion, the most feasible recharge mechanism for rainfall to Karoo fractured-rock aquifers is via vertical fractures.

Kirchner et al., (1991) showed that most recharge in the Dewetsdorp aquifer takes place along preferred pathways and in areas with no or a thin soil cover. They estimated that the annual rate of recharge from rainfall varies from 4-6% in the hilly areas where the soil cover is thin to as low as 1% in the valley areas where the soil cover is thicker and more clay-rich.

Most of the rivers and streams in the Karoo Basin are so-called 'gaining' rivers (groundwater flows towards the rivers), whilst the number of aquifers that are recharged directly from rivers are negligible. During infrequent episodes of flooding, the flowing rivers may directly recharge alluvial-bedrock composite aquifers developed along the course of the drainage system.

4.2.3.3 Water Quality Mass Balance

Chloride Method

The chloride method is represented by the equation:

$$RE_{av} = a.Rf_{av} \quad \text{Eq. 4.9}$$

Where

- a = $Cl_{rainfall} / Cl_{groundwater}$ represents the recharge coefficient
- RE_{av} = average recharge
- Cl = chloride concentration
- Rf_{av} = average rainfall

Application of this method assumes that the increase in chloride concentration has resulted from evapotranspiration losses and that no additional chloride has been added by contamination from or leaching of rocks or from the overburden. Unfortunately chloride concentrations of rainfall have only been measured at a few points in the Southern Africa, but could be estimated from measurements of Botswana rainfall (**Figure 4.66**). This indicates that the average chloride concentration is a function of the average precipitation. However, chloride concentrations decrease as mean annual rainfall increases, as indicated by the Lobatse chloride measurements (**Figure 4.67**) and conforms to the concept of a higher percentage recharge for higher rainfall. The chloride method allows point measurements of recharge to be obtained from chloride concentrations of individual boreholes and spatial variability from monitoring points spread over the recharge area. Based on chloride measurements in the Dewetsdorp area, a recharge of 2.6% of the rainfall is derived for this Karoo aquifer (**Table 4.15**).

The recharge could also be determined from the chloride concentration of uncontaminated springs issuing from the Karoo. Such estimates would represent recharge integrated over space and time. The following average recharge values have been obtained for different springs in Karoo Formations.

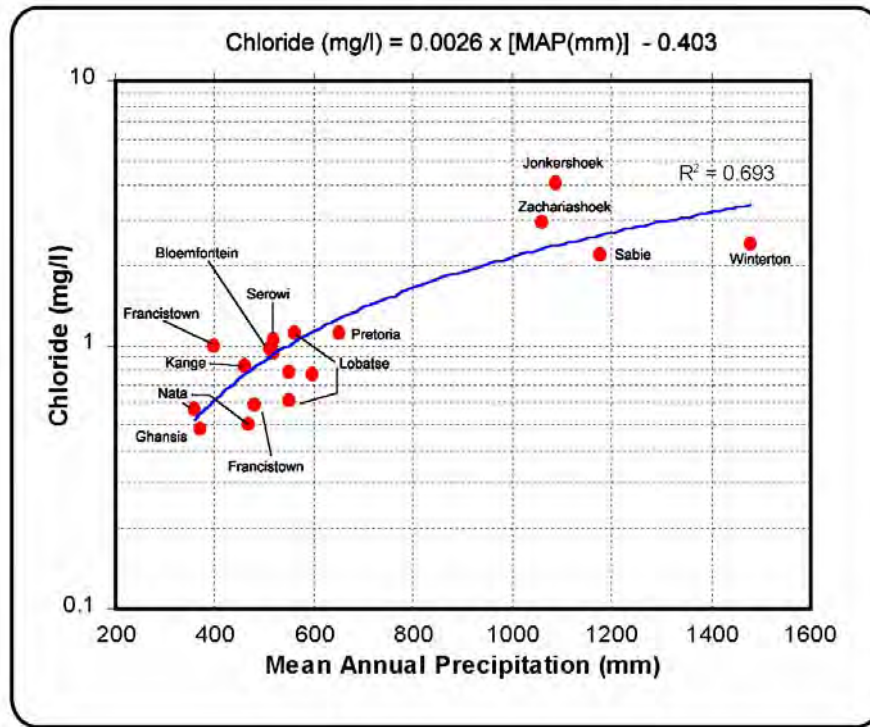


Figure 4.66: Relationship between mean annual rainfall and chloride content

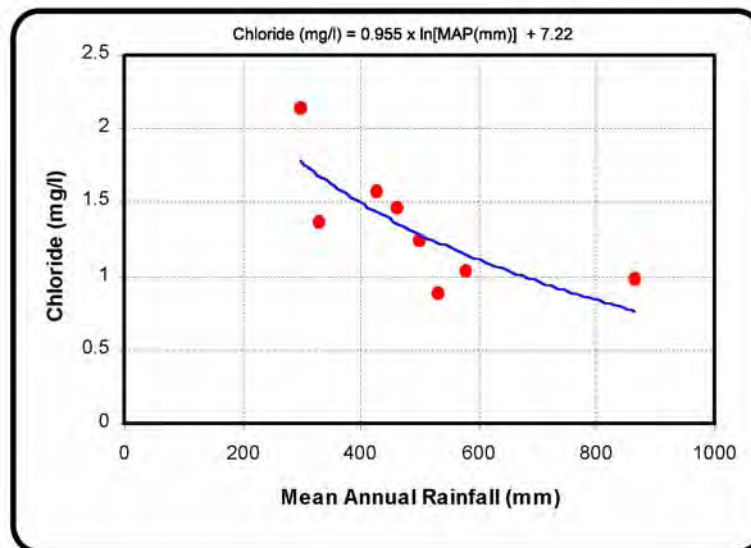


Figure 4.67: Lobatse – Relationship between average chloride content of rainwater and mean annual precipitation

Table 4.15: Recharge determined by means of the Chloride Method.

Locality	Mean average rainfall (Rf) (mm/a)	Cl _{rainfall} (mg/l)	Cl _{groundwater} (mg/l)	Recharge Cl method % Rf	Recharge SVF method % Rf
Dewetsdorp	600	1,0	39	2,6	4.3
De Aar	287	0,6			1,4 to 2,8
Trompsburg eye	580	0,85	23	3,7	-

4.2.3.4 Saturated Water Balance Method

Recharge to Karoo aquifers can be determined from the water-balance of a delimited aquifer by analysing the fluctuations of groundwater-levels over a specific time-interval dt , expressed as follows:

$$\text{Inflow} - \text{Outflow} + \text{RE} - Q = S \cdot dV/dt \quad \text{Eq. 4.10}$$

Where A is the aquifer area, and $dV = A \cdot dh$ is the fluctuation in saturated volume (SVF) of the aquifer based on groundwater level fluctuations (dh) integrated for monitoring points spread over the aquifer. RE represents the effective recharge as natural losses such as evapotranspiration, is not included in the term Q representing only artificial abstraction and outflow of springs. S is aquifer storativity.

Because of the fractured nature of the aquifer it is difficult to determine S in Karoo Formations from the usual interpretation of pumping tests. The latter indicates S to be dependent on the distance between the pumping borehole and the observation borehole. An empirical method to infer S has been derived by Bredenkamp et al., (1995), but by means of an adapted 3-dimensional hydrodynamic model the storativity of the aquifer and of the fractures could be determined (Van Tonder et al., 1997).

Recharge can be determined as the abstraction during periods of equal volume ($dV=0$ in **Equation 4.10**), in relation to the rainfall during the same period. This is known as the *Equal Volume Method* (EVM). The reliability of the recharge estimate would depend on correctly integrating the groundwater-level fluctuations occurring over the entire aquifer, which depends on the number and spatial distribution of groundwater monitoring points. In some cases, inflow and outflow can be assumed to cancel-out, but have to be accounted for if they are not the same. Inflow and outflow could be estimated from the following equation:

$$\text{Inflow} = T_{in} \cdot I_{in} \cdot L_{in}$$

$$\text{Outflow} = T_{out} \cdot I_{out} \cdot L_{out}$$

where subscript **in** refers to inflows and **out** to outflows across the aquifer boundary, while T = aquifer transmissivity, I = the hydraulic gradient and L = the length of the flow cross section.

Application of the EV-method to the Dewetsdorp Karoo aquifer yielded a curvi-linear relationship of recharge in relation to the monthly rainfall [Figure 4.68 after Kirchner et al., (1991)]. The recharge equation in this figure produces monthly estimates very similar to those obtained by CRD Method (Equation 4.13).

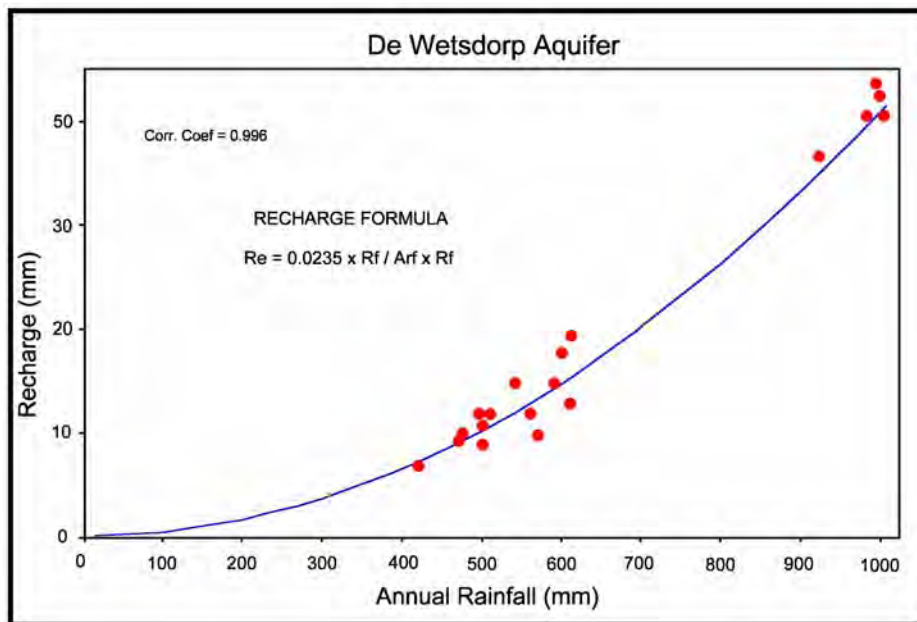


Figure 4.68: Relationship between recharge and annual rainfall for Dewetsdorp

4.2.3.5 Modified Hill Method

The normal *Hill Method* is based on a simplified version the groundwater balance by rewriting **Equation 4.10**, assuming inflow and outflow to each other cancel out (Inflow-Outflow = 0):

$$dV = -(1/S).Q + RE/ \quad \text{Eq. 4.11}$$

where

- dV = the change in saturated volume
- S = aquifer storativity
- RE = recharge
- Q = abstraction.

Equation 4.11 represents a linear equation with gradient = 1/S and RE/S representing the long-term average recharge which could be assumed constant (dV = 0). By dividing by the area of the aquifer the recharge in millimetres of precipitation is obtained.

In the *Modified Hill method* the linear equation is changed as follows:

$$dV = 1/S (RE - Q) \quad \text{Eq. 4.12}$$

This equation not only allows S to be determined more reliably, but would also indicate changes in S or inconsistencies in Q.

The SVF balance has been applied to the South-Western Aquifer at De Aar, which has been exploited for a long period of time (e.g. 10 years to 1995).

4.2.3.6 Cumulative Rainfall Departure (CRD) Method

Classical CRD method

The normal series of cumulative departures of rainfall has long been known to mimic groundwater level fluctuations quite accurately. The classic CRD-representation is as follows:

$$CRD(i) = Rf(i) - Rf_{av} + CRD(i-1) \quad \text{Eq. 4.13}$$

where

- i = a specific month
- Rf = rainfall
- Rf_{av} = average monthly rainfall based on the total rainfall record.

The relationship between waterlevel $h(i)$ and the cumulative rainfall departures can be expressed as:

$$h(i) = a \cdot CRD(i) \quad \text{Eq. 4.14}$$

where:

- a = regression constant, representing the water level rise per unit of recharge (= b/S)
- b = fraction of rainfall representing recharge, implying linear dependence between recharge and rainfall
- S = aquifer storativity

This leads to the relationship:

$$dh(i) = b/S[Rf(i) - Rf_{av}] \quad \text{Eq. 4.15}$$

where $dh(i)$ = the incremental water-level change in month- i effected by recharge which is determined by the following relationship:

$$RE(i) = b[Rf(i) - Rf_{av}] \quad \text{Eq. 4.16}$$

Using the CRD method in combination with an estimate of the average recharge coefficient (=b), which can be obtained by means of the chloride or the EV-method, the monthly variability of effective recharge could be derived.

Long- and Short-term Memory of an Aquifer System

The CRD relationship incorporating a characteristic short-term and long-term memory of a specific aquifer, can be represented by the following equation:

$${}^m_n CRD_i = \frac{1}{m} \sum_{j=i-m+1}^i Rf_j - \frac{k}{n} \sum_{j=i-n+1}^i Rf_j + {}^m_n CRD_{i-1} \quad \text{Eq. 4.17}$$

where

- CRD_i = cumulative rainfall departure for month i
- Rf_j = rain in month j
- m = short-term aquifer memory
- n = long-term aquifer memory
- k = factor indicating natural conditions ($k = 1$) or effect of abstraction ($k > 1$)

Figure 4.69 shows a high degree of comparison between the CRD series and the observed groundwater levels at De Aar.

The CRD method provides a useful check of the reliability of water level and of springflow records if reliable rainfall records are available.

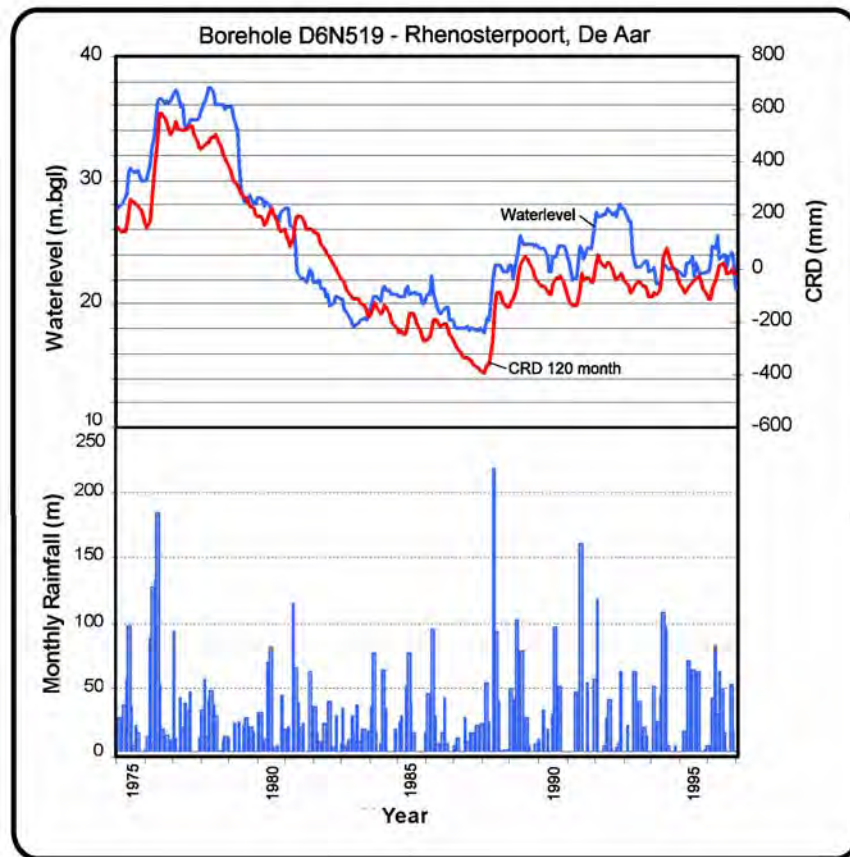


Figure 4.69: Relationship between the cumulative rainfall departure curve and waterlevel for borehole D6N519, at De Aar

Case Study: De Aar – Dewetsdorp

Kirchner et al., (1991) conducted a 3-year project, aimed at studying the natural groundwater recharge of aquifers in the Karoo formations of South Africa. Two typical Karoo aquifers, at Dewetsdorp and De Aar, were selected for study purposes. Data were collected from both the saturated and unsaturated zone. Neutron probe measurements showed there was no increase in the soil water content beneath a depth of about 1 m below the surface. Even with the exceptionally high rainfalls of

February 1988, neutron measurements indicated that very little soil water matrix flow occurred, which implies that most of the recharge occurred along preferred pathways.

Application of the SVF-method to the Dewetsdorp aquifer yielded the following three recharge equations:

$Re = 0.06(P-120)$ for areas with a thin soil cover

$Re = 0.023(P-51)$ for areas with a thick soil cover

$Re = 0.12(P-20)$ for areas with an alluvial cover

(Re = recharge in mm; P = precipitation in mm)

Kirchner et al. (1991) concluded that all recharge estimation methods that based upon the unsaturated zone theory, except for the CI-method, are not applicable to Karoo aquifers.

Weaver and Talma (1997) sampled a 2-km section of boreholes in Dewetsdorp, starting on the hillslope with a borehole that is situated close to an outcrop of Katberg Sandstone and continuing down slope to the Kareespruit stream, where a municipal borehole was sampled. **Figure 4.70** shows the age interpretation of the groundwater with the aid of CFC F-113 values. The CFC age determinations strongly support the chemistry results, with similar CFC-model recharge ages being obtained for boreholes G35432, G35435 and G35430. These three samples represent a mixture of the 1988 flood recharge water and older water thus producing an average groundwater age of 1980. Water from borehole G35436 hardly showed any movement on the Piper diagram, indicating it was not significantly affected by the flood recharge event. This water has the oldest CFC-model recharge age of early 1950s, which indicates that this part of the aquifer is confined and only marginally affected by such flood recharge events. The origin of the water in borehole G35436 is possible from a deeper-lying aquifer (G35436 is situated along a dyke).

4.2.3.7 Concluding Remark

Recharge in Karoo aquifers is highly variable due to varying thickness of the soil overburden, rock outcrops, collection of surface water in depressions and surface runoff. In addition spatial and temporal variations of rainfall are normally high. The most reliable methods of estimating recharge are therefore based on groundwater-balance methods and/or mass-balance methods (i.e. chloride method).

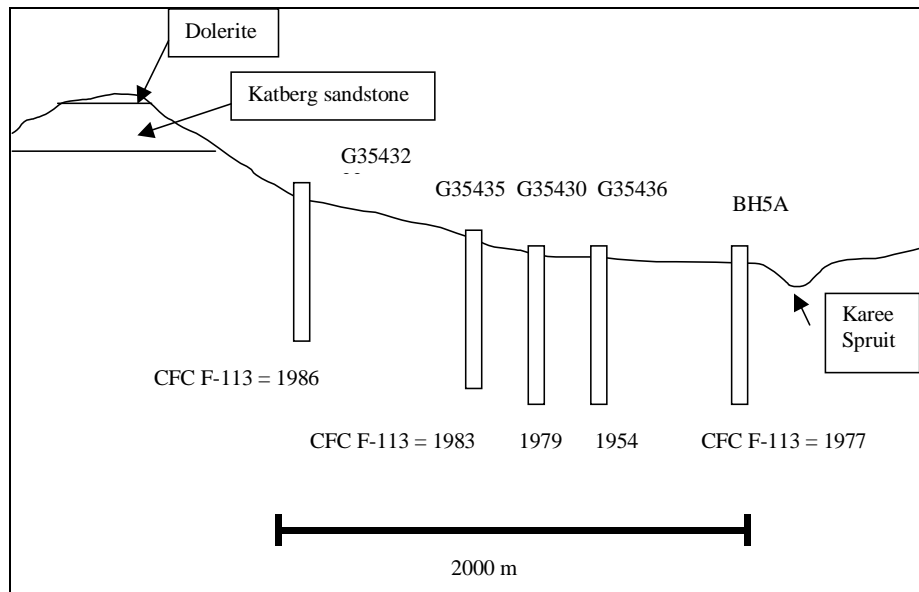


Figure 4.70: CFC groundwater age determinations in the Dewetsdorp aquifer

4.2.4 GROUNDWATER FLOW MODELLING

Predictive tools and techniques in geohydrology and hydrology have developed rapidly since 1970, when the use of computers for this purpose became common. Numerous models, all based on the same or similar mathematical, chemical and hydraulic principles were developed by many researchers in the field of geohydrology. The field of hydrology distinguishes itself from geohydrology in the sense that hydrological models are usually of a stochastic nature. Numerous hydrological models are currently also available and in use for the simulation and prediction of a vast array of circumstances.

In contrast to the rather precise development of predictive tools, data sets are often lacking. The reason for this discrepancy lies in:

- the inaccessibility of systems to measure values,
- the lack of time to measure, and
- the high cost of measurement.

Of these and particularly in the case of groundwater, the inaccessibility of the aquifer to measure parameters is probably the biggest constraint. This goes hand in hand with time and cost. In most instances, geohydrological systems can only be probed by a very limited number of boreholes. This usually requires input from a very experienced geohydrologist and interpretation of geohydrological systems is mostly very complex. Within the mining situation, geohydrological systems become even

more complex because they are usually of a dynamic nature, with flow regimes changing as mining progresses. Various possibilities for the classification of these predictive tools exist. These are, for instance:

- Geochemical/hydrochemical/kinetic models.
- Pathway models.
- Water/salt balance models.
- Flow models.
- Acid-base accounting.

A large number of computer models are available, but usually the following two models are used in South Africa for groundwater flow and mass transport modelling:

- MODFLOW 3D finite difference model (various pre-processors exist e.g. Modime, Pmwin)
- AQUAWIN (2D finite element model, including options for management, risk analysis and pump test analysis)

Three-dimensional models have the difficulty of assigning parameter values to each of the layers as well as spatially in the x-y directions. A lack of information usually necessitates researchers to abandon efforts for three-dimensional modelling and use 2D codes. Up to date no Karoo aquifers in South Africa are managed with the aid of 2D or 3D numerical models.

If a wellfield is to be managed, the only practical way to do it is by using:

- (1) an approximate 2D numerical model, or
- (2) a more sophisticated 3D model.

Both these models, however, will (i) underestimate the drawdown in the abstraction borehole because borehole losses are not included in these type of models and also (ii) the numerical solution at an abstraction node, underestimates the drawdown in the borehole. If a Green function approach is used in the vicinity of abstraction nodes, these types of numerical models will yield accurate solutions. However, models that are currently used in South Africa, do not use the Green function approach (e.g. MODFLOW, AQUAWIN, ASMWIN)

A very important aspect in catchment management, is the calculation of recharge. Bredenkamp et al., (1995) recommended three methods to be used in Karoo Formations:

- the CI- method (Chapter D.2.3.3),
- the water balance method (SVF) (Chapter D.2.3.4), and
- Groundwater flow modelling.

Kirchner et al., (1991) gave the following information for a first qualified guess of the recharge in Karoo Formations:

- Thick clayey soil cover: Recharge in the order of 1 – 2% of annual rainfall
- Thin soil cover: Recharge in the order of between 2 – 4% of annual rainfall
- No soil cover : Recharge between 4 – 7% of annual rainfall

For the case where a river or ‘spruit’ passes through the area, the recharge percentage will be higher than quoted above.

The map by Vegter (1995) can also be used as a first qualified guess of recharge in the Karoo (Figure 4.71). It is only in the case where satisfactorily long records on water level reactions and abstraction rates are available, that the groundwater balance method can be used to calculate the recharge.

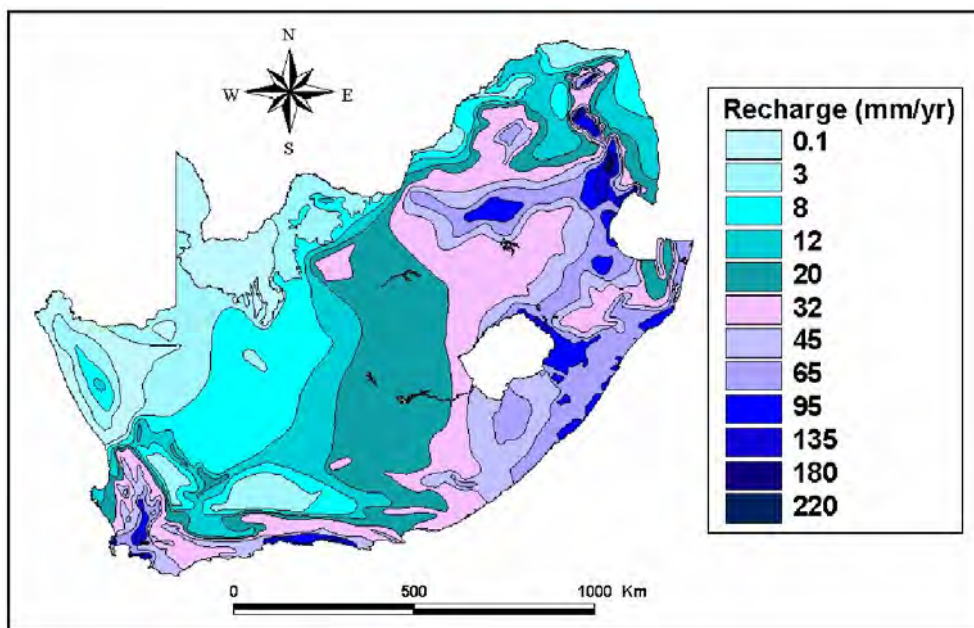


Figure 4.71: Mean annual groundwater recharge from precipitation (Vegter, 1995)

4.2.5 GROUNDWATER MANAGEMENT PRINCIPLES

For proper management of a borehole or an aquifer, the following two principles are important:

- The total amount of abstraction from an aquifer must be less than the long-term sustainable yield of the aquifer.
- A borehole must be operated in such a way that the waterlevel never reaches the position of the main water strike in the borehole (this will lead to a drastic decrease in the yield of the borehole and even drying up of a borehole). **Figure 4.72** illustrates an example what happens if ‘too much’ water is abstracted from a borehole.

The following important issues must be considered:

- Commonly, the complaint “*my borehole has dried up*” is heard. Usually this is due pumping a borehole at a rate that is in excess of the immediate yield of the production borehole (and not to a general lowering of the waterlevel in the aquifer) - enough water is still present in the aquifer just tens of meters from this borehole.
- A first estimation of a sustainable daily abstraction rate for an abstraction borehole, the late T-method, distance-to-boundary method or drawdown-to-boundary method could be used. In the case of deep water-strikes (more than 20 m below RWL), the late T-method will give an over estimation of the sustainable daily abstraction rate
- The two-layered radial pump test program RPTSOLV, will yield a more reliable sustainable daily abstraction rate. When a no-flow boundary is used in this model, a minimum sustainable abstraction rate will be obtained with this model.

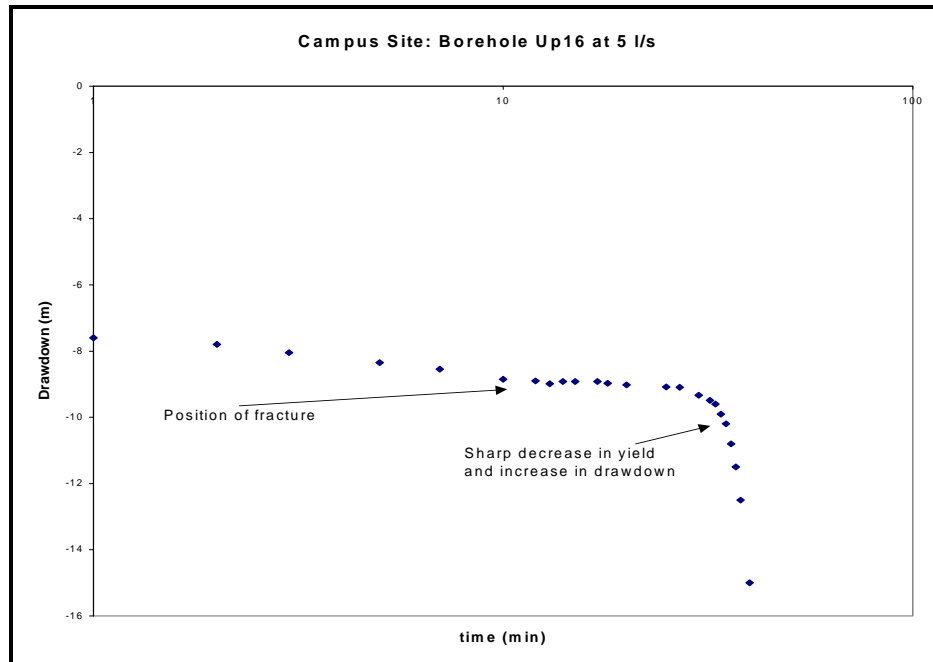


Figure 4.72: Reaction of waterlevel in a production borehole at pump rates in excess of the yield of the fractures

Case Study: Meadhurst Site

Figure 4.73 shows the geohydrological situation encountered at the Meadhurst Site. After 1 hour of abstraction from the production borehole (F4) at a rate of 1 ℓ/s , the waterlevel reached the position of the main fracture and the yield drastically decreased to less than 0.5 ℓ/s . However, the waterlevel in an observation borehole (F5), situated just 5 m from the abstraction borehole showed only a drawdown of 0.3 m. This illustrates the importance of the correct management of a production borehole.

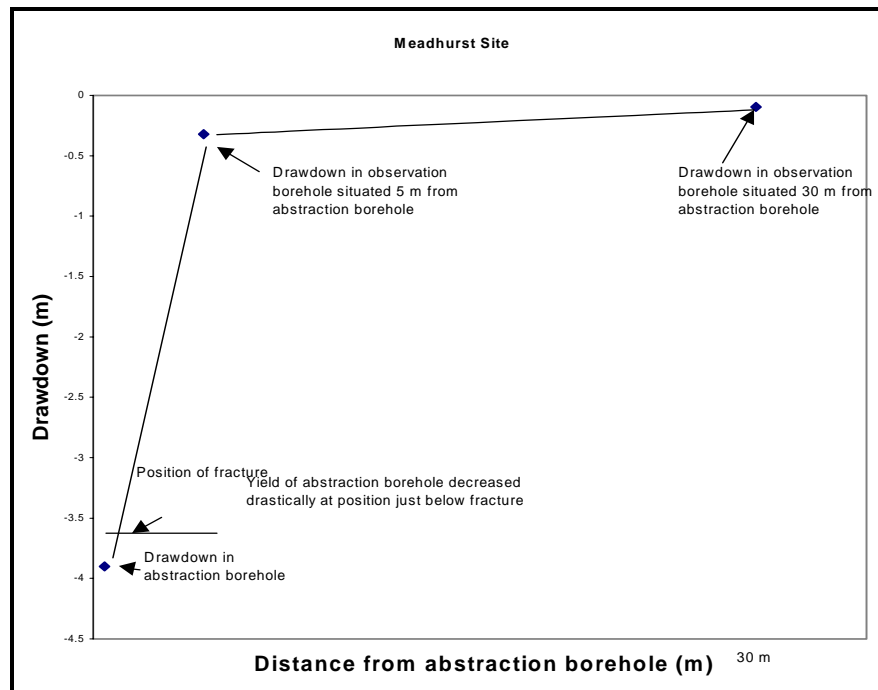


Figure 4.73: *Waterlevel decline in a production borehole that is being over-exploited*

Concluding Remarks

There is no doubt that up to now no perfect method has been developed for groundwater management purposes. The most reliable results will be obtained using a 3D groundwater flow model. However, these methods require extremely detailed field data that is very costly.

In Karoo aquifer systems, horizontal meso-fractures are one of the conduits for groundwater flow to a borehole, in which case it is possible that the dewatered fractures may 'collapse' and the borehole lost. It may well be that the compaction of the water-bearing fracture(s) in the vicinity of a borehole is irreversible. In this case, it would be imperative that such boreholes are not be pumped at a rate that causes the main horizontal, water-bearing fractures are de-watered. At this point, the yield of the borehole will decrease drastically. Moreover, if the hydraulic head gradient is very steep in the vicinity of the borehole and turbulent flow occurs, calcium carbonate (CaCO_3) may deposit due to a rapid change in partial CO_2 pressure. This calcification can also block the borehole and near well fractures, thereby decreasing the water yield. The *uncertainty in drawdown* therefore is of major importance in aquifer management. A sustainable pumping strategy in terms of probability (risk of failure) must ensure that the probability of drawing the piezometric head in the pumping borehole to the depth of the main water bearing fracture should be less than say 5%.

Major flow in Karoo aquifers occurs from the rock matrix to the fracture, which supplies the borehole with water. A highly permeable fracture quickly dewateres when pumped unless recharged through its surfaces. The recharge rate depends on the rate at which water can leak from the surrounding rock matrix to the fracture. A point can be reached when the aquifer cannot supply water fast enough to the fracture, to compensate for the losses due to pumping. There is thus a limit to the rate at which the rock-fracture system can supply water to a borehole. The immediate yield of a borehole is therefore not always limited by the amount of water stored in the aquifer, but more so by the finite rate at which water leaks from the matrix to the fracture system. The *uncertainty* of this leakage rate therefore must be quantified. In the case of a wellfield, an optimal pumping strategy must integrate the optimal *pumping rates* of *individual* boreholes and their recovery times (number and location of production boreholes) with the long-term sustainable yield of the *aquifer system*. A sustainable management strategy should employ the principle of utilising *more* production boreholes at *lower* abstraction rates.

4.3 POLLUTION POTENTIAL AND AQUIFER VULNERABILITY

4.3.1 AQUIFER VULNERABILITY AND RISK MANAGEMENT

The protection of groundwater quality is one of the most important facets of groundwater management. A number of potential or existing pollution sources could deteriorate groundwater to a point that it is no longer fit for its recognized use(s). The groundwater resources are thus vulnerable to contamination events because of contaminant loading and specific aquifer conditions. Internationally, mapping aquifer vulnerability became an essential part of groundwater protection strategy. In South Africa, the groundwater protection framework has been developing and institutionalizing only recently and the process is not yet complete.

Before discussing pollution and vulnerability, let us consider first what exactly pollution potential and aquifer vulnerability are. Groundwater protection approaches are usually based on the concepts of groundwater contamination / pollution risk and risk management. The risk of groundwater contamination depends upon the following elements (Daly and Warren, 1995):

1. the *hazard* posed by a polluting activity
2. the *vulnerability* of the medium to polluting activity
3. the existing or potential *consequences* of polluting activity.

Analysis of these three aspects followed by a response to risk is encompassed in the process known as risk management. In this context aquifer vulnerability is the sum of hydrogeologic, pedologic and hydrologic characteristics that determine the degree to which an aquifer can be polluted by contaminating activities.

Although aquifer vulnerability is most often associated with changes in groundwater quality, flow considerations (i.e. groundwater quantity) are also important. Groundwater mining is a prime example. However, further considerations deal for the most part with groundwater quality. Aquifer vulnerability is therefore considered as a contamination susceptibility of an aquifer.

4.3.2 POLLUTION HAZARD

The pollution hazard is a function of the type of pollutant and its loading. The pollution hazard is introduced into the aquifer through the release points. The release points posing as a main threat to Karoo aquifers represent point sources: waste disposal sites, septic systems, fuel spills at service stations, loading of agricultural chemicals and/or wastes. In the northern part of the Karoo Basin, with its rich coal and gold reserves, mining is also regarded as an important polluting activity. Due to the mainly pastoral character of agriculture in the Karoo, diffuse sources such as spreading of fertilizers and pesticides are believed to be relatively less significant. The main contaminant release sources believed to be significant under Karoo conditions are the following:

- waste management,
- large-scale mining, and
- fuel/oil spills

Several typical cases will be described in the section on case studies.

4.3.2.1 Vulnerability

As already discussed, aquifer properties determine the likelihood and, to a certain extent, the magnitude of a contamination event. The likelihood of aquifer contamination determines its contamination potential. Vulnerability mapping is the technique of assessing the geological and hydrogeological factors and presenting it in map format in an understandable manner.

The concept of vulnerability applies to groundwater in bedrock and/or weathered/decomposed residuum. Vulnerability is usually determined on the basis of transporting vertically the contaminants to the groundwater-table. By implication, the vulnerability assessment shows the susceptibility to contamination of the first groundwater encountered in the borehole, which may or may not be the main resource.

In the Karoo, the unsaturated part (vadose zone) and some sections of the saturated medium may have undergone varying degrees of weathering and (chemical) decomposition. Depending on the site-specific conditions, the bulk of groundwater resource may reside in this part of the subsurface lithology. The relatively unweathered bedrock then forms a 'deeper' aquifer, with often less significant groundwater storage. In parts of the Karoo where the level of weathering is low (Western Karoo), the 'upper' or 'shallow' aquifer may be missing and groundwater storage is attributable mainly to secondary porosity.

When conducting aquifer vulnerability mapping it is therefore important to distinguish which aquifer(s) are to be considered. Ideally, differences resulting from the level of decomposition and weathering should be eliminated and a concept of economically utilized domains should be adopted - using this concept the vulnerability will result in the assessment being confined to that section or subsystem of the aquifer that yields water (i.e. is of maximum beneficial use).

4.3.2.2 Exposure Consequences

The contaminant exposure consequences depend on the value of aquifer and its groundwater resources. The relative value of the groundwater resource depends not only upon the natural aquifer characteristics, but more so on its economic value. Even a relatively low-yielding groundwater resource may be the sole source of water for a community, which is often the case with Karoo aquifers. The aquifer classification system currently in use was developed by Parsons (1995).

According to this classification the aquifers can be categorized as follows:

1. Sole source aquifer system
2. Major aquifer system
3. Minor aquifer system
4. Non-aquifer system – we would prefer the term 'poor aquifer system'
5. Special aquifer system

It can be safely stated that Karoo aquifers can, in many instances, be classified within the first two categories. Out of 125 sole source aquifers currently proclaimed or proposed, for example, about 60% are situated in Karoo (Parsons and Conrad, 1997).

4.3.3 CONTAMINATION SUSCEPTIBILITY OF KAROO AQUIFERS

Vulnerability assessment and mapping has been carried out using various approaches in many countries. In South Africa, Reynders studied vulnerability mapping at a national scale, but this study unfortunately was not completed. Other studies relate to specific problems associated with aquifer vulnerability, such as waste disposal sites.

4.3.3.1 Main Factors Determining Vulnerability

The aquifer vulnerability depends on the time of travel of the infiltrating contaminant to the watertable. Strictly speaking, all aquifers are vulnerable, because in time the contaminants (in sufficient quantity) will reach the groundwater-table. Given the lithology of the Karoo Basin, infiltration rates through the unweathered rock mass may be very slow. The argillaceous and arenaceous character of the bulk of Karoo rocks inhibits the rapid and effective infiltration of contaminated water. On the other hand, the presence of secondary permeability, dyke and sill structures may allow for a preferential or focused infiltration and redistribution of contaminated water in the subsurface.

The time aspect cannot be the only factor determining the aquifer vulnerability. The contaminant attenuation capacity of the soil and aquifer material will have an effect on reducing or retarding the movement of the incoming contaminated. Groundwater is usually linked to the surface water system and it is the effectiveness of this link that determines the attenuation capacity, infiltration rate and ultimately the vulnerability status of the aquifer. The link physically consists of the soil cover (if any) and vadoze zone, which may encompass the decomposed and weathered regolith, as well as the bedrock extending down to the watertable.

Therefore, the most important geological/hydrogeological factors are:

- Presence or absence of soil cover, its thickness and clay content.
- Mode of recharge – diffuse (piston-like), focused (point, macro-pore)
- Thickness of unsaturated zone (depth to groundwater level).

In general, the nature of the soil overburden varies from east to west and is related to variations in the rainfall patterns across the Karoo Basin. In the Eastern Karoo, relatively thick soils develop in areas of high rainfall due to chemical weathering processes, whilst thin soils develop in the drier Western Karoo due to mechanical weathering processes. The western Karoo Basin is therefore more vulnerable to groundwater pollution than the eastern side.

It is very difficult to assess the mode of recharge in Karoo aquifers. Although some research into recharge of the Karoo aquifers has been done (**Chapter D.2.3**), the determination of recharge will always be site-specific and will contain large degrees

of uncertainty. However there are indications that recharge occurs via preferential pathways and is very variable with respect to the terrain. Recharge may be enhanced at in specific areas, i.e. along the contact of dyke, areas with thin soil cover (hilltops), bedrock outcrops, terrain depressions (rivers) etc.

Relatively deep watertable conditions (i.e. thick vadoze zone) reduce the probability of contamination as contaminants have to travel farther and hence travel-times are longer. Various degradation and/or retardation processes can then impact upon the flux of contaminants - thereby reducing the contaminant load reaching the aquifer. However, these retarding effects are often negated by the rapid movement of contaminants along preferential pathways in the aquifer. If fractures and joints extend to the surface and are not filled with low-permeability material (i.e. clay), then the aquifer vulnerability is relatively high, as it would be for an aquifer with overlying thin unsaturated zone.

4.3.3.2 Assessment Guidelines

There are presently no set guidelines for vulnerability guidelines for South African conditions. A vulnerability classification is usually subdivided into three or five classes. For example, the IAH guide to hydrogeological maps suggests five classes: extremely high (vulnerability), high, medium, low, very low. Zaporozec (1985) suggests three classes: best, moderate and least (subsurface attenuation potential). For Karoo conditions, the Irish model (Daly and Warren, 1995) may also be appropriate, where four classes are proposed – extreme, high, moderate, low.

The extreme class is characterized by no soil cover and ‘point’ recharge. The high class would apply to areas with 1 - 2 m of soil cover and a vadoze zone of 1 - 2 m thick. Moderate conditions can be applied to areas where the overburden is of low permeability (clay fraction more than 20%) and is at least 5 m thick, and cannot be applied to sandy and gravelly alluvium. Low permeability materials more than 10 m thick may be regarded as ‘low vulnerability’, provided diffuse recharge occurs and not to point recharge.

The vulnerability assessment is complicated by the secondary porosity/permeability of Karoo fractured-rocks. For instance, if the fracturing extends to the surface then all the above cases would fall into the extreme class, because the recharge is of a point type. On the other hand, Karoo fractured-aquifers consisting of shale and mudstone have certain characteristics that may place them in a low vulnerability class.

4.3.3.3 Uncertainty and Limitations

All methods of assessing groundwater vulnerability are limited in their precision and will contain various degrees of uncertainty. Vulnerability mapping is usually conducted with limited data, as a pre-requisite of further groundwater development. Therefore, the only way to improve the knowledge on the groundwater vulnerability of Karoo aquifer systems is by the way of site-specific investigations.

4.3.4 CASE STUDIES

4.3.4.1 Impact of Gold Mining in Free State

Water Research Commission funded research into the effects of gold-mining on Karoo aquifers (Project K5/224). The study area stretches from Allanridge to Theunissen in the northern OFS and covers approximately 2 100 km². The mining activities commenced in the early fifties. According to the project results the main sources of contamination were:

1. Solid waste rock (rock waste, scrap metal, domestic waste)
2. Slimes and return water dams
3. Evaporation facilities
4. Urban solid waste
5. Urban liquid waste
6. Industrial effluent

Two aquifer systems were considered during the project – (1) a shallow aquifer within the weathered and fractured zone of the Karoo sediments, and (2) a deep aquifer in Ventersdorp and Witwatersrand rocks. It was found that the occurrence of groundwater was geologically controlled (dolerite intrusions). The major results of this study with respect to aquifer vulnerability were as follows:

1. Contamination of the subsurface water resources occurred by mining, industrial and municipal activities.
2. Contamination of groundwater resources is generally contained within close proximity of the disposal site (extending approximately one km distance from the pollution source). The relatively low-levels of aquifer pollution is due to the favourable geological conditions (shale), despite the abundance of pollution sources.
3. Evaporation pans and slimes dams appear to be the main sources of pollution, although the spatial extent of the pollution plumes around these features appears to be limited. They do, however, pose a long-term pollution threat.

The scale of the gold-mining operations and its potential pollution threat to groundwater can be gauged by the fact that more than 5 000 hectares of land are used as evaporation areas for effluent water (155 000 m³/d), which either evaporates or infiltrates into the ground. It was also confirmed that chloride tends to spread to greater extent than any other relevant ions – due to its conservative transport characteristics. The surface water was found to be of a sodium chloride character, forcing ion-exchange processes in the infiltrated subsurface. As a result, groundwater appears to be enriched with calcium. Migration of heavy metals was limited to the zone of impact of acid mine drainage around the slimes dams.

A number of coal-mining operations are currently active in the northern section of the Karoo Basin, especially in the KwaZulu-Natal Province. The impacts of these operations are similar to that of goldmines with respect to the major pollution sources and their characteristics.

4.3.4.2 Municipal Waste Disposal

It is estimated that $\pm 1\ 400$ waste disposal sites exist in South Africa and that 95% of all solid waste is disposed of by land-filling or land-building. Permitting of waste sites has however been slow – only 7% of the waste sites have been investigated and/or reported, whilst only 15% of the identified waste disposal sites have been issued with permits or are in the process of obtaining permits (Engelbrecht, 1993). All towns in Karoo operate municipal waste disposal sites. With limited budgets and often limited expertise the level of monitoring and operation of these sites is quite variable. Parsons and Jolly (1994) in their Water Research Commission project K485 evaluated a number of waste disposal sites countrywide to test their site suitability evaluation system. Five sites out of the ten evaluated are situated on the Karoo aquifers.

Out of these five sites, three represent a threat to the local groundwater resources. In one case, the site has had a deteriorating impact on the sole source aquifer and was closed by the Department of Water Affairs and Forestry. The site is one kilometer from a production borehole supplying the town with water and is located on a dolerite dyke, with maximum soil thickness of 4 m. Although the water quality had not deteriorated to levels in excess of the SABS maximum limits, the long-term potential impact on the abstraction boreholes could not be ruled out.

A further example is cited, where a site is located on shale of the Pietermaritzburg Formation and the under-lying aquifer is relatively shallow (depth to watertable ~ 4 m) due to its proximity to a river. The unsaturated zone consists of a thin layer of alluvium. Based on limited geohydrological information the site was found to present a significant pollution threat due to the poor attenuation capacity of the unsaturated zone and the type of waste material. In this case, however, the groundwater potential of the area is limited and the perceived threat is directed towards the river.

In the north-facing valley on the edge of the Mgeni River floodplain there is a regional waste disposal site with a poorly functioning leachate collection system. Although the site is situated on black carbonaceous shale that are only slightly fractured, sandy alluvial deposits extend directly down gradient of the site. After 14 years of operation the site, contamination was detected 50 m down gradient of the waste site, but it then took only 1.5 years to travel a further 100 m. This site illustrates that even when waste site is located on a relatively 'suitable' geological material (shale), the poor functioning of the leachate-handling facilities may pose a great threat to aquifers further down gradient of the site. The site was therefore proclaimed unsuitable.

One of the two sites certified as suitable owes its suitability status to the fact that other land uses in the area have an even greater impact on groundwater (cemetery and informal settlements) and therefore the chance that the groundwater resources will be developed in the future is poor. Compared to the impacts of the settlement, the effects of the waste site are comparatively low.

A site in the Eastern Cape certified as suitable is situated in an old quarry (shale and sandstone of the Beaufort Group). Municipal by-laws in this case prevent groundwater from being used for drinking purposes. Although evidence for groundwater contamination was found and the buffer zone with potential attenuation capacity had been removed, this site is an example of the situation when the suitability is granted on the account of the relatively 'low' value of groundwater as a drinking water resource.

From the above examples, it appears that landfills do affect groundwater quality on a large scale and that the resulting deterioration in the groundwater quality may eventually be 'transferred' to the surface water resources. The pollution of Karoo aquifers can be greatly averted by applying proper waste disposal siting procedures (choice of low permeability bedrock, typical of the Karoo rocks) with relatively simple leachate-collecting and draining measures.

4.3.4.3 Fuel Leaks from Service Stations and Storage Facilities

Petroleum products, industrial thinners and mineral oils represent a category of potential pollutants that have been largely overlooked by regulatory agencies and legislature, despite their harmful effects at small concentrations. Because of their small miscibility with water, their transport in the subsurface is different from dissolved contaminants. These products, despite of their low miscibility, release small amounts of contaminants into the dissolution (water phase) and are carried in the groundwater system to potential receptors.

A small Karoo town in the Free State is situated on shale of the Volksrust Formation, which is dissected by numerous dolerite dykes and sills. The local aquifer system is classed as a 'sole aquifer', as the town derives all its domestic water from boreholes.

The dissolved phase by benzene (a well-known carcinogen) was detected in the central part of town, in close proximity of two petrol-service stations and an old depot. Benzene contamination was also found in a borehole some 50 m away from the town's production borehole. The boreholes within the affected zone do not show non-aqueous phase liquid (NAPL) as a separate phase floating on the top of groundwater-table, only dissolved aromatic hydrocarbons. The total petroleum hydrocarbon (TPH) content in the groundwater was 10 times greater than the maximum allowable limit of 0.6 mg/ℓ according to the Dutch C levels. The benzene concentrations were up to 170 times greater than the Dutch C maximum allowable limit of 0.03 mg/ℓ. Follow-up monitoring showed that a range of diesel organics eventually contaminated the town's production borehole. This shows that despite the relatively low permeability of the host rock there is potential for the development of a widespread contaminant plume originating from such fuel leaks.

In another town in the northern Free State, leaking petroleum products caused widespread contamination of the mudstone-sandstone (Adelaide Subgroup) fractured-rock aquifer underlying the town. Estimates of average flow velocities ranged between 0.009 to 1.084 m/day. The dissolved BTEX (Benzene-Toluene-Ethylbenzene-Xylene) plume of pollution extended beneath a large part of the town. Although the groundwater in the area is only used for irrigation purposes, it is possible that uninformed users will use the water for drinking purposes during drought periods.

4.3.5 EXPERIMENTAL WORK AT INSTITUTE FOR GROUNDWATER STUDIES

The Institute for Groundwater Studies (IGS) at Bloemfontein conducts various research programmes related to aquifer vulnerability issues.

Very interesting results on groundwater velocities, kinematic porosities, dispersivities and matrix diffusion were obtained during a WRC project entitled; '*Utilization of tracer experiments for the development of rural water supply management strategies for secondary aquifers*' (Van Tonder et al., 1998). A number of tracer tests were conducted at the well-known Campus Site of the University of the Free State and the Meadhurst test site, situated about 15 km from Bloemfontein. Karoo sediments underlie both of these sites.

Two types of tracer tests were conducted at the sites, namely, the Borehole Dilution test (BD) and the Radial Convergence (RC) tests. This type of experiment has two components, namely: (1) a borehole dilution test in the injection borehole and (2) recovery of a tracer from the abstraction well. A number of RC and BD tests were performed at the Campus Site.

4.3.5.1 Borehole Dilution Test

The BD test is a simple point-dilution tracer test that is conducted in a single borehole under (a) natural or (b) radial convergence conditions. The BD test aims to correlate the observed rate of tracer dilution in a borehole or in a segment of the borehole, to the average groundwater velocity in the aquifer. The groundwater through-flow gradually removes the tracer introduced to the borehole from the bore cavity to produce a time concentration relationship from which the Darcy velocity is computed.

Results from a number of BD tests on the Campus site yielded the following results:

Darcy velocity along fracture zone = 2.0 - 6.0 m/d.

Darcy velocity in matrix = 0.1 - 0.4 m/d.

4.3.5.2 Radial Convergence Test

A radial convergent flow regime is created by pumping a borehole until steady-state waterlevel conditions are reached. A tracer is then rapidly introduced into the injection borehole in the vicinity of the pumping borehole in such a way that it only results in minimal disturbance of the flow field, whilst the Tracer Breakthrough Curve (TBC) is monitored in the pumping borehole. Analysis of the resulting TBC's yields estimates of hydraulic conductivity (K), seepage velocity, kinematic porosity, dispersivity, effective thickness of the fracture zone and matrix diffusion (mass loss to the aquifer due to diffusion). The average transmissivity (T) of the aquifer at the Campus Site is in the order of 10 to 20 m²/d.

A number of RCT tests on the Campus site yielded the following range of parameters:

K along fracture	= 100 - 800 m/d
K of matrix	= 0.01- 0.1 m/d
Seepage velocity along fracture	= 22 - 77 m/d (for abstraction rates between 0.2 - 0.3 ℓ/s)
Seepage velocity in matrix	= 0.5 m/d
Kinematic porosity	= 0.03 - 0.06
Effective thickness of fracture zone	= 0.05 - 0.17 m (i.e. between 50 and 170 mm)
Dispersivity	= 0.08 - 3.00 m
Mass loss into aquifer	= 5 - 20 %

As can be seen from the tracer test results, groundwater flow velocities within the fractures can be very rapid, whilst flow in the matrix is relatively slow. Even under natural conditions flow velocities of up to 30 m/d is possible along fractures. The tracer test also showed that the 'parallel-plate' fracture flow model is not valid for Karoo fractured-aquifers and that the fracture system should rather be considered as a

porous medium with relatively a high kinematic porosity and a small effective thickness.

This study also revealed that the K-value obtained from standard hydraulic tests (e.g. slug tests) is scale dependent, i.e. the K value obtained from a slug test in an open borehole with saturated thickness D represents an average value for the entire length of the bore. During such tests, the smaller the distance between the straddle-packers the greater the calculated K value (**Figure 4.74**). For this reason it is proposed that the Cooper et al., method should be used to analyse slug-tests data and not the Hvorslev or Bouwer and Rice methods. The Cooper method yields an estimate of T and, if the effective thickness of the fracture zone is known (this can only be obtained from tracer tests), a K value for that zone can be estimated.

In conclusion, pollutants can move very rapidly along fractures and extremely slowly in the aquifer matrix. The loss of tracer mass into the aquifer also suggests that it could take a very long time (tens to hundreds of years) for aquifers to be cleaned up after being polluted.

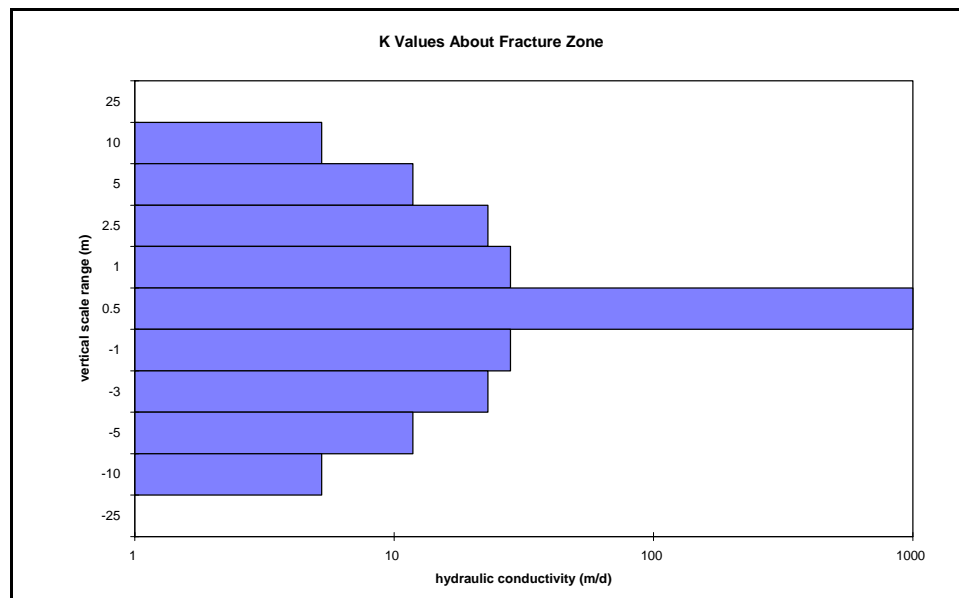


Figure 4.74: Scale dependency of Hydraulic Conductivity (K)

4.3.6 CAPTURE ZONES IN KAROO AQUIFERS

4.3.6.1 Purposes

A capture zone is the core of a Borehole Protection Area (BPA), which can be defined as the controlled surface area surrounding a production borehole (or wellfield) for preventing contaminants from reaching the borehole. A BPA may consist of a travel time-related capture zone, as well as a borehole catchment. The latter is also referred to as the Zone of Contributing Water (ZOC) (Todd, 1980; Reilly and Pollock, 1993), and represents the extreme case of a capture zone as shown in **Figure 4.75**.

In general, the capture zone is delineated to provide a buffer zone for the degradable contaminants to ‘die-off’ or degrade, whilst the borehole catchment is delineated to prevent the more persistent contaminants from entering into the borehole.

4.3.6.2 Conceptual Models

Three hydrogeological conceptual models are envisaged based upon information obtained from hydraulic tests, as well as later tracer experiments. In the following scenario analyses, the travel time-related capture zones are delineated to protect boreholes against the degradable contaminants such as faecal coliforms and viruses.

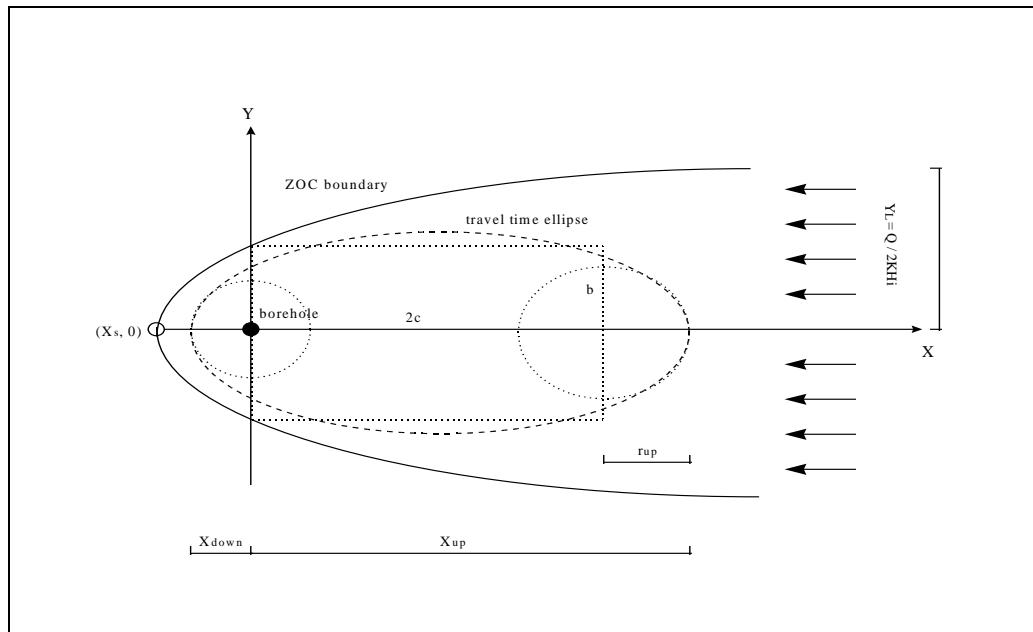


Figure 4.75: Approximation of the travel time ellipse and ZOC Boundary

Circular Zone

This approach assumes that the regional groundwater gradient is negligible. The radius of influence (R) may be calculated from the cylindrical flow model, i.e. $R = \sqrt[3]{Qt/hn\pi}$, where Q is the pumping rate, h the aquifer thickness, n effective porosity and t the travel time (Xu and Braune, 1995). As shown in **Figure 4.76**, this rudimentary approach is barely affected by the recharge rate within the 100 day of travel time. A circular zone of the R may thus be taken as a BPA.

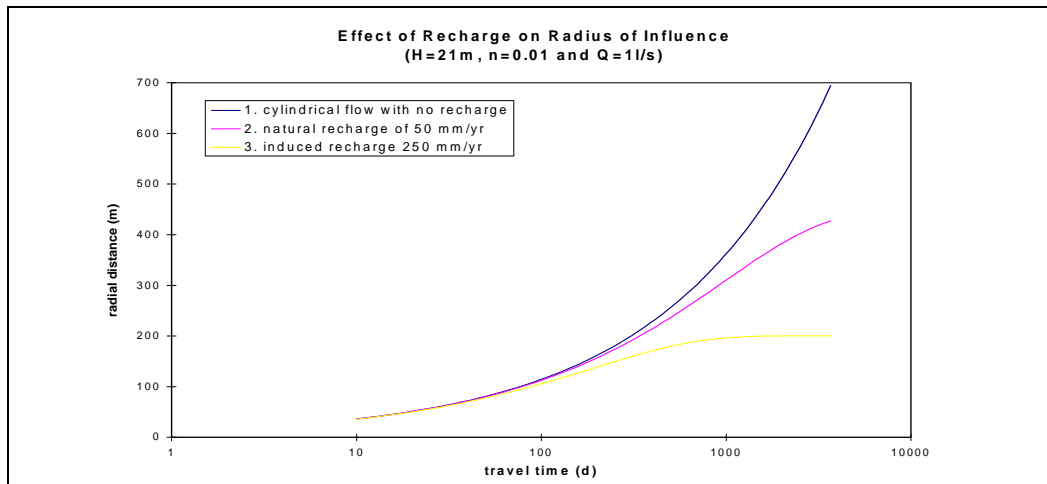


Figure 4.76: Effect of recharge on radius of influence

The radius of influence (R) may serve as a minimum distance between a borehole and pollution source. In the Karoo, this concept of ‘minimum distance’ may be adopted to provide groundwater quality protection against not only on-site sanitation but also other similar types of pollution sources including cattle-kraals, drinking-troughs (feedlots), graveyards (cemetery-sites) etc. This minimum distance is therefore regarded as an important concept for borehole source protection, especially within the Community Water Supply and Sanitation Programme.

Based on the local hydrogeological conditions, a set of formulae has been proposed for calculating this *minimum distance* (Xu and Braune, 1995). In general, the proposed minimum distance ranges from 15 m to 50 m. Actual values of the minimum distance for specific sites are dependent upon three factors, namely

- (i) soil material,
- (ii) depth to watertable, and
- (iii) type of aquifer.

The pollution hazards imposed by the above mentioned points would be greatly reduced by application of the proposed minimum distance during the water borehole siting stage. Because the method is simple and does not need complicated calculations, it is recommended as an initial basic protection measure and should be applied where no better protection measures are implemented.

Vertical Fracture (Dyke)

The capture zone for vertical fractures such, i.e. certain highly permeable dykes, may be simulated by using the line-sink concept. If the regional groundwater gradient is negligible, then the capture zone of such a dyke would take the form of an ellipse, which may be effectively represented by a rectangle flanked by two semi-circles (**Figure 4.77**). This approximation may be applied to dyke aquifers where the boreholes are located along the permeable dykes or fractured zones, and may also be extended to include certain wellfields.

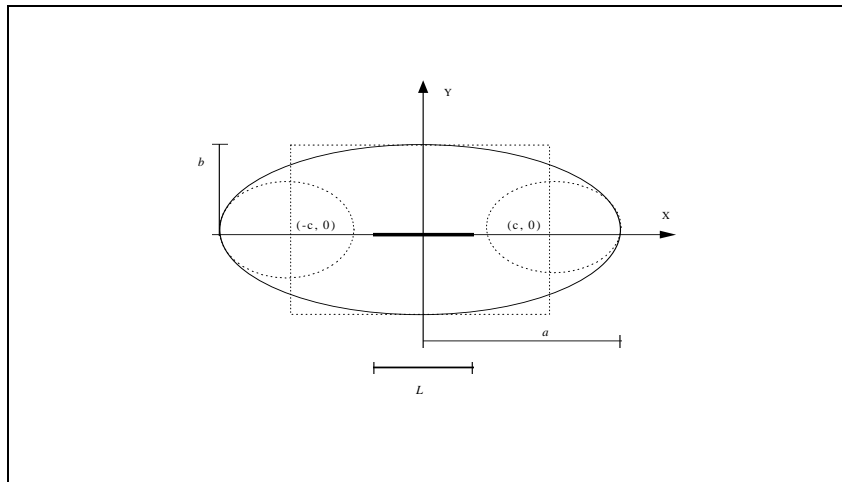


Figure 4.77: *Ellipsoidal protection zone along a vertical fracture or dyke*

As an example, a hypothetical wellfield consisting of two boreholes is discussed below. The hydraulic data is generalized from the campus-site aquifer at the University of the Orange Free State, Bloemfontein. The basic hydrogeological parameters of the wellfield include:

$$\begin{aligned}
 Q &= 1 \text{ } \ell/\text{s}, \\
 H &= 21 \text{ m}, \\
 n &= 0.01, \\
 t &= 30 \text{ d, and} \\
 L &= 15 \text{ m}.
 \end{aligned}$$

A simple water-balance indicates that the total required area
 $(A) = 1 \times 86.4 \times 30 \div (21 \times 0.01) = 12342.86 \text{ m}^2$. The two principal axes of the ellipse are $a = 70.18 \text{ m}$ and $b = 55.98 \text{ m}$. The internal circular area equals $\pi b^2 = 9845.73 \text{ m}^2$ and the outer conservative circular area $\pi a^2 = 1547.32 \text{ m}^2$.

- (1) *Scenario 1*: consider two production boreholes with the same yields.

If $Q_1 = Q_2 = 0.5 \text{ l/s}$, the two semi-circles with equal radius of 35.64 m were obtained. Area of the rectangle is $34.54 \times 55.98 \times 4 = 7734.2 \text{ m}^2$. The total protection area A_{app} would be 11725.09 m^2 .

- (2) *Scenario 2*: consider two production boreholes with different yields.

If $Q_1 = 0.6 \text{ l/s}$ and $Q_2 = 0.4 \text{ l/s}$, we will have the two different semi-circles with radii of 39.04 m and 31.88 m, respectively. The area of the rectangle is $34.54 \times 55.98 \times 4 = 7734.2 \text{ m}^2$. The total protection area A_{app} would be 11725.09 m^2 .

Horizontal Fracture

Horizontal fractures have been observed in high yielding boreholes in Karoo aquifers. The geological cause of such occurrence may be argued, but it is generally believed to be the result of unloading along the sedimentary bedding-planes during the process of weathering and erosion. Previously, vertical fractures were treated as a ‘line-sink’. An interbedded horizontal fracture may also be treated as a ‘line-sink’, although it is a complex mathematical process to compute the pathline distribution, because of the infinite number of image boreholes that are normally required to simulate the effect of impermeable boundaries. Therefore, a numerical approach should be used to simulate these capture zones.

To evaluate the effect of an interbedded horizontal fracture zone on the BPA, the campus site aquifer is conceptualised as a uniform, 3-layered aquifer (i.e. an upper layer of 10 m thick, a 1 m thick middle layer and a lower layer of 10 m). For the simulation of this 3D scenario, a model domain of 210 m x 210 m in the x, y plane is bounded by two fixed-head boundaries on right and left sides, with a waterlevel gradient of 0.005 and two no-flow boundaries as shown in **Figure 4.78**. The K and n values for all the three layers are taken as 1.5 m/d and 1%, respectively. A production borehole with its pump-inlet set at the centre of the middle aquifer layer is pumped at a rate of 86.4 m³/d. The resultant capture zone in the top layer of the aquifer under steady-state conditions is shown in **Figure 4.78**. The figure presents a capture zone for different hydraulic parameters under the same model and boundary conditions. In this case, the K value for the upper and lower layers is taken as 0.075 m/d, whilst a K

value of 30 m/d is assigned to the middle layer, which thus acts as a 1 m wide, horizontal fracture zone. This scenario was conceptualised from the results of a tracer experiment conducted on the campus-site aquifer. The capture zone in the upper layer of the aquifer under this scenario becomes much smaller than that of the former scenario (**Figure 4.78**). The reduction in the size of the capture zone is due to the pumping borehole removing groundwater mainly from the horizontal fracture zone, rather than from the upper and lower aquifer layers. Three-dimensional pathline tracking was simulated using a numerical model called PMWIN (Chiang, 1997). The larger capture zone will basically take on the form of an analytical ellipse, which can be adequately approximated using simple geometry, e.g. a rectangle flanked by two adjustable semi-circles (**Figure 4.79**).

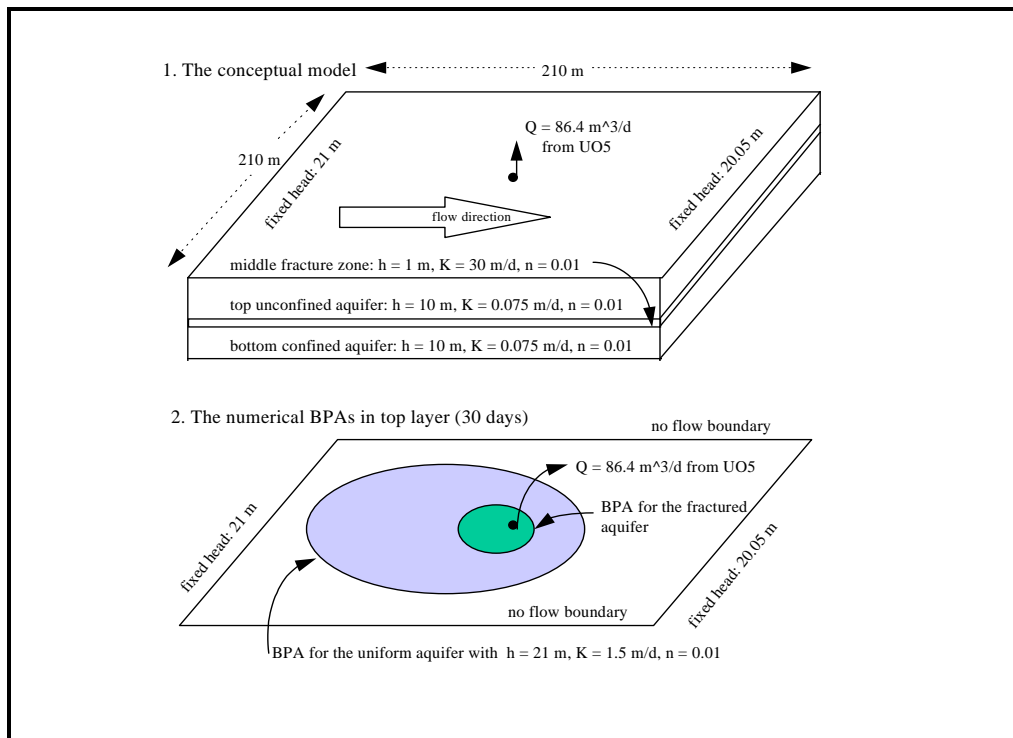


Figure 4.78: *Borehole protection area for an interbedded aquifer with a horizontal fracture zone*

4.3.6.3 Discussion

Establishing Regional Waterlevel Gradient

The regional waterlevel gradient is very gentle in most groundwater systems in the Karoo Basin and thus do not significantly influence the geometry of capture zones. However, should the gradient be significant, i.e. > 0.001 , then it must be accurately determined for the purpose of defining the capture zone, because the shape of a capture zone is very sensitive to the gradient.

Dealing with Parameter Uncertainty

In reality there are many uncertainties in terms of the input parameters required for calculating approximate BPAs. Two categories may be recognised, namely:

- (1) those associated with size of the capture zone, and
- (2) those associated with shape of the capture zone.

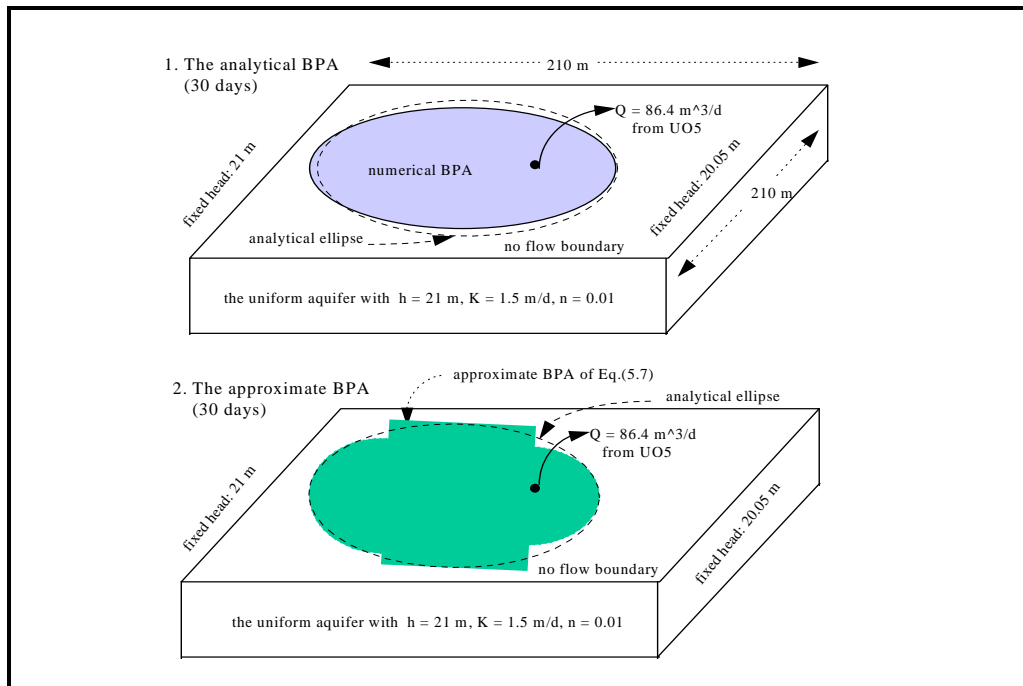


Figure 4.79: Comparison of analytical BPA with approximate BPA taken as a conservative approach

The former includes H , n , Q , t . The effect an error in these parameters on the size of the capture zone is demonstrated in **Table 4.16**, which was computed using the interval mathematics. For instance, if all the input parameters are associated with a 10% error, the average value for the size of the capture zone (A_{ave}) resulting from error propagation carries about a relative error of 8% (with respect to the conceptualised value $A = 12342.86 \text{ m}^2$). If the 10% error increases to 25%, the propagated error would be 57%. Clearly the latter would not be acceptable.

Table 4.16: Effect errors in input parameters on size of the BPA

Input parameters	Conceptualised	Error %	A_{low}	A_{high}	A_{ave}
H (m):	21	5	10103.79	15078.12	12590.95
n :	0.01	10	8262.574	18438.1	13350.33
t (d):	30	25	4443.429	34285.71	19364.57
Q (m ³ /d):	86.4	50	1371.429	111085.7	56228.57
A (m ²):	12342.86	95	8.114962	18773486	9386747

The second category is mainly associated with the hydraulic conductivity of the aquifer, which in reality often exhibits a wide range of values. In an aquifer, different methods of testing and repeated tests using the same method may well produce variable results. For instance, a conventional pumping-test on a borehole at the campus-site aquifer produced a K value of less than 1 m/d, whilst tracer tests produced K values in the order of about 1.5 m/d or even larger. In most rural water supply projects, only one of these methods may be actually be employed for estimating the K value.

To accommodate for possible drift in the K value, a stochastic treatment is required. For the sake of continuity, the campus-site aquifer example is used to demonstrate the effect of uncertainty in the K value on the shape of the capture zone. The following parameters are, as before, used: $H = 21 \text{ m}$, $n = 0.01$, $i = 0.005$, $Q = 86.4 \text{ m}^3/\text{d}$, $t = 30 \text{ d}$, but a K value of 1.5 m/d is used in the numerical simulation and is allowed to drift randomly according to a lognormal distribution (Freeze, 1975). Ten simulations were performed in which an error in the K value of 95% was introduced. The resultant capture zone ellipses are reflected in **Figure 4.80**, where only half of the ellipse is presented due to its symmetry. It must, however, be pointed out that the successful application of this stochastic approach under local conditions still requires further refinement.

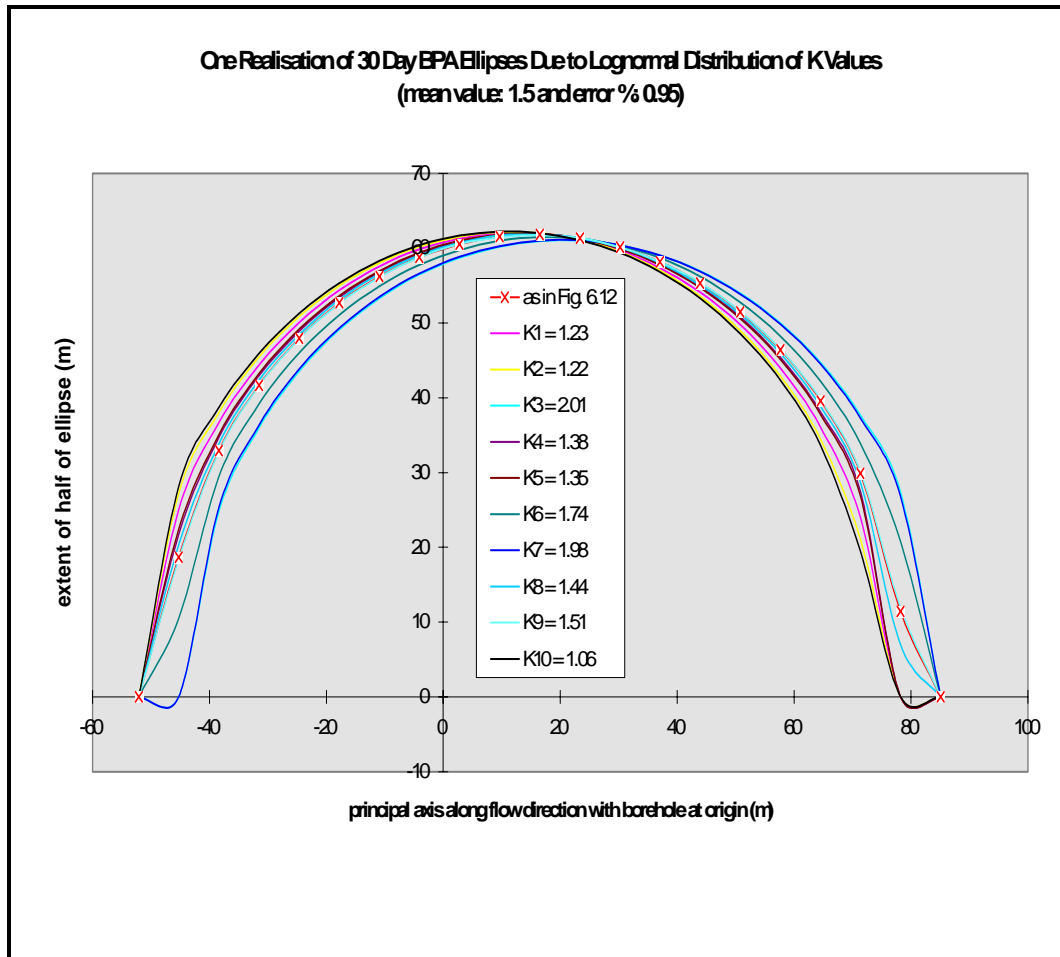


Figure 4.80: Effect of random *K* values on simulated BPA ellipses

4.4 NATIONAL GROUNDWATER QUALITY MONITORING IN KAROO AQUIFERS - PRELIMINARY RESULTS AND TRENDS

4.4.1 NATIONAL GROUNDWATER QUALITY MONITORING NETWORK

In 1994, the Department of Water Affairs & Forestry (DWAF) initiated the National Groundwater Quality Monitoring Programme (NGWQMP). The aim of NGWQMP was defined first and foremost to monitor broad, 'ambient' changes in groundwater quality at a national scale through a network of selected groundwater monitoring stations. This network monitors relatively shallow horizons, which are most readily exploited by various groundwater users.

The design of the NGWQMP network was performed under conditions of little prior information on spatial trends, using only existing (mostly private) boreholes. The boreholes were selected in areas where the impact of point source (and to a certain extent diffuse) pollution could be ruled out. The emphasis is therefore on discerning variations in groundwater quality with respect to lithology, climatology (especially rainfall patterns), soil types and thickness of soil cover and other spatially distributed factors.

The area broadly defined as Western Cape was selected as a pilot region for the NGWQMP. In time the network was extended into other areas of the country reaching now about 320 monitoring stations. Most of groundwater quality observations were, however, collected for the pilot region and the data spans 6 years (1994-1999). The boreholes were sampled twice a year, to discern changes in water quality between the onset of the rainy and dry seasons.

The groundwater samples were analysed for major cations and anions, which also included silica, pH and electrical conductivity (EC). Most recently other constituents were added into the sampling list for a 'once-off' scrutiny and included tritium, ^{18}O , and several trace elements. At the sampling site, on-site measurements form the part of the sampling protocol and include temperature, EC, pH and dissolved oxygen. The samples were analysed at the Instituted for Water Quality Studies at the Roodeplaat Dam, Pretoria. The analytical results were uploaded into the DWAF WMS database.

Until recently, very little work has been carried out on the monitoring data generated for the NGWQMP. Limited staff and budgetary conditions allowed channelling the resources only into the data collection. Nevertheless, with eleven completed sampling runs, it is now possible to conduct a preliminary evaluation of the NGWQMP results and identify trends using suitable evaluation techniques.

4.4.2 KAROO GROUNDWATER QUALITY

The WMS (DWAf water quality depository) NGWQMP database contains about 2 650 analyses for the whole country (at the end of 1999), over 700 of which lie within the Main Karoo basin. The database was checked for analytical errors by examining the ion balance error, pH values and apparent outliers. Where possible, corrections were made and the corrected dataset was used for subsequent evaluation. It appears that errors encountered may have been largely due to incorrect handling of output forms by the reporting programs.

Analytical data related to 78 Karoo-based sampling stations were drawn on for further trend analysis. The NGWQMP network in Karoo started with 31 sampled boreholes and was eventually extended to almost 80 (1999).

4.4.2.1 Determination of Regional Trends between 1994 and 1999

The significance of changes between two sampling events can be tested using various statistical techniques, both parametric and non-parametric. In principle, comparison is sought between analytical data taken from two sampling events. For a paired matched test both analytical sets have to contain the same monitoring stations. A null hypothesis is tested whereby zero difference between the mean of the two sets is postulated (i.e. a parametric test such as the *t*-test). Non-parametric tests are based upon evaluating the difference between ranks, rather than absolute values of data (Kolmogorov-Smirnov, Mann-Whitney, Wilcoxon test, etc.). The advantage of non-parametric tests is that they are not constrained by several assumptions that are required for parametric tests (e.g. normality). The power of non-parametric tests is usually sufficient for environmental applications and therefore they are widely used in the hydrological sciences.

Three scenarios were further considered, namely: (i) testing the difference between 1994 and 1999 (sampling event 1 and 11), (ii) 1994 and 1996 (sampling event 1 and 5) and (iii) 1996 and 1999 (sampling event 5 and 11). These intervals were chosen arbitrarily due to sizeable extension of the network during 1995-1996. All sampling events were carried out over the period April to May.

The following null hypothesis was tested - there was no significant net change in concentrations of water quality parameters between the selected sampling events. The alternative hypothesis was that there had been a significant change between the sampling events under consideration.

The results of the statistical analysis between events 1 and 11 are presented **Table 4.17**. At the considered significance level of 1%, a change between the two sampling events is apparent for pH, NH₄-N and F only. It is quite possible that especially for NH₄-N the changes are due to the fact that its concentrations are mostly

below the detection limit. The net effect between the 1994 and 1999 groundwater quality observations is thus rather small, suggesting that the observed system is in *equilibrium*. This must however be judged against the fact that only 31 matched pairs of observation points in the Karoo Basin could be used. This constitutes less than a half of the available stations.

Table 4.17: *Computed probability levels as a measure of the statistical significance of global change in groundwater quality between 1994 (event 1) and 1999 (event 11). Based on 31 matched sampling points*

	p (tT)	p (KS)	p (W)
TDS	0.75	>0.100	0.34
pH	0.00	<0.001	0.00
Ca	0.93	>0.100	0.07
Mg	0.78	>0.100	0.14
Na	0.50	>0.100	0.54
K	0.73	>0.100	0.14
NH4-N	0.00	<0.001	0.00
Alkalinity	0.56	>0.100	0.65
SO₄	0.89	>0.100	0.88
Cl	0.60	>0.100	0.14
NO_x-N	0.38	>0.100	0.12
F	0.00	<0.005	0.00
Si	0.32	>0.100	0.41

To improve the spatial statistics, a further analysis was conducted on the differences between the 1996 and 1999 datasets where 61 matched pairs could be utilised. The comparison between these two events did not show any statistically significant changes. This could mean that the observed changes are attributable to the early stages monitoring programme, after which the dynamics of system equilibrated. Another explanation may be that by increasing the sample size, changes attributable to individual stations were averaged out, resulting an insignificant net change.

The assessment of 1994 and 1996 datasets confirms the statistical results observed between 1994 and 1999 datasets, where only a sample of 31 matched pairs could be used. For this sample all or some of the selected statistical tests at a significance level of 1% confirmed the changes in pH, NH₄-N and F. No other changes were found to be significant.

It therefore appears that regional net changes in the groundwater quality of aquifers in the Karoo Basin are relatively small. Only parameters such as pH, NH₄-N and F were found to undergo statistically significant changes. This does not rule out the fact that

certain sub-domains may exhibit more significant trends than others. For that purpose it would be necessary to divide the network into sub-domains with relatively homogeneous properties and test the statistical significance of changes within each sub-domain separately.

4.4.2.2 Identification of Hydrochemical Classes

As proposed in the previous section, there is a need to subdivide the Karoo NGWQMP dataset into several sub-domains. This process was deemed necessary for the application of the trend-analysis, for in the absence of long-term records it is possible to apply these techniques to assess group variance as a measure of temporal trends.

Commonly applied hydrochemical methods aimed at grouping groundwater samples into classification systems rely only on few selected parameters, such as Ca, Mg, Na, HCO₃, SO₄, Cl (i.e. Piper diagram). It was felt that this type of classification would not be sufficient under relatively monotonous geological conditions of the Karoo Basin. The Dutch subdivided their monitoring network using fuzzy c-means cluster analysis (Frapporti and Vriend, 1993). The advantage of this technique is that it allows any number of parameters as classification criteria, which in turn makes the identification of the underlying hydrochemical processes possible and more reliable. The problem with traditional cluster techniques is that they attempt to group the hydrochemical data without any a priori knowledge. Fuzzy c-means clustering in contrast to 'hard' c-means clustering allows for a quantification of the compositional overlap between groups of groundwater samples. Certain levels of vagueness are to be anticipated for groundwater data where samples exhibit properties of two or more distinct groups. It is not possible to determine the level of ambiguity using the 'hard' approach only. On the other hand, fuzzy approach quantifies this vagueness by using a membership function. The membership value of an individual sample within a cluster can vary between 0 and 1, where zero indicates perfect similarity (visa versa).

A similar approach was applied to the Karoo NGWQMP data. The classification parameters included all major groundwater quality constituents analysed for by the IWQS, with the exception of pH. The data was log-transformed to reduce effects of the anticipated non-normal distribution, which is typical of hydrochemical datasets. Spatial parameters that may influence the groundwater chemistry (i.e. soil cover, geology, vegetation, rainfall zoning etc.) were not used during study, although there is a potential for a future research.

The choice of the initial number of clusters is largely arbitrary. In this case, a number was selected using the regional distribution patterns generated during hydro-geochemical mapping by Simonic (2000). Three cluster models were selected for analysis, namely a 3-, 5- and 7-cluster configuration, whilst the assessment of temporal trends was only performed on the 7-cluster model.

The classification model with only 3 clusters (**Figure 4.81**) is very crude for the purposes of more accurate spatial assessments. For example, monitoring points in cluster number 3 are spread over the entire study area and it is possible to visually distinguish more ‘refined’ homogeneous groups within this cluster. Even the 5-cluster model (**Figure 4.82**) did not sufficiently account for spatial variations of groundwater quality. The 7-cluster model appeared to more satisfactorily describe the major hydrochemical features of the Karoo aquifers (**Figure 4.83**). The spatial distribution of the boreholes within the different cluster groups seems to reflect the major compositional and concentration domains as they appear on the National Groundwater Quality Assessment maps (Simonic, 1999). The easternmost portion of the Karoo Basin (i.e. KwaZulu-Natal region) was not in this study as no monitoring stations were available. Future monitoring stations in the Kwazulu-Natal area may alter the cluster model and of station memberships may need to be re-assigned.

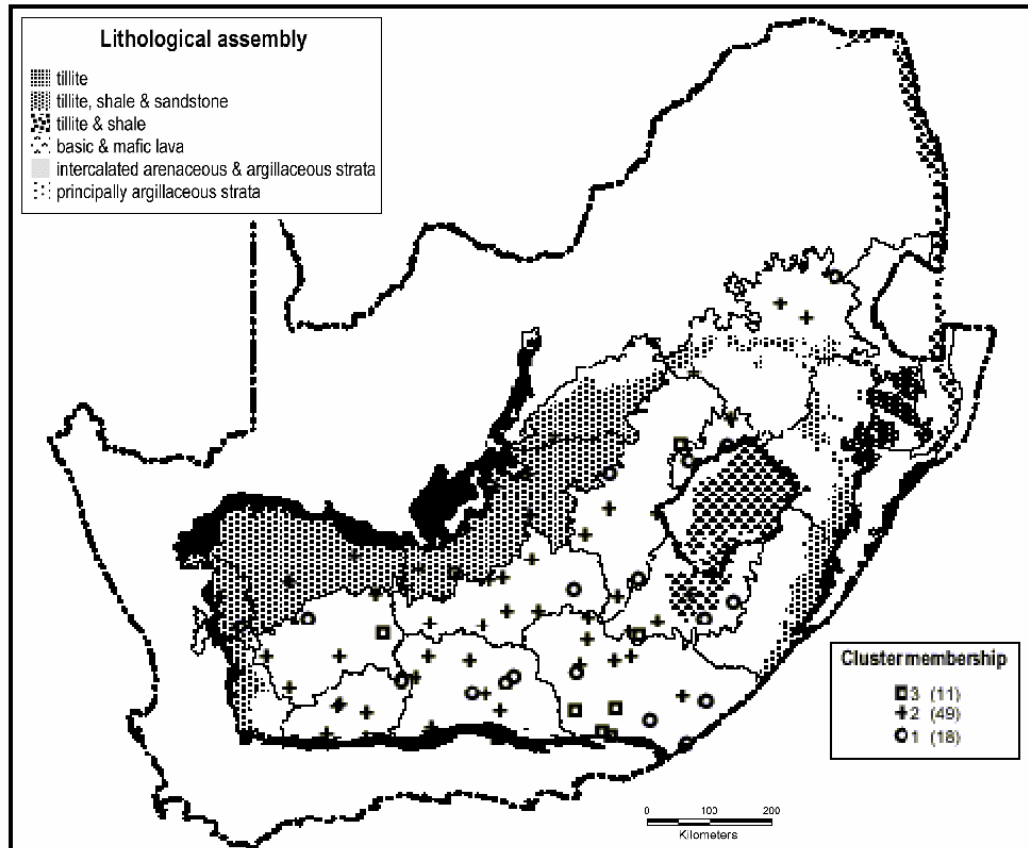


Figure 4.81: *Geographic distribution of sampled stations (1999) and their cluster membership for a 3-cluster model*

The fuzzy c-means clustering derived concentrations of seven cluster centres are presented in **Table 4.18**.

Table 4.18: *Hydrochemical parameters of cluster centres for a 7-cluster model*

cluster	pH	Ca	Mg	Na	K	Alk	SO ₄	Cl	NO _x -N	F	Si
1	6.70	81	42	77	1.9	311	71	84	4.51	0.59	17.1
2	7.30	156	67	235	3.9	351	186	408	4.07	0.86	12.3
3	7.37	132	43	148	2.2	293	186	241	0.02	0.77	11.1
4	7.68	58	25	38	1.7	271	23	25	1.82	0.34	15.4
5	7.88	76	33	73	1.9	296	62	78	2.84	0.53	14.9
6	8.16	23	6	66	1.0	186	19	31	0.02	0.94	9.6
7	9.02	27	0	215	1.1	20	7	339	0.01	5.94	10.2

Note: All concentrations in mg/ℓ (except for pH)

In addition the cluster centres are also portrayed on Schoeller (**Figure 4.84**) and Piper (**Figure 4.85**) diagrams, in order to examine the topological differences between the various clusters.

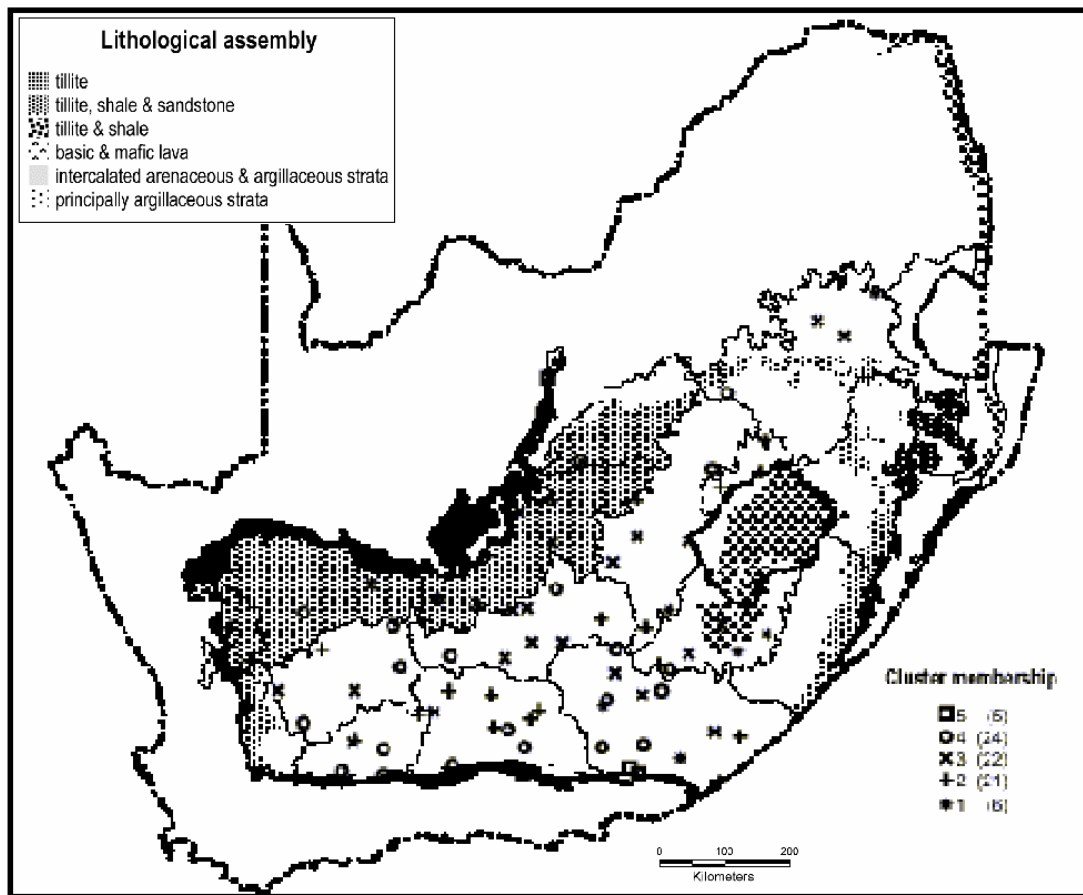


Figure 4.82: Geographic distribution of sampled stations (1999) and their cluster membership for a 5-cluster model

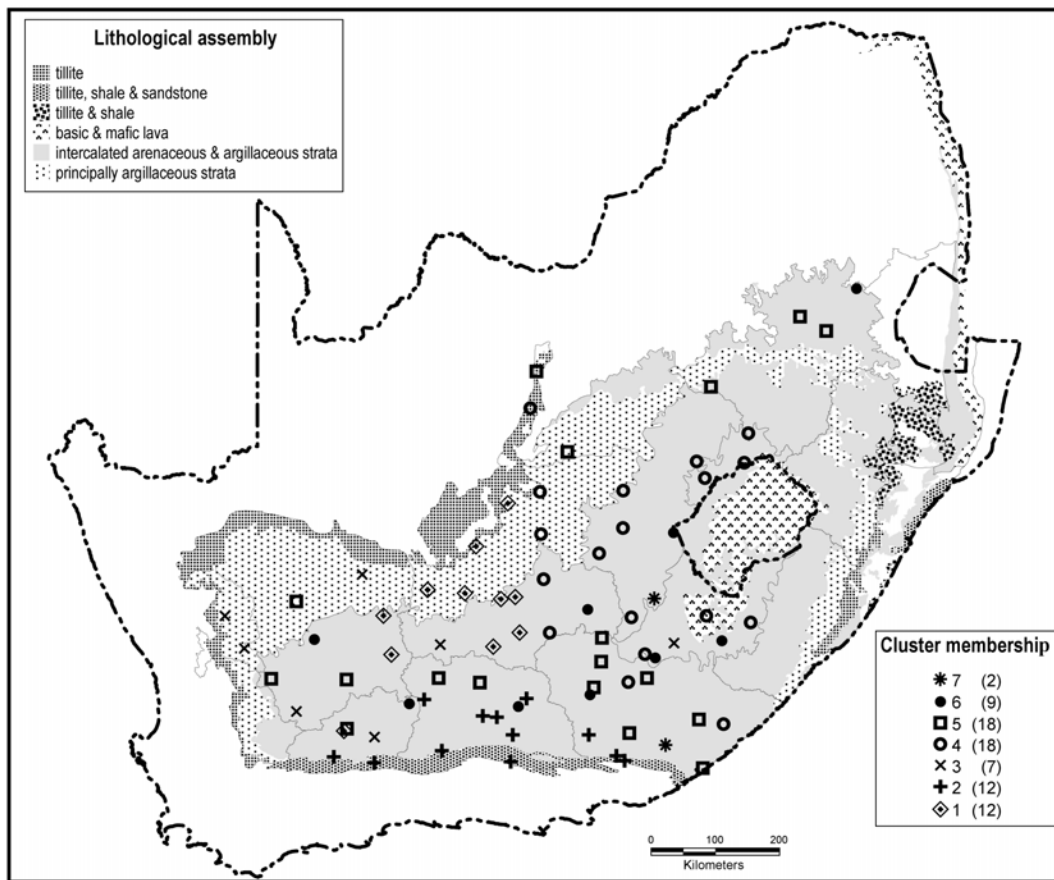


Figure 4.83: Geographic distribution of sampled stations (1999) and their cluster membership for a 7-cluster model

As indicated in both tabular and graphical forms, the differences between the cluster centres are due to different hydrochemical processes and/or concentrations of major ions. It is evident from Figure 4.85 that a pure Piper-based classification would not be properly delineate the various ‘homogeneous’ groupings identified using the fuzzy c-means clustering approach. It is also apparent that, cluster centres 1 to 5 form a ‘mixing’ line beginning at cluster 4 and extending to cluster 2, suggesting gradual transition between essentially fresh, recently recharged water to more stagnant groundwater formed by evaporite dissolution, ion exchange, silicate hydrolysis and other processes. On the other hand, cluster centres 6 and 7 have more distinct properties.

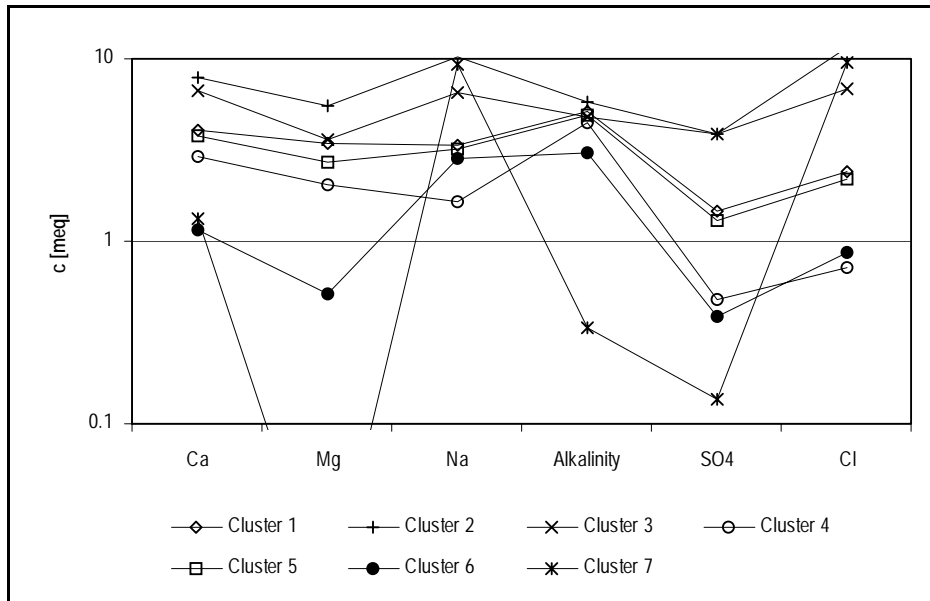


Figure 4.84: Schoeller diagram of cluster centres for the 7-cluster model

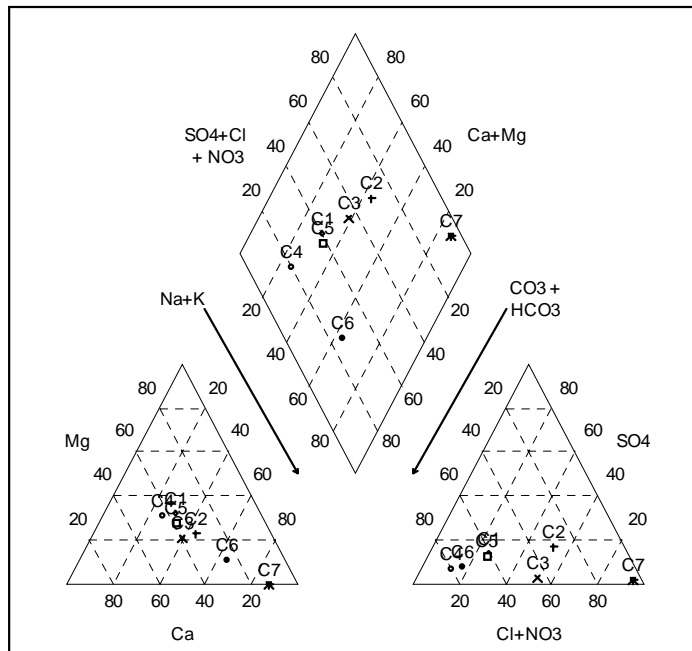


Figure 4.85: Piper diagram representation of cluster centres (7-cluster model)

The cluster-1 group is defined as mixed, Ca-Mg-Na-HCO₃-Cl type. The boreholes with this membership form a relatively 'tight' group limited to the northern parts of the eastern section of the winter rainfall area (Figure 4.83). This group has the highest silica concentrations pointing to active dissolution of silica minerals. Calcium dominates over magnesium and sodium. The pH value for this group is the lowest, being slightly acidic. The group has comparatively high nitrate concentrations, which are probably of natural origin.

The cluster-2 group has characteristically highest concentrations, especially of chloride, sulphate and sodium. The cluster centre water type is Na-Ca-Cl-HCO₃. Silica concentrations are slightly lower, but still higher than those in groups 3 to 7. Sodium is a product of cation exchange processes, which appears to influence the groundwater chemistry of almost all Karoo aquifers. A trend-line with a 2:1 slope was fitted to the clusters (Figures 4.86 and 4.87), which is typically indicates the dominance of ion exchange processes. The boreholes with this membership are located along the southern boundary of the Karoo Basin within the winter rainfall area. Nitrate concentrations are relatively high, suggesting active nitrification.

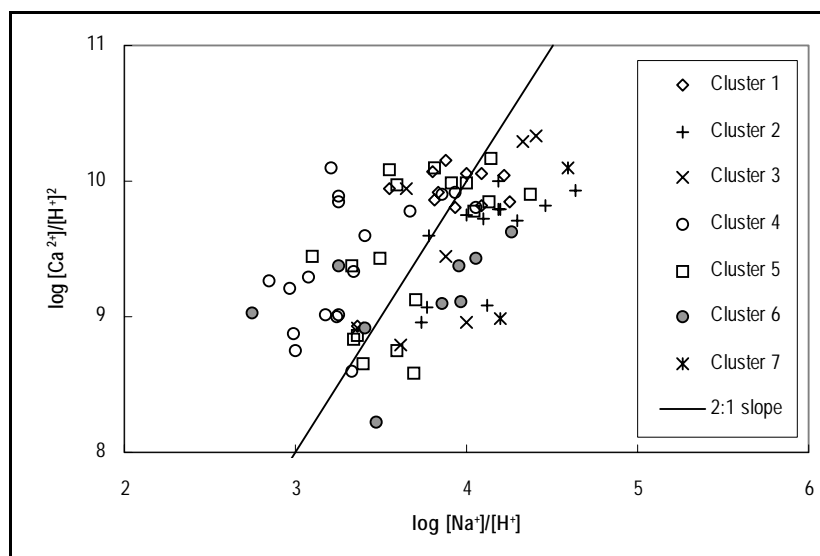


Figure 4.86: Relation between calcium and sodium, showing a trend-line with a 2:1 slope indicating ion-exchange processes

The cluster-3 group has the second highest concentrations, but comprise only $\pm 50\%$ of group 2. The dominant groundwater type is Ca-Na-Cl-HCO₃. The boreholes within this group are mostly located in the winter rainfall areas of the Karoo Basin. Several boreholes are concentrated in the westernmost section of the Basin. The low nitrate

concentrations (i.e. at detection limits) would indicate that reducing conditions may exist, but not at the prevailing sulphate/sulphide level.

The cluster-4 group comprises boreholes with relatively fresh groundwater quality and the dominant type is Ca-Mg-HCO₃. The boreholes in this group occur in the western half of the summer rainfall area, mostly in the Free State Province. The groundwater quality is largely controlled by that of the recharging water, resulting in comparatively higher (second highest) silica concentrations - which suggests active hydrolysis of silicates and an insignificant input from the dissolution of evaporates (low sulphate, chloride, fluoride etc.).

The cluster-5 group's dominant hydrochemical water type is Ca-Na-HCO₃-Cl. The boreholes of this group are distributed along a concentration-line that extends from the east coast towards the western Karoo. This group's chemical composition is similar to that of cluster 1, representing a mixing of recent recharge water and more stagnant components.

The boreholes in the cluster-6 group are located in approximately the same area as the group-5 boreholes, but they also occur further east than those in group-5. This group has the lowest concentrations with the dominant water type being Na-HCO₃. Silica concentrations are the lowest and nitrate is at its detection limit. As with group 4, the main process is dissolution of silicates within a very dynamic recharge environment, where groundwater residence times are probably very low.

The cluster-7 group consists of only two members and they consistently differ from all the other groups. This member represents deep-circulating groundwater with a Na-Cl hydrochemical type, with alkalinity being the lowest of all the groups, which affects the pH (most alkaline of all groups). Magnesium and nitrate concentrations are very low, zero for all practical purposes. The exchange processes in this case affect magnesium to such an extent that almost all magnesium is exchanged for sodium. The alkaline environment also favours dissolution of fluoride-containing minerals resulting in the highest fluoride concentrations of all groups. This redox character of this deep-seated environment is probably highly reducing, even below the sulphate/sulphide level. Although the group represents deep circulation conditions, the overall mineral contents are not high. This probably represents dissolution of minerals under stable conditions from a rock matrix that has already been largely depleted.

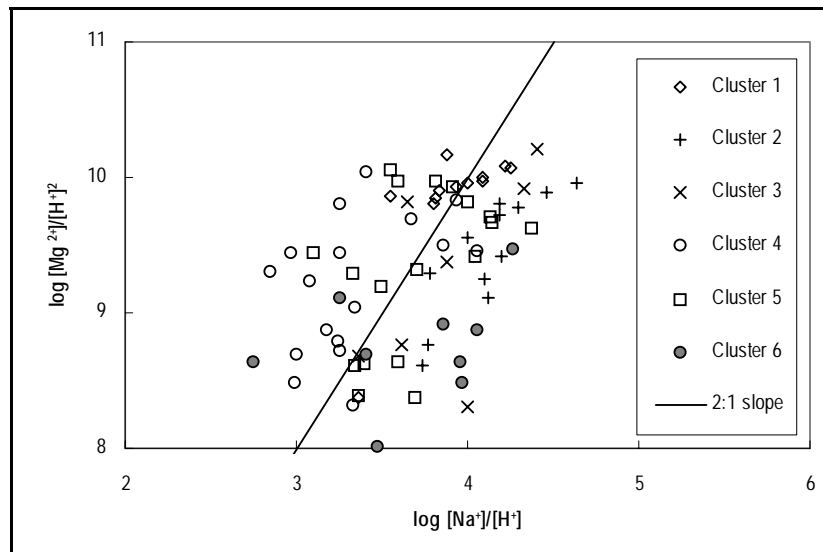


Figure 4.87: Relation between magnesium and sodium, with a trend line (2:1 slope) indicating ion-exchange processes

Interpretation of activity plots indicates that clay minerals are an important control on the cation composition of the groundwater in the Karoo Basin. Most groundwater data lie along the concentration-lines consistent with cation exchange, most likely occurring on the surface of secondary silicates such as clay minerals. The main product of the silicate mineral hydrolysis appears to be kaolinite (Figure 4.88), because the relationship between the major cations (calcium, magnesium, sodium) and silica produces values falling largely into the area defined by the kaolinite field.

Where values deviate from the 2:1 trend-line it is anticipated that different processes removing Ca (and Mg) may apply. For example, the precipitation of calcite may remove calcium from the solution. The carbonate dissolution processes do, however, appear to be active – where the saturation index with respect to calcite indicates largely under-saturated conditions (Figure 4.89). As will be shown later, this may be due to the fact that the most recently sampled pH values are rather low. It is believed that the saturation index values at saturation levels were higher at the beginning of the NGWQMP operation in 1994 than those measured in 1999. Therefore the present-day (1999) depletion of calcium and magnesium cannot function through carbonate precipitation.

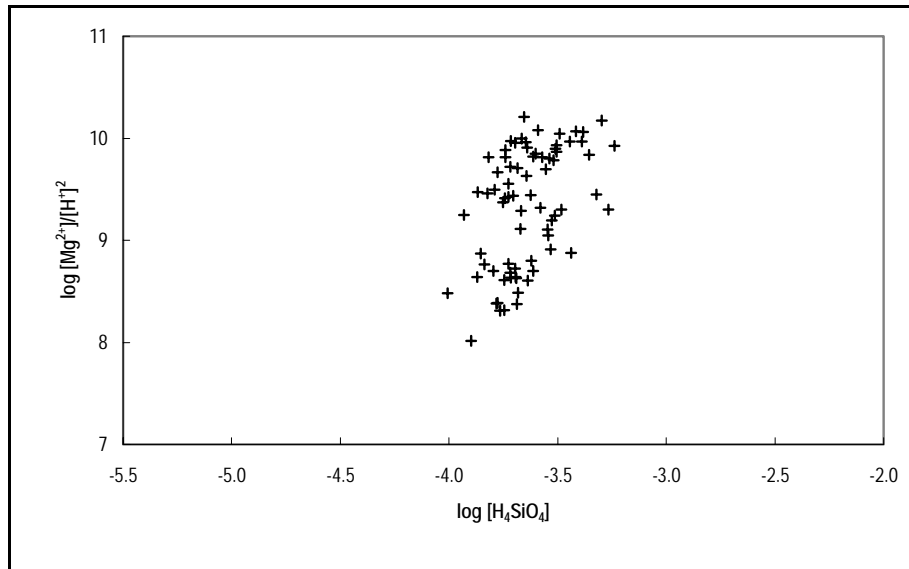


Figure 4.88: Relation between magnesium and silica indicating the precipitation of kaolinite (all Karoo monitoring points used up to the 1999 sampling run)

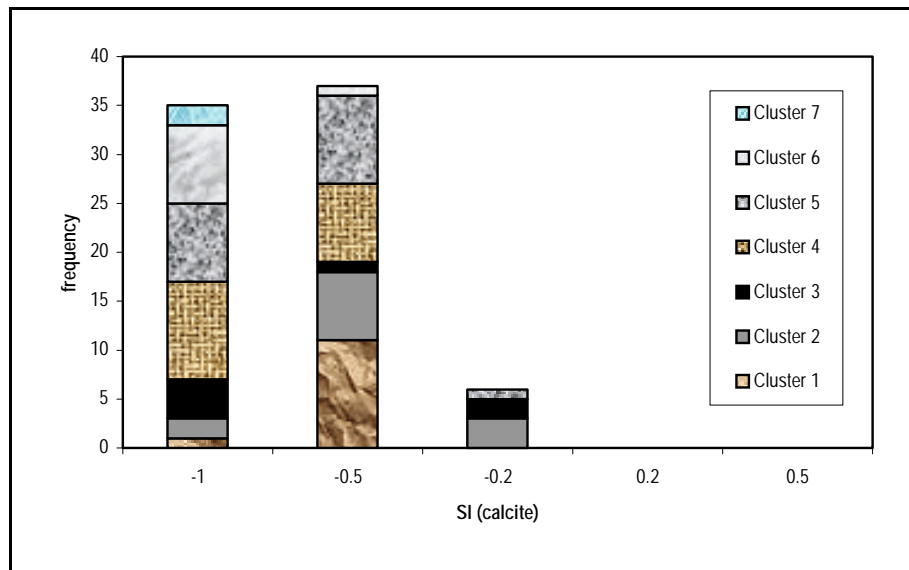


Figure 4.89: Saturation levels in groundwater with respect to calcite. Sub-zero levels indicate calcite dissolution processes, levels between -0.2 and 0.2 point to equilibrium conditions

4.4.3 TIME TREND DETECTION

4.4.3.1 Statistical Method

Due to the size of the NGWQMP network a robust and reliable method is required for a trend analysis. The non-parametric Spearman or Kendall-Tau statistical tests have been used for time trend detection without seasonality. Because of the global character and function of the NGWQMP the trend tests were applied to groups of monitoring data rather than the individual monitoring points. The low number of sampling events also supports the idea of station grouping – measurements from individual stations will not allow for reliable statistical testing. The confidence of a trend test statistic will be low for a low number of measurements (sampling events) – therefore a group statistics statistical approach was used.

Spearman rank correlation coefficients were used for statistical testing and the distribution correlation coefficients were compared to the zero correlation distribution using a Kolmogorov-Smirnov (K-S) statistic. Only one K-S is obtained for a cluster and for each parameter. The deviation from the zero distribution is evaluated at a 99% confidence level.

The Spearman ranks correlation coefficient, r_s , is computed between the ranks of two variables, with 1 assigned to the lowest value and N to the highest value - as follows:

$$r_s = 1 - \frac{6 * S}{N^3 - N}$$

where

$$S = \sum_{i=1}^N (x_i - y_i)^2$$

x_i and y_i are ranked variables.

The Spearman ranks zero correlation distribution is defined by computing all possible untied combinations of ranks x_i and y_i . The distribution ranges between -1 and 1 and is symmetrical about zero. Spearman rank correlation coefficients are available for a specific number of observations and Kendall (1975) tabulated these permutation distributions up to an N of 13. This is sufficient for this study as the maximum number of observations at this stage is 11.

4.4.3.2 Computed Temporal Trends

The dataset used for this analysis does not contain data for all stations, due to the specifics of the implementation process where certain stations had more analyses available per station than others. This is an unfortunate ‘teething’ problem that should be avoided at all costs in future. As a result two scenarios were evaluated: (1) trends detected for sampling events 3-11; and (2) trends detected for sampling events 1-11. The first scenario contains more stations for the slightly shorter period, whilst the second one is based upon fewer stations over the full period.

Detected trends for Scenario 1 (events 3-11)

The K-S statistics computed for sampling events 3-11 is presented in **Table 4.19**. The $K-S_{crit}$ represents the Kolmogorov-Smirnov critical level for a significant trend, ranks stand for the number of events available for a statistical evaluation for the specific cluster and number signifies the number of stations with the specific number of events available for the cluster under consideration.

As shown in **Table 4.19**, the pH trend is significant for all clusters. This is followed by the potassium trend, which is significant for all but one cluster (cluster 3). The trends for potassium and pH are probably interrelated, where a decrease in pH probably triggered changes in potassium as well.

Cluster 1 is the most dynamic in terms of detected temporal trends. Changes in pH, and concentrations of K, SO_4 and NO_3-N were found to be statistically significant. Other variables are also close to the level of significance and include at Na and Cl. The pH trend is however extremely ‘steep’ and for period under consideration its value declined by almost 2 units. Such acidification of the groundwater should warrant further investigation by the monitoring agency. It could either be the result of an ‘incoming’ wet period (with more carbonic acid available as a result of accelerated recharge) or a change in analytical method. The latter is, however, regarded as less likely. The nitrate trends point to a slight increase, whilst sulphate shows both downward and upward trends. The detected trends are not drastic (except for pH), but significant in relative rather than absolute terms. It must be noted that a change of only 1 mg/l for a particular variable with median concentration of 4 mg/l represents a 25% variation, which is then detected as significant.

The clusters 2 and 6 show trends in pH and K, which seem to be global. Cluster 3 only shows a change in pH, so the groundwater concentrations of this group are rather stable. Apart from pH and K, clusters 4, 5 and 7 show statistically significant trends in Ca, F and HCO_3 , respectively.

In summary, the water quality changes detected by the Karoo monitoring boreholes are only statistically significant for pH and K (decrease), whilst the change in other

elements varies from cluster to cluster. The detected changes are not great, but significant within the realm of an ambient groundwater quality monitoring network. If a network as well designed, the drastic changes in groundwater quality will be a matter of concern. The concentration changes in the ambient monitoring network are gradual, responding to hydrological events in a secular manner.

Table 4.19: *Computed trend statistics for all clusters (sampling event 3-11)*

cluster	1	2	3	4	5	6	7
K-S _{crit}	0.49	0.49	0.67	0.47	0.42	0.54	0.93
ranks	9	9	8	8	8	9	9
number	10	10	5	11	14	6	2
	K-S	K-S	K-S	K-S	K-S	K-S	K-S
TDS	0.34	0.32	0.45	0.42	0.25	0.21	0.75
pH	0.93	0.93	0.95	0.89	0.89	0.99	1.00
Ca	0.19	0.25	0.45	0.51	0.29	0.24	0.31
Mg	0.34	0.32	0.25	0.44	0.28	0.27	0.34
Na	0.42	0.32	0.25	0.33	0.37	0.46	0.53
K	0.87	0.75	0.20	0.58	0.73	0.71	0.99
NH ₄ -N	0.40	0.28	0.31	0.27	0.27	0.10	0.19
HCO ₃	0.22	0.15	0.25	0.29	0.34	0.27	0.97
SO ₄	0.52	0.19	0.52	0.29	0.16	0.26	0.12
Cl	0.42	0.18	0.41	0.26	0.21	0.37	0.47
NO ₃ -N	0.50	0.30	0.31	0.42	0.32	0.30	0.42
F	0.31	0.39	0.51	0.27	0.44	0.23	0.39
Si	0.21	0.18	0.42	0.29	0.18	0.12	0.49

Detected trends for Scenario 2 (events 1-11)

For this scenario, all sampling events were wherever possible in the analysis. As revealed in **Table 4.20**, clusters 4 and 7 could not be evaluated because their sampling record does not extend across all the sampling events. In such cases, the results from the previous scenario could have been used. The number of boreholes for which all the monitoring records are available is low, ranging from 33 to 67% of boreholes per cluster (zero boreholes in clusters 4 and 7).

The decreasing pH trends detected in the earlier 3 - 11 scenario analysis were again evident from the statistical analysis. The trend undetected by in previous scenario is that of a decline in the F concentrations. The noted trend in K concentrations also remained significant. Changes in other variables detected previously were not confirmed during this scenario analysis. This does not mean they are not significant,

it must be remembered that the total number of boreholes used in this scenario analysis is significantly less than in earlier 3 - 11 scenario. The results of this analysis are similar to the global test results, which also indicated statistically significant trends in pH, F and NH₄-N. The global test results, however, failed to detect the K trend.

Parameters close to the trend detection threshold include nitrate (cluster 1), TDS (cluster 2), bicarbonate (cluster 5). Nitrate (cluster 1) was detected in the previous scenario analysis, whilst TDS (cluster 2) and bicarbonate (cluster 6) were not. Different sample sizes thus seem to produce different results. It must be remembered that in both cases (scenario 3-11 and scenario 1-11) the evaluated datasets were incomplete and thus the composition of the datasets were different, which may produce inconsistent results.

This scenario analysis documents the fact that in order to obtain the most reliable results and to detect 'hidden' trends it is *absolutely necessary that stations be sampled every time and omissions are avoided.*

Table 4.20: Scenario 1-11 - Computed trend statistics for all sampling events

cluster	1	2	3	4	5	6	7
K-S _{crit}	0.54	0.58	0.83		0.62	0.62	
ranks	11	10	11		11	10	
number	8	7	3		6	6	
	K-S	K-S	K-S	K-S	K-S	K-S	K-S
TDS	0.35	0.54	0.65		0.29	0.27	
pH	0.91	0.86	0.98		0.79	0.90	
Ca	0.25	0.33	0.65		0.48	0.22	
Mg	0.24	0.33	0.58		0.28	0.31	
Na	0.35	0.49	0.42		0.29	0.21	
K	0.85	0.86	0.52		0.83	0.53	
NH ₄ -N	0.60	0.27	0.50		0.51	0.23	
HCO ₃	0.17	0.24	0.60		0.53	0.39	
SO ₄	0.39	0.35	0.65		0.29	0.19	
Cl	0.38	0.47	0.63		0.20	0.44	
NO ₃ -N	0.53	0.29	0.28		0.22	0.24	
F	0.70	0.55	0.85		0.73	0.34	
Si	0.15	0.27	0.47		0.29	0.16	

As already discussed, in spite of the fact that this scenario analysis is based on more events than the previous one, it failed to detect trends for specific clusters. This was probably due to the small number of sampling events per borehole. It will therefore be necessary to re-evaluate the network design and its specific stations.

4.4.4 CONCLUSIONS

The first detailed evaluation of the NGWQMP dataset was carried out to assess the variable hydrochemical conditions, both spatial and temporal, in Karoo aquifer systems and the process described above can serve as the basis for a pilot study of the performance of the NGWQMP system and to assess groundwater quality trends for the rest of the country.

This study indicated that no sampling points within a monitoring network should be bypassed during a routine sampling run, as it reduces the statistical power of any subsequent analysis. This does not rule out variance reduction designs, when certain stations are either added or removed from the network after careful statistically-based consideration.

The comparison between global tests on the entire database and pre-classified groups of data has shown that sub-division of the sampling stations is necessary, otherwise trends significant in certain sub-domains may go undetected. A hierarchical approach based on fuzzy *c*-means clustering was used to structure the station set into homogeneous groups. The structuring was based only upon water quality data and, in the future, it is recommended that other factors (i.e. rainfall, soil type, lithology, land use) be used in the classification process.

The trend detection method was applied to group of monitoring points, rather than individual monitoring points. Group-based statistical methods, in this case the Spearman ranks correlation coefficient, was shown to overcome the limitations of obtaining statistically significant results from relatively small datasets. The group-based results can also be used to detect anomalous classes, which can then be investigated at a local or individual monitoring station level.

All tests detected statistically significant decrease in pH and K over time. An overall decrease in the pH levels of almost 2 units, from 8.5 to 6.5, was detected. Global tests also revealed a decrease in F concentrations, which is probably related to the pH decrease. Analysis of individual clusters showed changes in other components such as NO₃, Ca, HCO₃, SO₄, which were not detected during the global analysis. The detected trends did not reveal any abrupt changes in groundwater quality, confirming that the network is correctly designed to fulfil its objective of monitoring the ambient groundwater quality at a national scale. The detected trends need to be further investigated and accounted for by means of specialist studies and/or further more detailed follow-up investigations.

Additional research is recommended aimed at identifying the factors responsible for detected changes in groundwater quality. Apart from other techniques, there is a tremendous potential for the application of fuzzy c-means clustering in uncovering 'hidden' spatial correlations and trends.

Chapter 5

RECOMMENDATIONS FOR FUTURE RESEARCH

The Karoo Basin is characterised by fractured-rock aquifers that are bisected by numerous vertical and horizontal dolerite intrusions. These conditions produce a unique and complex hydrogeological system, which complicates the study and development of the groundwater.

Water Research Commission (WRC) has funded a number of research projects aimed at providing a better insight into Karoo fractured-rock aquifers. This research has been varied and many aspects of the Karoo hydrogeology have been studied by various concerns. Projects have often dealt with specific problems, which were normally within the field of specialisation of the organisation conducting the research. They can be categorized as (1) regional projects (national mapping, chemistry, water evaluation and strategy), (2) exploratory projects (ground water occurrences), (3) experimental and localised projects (fracture behaviour and aquifer potential) and (4) technological development (geophysics, isotopes). Both local- and regional-scale geohydrological studies often require input from a number of related disciplines, each with its own field of specialisation. The costs of setting up and conducting these projects and the field-based studies during such research programmes are high (i.e. geophysical surveys, exploration drilling, pump-testing etc.).

Although the research has generally been of a high standard, little effort was made to collaborate or exchange results between the different teams. It is clear from a number of these reports that, had other aspects been considered or specialist inputs sought, the research results would have been enhanced. Many of these projects were in fact complementing each other. Strong divergences of opinions also rose that were never really resolved within the framework of a global programme. Besides, the lack of tight collaboration and communication between the different teams was not conducive to practical results i.e. bringing the water to the people.

Future WRC funded groundwater research programmes should therefore adopt a *multi-disciplinary programme-based approach*, both in terms of project conceptualisation and realisation (i.e. requiring a multi-disciplinary team). Convergence and divergence of opinion, expertise in specific field and practical results should now be brought together in order to synthesise and consolidate our knowledge, and transfer it to other people.

The need for future research is therefore two folded:

- *Water Resource Management*: to develop a program that will assess the resources of the main Karoo basin by applying the scientific results that were gathered for the last 15 years and therefore answer to the people's needs as well as evaluate the consequences on their environment
- *Technology transfer*: to pass the knowledge onto water users, practitioners or decision makers and sensitise / educate people on groundwater exploitation.

5.1 **WATER RESOURCE MANAGEMENT**

This applied research programme on main Karoo fractured-rock aquifer resource should address two fundamental problems and fill two major gaps in the present book:

How much water is available and abstractable: groundwater quantification
What are the needs for water: development and environment

5.1.1 **GROUNDWATER QUANTIFICATION**

The Main Karoo basin can be defined as a compartmented fractured-rock aquifer due to the vertical, transgressive and horizontal dolerite intrusions dissecting the flat-lying sediments, which are characterised by different permeability and porosity. Very little is known about the dynamics of the groundwater: water flow on regional scale, flow from one compartment to the other, depth, size and sustainability of various aquifers. Yet, significant advances could be made in that domain by combining the knowledge and results accumulated during the last 10 years and described in the present book, with a unique structured research programme.

Three key parameters have to be quantified:

- The depth of the various aquifers and the way they interact: hydrostratigraphy
- The reserve of the water available for abstraction
- The flow dynamics of groundwater on the regional scale

5.1.1.1 Hydrostratigraphy

The occurrence of deep-seated groundwater should be investigated with the purposes of proving or disproving:

- The presence of deeper, more regional groundwater flow system
- The presence of connate or fossils waters
- Aquifer stratification or hydrostratigraphic controls
- Possible inter-connectivity between aquifers
- Old ages

5.1.1.2 Reserves

Aquifer Geometry

Stratigraphy and structure of the Karoo basin are the main factors that control groundwater occurrences and shape and size of fractured-rock aquifers.

Primary storativity and permeability of the different sediments layers are known, although poorly constrained in some areas and especially at depth. Storativity of shallow flat-lying fractures in the sediments has been investigated but the water bearing potential of deeply buried fractures is unknown

The intrusion of dolerite was instrumental in the formation of fractured-rock aquifers and interconnectivity between reservoirs. They have been proven to form good traps for deep aquifers. Highresolution aero-magnetic surveys can be used to investigate the geometry and extension of the aquifers at depth.

Sustainability and Recharge

The research would include:

Development of methods to delineate preferential recharge zones within a Karoo fractured-rock aquifer and to assess recharge rates within each zone.

Pump-test method evaluation for the Karoo aquifers

Mapping aquifer recharge / discharge zones on a catchment scale using air- and satellite-borne sensors, i.e. radar.

Dating and tracing of deep water (below 200 m)

5.1.1.3 Flow Dynamics

Flow dynamics on the regional scale and meso-scale is still unknown. It requires studies on:

- Interconnectivity (remote sensing and spatial analysis of lineaments)
- Regional directional permeability
- Quantification of the transmissivity of the aquifer rock-matrix.
- Hydrochemistry: movement of pollutants in fractured-rock aquifers.

At a local scale the application of high resolution tomographic techniques to the study of fractures in Karoo sedimentary rocks, should be further investigated

5.1.2 GROUNDWATER DEVELOPMENT AND ENVIRONMENT

5.1.2.1 Availability and Needs

In the present book the problem of how groundwater can contribute to the needs of the people has not been addressed. Research in that domain should therefore be implemented such as methods of determining groundwater allocations (as part of the *groundwater reserve*) and improving the management of Karoo aquifers within the context of the catchments, as required in the new Water Act.

5.1.2.2 Environmental Issues

Groundwater and Ecosystems

Ecosystem dependency to shallow or deep aquifers and vulnerability to groundwater abstraction is a complex problem requiring a multidisciplinary approach:

- Hydrostratigraphy and aquifer quantification
- Spring evaluation, rainfall and recharge
- Geomorphology and catchment calculation
- Biosystems and temporal evolution
- Hydrochemistry and flow dynamics

The establishment of time series becomes a crucial issue. Remote sensing can be used to study the evolution of the ecosystems, vegetation, springs over the last 15 years. It can therefore be combined with hydrostratigraphy, geomorphology, rain fall history and recharge estimation in order to make prediction on the response of the ecosystem to high-volume abstraction schemes.

Water Quality

Additional research is recommended in ambient water quality monitoring in the Karoo basin. The research should be aimed at identifying the factors responsible for changes detected in groundwater over time.

There is a tremendous potential in the application of fuzzy C-means clustering in uncovering hidden spatial correlation and temporal trends.

Isotopes

The potential of environmental isotopes has not properly been exploited in the main Karoo Basin, and their use in research programmes should be encouraged. In addition, more research is required in different aspects of Karoo hydrogeology in order to establish the general principles and guidelines for their use in this environment. Some of the most important topics are enumerated below:

The exploitation potential of Karoo aquifers and evolution of the ecosystems;

An environmental isotope study of the origins of (high) nitrates in Karoo aquifers, with special reference to nitrogen isotopes;

Interdisciplinary studies involving environmental isotopes of mineralisation processes of Karoo groundwater;

Detecting pollution plumes entering rivers and estuaries using high-resolution airborne sensors;

5.2 TECHNOLOGY TRANSFER

5.2.1 INFORMATION TECHNOLOGY

5.2.1.1 Data Archiving and Accessibility

Each WRC project is archived by the organisation in charge of the research. The WRC should compile a GIS or digital data-base of information collected during these projects.

The information thus gathered should be stored and maintained by the WRC (or suitable organisation) and made available to WRC funded researchers and used for technology transfer or educational programmes. This data acquisition, compilation and management could be accomplished via small projects requiring an initial capital outlay, but with low-running costs.

5.2.1.2 Access to Technology

Development of user-friendly programs should be implemented.

Ex: analyse of pump-tests conducted in fractured-rock aquifers.

5.2.1.3 Layman Book

The book could be a simplified version on the present one with basic concepts illustrated with simple figures.

The targeted audience:

- Town planners and decision makers
- Farmers
- Schools

5.2.1.4 Website

The design of a Website should be put under the responsibility of the WRC.

5.2.2 EDUCATION

The design of a proper educational programme constitutes a research project on its own. The content of the programme and the items to be addressed are therefore difficult to lay out at this stage.

Should it be addressed to groundwater practioners only, or should it be extended to schools or to the whole population?

Two media forms should be used: formal courses and internet based 'online' training.

5.2.2.1 Training Courses

Courses for hydrogeologists on flow characterisation method and recharge are already available at IGS at the University of the Free State.

Other subjects should be considered like:

- Groundwater occurrence
- Methods to site successful boreholes
- Regional characterisation of fractured rock aquifers
- Environmental issues

5.2.2.2 Internet ‘Online’ Training

Online formation would be a follow up of the courses. It should be aimed at further assisting hydrogeologists and decision makers in their exploration search and planning and could be geared towards:

- Helping with general information on their region
- Provide advice or solutions to specific and localised problems

5.3 CONCLUSION

It is therefore recommended that the WRC establish a more formal working-group that will ensure that this approach is successfully implemented within its so-called “fractured-rock aquifer” research programme. The working group members should be primarily drawn from WRC-funded researchers and other role players within this field of research. The working-group should assist the WRC in developing a broader framework for future research into fractured-rock aquifers in South Africa.

In this approach, smaller specialised research projects would continue to be funded individually by the WRC, but would form part the broader research framework, being directed by the working-group. For instance, a WRC project aimed at studying the hydrostratigraphy may be coupled with other projects aimed at studying the isotopic character of Karoo aquifers, or evaluating the use of specific geophysical or remote-sensing techniques for locating groundwater. These projects may all form part of a broader research programme aimed at assessing the development and exploitation potential of a specific catchment.

These regional-scale research projects will require a multi-disciplinary approach, with specialist inputs from geologists (stratigraphy, structure, tectonics), geophysicists (deep depth-soundings, regional evaluation of spatial geophysical information), hydrogeologists (conceptualisation of flow systems and modelling), chemists (study of groundwater / rock chemistry, isotopes and groundwater dating studies), environmentalists (ecosystems), groundwater developers / users, and education specialists.

References

- Allsopp, H.L., Bristow, J.W., Smith, C.B., Brown, R., Gleadow, A.J.W., Kramers, J.D. and Garvie, O.G. (1986): *A summary of radiometric dating methods applicable to kimberlites and related rocks*. Fourth Intern. Kimberlite Conf., Perth, J. Ross ed., Vol.1, GSA special Publ. No 14, pp343 - 357.
- Andersen, N.J.B. and Ainslie, L.C., (1994): *Neotectonic reactivation - an aid to the location of ground water*. Afr. Geo. Rev. VI, pp1-10.
- Andrews, J. N., (1972): *Mechanism of radon release in rock matrices and entry into ground water*. Trans. Inst. Min. Metal. Section B81, pp198.
- Andreoli M.A.G., Doucouré M., Van Bever Donker J., Brandt D. And Andersen N.J.B. (1996): *Neotectonics of Southern Africa - A review*. Africa Geoscience Review, Vo.3, No1, 1-16.
- Bangert, B., Lorenz, V. and Armstrong, R., (1998): *Bentonitic tuff horizons of the Permo-Carboniferous Dwyka Group in southern Africa: volcanoclastic deposits as ideal time markers*. Abstracts, Gondwana 10 Proceedings, Cape Town, South Africa - Journal of African Earth Sciences, 27 (1A): 18-19.
- Barnes, C. J., Jacobson, G. & Smith, G. D.(1992): *The origin of high-nitrate ground waters in the Australian arid zone*, Journal of hydrology; V. 137, Issue 4, Issue 1, pp.181-197.
- Beekman, H. E., Gieske, A. and Selaolo, E. T; (1996): *GRES: Groundwater recharge studies in Botswana 1987-1996*. Botsw. Jnl of Earth Sci. 3, pp1-17.
- Beukes, N. J., (1969): *Die Sedimentologie van die Etage Holkranssandsteen, Sisteem Karoo*. Unpublished M.Sc. Thesis. Department of Geology, P.O. Box 339, Bloemfontein.
- Beukes, N.J., (1970): *Stratigraphy and sedimentology of the Cave Sandstone Stage, Karroo System*. Proceedings and Papers, 2nd Gondwana Symposium, Johannesburg, South Africa, p. 321-342.
- Binnie and Partners (1971) from Alan**
- Bodmer H.P., (1994): *The use of seismological data to predict overpressures*. Bull. Swiss. Assoc. Petroleum Geol, und-Eng., vol.61, 139, 69-81.
- Boehmer, W.K. and Boonstra, J. (1986): *Flow to wells in Intrusive Dykes*, Akademisch Proefskrif. Vrije Universiteit, Amsterdam.
- Bond, G.W., (1946): *A geochemical survey of the underground water supplies of the Union of South Africa*, Dept. of Mines, Geological survey Memoir, V41, pp.216.
- Botha, W. J., Wiegmans, F. E., van der Walt, J. J. and Fourie, C. J. S., (1992): *Evaluation of electromagnetic exploration techniques in groundwater exploration*. Water Research Commission Report no. 212/1/92.
- Botha, J.F., Vivier, J.J.P. & Verwey, J.P., (1996): *Grondwaterondersoek te Philippolis*. Verslag opgestel vir die Firma Cahi De Vries. Instituut vir Grondwaterstudies, Universiteit van die Oranje-Vrystaat, PO Box 339, Bloemfontein.

-
- Botha, J. F., Verwey, J. P., Van der Voort, I., Vivier, J. J. P., Colliston, W. P. and Looock, J. C. (1998): ***Karoo Aquifers. Their Geology, Geometry and Physical Behaviour***. WRC Report No 487/1/98. Water Research Commission, P.O. Box 824, Pretoria 0001.
- Bourdet, D., Ayoub, J.A. and Pirard, Y.M. (1984): ***Use of pressure derivative in well test interpretation***. Paper SPE 12777 presented at the 1984 SPE California Regional meeting, Long Beach, April 11-13.
- Bredenkamp, D. B; (1978): ***Quantitative estimation of groundwater recharge with special reference to the use of natural radioactive isotopes and hydrological simulation***. Unpub. PhD thesis, University of the Orange Free State.
- Bredenkamp, D. B., Verhagen, B. Th. and Botha, L; (1998): ***Hydrogeological and isotopic assessment of the response of a fractured multi-layered aquifer to long-term abstraction***. Final report on project K5/565 to the Water Research Commission.
- Brink, A.B.A., (1983): ***Engineering Geology of Southern Africa.***, Volume 3, The Karoo Sequence. Building Publications, Pretoria, South Africa, 320 pp.
- Brink A.B.A., (1985): ***Engineering geology of Southern Africa***, Post-Gondwana deposits. Vol. 4, Building Publication Pretoria, 332 pp.
- BRGM., (1978): ***Groundwater investigation at Beaufort West (Salt River)***, Bureau de Recherches Geologiques et Minières, Technical Report for DWAF, Contract No. W6018, Paris.
- Burger, C.A.J., Hodgson F.D.I. and Vand der Linde P.J. (1981): ***Hidrouliese eienskappe van akwifere in die Suid-Vrystaat. Die ontwikkeling en evaluering van tegnieke vir die bepaling van die ontginningspotensiaal van grondwaterbronne in die Suid-Vrystaat en in Noord-Kaapland***, Volume 2, Institut vir Grondwaterstudies.
- Burke, K. (1996): ***The African Plate***. S.afr.J.Geol., 99 (4), 341 - 409.
- Busenberg, E. and Plummer, L. N; (1992): ***Use of chlorofluorocarbons (CCl_3F and CCl_2F_2) as hydrologic tracers and age-dating tools: the alluvial and terrace system of central Oklahoma***. Water Res. Res; V28, No.9. pp2257-2283.
- Cadle, A.B. and Hobday, D.K., (1977): ***A subsurface investigation of the Middle Ecca and Lower Beaufort in northern Natal and the south-eastern Transvaal***. Transactions Geological Society of South Africa, Vol. 80, pp 111-115.
- Campbell, G.D.M., (1975): ***Groundwater Investigation at Beaufort West***, Technical Report Gh3235, Directorate: Geohydrology, Department Water Affairs & Forestry, Pretoria.
- Catuneanu, O., Hancox, P.J. and Rubidge, B.S., (1998): ***Reciprocal flexural behaviour and contrasting stratigraphies: a new basin development model for the Karoo retroarc foreland system, South Africa***. Basin Research, Vol.10, pp 417-439.
- Chevallier, L., (1997): ***Distribution and tectonics of kimberlites; a craton / off craton study from South Africa***. In: N.V. Sobolev and R.H. Mitchell Eds, Proceedings of the sixth International Kimberlite Conference, Novosibirsk, Russia, Vol.2,
- Chevallier, L. (1998): ***Karoo dolerites to Drakensberg basalts: structure, volcanics and seismicity***. In: Melis and Duplessis consulting Engineers (eds), Review of the current stage of knowledge
-

of the seismotectonic setting of Lesotho and its significance in predicting seismic design parameters for the Katse and Mohale Dams and further phases of the LHWP. Lesotho Highlands Water Project contract No 1028., Workshop in Maseru, 25 may, 1998. 17pp.?

Chevallier L. and Woodford A.C. (1999): *Morpho-tectonics and mechanism of emplacement of the dolerite rings and sills of the Western Karoo, South Africa.*, S.Afr.J.Geol., Vol. 102 (1), pp. 43-54.

Chevallier L., Goedhart, M. and Woodford A.C. (2001): *Influence of dolerite ring-structures on the occurrence of groundwater in Karoo Fractured Aquifers: a morpho-tectonic approach*, Project Number K937, Water Research Commission, Pretoria, p146.

Chorley, R. J. (1969): *Water, Earth and Man.*, Methuen & Co. Ltd., London.

Coetzee, D.S., (1983): *The deformation style between Meirings Poort and Beaufort West.* In: A.P.G. Söhnge and I.W. Hälbig (eds), Geodynamics of the Cape Fold Belt. Geol. Soc. S. Afr. Spec. Publ., No 12, 101 - 113.

Cogho, V.E., van Niekerk, L.J., Pretorius, H.P.J. and Hodgson, F.D.I., (1992): *The development of techniques for the evaluation and effective management of surface and ground-water contamination in the Orange Free State Goldfields*, Water Research Commission, Project Number K5/224, Pretoria.

Cole, D.I. and McLachlan, I.R., (1991): *Oil Potential of the Permian Whitehill Shale Formation in the Main Karoo Basin, South Africa.* In: Ulbrich, H. and Rocha Campos, A.C. (Eds). Gondwana Seven Proceedings. Instituto de Geociências, Universidade de Sao Paulo, Sao Paulo, Brazil, pp. 379-390.

Cole, D.I., Labuschagne L.S., Söhnge, Stettler E.H. and Scheinder G.I.C., (1991): *Aeroradiometric survey for uranium and ground follow-up in the Main Karoo Basin.* Geol. Surv., Memoir 76, 172 pp + map.

Cole, D.I. (1992): *Evolution and development of the Karoo Basin.* In: de Wit M.J. and Ransome I.G.D. (eds) Inversion tectonics of the Cape Fold Belt, Karoo and Cretaceous Basins of Southern Africa. Balkema, Rotterdam, pp87 - 99.

Cole, D.I. and Wipplinger, P.E., (in press): *Molybdenum in the Beaufort Group of the main Karoo basin.* Bulletin of the Council for Geoscience of South Africa.

Dally, D. and Warren, W.P., (1995): *Mapping Groundwater Vulnerability – The Irish Perspective.* Proceed (MILO).

Dawson J.B. (1962): *Basutoland kimberlites.* Geol. Soc. Am. Bull., v.73, 545 560.

Dawson, J.B., (1970): *The structural setting of African Kimberlite magmatism;* in Clifford T.N and Gass I.G., eds, African magmatism and tectonics: Oliver and Boyd, Edinburgh, Scotland, p 321 - 335.

De Beer, J. H., (1983): *Geophysical studies in the southern Cape Province and models of the lithosphere in the Cape Fold Belt.* In Söhnge, A P G and Hälbig, I W (1983) "Geodynamics of the Cape Fold Belt", Spec. Publ. geol. Soc. S. Afr. V12, 65-74.

-
- de la Rue Winter, H. and Venter, J.J., (1970): *Lithostratigraphic correlation of recent deep boreholes in the Karoo - Cape sequence*. In: Proceedings of the 1970 Gondwana Symposium. pp395 - 408.
- Department of Water Affairs, (1986): *Water Resources of the Republic of South Africa*. Department of Water Affairs and Forestry, Pretoria.
- D'Hoore, J., (1954): *Proposed classification of the accumulation zones of free sesquioxides on a genetic basis*. African Soils, Vol.3, 66 - 81.
- De Wit, M.C.J. (1996): *The distribution and stratigraphy of inland alluvial diamond deposits in South Africa*. Afr. Geos. Rev., 3, No2, 175 - 189.
- De Villiers, S B (1961). *Boorplekaanwysing vir water in Suidwes-Transvaal*. Bull. 34, Geol. Surv. SA, Pretoria.
- Driscoll, F. G., (1986): *Groundwater and Wells*. Johnson Division, St. Paul, Minnesota.
- Duane, M.J. and Brown, R., (1992): *Geochemical open-system behaviour related to fluid-flow and metamorphism in the Karoo Basin*. In: de Wit M.J. and Ransome I.G.D. (eds) Inversion tectonics of the Cape Fold Belt, Karoo and Cretaceous Basins of Southern Africa. Balkema, Rotterdam, 127 - 140.
- Duncan R.A., Hargraves R.B. and Brey G.P. (1978) Age, *paleomagnetism and chemistry of melilite basalts in the Southern Cape, South Africa*. Geol. Mag., 115, 317 - 327.
- Duncan, R.A., Hooper, P.R., Ehacek, J., Marsh, J.S. and Duncan, R.A., (1997): *The timing and duration of the Karoo igneous event, Southern Gondwana*. J. Geophys.Res., 102, 18127 - 18138.
- Du Plessis, A., Hartnady, C.J.H. and Partridge, T.C., (1997): *Causes of Southern African Seismicity*. Abstract. 29th International Union of Seismology and Physics of the Earth's Interior (IASPEI) General Assembly (Thessalonika, Greece, August 18 -28). Abstract Volume, Page xxx.
- Du Toit, A.L., (1954): *Geology of South Africa*. Oliver and Boyd, Edinburgh, 611 pp.
- Dunkle, S. A., Plummer, L. N., Busenberg, E., Phillips, P. J., Denver, J. M., Hamilton, P. A., Michel, R. L. and Coplen, T. B; (1993): *Chlorofluorocarbons (CCl₃F and CCl₂F₂) as dating tools and hydrologic tracers in shallow groundwater of the Delmarva Peninsula, Atlantic coastal plain United States*. Wat. Res. Res., V29, No.12, pp3837-3860
- Du Toit, A.L. (1905). *Geological survey of Glen Grey and parts of Queenstown and Woodehouse, including the Indwe area*. Geological Commission of the Cape of Good Hope, tenth annual report, 95-140.
- Du Toit, A.L. (1920) *The Karoo Dolerites- a study in Hypabyssal Intrusion*. Trans. Geol. Soc. S. Afr., V23, pp1-42.
- Du Toit A.L. (1929) *The geology of the major portion of East Griqualand. An explanation of Cape sheet No 35 (Matatiele)*. Geological Survey of the Union of South Africa. 36pp
- Ellis, F. and Schloms, B.H.A., (1981): *A note on the dorbanks (duripans) of South Africa*. Palaeoecology of Africa and the surrounding islands, vol. 15, 149 - 158.

-
- Engelbrecht, J.F.P., (1993): *An assessment of health aspects of the impact of Domestic and Industrial waste disposal activities on groundwater resources*, Water Research Commission, Report No. 371/1/93, Pretoria.
- Enslin, J.F., (1943): *Basins of decomposition in igneous rocks: their importance as underground water reservoirs and their location by the electrical resistivity method*. Trans. geol. Soc. S. Afr. V46, pp1-12.
- Enslin, J. F., (1949): *Die beperkte ondergrondse watervoorraad van die Unie*. Tydskrif vir Wetenskap en Kuns, October 1949, pp143-164.
- Enslin, J.F., (1950): *Geophysical methods of tracing and determining contacts of dolerite dykes in Karoo sediments in connection with the siting of boreholes for water*. Trans. geol. Soc. S Afr., V53, pp193-204.
- Enslin, J.F., (1955): *A new electromagnetic field technique*. Geophysics, V20, (2), pp318-314.
- Enslin, J.F., (1963): *The hydrological interpretation of electrical resistivity depth-probe surveys*. Ann. geol. Surv. S. Afr., V2, (2), pp83-122.
- Erdas Inc., 1997: *Erdas Field Guide*, Erdas Inc., Erdas Imagine 8.3, 4rd Edition, Atlanta, Georgia, 655p.
- Eriksson, P.G., (1981): *A palaeoenvironmental analysis of the Clarens Formation in the Natal Drakensberg*. Transactions Geological Society of South Africa, Vol.84, pp 7-17.
- Fahrig W.F. (1987) *The tectonic settings of continental mafic dyke swarms: failed arm and early passive margin*. In: H.C. Halls and W.F. Farhig (Eds), Mafic dyke swarms. Geol. Ass. Can. Spec. Pap., No 34, 331-348.
- Fatti, J.L. and du Toit, J.J.L., (1970): *A reflection seismic line in the Karoo Basin near Beaufort West*. Trans. geol. Soc. S. Afr., V73, pp17-27 + 3 plates.
- Faure K. and Cole, D.I., (1998): *Stable isotope evidence for a freshwater algal bloom in the Permian Karoo and Paraná Basins of southwestern Gondwana*. Abstracts, Gondwana 10 Proceedings, Cape Town, South Africa - Journal of African Earth Sciences, Vol. 27 (1A), pp. 70-71.
- Faure K. and Cole, D.I., (1999): *Geochemical evidence for lacustrine microbial blooms in the vast Permian Main Karoo, Paraná, Falkland Islands and Huab basins of southwestern Gondwana*, Paleogeography, Paleoclimatology, Palaeoecology, Vol. 152, pp. 189-213.
- Fernandez, L.M. and du Plessis, A., (1992): *Seismic hazard maps for Southern Africa*., Geological Survey of South Africa, Pretoria.
- Finch, J.W., 1990: *Location of high-yielding groundwater sites in Zimbabwe by use of remotely sensed data*., in Remote Sensing: An operational technology for the mining and petroleum industries, organized by the IMM in October 1990, London.
- Fontes, J-C., (1980): *Environmental isotopes in groundwater hydrology*., In: Handbook of environmental isotope geochemistry 1 P Fritz & J-C Fontes (Eds.) Elsevier, pp. 75-140.
-

-
- Freeze, A. L. and Cherry, J. A., (1979): *Groundwater*. Prentice-Hall Inc., Englewood Cliffs, New Jersey.
- Gordon, R.G., (1995): *Plate motions, crustal and lithospheric mobility, and palaeomagnetism: prospective viewpoint.*, *J. geophys. Res.*, V100, 24367-24392.
- Gordon, R.G., and Stein S., (1992): *Global tectonics and space geodesy*. *Science*, **256**, 333-342.
- Gordon-Welsh, J.F., (1974): *Hydrological phenomena in the southwestern Cape associated with the Ceres earthquake.*, In "The Earthquake of 29 September 1969 in the Southwestern Cape Province, South Africa", *Geol. Surv. S. Afr. Seismol. Ser. 4*, p.25-30.
- Greeff, G.J. (1968): *Fracture systems and the kimberlite intrusions of Griqualand West*. M.Sc. Thesis, Stellenbosch Univ., 126 p.
- Greenough J.D. and Hodych J.P. (1990) *Evidence of lateral magma injection in the Early Mesozoic dykes of eastern North America*. In: A.J. Parker, P.C. Rickwood and D.H. Tucker (Eds) *Mafic dykes and emplacement mechanisms*. A.A. Balkema, Rotterdam. 35 - 46.
- Groenewald, G.H., (1989): *Stratigrafie en sedimentologie van die Groep Beaufort in die Noordoos-Vrystaat*. *Bull. Geol. Surv. S. Afr.*, 96, 62 pp.
- Hälbich, I.W., (1992): *The Cape Fold Belt Orogeny: State of the art 1970' - 1980'*. In: de Wit M.J. and Ransome I.G.D. (eds) *Inversion tectonics of the Cape Fold Belt, Karoo and Cretaceous Basins of Southern Africa*. Balkema, Rotterdam, 141 - 158.
- Hälbich, I.W., Fitch F.J. and Miller, J.A., (1983): *Dating the Cape Orogeny*. In A.P.G. Söhngge and I.W. Hälbich (eds), *Geodynamics of the Cape Fold Belt*. *Geol. Soc. S. Afr. Spec. Publ.*, No 12, 149 - 164.
- Hälbich, I.W. and Swart, J., (1983): *Structural zoning and dynamic history of the cover rocks of the Cape Fold Belt*. In: A.P.G. Söhngge and I.W. Hälbich (eds), *Geodynamics of the Cape Fold Belt*. *Geol. Soc. S. Afr. Spec. Publ.*, No 12, 75 - 100.
- Hallbauer D.K., Chevallier L. and Woodford A.C. (1995) *The application of capillary ion analysis to the geochemistry of ground water from Western Karoo Aquifers*. *Ground Water Recharge and Rural Water Supply*, 26 -28 sept 1995, Midrand. Extended Abstract.
- Handcock, P.L. and Engelder, T., (1989): *Neotectonic joints*. *Soc. Am. Bull.*, V101, 1197 - 1208.
- Hartnady, C.J.H., (1990): *Seismicity and plate boundary evolution in southeastern Africa*. *S Afr. J. Geol.*, V93, pp473 - 484.
- Hartnady, C.J.H., (1998): *A review of the earthquake history and seismotectonic interpretation of the kingdom of Lesotho*. In: Melis and Duplessis consulting Engineers (eds), *Review of the current stage of knowledge of the seismotectonic setting of Lesotho and its significance in predicting seismic design parameters for the Katse and Mohale Dams and further phases of the LHWP*. Lesotho Highlands Water Project contract No 1028., Workshop in Maseru, 25 may, 1998. 37pp.
- Hartnady, C.J.H. and Woodford, A.C., (1996): *A feasibility investigation of the relationship between near-surface neotectonic crustal stress and groundwater occurrence in a Karoo fractured-rock aquifer*. Research proposal to the Water Research Commission.
-

-
- Hattingh, J. and Goedhart, M.L., (1997): *Neotectonic control on drainage evolution in the Algoa basin, southeastern Cape Province*. S. Afri. J. Geol., 100, 43- 52.
- Haxby, W.F. and Turcotte, D.L., (1976): *Stresses induced by the addition or removal of overburden and associated thermal effects*. Geology, 4, N03, 181-184.
- Heaton, T.H.E., (1986): *Isotopic studies of nitrogen pollution in the hydrosphere and atmosphere: a review*. Chem. Geol. (Isot. Geosc. Sect.) V59, pp87-102.
- Hem, JD, (1970): *Study and interpretation of chemical characteristics of natural waters*, U.S. Geological Survey Water Supply Paper, 1473, U.S. Govt. Printing Office, Washington.
- Hobday, D.K., (1973): *Middle Ecca deltaic deposits in the Muden-Tugela Ferry area of Natal*. Transactions Geological Society of South Africa, Vol.76, pp.309-318.
- Hodgson, F., Verhagen, B. Th. and van der Linde P. J; (1977): *The use of groundwater chemistry in detemining the relative age of groundwater occurrences in the southern Orange Free State*. Unpub. Rep. IGS, UOFS.
- Holmes, P.J. and Reynhardt, J.H., (1989): *Late Cenosoic alluvial gravels in the vicinity of Aliwal North*. Suid- Afrik. Tydsk. vir Wetenskap. Vol. 85, 65 - 68.
- Hooper, P.R., Rehacek, J., Duncan, R.A., Marsh, J.S., and Duncan, A.R., (1993): *The basalts of Lesotho, Karoo Province, Southern Africa*. EOS, Vol. 74, 553.
- Horne, R.N. (1997): *Modern Well Test Analysis. A computer-aided approach*. Petroway Inc., Palo Alto, USA. 257 p.
- Hübner, H., (1986): *Isotope effects of nitrogen in the soil and biosphere*. In: Handbook of Environmental Isotope Geochemistry 2 (P Fritz & J-C Fontes, Eds) Elsevier. pp.361-426.
- Hunter D.R. and Reid D.L., (1987): *Mafic dykes swarms of Southern Africa*. In: Halls H.C. & Fahrig W.F. (Eds.), Mafic Dyke Swarms. Spec. Pap. geol. Assoc. Canada, 34, 445-456.
- IAEA, (1983): *Guidebook on nuclear techniques in hydrology*. Tech. Rep. Series 206. IAEA, Vienna.
- IAEA, (1992): *Statistical treatment of data on environmental isotopes in precipitation*. Techn. Rep. Series No.331, IAEA, Vienna.
- Johnson, M.R., Van Vuuren, C.J., Visser, J.N.J., Cole, D.I., Wickens, H. de V., Christie, A.D.M., Roberts, D.L., and Brandl, G., (1997): *The foreland Karoo Basin, South Africa*. In: R.C. Selley (Ed.), African Basins. Sedimentary Basins of the World, 3. Elsevier, Amsterdam.
- Kent, L.E., (1972): Springs, In Eeden, O.R., 1972, *The geology of the Republic of South Africa*. An Explanation to the 1:1 000 000 map, 1970. Special publication 18, Geological Survey, Department of Mines, p. 71-74.
- Kent, L.E. and Enslin, J.F., (1965): *Ground-water prospecting methods used in the Republic of South Africa*. Ann. Geol. Surv. SA, V4, pp151-156 + 4 folders.
- Keys, W.S., (1989): *Borehole geophysics applied to ground-water investigations*. National Water Well Ass., Dublin, Ohio, pp.314.

-
- Kingsley, C.S., (1981): *A composite submarine fan-delta-fluvial model for the Ecca and lower Beaufort Groups of Permian age in the eastern Cape Province, South Africa*. Trans. Geol. Soc. S. Afr., 94, 27–40.
- Kirchner, J. O. G., Van Tonder, G. J. and Lukas, E., (1991): *Exploitation Potential of Karoo Aquifers*. WRC Report No 170/1/91. Water Research Commission, P.O. Box 824, Pretoria 0001.
- Kok, T.S., (1982): *Municipal Water Supply from Jagersfontein Mine, Orange Free State*, Department of Water Affairs & Forestry, Directorate Geohydrology Technical Report GH1482, Pretoria, South Africa.
- Kok, T.S., (1981): *Bibliography of publications and theses on southern African groundwater subjects*. Dept. Of Water Affairs and Forestry, Technical Report GH 3160, Pretoria.
- Kokelaar B.P. (1983) *The mechanism of Surtseyan volcanism*. J. Geol. Soc., 140, 939 - 944.
- Kruger, J.C. and Kok, T.S., 1976: *Die voorkoms van grondwater in dolerietgange in dele van noordoos-vrystaat*, Department of Water Affairs & Forestry, Directorate Geohydrology Technical Report GH1482, Pretoria, South Africa.
- KwaZulu-Natal Hydrogeological mapping project (1995): Units 8, 9, 10 and 11. Department of Water Affairs and Forestry, Pretoria, Empangeni. 11 reports (geographic units 1 to 11) + maps.
- Leskiewicz, A.F., (1979): Nelspoort – *Salt River groundwater investigation.*, Technical Report GH3124, Department of Water Affairs and Forestry, Pretoria.
- Maclear, L.G.A. and A.C. Woodford, A.C., (1995): *Factors affecting spring-flow variations at Uitenhage Springs, Eastern Cape*. In Groundwater 95 - Groundwater Recharge and Rural Water Supply, 26-28 September 1995, Volkswagen Conference Centre, Midrand, South Africa.
- Marsh, G., (1991): *Inaugural field trip to the Northern Cape. The volcanology Group of the Mineralogical Association of South Africa.*, 11 - 13 October 1991. Guide book. Rhode University, Grahamstown
- Marsh, J.S., Hooper, P.R., Rehacek, J., Duncan, R.A. and Duncan, A.R., (1997): *Stratigraphy and age of Karoo basalts of Lesotho and implications for correlations within the Karoo igneous Province*. In: Mahomey J. & Coffin M. (eds) Large Igbeous Provinces: continental, Oceanic and Planetary Flood Volcanism. Am. Geoph. Un., Geophys. Mono. No 100, 247 - 272.
- Marshall, J.E.A., (1994): *The Falkland Islands: A key element in Gondwana paleogeography*, Tectonics, Vol.13, No2, 499 - 514.
- Maske S., (1966): *The petrography of the Ingeli Mountain Range*. Annale Universiteit van Stellenbosch, Vol. 41, 108 pp.
- Maree, B.D., (1943): *Notes on some magnetometric surveys, with special reference to anomalies on Karoo dolerites*. Trans. geol. Soc. S. Afr., V46.
- Mazor, E. and Verhagen, B. Th; (1983): *Dissolved ions, stable and radioactive isotopes and noble gases in thermal waters of South Africa*. J. of Hydrology V63, pp315-329.

-
- Mazor, E., (1991): *Applied chemical and isotopic groundwater hydrology*. Open University Press. 274 pp.
- Meyboom, A.F. and Wallace, R.C., (1978): *Occurrence and origin of ring-shaped dolerite outcrops in Eastern Cape Province and Western Transkei*, Trans. Geol. Soc. S. Afr., 81, 95-99.
- Meyer, R. en van Zijl, J.S.V., (1980): *Die ontwikkeling en evaluasie van tegnieke vir die bepaling van die ontginningspotensiaal van grondwaterbronne in die Doornberg-breuksone*. Finale verslag Deel 2(b): Venterstad-omgewing - Geofisiese studies. Water Research Commission Project K5/28.
- Meyer, R, van Zijl, J.S.V. en de Beer, J.H., (1980): *Die ontwikkeling en evaluasie van tegnieke vir die bepaling van die ontginningspotensiaal van grondwaterbronne in die Doornberg-breuksone. Finale verslag Deel 3(b): De Aar- en Prieska-omgewing - Geofisiese en geohidrologiese ondersoek van die Prieskagebied*. Water Research Commission Project K5/28.
- Mohale Consultants Group (2000): *Seismo-tectonic setting of Lesotho and the assessment of the maximum regional earthquake (M_{max}) for Katse, Mohale and Mashai dam sites of the Lesotho Highlands Water Project*, Lesotho Highlands Development Authority, Report No. 1017-08-01, Vol. 1.
- Murray, E.C., (1996): *Masakala Borehole Yield Assessment*. Unpublished Technical Report by Rural Support Services, East London.
- Murray, E.C., (1996): *Guidelines for assessing borehole yields in secondary aquifers*. Unpublished M.Sc. thesis, Univ. of Rhodes, Grahamstown.
- Newton, A.R., (1993): *Thrusting on the northern margin of the Cape Fold Belt, near Laingsburg*. S.Afr.J.Geol., 96 (1/2), 22 - 30.
- Nixon P.H., Boyd F.R. and Boctor N.Z. (1983) *East Griqualand kimberlites*. Trans. Geol. Soc. S. Afr., 86, 221 - 236.
- Nixon P.H. and Kresten P. (1973) *Butha-Buthe swarm and associated kimberlite blows*. In: *P.H. Nixon Ed., Lesotho kimberlites*. Lesotho National Development Corporation. 197 - 206.
- Norman J.L., Price N.J. and Petres E.R. (1977) *Photogeological fracture trace study of controls of kimberlite intrusion in Lesotho basalts*. Mining and Metallurgy, Mai 1977, 78 - 90.
- Oelofsen, B.W. and Araujo, D.C., (1987): *Mesosaurus tenuidens and Stereosternum tumidum from the Permian Gondwana of both southern Africa and South America*. South African Journal of Science, Vol. 83, pp. 370-372.
- Olivier H.J. (1972): *Geohydrological investigation of the flooding of shaft 2, Orange - Fish tunnel, North eastern Cape Province*. Trans. Geol Soc. S. Afri., 75, pp197- 219.
- Parsons, R.P. and Jolly, J.L. (1994): *The development of a systematic method for evaluating site suitability for waste disposal based on geohydrological criteria*; WRC Report No. 485/1/94, Water Research Commission, Pretoria.

-
- Partridge, T.C., (In press): *Of diamonds, Dinosaurs and diastrophism: 150 million years of landscape evolution in Southern Africa*. The 25th Alex Du Toit memorial lecture 1997.
- Partridge, T.C. and Maud, R.R., (1987): *Geomorphic evolution of Southern Africa since the Mesozoic*. South African Journ. Geol., 90, 179 - 208.
- Parsons, R.P., (1986): *The exploration and evaluation of groundwater ubits south and west of Graaff-Reinet, Cape Province, South Africa.*, Unpubl. MSc. Thesis, Rhodes University, Grahamstown.
- Parsons, R.P., (1995): *A South African aquifer system management Classification*. **Water (MILO)**.
- Parsons, R.P. and Conrad, J., (1997): *Explanatory notes for the development of a groundwater contamination susceptibility map of South Africa*, Draft report for Water Research Commission & SA Oil Industry Environmental Committee.
- Paver, G.L., Simpson, D.J., Freeman, C.J., and Clark, M.A. (1943): *The location of underground water by geological and geophysical methods*, Compiled from Technical Work of the Unit 42nd Geological Section, South African Engineering Corps, U.D.F., M.E.F. April 1943, published by G.H.Q and printed M.M.P. & P Coy., S.A.E.C.
- Potgieter, G.J.A., (1981): *Die ontwikkeling en evaluering van tegnieke vir die bepaling van die ontginningspotensiaal van grondwaterbronne in die Suid-Vrystaat en in Noord-Kaapland*. Volume 3: Grondwaterondersoeke in Nooord-Vrystaat en Noord-Kaapland. Instituut vir Grondwaterstudies, Universiteit van die Oranje Vrystaat.
- Repsold, H., (1989): *Well logging in groundwater development*. Int. Contributions to Hydrogeology, Vol. 9, pp. 165, Int. Ass. of Hydrogeol., Verlag Heinz Heise, Hannover, Germany.
- Rowell, D.M. and de Swart, A.M.J., (1976): *Diagenesis in Cape and Karoo sediments, South Africa and its bearing on their hydrocarbon potential*. Trans. geol. Soc. S. Afr., pp81-145.
- Rogers, A.W. and Du Toit A.L. (1903). *Geological Survey of parts of the divisions of Ceres, Sutherland and Calvinia*. Ann. Report of Cape Geol. Comm., 36-43.
- Rust, I.C., Shone, R.W. and Siebrits, L.B., (1991): *Carnarvon Formasie: golf-oorheersde sedimentasie in 'n vlak Karoosie*. South African Journal of Science, Vol.87, pp.198-202.
- Salman, A. B., 1983: *Using Landsat imagery interpretation for underground water prospection around Quena Province Egypt.*, Int. J. Remote Sensing, Vol. 4, No 2, pp. 179-189.
- Self, S. and Thordarson, T., (1998): *Eruption dynamics and volatile release in floodbasalts eruptions*. Abstract. IAVCEI, International Volcanological Congress, Cap Town, July 1998. Abstract Volume, 55.
- Seward, P., (1982): *Possibilities for groundwater development in the Vanwyksvlei area*, Technical Report GH3225, Department of Water Affairs and Forestry, Pretoria.
- Siebrits, L.B., (1987): *Die sedimentologie van die Formasie Carnarvon in die omgewing van Carnarvon*. Unpublished M.Sc. thesis, University of Port Elizabeth, 92pp.
- Siegal, B.S. & Gillespie, A.R. (Eds), 1980: *Remote Sensing in Geology.*, Wiley & Sons, New York.
-

-
- Shudofsky, G.N., (1985): *Source mechanism and focal depths of East African earthquakes using Rayleigh-wave inversion and body-wave modelling*. Geophys. J. R. astr. Soc., 83, 563-614.
- Sibson, R.H., (1990): *Rupture nucleation on unfavorably oriented faults*. Bull. Seism. Soc. Am., 80/6, 1580-1604.
- Smart, M.C., (1994): *Mimosadale wellfield long term yield and future groundwater development at Graaff Reinet.*, DWAf Technical Report GH 3836, Pretoria.
- Smith C.B., Allsopp, H.L., Kramers, J.D., Hutshinson, G. and Roddick, J.C. (1985) *Emplacement ages of Jurassic - Cretaceous South African kimberlites by Rb - Sr method on phlogopite and whole-rock samples*. Trans. Geol. Soc. S. Afr., 88, 249 - 266.
- Smith, R.H.M., (1990): *A review of stratigraphy and sedimentary environments of the Karoo Basin of South Africa*. J. Afr. Earth Sc., 10, 117–137.
- Smith, R.M.H., Eriksson, P.G., & Botha, W.J., (1993): *A review of the stratigraphy and sedimentary environments of the Karoo-aged basins of Southern Africa*. J. Afr. Earth Sc., 16, 143–169.
- Smith C.B., Clark T.C., Barton E.S. and Bristow J.W. (1994): *Emplacement ages of kimberlite occurrences in the Prieska region*, Southwest border of the Kaapvaal Craton, South Africa. Chem. Geol., 113, 149-169.
- Stear, W.M., (1980): *Sedimentary environment of the Beaufort West Group uranium province in the vicinity of Beaufort West, South Africa*. PhD thesis, Univ. Port Elizabeth (unpubl.).
- Steffen, Robertson and Kirsten (SRK), (1987). *Wellfield development at Graaff-Reinet; Phase 1*. Unpublished Technical Report CE 5892/1, Cape Town.
- Steffen, Robertson and Kirsten (SRK), (1988). *Wellfield development at Graaff-Reinet; Phase 2*. Unpublished Technical Report CE 5892/2, Cape Town.
- Steffen, Robertson and Kirsten (SRK), (1991 – 1993). *Wellfield monitoring: Graaff-Reinet*. Unpublished Quarterly reports 164555/M, Cape Town.
- Steffen, Robertson and Kirsten (SRK), (1997): *Beaufort West Municipality: Brandwacht Aquifer and Wellfield Groundwater Flow Model.*, (Kotze J C and Rosewarne P N), Steffen, Robertson & Kirsten report: 227331/3, Cape Town.
- Storey, B.C. and Kyle, P.R., (1997): *An active mantle mechanism for Gondwana breakup.*, South Africa. S.Afr.J.Geol., 100 (4), 283 - 290.
- Tankard, A.J., Eriksson, K.A., Hunter, D.R., Jackson, M.P.A., Hobday, D.K., and Minter, W.E.L., (1982): *Crustal Evolution of Southern Africa*. Springer-Verslag, New York, 523 pp.
- Tavener-Smith, R., Cooper, J.A.J., and Rayner, R.J., (1988): *Depositional environments in the Volksrust Formation (Permian) in the Mhlathuze River, Zululand*. S. Afr. J. Geol., 91, 198–206.
- Theron, A.C., (1967): *The Sedimentology of the Koup Subgroup near Laingsburg*. Unpublished M.Sc. thesis, Geology Department, University of Stellenbosch, Stellenbosch, South Africa, 22 pp.

-
- Theron, J.N. and Blignault, H.J., (1975): *A model for sedimentation of the Dwyka glacials in the south-western Cape*. In: Campbell, K.S.W. (Ed.). *Gondwana Geology*. Australian National University Press, Canberra, pp. 347-356.
- Thomas R.J., Du Plessis A., Fitch F.J., Marshall C.G.A., Miller J.A, von Brunn V. and Watkeys M.K. (1992): *Geological studies in southern Natal and Transkei: implication for Cape Orogen*. in De Wit M.J. and Ransome I.G.D. (Eds), Inversion tectonics of the Cape Fold Belt, Karoo and Cretaceous Basins of Southern Africa. Conference on inversion tectonics of the Cape Fold Belt Proceedings, South Africa. Balkema, Rotterdam. 229 - 236.
- Tordiffe, E.A.W., 1978:, unpubl. Ph.D. Thesis *Aspects of the hydrochemistry of the Karoo Sequence in the Great Fish River Basin, Eastern Cape Province, with special reference to the groundwater quality*, Univ. O.F.S.
- Turner, B.R. & Thomson, K., 1998: *Tectonostratigraphical development of the Upper Karoo foreland basin: orogenic unloading versus Gondwana rifting*, Implications for the Mesozoic evolution of the Falkland Plateau and Wets Gondwana, *Journal of African Earth Sciences*, Vol 27 (1A), p.201-202.
- Van Copenhagen, J.D., (1953): *Groundwater in the Karoo System rocks of the Eastern Cape and the application of various geophysical and geological methods to borehole siting*. Geol. Surv. S. Afr., Technical Report GH 888.
- Van der Merwe, D.H., (1961): *Weathering of various types of Karoo Dolerite, in the Middelburg area*, Cape Province., *Trans. Geol. Soc. S. Afr.*, V65(2), pp119-138.
- Vandoolaeghe, M.A.C., (1979): *Middelburg geohydrological investigation.*, Unpublished Technical Report GH3072, Directorate:Geohydrology, Department of Water Affairs, Cape Town.
- Vandoolaeghe, M.A.C., (1980): *Queenstown geohydrological investigation.*, Unpublished Technical Report GH3135, Directorate:Geohydrology, Department of Water Affairs, Cape Town.
- Van Tonder, G.J., Woodford, A.C., and Van Wyk, A. (1998): *The Flow Characteristic Method: a new method for the estimation of the long-term sustainable yield of a borehole*, in press.
- Van Wyk, W.L., (1963): *Groundwater studies in northern natal, zoland and surrounding areas*, Memoir 52, Geological Survey of South Africa, pp133.
- Van Zijl, J.S.V., (1977): *A practical manual on the resistivity method.*, CSIR report FIS 142, 1st edition, 132pp.
- Van Heerden, W.L., (1976): *Practical application of the CSIR triaxial strain cell for rock stress measurements*. In: Bieniawski, Z.T. (ed.). *Exploration for Rock Engineering, Vol. 1*. A.A. Balkema, Cape Town, p. 189-194.
- Van Vuuren, C.J. and Cole, D.I., (1979): *The stratigraphy and depositional environments of the Ecca Group in the northern parts of the Karoo basin*. In: Anderson A.M. and Van Biljon, W.J. (Eds.). *Some Sedimentary Basins and Associated Ore Deposits of South Africa*. Special Publication Geological Society of South Africa, Vol.6, pp.103-111.
- Van Zijl, J.S.V., (1979): *A resistivity study of the Karoo basin.*, Proc. 18th Geol. Congr. Geol. Soc. S. Afr., Part 1, pp400-401.
-

-
- Veevers, J.J., Cole, D.I. and Cowan, E.J., (1994): *Southern Africa: Karoo Basin and Cape Fold Belt*. In: Veevers, J.J. & Powell, C. McA. (Eds.), Permian-Triassic Pangean Basins and Foldbelts Along the Panthalassan Margin of Gondwanaland. Mem. Geol. Soc. Am., 184, 223–279.
- Vegter, J.R., 1984: *Opening Address by the Minister of Agricultural Economics and Water Affairs*, drafted by J.R. Vegter, Groundwater Conference arranged by NGWA (now Water Borehole Association) and Groundwater Division of the Geological Society of South Africa, Pretoria, Directorate:Geohydrology File Reference BG 3/10/1, Department of Water Affairs.
- Vegter, J.R., (1992): *An evaluation of ground water exploitation and its potential for urban use, De Aar*, hydrogeological consulting report to the Directorate of Geohydrology, Department of Water Affairs and Forestry, Pretoria, South Africa.
- Vegter, J.R., (1995): *An explanation of a set of national groundwater maps.*, Water Research Commission, Report 483, TT74/95, Pretoria.
- Verhagen, B. Th. and Smith, P.E; (1978): *Brief report on a preliminary isotope and chemical study of ground water and river water in the Great Fish River valley*. Unpub. report to the NIWR, CSIR.
- Verhagen, B. Th., (1984): *Environmental isotope study of a groundwater supply project in the Kalahari of Gordinia.*, Isotope Hydrology 1983. IAEA Vienna. pp. 415-432.
- Verhagen, B. Th., Geyh, M. A., Froehlich, K. and Wirth, K; (1991): *Isotope hydrological methods for the quantitative evaluation of ground water resources in arid and semi-arid areas*. Research reports: Fed. Ministry for Econ. Coop., FRG. ISBN 3-8039-0352-1.
- Verhagen, B. Th., (1993): *Jwaneng ground water: an isotopic model*. In: Africa Needs Ground Water. Convention Papers Vol.1. Paper 22. ISBN 0-620-17829-5
- Verhagen, B. Th., Butler, M. J., Levin, M. and Walton, D.G; (1996): *Investigation of ground water pollution associated with waste disposal: development of an environmental isotope approach*. Final report to the Water Research Commission on Project K5/311.
- Viljoen, J.H.A., (1994): *Sedimentology of the Collingham Formation, Karoo Supergroup*. South African Journal of Geology, Vol.97, pp.167-183.
- Visser, J.N.J., (1986): *Lateral lithofacies relationships in the glaciogene Dwyka Formation in the western and central parts of the Karoo Basin*. Trans. Geol. Soc. S. Afr., 89, 373–383.
- Visser, J.N.J., (1987): *The palaeogeography of part of the southwestern Gondwana during the Permo-Carboniferous glaciation*. Palaeogeography Palaeo-climatology Palaeogeography, Vol.61, pp.205 – 219.
- Visser, J.N.J., (1991): *Geography and climatology of the Late Carboniferous to Jurassic Karoo Basin in south-western Gondwana*. Annals South African Museum, Vol.99 (12), pp. 415-431.
- Visser, J.N.J., (1992): *Deposition of the Early to Late Permian Whitehill Formation during a sea-level highstand in a juvenile foreland basin*. South African Journal of Geology, Vol.95, pp.181-193.

-
- Visser, J.N.J., (1993): *Sea-level changes in a back-arc - foreland transition: the late Carboniferous - Permian Karoo Basin of South Africa*. Sedimentary Geology, Vol.83, pp.115-131.
- Visser, J.N.J., (1997): *Deglaciation sequences in the Permo-Carboniferous Karoo and Kalahari basins of southern Africa: a tool in the analysis of cyclic glaciomarine basin fills*. Sedimentology, Vol.44, pp.507-521.
- Visser, J.N.J. and Botha, B.J.V., (1980): *Meander channel, point-bar, crevasse splay and aeolian deposits from the Elliot Formation in Barkly Pass, northeastern Cape*. Trans. Geol. Soc. S. Afr., 83, 55–62.
- Visser, J.N.J. and Looock, J.C., (1978): *Water depth in the main Karoo Basin, South Africa, during Ecca (Permian) sedimentation*. Transactions Geological Society of South Africa, Vol.81, pp.185-191.
- Visser, J.N.J. and Praekelt, H.E., (1996): *Subduction, mega-shear systems and Late Palaeozoic basin development in the African segment of Gondwana*. Geologische Rundschau, Vol.85, pp.632-646.
- Visser, J.N.J., Van Niekerk, B.N. and Van der Merwe, S.W. (1997): *Sediment transport of the Late Palaeozoic glacial Dwyka Group in the southwestern Karoo Basin*. South African Journal of Geology, Vol.100, pp.223-236.
- Visser, H.N; von Backström, J.W; Keyser, U; van der Westhuizen, J.M; Marais, J.A.H; Coetzee, C.B; Schumann, F.W; van Wyk, W.L; de Villiers, S.B; Coertze, F.J; Wilke, P.P; de Jager, D.H; Rilett, M.H. and Toerien, B., (1963): *Gips in die Republiek van Suid Afrika.*, Geological Survey Handbook No 4, pp 134 + maps.
- Vogel, J.C., (1970): *Carbon-14 dating of ground water*. In: Isotope Hydrology 1970. pp225-240. IAEA, Vienna.
- Vogel, J. C. and van Urk, H; (1975): *Isotopic composition of groundwater in semi-arid regions of southern Africa*. J. of Hydrol. V25, pp23-36.
- Vogel, J.C., and Heaton, T.H.E; (1980(a)): *The isotopic, chemical and dissolved gas concentrations in groundwater near Venterstad, Cape Province.*, CSIR, Technical report 391, Natural Isotopes Division, Pretoria.
- Vogel, J.C., Talma, A.S. and Heaton, T.H.E; (1980(b)): *Natural isotope studies of the groundwater in the Beaufort West area*. CSIR, Pretoria. Final report Kon/Gf/74/1; K 5/28
- Von Hoyer, M., & Rinkel, M.W., (1976): *Ground Water development in the area southwest of De Aar.*, Unpublished Technical Report GH2886, Directorate:Geohydrology, Department of Water Affairs, Pretoria.
- Von Hoyer, M., & Rinkel, M.W., (1976): *Ground Water development in the southeast of De Aar.*, Unpublished Technical Report GHXXX, Directorate:Geohydrology, Department of Water Affairs, Pretoria.
- Walton, J. (1998): *Windpumps in South Africa*. Human & Rousseau, Cape Town.

-
- Weaver, J.M.C., Conrad, J.E. and Eskes, S.J.T., (1993): *Valley calcretes: another Karoo ground water exploration target*. Proc. Convention: Africa needs ground water. Ground Water Division, GSSA, Univ. of the Witwatersrand, Johannesburg, Vol. I, Paper 8.
- Weaver, J.M.C. and Talma, S., (1997): *CFC-s and Groundwater age-dating in South Africa's fractured rock aquifers*. Progress Report to the Water Research Commission, Pretoria.
- Weinert, H.H., (1974): *A climatic index of weathering and its application in road construction*, Geotechnique, 24 (4), pp475-488.
- Wending, J., Fillion, E. and Trouillard, J.M., (1994): *Geometrie de la fracturation et écoulements. Perméabilité et porosité directionnelles en milieu sédimentaire fracturé. Sites de Tabuk et Tayma (Arabie Saoudite)*. Report BRGM A 01865 (Orléans), 54pp.
- White, R.S., (1997): *Mantle plume origin for the Karoo and Ventersdorp flood basalts, South Africa*. S.Afr.J.Geol., 100 (4), 271 - 282.
- Wickens, H. de V., (1994): *Basin Floor Fan Building Turbidites of the southwestern Karoo Basin, Ecca Group, South Africa*. Ph.D. thesis (unpublished), Geology Department, University of Port Elizabeth, Port Elizabeth, South Africa, 233 pp.
- Winter, H. de la R., and Venter, J.J., (1970): *Lithostratigraphic correlation of recent deep boreholes in the Karoo-Cape sequence.*, Proc. 2nd. Gondwana Symp., IUGS Commission on Stratigraphy, pp395-408.
- Woodford, A.C. (1984): *Possibilities for groundwater development in the Graaff-Reinet area. Part I: The Van Rhyneveldspas Basin*. Department of Water Affairs & Forestry, Technical Report GH3341, Pretoria.
- Woodford, A.C. (1989): *Preliminary evaluation of aquifer tests conducted in the South-Eastern / Burgerville areas, southeast of De Aar.*, Department of Water Affairs & Forestry, Technical Report GH3645, Pretoria.
- Woodford, A.C., (1989): *The Exploration and Evaluation of Groundwater Units in Van Rynevelds Pass Dam Basin, North of Graaff-Reinet, Cape Province*, Unpublished MSc Thesis, Rhodes University, Grahamstown.
- Woodford, A.C., (1992): *Comments on the Mimosadale wellfield for meeting 08/12/1992*. Directorate of Geohydrology, Letter to Graaff-Reinet Municipality, Department of Water Affairs and Forestry.
- Woodford A.C. and Chevallier L., (2000): *Regional characterization and mapping of Karoo fractured aquifer systems - An integrated approach using a geographical information system and digital image processing*, Water Research Commission, Project Report K653, Pretoria, p209.
- Woodford, A.C. and Chevallier, L (in press): *Hydrogeology of the dolerite breccia-plugs of the Western Karoo*, In preparation.
- Wright, E.P. and Burgess, W.G. (eds.) (1992): *Hydrogeology of Crystalline Basement Aquifers in Africa*, Geol. Soc. Spec. Publ. No.66, pp 77-85.

-
- Zoback, M.L., (1992): *First- and second-order patterns of stress in the lithosphere: The World Stress Map Project*. J. geophys. Res., V97, pp 11702-11728.
- Zoback, M.L. and Zoback, M.D., (1980): *State of stress in the conterminous United States*. J. Geophys. Res., V85, pp6113 - 6156.
- Zoback, M.L., Zoback, M.D., and the World Stress Map Team, 1989: *Global patterns of tectonic stress*. Nature, V341, pp291-298.
- Zumberge, J. H. and Nelson, C. A., (1984): *Elements of Physical Geology*. John Wiley & Sons Inc., New York